UNIVERSITY OF ALBERTA

# Flow of Formation Water in the Alberta Basin Adjacent to the Rocky Mountains Thrust and Fold Belt, West-Central Alberta, Canada

by

**Karsten Michael** ©

A thesis submitted to the Faculty of Graduate Studies and Research in partial fulfilment of the requirements for the degree of Doctor of Philosophy.

Department of Earth and Atmospheric Sciences

Edmonton, Alberta

Fall, 2002

Reproduced with permission of the copyright owner. Further reproduction prohibited without permission.

National Library of Canada

Acquisitions and Bibliographic Services

395 Wellington Street
Ottawa ON K1A 0N4
Canada

Bibliothèque nationale du Canada

Acquisitions et services bibliographiques

395, rue Wellington
Ottawa ON K1A 0N4
Canada

Your file Votre référence

Our file Notre référence

The author has granted a non-exclusive licence allowing the National Library of Canada to reproduce, loan, distribute or sell copies of this thesis in microform, paper or electronic formats.

L'auteur a accordé une licence non exclusive permettant à la Bibliothèque nationale du Canada de reproduire, prêter, distribuer ou vendre des copies de cette thèse sous la forme de microfiche/film, de reproduction sur papier ou sur format électronique.

The author retains ownership of the copyright in this thesis. Neither the thesis nor substantial extracts from it may be printed or otherwise reproduced without the author's permission.

L'auteur conserve la propriété du droit d'auteur qui protège cette thèse. Ni la thèse ni des extraits substantiels de celle-ci ne doivent être imprimés ou autrement reproduits sans son autorisation.

0-612-81241-3

Canada

Reproduced with permission of the copyright owner. Further reproduction prohibited without permission.

UNIVERSITY OF ALBERTA

## Library Release Form

Name of the Author: **Karsten Michael**

Title of Thesis: **Flow of Formation Water in the Alberta Basin Adjacent to the Rocky Mountains Thrust and Fold Belt, West-Central Alberta, Canada**

Degree: **Doctor of Philosophy**

Year this Degree Granted: **2002**

Permission is hereby granted to the University of Alberta Library to reproduce single copies of this thesis and to lend or sell such copies for private, scholarly, or scientific research purposes only.

The author reserves all other publication and other rights in association with the copyright in the thesis and except as herein before provided, neither the thesis nor any substantial portion thereof may be printed or otherwise reproduced in any material form whatever without the author's prior written permission.

K. Michael

Karsten Michael
# 302, 9950 90 Ave
Edmonton, Alberta
Canada, T6E 5A4

Date: June 10, 2002

Reproduced with permission of the copyright owner. Further reproduction prohibited without permission.

UNIVERSITY OF ALBERTA

**Faculty of Graduate Studies and Research**

The undersigned certify that they have read, and recommend to the Faculty of Graduate Studies and Research for acceptance, a thesis entitled **Flow of Formation Water in the Alberta Basin Adjacent to the Rocky Mountains Thrust and Fold Belt, West-Central Alberta, Canada**

by Karsten Michael in partial fulfillment of the requirements for the degree of **Doctor of Philosophy**

Dr. S. Bachu

Dr. H.G. Machel

Dr. C.A. Mendoza

Dr. J. Richards

for

Dr. M. Person

Dr. F.W. Jones

Date: June 10 2002

Reproduced with permission of the copyright owner. Further reproduction prohibited without permission.

## Abstract

The hydraulic communication between the deformed and undeformed parts of the Alberta Basin, as well as the vertical hydraulic communication, flow-driving mechanisms, and the evolution of formation waters in the deep basin, are still poorly understood. Therefore, flow patterns of formation waters in west-central Alberta in the vicinity of the Rocky Mountains were investigated using publicly-available, standard industry, chemical analyses of formation waters and fluid pressure data from drillstem tests.

Hydraulic analysis of DST data shows that only flow in the post-Colorado aquifers has adjusted to local to regional-scale ground surface topography. Flow in the Colorado and Mannville (Lower Cretaceous) aquifers is mostly towards sinks created by erosional and post-glacial rebound of the intervening shales, and towards the receding hydrocarbon-saturated regions along the Rocky Mountains. The Jurassic to Cambrian aquifers appear to be influenced only marginally by mixing with freshwater, carried predominantly by a long-range, gravity-driven flow system originating in the south of the study area in Montana. A contribution of freshwater from the adjacent Rocky Mountains appears to be restricted to channelled flow along relatively high-permeable strata, i.e., Middle Devonian platform margins. The main reasons for the isolation of "relict" formation waters in the Jurassic-Cambrian aquifers are: 1) effective confining aquitards; 2) hydrocarbon-saturated zones in the overlying Cretaceous; and 3) buoyancy effects between less saline formation water located downdip of heavy connate brine.

Based on salinity and Na/Cl-ratios, the formation waters in west-central Alberta can be grouped with partial overlap into: 1) mainly meteoric, Tertiary-Upper Cretaceous

Reproduced with permission of the copyright owner. Further reproduction prohibited without permission.

groundwater (TDS < 15 g/L, $Na/Cl_{molar}$: 0.9-1.5); 2) Lower Cretaceous waters with various degrees of mixing between seawater and meteoric water (TDS <100 g/L, $Na/Cl_{molar}$: 0.9-1.5); 3) Jurassic-Mississippian, evaporated seawater that was altered by halite dissolution and dolomitization (TDS: 50-160 g/L, $Na/Cl_{molar}$: 0.8-1.0); and 4) Devonian-Cambrian, evaporated seawater that underwent a high degree of water-rock interaction, i.e., dolomitization, halite dissolution, and predominantly albitization of feldspar (TDS: 125-300 g/L, $Na/Cl_{molar}$: 0.5-0.9).

The analysis of fluid and pressure distributions in the Tertiary-Cretaceous succession in west-central Alberta demonstrates that the hydrocarbon-saturated zones have a major effect on basin-scale fluid flow in the Alberta Basin, forming both, an effective barrier and a sink for formation water flow. Furthermore, the integration of hydrodynamics and formation water chemistry shows evidence of only marginal mixing of formation waters with meteoric water in the deeper parts of the basin.

Reproduced with permission of the copyright owner. Further reproduction prohibited without permission.

## Acknowledgments

This thesis was mainly funded through a scholarship from the Alberta Geological Survey of the Alberta Energy and Utilities Board. Additional financial support was provided through funds from a Natural Science and Engineering Research Council (NSERC) operating grant to Hans G. Machel (University of Alberta), supplemented by contributions from Chevron Canada Resources Ltd. A travel grant was provided by the University of Alberta to enable the author to present parts of this thesis at a conference.

I am grateful to Stefan Bachu and I would like to thank Hans Machel for valuable discussions and editorial suggestions throughout many stages of the completion of this thesis. Discussions with Ben Rostron, Jennifer Adams, Carl Mendoza, Kevin Parks, Maja Buschkuehle, Pat Cavell, Matt Grobe, Willem Langenberg, Hugh Reid and Tony Lemay provided many helpful insights and ideas. I am indebted to Kelly Roberts, Michel Brulotte, Barry Fildes, Sheila Stewart, Dan Magee, Andre Lytviak and all of the Alberta Geological Survey staff for providing logistic, computer and database support.

I owe my warmest thanks to my parents for their moral support and for having that "money-printing machine" in their basement. A loving thank-you goes to Maja for sharing the ups and downs of life as a grad student and the adjustment to a new life in Canada.

Reproduced with permission of the copyright owner. Further reproduction prohibited without permission.

# Table of Contents



Reproduced with permission of the copyright owner. Further reproduction prohibited without permission.

Reproduced with permission of the copyright owner. Further reproduction prohibited without permission.

# List of Tables



Reproduced with permission of the copyright owner. Further reproduction prohibited without permission.

# List of Figures



Reproduced with permission of the copyright owner. Further reproduction prohibited without permission.

Reproduced with permission of the copyright owner. Further reproduction prohibited without permission.

Reproduced with permission of the copyright owner. Further reproduction prohibited without permission.

# CHAPTER 1: INTRODUCTION

## 1.1 Rationale

Formation water is an important agent in most geological processes and regional water flow affects the formation and distribution of mineral and hydrocarbon deposits during the evolution of sedimentary basins (e.g., Garven, 1995; Tóth, 1999; Ingebritsen and Sanford, 1998). The two basic aspects of the influence of formation water in the subsurface are the interaction between water and the surrounding rock framework, and water flow as a transport and distribution mechanism (Tóth, 1999). Therefore, studying the hydrochemical and hydrodynamic patterns is essential for understanding the spatial and temporal distribution of fluids, solutes and precipitates in sedimentary basins, and for the emplacement of energy and mineral resources.

The Alberta Basin in western Canada (Fig. 1.1a) is a representative example of a foreland basin that has been studied extensively. The Alberta Basin, spanning from ~49$^{O}$N to ~61$^{O}$N and from ~109$^{O}$W to the Rocky Mountains, consists of a northeasterly tapering wedge of sedimentary rocks that varies in thickness from > 6000 m in the west, at the thrust and fold belt of the Rocky Mountains, to zero in the northeast, at the exposed Precambrian Shield (Fig. 1.1b). Ongoing erosion since the Eocene created the current topographic relief, with elevations ranging in the undeformed part of the Alberta Basin from > 1400 m above sea level (a.s.l.) in the west-southwest to ~200 m a.s.l. at the Great Slave Lake in the north-northeast.

Formation water flow and hydraulic characteristics of the rock framework affect(ed) the migration and accumulation of hydrocarbons, terrestrial heat flow, ore genesis, and the suitability for deep waste disposal in the Alberta Basin (Bachu, 1999). Many basin- to regional scale hydrogeological studies have been performed during the last four decades that have led to a significant improvement in the understanding of the hydrogeological regime in the basin.



Reproduced with permission of the copyright owner. Further reproduction prohibited without permission.

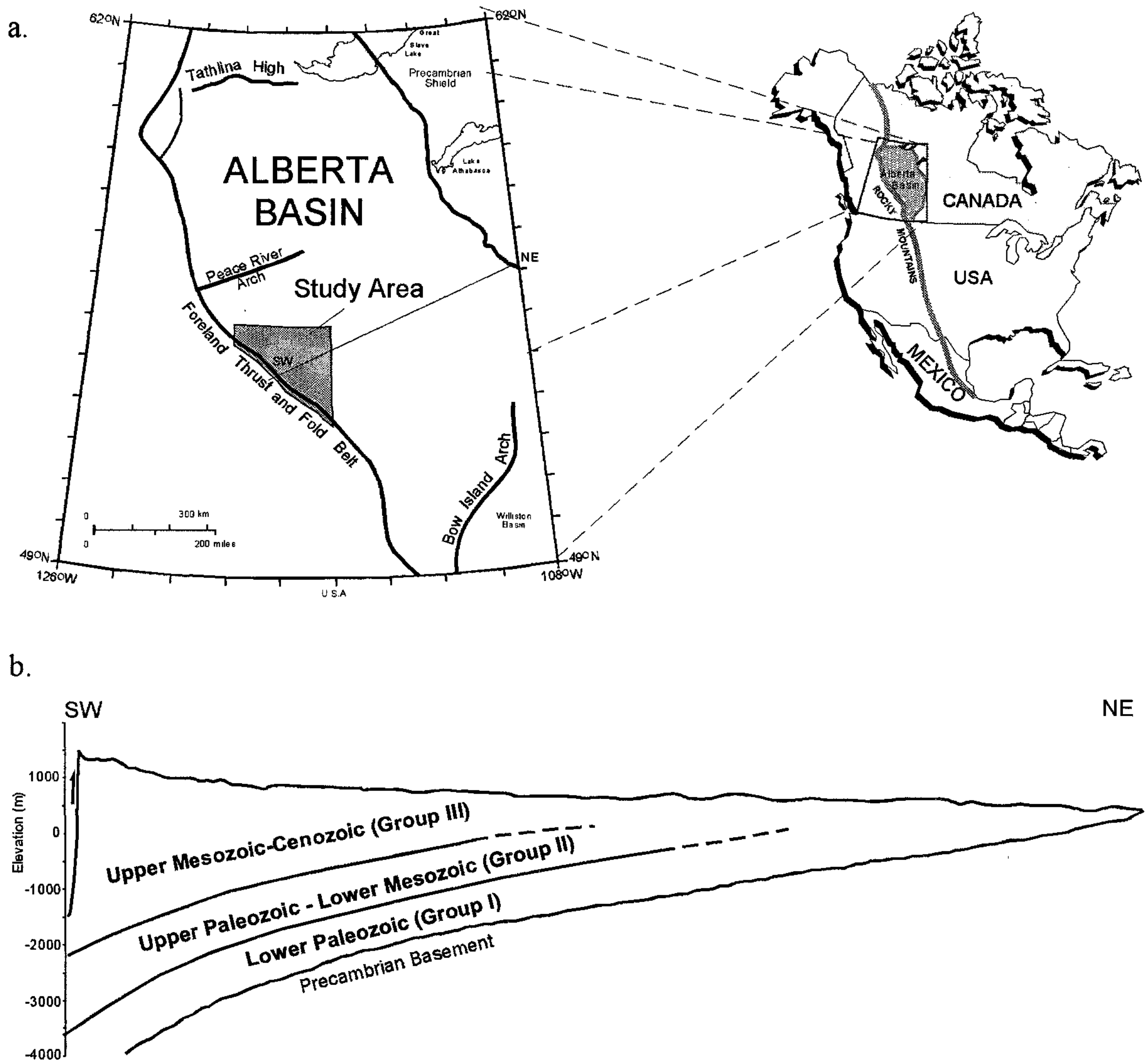


Figure 1.1: a) Location of the study area in the Alberta Basin, and b) cross section showing general subdivision of the sedimentary succession into three main hydrostratigraphic groups (after Tóth, 1978; Hitchon et al., 1990).

Following Tóth (1963), Hitchon (1969) developed the first concept of a basin-wide, topography-driven flow system in the Alberta Basin. Further studies revealed much greater complexity of the hydrostratigraphy and flow patterns in the basin, which led to the currently accepted model of formation water flow (Bachu, 1995a and references therein). According to this conceptual model, flow systems of various scales, and in



Reproduced with permission of the copyright owner. Further reproduction prohibited without permission.

different parts of the Alberta Basin, are driven by topography, erosional rebound, and/or past tectonic compression, and may interact with each other to varying degrees (Bachu 1995a; 1999). Although the understanding of regional-scale flow in the basin is relatively high, several issues regarding the basin- to regional-scale hydrogeology in the Alberta Basin remain to be further investigated. These include: 1) focused flow along high-permeability pathways, 2) the degree of hydraulic communication between the deformed and undeformed parts of the basin, 3) hydraulic communication between the crystalline basement and the sedimentary succession, 4) the interaction between the hydrocarbon- and water-saturated parts, and 5) the recharge of and the nature of the flow-driving mechanisms in deep-basin aquifers (Bachu, 1999).

The deeper parts of the Alberta Basin near the deformation front of the Rocky Mountains are of particular interest because this region is currently an exploration target for natural gas in the Devonian and for coal bed methane in the Cretaceous systems. It was proposed that tectonic expulsion of fluids during the Laramide orogeny has affected flow in the Devonian aquifers in west-central Alberta (Machel et al., 1996; Machel and Cavell, 1999). Although numerical studies by Ge and Garven (1989, 1994) suggest that the resulting excess pressures should have dissipated after several million years, relatively weak remnants of the tectonically induced flow might still be active in this part of the Alberta Basin (Bachu, 1995a).

Hydrocarbons displaced formation water, to form hydrocarbon-saturated regions in the Cretaceous succession along the Rocky Mountain trust and fold belt, downdip of the water-saturated parts of the basin (Masters, 1979). Yet, it has not been investigated how these hydrocarbon accumulations affect the present regional flow of formation waters. Currently, erosional rebound of shales is believed to be the main mechanism that creates observed underpressures in Cretaceous aquifers (Bachu, 1995a; Parks and Tóth, 1995; Bekele et al., 2000).



Reproduced with permission of the copyright owner. Further reproduction prohibited without permission.

The extent of mixing of connate formation water with meteoric recharge is of interest from a scientific point of view. Especially, the hydraulic communication of meteoric recharge in the Rocky Mountain thrust and fold belt with the undeformed parts of the Alberta Basin is not well understood. While basin-scale recharge from the thrust and fold belt was shown for the northern part of the Alberta Basin (Bachu, 1997), lack of hydraulic communication was inferred south of the Peace River region (Fig. 1.1) on the basis of flow patterns (Bachu, 1995a; 1999), and it was also suggested in a hydrogeological study of Devonian aquifers in southern Alberta (Wilkinson, 1995). On the other hand, freshwater is believed to have infiltrated down to Mississippian aquifers via convoluted pathways in the over-thrust fault systems (Underschultz and Bartlett, 1999).

## 1.2 Study Area

The location of the study area (Fig. 1.2) was chosen to investigate specifically the hydrogeology of strata suspected to be influenced by tectonic fluid expulsion (Bachu 1995a, Machel and Cavell, 1999) in the area of the Upper Devonian Southesk-Cairn carbonate complex, and to elucidate the influence of 'deep basin' hydrocarbon accumulations (Masters, 1979) on formation water flow in the Cretaceous succession. Also, due to the vicinity of the study area to the Rocky Mountain thrust and fold belt, a study of the hydrogeology in this area could produce new information on the hydraulic communication between deformed and undeformed parts in this part of the Alberta Basin.

The boundaries of the study area are defined by $52.3^0$ - $55^0$ latitude N and $116^0$ - $120^0$ longitude W, and by the SE-NW trending deformation front of the Rocky Mountains in the west (Fig. 1.2). In places, the hydrogeological interpretations are extended into the foothills region, where hydrogeological data are available. The study area comprises 510 townships and covers approximately 50,000 km$^2$.



Reproduced with permission of the copyright owner. Further reproduction prohibited without permission.

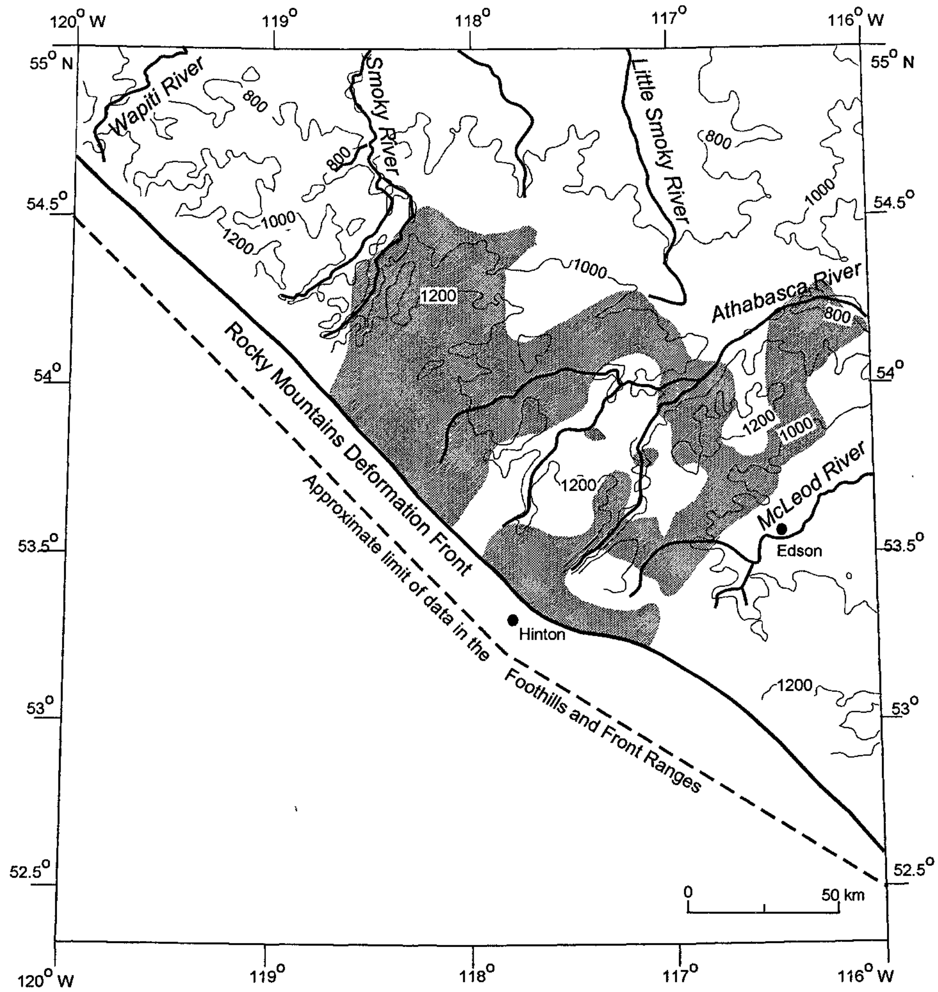


Figure 1.2: Topographic map of the study area, showing outline of the Devonian Southesk-Cairn Complex (grey shading) in the subsurface (outline from Buschkuehle and Machel, 2001).

The topography in the study area ranges from over 1400 m in the foothills region down to 700 m above the sea level in the plains. Major population centers are Hinton in the foothills region and Edson near the eastern boundary. The largest rivers, flowing across the study area from the mountains to the northeast, are the Athabasca River in the south and the Smoky River in the north.



Reproduced with permission of the copyright owner. Further reproduction prohibited without permission.

## 1.3 Previous Work

The Alberta Basin is an important petroleum province, with extensive exploration and exploitation using more than 300,000 wells drilled since the early 1950s. Thus, there is an extensive collection of geological as well as hydraulic and hydrochemical data, which were used in various hydrogeological studies to interpret regional fluid flow in the basin. The locations of the studies that were fundamental for the development of hydrogeological concepts in the basin and those that are most relevant with respect to their geographic location and hydrogeological results as related to this study are shown in Figure 1.3.

*Hydrochemistry of Formation Waters*

Hitchon and Friedman (1969), Billings et al. (1969) and Hitchon et al. (1971) concluded that the formation waters in the Alberta Basin represent ancient seawater that has been diluted and/or concentrated by meteoric water and membrane filtration, respectively. Their study was based on the distribution of major ions, alkali metals, and stable isotopes of hydrogen and oxygen in formation waters. Schwartz et al. (1981) confirmed the mixing with present-day meteoric water in the Taber area in southern Alberta and depicted flow patterns in Cretaceous aquifers, using stable isotope data of hydrogen and oxygen. $Cl^{36}$-dating of Late Cretaceous Milk River formation waters estimated the residence time of these waters to be approximately 2 m.y. (Phillips et al., 1986). Spencer (1987) characterized the majority of Devonian formation waters as Ca – Cl brines that initially formed from the evaporation of seawater and were modified by water – rock interaction with basement rocks and mixing with freshwater. Also, the pervasive, replacive dolomitization of limestones in the Devonian succession indicates that large amounts of fluids must have passed through these rocks (e.g., Machel and Mountjoy, 1987; Mountjoy et al., 1999), which probably has significantly influenced the formation water chemistry.



Reproduced with permission of the copyright owner. Further reproduction prohibited without permission.

To date the most comprehensive hydrochemical study in the Alberta Basin is by Connolly et al. (1990a,b). These authors were able to distinguish between three groups of formation waters (Tab. 1.1), using comprehensive hydrochemical data (major ions, isotopes, organic chemistry) from throughout the entire stratigraphic column, in a local- to regional-scale study in central Alberta (Fig. 1.3).

<table>
<tr><th>Era</th><th>Hydrochemistry<br>(Connolly et al. 1990)</th><th>Regional Hydrogeology<br>(Tóth, 1978)</th><th>Basin Hydrogeology<br>(Bachu, 1995a)</th></tr>
<tr><td>Tertiary</td><td rowspan="2">Group 3<br>Dilute, meteoric waters</td><td rowspan="3">Group III<br>Local flow system</td><td rowspan="5">Post-Jurassic<br>- topography-driven flow (local-scale)<br>- flow driven by erosional rebound (regional-scale)</td></tr>
<tr><td rowspan="3">Cretaceous</td></tr>
<tr><td rowspan="3">Group 2<br>Brines isolated from present meteoric recharge (in clastics)</td></tr>
<tr><td rowspan="6">Group II<br>Intermediate flow system</td></tr>
<tr><td>Jurassic</td></tr>
<tr><td>Triassic</td><td rowspan="6">Group 1<br>Brines isolated from present meteoric recharge (in carbonates)</td><td rowspan="6">Pre-Cretaceous<br>- topography-driven flow (basin-scale)<br>- tectonically-induced flow with buoyancy effects (basin-scale)</td></tr>
<tr><td>Permian</td></tr>
<tr><td>Mississip.</td></tr>
<tr><td rowspan="2">Devonian</td></tr>
<tr><td rowspan="2">Group I<br>Regional flow system</td></tr>
<tr><td>Cambrian</td></tr>
</table>

Table 1.1: Various hydrogeological sub-divisions of the Alberta Basin.



Reproduced with permission of the copyright owner. Further reproduction prohibited without permission.

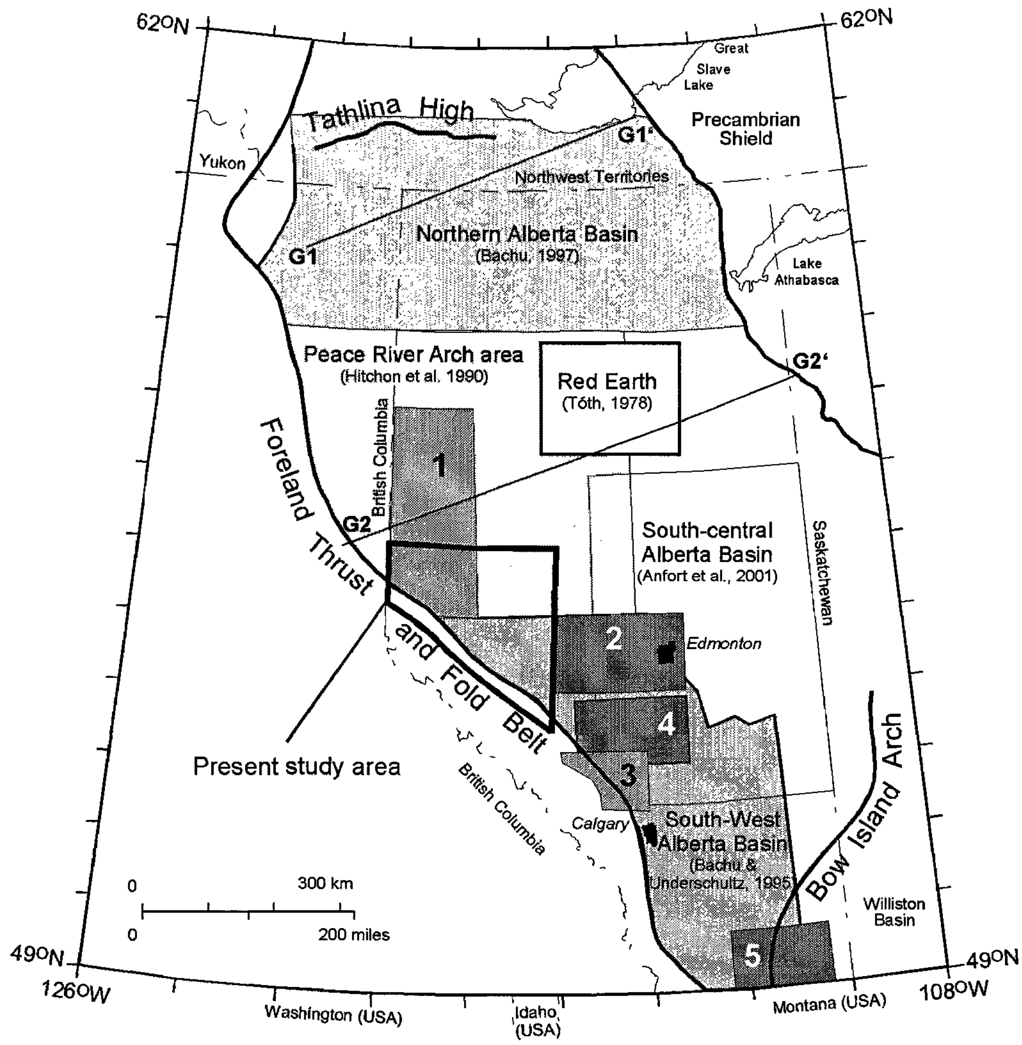


1 Peace River Region (Thompson, 1989)
2 Central Alberta (Connolly et al., 1990)
3 Thrust Belt (Wilkinson, 1995)
4 Bashaw Region (Rostron, 1990; Rostron & Tóth, 1997)
5 Taber Region (Schwartz et al., 1981)
G1G1' Line of 'Pine Point' modeling cross section (Garven, 1985)
G2G2' Line of 'Athabasca Tar Sands' modeling cross section (Garven, 1989)

Figure 1.3: Location of former local- to regional-scale hydrogeological studies in the Alberta Basin that are relevant to the present study.

Connolly et al. (1990a,b) suggested that water from deep, hydraulically isolated, carbonate (Group 1) and sandstone (Group 2) aquifers is represented by evaporated seawater that was diluted by post-Laramide meteoric water, whereas Group 3 is characterized by dilute, meteoric waters from Upper Cretaceous aquifers. However, the



Reproduced with permission of the copyright owner. Further reproduction prohibited without permission.

above study covered only a part of the Alberta Basin, and the evolution history of formation waters for the remainder of the basin has not yet been clarified.

*Flow of Formation Waters*

An earlier interpretation of the flow in the Alberta Basin suggested a basin-wide, topography-driven flow system (Fig. 1.4) that is recharged in the Rocky Mountain Foothills in the southwest, channeled updip mainly along Devonian carbonate aquifers, and discharges in the northeast along the "feather-edge" of the basin (Hitchon, 1969, 1984). This interpretation was used to explain the Pine Point Pb-Zn and the Athabasca oil sands deposits in the Alberta Basin, whereby a relatively high permeability was assumed for the Upper Devonian carbonates that were thought to be the major regional aquifer (Hitchon, 1984; Garven, 1985; 1989). One implication of this hydrogeological interpretation is that the basin-scale flow system should have flushed the connate brines from the deep Devonian aquifers within only about two million years, as shown by numerical models of topography-driven flow (Deming and Nunn, 1991; Adams et al. 2000). However, the presence of high-salinity brines in the Paleozoic formations indicates that the basin has not been flushed, and that a single, basin-scale topography-driven flow system, as described above, is not likely to be active in the Alberta Basin (Bachu, 1995a).

Tóth (1978) in the Red Earth region and Hitchon et al. (1990) in the Peace River Arch area (Fig. 1.3) divided the stratigraphic succession into three main hydrogeological groups: I) Lower Paleozoic, II) Upper Paleozoic-Lower Mesozoic, and III) Upper Mesozoic-Cenozoic (Fig. 1.1b), each separated by regional aquitards. According to their interpretation, the flow systems in Groups II and III generally have adjusted to the overlying intermediate- and local-scale ground surface topography, respectively. However, some areas may contain superimposed local flow systems originating in the Pleistocene-Holocene (Tóth, 1978). Flow systems in Group I were interpreted to be maintained by "relict energy differences" originating in the Pliocene, with the flow in a



Reproduced with permission of the copyright owner. Further reproduction prohibited without permission.

transient process of equilibrating to the present-day ground surface (Tóth, 1978; Tóth and Millar, 1983; Tóth and Corbet 1986). On the other hand, Hitchon et al. (1989; 1990) attributed flow patterns in Group I that are not in equilibrium with the ground surface to be caused by the drainage effect of the underlying, high-permeable Grosmont carbonate aquifer with basin-scale northeastward flow. Subsequent studies have shown that the erosional rebound of shales is the most likely mechanism creating underpressures in Group III aquifers (Corbet and Bethke, 1992; Parks and Tóth, 1995; Bachu and Underschultz, 1995), as opposed to the former concept of "relict pressures".

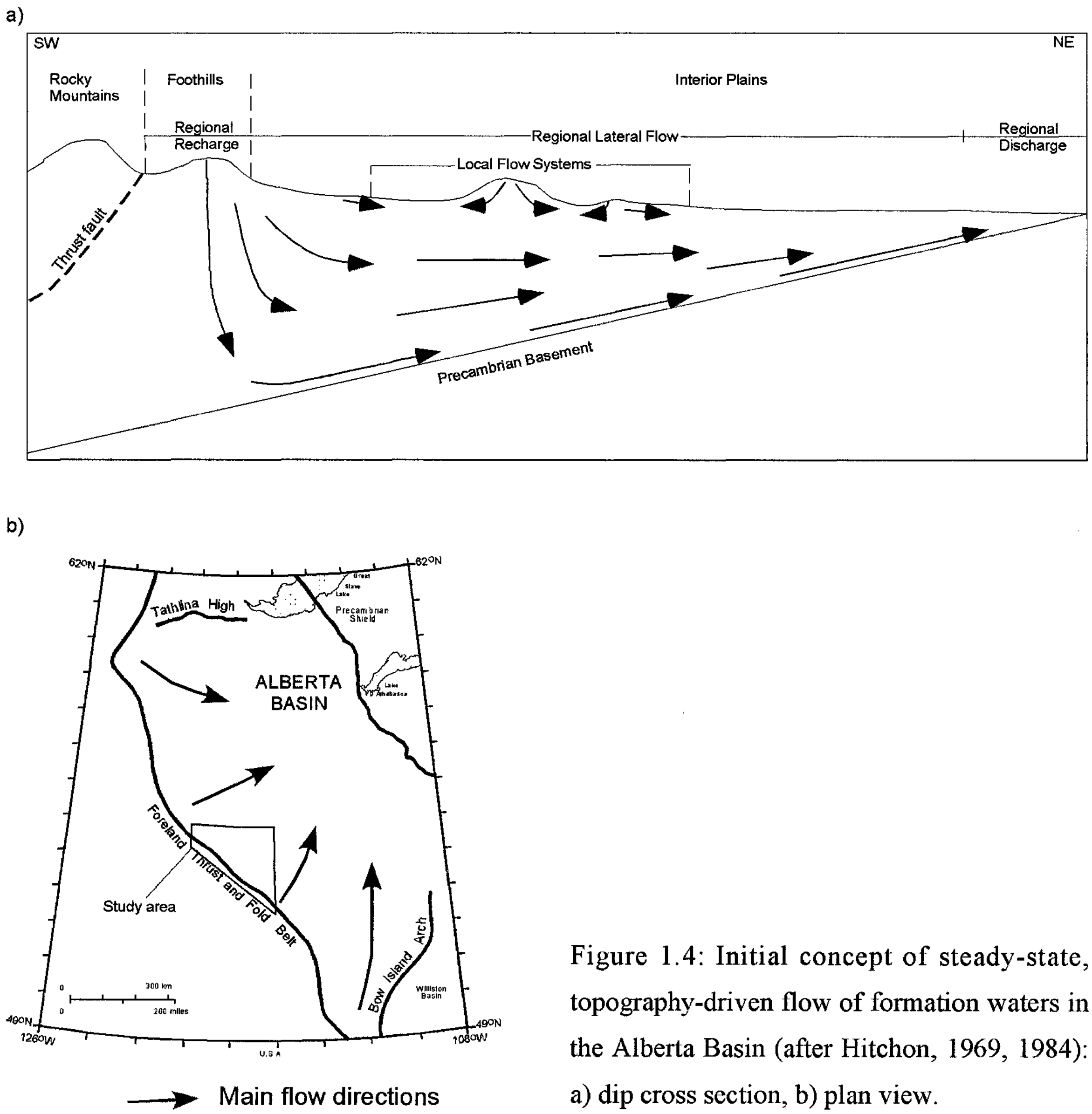


Figure 1.4: Initial concept of steady-state, topography-driven flow of formation waters in the Alberta Basin (after Hitchon, 1969, 1984): a) dip cross section, b) plan view.



Reproduced with permission of the copyright owner. Further reproduction prohibited without permission.

At present, different driving mechanisms are thought to drive flow in two megahydrostratigraphic groups (MHG), the pre-Cretaceous and post-Jurassic (Bachu, 1995), in various parts of the Alberta Basin (Fig. 1.5, Tab. 1.1). In the northern part, flow in the entire stratigraphic succession is driven by ground surface topography in local to regional systems. The general flow direction is northeastward, with recharge in the thrust and fold belt of the Rocky Mountains and discharge at the Great Slave Lake, where the respective aquifers subcrop beneath the Quaternary cover (Bachu, 1997).

a)

b)

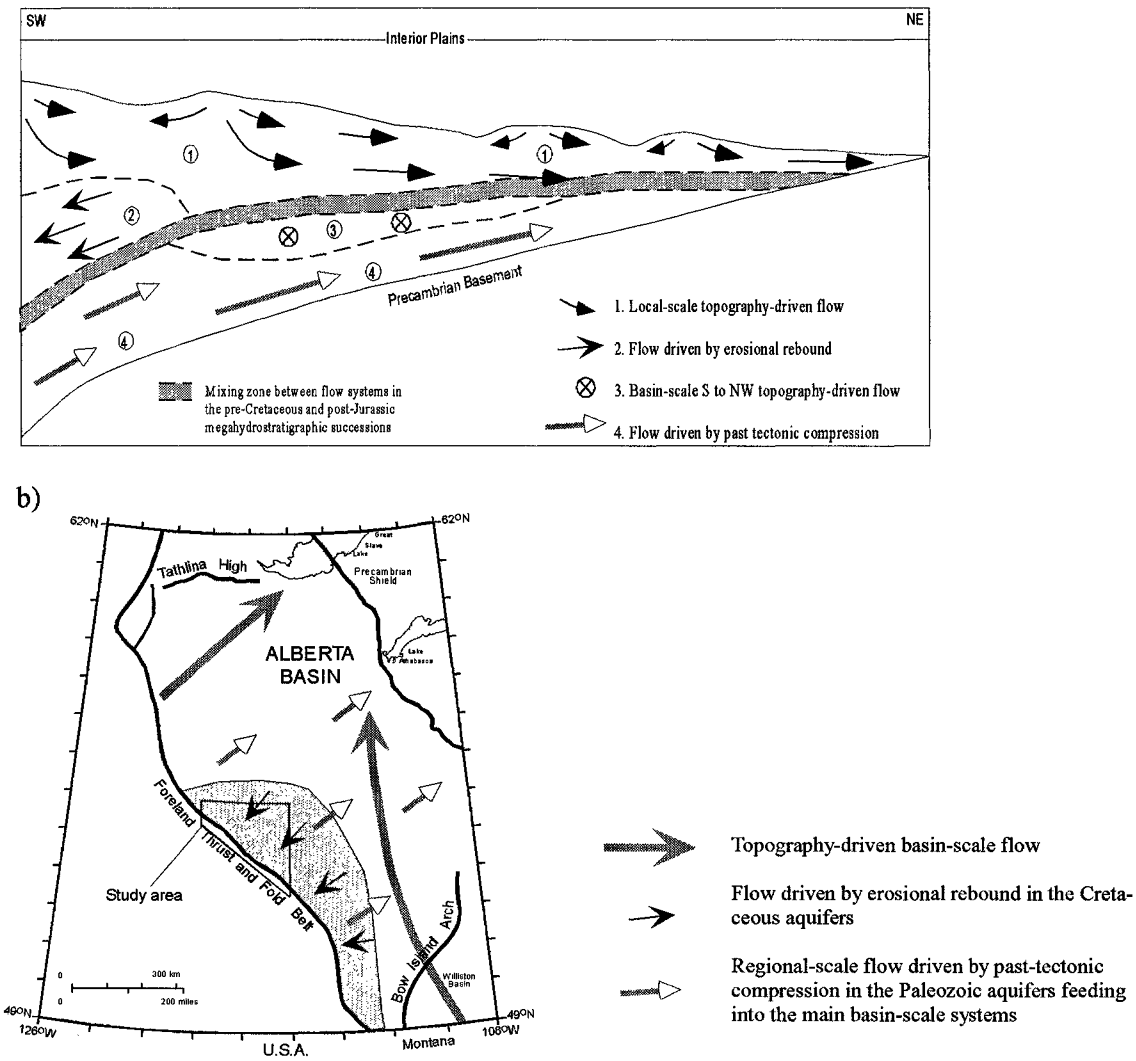


Figure 1.5: Recent diagrammatic representation of flow systems and pattern in the Alberta Basin after a compilation of hydrogeological studies by Bachu (1995a; 1999, and references therein): a) dip cross section, and b) plan view.



Reproduced with permission of the copyright owner. Further reproduction prohibited without permission.

In contrast, in the southern and central parts of the basin the general flow direction in the pre-Cretaceous MHG is northward, driven also by topography, with recharge occurring in areas of Devonian outcrop at high elevations in the south in Montana and discharge at formation outcrop in the north along the Peace River (Bachu, 1995a; 1999; Anfort et al., 2001). Hydraulic heads in the various aquifers in the pre-Cretaceous MHG in the west-central part of the basin indicate east-northeastward flow from the Rocky Mountain deformation front (Hitchon et al., 1990), but relatively high formation water salinity suggests that the flow in these aquifers is disconnected from any mixing with low-salinity meteoric recharge (Bachu, 1995a). Also, a study of flow in Devonian aquifers in southern Alberta revealed that flow systems in the thrust and fold belt of the Rocky Mountains appear to be disconnected from flow systems in the adjacent undeformed part of the basin (Wilkinson, 1995). Past tectonic compression was proposed as the mechanism that drives the flow in this region (Bachu, 1995a; 1999; Machel et al., 1996), but strontium isotope studies indicate that fluids expelled by this mechanism migrated only 100 km from the deformation front (Machel and Cavell, 1999; Buschkuehle and Machel, 2001). In addition, numerical modeling studies suggest that excess pressures generated by tectonic loading would have occurred in pulses and dissipated after several million years (Ge and Garven, 1989; 1994). On the other hand, freshwater is believed to have infiltrated down to Mississippian aquifers via convoluted pathways in the over-thrust fault systems (Underschultz and Bartlett, 1999). Thus, the flow-driving mechanism(s) of brines in the pre-Cretaceous MHG in the west-central part of the basin is not yet understood.

Fluid flow in the lower part of the post-Jurassic MHG in the northern part of the Peace River region is driven by regional- and local-scale topography, respectively, while flow in the southern part is hindered by "deep basin" gas accumulations that act as a barrier to fluid flow (Thompson, 1989). Recharge of the lower Cretaceous by meteoric water from the topographic highs in the Rocky Mountain thrust and fold belt north of the Peace River (Thompson, 1989) is consistent with basin-scale recharge from the thrust and fold belt in the northern part of the Alberta Basin (Bachu, 1997). Lack of hydraulic communication



Reproduced with permission of the copyright owner. Further reproduction prohibited without permission.

was inferred south of the Peace River region on the basis of flow patterns (Bachu, 1995a, 1999). The observed underpressuring and the flow in the Cretaceous units in the central and southern parts of the basin were attributed to erosional rebound in thick shale successions after the peak of the Laramide orogeny (Corbet and Bethke, 1992; Bachu, 1995a; Bachu and Underschultz, 1995; Parks and Tóth, 1995; Bekele et al., 2000).

Aside from the basin- to regional separation of various hydrostratigraphic groups in the Alberta Basin by competent aquitards, cross-formational flow may occur where intervening aquitards are locally thin or absent. Locations with vertical hydraulic communication were identified previously across the thin Cretaceous Clearwater and the Devonian Watt Mountain aquitards in northeastern Alberta (Bachu and Underschultz, 1993); across the Devonian Calmar aquitard in southeastern Alberta (Rostron and Tóth, 1997; Anfort et al., 2001); and in places where the Ireton aquitard is thin or absent above reef complexes in the Cheddarville and Bashaw areas in southern Alberta (Wilkinson, 1995; Rostron et al., 1997; Anfort et al., 2001) and along the Rimbey-Meadowbrook reef trend further to the north (Bachu and Underschultz, 1993). The identification of areas of cross-formational flow is important, because they are potential pathways for hydrocarbon migration.



Reproduced with permission of the copyright owner. Further reproduction prohibited without permission.

## 1.4 Thesis organization and main objectives

This thesis investigates the regional hydrogeology in the west-central part of the Alberta Basin and is organized into eight chapters. The first four chapters establish the methodological and geological framework of this study:

- former hydrogeological work in the Alberta Basin, resulting concepts, remaining issues, and main objectives and rationale for this study (this chapter);
- theoretical principals of formation water flow in sedimentary basins (Chapter 2);
- data processing, culling methods and data accuracy (Chapter 3);
- regional geological framework (Chapter 4).

The hydrogeological observations and interpretations are presented in the last four chapters. The main objectives are:

- to investigate the distribution and interaction of hydrocarbon- and water-saturated regions and the extent of topography-driven flow versus flow driven by erosional rebound in the Tertiary-Cretaceous succession (Chapter 5);
- to establish the origin and flow-driving mechanisms of formation water in the Jurassic-Mississippian succession (Chapter 6);
- to investigate the possibility of tectonically-induced flow, the displacement of connate brines by meteoric waters, and preferential flow paths in the Cambrian-Devonian succession (Chapter 7);
- to characterize the interaction of flow systems and evolution of formation waters in the entire succession from the ground surface to the Precambrian basement, and to compare the results to the currently accepted interpretation of formation water flow in the Alberta Basin (Chapter 8).



Reproduced with permission of the copyright owner. Further reproduction prohibited without permission.

# CHAPTER 2: REPRESENTATION METHODS FOR FLOW OF AQUEOUS FLUIDS IN SEDIMENTARY BASINS

## 2.1 Introduction

The purpose of this chapter is to find a suitable method for accurately interpreting the flow of formation waters in the west-central part of the Alberta Basin, using pressure and hydrochemical data collected by the petroleum industry. The ability to evaluate the direction and rate of flow depends on the availability, distribution and quality of the required hydrogeological data, knowledge of the aquifer geometry, and on the understanding of driving mechanisms for formation water flow in sedimentary basins. Therefore, the first section of this chapter introduces the physical principles and equations for fluid flow and how they account for the various flow-driving mechanisms.

Traditionally, freshwater hydraulic heads have been used to interpret fluid flow in sedimentary basins. However, there are errors associated when applying this method to the case of variable-density fluid flow in sloping aquifers (Lusczynski, 1961; Davies, 1987; Dorgarten and Tsang, 1991; Bachu, 1995b). Therefore, limitations for the usage of hydraulic heads and possible alternatives are evaluated in the second section of this chapter.

In contrast to near-surface groundwater flow, which is almost solely driven by gravity in most cases, regional flow in sedimentary basins is driven by a combination of various mechanisms such as: a) topography (gravity), b) sediment compaction, c) tectonic loading, d) erosional rebound, e) buoyancy, f) overpressures due to hydrocarbon generation, and g) osmosis or mineral phase changes (e.g., Kreitler, 1989; Garven, 1995; Ingebritsen and Sanford, 1998). During the geologic history of a sedimentary basin various driving mechanisms may dominate in various stages of basin evolution. Because of the large size of sedimentary basins, properties of the fluids and solids can also vary



Reproduced with permission of the copyright owner. Further reproduction prohibited without permission.

significantly in space and with time. These changes have to be considered when interpreting present-day hydrogeological data. The individual driving mechanisms, as well as fluid and rock properties with respect to their influence on basin-scale fluid flow are reviewed in Appendix A.

## 2.2 Equations describing flow in sedimentary basins

Fluid flow in sedimentary basins can be described by three equations based on the conservation laws for mass and energy and on the empirical equation of Darcy's Law (Eqs. 2.1 – 2.3). Hubbert (1940) defined fluid flow in porous media as a mechanical process that is dominantly influenced by friction, and during which the mechanical energy initially contained in the fluid is continuously dissipated along the flow path from high to low energy potentials. The energy of a fluid is defined by its relative elevation (potential energy), the fluid pressure at that elevation (pressure energy), and the kinematic energy so that, for a non-compressible fluid and a conservative flow field, the law for the conservation of energy can be expressed by (Hubbert, 1940):

$$\Delta\left(gz + \frac{p}{\rho} + \frac{v^2}{2}\right) + \Delta\varepsilon = 0 \tag{2.1a}$$

where g = acceleration due to gravity ($m/s^2$), z = elevation (m), p = fluid pressure (Pa), ρ = fluid density ($kg/m^3$), v = flow velocity (m/s), Δε = dissipated energy per unit mass ($m^2/s^2$) due to friction along the flow path.

The kinematic energy term ($v^2/2$) is negligible with respect to the other terms, because of the generally low velocities of groundwater flow, and Equation 2.1a simplifies to:

$$\Delta\left(gz + \frac{p}{\rho}\right) + \Delta\varepsilon = 0 \tag{2.1b}$$



Reproduced with permission of the copyright owner. Further reproduction prohibited without permission.

The combination of the two terms within the brackets in this relation explicitly shows that fluids flow from high to low energy levels, and not just from high to low pressures. Therefore, fluid pressure, fluid density and the measurement elevation are the three basic parameters for analyzing the energy available to cause flow of formation water.

Darcy's Law is an empirical formulation for the law of momentum conservation for flow in porous media. For coupled flow and a reference state of formation water regarding fluid density and viscosity for respective pressure-temperature-concentration conditions, Darcy's Law can be expressed as (Bear, 1972; de Marsily, 1986; Bachu, 1995b):

$$q = -\frac{k\,\rho_0\,g}{\mu}\left[\nabla\left(\frac{p}{\rho_0 g} + z\right) + \frac{\rho - \rho_0}{\rho}\nabla z\right] - K_T \nabla T - K_C \nabla C \qquad (2.2)$$

where q = specific discharge (m/s), k = permeability ($m^2$), ρ = fluid density ($kg/m^3$), $\rho_0$ = reference density ($kg/m^3$), μ = fluid viscosity (Pa s), T = temperature (°C), C = concentration (kg/kg), and $K_T$, $K_C$ = phenomenological coefficients representing the hydraulic conductivity to thermal ($m^2/°C/s$) and chemical osmosis ($m^2/s$), respectively.

Equation 2.2 shows that flow of a variable-density fluid is driven by a combination of forces resulting from potential differences, buoyancy, and thermal and chemical osmosis. The potential differences are a result of pressure and/or elevation (topography) differences that combine to the expression of the "hydraulic gradient" for a fluid with constant density: $\nabla H_0 = \nabla\left(z + \frac{p}{\rho_0 \cdot g}\right)$, (2.3)

where $$H_0 = z + \frac{p}{\rho_0 \cdot g} \qquad (2.4)$$

is defined as 'hydraulic head' in units of metres above mean sea level (e.g., Hubbert, 1956).



Reproduced with permission of the copyright owner. Further reproduction prohibited without permission.

The density variations in the fluid are accounted for in the buoyancy term: $\frac{\rho - \rho_0}{\rho} \nabla z$.

Thermal and chemical osmosis are generally negligible, because the phenomenological coefficients $K_T$ and $K_C$ are much smaller than the hydraulic conductivity $K_H$ (Bear, 1972; de Marsily, 1986; Neuzil, 1986), where $K_H = \frac{k\ \rho_0 g}{\mu}$. Nevertheless, the temperature distribution and the concentration of solutes affect the fluid density and may cause buoyancy effects.

The distribution of the permeability k of the rock framework (Eq. 2.2), hence the hydraulic conductivity $K_H$, largely controls pressure transmission and fluid flow in sedimentary basins. In the most generalized form the permeability is represented by a second-rank symmetric tensor (Bear, 1972), but the nine components reduce to three if the principal directions of anisotropy coincide with the respective coordinate axes in three dimensions. This is usually considered to be the case for layered sedimentary sequences, with a horizontal to vertical anisotropy between 1 : 1 and 10 : 1 (Freeze and Cherry, 1979, p. 32).

The law of mass conservation of the fluid contained in a volume unit of a porous medium can be expressed in the form of the continuity equation (de Marsily, 1986):

$$\nabla \cdot (\rho\ \vec{q}) + \frac{\partial}{\partial t}(\rho\ n) + \rho\ \xi = 0 \qquad (2.5)$$

where n = porosity (-), $\xi$ = source term (-).

Combining Darcy's Law (Eq. 2.2) and the continuity equation (Eq. 2.5) results in various forms of a partial differential equation, generally known as the diffusion equation, which describes various types of flow, and which can be solved as an initial and boundary-value problem. A comprehensive form of the diffusion equation for transient, saturated flow in a heterogeneous, anisotropic porous medium can be found in Neuzil (1995), which in addition to the hydraulic driving force accounts for changes in pressures as a result of: a)



Reproduced with permission of the copyright owner. Further reproduction prohibited without permission.

changes in total stress due to compaction, decompaction, or tectonic loading, b) changes in porosity due to mineral dissolution and precipitation, and/or density changes caused by mineral and hydrocarbon phase changes, c) thermal expansion/shrinking of the fluid and rock matrix, and d) external fluid sources, such as derived from magmatic intrusions or the basement (Bredehoeft and Hanshaw, 1968; Neuzil, 1995). The effects on fluid pressure described by the last four processes (a-d) can be maintained only over a geological significant period of time in a low-permeability environment (Bredehoeft and Hanshaw, 1968; Neuzil, 1995).

Darcy's Law and the diffusion equation can be solved quantitatively only with numerical models, because many variables vary spatially and in time. These models typically discretize a study area into blocks and time steps in which the variables are assumed to be constant. For each block and time step the equation has to be solved separately. A comprehensive discussion of groundwater modeling in sedimentary basins is beyond the scope of this thesis and the reader is referred to corresponding literature on that topic (e.g. Bethke, 1985,1989; Deming and Nunn, 1991; Garven, 1985, 1989; Ge and Garven, 1992; Nunn and Deming, 1991; Person et al., 1996).

Only present-day pressure and hydrochemical data are available for this study, hence a more qualitative approach has to be taken to analyze and interpret fluid flow. Therefore, the next section discusses representation methods that only require data sets of pressure, density, and aquifer geometry.

*Fluid Potential and Hydraulic Head*

The most important method to represent and interpret regional-scale fluid flow in the subsurface is by using potentiometric surface maps of hydraulic heads to infer flow direction and strength. Hydraulic heads are calculated according to Equation 2.4 and flow is inferred to occur from high to low hydraulic heads. Although the use of hydraulic heads in potentiometric surface maps is a powerful and often the only available tool to



Reproduced with permission of the copyright owner. Further reproduction prohibited without permission.

investigate fluid movement in the subsurface, it is applicable only under certain conditions.

To infer fluid flow from differences in hydraulic head it must be shown that $H_0$ is indeed a parameter that represents the energy potential of the fluid. Hubbert (1940) defined the fluid potential per unit mass as (see also Eq. 2.1a):

$$\Phi = gz + \frac{v^2}{2} + \int_{p_0}^{p} \frac{dp}{\rho} \tag{2.6}$$

For a fluid potential to exist, the work along any distance, ds, in a closed path, in the flow field must equal zero. Neglecting the kinetic energy term, justified for the very slow velocities encountered in groundwater flow, Hubbert (1940) expressed this mathematically as:

$$\oint \left( \frac{\partial (gz)}{\partial s} + \frac{1}{\rho} \frac{\partial p}{\partial s} \right) ds \overset{!}{=} 0 \tag{2.7}$$

("!" in combination with "=" translates to "must equal")

and, since the gravity field is a potential field, this leads to:

$$\oint \left( \frac{1}{\rho} \frac{\partial p}{\partial s} \right) ds \overset{!}{=} 0 \tag{2.8}$$

To satisfy this condition, the fluid density has to be either constant or vary uniquely-dependent on pressure. For groundwater flow that complies with these conditions, and neglecting $v^2/2$, a fluid potential $\Phi$ exists, and combining Equations 2.1b and 2.8 leads to:

$$\Phi = g\ H_0 \tag{2.9}$$



Reproduced with permission of the copyright owner. Further reproduction prohibited without permission.

This mathematically justifies rewriting Darcy's Law (Eq. 2.2) in terms of equivalent hydraulic heads $H_0$ (Eq. 2.4) as (Bachu, 1995b):

$$\vec{q} = -\frac{\mu_0}{\mu} K_{H_0}\left[\nabla H_0 + \frac{\Delta\rho}{\rho_0}\nabla z\right] - K_C \nabla C - K_T \nabla T \qquad (2.10)$$

where $K_{H_0}$ is the hydraulic conductivity for a reference fluid with $\rho_0$ and $\mu_0$.

Similarly to the considerations for the work along a closed path in the force field (Eq. 2.7), the fluid flux should only be dependent on the difference in fluid potential (or hydraulic head) between two points, and therefore should not be affected by the actual flow path between these two points. For the flux vector to be actually derived from a potential field, it has to be irrotational in a mathematical sense (Bachu, 1995b):

$$\nabla \times \vec{q} = \underbrace{-\mu_0 \nabla\left(\frac{1}{\mu}\right) \times \left[K_{H_0}\left(\nabla H_0 + \frac{\rho - \rho_0}{\rho_0}\nabla z\right)\right]}_{I} \underbrace{- \frac{\mu_0}{\mu}\nabla K_{H_0} \times \left(\nabla H_0 + \frac{\rho - \rho_0}{\rho_0}\nabla z\right)}_{II}$$
$$\underbrace{-\frac{\mu_0}{\mu} K_{H_0} \cdot \nabla\left(\frac{\rho - \rho_0}{\rho_0}\right) \times \nabla z}_{III} - \underbrace{\nabla K_T \times \nabla T}_{IV} - \underbrace{\nabla K_C \times \nabla C}_{V} \overset{!}{=} 0$$

(2.11)

For this equation to equal zero, every one of the five expressions (I - V) or a combination thereof has to be zero, with the following implications for each term (Bachu, 1995b): (I) $\mu$ = const. or $\nabla\mu$ parallel to $\nabla H_o$ and $\nabla z$; <u>and</u> (II) $K_{H_0}$ = const. or $\nabla K_{H_0}$ parallel to $\nabla H_o$ and $\nabla z$; <u>and</u> (III) $\rho$ = const. or $\nabla\rho$ parallel to $\nabla z$; <u>and</u> (IV) $\nabla K_T$ parallel $\nabla T$; <u>and</u> (V) $\nabla K_C$ parallel $\nabla C$. Physically speaking, these conditions require that fluid density ($\rho$), viscosity ($\mu$), temperature (T) and salinity (C), as well as rock permeability (k) and the phenomenological coefficients $K_T$ and $K_C$, are either constant or vary with depth only (vertical stratification). Only when all these conditions are being simultaneously met the



Reproduced with permission of the copyright owner. Further reproduction prohibited without permission.

flow is irrotational and derives from a potential, which allows the use of hydraulic heads for a correct representation of the flow field.

Due to the large size of sedimentary basins, the density and viscosity of the fluid, the permeability of the rock framework, and the temperature and concentration fields vary significantly in any direction (Hanor, 1994). Therefore, the restrictions for the properties of the fluids and the porous medium derived above show that, senso-stricto, it is mathematically incorrect to use potentiometric surface maps of hydraulic heads for the representation, analysis and interpretation of the flow of formation water in sedimentary basins. Nevertheless, if coupled flow processes are neglected ($K_T$, $K_C$ << $K_H$), Darcy's Law becomes:

$$q = -\frac{\mu_0}{\mu} K_{H_0} \left[ \nabla H_0 + \frac{\Delta \rho}{\rho_0} \nabla z \right] \tag{2.12}$$

and assuming constant fluid properties ($\rho$ = const., $\mu$ = const.) and isotropic permeability

$$q = -K_{H_0} \nabla H_0 \tag{2.13}$$

with flow along $\nabla H_0$ (maximum slope on maps of hydraulic head distribution).

For this reason, contour maps of equivalent hydraulic heads are extensively used in hydrogeological studies, even for variable-density fluids and anisotropic permeability distributions, because they are often the only interpretative tools available (Bachu, 1995b). It remains to be investigated however, how sensitive Equation 2.12 is to variations in fluid density. It might be possible to define a range in which, although the density may vary, the rotational component in Equation 2.13 remains small enough so that hydraulic heads provide an adequate and meaningful representation of the fluid flow.



Reproduced with permission of the copyright owner. Further reproduction prohibited without permission.

## 2.3 Methods for fluid flow representation and analysis

*Pressure variation versus depth and elevation*

Plots of pressure versus depth, p(d), and pressure versus elevation, p(z), are important tools to investigate fluid pressure – topography relations and fluid flow in general. The pressure in a static, continuous column of water in contact with the ground surface is:

$$P = \rho \cdot g \cdot d = \gamma \cdot d \tag{2.14}$$

with d = depth (m); $\gamma$ = vertical pressure gradient (Pa/m).

Therefore, plotting pressure data versus depth allows characterizing the pressure conditions of subsurface fluids by comparing the measured fluid pressures to freshwater hydrostatic pressure. Deviations from freshwater hydrostatic pressure may be caused by: a) vertical flow in the aquifer (Fig. 2.1a), b) lack of hydraulic continuity with hydrostatically pressured aquifers and the ground surface (Fig. 2.1b and c); c) density variations, and d) fluid sinks or sources within the aquifer or bounding aquitards. A distinction can be made between "sub- and above-hydrostatic pressures" for pressures that are solely caused by topography, density variations and fluid flow, and "under- and overpressured", for pressures that cannot be explained by the previous causes alone (Orr and Kreitler, 1985). These causes have to be identified before a proper characterization of the flow is possible.

The vertical component in Darcy's Law can be expressed as (Bachu 1995b):

$$q_z = -\frac{k}{\mu}\left(\frac{\partial p}{\partial z} + \rho\, g\right) \tag{2.15}$$



Reproduced with permission of the copyright owner. Further reproduction prohibited without permission.

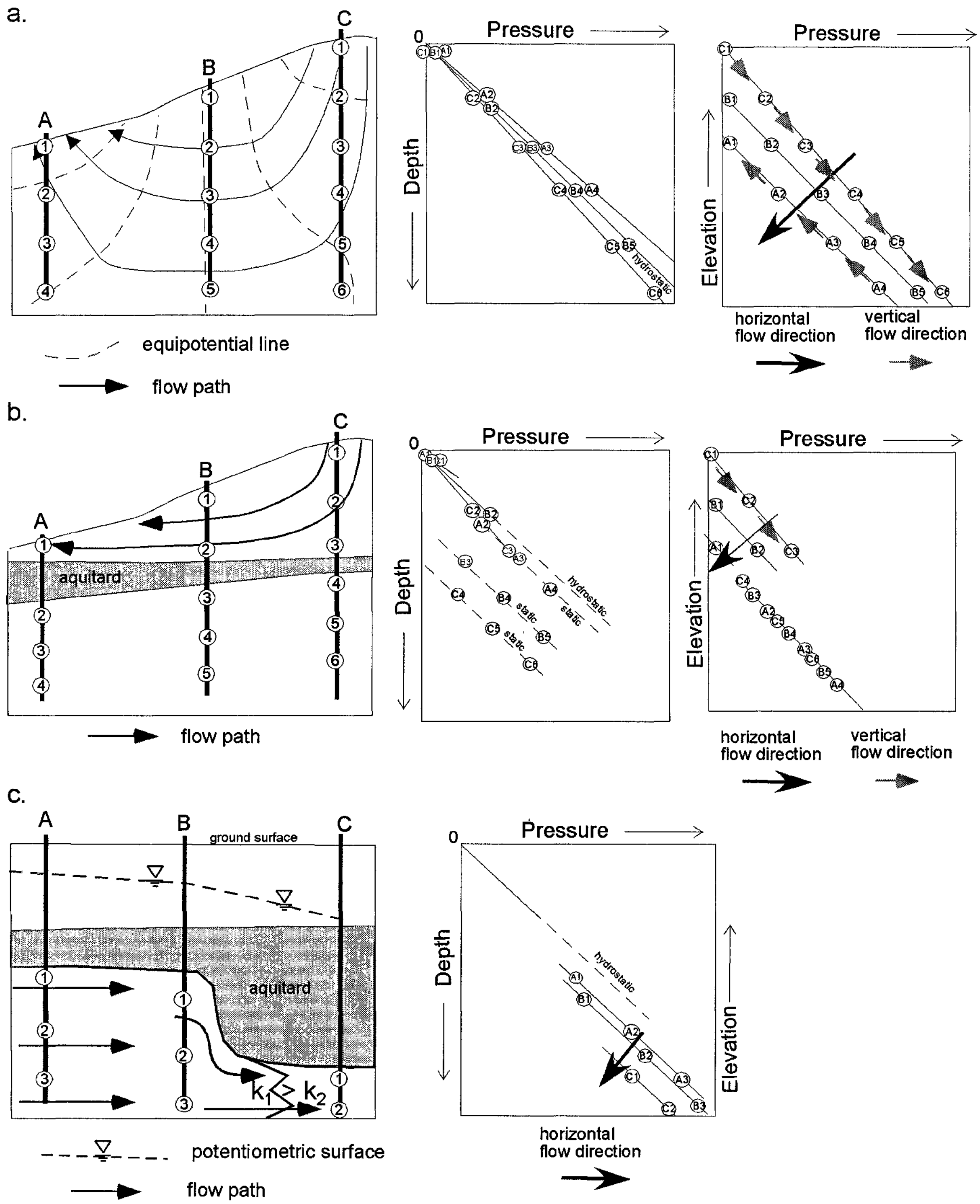


Figure 2.1: Schematic patterns of flow in the subsurface and respective distributions of fluid pressure versus depth and elevation: a) Topography-driven flow in a continuous, homogeneous aquifer; b) aquitard separating shallow, topography-driven flow system from deep aquifer with static flow conditions (after Tóth, 1978; Orr & Kreitler, 1985); c) horizontal flow in an thinning aquifer with decreasing permeability .



Reproduced with permission of the copyright owner. Further reproduction prohibited without permission.

Hence, vertical flow directions can be determined by $\frac{\partial p}{\partial z} = \rho g$, $\frac{\partial p}{\partial z} > \rho g$ or $\frac{\partial p}{\partial z} < \rho g$, indicating no vertical flow, and upward or downward flow, respectively as shown in Figure 2.1a (upward flow in well A, no vertical flow in well B, and downward flow in well C). To calculate the actual fluid flux in the vertical direction, this method is valid only if the pressure measurements are from the same well or from an unconfined, homogeneous aquifer. For confined hydrogeological conditions, the potentiometric surface rarely follows the ground surface topography. Instead, the potentiometric surface lies above or below the ground surface, indicating above-hydrostatic or sub-hydrostatic pressure conditions in the subsurface, respectively, depending on the locations of the recharge and discharge areas.

If $\rho$ = const., then the vertical pressure gradient is constant, and the distribution of pressures versus depth plot along a straight line. Otherwise the pressure gradient varies with depth according to the vertical density variation. If the salinity increases significantly with depth, then this dominates the density distribution, as opposed to the density decrease due to elevated temperatures at depth (McCain, 1991). Pressure versus depth distributions for formation waters of various constant densities, and a non-constant increase in pressure for a gradual increase in density with depth are shown in Figure 2.2.

Generally, purely hydrostatic pressures are present only in an unconfined aquifer with no flow or strictly horizontal flow ($q_z = 0 \Rightarrow \frac{\partial p}{\partial z} = \rho\, g$, well B in Figure 2.1a). Pressures in a confined aquifer with no horizontal flow that is connected to the ground surface at some lower elevation than the directly overlying ground elevation do not plot along a single straight line in a p(d)-plot. Instead, the vertical pressure distributions in each well follow different straight lines, each with a static gradient, that do not extrapolate to zero pressure at zero depth (Fig. 2.1b); hence making it difficult to draw conclusions on the flow conditions.



Reproduced with permission of the copyright owner. Further reproduction prohibited without permission.

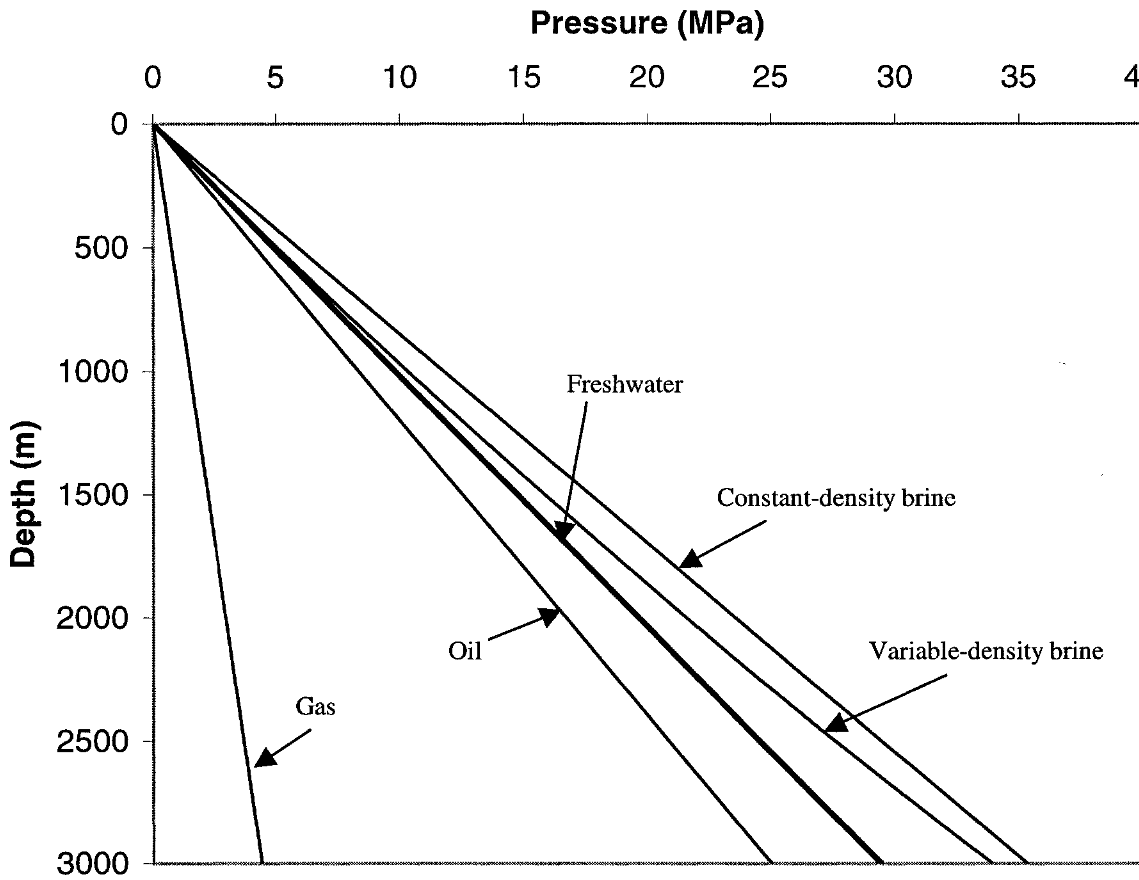


Figure 2.2: Static pressure distributions versus depth for various fluid densities: $\rho_{Gas}$ = 120 kg/m$^3$, $\rho_{Oil}$ = 850 kg/m$^3$, $\rho_{Freshwater}$ = 1000 kg/m$^3$, $\rho_{Brine}$ = 1200 kg/m$^3$. Starting with 1000 kg/m$^3$, the density was increased by 5 kg/m$^3$ every 100 m ($\rho$ = 1150 kg/m$^3$ at 3000 m depth) to calculate the theoretical pressure distribution of a variable-density brine with linearly increasing density versus depth.

In contrast, the p(z)-plots compare fluid pressure variations to a reference elevation (sea level). The pressure value at any point in the subsurface extrapolated along a hydrostatic gradient to pressure conditions at the ground surface (p = 0) indicates the hydraulic head with respect to the sea level as datum, which, in a conventional topography-driven flow system, is approximately equal to the ground surface elevation. For example, pressures measured in well B in Figure 2.1a plot along a straight line with a static water gradient that crosses the y-axis at the respective ground surface elevation for zero pressure in the p(z)-plot. Pressures in wells A and B also plot lines with pressure gradients slightly higher and lower than hydrostatic, indicating upward and downward flow, respectively.



Reproduced with permission of the copyright owner. Further reproduction prohibited without permission.

For the case of two separate aquifers in Figure 2.1b, all pressures in the confined aquifer lie on a straight line with a static gradient, correctly indicating no horizontal flow.

Pressure-elevation plots may be used also to assess the homogeneity of a specific aquifer. Consider horizontal flow of a constant-density fluid in an aquifer with homogeneous thickness and permeability distribution. Then in each well, pressures plot on a straight line with a static gradient (Fig. 2.1c; wells A and B), and the offset of each line is dependent on the constant hydraulic gradient between wells according to Darcy's Law (Eq. 2.13). If the permeability decreases along the flow path, the hydraulic conductivity term decreases accordingly:

$$K_{H_1} = \frac{k_1 \cdot \rho \cdot g}{\mu} > K_{H_2} = \frac{k_2 \cdot \rho \cdot g}{\mu} \quad \text{for } k_1 > k_2. \tag{2.16}$$

Thus, if there are no fluid sinks or sources within the aquifer, the horizontal flux q is constant, and the hydraulic gradient increases accordingly across the zone of permeability change.

Similarly, if the aquifer becomes thinner and the extent stays constant, the same amount of fluid must pass through a reduced area of the original aquifer; hence the hydraulic gradient has to increase according to (e.g., Freeze and Cherry, 1979):

$$Q = -K_H \cdot \nabla H_0 \cdot A \tag{2.17}$$

where, Q = flow rate ($m^3/s$), A = a b = area of the aquifer ($m^2$), b = aquifer thickness (m), a = lateral extent of the aquifer perpendicular to the flow direction (m). The hydraulic conductivity multiplied by the aquifer thickness is defined as transmissivity T (e.g., Freeze and Cherry, 1979):

$$T = K_H \cdot b \tag{2.18}$$

In the example in Figure 2.1c, a decrease in permeability and/or transmissivity along the flow path results in an increase in hydraulic gradient between wells B and C, which is exemplified by an increase in the slope of the potentiometric surface and larger offset of lines through pressure measurements between wells B and C than between wells A and B, yet constant well spacing.



Reproduced with permission of the copyright owner. Further reproduction prohibited without permission.

For regional-scale hydrogeological investigations, pressure-elevation plots generally seem to have more useful information on pressure conditions in the subsurface than pressure-depth plots. First, they always indicate the direction of flow and the approximate elevation of the potentiometric surface. Secondly, deeper, confined aquifers are at least partly disconnected by major aquitards from recharge from the directly overlying ground surface, so that the p(d)-plot using the ground surface as datum will only indicate over- or underpressured conditions. In the pressure-depth analysis for individual aquifers in this study, a pressure gradient is used that represents the average water density in each aquifer.

*Representation of variable-density fluid flow using hydraulic heads and driving force vectors*

Typically, lateral fluid flow is interpreted by using 'freshwater hydraulic head' distributions. Flow is inferred to be from high to low hydraulic heads, and freshwater hydraulic heads $H_f$ are calculated using the density of freshwater at standard conditions ($\rho_f$ = 1000 kg/m$^3$) as reference density in Equation 2.4. To be able to distinguish in this study between the general definition of hydraulic heads, in which any density may be used as reference density and the special case of freshwater hydraulic heads, subscripts "0" and "f" refer to a general and freshwater density, respectively.

With x, y, z representing the principal axes of anisotropy, and horizontal permeability components $k_x$, $k_y$ and vertical permeability component $k_z$, Darcy's Law can be decomposed into its horizontal ($q_x$, $q_y$) and vertical ($q_z$) components (de Marsily, 1986, p. 64):



Reproduced with permission of the copyright owner. Further reproduction prohibited without permission.

$$q_x = -\frac{k_x \cdot \rho \cdot g}{\mu} \cdot \frac{\partial H_0}{\partial x}, \qquad q_y = -\frac{k_y \cdot \rho \cdot g}{\mu} \cdot \frac{\partial H_0}{\partial y},$$

$$q_z = -\frac{k_z \cdot \rho \cdot g}{\mu}\left(\frac{\partial H_0}{\partial z} + \frac{\rho - \rho_0}{\rho_0}\right) \tag{2.19}$$

Hence, using only hydraulic heads results in a correct interpretation of flow in the horizontal plane. On the other hand, if the flow has a vertical component, as in the case of sloping aquifers, the representation of flow using only hydraulic heads introduces errors, because the density term in the $q_z$ component is neglected.

Even if the density is constant but different from freshwater, errors result from the use of freshwater hydraulic heads as shown in the following theoretical example (Jorgensen et al. 1982). In Figure 2.3 static conditions and a constant brine density, higher than freshwater, are assumed. The ground surface coincides with the sea level elevation, so that plots of fluid pressure versus depth and pressure versus elevation are identical. Freshwater hydraulic heads can be calculated for the two test locations in the aquifer:

$$H_{f1} = z_1 + \frac{p_1}{\rho_f g} \quad ; \quad H_{f2} = z_2 + \frac{p_2}{\rho_f g}$$

As can be seen from the extrapolation in the p(z)- plot (Fig. 2.3), these head values are not the same, $H_{f2} > H_{f1}$, implying flow from left to right, which obviously is wrong because there is no flow in the aquifer (hydrostatic conditions assumed a priori). If the actual water density is used as a reference density instead of freshwater, then $H_1 = H_2$ and the system correctly shows no flow.



Reproduced with permission of the copyright owner. Further reproduction prohibited without permission.

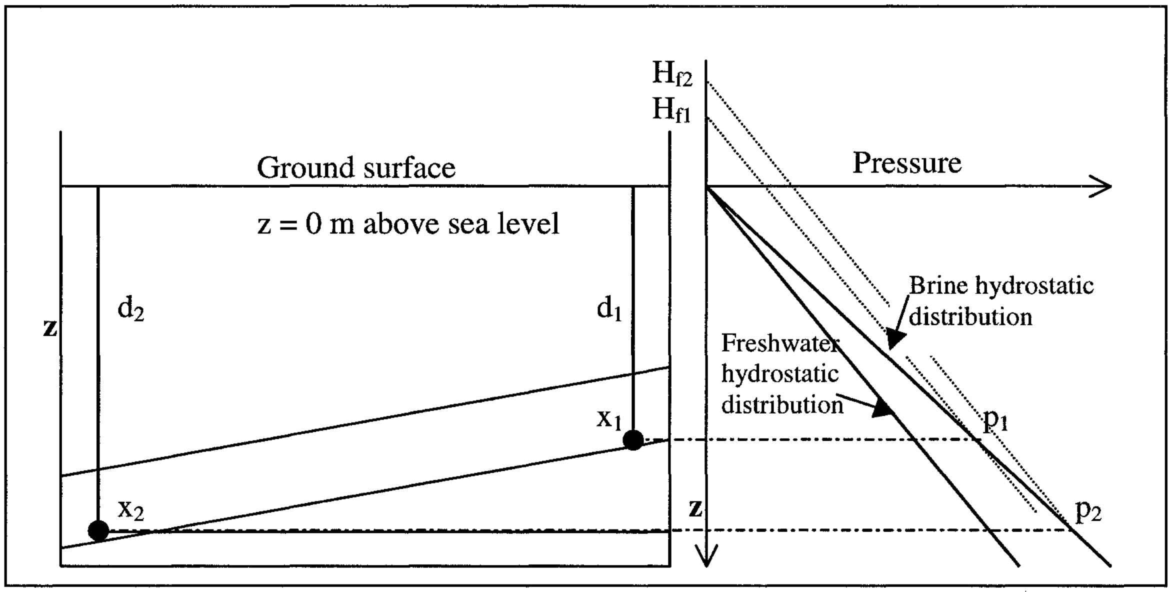


Figure 2.3: Cross sectional view of an aquifer saturated with a constant-density brine and penetrated by two wells aligned along the z-axis, and corresponding pressure-elevation plot (z = elevation, d = depth, x = location of pressure measurement, p = pressure).

This result can be extended to the case of a static system containing variable-density water. The assumption of static conditions can be mathematically expressed by setting the fluid flux q = 0 (Eq. 2.12):

$$
\begin{aligned}
q &= -\frac{k\,\rho_0\,g}{\mu}\cdot\left(\nabla H_0 + \frac{\rho-\rho_0}{\rho_0}\nabla z\right) = 0 \\
\Rightarrow \nabla H_0 &= -\frac{(\rho-\rho_0)}{\rho_0}\nabla z
\end{aligned}
\tag{2.20}
$$

Only if the actual fluid density is used as reference density in Equation 2.20, the gradient becomes 0, and Darcy's Law correctly shows no flow. Thus, using freshwater hydraulic heads calculated from pressure data measured at different elevations introduces an error into the interpretation of fluid flow that is represented by the term $-\frac{(\rho-\rho_0)}{\rho_0}\cdot\nabla z$ that, in the case presented above, wrongly indicates flow. Generally, this term could be considered as an 'artificial' buoyancy term that is always introduced when choosing a reference fluid density other than the actual fluid density.



Reproduced with permission of the copyright owner. Further reproduction prohibited without permission.

On the other hand, using the actual fluid density ρ in a variable-density system at every point where the hydraulic head is calculated also results in a wrong interpretation of the flow direction, as illustrated again in the case of a static system (Fig. 2.4). The variable-density head can be expressed as:

$$H_v = \frac{p}{\rho g} + z \tag{2.21}$$

where ρ is the actual fluid density and, if ρ is not constant, then $H_v$ is a function of p, z and ρ, as opposed to $H_0$, which is only a function of p and z.

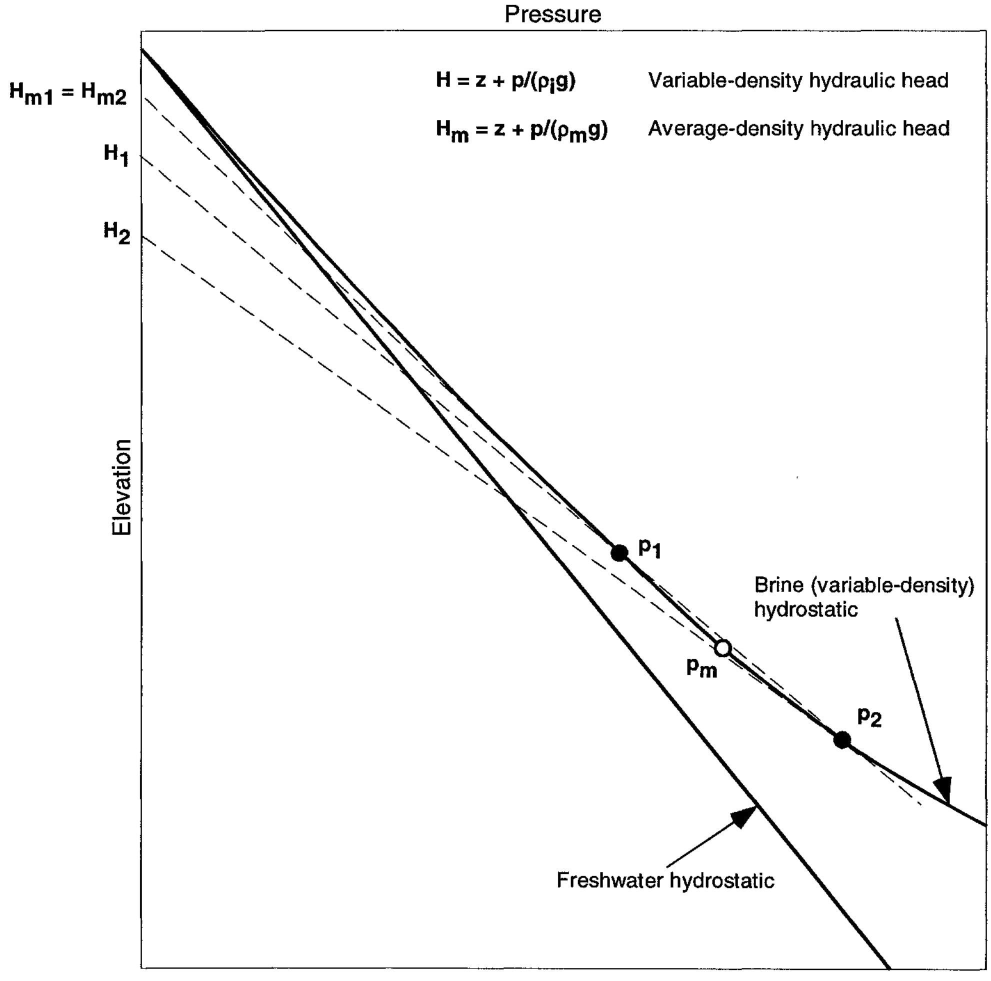


Figure 2.4: Pressure-elevation plot for static conditions in an aquifer containing variable-density formation water (linear density increase with depth), schematically showing differences in hydraulic head calculations for various densities. For the spatial relationship between $p_1$ and $p_2$ see cross section in Figure 2.3.



Reproduced with permission of the copyright owner. Further reproduction prohibited without permission.

There is a difference in variable-density heads $\Delta H_v$ between points $x_1$ and $x_2$, and flow down-slope is implied from right to left, although static conditions are assumed a priori. Nevertheless, for any linear density variation with depth, a correct result and flow interpretation would be achieved by using an average density $\rho_m = (\rho_2 + \rho_1)/2$ in the hydraulic head calculation, which, in this case results in $H_{m1} = H_{m2}$, correctly indicating no flow.

Gupta and Bair (1997) modeled steady-state, variable-density fluid flow using a numerical code based on Equation 2.12 (Kuiper, 1983). They compared calculated fluid flux vectors and variable-density heads in the Mt. Simon Sandstone aquifer, which showed implicitly that the actual flow direction and magnitude do not correspond to the variable-density head gradient, hence that variable-density heads wrongly represent fluid flow. Mathematically, this can be shown by substituting the expression for the variable-density head (Eq. 2.16) into Equation 2.13:

$$- K\, \nabla H_v = -K\left(\frac{\nabla p}{\rho\, g} + \nabla z - \frac{p}{\rho^2 g}\nabla\rho\right) = -\frac{k}{\mu}\left(\nabla p + \rho\, g \nabla z - \frac{p}{\rho}\nabla\rho\right) \\ = q + \frac{k\, p}{\mu\, \rho}\nabla\rho \tag{2.22}$$

which adds a term to, and therefore contravenes, Darcy's Law.

In order to consider any density variation with depth, Lusczynski (1961) introduced the concept of "environmental hydraulic heads", $H_e$, which he defined as:

$$H_e = H_f + \frac{\rho_f - \rho_a}{\rho_f} \cdot \left(z_g - z\right) \tag{2.23}$$

where $z_g$ = ground surface elevation, $\rho_f$ = freshwater density, $H_f$ = freshwater hydraulic head, and $\rho_a$ = average fluid density, defined as:



Reproduced with permission of the copyright owner. Further reproduction prohibited without permission.

$$\rho_a = \frac{1}{z_g - z} \int_z^{z_g} \rho \, dz \qquad (2.24)$$

The environmental hydraulic head considers the hydrostatic pressure within a column of variable-density water connected to the ground surface, and would correctly describe the hydrostatic pressure distribution in Figure 2.4 for a hydraulically continuous aquifer system. Environmental hydraulic heads correctly indicate the vertical flow component, but misrepresent the horizontal components of fluid flow, because, similar to variable-density heads, they contravene Darcy's Law when introduced in Equation 2.12 (Bachu, 1995b). In addition, they are difficult to calculate for natural settings, even if only the vertical flow component is sought, because the exact density distribution is usually not known and the pressure distribution in the aquifers is not necessarily vertically continuous to the ground surface, if they are confined by intervening aquitards.

It is instructive to split the driving force acting on the fluid into its pressure-related and density-related force components. From Darcy's Law, the total driving force F* per unit volume acting on the fluid can be expressed as (Hubbert, 1940; Bachu 1995b):

$$F^* = -\rho_0 \cdot g\left(\nabla H_0 + \frac{\rho - \rho_0}{\rho_0} \cdot \nabla z\right) = \frac{\mu}{k}\vec{q} \qquad (2.25)$$

The driving force only indicates the potential for fluid flow, but it does not identify the acting driving mechanism(s).

In sloping aquifers flow is along the confining layers. Kuiper (1983) developed a numerical model for simulating flow in these aquifers by decomposing the flow rate into two orthogonal components in the bedding plane and a vertical component. Similarly, for the two-dimensional case of a sloping aquifer at the angle Θ (Fig. 2.5a), the flow driving force per unit volume along the aquifer slope is (Dorgarten and Tsang, 1991):



Reproduced with permission of the copyright owner. Further reproduction prohibited without permission.

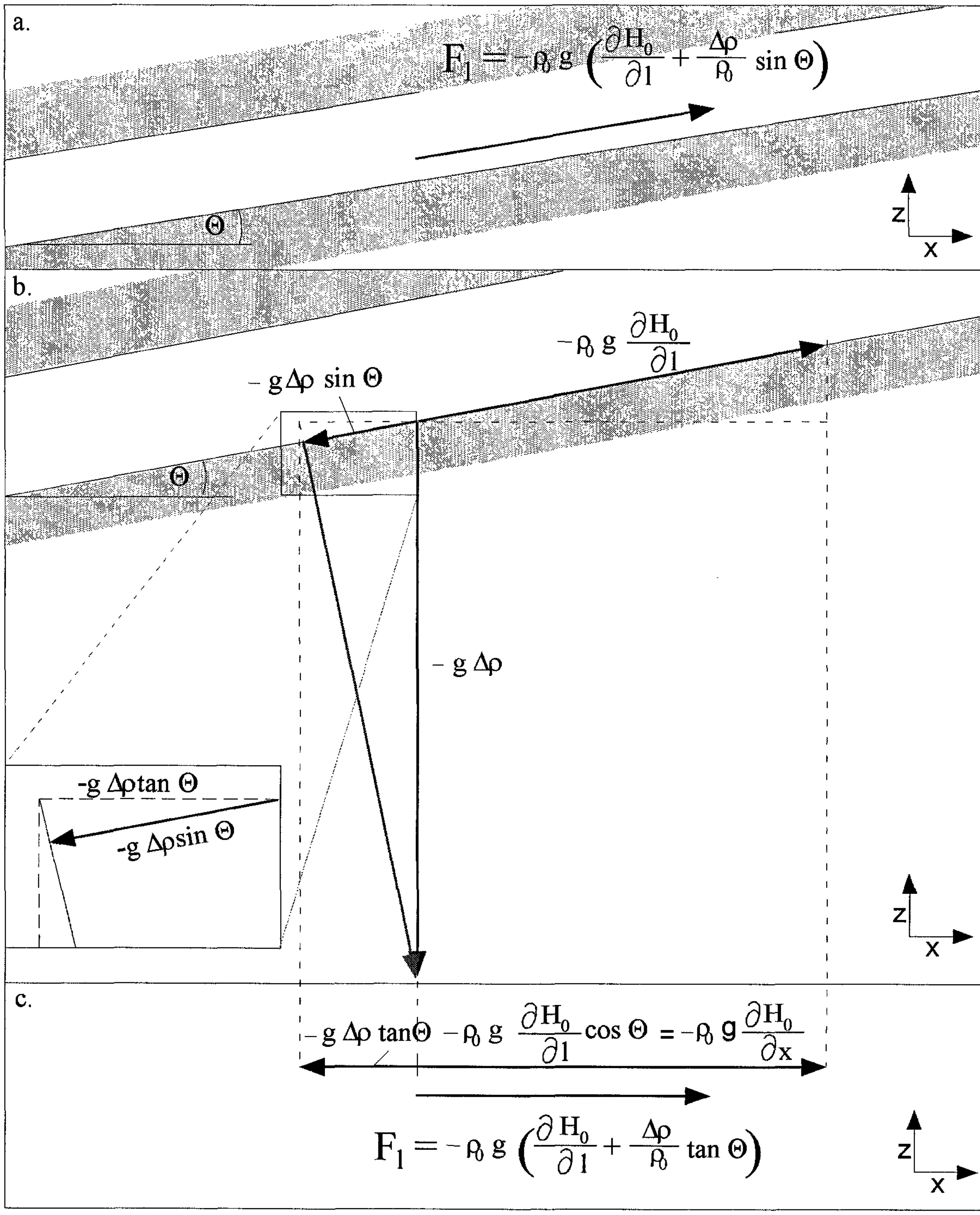


Figure 2.5: Diagram of the two-dimensional decomposition of the driving force vector along a sloping aquifer and the approximation of its components in Cartesian coordinates (H decreases along the x-axis): a) total driving force along the aquifer slope ($\tan\Theta = \nabla E$), b) pressure- and density related force components, c) horizontal driving force and its components.



Reproduced with permission of the copyright owner. Further reproduction prohibited without permission.

$$F_l = -\rho_0 \; g\left(\frac{\partial H_0}{\partial l} + \frac{\Delta\rho}{\rho_0}\sin\Theta\right) \tag{2.26}$$

Short of numerical modeling, and because $\frac{\partial H_0}{\partial l}$ and sin Θ are difficult to evaluate, this force is decomposed in Figure 2.5 into its horizontal (x) and vertical (z) components (Cartesian coordinates). If the angle Θ of the aquifer slope, defined as $\nabla$ E, is small, then:

$$\frac{\Delta\rho}{\rho_0}\sin\Theta \cong \frac{\Delta\rho}{\rho_0}\tan\Theta \qquad \text{and} \qquad \frac{\partial H_0}{\partial l} \cong \frac{\partial H_0}{\partial x}, \qquad \text{so that}$$

$$F_l \cong -\rho_0 \cdot g\left(\frac{\partial H_0}{\partial x} + \frac{\rho - \rho_0}{\rho_0}\tan\Theta\right) \tag{2.27}$$

is a good approximation for the driving force acting on the fluid along the confining layers of a dipping aquifer. For three dimensions Equation 2.27 becomes:

$$F_l \cong -\rho_0 \; g\left(\nabla_{xy} H_0 + \frac{\rho - \rho_0}{\rho_0}\nabla E\right) \tag{2.28}$$

where $\nabla_{xy}$ = gradient in the horizontal plane only (x and y components).

When solely using equivalent hydraulic heads ($H_o$), only the pressure-related force component of the total fluid driving force is being considered, which results in the prediction of a wrong flow direction (by the angle ψ) and erroneous flow magnitude (Fig. 2.6).



Reproduced with permission of the copyright owner. Further reproduction prohibited without permission.

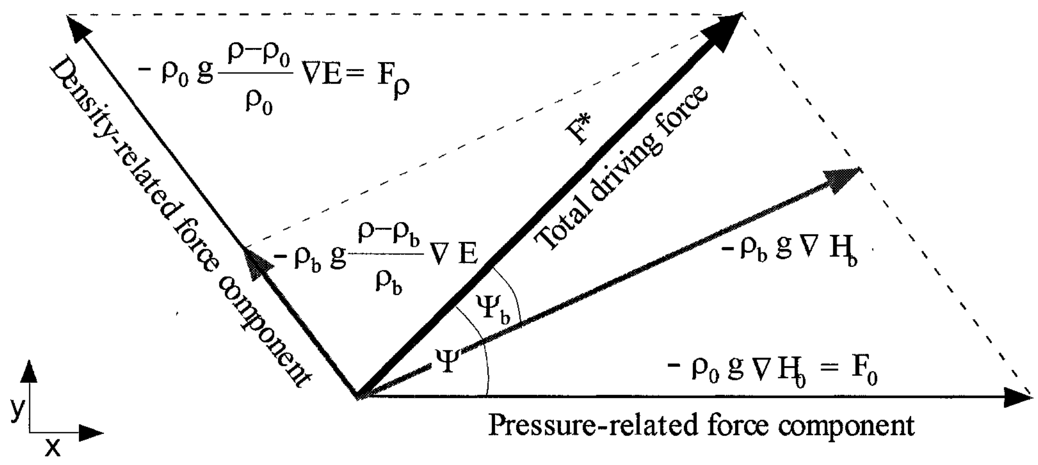


Figure 2.6: Vector diagram of driving force components in plan view for various reference densities (modified after Davies, 1987).

The schematic vector diagram (Fig. 2.6) shows that basically any value may be chosen for the reference density, which results in an infinite number of combinations into which the driving force vector can be decomposed. Thus, the "buoyancy" term in Darcy's law (Eq. 2.12) and in the driving force vector equation (Eq. 2.25) corrects for errors that are introduced by using a reference density different from the actual formation water density in the representation of a variable-density fluid system.

According to Equation 2.25, the following parameters are needed to describe fluid flow using driving force vectors: a) pressure, b) measurement elevation, and c) fluid density. In addition, permeability and fluid viscosity are needed for the calculation of fluid fluxes (see following section). In plan view, the driving force vector method represents the lateral driving force acting on the fluid in an aquifer. When constructing driving force vectors, only the hydraulic head and elevation are introduced spatially by the differentiation of their values, thus considering the hydraulic gradient between adjacent points of possibly different elevation. On the other hand, the density values are introduced only at the point under consideration and are individually compared to a reference value but not to each other. Thus, the relative buoyancy of adjacent points is not actually taken into account.



Reproduced with permission of the copyright owner. Further reproduction prohibited without permission.

Although mathematically more accurate, the construction of driving force vector maps still requires considerably more work than the calculation and mapping of hydraulic heads. Also, the aquifer slope has to be averaged over a certain distance, and the fluid density at the points for which the driving force is determined is calculated from contour maps of salinity and subsurface temperature. This introduces technical and averaging errors in addition to the ones that already exist for the pressure data used in the calculation of hydraulic heads (see Chapter 3).

Therefore, the validity and applicability of hydraulic head interpretations compared to the driving force is examined more closely. Davies (1987) defined the driving force ratio (DFR) as the ratio of the pressure- and density-related components of the driving force:

$$DFR = \frac{\rho - \rho_0}{\rho_0} \cdot \frac{|\nabla E|}{|\nabla_{xy} H_0|} \tag{2.29}$$

Based on numerical simulations that actually calculated the flux vector q in a homogeneous and isotropic aquifer, Davies (1987) suggested a value DFR = 0.5 as a threshold above which the distribution of freshwater hydraulic heads gradient alone does not sufficiently represent lateral flow in the aquifer, and density variations have to be explicitly accounted for. He also pointed out that this threshold value might vary depending on the scale and the required accuracy of a particular study. A DFR = 0.5 infers a difference of up to 50 % in magnitude between the actual driving force and its pressure-related component, and a deviation from the actual flow direction of up to $30^{\circ}$. The maximum difference in magnitude and direction cannot occur simultaneously. The maximum of the magnitude error occurs for zero deviation ($\psi = 0$), whereas the maximum deviation occurs for a minimum of the magnitude error. The relationship between force components and total force on the fluid is shown in Figure 2.7.



Reproduced with permission of the copyright owner. Further reproduction prohibited without permission.

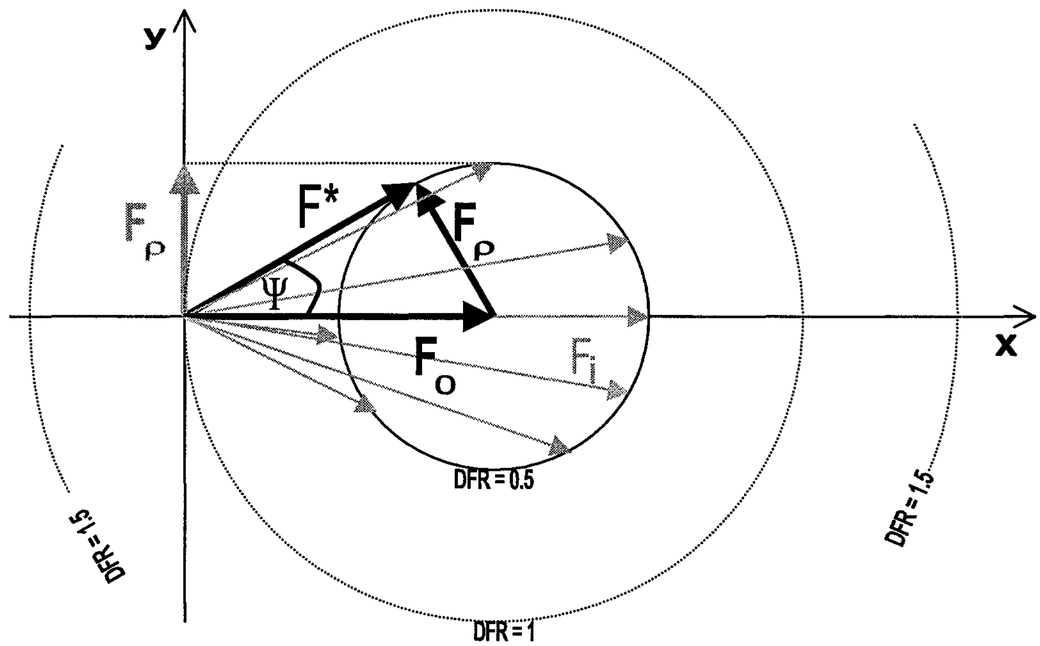


Figure 2.7: Schematic vector diagram of the driving force components in the horizontal plane. The circles define the possible end points of driving total force vectors for a given DFR value. Vectors in grey are examples of total force vectors for DFR = 0.5. The bold vectors represent the driving force and its components, $F_0$ (pressure-related component) and $F_\rho$ (density-related component) at a maximum deviation between $F_0$ and F* of $\Psi = 30^O$. See Figure 2.6 for the definition of $F_0$ and $F_\rho$.

Many driving forces $F_i$ decompose in components that have the same force ratio. This group of possible force vectors $F_i$ is defined by a circle around the tip of the pressure-related force vector $F_0$. The radius of the circle is the magnitude of the density-related force component $F_\rho$. The maximum deviation $\Psi_{max}$ between the driving force and its pressure-related component occurs when F* is tangential to the circle defined by the respective DFR. Hence:



Reproduced with permission of the copyright owner. Further reproduction prohibited without permission.

$$\sin\Psi_{\max} = \frac{\rho-\rho_0}{\rho_0}\cdot\frac{|\nabla E|}{|\nabla H_0|} \text{ for } DFR \leq 1 \tag{2.30}$$

and $\Psi_{max}$ = 180$^{O}$ for DFR > 1, which is also the maximum possible deviation max ($\Psi_{max}$).

It is helpful to examine both the DFR and the orientation of the pressure- to the density-related force components in order to identify whether the prediction of the magnitude and/or the direction of the driving force are significantly in error. When using freshwater density as the reference density, the density-related component of the driving force is directed downdip for water densities > 1000 kg/m$^3$, which is the case for most sedimentary basins with high-salinity formation water. There are various extreme cases to be considered:

(a) The pressure-related force component is directed downdip, along the aquifer slope. In this case, using only the pressure component underestimates the magnitude of the driving force, but it does not misrepresent its direction. Hence, by using only equivalent freshwater hydraulic heads, the magnitude of the driving force will always be underestimated, but the predicted flow direction is correct.

(b) The pressure-related force component is directed updip, again parallel to the aquifer slope By using only freshwater hydraulic heads for DFR < 1, the magnitude of the driving force is overestimated. For DFR > 1 the flow direction is actually opposite (downdip) to the updip one indicated by the pressure component.

(c) If a different density than that of freshwater is chosen as a reference state, the direction of the density-related force component is directed updip for actual densities smaller than the reference density, and downdip for actual densities larger than the reference density. The equivalent hydraulic gradient is opposed (updip or downdip) to the driving force vector only in the cases of DFR > 1 and opposed density- and pressure-related force components.

In cases a) – c) the DFR is equal to the percentage of error in the magnitude between the equivalent hydraulic gradient and the actual total force acting on the fluid.



Reproduced with permission of the copyright owner. Further reproduction prohibited without permission.

The previous examples represent special flow conditions, whereas in the general case the aquifer slope and the pressure-related force component are at an angle. A DFR = 1 is still the threshold above which there is the possibility that the flow direction, as inferred from the gradient of equivalent hydraulic heads, is reversed, or opposed to the actual flow direction.

As explained earlier, any value may be chosen as reference density $\rho_0$, but, for the same flow conditions, different reference densities result in different DFRs. Therefore, it should be possible to find a suitable reference density for which the DFR is minimal and hydraulic heads alone are sufficiently accurate to represent flow. Figure 2.8 illustrates how, under the same flow conditions ($F^*$ = const.) in a variable-density system, different reference densities and the direction of the density-related component affect the difference between the driving force and its pressure-related component. It considers cross-sectional (2-D) flow along a sloping aquifer ($\nabla E$ = const.), for various values for the reference density $\rho_o$ and a fluid density range 1000 –1200 kg/m$^3$ commonly observed in sedimentary basins. The value on the y-axis compares the total driving force $F^*$ to its pressure-related component $F_0$:

$$\frac{F^*}{F_0} = \frac{\left| -\rho_0\, g \left( \nabla H_0 + \frac{\Delta\rho}{\rho_0} \nabla E \right) \right|}{\left| -\rho_0\, g\, \nabla H_0 \right|} = 1 \pm DFR \tag{2.31}$$

depending on whether $\Delta\rho > 0$ or $\Delta\rho < 0$.

Regardless of the flow direction, the ratio $F^*/F_0$ is given by 1 - DFR for flow opposite to its density-related component, and by 1 + DFR for flow where the two are in the same direction. Thus the flow magnitude is over- or underestimated, respectively, when using hydraulic heads only in the flow representation, depending on the relative position of the driving force and its density-related component.



Reproduced with permission of the copyright owner. Further reproduction prohibited without permission.

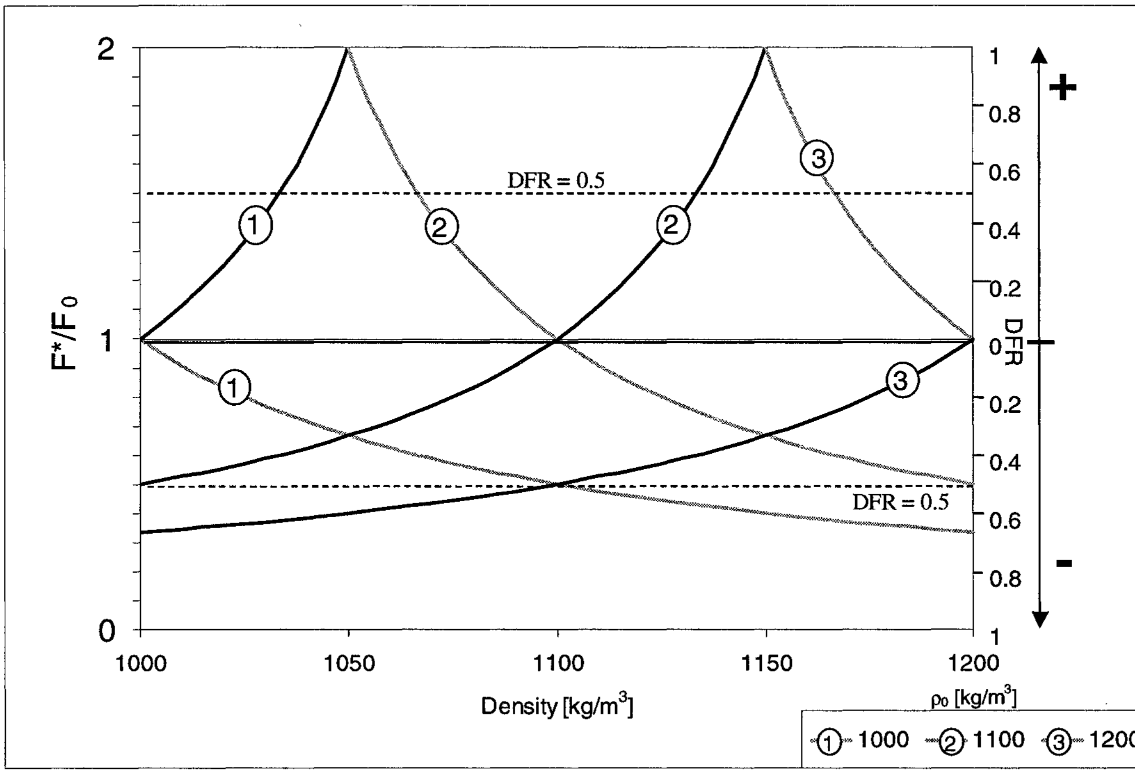


Figure 2.8: Graph showing the error introduced when interpreting the driving force as derived from equivalent hydraulic head gradients only, versus the driving force (for 2-D flow along the slope of the aquifer; +/- indicate over- or underestimation of the actual driving force acting on the fluid, respectively). The grey and black curves represent updip flow and downdip flow, respectively. $F^*/F_0$ was calculated according to Equation 2.31 for $\nabla E = 0.01$ and $\nabla H_0 = \frac{F^*}{-\rho_0 \cdot g} - \frac{\rho - \rho_0}{\rho_0} \nabla E$, where the constancy of the arbitrarily chosen flow driving force is expressed by $\frac{F^*}{g} = 1 \frac{m^3}{kg}$.

As expected, DFR = 0 and $F^*/F_0 = 1$ if the fluid density $\rho$ is constant and the reference density is chosen as $\rho_o = \rho$, which means that the distribution of equivalent hydraulic heads accurately describes the lateral flow in the aquifer. In the case of a variable density distribution, for any reference density $\rho_o$ and predefined critical DFR value ($DFR_{crit}$), the density range $\rho_{min}$ - $\rho_{max}$ for which DFR < $DFR_{crit}$ is constant, but asymmetrically distributed around $\rho_o$, depending on the flow direction. Therefore, choosing a reference density at the lower or upper end of the naturally observed density range in sedimentary



Reproduced with permission of the copyright owner. Further reproduction prohibited without permission.

basins limits the use of hydraulic heads alone, because parts of the theoretically available density range are practically ignored. For example, arbitrarily choosing a $DFR_{crit} = 0.5$ in a system where ρ ranges between 1000 and 1200 kg/m$^3$, shows that using the average density as reference density ($\rho_0$ = 1100 kg/m$^3$) allows for the widest range of fluid density variation, within which flow can still be satisfactorily interpreted with equivalent hydraulic heads (Tab. 2.1).

| $\rho_o$ (kg/m$^3$) | Flow direction | $\rho_{min}$ (kg/m$^3$) | $\rho_{max}$ (kg/m$^3$) |
|---|---|---|---|
| 1000 | Updip | 1000 (970) | 1100 |
| | Downdip | 1000 (900) | 1030 |
| 1100 | Updip | 1070 | 1200 |
| | Downdip | 1000 | 1130 |
| 1200 | Updip | 1170 | 1200 (1300) |
| | Downdip | 1100 | 1200 (1230) |

Table 2.1: Example of minimum and maximum density values from Figure 2.8 for which DFR < 0.5. The numbers in brackets refer to the theoretically minimum and maximum density values, which are not commonly observed in sedimentary basins.

Because formation water densities significantly below 1000 kg/m$^3$ or above 1200 kg/m$^3$ usually do not occur in sedimentary basins, the allowable density range for freshwater ($\rho_f$ = 1000 kg/m$^3$) or high-saline brine (1200 kg/m$^3$) as reference density is smaller. When examining the flow of high-density brines, the DFR values, hence the errors introduced by using only hydraulic-head distributions, are minimized, if an appropriate reference density that reflects the average brine density is chosen. This allows for a better application of equivalent hydraulic heads and for a wider density range, while the use of equivalent freshwater hydraulic heads would actually maximize the error.

When a theoretically accurate representation and analysis is required for a flow domain with varying fluid density, it is necessary to calculate driving force vectors to account for effects of density variation. Nevertheless, one should be aware of the practical errors in this procedure. As shown earlier, the driving force is unique at every point in the aquifer



Reproduced with permission of the copyright owner. Further reproduction prohibited without permission.

and it can be decomposed in an infinite number of pressure- and density-related components by choosing different values for $\rho_0$. Therefore, at least theoretically, adding the pressure-related force components, derived from hydraulic head distributions, to the density-related force components should result in the same, unique force vector field, independent from the reference density. It should be emphasized that "unique" does not automatically imply that it is the "correct" driving force, because the accuracy of the force vectors still depends to a large extent on the original data quality used in its calculation. Practically, when calculating the force field on a regular grid from irregularly distributed data (hydraulic heads, formation water density, aquifer slope) the force vector field is not necessarily unique, because the gridding process introduces errors due to the inter-, and extrapolation of data points. The effect of data accuracy on the representation of flow will be discussed further in Chapter 3.

In some cases, especially in regional-scale hydrogeological studies, it might be less important to know the exact flow direction and magnitude, and the use of equivalent hydraulic heads gives satisfactory results for the interpretation of the general flow field. Calculating the DFR at critical points in the study area helps in determining the potential error of this analysis. Depending on the required accuracy for the particular study, a threshold value for the DFR has to be chosen above which the errors in the equivalent hydraulic head interpretation become unacceptable. This threshold value can basically range between DFR = 0 (exact solution) and DFR = 1 (possibility of opposed flow and 100 % error in force magnitude). By predefining an acceptable error in the deviation of the flow direction, and/or its magnitude, the threshold DFR value can be calculated either directly from Equation 2.29, or using Table 2.2.



Reproduced with permission of the copyright owner. Further reproduction prohibited without permission.

| Max. Error in Force Magnitude [%] | Max. Deviation [ $^{o}$] | DFR |
|---|---|---|
| 0 | 0.0 | 0 |
| 10 | 5.7 | 0.1 |
| 20 | 11.5 | 0.2 |
| 30 | 17.5 | 0.3 |
| 40 | 22.6 | 0.4 |
| 50 | 30.0 | 0.5 |
| 60 | 36.9 | 0.6 |
| 70 | 44.4 | 0.7 |
| 80 | 52.1 | 0.8 |
| 90 | 64.2 | 0.9 |
| 100 | 90.0 | 1 |
| < 100 | 180 | < 1 |

Table 2.2: Driving force ratio (DFR) as a function of maximum errors of force magnitude and direction resulting from the interpretation of equivalent hydraulic heads without accounting for density variations.



Reproduced with permission of the copyright owner. Further reproduction prohibited without permission.

The distributions of driving forces and/or hydraulic heads are indicative only of the potential for fluid flow and of the flow direction. The actual flow rate is given by Darcy's Law (Eq. 2.12), that can be also written as:

$$\vec{q} = \frac{k}{\mu} \cdot F^* \tag{2.32}$$

Equation 2.29 shows that the flow is largely controlled by the permeability of the porous medium, because k varies within several orders of magnitude (e.g., Freeze and Cherry, 1979, p. 29), while μ changes usually by less than one order of magnitude (de Marsily, 1986).

In a homogenous aquifer, F* correctly indicates the flow direction (if known and calculated correctly). The driving force F* calculated based on $\nabla_{xy} H_0$ and $\frac{\Delta\rho}{\rho_0}\nabla E$ is still good for indicating the flow direction (first approximation), while $\nabla_{xy} H_0$ alone (second approximation) is acceptable only if the DFR value is below a predetermined critical value. The flow magnitude is still not known unless multiplied by a constant k and divided by a constant μ. The same holds for a heterogeneous aquifer, only that F* has to be multiplied by the respective k /μ, depending on its distribution in the aquifer. In an anisotropic aquifer even the directions of driving force and flux vector are different from each other and delineating flow paths becomes very difficult without knowledge of the permeability distribution and anisotropy characteristics.



Reproduced with permission of the copyright owner. Further reproduction prohibited without permission.

## 2.4 Illustrative example of optimizing the reference density in the hydraulic-head calculation

For illustration, the effect of selecting different reference densities in the calculation of hydraulic heads is presented in the following for the flow representation in a part of the Elk Point aquifer in the study area. This aquifer is a good example, because, besides the slope of the aquifer, it contains high-salinity formation water and low hydraulic gradients so that the water density and the reference density used in the calculation of hydraulic heads have a significant effect on the flow representation. An 80 x 130 $km^2$ area defined by 116 – 118$^O$ W and 54.25 – 55.0$^O$ N was chosen because of the data distribution and the erosional limit of the Elk Point Group. The top of the Elk Point aquifer varies from -1270 m in the southwest to -1680 in the northeast, with an average slope of 10.9 m/km (Fig. 2.9). The density of the formation water, calculated on the basis of salinity and the average geothermal gradient (Bachu and Burwash, 1991, 1994), increases north-northwestward from approximately 1090 to 1135 kg/$m^3$ (Fig. 2.10). Figures 2.11 – 2.14 show the distributions of hydraulic heads and of the Driving Force Ratios (DFR), which were calculated with the following reference densities: $\rho_f$ = 1000 kg/$m^3$ (freshwater), $\rho_{min}$ = 1090 kg/$m^3$, $\rho_{max}$ = 1135 kg/$m^3$, and $\rho_{av}$ = 1120 kg/$m^3$ (field average). The flow-driving force field is superimposed on each hydraulic-head map to illustrate the errors made by inferring flow on the basis of hydraulic heads only and by neglecting the density-related force component. If hydraulic heads correctly represent the flow direction, the force vectors should be perpendicular to the hydraulic head contour lines, and the DFR ideally should be zero, but definitely significantly smaller than 1.



Reproduced with permission of the copyright owner. Further reproduction prohibited without permission.

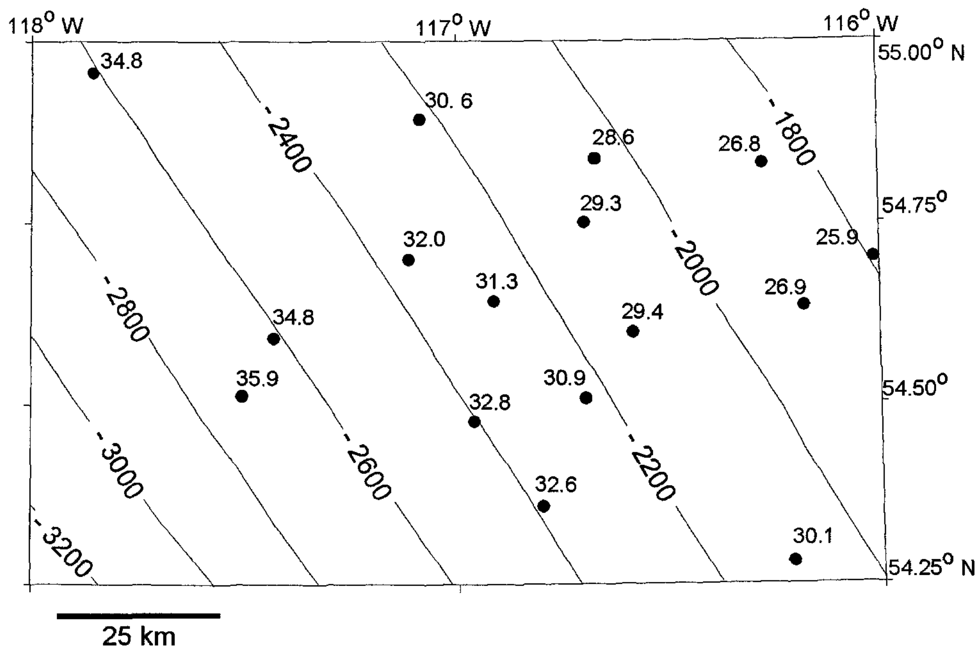


Figure 2.9: Structure top of the Elk Point aquifer (m.a.s.l.) and observed formation water pressures (MPa) at the top of the aquifer.

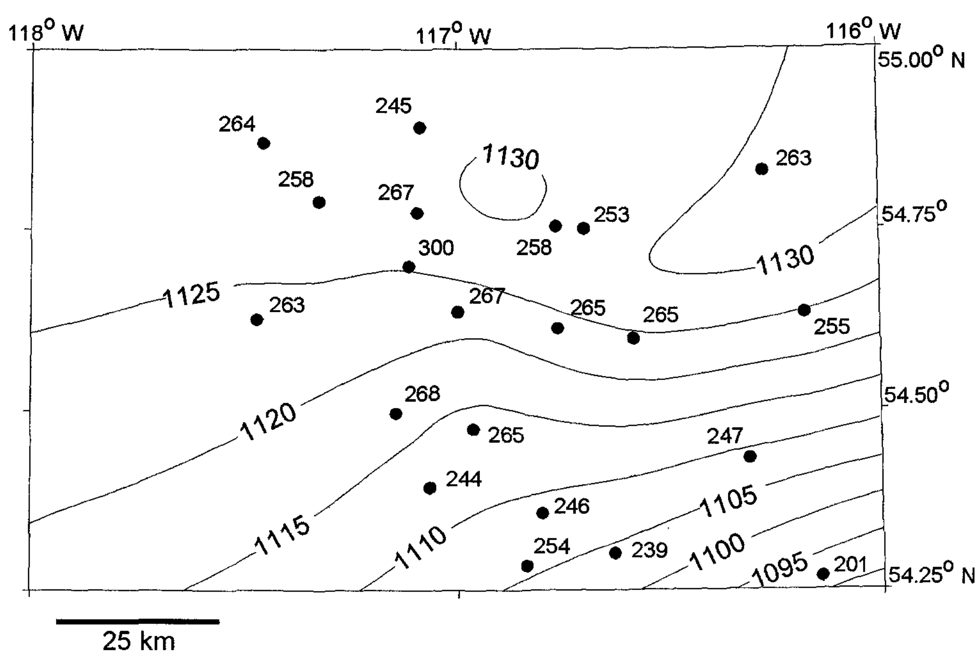


Figure 2.10: Density distribution (kg/m³) and salinity values (g/l) of formation water in the Elk Point aquifer.



Reproduced with permission of the copyright owner. Further reproduction prohibited without permission.

a.

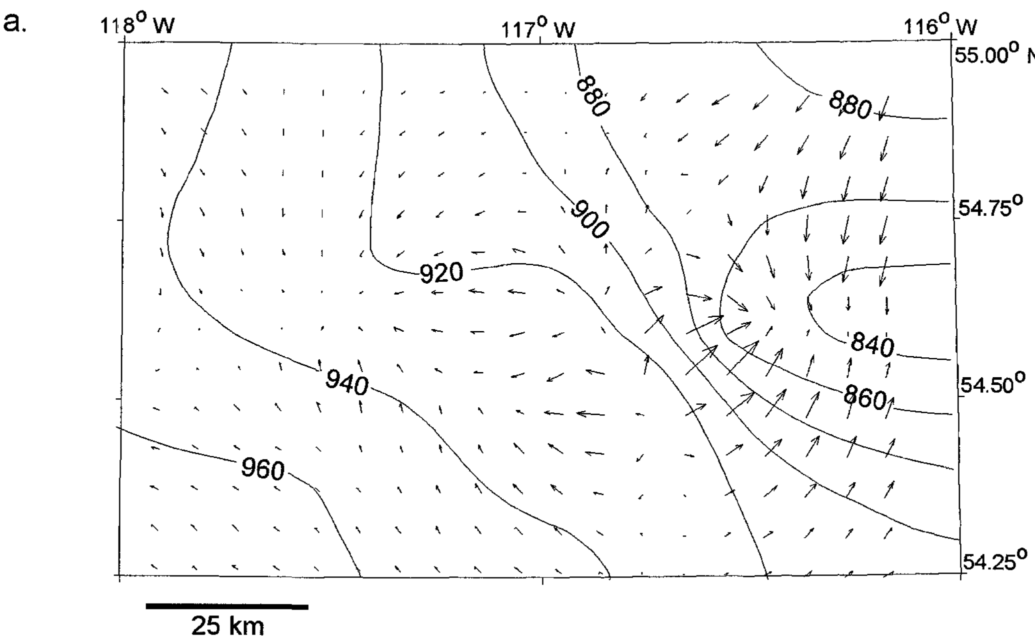


b.

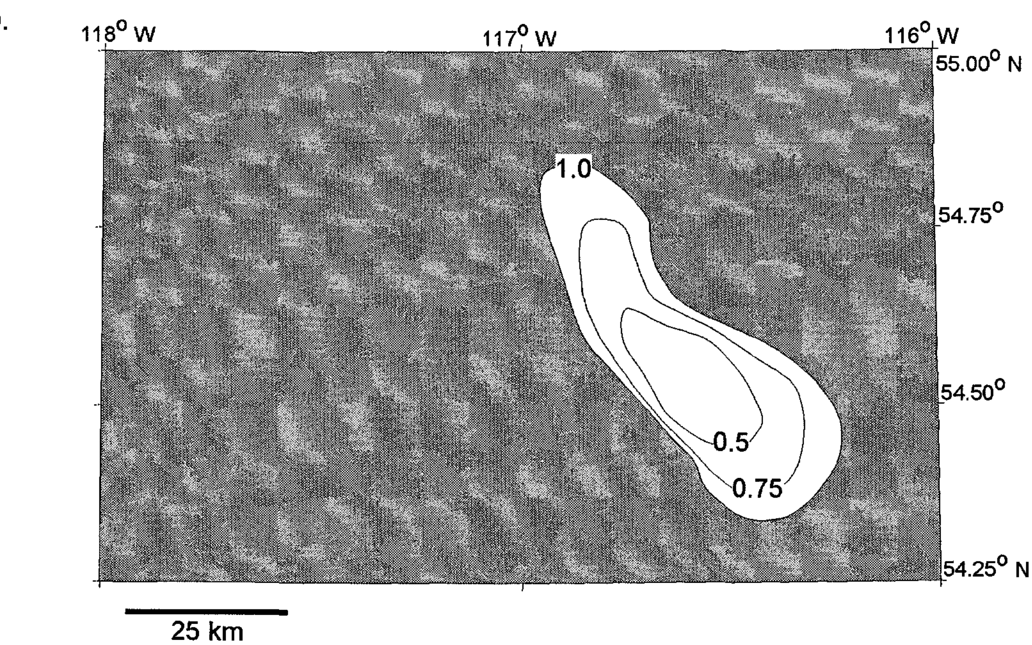


Figure 2.11: Flow representation in the Elk Point aquifer using $\rho_0 = 1000$ kg/m³ as reference density: a) Freshwater hydraulic head distribution (m) overlain by driving force vector field, b) DFR distribution, area where DFR > 1 is shaded in grey.



Reproduced with permission of the copyright owner. Further reproduction prohibited without permission.

a.

b.

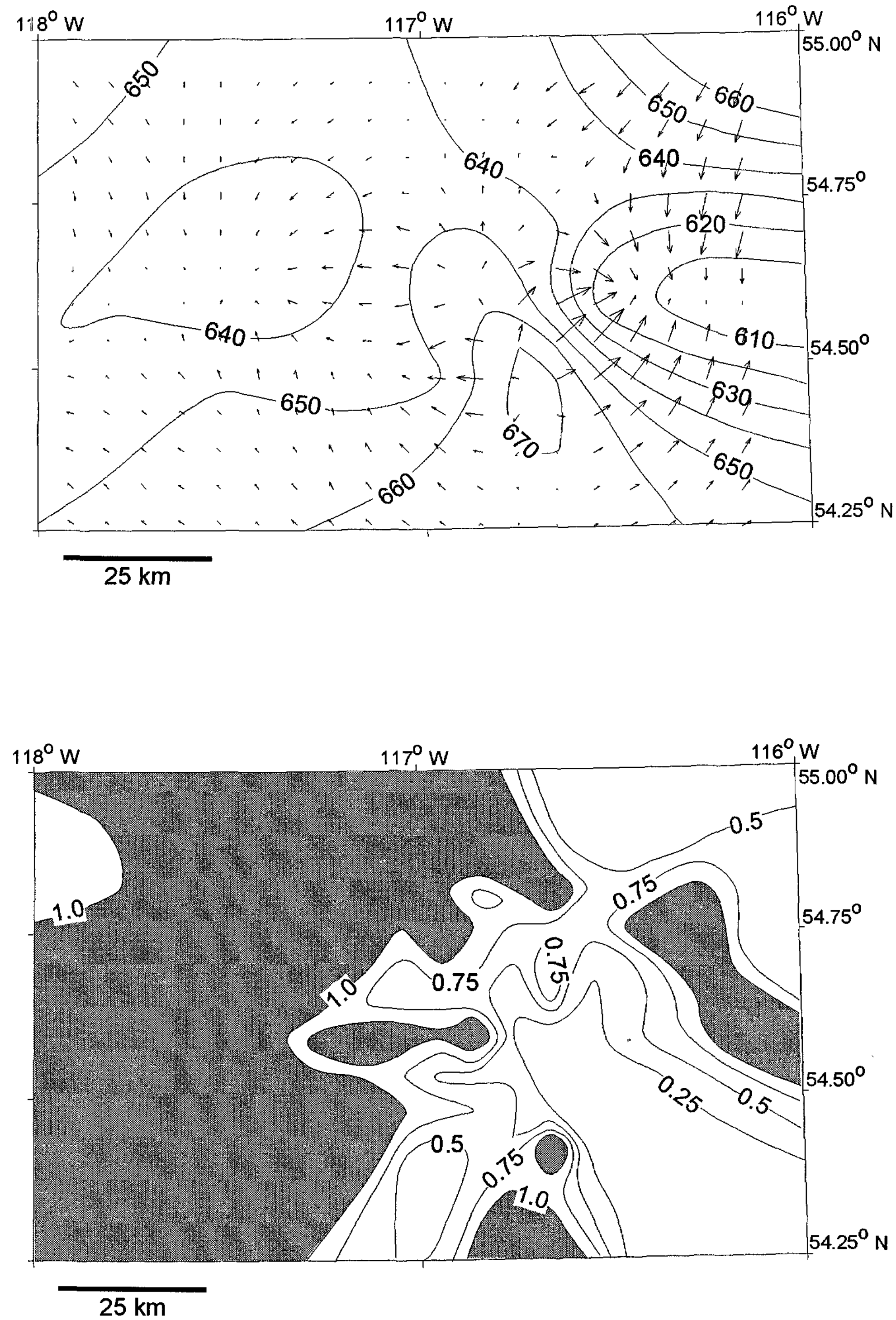


Figure 2.12: Flow representation in the Elk Point aquifer using $\rho_{min}$ = 1090 kg/m³ as reference density: a) Hydraulic head distribution (m) overlain by driving force vector field, b) DFR distribution, area where DFR > 1 is shaded in grey.



Reproduced with permission of the copyright owner. Further reproduction prohibited without permission.

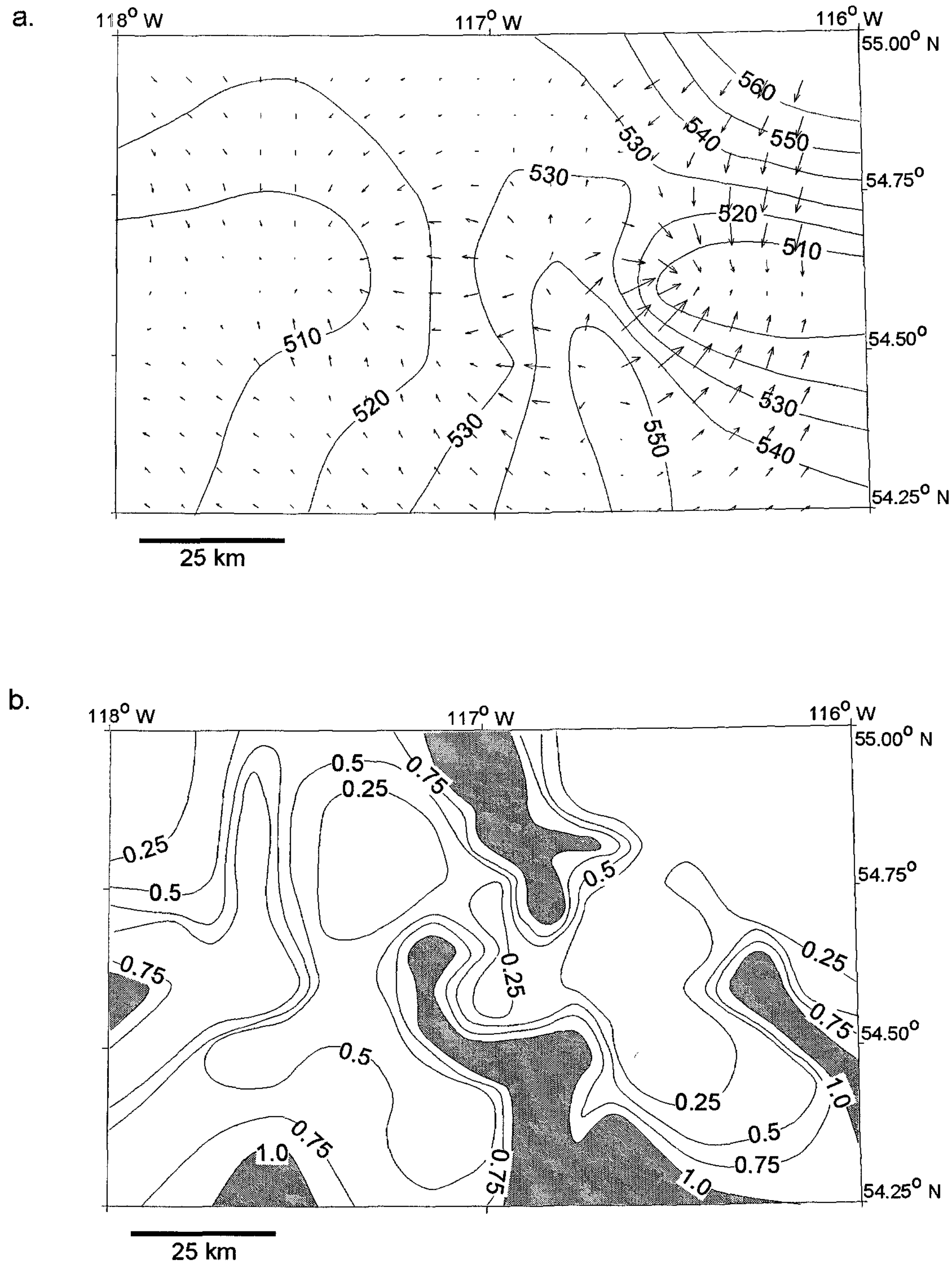


Figure 2.13: Flow representation in the Elk Point aquifer using $\rho_{max}$ = 1135 kg/m³ as reference density: a) Hydraulic head distribution (m) overlain by driving force vector field, b) DFR distribution, area where DFR > 1 is shaded in grey.



Reproduced with permission of the copyright owner. Further reproduction prohibited without permission.

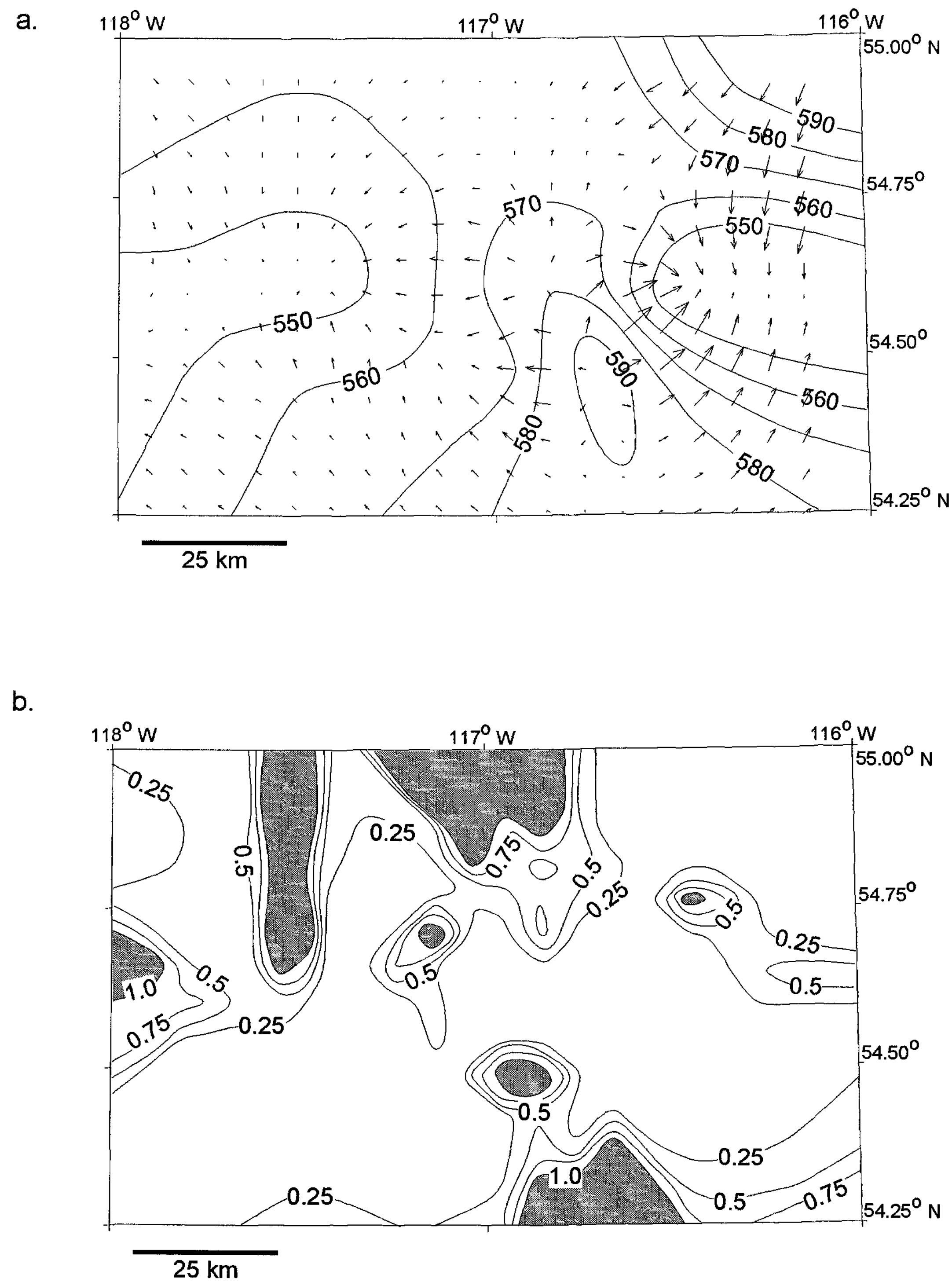


Figure 2.14: Flow representation in the Elk Point aquifer using $\rho_{av}$ = 1120 kg/m³ as reference density: a) Hydraulic head distribution (m) overlain by driving force vector field, b) DFR distribution, area where DFR > 1 is shaded in grey.



Reproduced with permission of the copyright owner. Further reproduction prohibited without permission.

Freshwater hydraulic heads generally decrease from above 940 m in the south and in the west to less than 840 m in the east, suggesting north- and eastward directions of formation water flow (Fig. 2.11 a). On the other hand, the force vectors indicate westward flow in the western two thirds of the study area and eastward flow in the eastern third. This shows that only in the east, where the hydraulic gradient is relatively steep, flow directions inferred from freshwater hydraulic heads are more or less comparable to the force vectors. In the remainder of the study area the hydraulic head contours are mainly parallel (in the SW) or even opposite (in the N) to the force vectors, hence significantly misinterpreting the direction of formation water flow. The respective DFR values are larger than 1 for most parts of the study area, with an areal average of 4.5 (Fig. 2.11 b), showing that hydraulic heads calculated with a freshwater reference density are not appropriate to represent flow in this part of the Elk Point aquifer.

Hydraulic heads calculated with $\rho_o = \rho_{min}$ vary in the 610 - 670 m range (Fig. 2.12 a) and correctly predict the flow direction and strength in the eastern third of the study area. The flow in the western two thirds is better represented than for the freshwater reference density case, although errors in direction are still present, particularly in the W-NW. This is consistent with the DFR distribution (Fig. 2.12 b), where the DFR < 1 in most of the eastern third of the study area, and > 1 in the western two thirds. The areal DFR average of 2.3 is overall lower than in the case for $\rho_o = \rho_f$. The inferred flow radiates from a local hydraulic-head high of 670 m in the southeast, and converges toward the 610 m low in the east and the low (< 640 m) in the west (Fig. 2.12 a).

Hydraulic heads calculated with $\rho_o = \rho_{max}$ vary in the 510 to 560 m range (Fig. 2.13 a) and correctly predict the flow direction and strength over most of the study area. In the southwest, hydraulic heads suggest flow from a tongue of high hydraulic heads, as opposed to the radiating flow pattern indicated by the flow-driving force, while in the west flow is toward a <510 m low, west of the 510 m contour line. The DFR values are generally lower than in the case of $\rho_o = \rho_{min}$ (Fig. 2.13 b), with an areal average of 1.2. The regions where the flow is still incorrectly depicted by hydraulic-head distributions, particularly in terms of local direction, correspond to a DFR > 1.



Reproduced with permission of the copyright owner. Further reproduction prohibited without permission.

Finally, hydraulic heads calculated with the field density average $\rho_o=\rho_{av}$, which vary in the 550-590 m range, seem to be most appropriate to infer flow direction and strength (Fig. 2.14 a), correctly showing, beside the strong features, the radiating flow from the hydraulic-head high in the southwest, and the flow towards the < 550 m low west of the 550 m contour line. The DFR values are generally the lowest of all cases presented, with an areal average of 0.6 (Fig. 2.14 b).

The previous example shows that, when using only hydraulic heads in the representation of variable-density fluid flow in sloping aquifers, choosing a reference density value within the observed range of formation water densities helps to minimize the errors in the flow interpretation caused by the neglect of the density-related force component. It is difficult to define an optimal reference density, because the DFR depends on the actual density variation, the reference density and the ratio between aquifer slope and hydraulic gradient. Nevertheless, in cases with a more or less constant hydraulic gradient and a relatively constant aquifer slope the field average of the observed fluid densities is probably the best choice for the reference density. On the other hand, using the freshwater density in the calculation of hydraulic heads maximizes the DFR, hence the error in the flow interpretation, because in almost all cases it lies at the lower end or outside the spectrum of formation water densities in the aquifers to be investigated.

## 2.5 Summary and conclusions

Flow in sedimentary basins is driven by a combination of various mechanisms, such as a) topography (gravity), b) sediment compaction, c) tectonic loading, d) erosional rebound, e) buoyancy, f) overpressures due to hydrocarbon generation, g) osmosis and h) mineral phase changes. The internal and boundary conditions for fluid flow change with time and various driving mechanisms may be active during different stages of the basin history. Pressure dissipation and fluid flow as a result of the various flow-driving mechanisms are transient processes, and their rates largely depend on the permeability distribution. Aquitards and lateral low-permeability barriers retard these processes so that the present-day pressures in the subsurface have not necessarily equilibrated to the present-day



Reproduced with permission of the copyright owner. Further reproduction prohibited without permission.

internal and boundary conditions. Flow systems at shallow depth usually have adjusted to the current ground surface relief and are topography-driven, while flow in deeper, low-permeability environments, which are relatively isolated from the ground surface, may be controlled by other driving mechanisms or reflect a paleo-flow regime. In regional-scale hydrogeological studies, the effect of osmosis is usually negligible and the flow can be represented and analyzed by the driving force acting on the fluid, which combines all fluid driving mechanisms introduced by the diffusion equation.

Numerical modeling is the only tool to represent the transient flow and the interaction between various flow-driving mechanisms in a sedimentary basin, but modeling requires a large amount of data input and knowledge of the distribution of many variables in space and in time. The time needed for data collection, data availability and quality, and computational limits largely restrict the applicability of numerical models in the representation of flow in sedimentary basins to theoretical and conceptual studies.

The calculation of driving forces requires data of present-day distributions of pressure and fluid densities, and values for the aquifer slope; thus, a quasi-steady-state flow regime has to be inferred in any hydrodynamic analysis that uses this method. Driving force vectors deliver the theoretically most accurate solution for the magnitude and direction of current fluid flow based on actual data distributions, but their implementation is still relatively cumbersome, because three different data sets ($\nabla H_0$, $\rho$, $\nabla E$) are needed and have to be combined to calculate the driving force. Practically, this increases the potential sources for inaccuracies due to errors in the various data sets. Determining the fluid fluxes is even more complicated, because this requires the knowledge of the fluid properties ($\rho$, $\mu$) and the permeability distributions, which are usually insufficiently known.

A less complicated method to represent and analyze flow is to use only the distribution of equivalent hydraulic heads ($H_0$). The driving force can be decomposed into its pressure-



Reproduced with permission of the copyright owner. Further reproduction prohibited without permission.

and density related components, which are represented by the equivalent hydraulic-head gradient ($\nabla H_0$) and $\frac{(\rho - \rho_0)}{\rho_0}\nabla E$, respectively. The magnitude of each of these components varies, depending on the value of the reference density ($\rho_0$), while their vectorial sum (the driving force) is constant. Hence, when using driving force vectors, any density value may be chosen as reference density. The use of equivalent hydraulic heads in variable-density fluid flow is only valid for strictly horizontal flow. In sloping aquifers, the use of hydraulic heads alone introduces an error because the effects of density variation on the flow are neglected. The significance of this error can be evaluated by the DFR, which is defined as the ratio of the pressure- and density-related components of the total driving force. It has been demonstrated theoretically and with an example from the study area that choosing the average water density in the aquifer as the reference density minimizes the DFR to such an extent that the density-related force component may become negligible. The advantages and disadvantages of using driving force vectors versus hydraulic heads for the representation of flow in the study area are discussed further in Chapter 3, in which theoretical and practical aspects of both methods will be compared.

Constructing a hydrostratigraphic framework, by subdividing the sedimentary succession into various units, is intended to generate a framework in which the concept of using hydraulic heads and driving force vectors can be applied. Strict assumptions that have to be made for each hydrostratigraphic unit in order to be able to correctly apply these concepts, but that can be rarely realized, are: horizontal layering, a homogeneous, isotropic permeability distribution and a homogeneous fluid. When loosening these restrictions, flow directions are not necessarily perpendicular to contours of hydraulic heads or in the direction of the driving force vectors, and the interpretation of fluid flow is limited to a more qualitative analysis of hydrogeological data. It still has to be determined how large the error of the obtained solution is, and if the solution is, at least in general, representative of the actual fluid flow system. The margin for the change in aquifer slope and fluid density variations in relation to the hydraulic gradient can be determined by the DFR.



Reproduced with permission of the copyright owner. Further reproduction prohibited without permission.

# CHAPTER 3: DATA SOURCES AND PROCESSING

This chapter describes the sources and the processing of the various hydrogeological data that were used in this study. Also, data accuracy is discussed, especially with respect to how it affects the reliability of the hydrogeological interpretation methods.

## 3.1 Data sources

More than 150,000 wells have been drilled in the Alberta Basin by the petroleum industry, of which approximately 11,000 wells are located in the study area. By provincial law, all well data have to be submitted to the Alberta Energy and Utilities Board (EUB) and become part of the public domain after one year. For this study, stratigraphic picks of formation tops from the EUB well database and from data sets assembled for the Atlas of the Western Canada Sedimentary Basin (Mossop and Shetsen, 1994) were used to establish the geological and hydrostratigraphic framework. The hydrogeological data consist of pressure data from drillstem tests (DSTs) and hydrogeochemical analyses of formation waters. All of these data were collected by the petroleum industry in Alberta and were captured in electronic form in databases at the Alberta Geological Survey (AGS). No personal sampling or testing was performed.

## 3.2 Data culling

The EUB databases consist mainly of unprocessed data that contain errors due to: a) mechanical problems of testing methods and analyzing techniques, b) external influences on tests, such as production influence from surrounding wells, c) human error in sampling, analyzing techniques, and data interpretation, and d) human error in recording and electronic data entry. Therefore, the original data sets had to be culled for erroneous data before they were used in (hydro-)geological interpretations. The three main data sets: a) stratigraphic picks, b) pressure data, and c) formation water analyses, are affected by different error sources, and the culling procedure for each individual set is therefore presented separately.



Reproduced with permission of the copyright owner. Further reproduction prohibited without permission.

*Stratigraphic picks of geological formation tops*

The depth of geological formation tops usually are assigned by a geologist during and after the drilling of a well, on the basis of drill cuttings, cores, and geophysical logs. The main errors introduced during this process are: a) report of a wrong ground surface elevation or kelly bushing (KB) for the well, b) a wrong stratigraphic pick based on personal judgment, c) wrong unit conversions (i.e., from ft to m), or d) erroneous electronic data entry.

Where available, the data used for the Geological Atlas of the Western Canada Sedimentary Basin (Mossop and Shetsen, 1994), stored at the AGS, were considered to be reliable, because the contributing authors of this volume had already individually checked and validated them. The remaining data were culled through an iterative process of gridding and mapping, i.e., checking the respective grids and maps for inconsistencies, and correcting single data points. The results were compared to existing structural maps, in the Geological Atlas of the Western Canada Sedimentary Basin (Mossop and Shetsen, 1994), for which one well per township, where available, was used for mapping. Depending on the data density for the respective stratigraphic units, between 31 and 355 stratigraphic picks of the Atlas set are in the present study area, which consists of approximately 380 townships. The gridding resolution of the Atlas maps (25 km increments) is lower than that of the maps in this study (12.5 km increments), in which a much larger number of stratigraphic picks was used (see Chapter 4, Tab. 4.1). Hence, when the newly created maps of this study matched the Atlas maps, differences of the order of metres were deemed acceptable, and the culling process was ended. Correcting and culling of single data points was either achieved by checking the original well logs, or by simply removing the well from the data set for areas where sufficient data exist and/or where the cause of error could not be determined.



Reproduced with permission of the copyright owner. Further reproduction prohibited without permission.

*Formation water analyses*

The hydrochemical analyses in the AGS database were already culled prior to this study using the procedures described in Hitchon and Brulotte (1994). In this "automatic" culling process, analyses are sequentially rejected on criteria such as: incomplete analysis, drilling mud contamination, poor chemical analysis, sampling and production method, and fluid recovery. In addition, the analyses were culled manually based on the regional hydrogeochemistry (Table 3.1).

| Flag # | Culling Criteria |
|---|---|
| 1 | Any of Ca, Mg, Cl, $HCO_3$ (or alkalinity), or SO4 missing |
| 2 | Mg-concentration > Ca-concentration |
| 3 | 10.0 < pH < 5.0 |
| 4 | OH reported |
| 5 | $CO_3$ reported |
| 6 | Calculated Na-concentration < 0 |
| 7 | Density < 1000 kg/m3 |
| 8 | ([cation] - [anion]) / ([cation] + [anion]) > 0.15 |
| 9 | No sample depth interval reported |
| 10 | Method of production from excluded class |
| 11 | Sampling point from excluded category |
| 12 | Analysis from multiple drillstem tests |
| 13 | Only fluids which are dominantly non-aqueous recovered |
| 14 | DST recovered fluids where the water dominated fluid is < 10% of the total recovery |
| 15 | KCl mud contamination, [K] / [Na] * 1000 > threshold for individual formation |
| 16 | Culled manually by hydrogeochemist (e.g., Duplicate chemistry, values out of range for individual formation in given area, analytical problems...) |

Tab. 3.1: Culling criteria for formation water analyses used in the automatic culling procedure (from Hitchon and Brulotte 1994).



Reproduced with permission of the copyright owner. Further reproduction prohibited without permission.

These rejection criteria act on the data set in successive order of their individual importance. Herein, incomplete analyses for example are considered of the highest culling priority, because important ion concentrations are missing and these analyses cannot be hydrochemically balanced. This will affect mainly analyses where only one component (most often chloride) is reported. Drilling and production methods are considered of a lesser priority, because they might suggest a high possibility of sample contamination due to their technical nature, but the quantitative influence on the analysis cannot be defined. In the AGS database there are 9593 water chemistry analyses for the entire stratigraphic succession in the study area performed up to 1992, of which only 1100 (11%) passed the mechanical culling criteria. This set was augmented by another 267 analyses performed since 1992, and acquired from the Geofluids™ database licensed by Rakhit Petroleum Consulting Ltd. Distribution maps of total dissolved solids (TDS) and bicarbonate ($HCO_3^-$) concentrations were used in a unit-by-unit analysis. Examination of the anomalies that could not be reasonably explained by natural processes led to their rejection. The final number of formation water analyses used in the hydrogeological interpretations is shown in Table 3.2. Chemical analyses of gas and oil were not used in this study.

In many standard industry chemical analyses only the concentrations of the major ions (e.g., $Cl^-$, $SO4^{2-}$, $HCO^{3-}$, $CO3^{2-}$, $Mg^{2+}$, and $Ca^{2+}$) are measured, and $Na^+$ is calculated by charge balance. The amount of total dissolved solids is calculated based on the calculated $Na^+$ and the remainder of the major ions. These calculations do not account for the $K^+$ concentrations in the formation waters, which in the study area generally are less than 10 % of the $Na^+$ concentrations, and therefore only introduce a small error in the TDS calculation. However, when interpreting formation water origin based on $Na^+$ concentrations these errors might become significant. Therefore, a subset of chemical analyses containing measured values for $Na^+$ and $K^+$ was used for the plotting of various ion relations in the formation waters. For these analyses the $N^+$ concentration was recalculated incorporating $K^+$ in the charge balance, to at least partly account for the relatively large analytical errors associated with $Na^+$.



Reproduced with permission of the copyright owner. Further reproduction prohibited without permission.

| Formation | Chemistry # after cull | Original DST # | DST # after cull | A & B Quality | C Quality |
|---|---|---|---|---|---|
| Paskapoo / Coalspur | 1 | 10 | 10 | 8 | 2 |
| Brazeau | 51 | 143 | 100 | 54 | 46 |
| Cardium | 40 | 131 | 80 | 34 | 46 |
| Dunvegan | 14 | 88 | 49 | 18 | 31 |
| Viking | 64 | 264 | 144 | 75 | 69 |
| U. Mannville | 35 | 198 | 89 | 56 | 33 |
| L. Mannville | 193 | 473 | 131 | 131 | - |
| Total post-Jurassic | 398 | 1307 | 603 | 376 | 227 |
| Nordegg | 11 | 41 | 22 | 15 | 7 |
| Triassic | 102 | 325 | 153 | 86 | 67 |
| Permian (Belloy) | 45 | 86 | 49 | 22 | 27 |
| Carboniferous | 140 | 293 | 167 | 90 | 77 |
| Total Miss.-Jurassic | 298 | 745 | 391 | 213 | 178 |
| Wabamun | 25 | 74 | 36 | 17 | 19 |
| Winterburn | 46 | 113 | 54 | 22 | 32 |
| Woodbend | 145 | 167 | 52 | 15 | 37 |
| Beaverhill Lake | 66 | 159 | 45 | 15 | 30 |
| Elk Point | 37 | 42 | 18 | 7 | 11 |
| Cambrian | 6 | 12 | 3 | 0 | 3 |
| Total Cambr.-Devon. | 325 | 567 | 208 | 76 | 132 |
| Total | 1021 | 2619 | 1202 | 665 | 537 |

Table 3.2: Distribution of valid formation water analyses and drill stem tests by hydrostratigraphic unit in the study area. Only DSTs of high quality (A, B and C) were used, except for the Lower Mannville, where only A and B quality tests were considered.

*Pressure data*

It is important for hydrogeological studies to use only good-quality pressure data. Therefore, only data that are derived from well-performed and interpreted DSTs, and from which stable formation pressures were calculated, should be used. Due to the mechanical complexity of the drillstem test procedure, there are many potential sources for error (Bredehoeft, 1965; Timmerman and van Poollen, 1972). The initial pressure data from a DST are transient pressures that are recorded during the test as the formation pressure recovers (pressure-"build-up" phase), and have to be converted into the stable formation pressures. Assuming radial flow in a homogenous medium to the well bore, the



Reproduced with permission of the copyright owner. Further reproduction prohibited without permission.

solution of pressure recovery over time has a logarithmic form that ideally produces a straight line in semi-logarithmic coordinates (Horner-Method). By extrapolating the straight line to the origin (infinite time), the formation pressure is estimated (e.g., Dahlberg, 1995).

The pressure data available from the AGS database are extrapolated to the formation pressure from sources specialized in DST interpretations, such as the Canadian Institute of Formation Evaluation (CIFE), Digitech, or Hydro-Fax Resources Ltd. These companies assign an overall quality rating to each test, which describes the quality of the test, and, implicitly, a degree of reliability of the pressure value (Tab. 3.3). The fluid recovery is also reported.

| | |
|---|---|
| 'A' | best quality |
| 'B' | nearing stabilization |
| 'C' | caution (plugging) |
| 'D' | questionable |
| 'E' | low permeability, low pressure |
| 'F' | low permeability, high pressure |
| 'G' | misrun (flow only) |

Table 3.3: Standard-industry data quality classes for DSTs.

Drill stem test data of quality A and B (665) were used preferably in the hydrogeological interpretation (Tab. 3.2). Due to increasing data scarcity towards the deeper parts of the basin, C quality data (537) were added to most of the units, but these data were checked for their accuracy by examining the individual drill reports and build-up curves, and by removing non-reliable tests. This led to the rejection of 54 % of the DST data, leaving 1202 DSTs from an original number of 2619 (Tab. 3.2).

In addition to the testing problems, in the study of the natural flow regime in the basin it has to be ensured that the measured pressures are not influenced by production-induced



Reproduced with permission of the copyright owner. Further reproduction prohibited without permission.

drawdown (PID) from adjacent wells. Production from the same aquifer and contained reservoirs leads locally to lower pressures than the undisturbed, "virgin" formation pressure, whereas injection of fluids increases formation pressures. The PID depends on: the distance r between tested and pumped wells, time t since the start of pumping, production rates Q, hydraulic conductivity K and specific storage $S_S$ (deMarsily, 1986). The magnitude of drawdown s expressed in terms of drop in hydraulic head caused by production in a well, as a function of radial distance from the DST well and the duration of pumping, can be calculated by using the Theis equation:

$$s = \frac{Q \cdot b \cdot W(u)}{4 \cdot \pi \cdot K} \tag{3.1}$$

with:

$$W(u) = \int_u^\infty \frac{e^{-u} du}{u} \quad \text{(well function);} \tag{3.2}$$

and

$$u = \frac{r^2 S_s}{4K \cdot t} \tag{3.3}$$

where: s = drawdown (m), $S_s = \rho\, g\, (\alpha + \beta\, n)$ = specific storage (1/m), $\alpha$, $\beta$ = aquifer -and fluid compressibility (1/Pa), n = porosity (-), Q = production rate ($m^3/s$); K = hydraulic conductivity (m/s), r = radial distance between DST well and producing well (m), b = aquifer thickness (m), t = time period of production prior to DST (s).

There are two major complications to this method, one regarding the Theis equation itself and the other regarding the hydraulic parameters K and $S_S$. The Theis equation is strictly valid only under certain idealized conditions (e.g., Freeze and Cherry, 1979, p. 315-317; Langguth and Voigt, 1980, p. 150-151), that include a perfectly confined, homogeneous and isotropic aquifer with infinite extent. The values of n, K, Q, $\alpha$ and $\beta$, and hence $S_s$, generally are not known and must be estimated. Because of the integral form of the well function, the Theis method has to be applied manually and individually to each test. An



Reproduced with permission of the copyright owner. Further reproduction prohibited without permission.

additional limiting factor is, therefore, the amount of time needed for data processing, particularly for a very large database.

To overcome the difficulties and lack of data, in applying the Theis solution, Tóth and Corbet (1986) assumed that, all other factors being constant, the effect of production is directly proportional to an interference index, I, defined as:

$$I = \log (t/r^2) \tag{3.4}$$

Several neighboring producing wells may influence the drawdown in a single DST. The nearest producing well does not necessarily have the biggest influence on the drawdown in the DST well, because production rates from wells farther away might be significantly larger. Based on the linearity of Equation 3.1, a cumulative interference index $I_C$ is calculated as the sum of interference indices ($\Sigma$ I) for all producing wells located within a defined minimum radial distance:

$$I_C = \Sigma [\log (t/ r^2)] \tag{3.5}$$

Application of this equation requires knowledge of the distance between wells, and DST and production dates, information recorded by the industry and captured in the EUB and private databases. Thus, calculation of the interference index $I_C$ can be easily automated and applied to large databases. The minimum radial distance from the DST well within which producing wells have an effect on the drawdown largely depends on aquifer permeability. Permeability heterogeneity, for example due to changes in lithology, fracturing, or faults, causes a wide range, commonly 2 – 20 km, in the value of the radius of influence (Rostron et al., 1995).

For all practical purposes, taking into account aquifer heterogeneity and possible missing or inconsistent data from producing wells, a semi-quantitative culling approach was used in this study. Considering only the well locations with the respective DST or production dates, an interference index was calculated for each DST well and the nearest producing



Reproduced with permission of the copyright owner. Further reproduction prohibited without permission.

well according to Equation 3.4 using a computer code described by Rostron et al. (1995). In addition, the number of producing wells predating the DST within a radius of up to 50 km from each DST well were reported. This procedure was applied, on an aquifer-by-aquifer basis, only to the water-saturated zones, assuming that drawdown effects propagating vertically across aquitards are negligible. Hydraulic heads were calculated from the formation pressure for all DSTs (see chapter 2, Eq. 2.7) and contoured for each aquifer. Generally, a data point that creates closed contour lines indicates a source or sink for formation water flow, which could be due to: a) a natural fluid sink or source within the aquifer itself b) vertical flow into or out of an adjacent aquitard); c) vertical cross-formational flow into or out of an adjacent aquifer; or d) producing or injecting wells in the vicinity. Therefore, DSTs with a high interference index and/or a large number of producing wells in their vicinity were individually examined and rejected if they caused anomalies in the hydraulic head contours. Also, tests in the near vicinity of heavily producing hydrocarbon fields were checked more thoroughly, even if the DST was not from a producing unit, and rejected if the reported initial reservoir pressure was higher than that measured in the DST for a comparable depth, or an associated anomaly could not be explained by natural flow processes (a, b or c). Natural flow processes were deemed unlikely to have caused anomalies if there was no known mechanism to create a sink or source in the particular aquifer or confining aquitard, and if hydraulic head distributions in the directly adjacent aquifers did not show a corresponding source or sink that would support the possibility of cross-formational flow.

## 3.3 Data processing

### 3.3.1 Structure maps

The irregular distributions of well picks for each formation were transformed into a regular grid distribution using a least-squares gridding algorithm implemented by the Radian Mapping Software CPS-3. The computer grid was smoothed by a bi-harmonic filter and tied back to the control point data (Graf and Thomas, 1988), to achieve



Reproduced with permission of the copyright owner. Further reproduction prohibited without permission.

maximum honoring of the original well data picks. To obtain a consistent framework of the general geology in the study area, a relatively coarse grid was used (24 x 24 nodes spaced 12.5 km apart). The number of picks generally increases from SW near the thrust and fold belt to the NE, and from the Precambrian up to the Cretaceous. Therefore, the computed surfaces might represent a relatively rough approximation of the stratigraphy, especially of deeper strata and in the area close to the thrust and fold belt.

The result is a three-dimensional representation of the succession of major stratigraphic surfaces in the undeformed part of the study area. The stratigraphic surfaces were used to allocate the hydrochemical and pressure data to the respective formations. The complete set of DST and chemistry data was run against the bounding surfaces of all aquifer units (Tab. 3.2) by comparing location and the elevation of each test interval against the interpolated surface grid elevation at each point. This process resulted in separate DST and chemistry files for each aquifer unit. Data points were checked individually for the reported driller's allocation of the respective test interval in cases of thin aquifers or thin confining units between aquifers (e.g., Viking aquifer: 5 – 50 m thickness), for which the resolution of the gridded surfaces was inadequate. Data were re-allocated if the driller's allocation conflicted with the mechanical allocation using the surface grids. The combination of a grid-based allocation of data and using the driller's stratigraphic allocation from the DST or chemistry report guarantees a higher reliability than using only one of the two methods.

### 3.3.2 Hydrogeochemical representation methods

The hydrochemical data in this study were used to: a) determine the origin and evolution of formation waters; b) in conjunction with hydraulic data, delineate flow paths; and c) calculate the in-situ density of formation waters.

Variations in the major ion hydrochemistry can be used to determine the origin and evolution of formation waters in sedimentary basins (i.e., Carpenter, 1978; Land, 1987;



Reproduced with permission of the copyright owner. Further reproduction prohibited without permission.

Hanor, 1994 a, b). As most sediments are deposited in marine or marginal-marine environments, seawater is a useful reference solution against which formation waters are compared (Land, 1987). While salinity lower than that of seawater (35 g/L) usually is caused by mixing with meteoric water, the increase in the concentration of dissolved solids in brines (> 35 g/L) is mainly attributed to the evaporation of seawater and the dissolution of evaporites (Hanor, 1994).

During the evaporation of seawater various salts precipitate from solution, depending on their solubility, and causing a change in the relative concentration of ions in the remaining fluid. Generally, the trends of relative changes in concentration of any two dissolved ions during the evaporation of seawater is termed seawater evaporation trajectory (SET). Bromide-versus-chloride concentrations are a commonly used indicator for dissolved salts in formation waters (Carpenter, 1978). The Cl/Br-ratio remains constant during the evaporation of seawater until the point of halite saturation, after which Cl is preferentially precipitated, causing a decrease in the Cl/Br-ratio (Carpenter, 1978). Subsequent dilution by meteoric water does not change the Cl/Br-ratio any further, only both concentrations decrease, so that the dilution trend of Cl versus Br falls parallel and above the SET (Connolly et al., 1990; Hanor, 1994). On the other hand, halite dissolution causes a concentration of Cl in the residual solution, and the respective Br/Cl-ratios are lower than those along the SET. However, Br is rarely measured in standard industry analysis. The major cations also follow a distinct seawater evaporation-dilution trend (Carpenter, 1978). From the major ions, chloride acts as the most conservative, because, except for the dissolution and precipitation of Cl-salts, Cl is not involved in processes of water-rock interaction in the subsurface. Therefore, plots of the major cation concentrations of Na, Mg, and Ca against Cl concentrations in the formation waters were compared to experimentally derived evaporation-dilution trends (McCaffrey et al., 1986), to investigate whether the formation waters are evaporated or diluted seawater. If the data followed different trends, other processes had to be considered that might have affected the major ion chemistry (i.e., dissolution of evaporites, dolomitization, albitization).



Reproduced with permission of the copyright owner. Further reproduction prohibited without permission.

Another useful method in the investigation of basinal brines is the comparison of Na, Ca, and Cl concentrations between formation waters and seawater. Davisson and Criss (1996) introduced a mathematical transformation of Na, Ca, and Cl concentrations that produces a linear slope of unity between the milliequivalencies of Na and Ca cations in numerous basinal fluids, including the Alberta Basin. The excess Ca and the Na deficit relative to seawater reference ratios are defined as (Davisson and Criss, 1996):

$$Ca_{excess} = \left[ Ca_{meas} - \left( \frac{Ca}{Cl} \right)_{sw} \cdot Cl_{meas} \right] \cdot \frac{2}{40.08}$$

$$Na_{deficit} = \left[ \left( \frac{Na}{Cl} \right)_{sw} \cdot Cl_{meas} - Na_{meas} \right] \cdot \frac{1}{22.99}$$

where the concentrations (in mg/L) of the ions measured (meas) in a sample are referred to those in seawater (sw), and the numerical constants convert the results to meq/L. Plotting $Ca_{excess}$ versus $Na_{deficit}$ values of more than 800 samples from various basins and aquifer lithologies, Davisson and Criss (1996) derived a highly correlated regression line that they termed Basinal Fluid Line (BFL):

$$Ca_{excess} = 0.967(Na_{deficit}) + 140.3,$$

where the unit slope is interpreted to indicate that the albitization of plagioclase (2 Na for 1 Ca exchange ratio) is the predominant reaction to control the chemistry of deep formation waters. The intercept of 140.3 for the BFL can be attributed to the dissolution of halite prior to albitization, whereas the trend of albitization of seawater only would start at the origin of the excess-deficit graph (Davisson and Criss, 1996).

### 3.3.3 Contouring of hydrochemical data

The distributions of salinity and selected ion concentrations (g/L) were contoured manually, which allowed for the better integration of geological and hydraulic information for extra- and interpolation purposes in areas of low data density. For



Reproduced with permission of the copyright owner. Further reproduction prohibited without permission.

example, geological boundaries, like the extent of carbonate platforms, represent discontinuities in the aquifer geometry, which affect the distribution and flow paths of formation fluids and which is difficult to account for in mechanical contouring procedures. A typical gridding algorithm does not recognize aquifer heterogeneity and the resulting contours would likely cross geological boundaries, which subsequently would have to be changed in order to achieve an interpretation of flow patterns that is consistent with the geology. Plots of the study area showing data locations and concentration values were generated for each aquifer, using the Aberta Geological Survey cartographic system (AGSSYS). These maps were imported in the CANVAS graphics program, in which the data points were hand-contoured. Contours were interpolated in areas of low data density data by comparing and fitting the distribution of chemical data to patterns observed in the complementary hydraulic and geological maps. All data points were honoured within their range of accuracy as manifested in the respective contouring interval.

Usually, the analytical errors in the chemical analyses are significantly smaller than errors introduced by sampling techniques and potential dilution with drilling mud. It is difficult to estimate the magnitude of practical errors in the remaining hydrochemical data that passed the mechanical culling process because the potential mixing or dilution of formation water samples with drilling fluids cannot be determined quantatively from the analytical report. Therefore, a conservative error of 10 % for salinty was chosen, based on the variance of concentrations in chemical analyses from the same water sample or different samples from the same well and depth range. This translated to a contour interval of at least 10 % of the average concentration, which was used for the mapping of salinity (TDS) in the various aquifers.

### 3.3.4 Processing of pressure data

The pressure data from DSTs were plotted versus depth (p(d)-plot) and versus elevation (p(z)-plot), and equivalent hydraulic heads were calculated and contoured. In addition, in



Reproduced with permission of the copyright owner. Further reproduction prohibited without permission.

the Elk Point aquifers the impelling force vectors acting on the fluid were constructed. Due to the complexity and controversies regarding the representation of variable-density fluid flow in sedimentary basins, Chapter 2 presented a detailed discussion on the theoretical aspects and defined the variables and equations for the calculation of the hydraulic gradient and the impelling force. The measurement accuracy and mechanical errors associated with formation pressures determined from DSTs have to be taken into account in addition to the theoretical errors associated with using equivalent hydraulic heads in the flow representation. Only then, the accuracy in the flow representation, using hydraulic head maps versus impelling force vectors, can be evaluated. Following parameters may have errors associated with them: fluid pressure p and measurement elevation z for calculating hydraulic heads, and in addition fluid density $\rho$ and aquifer slope $\nabla E$ for calculating force vectors.

The accuracy as specified by various manufacturers ranges between 0.025 and 0.25 % of the full scale for newer pressure gauges (1970 – 2000) and was as low as 0.5 % for gauges from the 50's and 60's (from H. Reid, course manual for DST interpretation). This translates to a maximum error of approximately to +/- 200 kPa (accepted pressure difference between first and second shut-in measurement for a C quality DST) or +/- 20 m of hydraulic head. On the other hand, errors introduced by the mechanical procedure of the test are much larger, and empirically determined errors in pressure measurements generally increase with depth and range between 170 and 650 kPa (Bradley, 1975; Bredehoeft, 1965; Dahlberg, 1995). Assuming freshwater density, this translates to a hydraulic head difference that varies approximately between 17 m for shallow aquifers and a maximum of 65 m for deep aquifers. This relatively large methodology error may be reduced by only using DSTs of A, B, and C quality and Horner-extrapolated pressures. Errors associated with the depth measurement and the land surveying of the kelly bushing (KB) elevation are comparably small, but only can be estimated to be in the range of a few metres. A contour interval of 50 m was therefore chosen in most of the hydraulic head maps for representation and analysis, which is the contour interval that typically has been used in many previous regional-scale hydrogeological studies, based on industry



Reproduced with permission of the copyright owner. Further reproduction prohibited without permission.

pressure data in the Alberta Basin (e.g., Tóth, 1978; Bachu and Underschultz, 1993; Rostron and Tóth, 1997; Rostron et al., 1997; Anfort et al., 2001).

The fluid density was calculated based on the salinity of the formation water, pressure, and temperature using empirical equations that were fit to laboratory experiments (Rowe and Chou, 1970; Kestin et al., 1981; Appendix D). This expression was used in various numerical models of formation water flow in sedimentary basins (e.g., Garven, 1985, 1989; Raffensberger and Garven, 1995; Person and Garven, 1994; Appold and Garven, 1999). Kestin et al. (1981) estimate the accuracy of the calculated densities to be +/- 0.5%, which translates to +/- 5 kg/m$^3$ for freshwater (1000 kg/m$^3$). However, errors associated with the measured pressure, salinity, and temperature values have to be added. The pressure was obtained from the DST itself and salinities from distribution maps (grids). In-situ temperatures were calculated from integral geothermal gradients in the Western Canada Sedimentary Basin within an estimated accuracy of a few degrees Celsius (Bachu and Burwash, 1994).

The sensitivity of the calculated formation water density was determined by changing pressure, salinity and temperature in the empirical density equation (Rowe and Chou, 1970; Kestin et al., 1981) within the respective error ranges for three theoretical cases of representative pressure, salinity and temperature conditions (Table 3.4). Generally, the error in salinity causes the largest difference in the value of the calculated formation water density (~ +/- 7 kg/m$^3$), except for formation water with low salinity, which is slightly more affected by errors in temperature (+/- 1.0 kg/m$^3$) than errors in salinity (+/- 0.7 kg/m$^3$). In comparison, changes in pressure within a range of 400 kPa have almost no affect on the calculated density (+/- 0.1 kg/m$^3$). An overall error of at least +/- 15 kg/m$^3$ in the calculated formation water density results from adding the mathematical error of +/- 5 kg/m$^3$ (Kestin et al., 1981) to the confidence range of approximately +/- 10 kg/m$^3$ that is caused by the inaccuracy in salinity, temperature and pressure.



Reproduced with permission of the copyright owner. Further reproduction prohibited without permission.

| | Ref. | Salinity: +/- 10 % | | Temperature: +/- 5°C | | Pressure: +/- 200 kPa | |
|---|---|---|---|---|---|---|---|
| **Shallow depth** | | | | | | | |
| Pressure (MPa) | 5 | 5 | 5 | 5 | 5 | 4.8 | 5.2 |
| Salinity (wt%) | 0.01 | 0.009 | 0.011 | 0.01 | 0.01 | 0.01 | 0.01 |
| Temperature (°C) | 20 | 20 | 20 | 15 | 25 | 20 | 20 |
| Density ($kg/m^3$) | 1008 | 1007 | 1008 | 1009 | 1006 | 1008 | 1008 |
| $\Delta \rho$ ($kg/m^3$) | | 1 | 0 | -1.0 | 2 | 0 | 0 |
| **Intermediate depth** | | | | | | | |
| Pressure (MPa) | 18 | 18 | 18 | 18 | 18 | 17.8 | 18.2 |
| Salinity (wt%) | 0.12 | 0.11 | 0.13 | 0.12 | 0.12 | 0.12 | 0.12 |
| Temperature (°C) | 65 | 65 | 65 | 60 | 70 | 65 | 65 |
| Density ($kg/m^3$) | 1071 | 1064 | 1079 | 1074 | 1068 | 1071 | 1071 |
| $\Delta \rho$ ($kg/m^3$) | | 7 | -8 | -3 | 3 | 0 | 0 |
| **Large depth** | | | | | | | |
| Pressure (MPa) | 29.5 | 29.5 | 29.5 | 29.5 | 29.5 | 29.3 | 29.7 |
| Salinity (wt%) | 0.2 | 0.19 | 0.21 | 0.2 | 0.2 | 0.2 | 0.2 |
| Temperature (°C) | 95 | 95 | 95 | 90 | 100 | 95 | 95 |
| Density ($kg/m^3$) | 1116 | 1108 | 1124 | 1119 | 1113 | 1116 | 1116 |
| $\Delta \rho$ ($kg/m^3$) | | 8 | -8 | -3 | 3 | 0 | 0 |

Table 3.4: Sensitivity of the calculated density with changing salinity, temperature and pressure. Only one parameter was changed from the reference conditions (Ref.) in each column within its respective error range, while the other two were kept constant.

*Accuracy of equivalent hydraulic heads and flow-driving force vectors*

According to the theoretical discussion in Chapter 2, the effect of density variations on the flow representation becomes significant only when the pressure-related force component is small compared to the density-related force component, i.e. $\nabla H_0 \approx 0$ and the aquifer slope and difference between water density and reference density are large. However, the hydraulic gradient is calculated using DST pressures measurements that contain a certain degree of error. The force vectors have an even higher degree of uncertainty because errors in the pressure-related force component (hydraulic gradient) have to be added to errors in the density-related force component due to the inaccuracy in



Reproduced with permission of the copyright owner. Further reproduction prohibited without permission.

the density calculation. Therefore, it is critical to compare the magnitude and accuracy of the hydraulic gradient to the magnitude and accuracy of the density-related force component, before the impact of density variations on the flow representation can be assessed.

According to Equations 2.25 and 2.28, the driving force along the aquifer slope can be represented by the sum of its pressure- and density-related components:

$$F^* = -\rho_0 \cdot g(\nabla H_0 + \frac{\rho - \rho_0}{\rho_0} \cdot \nabla E = -\rho_0 \cdot g\left(F_p + F_\rho\right), \tag{3.6}$$

Therefore, the error in the force magnitude ΔF is the sum of the errors in its two components:

$$\Delta F = \Delta F_p + \Delta F_\rho . \tag{3.7}$$

The four steps for constructing the impelling force vector are:

(1) Equivalent hydraulic heads $H_0$ and hydraulic gradients grad $H_0$ are calculated for each point using a reference fluid density and DST pressures.

(2) A value for the elevation gradient grad z is calculated either from a grid of DST test elevations or a grid of the aquifer structure. Resulting gradients from these two grids are comparable for an aquifer with a large lateral extent compared to its thickness. However, using the grid of the aquifer structure is preferred because the coverage of stratigraphic data is better than that of DST data for any aquifer.

(3) A relative density term $\rho^* = \frac{(\rho - \rho_0)}{\rho_0}$ is calculated for each point and multiplied with the value of the elevation gradient.

(4) The resulting impelling force vector is constructed by adding the x and y components of grad $H_0$ and $\frac{(\rho - \rho_0)}{\rho_0} \cdot \nabla z$ at every point.



Reproduced with permission of the copyright owner. Further reproduction prohibited without permission.

Practically, the hydraulic gradient between two points (wells or grid points) in an aquifer is approximated by the difference in hydraulic heads divided by the distance l between the two points: $\nabla H_0 = \frac{H_{01} - H_{02}}{l}$. (3.8)

A maximum error in equivalent hydraulic head $\Delta H_0$ of +/- 25m causes the error in the pressure-related force component to be:

$$\Delta F_p = \frac{2 \cdot \Delta H_0}{l} = \frac{50m}{l} \tag{3.9}$$

Practically, the slope of the aquifer is approximated by the difference in elevation of the aquifer top or bottom between two points: $\nabla E = \frac{z_1 - z_2}{l}$ (3.10)

A maximum error $\Delta\rho$ of +/- 15 kg/m$^3$ in the density values and $\Delta z$ = +/- 2.5 m in elevations results in an uncertainty in the maximum pressure-related force component of approximately:

$$\begin{aligned} \Delta F_\rho &= \frac{\partial F_\rho}{\partial \rho} \cdot \Delta\rho + \frac{\partial F_\rho}{\partial E} \cdot \Delta z = \frac{1}{\rho_0} \cdot \frac{z_1 - z_2}{l} \cdot \Delta\rho + \frac{2 \cdot \Delta z}{l} \cdot \frac{\rho - \rho_0}{\rho_0} \\ &= \frac{15 \cdot (z_1 - z_2)}{1000 \cdot l} + \frac{5\ m \cdot 150}{1000 \cdot l} = \frac{0.015 \cdot (z_1 - z_2) + 0.75\ m}{l} \\ &= 0.015 \cdot \nabla E + \frac{0.75\ m}{l} \end{aligned} \tag{3.11}$$

for a maximum density difference $\rho - \rho_0 = 150$ kg/m$^3$.

The dependence on the distance l of the errors in the force and force components infers that practically it is impossible to accurately determine low force magnitudes over relatively short distances as shown in the following example, assuming a maximum value



Reproduced with permission of the copyright owner. Further reproduction prohibited without permission.

for the density-related force component and relatively low value for the pressure-related force component.

Example 1:

$\rho_0 = 1000\ kg/m^3$, $\rho = 1150\ kg/m^3$ (maximum density difference in the study area),

$\nabla E = 0.02$ (maximum aquifer slope in the study area)

$\nabla H_0 = - F_\rho/2 = - 0.0015$ (DFR = 2)

a) l = 10 km

$$\frac{F^*}{-\rho_0 \cdot g} = F_p \pm \Delta F_p + F_\rho \pm \Delta F_\rho = -0.0015 \pm 0.005 + 0.0030 \pm 0.0004$$

$$= 0.0015 \pm 0.0054$$

$$DFR = \frac{|F_\rho|}{|F_p|} \pm \left( \frac{\Delta F_\rho}{F_\rho} + \frac{\Delta F_p}{F_p} \right) \cdot DFR = 2 \pm 7$$

b) l = 50 km

$$\frac{F^*}{-\rho_0 \cdot g} = -0.0015 \pm 0.001 + 0.0030 \pm 0.0003$$

$$= 0.0015 \pm 0.0013$$

$$DFR = 2 \pm 1.5$$



Reproduced with permission of the copyright owner. Further reproduction prohibited without permission.

c) l = 100 km

$$\frac{F^*}{-\rho_0 \cdot g} = -0.0015 \pm 0.0005 + 0.0030 \pm 0.0003$$

$$= 0.0015 \pm 0.0008$$

$$DFR = 2 \pm 0.9$$

The previous example shows that:

1) the error in the pressure-related force component ('hydraulic gradient') increases with decreasing distance over which it is determined. The relative error is larger than 1 to a distance l of approximately 40 km (Fig. 3.1 a);
2) the maximum error in the density-related force component for the case of maximum density difference and aquifer slope is ± 0.0003, increasing only slightly with decreasing distance. The relative error is approximately 10 %. This error is smaller than the error in the pressure-related force component for measurement distances l < 300 km (Fig. 3.1 a);
3) small differences in equivalent hydraulic heads; in this case a pressure-related force component having half the magnitude of the density-related force component, cannot be accurately determined over distances < 50 km (Fig. 3.1 a) due to the large errors associated with the pressure measurements. Over these distances, it also is not meaningful to calculate the force vector by adding its density-related component, because the magnitude of the total force is still smaller than its total error.



Reproduced with permission of the copyright owner. Further reproduction prohibited without permission.

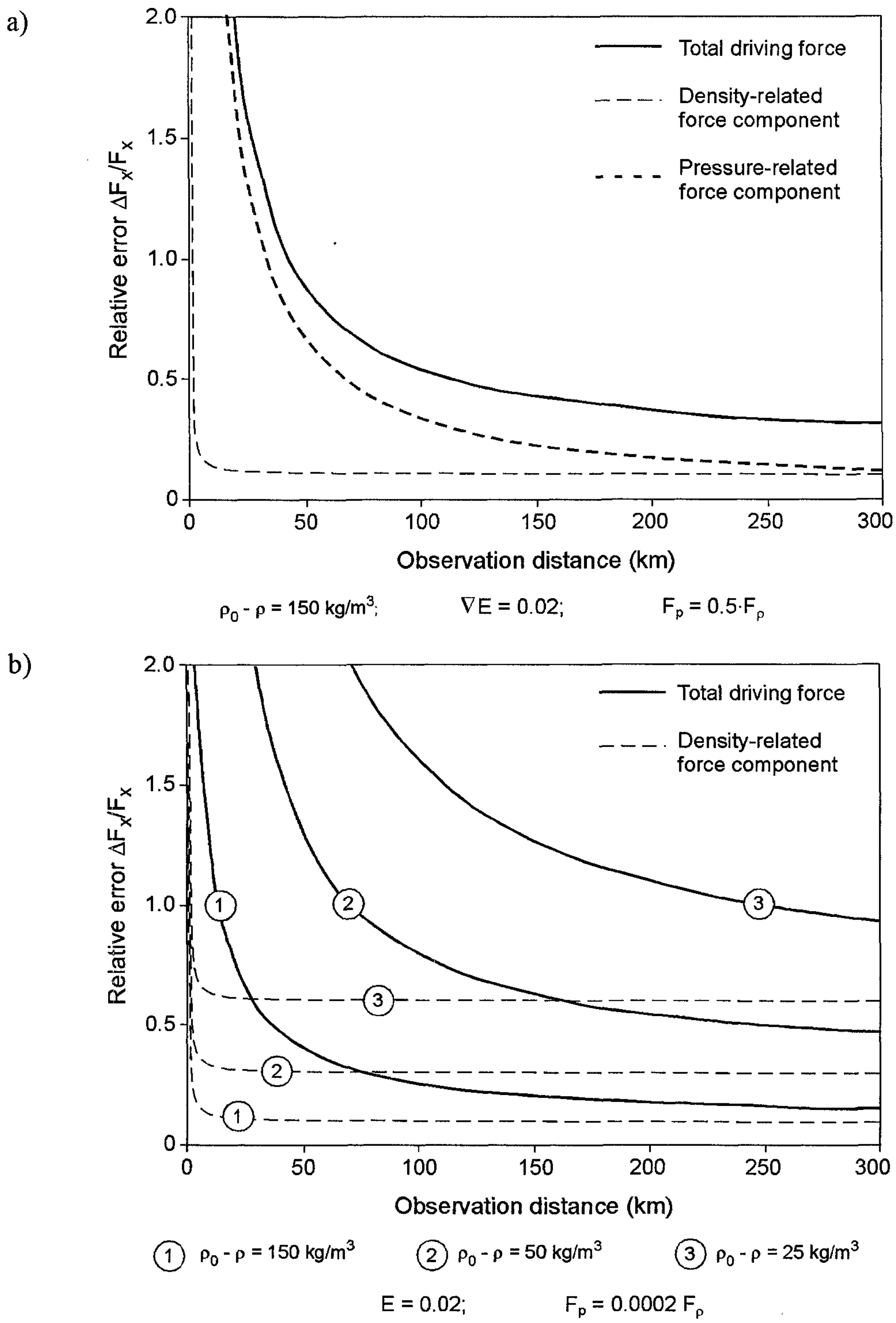


Figure 3.1: Change of the relative errors of the driving force magnitude and its pressure- and density-related components with distance over which the force was calculated for: a) Maximum density difference in the study area, maximum aquifer slope and a DFR = 2, and b) three difference density ranges, maximum aquifer slope, and $F_p << F_\rho$. Equations 3.6, 3.7, 3.9, and 3.11 were used to calculate the relative error for the driving force and its components.



Reproduced with permission of the copyright owner. Further reproduction prohibited without permission.

More generally speaking, the theoretical gain of accuracy in the representation of flow by calculating force vectors is limited to a certain scale of observation by the measurement errors in the pressure-related force component. Even for the most extreme case, when equivalent hydraulic heads cannot be used to represent water flow in the study area (i.e., 150 $kg/m^3$ difference between actual formation water density and reference density, a maximum aquifer slope of 0.02, and $F_p >> F_\rho$), the general direction of flow can be inferred accurately from driving force vectors only if the relative error is smaller than 1.0; hence if the force is determined of a distance larger than 20 km (Fig. 3.1 b, Case 1). However, if the difference between formation water density and reference density is only 50 $kg/m^3$ for the same pressure conditions in the aquifer, the threshold for the observation distance beyond which the general flow direction may be determined accurately from force vectors is approximately 65 km (Fig. 3.1 b, Case 2). Obviously, if the pressure-related force component is close to zero and the density-related force component is small (Fig. 3.1 b, Case 3), the flow direction in the aquifer cannot be clearly determined by either equivalent hydraulic heads or force vectors under 250 km, approximately the range of the study area. Consequently, within the appropriate error margins of the impelling force, the flow can be characterized only as +/- stagnant.

*Consequences from theoretical and practical considerations for the interpretation of pressure data*

Two aspects have to be considered when choosing the appropriate representation method, equivalent hydraulic heads versus driving force vectors, for the flow of variable-density formation water in sloping aquifers: 1) the magnitude of the theoretical error that is due to the neglect of the density-related force component in equivalent hydraulic head interpretations (see Chapter 2), and 2) the effect of practical errors on equivalent hydraulic heads and force vectors that is caused by the inaccuracies in pressure measurements and density calculations. Ideally, theoretical errors should be avoided and the level of uncertainty should be incorporated in the method of flow representation. The previous section showed that the errors associated with the pressure measurements are the



Reproduced with permission of the copyright owner. Further reproduction prohibited without permission.

principal cause for the inaccuracies in both, gradients calculated from equivalent hydraulic heads and driving force vectors, and that the relative error depends on the distance over which these two are measured. Consequently, only general flow directions can be inferred from any method that uses pressure measurements from DSTs. Theoretically, driving force vectors are the accurate method for the representation of variable-density flow in sloping aquifers (see Chapter 2). However, the driving force vector at a specific point can be calculated practically only between two wells or within a grid, because the vector is composed of gradients of hydraulic heads and aquifer structure. Thus, for low hydraulic gradients and DFR > 1, the spacing between wells or grid points would have to be relatively wide (20 – 250 km) compared to the dimensions of the study area, depending on the reference density and aquifer slope, before force vectors accurately indicate the general flow direction within the appropriate error range (Fig. 3.1). The appropriate result would be either a coarse grid with even spacing between flow vectors that indicates the general flow direction in the study area, but has a bad resolution in areas with high hydraulic gradients, or an uneven distribution of grid points (high resolution in area of high hydraulic gradients and low resolution in areas of low hydraulic gradients), for which the errors vary depending on the grid spacing, and which is cumbersome to construct. Contour maps of equivalent hydraulic heads have the advantage that they are easy to construct and that the contour interval, if chosen accordingly, directly reflects the accuracy of the point data. The disadvantage is the theoretical error that is made when inferring flow directions from hydraulic gradients and ignoring the density effects. Nevertheless, this theoretical error is critical only if hydraulic gradients are low compared to the density-related force component, and the error can be minimized by reducing the difference between the reference density and the actual formation water density (see Chapter 2).

In summary, the measurement errors associated with pressure data from DSTs cause inaccuracies in both equivalent hydraulic heads and driving force vectors. This imprecision outweighs the theoretical accuracy of the driving force vectors compared to equivalent hydraulic heads for most pressure-, density- and aquifer slope conditions and scales of observation in the study area. As a consequence, contour maps of equivalent hydraulic heads were used for the interpretation of flow in this study. The maximum



Reproduced with permission of the copyright owner. Further reproduction prohibited without permission.

difference between reference density and formation water density in each of the three hydrostratigraphic groups in the study area is 50 kg/m$^3$, when choosing as reference density the average between the respective minimum and maximum densities (Tab. 3.5). Reference densities of 1040 kg/m$^3$, and 1090 kg/m$^3$ were used to calculated equivalent hydraulic heads in the Jurassic-Mississippian, and the Cambrian-Devonian hydrostratigraphic groups, respectively. Because of the relatively small difference of formation water density in the Tertiary-Cretaceous hydrostratigraphic group ($\rho_{min} - \rho_{max}$ = 50 kg/m$^3$) freshwater density could be used as a reference density, still resulting in the same level of accuracy as in the other hydrostratigraphic groups.

| Hydrostratigraphic Group | Salinity Range (g/L) | Density Range (kg/m$^3$) |
|---|---|---|
| Tertiary-Cretaceous | 1.7 - 10.5 | 995 - 1045 |
| Jurassic-Mississippian | 35 – 165 | 1000 - 1080 |
| Cambrian-Devonian | 115 – 300 | 1040 - 1140 |

Table 3.5: Salinity and density range in the various hydrostratigraphic groups in the study area. The fluid density was calculated based on the salinity of the formation water, pressure, and temperature using empirical equations that were fit to laboratory experiments (Rowe and Chou, 1970; Kestin et al., 1981; Appendix D).

The distribution of equivalent hydraulic heads was contoured manually, for the same reasons and the using the same procedure as described for the conturing of hydrochemical data (Section 3.3.3). All data points were honoured within their range of accuracy as manifested in the contouring interval of 50 m. Therefore, hydraulic head differences can be calculated only to a resolution of 50 m over any distance l (Eq. 3.9). Hydraulic gradients accurately indicate the general flow direction, for $\nabla H_0 > F_\rho$ (DFR $< 1$) <u>and</u> $l < \dfrac{50\ m}{F_\rho}$. The critical distance beyond which the flow direction inferred from a hydraulic head difference of 50 m might be reversed due to density effects exists for a maximum aquifer slope of 0.02 and maximum difference between reference and



Reproduced with permission of the copyright owner. Further reproduction prohibited without permission.

formation water density of 50 kg/m$^3$: $l_{crit} = \frac{50\ m}{\max\ F_\rho} = \frac{50\ m}{0.001} = 50\ km$. For the same conditions, driving force vectors accurately indicate the general flow direction if measured over at least 65 km (Fig. 3.; Case 2). These critical distances will be larger for less extreme density differences and aquifer slopes. For all practical purposes, areas in which the lateral distance between 50 m contour lines larger than 50 km have to be examined more closely with respect to the actual aquifer slope and formation water density.

Note: The impelling force vectors that were calculated for the Elk Point example in Chapter 2, only considered the theoretical aspects of the difference between equivalent hydraulic heads and impelling force vectors for the representation of formation water flow. If data accuracy were considered in the Elk Point example, a 50 m contour interval instead of 10 m would be appropriate. Then, the general flow direction could be inferred only in the area of relatively high hydraulic gradients and large force magnitudes in the east, while flow in the west would have to be interpreted as +/- stagnant.



Reproduced with permission of the copyright owner. Further reproduction prohibited without permission.

# CHAPTER 4: GEOLOGICAL AND TECTONIC SETTING

## 4.1 Introduction

The study area is located at the western edge of the Alberta Basin, which is part of the Western Canada Sedimentary Basin (WCSB) (Fig. 4.1). The undeformed part of the Alberta Basin is bounded by the Tathlina High in the north, the Bow Island Arch, separating it from the Williston Basin, in the southeast, the Precambrian Shield in the northeast and the Rocky Mountain thrust and fold belt in the west. The basin consists of a wedge of Phanerozoic sediments thickening southwestward from the exposed Precambrian Shield to a thickness of more than 6 km along the Cordilleran deformation front.

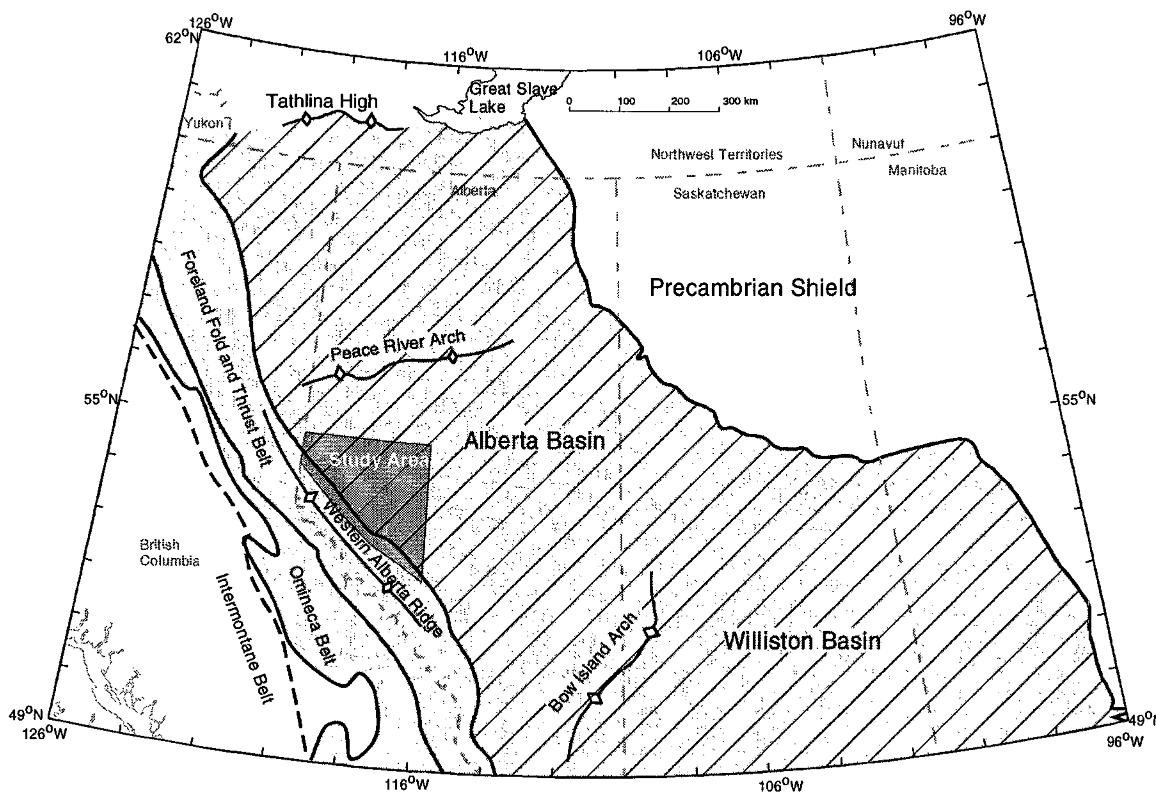


Figure 4.1: Structural elements of the Western Canada Sedimentary Basin. The grey shading represents the area of preserved sedimentary rocks of the WCSB; the hatched area shows the undeformed part of the basin (modified after Wright et al., 1994).



Reproduced with permission of the copyright owner. Further reproduction prohibited without permission.

The study area extends from the Foothills within the Rocky Mountain thrust and fold belt to about 200 km into the undeformed part of the basin (Fig. 4.2). The sediment thickness ranges between approximately 3 km in the northeast to 6 km in the southwest.

The sedimentological history of the Alberta Basin can be differentiated into two main phases. The "platform stage" (Proterozoic to Jurassic) represents a mainly transgressive onlap of dominantly marine sediments along the passive margin of the North American Craton. The boundary between the craton and allochthonous terranes lies approximately between the Omineca Belt and the Intermontane Belt (Fig. 4.1). In the "foreland stage" (Jurassic to Paleocene) the former sediments were compressed as a result of the Columbian (Jurassic-Early Cretaceous) and Laramide (Mid-Late Cretaceous-Tertiary) Cordilleran orogenies, and syn- as well as post-orogenic, dominantly clastic, deltaic to fluvial sediments were deposited (Porter et al., 1982).

## 4.2 Regional structural geology

The study area can be divided into two structural provinces: 1) Interior Plains (Bally et al., 1966), which represents the undisturbed part, and 2) the deformed part of the basin, i.e., the Rocky Mountain Thrust and Fold Belt (Monger, 1989). These two parts of the basin are separated by the Paleozoic and Mesozoic deformation fronts that represent the limit of Cordilleran deformation in the two major sedimentary assemblages, respectively. The boundary between the Foothills and Front Ranges in the southern part of the study area is the McConnell Thrust (Fig. 4.2), whereas the Nikanassin Thrust is considered the boundary further north (Lebel et al. 1996).



Reproduced with permission of the copyright owner. Further reproduction prohibited without permission.

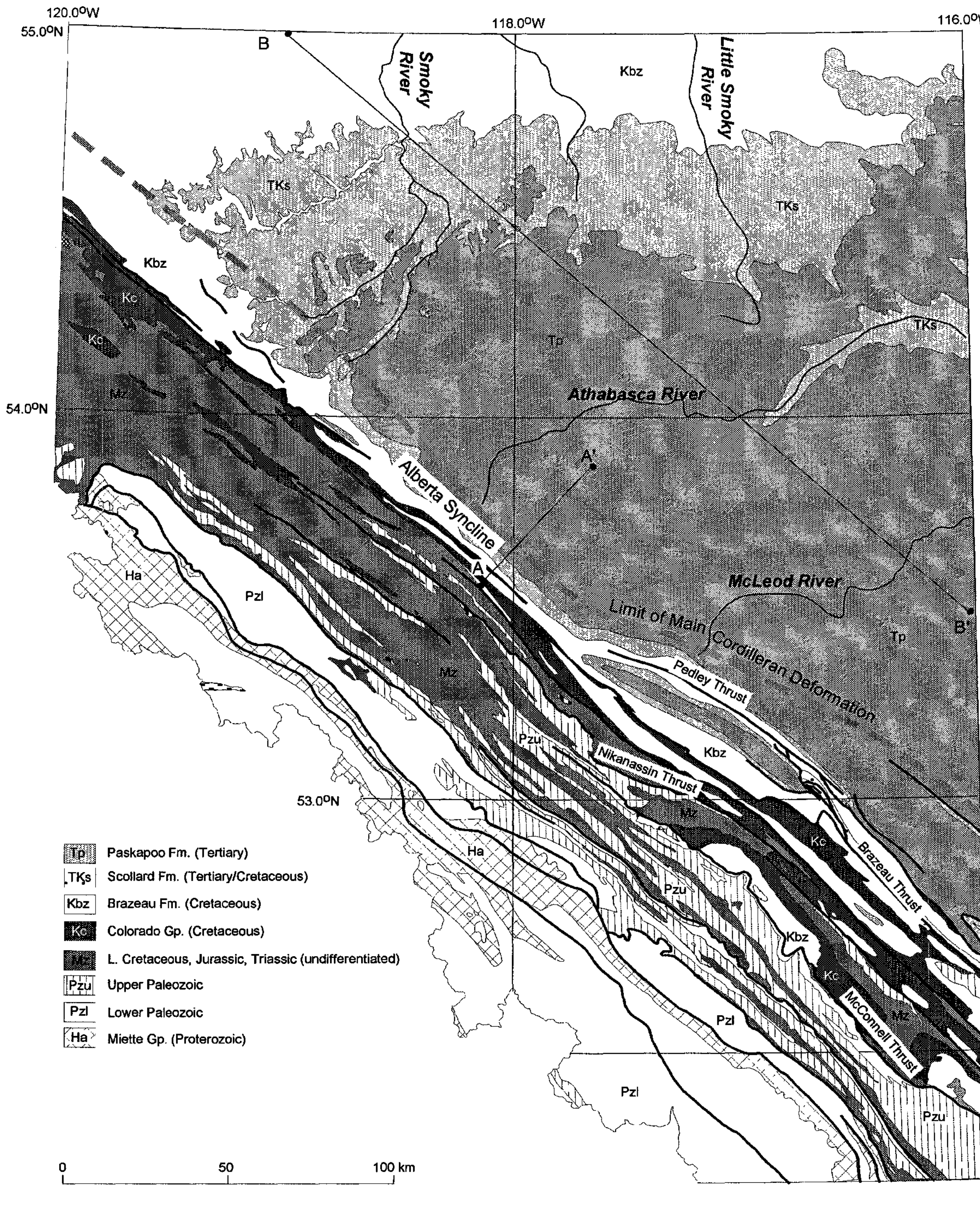


Figure 4.2: Bedrock geology in the study area (modified from Hamilton et al., 1997). Cross sections A - A' and B - B' are shown in Figures 4.3 & 4.5, respectively.



Reproduced with permission of the copyright owner. Further reproduction prohibited without permission.

The structure of the Foothills is formed by east-to-northeast verging listric thrusts and associated decollement folds. Thrust sheets consist mainly of Paleozoic carbonates, overlain by folded Mesozoic clastic rocks (Bally et al., 1966; Price, 1986). Differences in the structural style of the thrusting are largely controlled by lithology and, hence, competence of the involved strata. Thick, competent carbonate and sandstone successions cause the development of thick, laterally extensive thrust sheets, whereas less competent assemblages of inter-layered sandstone and shales or carbonates and shale show the development of folds (Monger, 1989).

Within the eastern edge of the thrust and fold belt, a triangle zone is defined, which is underlain by a subhorizontal foreland-verging thrust that ends against a foreland-dipping thrust (Charlesworth et al., 1987). The eastern boundary of this triangle zone is represented by the Pedley Thrust (Fig. 4.3), which back-steps northeastward into the Robb Fault (Lebel et al., 1996). These thrust faults die out northeastwards in the Alberta Syncline, which forms the transition zone between the Foothills and Plains regions.

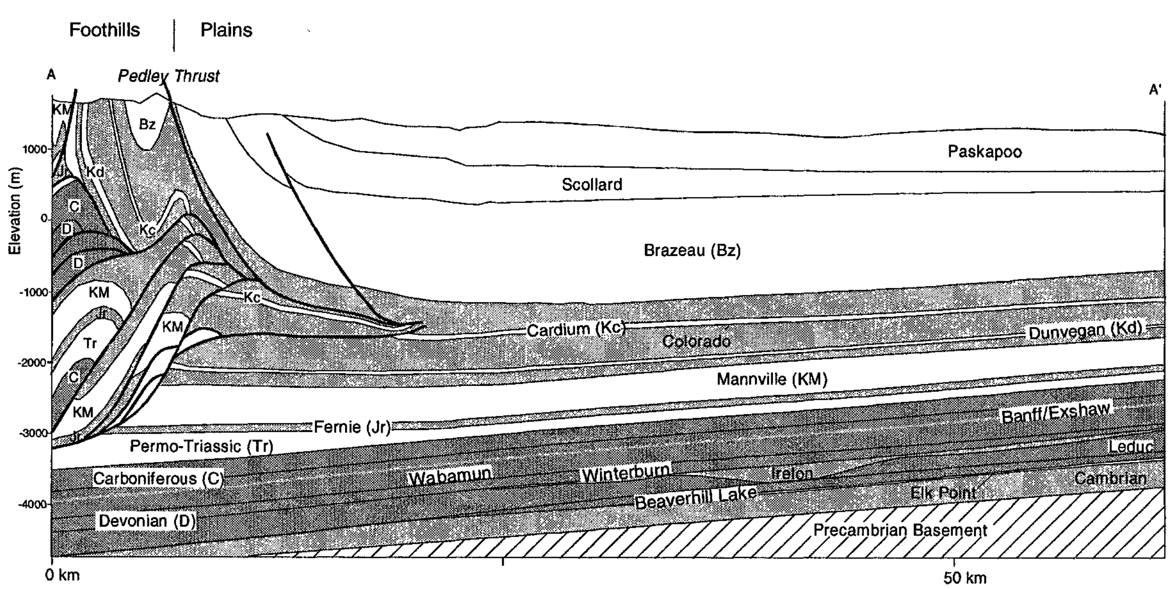


Figure 4.3: Geological dip cross section showing general lithology in the undeformed part of the basin and the structure of the triangle zone (structural part modified from Langenberg, 1992). See Fig. 4.2 for line of cross section.



Reproduced with permission of the copyright owner. Further reproduction prohibited without permission.

### 4.3 Passive margin succession (Proterozoic – Jurassic)

The crystalline Precambrian basement forms the base of the passive margin sedimentary succession (Fig. 4.4). Structural features of the basement that affected sedimentation in the study area are the Peace River Arch to the north and the Western Alberta Ridge along the deformation front in the west (Fig. 4.1). The extent of the latter is not very well defined because of Paleozoic and Mesozoic deformation. Both structures formed topographic highs during the Paleozoic and, therefore, played an important role for the control of sedimentation during that time. Proterozoic sediments are exposed only in the mountain ranges and consist of coarse clastics of the Gog and Miette Groups (Rickets, 1989; Ross et al., 1989).

Cambrian sediments accumulated on the ancestral continental shelf during periods of rifting and extension (Cecile et al., 1997). Quartz sandstone forms the base of the Cambrian ('Basal Sandstone'), whereas the middle and late Cambrian mainly consists of mixed carbonates and clastics (Slind et al., 1994; Hein and Nowlan, 1998). The top of the Cambrian represents a major hiatus, as the Silurian to Lower Devonian strata are absent in the study area due to either erosion or non-deposition. Parallel to the axis of the Peace River Arch, the Cambrian was completely eroded as well, and is absent in the northwestern corner of the study area (Fig 4.5a).

The Middle to Upper Devonian succession was deposited during a major marine transgression. This succession can be broken down into a number of cycles, as represented respectively by the sediments of the Elk Point, Beaverhill Lake, Woodbend, Winterburn and Wabamun Groups (Moore, 1989).



Reproduced with permission of the copyright owner. Further reproduction prohibited without permission.

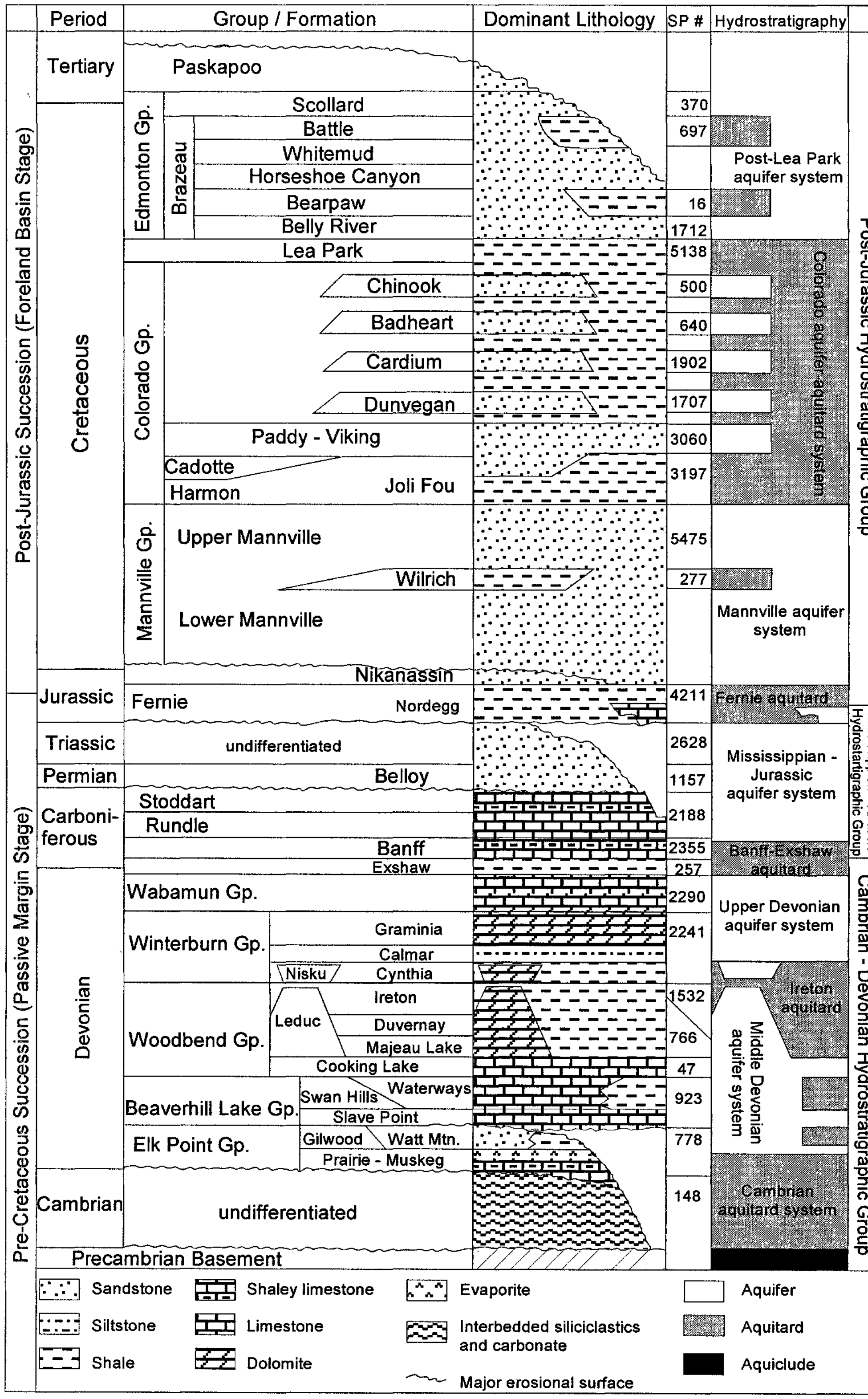


Figure 4.4: Stratigraphy, general lithology and general hydrostratigraphy of the sedimentary bedrock succession in the study area. SP # = Number of stratigraphic picks used for the construction of formation surfaces.



Reproduced with permission of the copyright owner. Further reproduction prohibited without permission.

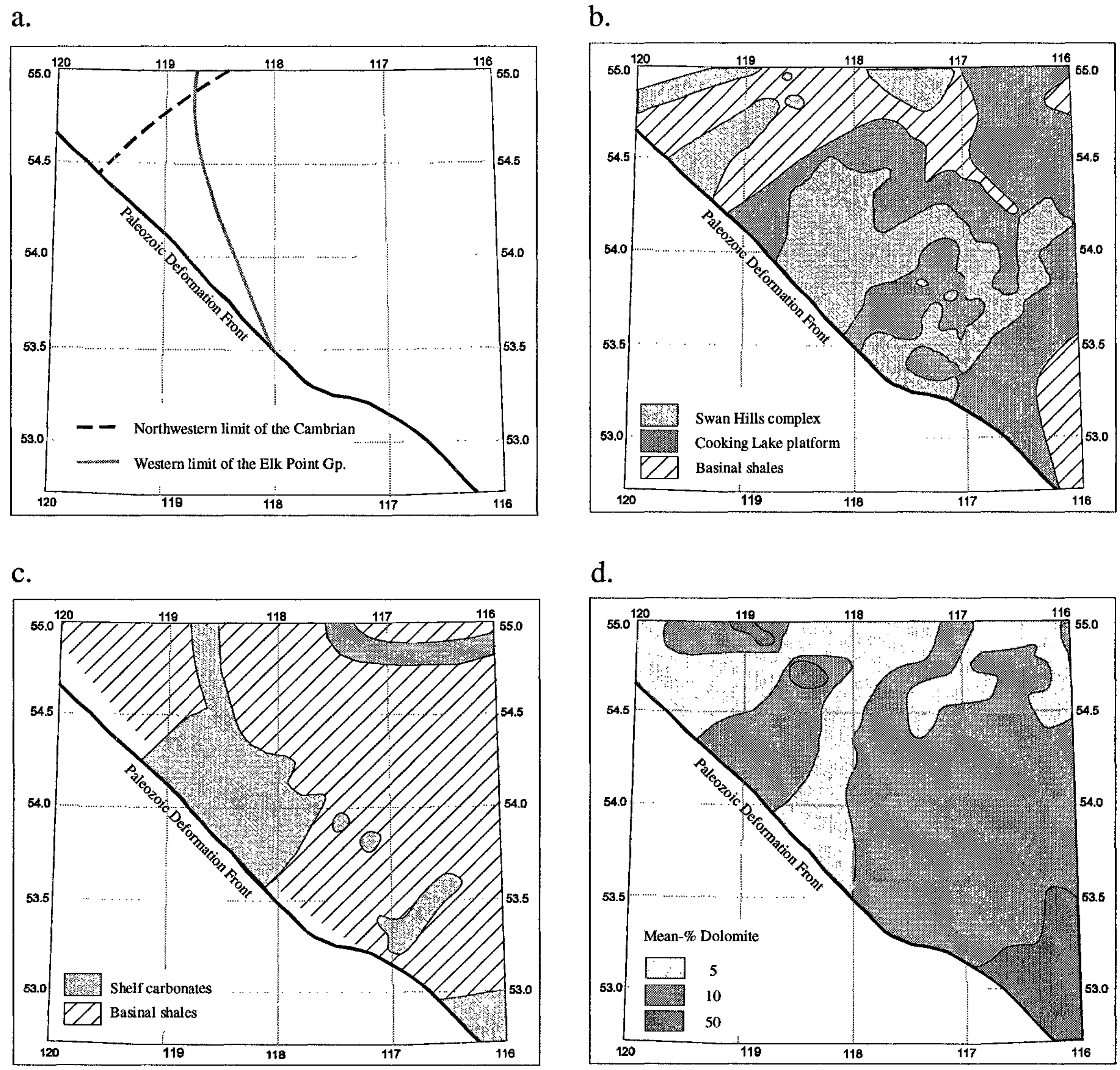


Figure 4.5: Various boundaries of Paleozoic strata in the study area in ascending order: a) erosional limits of the Cambrian and the Middle Devonian Elk Point Group., b) extent of carbonate platforms in the Middle Devonian Beaverhill Lake and Upper Devonian Woodbend groups, c) Lower Winterburn Group lithofacies, d) distribution of dolomite in the Wabamun Group. (modified from Mossop and Shetsen, 1994).



Reproduced with permission of the copyright owner. Further reproduction prohibited without permission.

Elk Point Group sediments were not deposited in the areas of the former Peace River landmass and the Western Alberta Ridge. The youngest formation of this group, the Prairie, is present only in the northeastern part of the study area. The Prairie Formation consists of mixed clastics and carbonates and is overlain by interbedded anhydrites and dolostones of the Muskeg Formation, which are overlain by interbedded shales, sandstones and dolostones of the Watt Mountain/Gilwood Formation (Meijer Drees et al., 1994).

Platform (Slave Point Fm.) and reef (Swan Hills Fm.) carbonates of the Beaverhill Lake Group successively onlap the Precambrian basement and the Cambrian and Elk Point Group sediments (Fig. 4.6). In the study area these carbonates form the Swan Hills Complex (Fig. 4.5b), which is capped by carbonaceous shales of the Waterways Formation (Oldale and Munday, 1994).

There is a transition from Swan Hills carbonates into platform carbonates (Cooking Lake Fm.) of the Woodbend Group (Fig. 4.5b) with overlying reefs (Leduc Fm.). The latter two form the Southesk Cairn Complex, which is overlain by shales and carbonaceous shales of the Majeau Lake, Duvernay and Ireton formations. Where the Ireton shales are thin or absent, the Leduc reefs are in direct contact with the overlying Nisku Formation, the lowest part of the Winterburn Group (Switzer et al., 1994).

The lower Winterburn Group represents a continuation of shale deposition (Cynthia Fm.) with the exception of isolated Nisku pinnacle reefs and a narrow band of shallow shelf carbonates (Fig. 4.5c), all being overlain by a thin siltstone layer (Calmar Fm.). The upper part of the succession is formed by thick carbonates of the Blue Ridge Member and Graminia Formation, of which the uppermost part consists of a thin, regional extensive silt layer that represents the boundary to the upper Devonian Wabamun Group (Switzer et al., 1994).



Reproduced with permission of the copyright owner. Further reproduction prohibited without permission.

Reproduced with permission of the copyright owner. Further reproduction prohibited without permission.

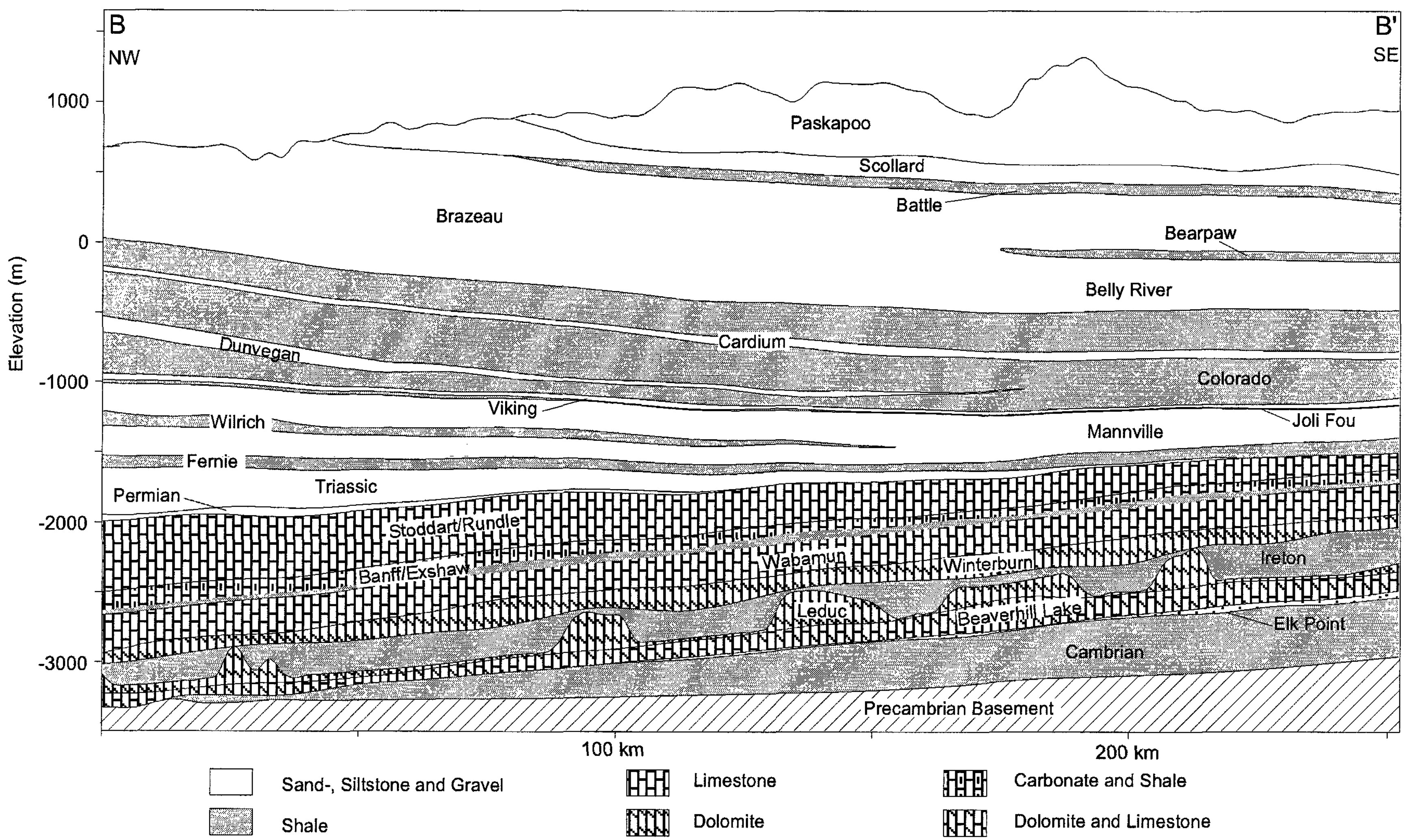


Figure 4.6: Geological cross section (B - B') sub-parallel to the deformation front showing general lithology distribution. See Figure 4.2 for line of cross section.

The Wabamun Group consists of massive, partly dolomitized carbonates. Generally, the lithofacies in the Wabamun Group change basin-wide southeastward from limestone to dolomite to evaporites (Andrichuk, 1960) (Fig. 4.5d). The limestone content increases upward, while dolomite and evaporites decrease (Saller and Yaremko, 1994). The boundary between the Devonian and Carboniferous systems lies in the overlying dark shales of the Exshaw Formation.

The Carboniferous succession was deposited on the, by that time downwarped and downfaulted, western margin of the North American plate, caused by the Antler orogeny, and continued southward into the Antler Foreland basin of the western United States (Richards, 1989). The Exshaw Formation is a rather thin layer (< 50 m) of dark, organic shales and siltstones. The shales continue in the much lower part of the Banff Formation, whereas the upper two thirds consist of heterogeneous carbonate ramp deposits and siliciclastics (Richards et al., 1994). The overlying Rundle Group represents a transgressive-regressive sequence, which mainly consists of carbonate platform and ramp deposits, as well as minor evaporites and siliciclastics (Richards, 1989). The dominantly sand- to siltstones of the Stoddart Group at the top of the succession probably were deposited in an estuarine environment with associated deltas (Richards, 1989). The top of the Carboniferous forms a major unconformity due to subaerial erosion that cuts through several formations and started during the Late Carboniferous.

Permian, Triassic and Jurassic strata successively overlie the Carboniferous formations. Sediments of the Permian Belloy Formation cover only about 50 % of the study area (Fig. 4.7a) and consist dominantly of siliciclastics that become increasingly carbonaceous towards the deformation front. The top of the Permian forms an erosional boundary with the Triassic strata, but may be directly overlain by Jurassic sediments in small zones in the east, along the Triassic erosional edge (Fig. 4.7a).

The Triassic succession represents a coarsening-upward cycle deposited on a topographically low, tectonically stable continental shelf along the western margin of the



Reproduced with permission of the copyright owner. Further reproduction prohibited without permission.

North American craton (Gibson and Barclay, 1989). Shales and siltstones form the base, overlain by silt- to sandstones, followed by sandstones and evaporites (Edwards et al., 1994). The top of the Triassic succession is a major erosional unconformity, with increasingly older formations subcropping underneath Jurassic strata from west to east. The Triassic is completely eroded at the eastern boundary of the study area.

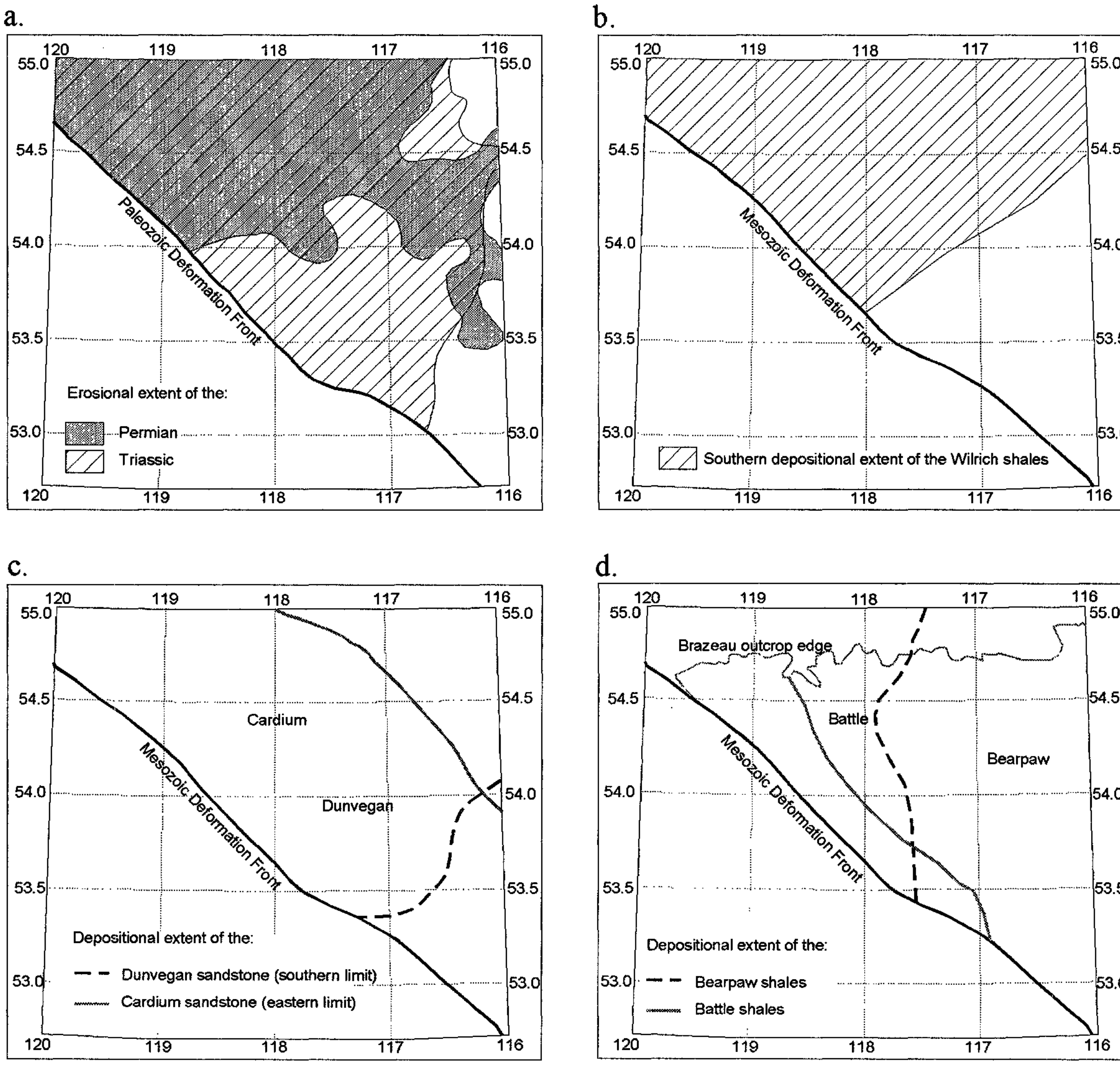


Figure 4.7: Boundaries of Late Paleozoic to Cretaceous strata in the study area: a) Permian and Triassic (Mossop & Shetsen, 1994), b) Wilrich shales (after Connolly, 1989), c) Cardium and Dunvegan sandstones (Mossop and Shetsen, 1994), and d) Bearpaw and Battle shales.



Reproduced with permission of the copyright owner. Further reproduction prohibited without permission.

The Jurassic succession represents the transition from a passive to an active continental margin (Poulton, 1989). The main part of the Jurassic is formed by an assemblage of dominantly shales interbedded with thin sandstone layers of the Fernie Group. At the base of the Jurassic, a thin phosphatic siltstone layer is found, which becomes a limestone with chert lenses (Nordegg Mbr.) in the east of the study area (Poulton, 1989). The Fernie shales coarsen upward into sandstones of the Nikanassin Formation, which are late Jurassic to lower Cretaceous in age, and which are interbedded with thin coal seams. The entire succession is unconformably overlain by the Cretaceous Mannville Group.

## 4.4 Foreland basin succession (Late Jurassic – Recent)

With respect to global plate tectonics, the evolution of the Alberta Basin is closely related to the formation of the Cordillera (Price, 1994). Terrane accretion during the Columbian (Jurassic-Early Cretaceous) and Laramide (Mid-Late Cretaceous-Tertiary) orogenies controlled the sedimentation of the foreland succession (Porter et al., 1982).

The Mannville Group was deposited during the Columbian orogeny. The Lower Mannville Group is formed by dominantly fluvial sandstones and conglomerates grading upwards into delta and open marine sandstones and shales (Cant, 1989). Marine shales of the overlying Wilrich Formation thin out towards the southeast and the depositional facies changes to near-shore silt- and sandstones in the center of the study area, defining the boundary between Lower and Upper Mannville Groups (Fig. 4.7b). The Upper Mannville Group consists mainly of non-marine to marginal marine sandstone to shale units (Cant, 1989). Regionally extensive coal seams are found in both the Upper and the Lower Mannville Group (Smith et al., 1994).

The overlying Upper Cretaceous Colorado Group represents a thick wedge of marine shales with progradational packages of sandstones and conglomerate of different extent (Leckie, 1989), deposited during a lull in plate convergence and tectonic activity. Major



Reproduced with permission of the copyright owner. Further reproduction prohibited without permission.

and regionally extensive sandstone units are Viking, Dunvegan, Cardium (Figs. 4.6 & 4.7c), and Badheart Formations. The shales continue at the top of the Colorado Group into the Lea Park Formation, which forms the boundary to the overlying Upper Cretaceous sediments of the Edmonton Group.

The overlying Upper Cretaceous to Tertiary succession was deposited during the Laramide orogeny. The Edmonton Group begins with an interval of clastic detritus of the mostly non-marine Brazeau and Wapiti Formations in the west, and with the Belly River Formation at the base in the east of the study area (Leckie, 1989). These formations successively crop out parallel to the northern boundary of the study area (Fig. 4.2). In the eastern part of the study area, the marine shales of the Bearpaw Formation (Fig. 4.7d) separate the underlying Belly River Formation from overlying terrestrial deposits of the Horseshoe Canyon Formation. The boundary with the coal-bearing strata of the Scollard Formation, better defined in the east by shales of the Battle Formation and the Kneehills Tuff Zone (Fig. 4.7d), is represented in the west by finer grained sandstones at the top of the Brazeau Formation. The youngest unit in the Edmonton Group is the Scollard Formation, which contains mostly clastic, alluvial plain deposits, shallow water and lake sediments, and regionally extensive coal seams up to 7 m thick (Smith, 1989). It crops out in the northern half of the study area (Fig. 4.2).

The Tertiary in the study area is represented by the Paskapoo Formation, the K/T - boundary itself being located in the underlying Scollard Formation. The deposits of the Paskapoo Formation are mostly sandstones and conglomerates, representing a continuing sedimentation of large alluvial fans. The deposition of Tertiary sediments lasted approximately to the peak of the Laramide orogeny (~53 Ma).

A major period of erosion, starting after the peak of the Laramide orogeny, has been responsible for shaping the basin relief until the present. Figure 4.8a shows that approximately 1.5 – 3.5 km of sediments were removed by erosion to the present-day bedrock topography (Magara, 1976b; Connolly, 1989; Bustin, 1991).



Reproduced with permission of the copyright owner. Further reproduction prohibited without permission.

The thickness of the Quaternary cover in the study area ranges between approximately 0 and 120 m and consists mainly of glacial tills, and to a lesser degree of lacustrine and fluvial sediments (Fenton et al., 1994). At least five major southward advances of the Laurentide ice sheet in the plains region (Fenton, 1984) and four glaciations in the Canadian Cordillera (Fulton, 1984) are represented by the Pleistocene sediments. During its maximum advancement (~ 20 ka), the Laurentide ice sheet covered almost the entire study area (Fig. 4.8b) reaching a maximum thickness of 1 to 2 km (Matthews, 1974). An approximately 100 km wide, ice-free corridor might have existed during maximum Pleistocene glaciation between the Cordilleran and Laurentide glaciers in the southern part of the study area, sub-parallel to the deformation front (Rutter, 1984). The Laurentide ice-sheet had receded from the plains region about 7 ka ago, while the Cordilleran glacier cover reached a little more than its present extent by 10 ka (Fulton et al., 1984), allowing for the development of the current topography and drainage system.

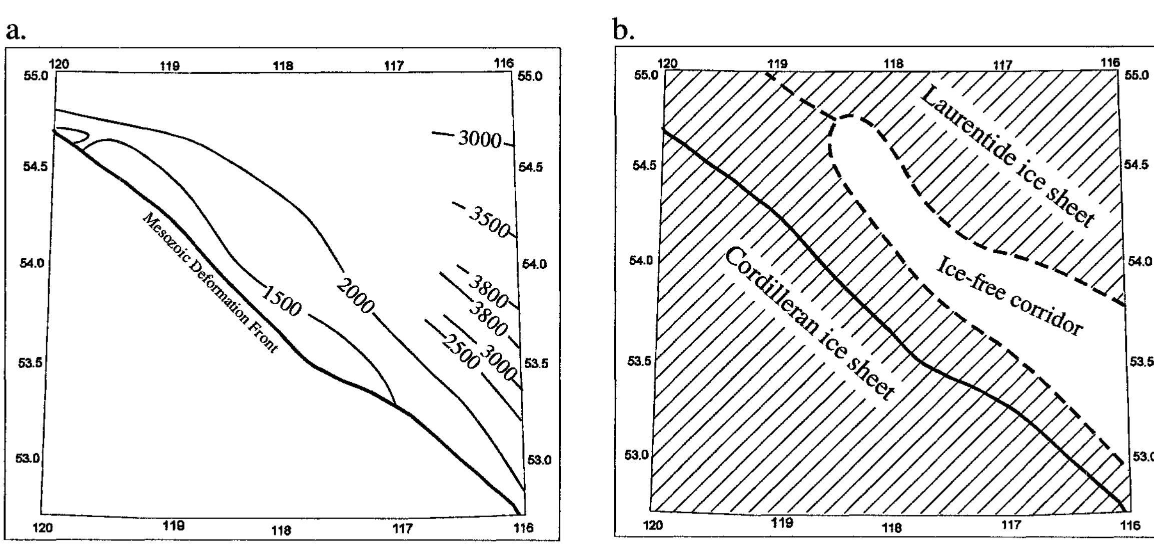


Figure 4.8: a) Schematic and generalized map of reconstructed thickness of overburden (in metres) in the study area (modified from Bustin, 1991), b) approximate maximum extent of the Cordilleran and Laurentide ice sheets during the Late Wisconsinan (modified from Fenton, 1984).



Reproduced with permission of the copyright owner. Further reproduction prohibited without permission.

## 4.5 General hydrostratigraphy

A hydrostratigraphic framework was constructed by subdividing the entire stratigraphic succession into aquifers, aquitards and aquicludes (for definitions see Chapter 2, 2.3) based on the permeability inferred from the general lithology of the stratigraphic units (Fig. 4.4). Generally, coarse siliciclastics (gravels – sandstones) and carbonates were considered to be aquifers, whereas shales and evaporitic sequences form aquitards. The crystalline Precambrian basement was considered to be an aquiclude, but currently there are insufficient hydraulic data to definitively characterize it as such. The general subdivision of the stratigraphic succession into three hydrostratigraphic groups, each containing several aquifer and aquitard systems, is based on previous work in the west-central part of the Alberta Basin (Hitchon et al., 1990; Bachu 1995b). This hydrostratigraphic framework will be discussed in detail and individually for each hydrostratigraphic group in Chapters 5, 6, and 7, respectively.



Reproduced with permission of the copyright owner. Further reproduction prohibited without permission.

# CHAPTER 5: FLUID AND PRESSURE DISTRIBUTION IN THE FORELAND BASIN (TERTIARY-CRETACEOUS) SUCCESSION

## 5.1 Introduction

The post-Jurassic sedimentary succession in west-central Alberta is of special interest regarding its hydrogeology for the following reasons:

1) Severe underpressuring is observed in large parts of various Cretaceous aquifers, which has been attributed to the erosional rebound of thick intervening shale units (Bachu and Underschultz, 1995; Bachu, 1995a; Parks and Tóth, 1995). On the other hand, flow in shallower aquifers has adjusted to present-day ground surface topography. This study investigates the driving mechanisms for fluid flow in the succession, in an attempt to identify causes for abnormal fluid pressures, and examines to what extent the post-Jurassic succession has been flushed by meteoric water.
2) The deep part of the Cretaceous succession is mainly saturated with hydrocarbons (Fig. 5.1) and is referred to as the "deep basin gas trap" (Masters, 1979). The interaction between formation water flow and hydrocarbon generation and migration has been addressed so far in very few local-scale studies only (Pendergast, 1969; Putnam 1993; Putnam and Ward, 2001), and is further investigated in this study.



Reproduced with permission of the copyright owner. Further reproduction prohibited without permission.

a.

b.

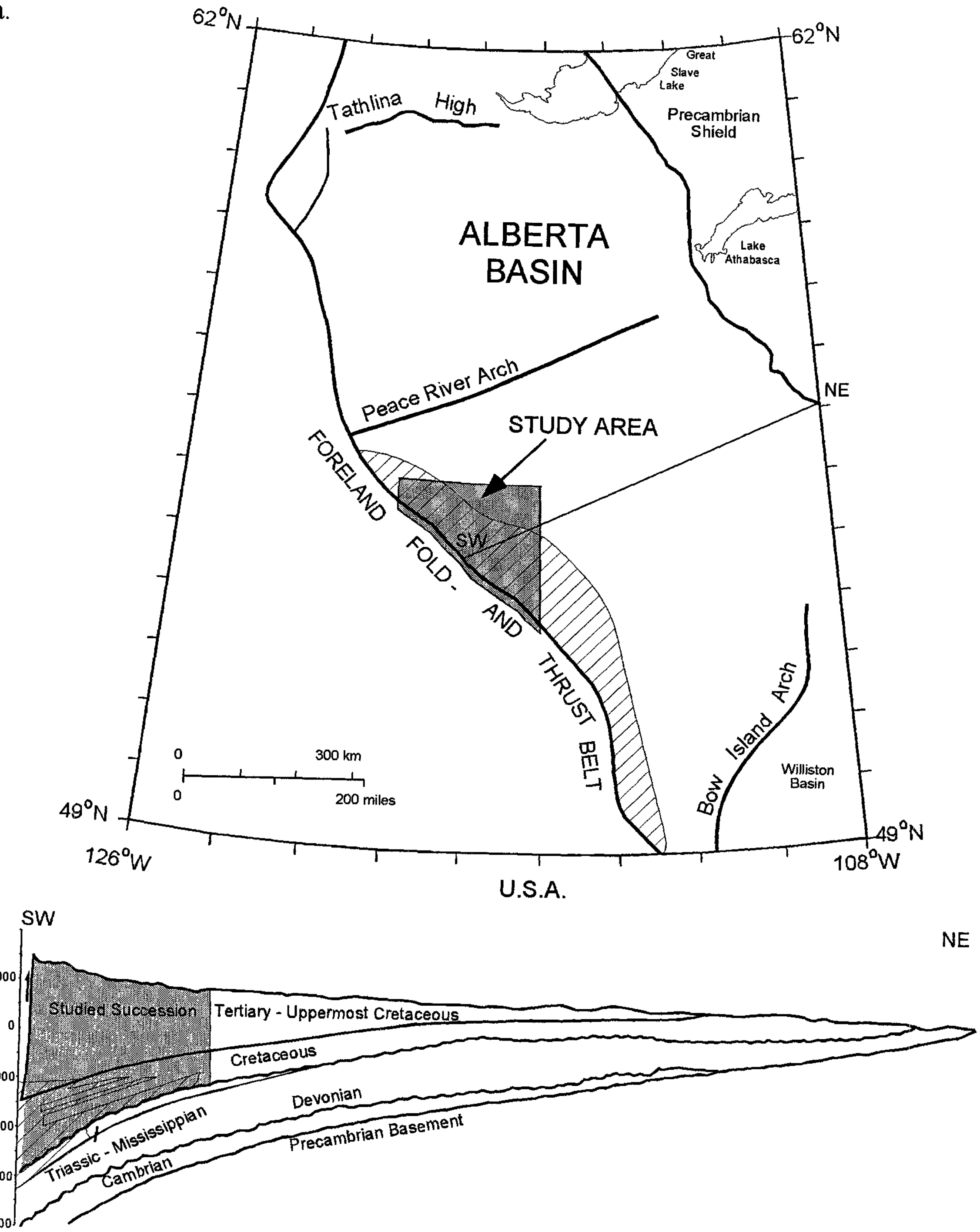


Figure 5.1: Location of the study area in the Alberta Basin: a) in plan view, and b) stratigraphically along a dip cross section. The hatched area represents the approximate extent of the gas-saturated "deep basin" (after Masters, 1984).



Reproduced with permission of the copyright owner. Further reproduction prohibited without permission.

3) The question of hydraulic communication between flow in the thrust and fold belt and flow in the plains region is still not satisfactorily answered, as different interpretations exist for various areas along the deformation front. Recharge of the Cretaceous Mannville aquifer by meteoric water from the thrust and fold belt was identified in the northern part of the Peace River region (Thompson, 1989), north of the study area, consistent with basin-scale recharge from the thrust and fold belt in the northern part of the Alberta Basin (Bachu, 1997). In the southern part of the Peace River region flow appears to be hindered by the "deep basin" gas accumulations that act as barrier to fluid flow (Thompson, 1989). Lack of hydraulic communication between the deformed and undeformed parts of the Alberta Basin was inferred also south of the Peace River region based on flow patterns (Bachu, 1995a, 1999).

Answering the above questions may help to better understand the basin-scale flow patterns and their driving mechanisms in the Alberta Basin as a whole, and to identify fluid origins. Understanding the interaction between hydrocarbon- and water-saturated regions is of particular interest because the Cretaceous succession is a major target for petroleum exploration and exploitation in this part of the basin, and the flow of formation waters has affected and still influences to a large extent the migration and accumulation of hydrocarbons.

### 5.2 Hydrostratigraphic framework

The Tertiary-Cretaceous sedimentary succession consists of fluvio-deltaic and marine to marginal marine siliciclastics (Smith, 1994). The Jurassic Fernie shales form a regional extensive aquitard (Bachu, 1995a) and represent the base of this hydrostratigraphic group (Fig. 5.2), which can be divided into three major hydrostratigraphic systems: I) the post-Colorado aquifer system, II) the Colorado aquitard system, and III) the Mannville aquifer system. Herein, sandstone dominated formations form aquifers, whereas shale formations act as aquitards. The hydrogeology of the three hydrostratigraphic systems will be discussed in descending stratigraphic order.



Reproduced with permission of the copyright owner. Further reproduction prohibited without permission.

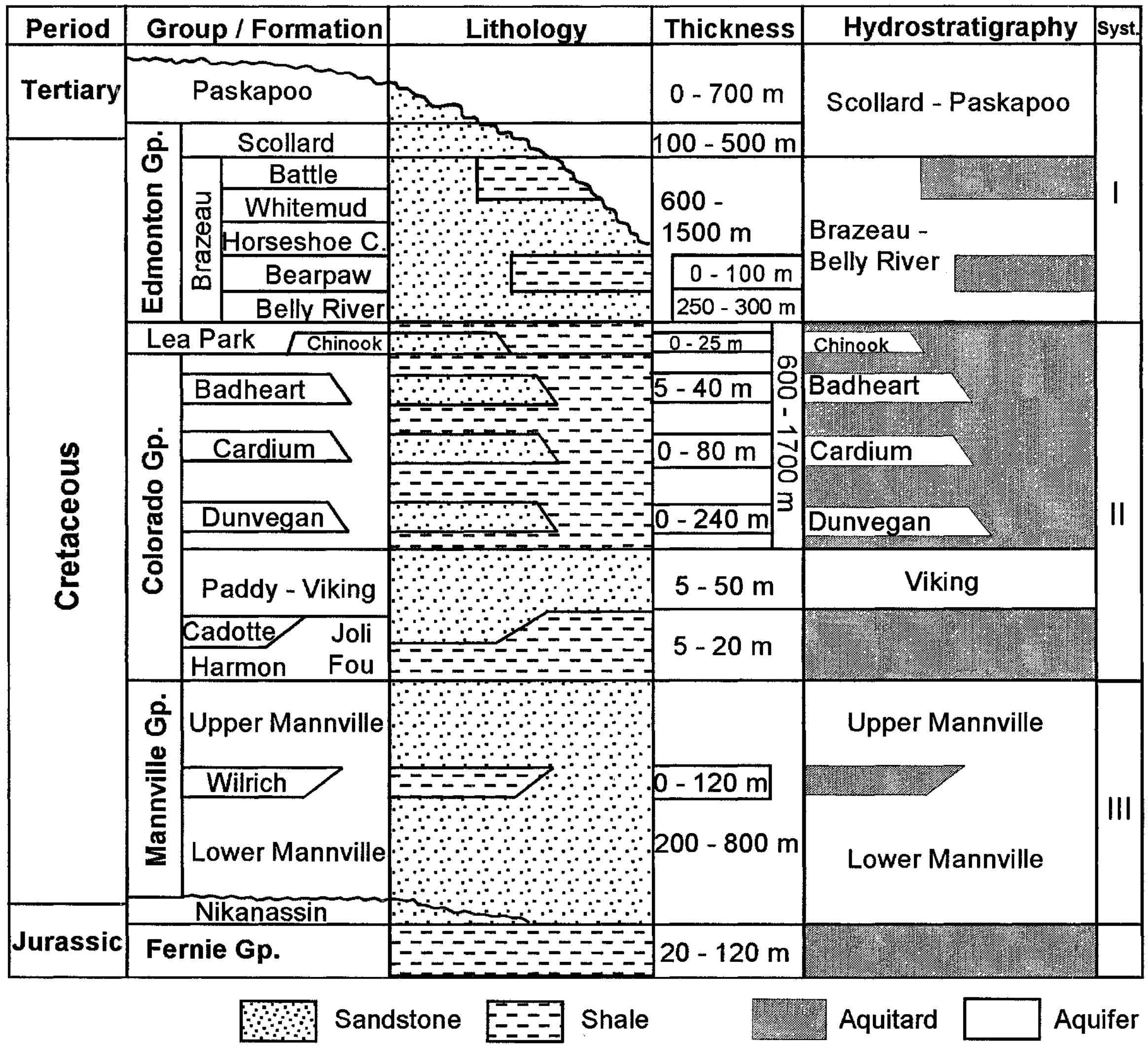


Figure 5.2: General lithology and hydrostratigraphy of the Tertiary-Cretaceous succession in the study area.

*Post-Colorado aquifer system*

The post-Colorado aquifers crop out underneath the Quaternary cover, where these aquifers are replenished by meteoric water, and discharge at the valleys of the Athabasca and Smoky Rivers and their tributaries (Fig. 5.3) that cut into the unconsolidated Quaternary sedimentary cover and the top of the bedrock (Barnes, 1977; Tokarsky, 1997; see Chapter 4, Fig. 4.2). Based on the general lithology distribution, the post-Colorado represents a relatively continuous aquifer system from the ground surface down to the



Reproduced with permission of the copyright owner. Further reproduction prohibited without permission.

Lea Park shales, the latter defining the lower boundary. Regional-scale aquitards are the shales of the Battle Formation and the Bearpaw Formation, which are both absent in parts of the study area (see Chapter 4, Fig. 4.7 d). The western depositional edge of the Battle aquitard runs at some 25 km distance sub-parallel to the deformation front, such that the Brazeau aquifer is in direct contact with the overlying Scollard-Paskapoo aquifer. The Bearpaw Formation is deposited only in the eastern part of the study area, and its thickness reaches up to 100 m. Here the Bearpaw aquitard subdivides the Brazeau-Belly River aquifer into the Belly River and Horseshoe Canyon aquifers.

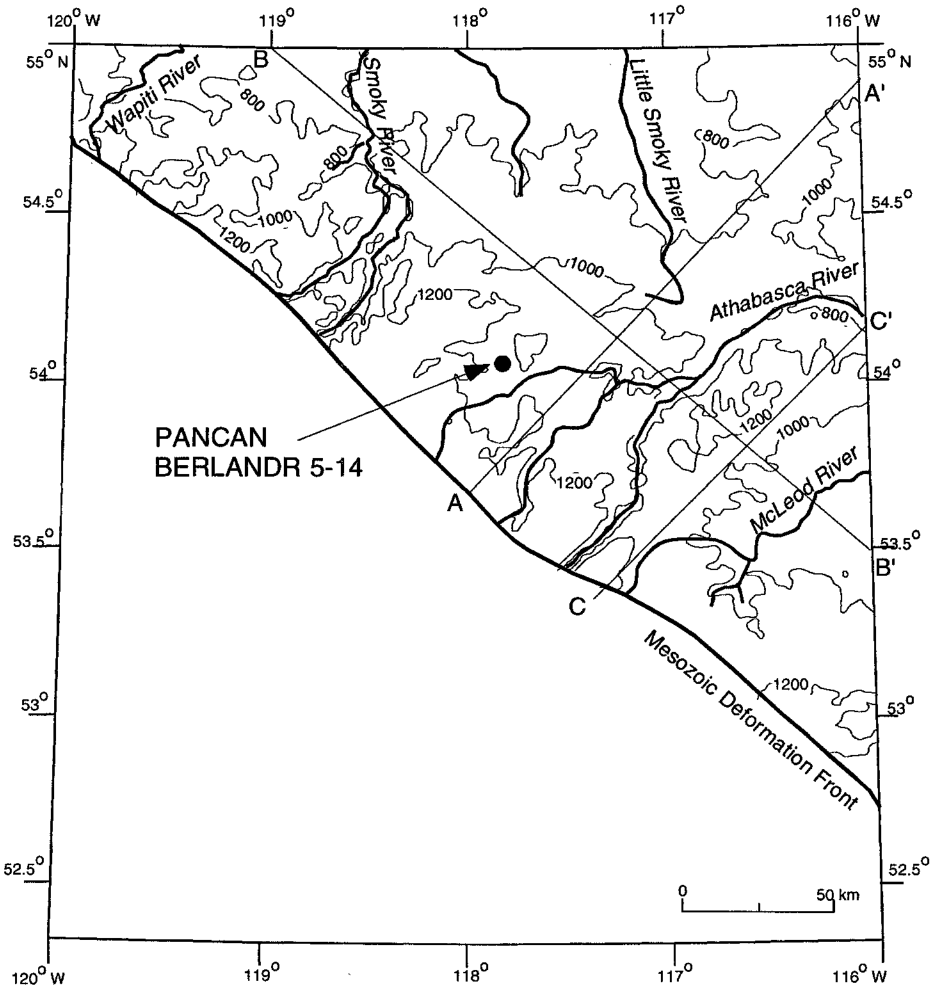


Figure 5.3: Topographic map of the study area showing lines of cross sections and location of a PanCan well (s. Fig. 5.33).



Reproduced with permission of the copyright owner. Further reproduction prohibited without permission.

*Colorado aquifer-aquitard system*

The lithology of the Colorado aquitard system is dominated by the up to 1500 m thick Colorado Group shales, which represent a major continuous aquitard system throughout the Alberta Basin (Bachu, 1995a). Five embedded sandstone units form isolated aquifers: Chinook, Badheart, Cardium, Dunvegan, and Viking. The Viking aquifer at the base of the system is separated from the underlying Mannville aquifer system by the relatively thin Joli Fou aquitard.

*Mannville aquifer system*

The Mannville aquifer system is subdivided by the Wilrich aquitard into the Upper and Lower Mannville aquifers in the northwestern half of the study area, where the former is present (see Chapter 4, Fig. 4.7 b). Along the Rocky Mountain Foothills, the Mannville sandstones directly overlie the sandstones of the Jurassic – Lower Cretaceous Nikanassin Formation, thus forming a single hydrostratigraphic unit that will be referred to as the Lower Mannville aquifer. The underlying continuous shales of the Jurassic Fernie Group represent the lower boundary of the Mannville aquifer system.

## 5.3 Hydrogeological patterns

Contour maps of equivalent freshwater hydraulic heads (reference density $\rho_0$ = 1000 kg/m$^3$), as well as p(d)- and p(z)-plots were used to interpret the flow in the foreland-basin succession. Only pressure data from DSTs in which water was dominantly recovered were used to calculate hydraulic heads and contoured. Water, gas and oil pressure data are presented in the p(d)- and p(z)-plots. The DFR in the studied aquifers is everywhere < 0.35 due to a combination of: a) relatively low salinity, b) strong hydraulic gradients, and c) location of the water-saturated zones in the shallower part of the study



Reproduced with permission of the copyright owner. Further reproduction prohibited without permission.

area, where the aquifer slope is relatively mild (< 8m/km). The small DFR indicates that the errors in flow representation are small, and therefore the use of freshwater hydraulic heads in interpreting the flow is justified (s. Chapter 2). Hydrogeochemical data are presented in the form of contour maps of salinity and bicarbonate concentrations to supplement the pressure data, and to identify fluid sources and pathways.

The aquifers were subdivided into water-saturated and hydrocarbon-saturated zones, I and II, respectively. Hydrostatic-to-subhydrostatic pressures (subzone Ia) and underpressures (subzone Ib) can be distinguished in the water-saturated zone. The boundary between these subzones was obtained by mapping pressure data that plot along different, offset lines in the p(z)-plot, indicating some sort of permeability barrier or transmissivity change between the two pressure populations (see Chapter 2, 2.3). The hydrocarbon-saturated zone in some aquifers could be further subdivided into underpressured gas (or overpressured oil in the Cardium), being located directly downdip of the underpressured water-saturated zone. Gas and oil pressures from the hydrocarbon-saturated zones plot along various lines with static gas and oil gradient, respectively. This hydrocarbon-saturated subzone is respectively denoted as IIa or IIb, depending on whether or not it is adjacent in turn to a normally-to-overpressured subzone IIc further downdip. The zonation of the various aquifers and the range of the hydrogeological data in the water-saturated zone are summarized in Table 5.1.



Reproduced with permission of the copyright owner. Further reproduction prohibited without permission.

| Unit | Zone | Subzone | Fluid | Pressure Regime | $H_f$ (m) | TDS (g/L) |
|---|---|---|---|---|---|---|
| Scollard-Paskapoo | | | Water | (sub-)hydrostatic | | |
| Brazeau-Belly River | I | a | Water | (sub-)hydrostatic | 625 - 825 | 1.7 – 10.5 |
| | | b | Water | Underpressured | 500 - 625 | |
| | II | | Oil | Underpressured | | |
| Cardium | I | a | Water | (sub-)hydrostatic | 350 - 500 | 15 - 26 |
| | | b | Water | Underpressured | 700 - 800 | 7 – 14 |
| | II | a | Oil | Overpressured | | |
| | | b | Oil | Overpressured | | |
| | | c | Gas | Normally-pressured | | |
| Dunvegan | I | a | Water | (sub-)hydrostatic | 450 - 550 | 7 – 13 |
| | | b | Water | Underpressured | 200 - 400 | |
| | II | | Gas | Normally-pressured | | |
| Viking | I | a | Water | (sub-)hydrostatic | 500 | 10 - 25 |
| | | b | Water | Underpressured | 350 - 500 | |
| | II | a | Gas | Underpressured | | |
| | | b | Gas | Underpressured | | |
| | | c | Gas | Over- and Normally-pressured | | |
| Upper Mannville | I | a | Water | (sub)-hydrostatic | 550 - 700 | 9 - 36 |
| | | b | Water | Underpressured | 300 - 500 | |
| | II | a | Gas | Underpressured | | |
| | | b | Gas | Underpressured | | |
| | | c | Gas | Over- and Normally-pressured | | |
| Lower Mannville | I | Ia | Water | (sub-)hydrostatic | 500 - 650 | 35 - 90 |
| | | Ib | Water | Underpressured | 350 - 500 | |
| | II | IIa | Gas | Underpressured | | |
| | | IIb | Gas | Underpressured | | |
| | | IIc | Gas | Over- and Normally-pressured | | |

Table 5.1: Summary of fluid distribution, pressure regimes and ranges in hydraulic heads and salinity in the post-Jurassic aquifers in the study area.



Reproduced with permission of the copyright owner. Further reproduction prohibited without permission.

The hydrogeological data in the Scollard – Paskapoo aquifers are relatively sparse and cannot be contoured areally. Therefore, flow is only interpreted along selected cross sections, and the pressure data are compared to the ground surface and to data from the directly underlying Brazeau-Belly River aquifer. Figures 5.4 to 5.7 present, respectively, the distribution of freshwater hydraulic heads, p(d)- and p(z)-plots, and distributions of salinity and bicarbonate in the Brazeau-Belly River aquifer.

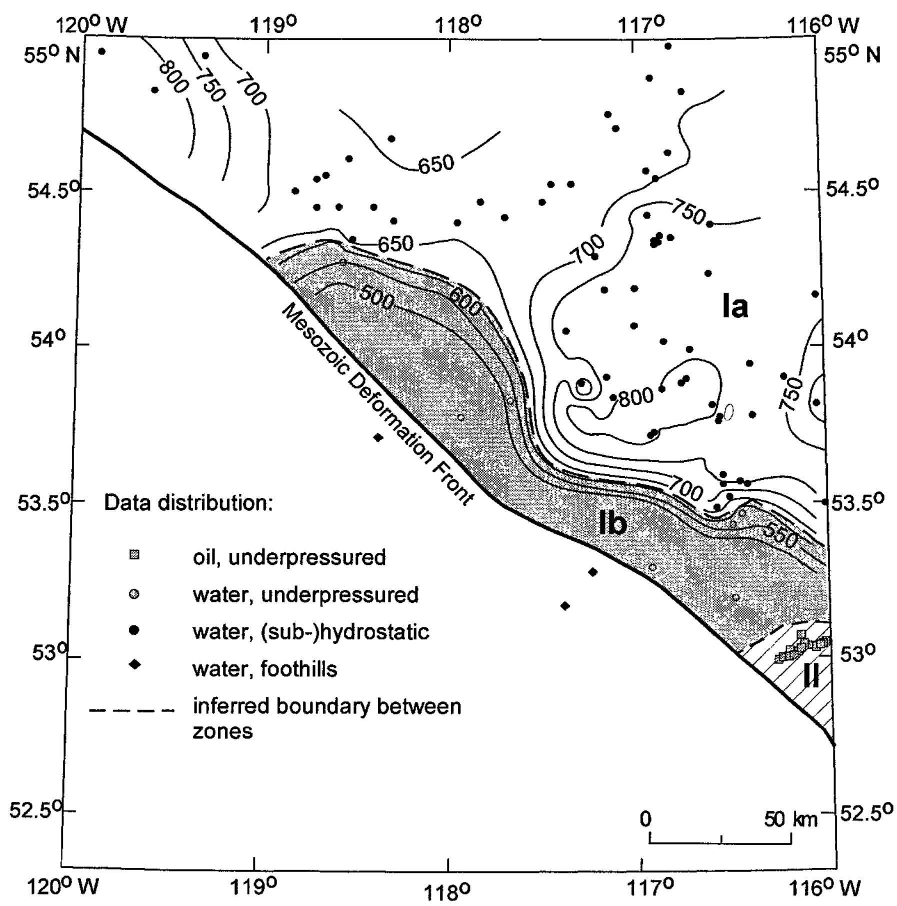


Figure 5.4: Freshwater hydraulic head distribution and aquifer zonation in the Brazeau-Belly River aquifer (50 m contour interval). For better visualization purposes, subzone Ib is shaded grey and the hydrocarbon-saturated zone II is hashed.



Reproduced with permission of the copyright owner. Further reproduction prohibited without permission.

Reproduced with permission of the copyright owner. Further reproduction prohibited without permission.

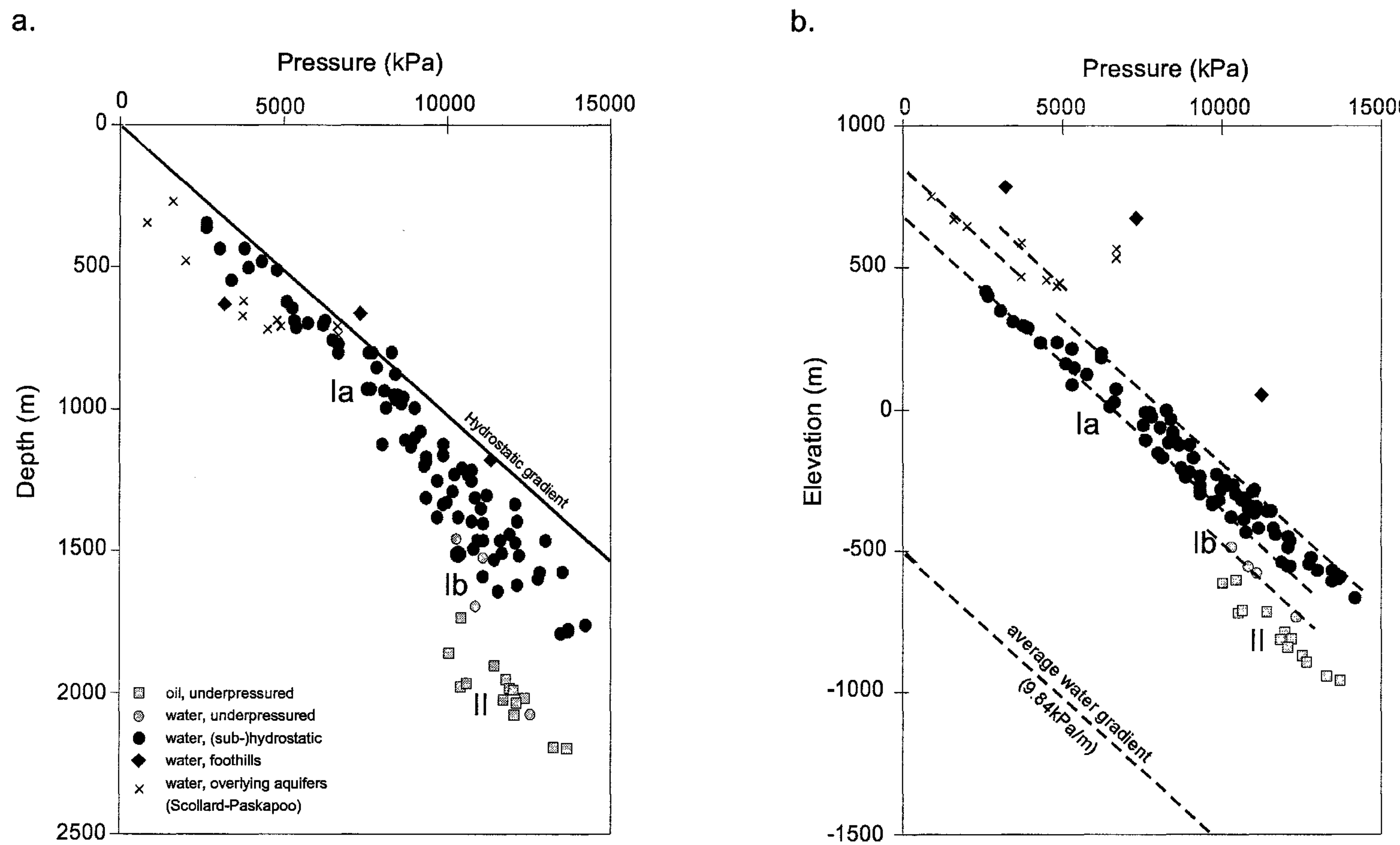


Figure 5.5: Pressure variation with: a) depth and b) elevation, in the post-Colorado aquifers (Brazeau-Belly River and Scollard-Paskapoo). The data groups denoted by roman numbers correspond to the geographic distributions shown in Figure 5.4.

Reproduced with permission of the copyright owner. Further reproduction prohibited without permission.



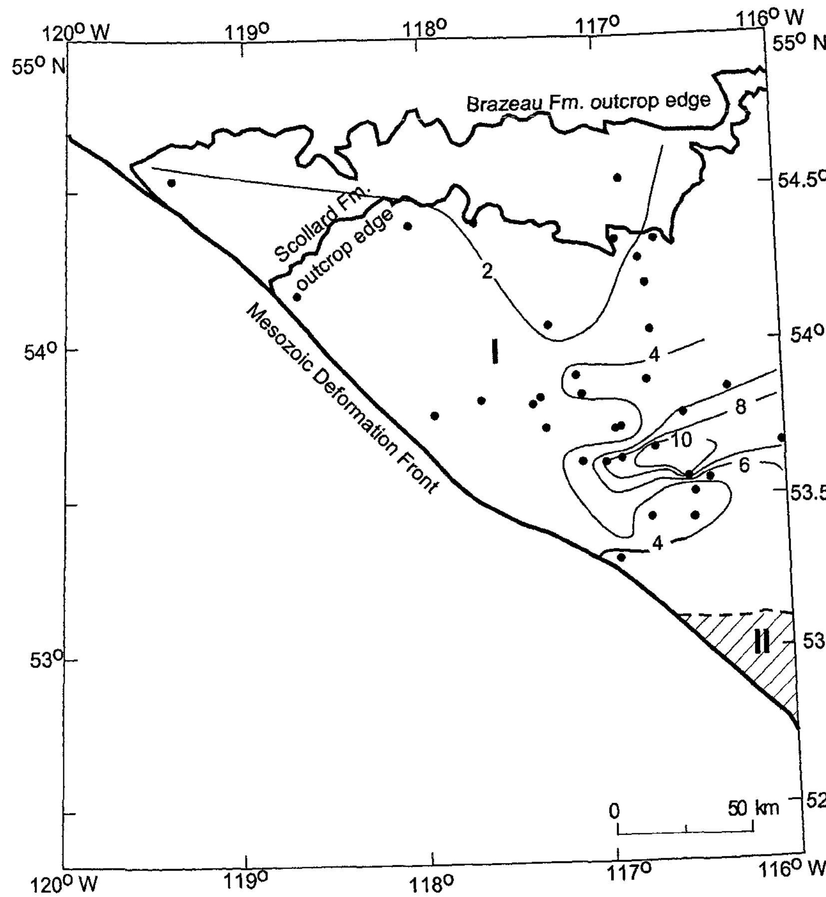


Figure 5.6: Salinity distribution in the Brazeau-Belly River aquifer (2 g/l contour interval). Zones I and II correspond to the zonation in Figure 5.4.

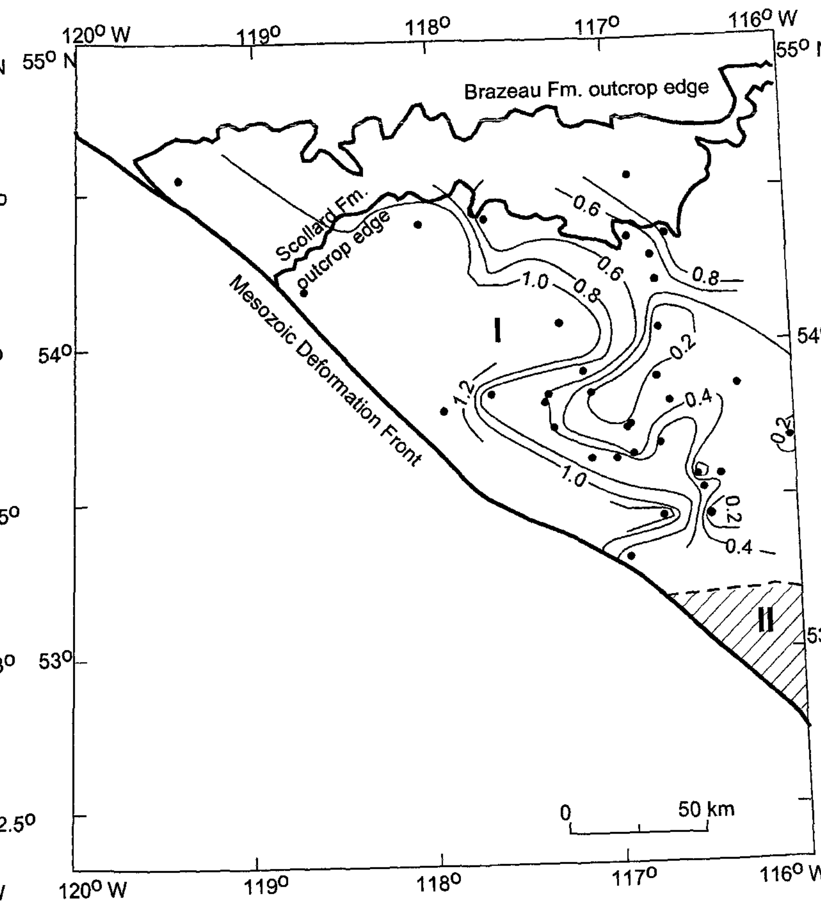


Figure 5.7: Bicarbonate distribution in the Brazeau-Belly River aquifer (0.2 g/l contour interval). Zones I and II correspond to the zonation in Figure 5.4.

Pressure data from the Brazeau-Belly River are mainly from depths close to the Lea Park shales and can be divided into two groups: I) data where the DST recovery was dominantly water and II) data with oil but almost no water recovered. The two groups distribute areally into two corresponding zones (Fig. 5.4). Freshwater hydraulic heads in the larger part of the water-saturated zone (Ia) of the aquifer range between approximately 650 and 830 m. The general inferred flow direction is from two areas: a topographic high at $53.8^{O}$ N and $116.8^{O}$ W, and in the northwestern corner of the study area (Fig. 5.3), towards the Smoky and Little Smoky river valleys at the northern boundary. An area with very low hydraulic heads (less than 600 m in subzone Ib) is situated in the deep parts of the Brazeau-Belly River aquifer, sub-parallel to the deformation front. Relatively steep hydraulic gradients along the boundary between aquifer zones Ia and Ib are in opposite direction to the regional ground surface slope, and therefore suggest the potential for inward flow towards the foothills region.

On the p(d)-plot (Fig. 5.5a) almost all data points plot below hydrostatic, becoming increasingly underpressured with depth, which indicates a general downward direction of fluid flow. Pressure data from DSTs with oil as the dominant fluid phase plot separately, and show significant underpressuring. The oil pressure data plot approximately along the static oil gradient (Fig. 5.5b). Extrapolating this gradient to the line that represents the water gradient in subzone Ia suggest a regional oil – water contact at –500 m elevation. Hydraulic heads drop from the ground surface to the Scollard-Paskapoo aquifer, and even farther in the Brazeau-Belly River aquifer (Fig. 5.5b), indicating the potential for downward flow, and that the intervening major aquitards (Battle and Bearpaw) and other minor and localized, but frequent shaly aquitards provide a significant resistance to flow. Hence, the Brazeau-Belly River presents the characteristics of an aquifer confined by leaky and tight aquitards at the top and bottom, respectively.

The concentration of total dissolved solids (TDS) ranges between 1.7 and 10 g/L (Fig. 5.6). The salinity is lowest in the discharge region in the area of Brazeau outcrop, where the main aquitards, Battle and Bearpaw, are thin or absent, and deep formation waters can mix with shallow, meteoric groundwater. The value of 1.7 g/L is still relatively high



Reproduced with permission of the copyright owner. Further reproduction prohibited without permission.

compared to the salinity usually observed in shallow aquifers (~ 0.5 g/L). The discharge of the more saline formation water from the deep parts of the Brazeau-Belly River aquifer causes an increase in salinity in shallow aquifers in that region (Barnes, 1987; Tokarsky, 1977). Salinity increases with depth, and a plume of maximum TDS values up to 10 g/L can be observed in the region at $53.8^{O}$ N and $116.8^{O}$ W, which corresponds to high ground surface elevation (Fig. 5.3) and high hydraulic heads (Fig. 5.4).

The distribution of bicarbonate concentrations (Fig. 5.7) complements the TDS map. The main bicarbonate input in shallow groundwater systems comes from dissolved carbon dioxide from the air, and dissolution of carbonate mineral (Freeze and Cherry, 1979; p. 241-243). The concentration decreases with increasing residence time of the formation water due to adsorption processes and flushing from the active flow zone (Freeze and Cherry, 1979). Bicarbonate values in the study area are highest in the region of shallow groundwater influence in the northeast and along the foothills.

*Colorado aquifers*

The flow in the Chinook and Badheart aquifers could not be analyzed and interpreted because of the lack of data. Figures 5.8 to 5.11 present, respectively, the distribution of freshwater hydraulic heads, p(d)- and p(z)-plots, and distributions of salinity and bicarbonate in the Cardium aquifer.

Hydraulic heads in the 700 – 800 m range in subzone Ia in the Cardium aquifer (Fig. 5.8) correspond to the elevation of the Cardium Formation outcrop some 50 km north of the study area to which this part of the aquifer appears to be hydraulically connected. Pressures are hydrostatic in the northern, shallow part of subzone Ia and develop into sub-hydrostatic pressures with increasing depth (Fig. 5.9 a) and towards the southeast. Hydraulic heads in the 350 – 500 m range in subzone Ib are significantly lower than the heads in subzone Ia (Fig.5.8), and the corresponding pressures plot along a separate, underpressured gradient (Fig. 5.9 b). The dominantly hydrocarbon-saturated zone II in



Reproduced with permission of the copyright owner. Further reproduction prohibited without permission.

the Cardium aquifer can be subdivided into an oil- and a gas-saturated subzone, IIa & b and IIc, respectively. The pressures in these subzones, although similarly located downdip of the water-saturated zones as in the Brazeau-Belly River aquifer, fall approximately on the hydrostatic gradient (subzones IIc) or plot above hydrostatic (subzone IIa & b) (Fig. 5.9).

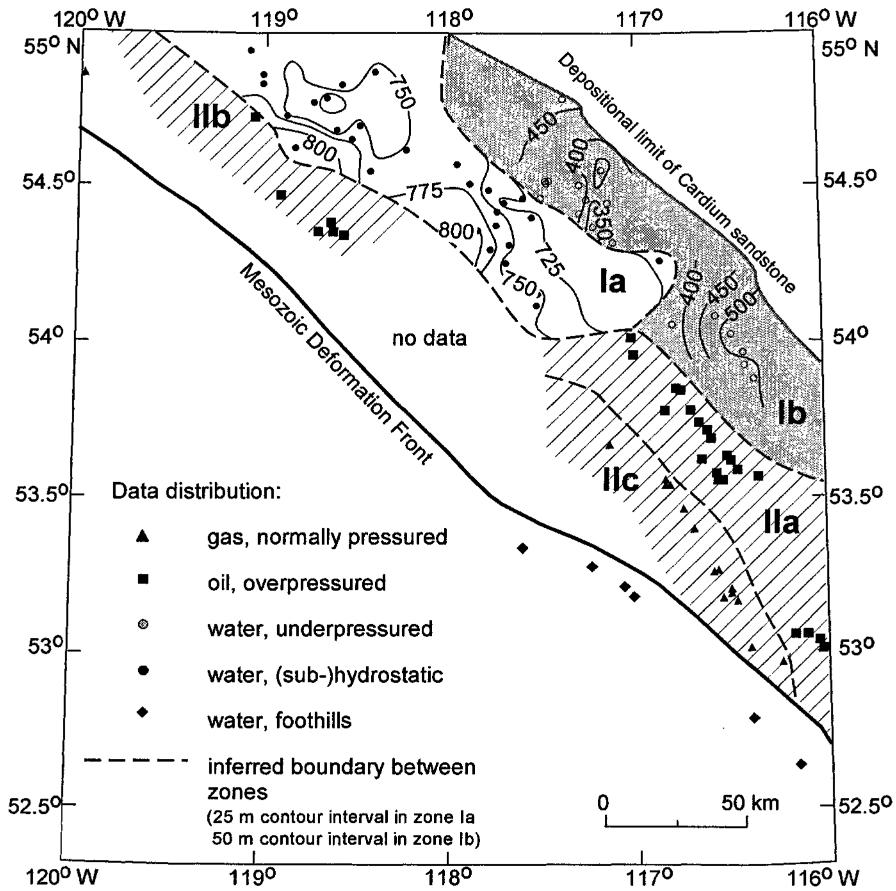


Figure 5.8: Freshwater hydraulic head distribution and aquifer zonation in the Cardium aquifer (note the different contour intervals).



Reproduced with permission of the copyright owner. Further reproduction prohibited without permission.

Reproduced with permission of the copyright owner. Further reproduction prohibited without permission.



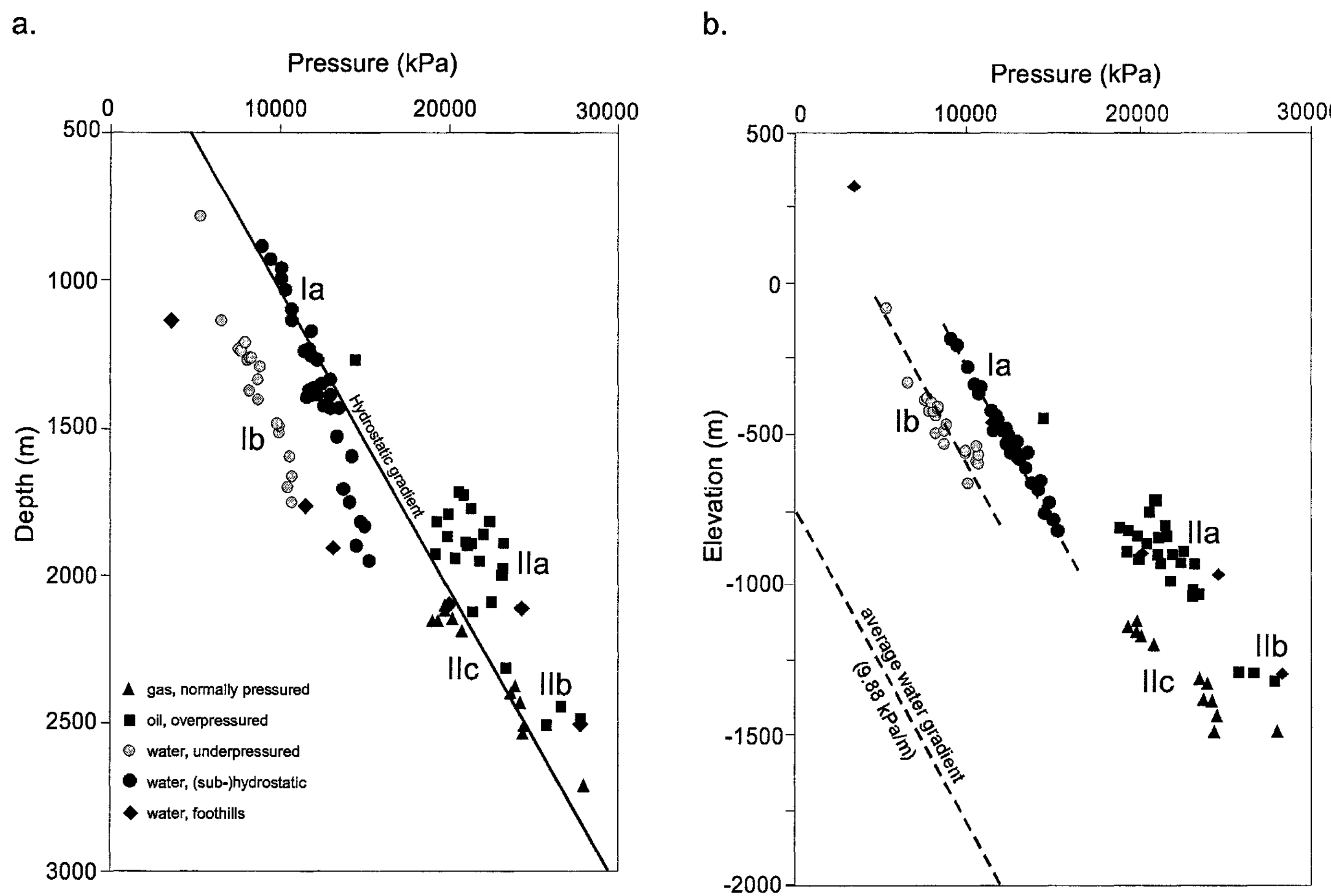


Figure 5.9: Pressure variation with: a) depth and b) elevation in the Cardium aquifer. The data groups denoted by roman numbers correspond to the geographic distributions shown in Figure 5.8.

Reproduced with permission of the copyright owner. Further reproduction prohibited without permission.

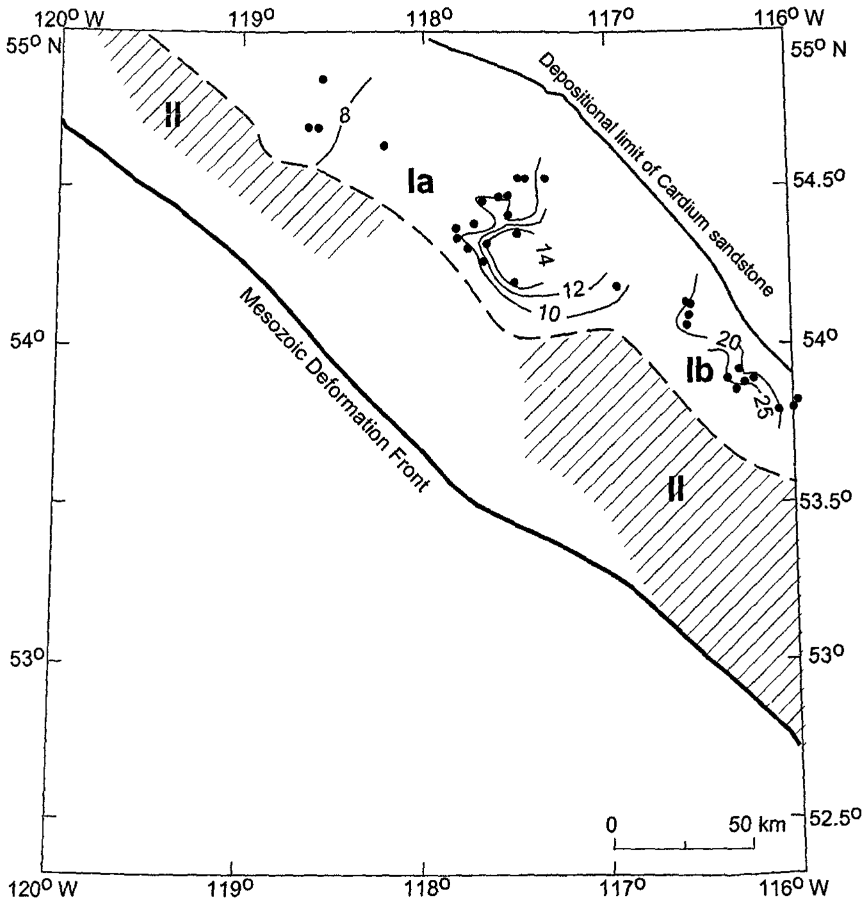


Figure 5.10: Salinity distribution in the Cardium aquifer (note the different contour intervals). (Sub-)zones Ia, Ib and II correspond to the zonation in Figure 5.8.

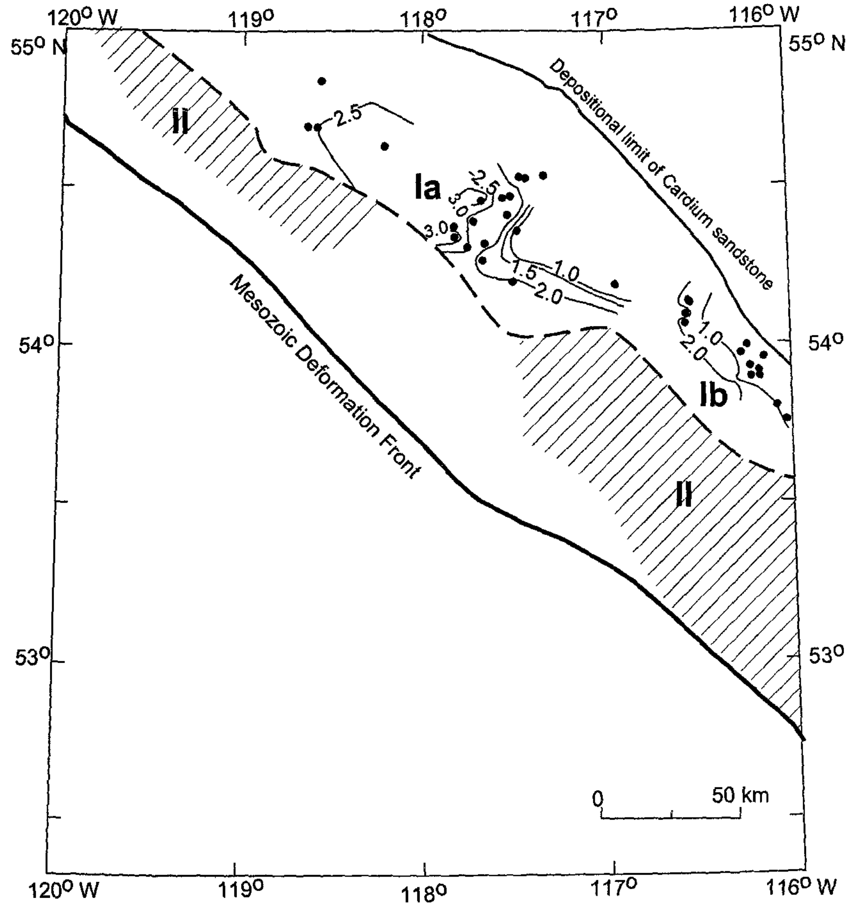


Figure 5.11: Bicarbonate distribution in the Cardium aquifer (0.5 g/l contour interval). (Sub-)zones Ia, Ib and II correspond to the zonation in Figure 5.8.

The salinity of formation waters in subzone Ia increases from 7 g/L to approximately 14 g/L (Fig. 5.10) in the direction of southeastward decreasing hydraulic heads (Fig. 5.8). Higher salinities in subzone Ib, in the 20 – 25 g/L range, suggest that this part of the aquifer is largely cut off from meteoric recharge. This is supported by the slightly higher range in bicarbonate concentrations (1 – 3 g/L) in subzone Ia compared to 1 – 2 g/L in subzone Ib (Fig. 5.11).

Figures 5.12 to 5.15 present, respectively, the distribution of freshwater hydraulic heads, p(d)- and p(z)-plots, and the distributions of salinity and bicarbonate in the Dunvegan aquifer. Hydraulic heads in subzone Ia show only a small variation between 500 and 550 m (Fig. 5.12) so that flow directions cannot easily be established. The Dunvegan aquifer crops out at elevations of 455 to 610 m along the Peace River some 100 km north of the study area and, therefore, a hydraulic connection of subzone Ia to the ground surface seems likely. Pressures (Fig. 5.13) and hydraulic heads in subzone Ib are significantly lower and appear to be isolated from other aquifer zones, as well as from the ground surface. Zone II in the deeper parts of the Dunvegan aquifer is dominantly gas-saturated, with slightly sub- to slightly above-hydrostatic pressures (Fig. 5.13). The salinity in the water-saturated zone is in the range of 7 to 13 g/L (Fig. 5.14) and bicarbonate concentration ranges between 0.9 to 2.8 g/L (Fig. 5.15), but data are too scarce to construct meaningful contour maps.



Reproduced with permission of the copyright owner. Further reproduction prohibited without permission.

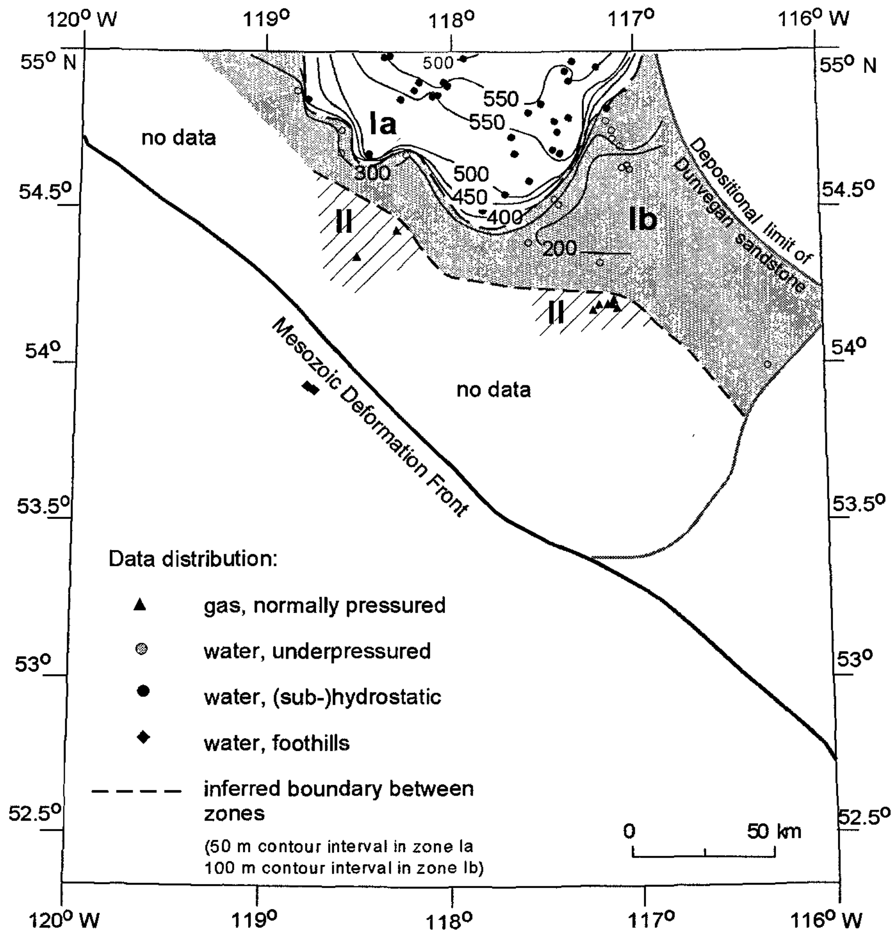


Figure 5.12: Freshwater hydraulic head distribution and aquifer zonation in the Dunvegan aquifer (note the different contour intervals).



Reproduced with permission of the copyright owner. Further reproduction prohibited without permission.

Reproduced with permission of the copyright owner. Further reproduction prohibited without permission.



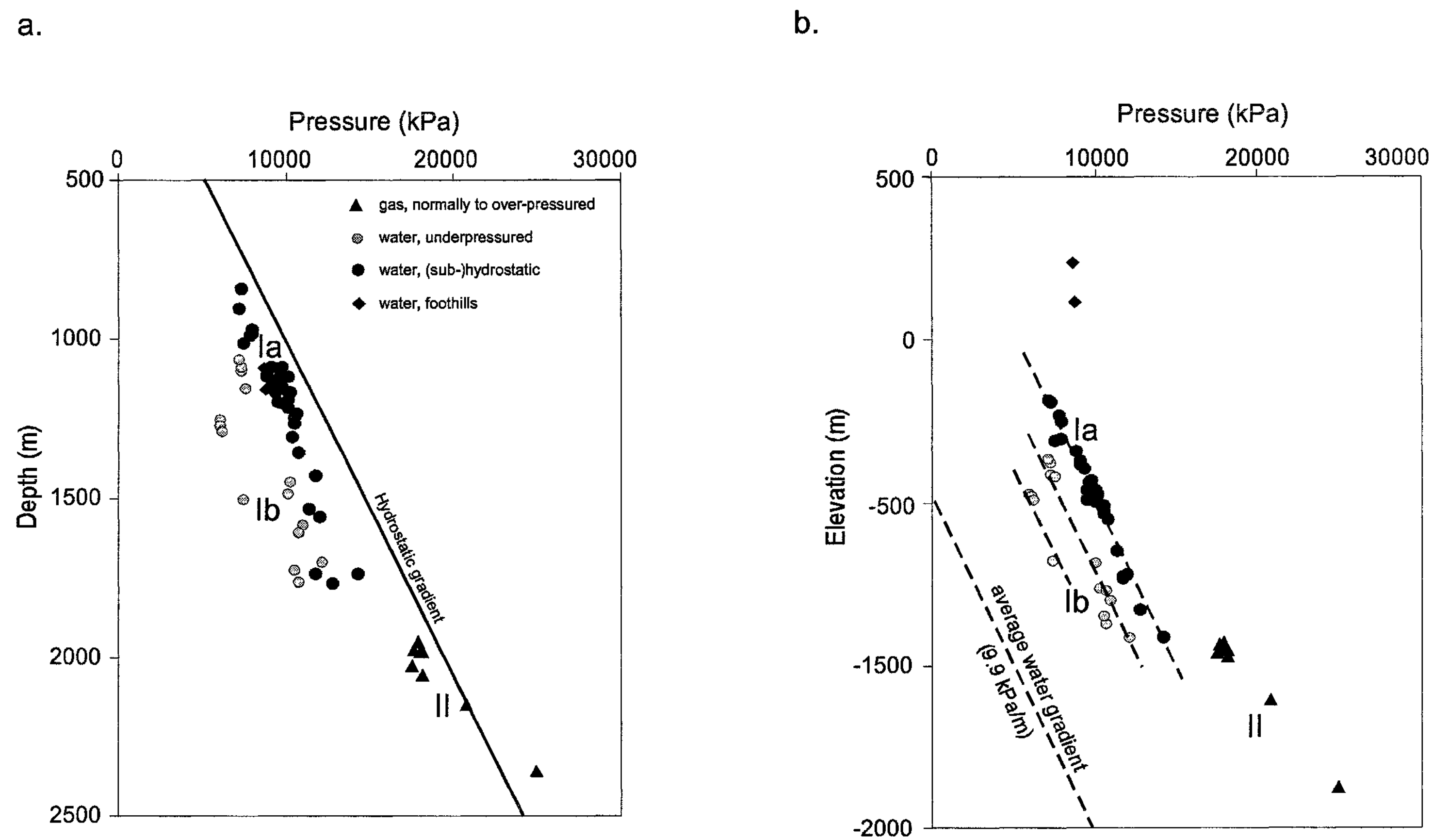


Figure 5.13: Pressure variation with: a) depth and b) elevation in the Dunvegan aquifer. The data groups denoted by roman numbers correspond to the geographic distributions shown in Figure 5.12.

Reproduced with permission of the copyright owner. Further reproduction prohibited without permission.



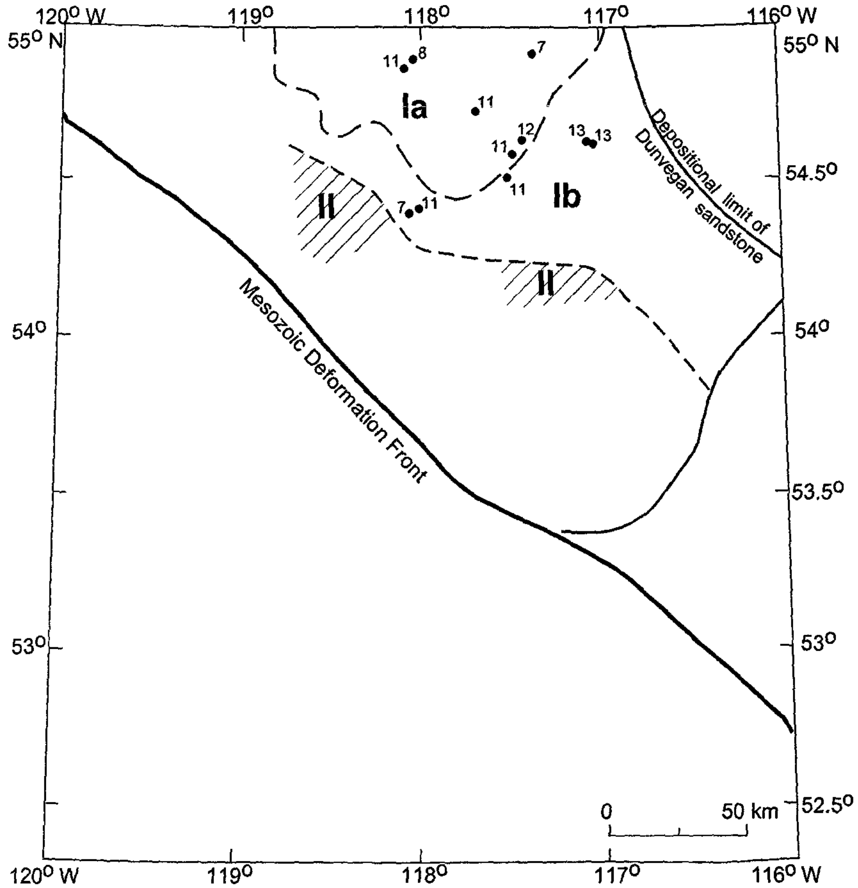


Figure 5.14: Salinity distribution in the Dunvegan aquifer (point values in g/l). (Sub-)zones Ia, Ib and II correspond to the zonation in Figure 5.12.

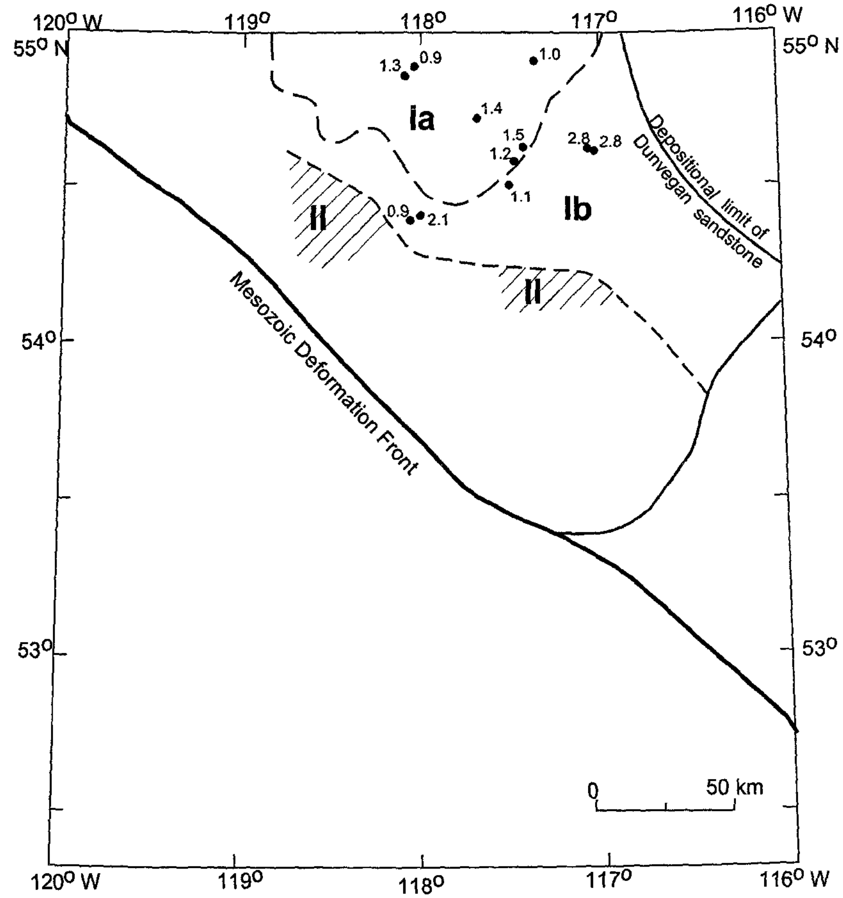


Figure 5.15: Bicarbonate distribution in the Dunvegan aquifer (point values in g/l). (Sub-)zones Ia, Ib and II correspond to the zonation in Figure 5.12.

Figures 5.16 to 5.19 present, respectively, the distribution of freshwater hydraulic heads, p(d)- and p(z)-plots, and distributions of salinity and bicarbonate in the Viking aquifer. Hydraulic heads (Fig. 5.16) are also in the 500 m and 300 to 450 m range in subzones Ia and Ib, respectively, like in the overlying Dunvegan aquifer, but the respective subzones in both aquifers do not overlap. The change in the hydraulic gradient and the difference between the sub-hydrostatically pressured (Ia) and underpressured (Ib) subzones (Figs. 5.16 & 5.17) are not as sharp as the changes in the Cardium and Dunvegan aquifers.

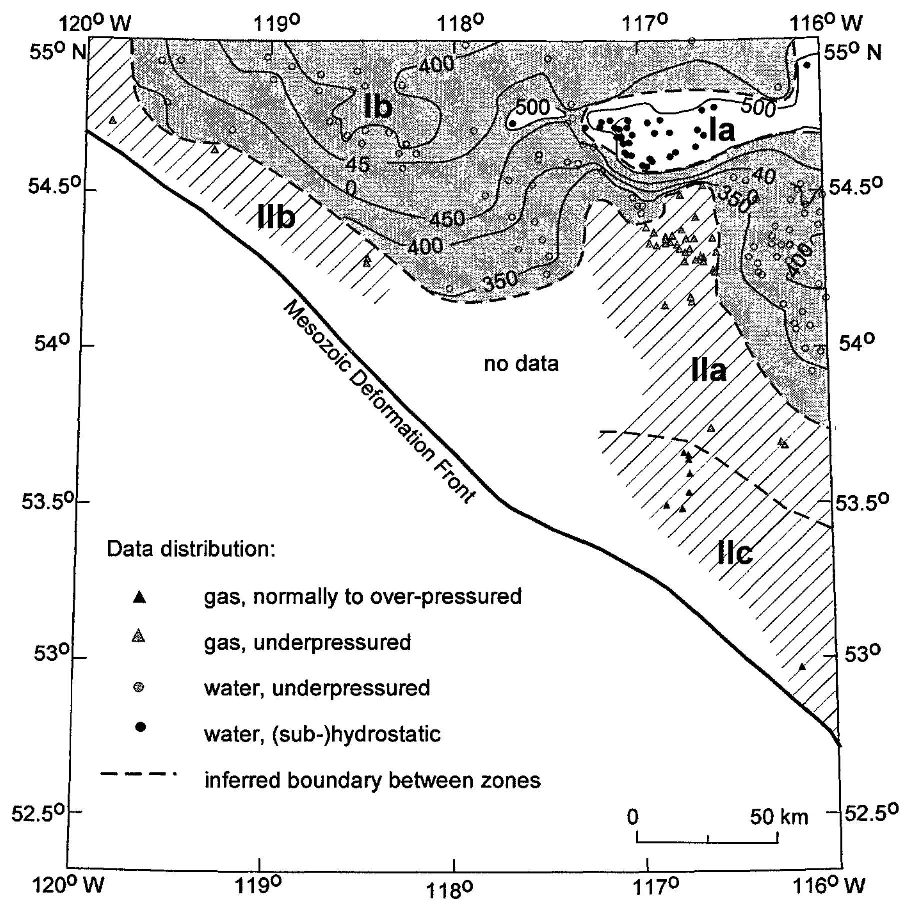


Figure 5.16: Freshwater hydraulic head distribution and aquifer zonation in the Viking aquifer (50 m contour interval).



Reproduced with permission of the copyright owner. Further reproduction prohibited without permission.

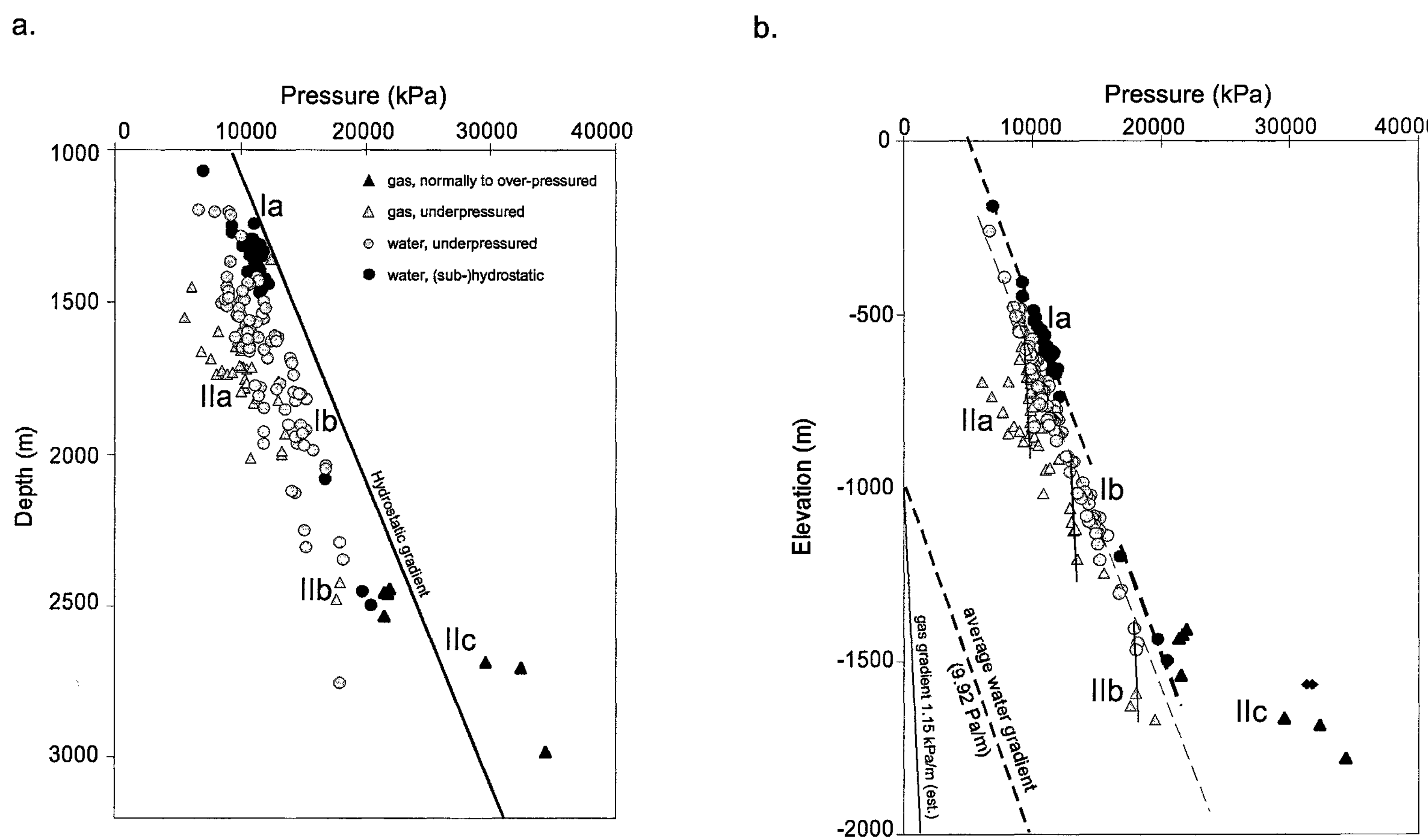


Figure 5.17: Pressure variation with: a) depth and b) elevation in the Viking aquifer. The data groups denoted by roman numbers correspond to the geographic distributions shown in Figure 5.16.



Reproduced with permission of the copyright owner. Further reproduction prohibited without permission.

Reproduced with permission of the copyright owner. Further reproduction prohibited without permission.



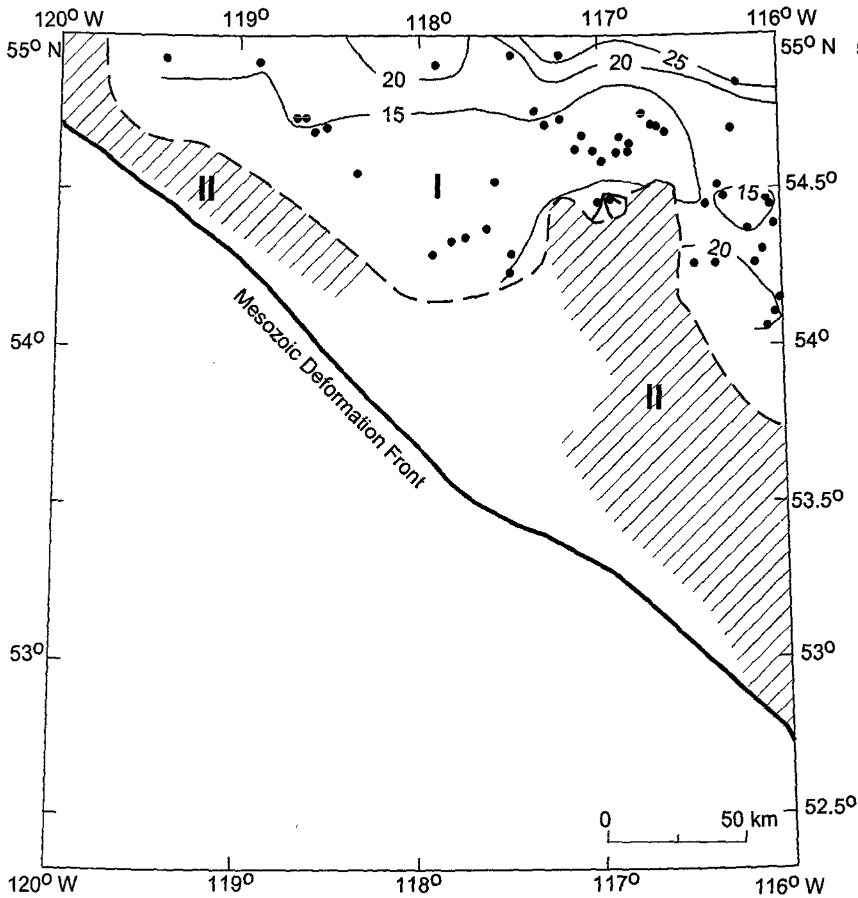


Figure 5.18: Salinity distribution in the Viking aquifer (5 g/l contour interval). Zones I and II correspond to the zonation in Figure 5.16.

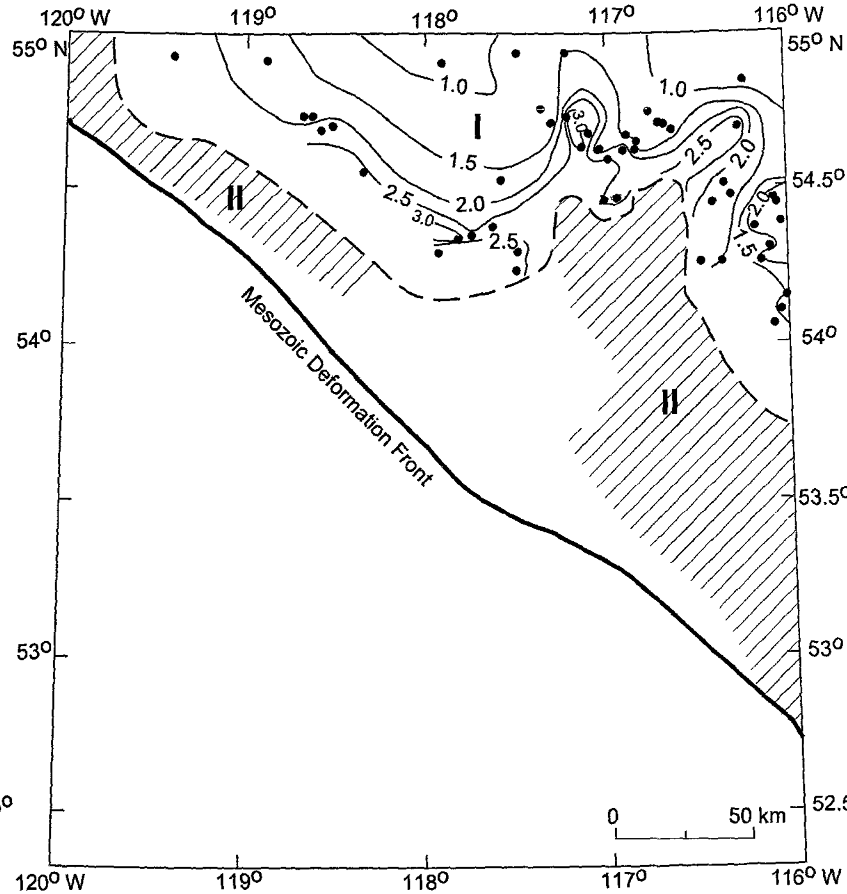


Figure 5.19: Bicarbonate distribution in the Viking aquifer (0.5 g/l contour interval). Zones I and II correspond to the zonation in Figure 5.16.

Maximum hydraulic heads in the Viking aquifer (~500 m) can be observed in subzone Ia, which appears to be rather isolated, except for a possible continuation of this subzone beyond the northeast corner of the study area (Fig. 5.16). Hence, the flow in subzone Ia may be either laterally from or to the northeast, or vertical from over- or underlying aquifers. The gas-saturated zone in the deep parts of the Viking can be further subdivided into subzones IIa & b and IIc, with sub-hydrostatic and slightly sub-hydrostatic to above-hydrostatic pressures, respectively (Fig. 5.16 & 5.17). Pressures in subzones IIa & b plot approximately along a static gas gradient, suggesting that this zone represents an unconventional gas accumulation downdip of a water leg.

The salinity decrease from 25 g/L in the northeast to < 15 g/L in the center, along the boundary to the gas-saturated zone II (Fig. 5.18), coincides with the general flow direction, which is unexpected because salinity generally increases along the flowpath and downdip in other units. Bicarbonate concentrations, increasing towards the south, range between 1 and 3 g/L (Fig. 5.19) and, are similar to concentrations in the overlying aquifers.



Reproduced with permission of the copyright owner. Further reproduction prohibited without permission.

*Mannville aquifers*

Figures 5.20 to 5.27 present, respectively, the distribution of freshwater hydraulic heads, p(d)- and p(z)-plots, and distributions of salinity and bicarbonate in the Mannville aquifers. Hydraulic heads in subzone Ia of the Upper and Lower Mannville aquifers vary from 700 to 550 m, and 600 to 550 m, respectively (Figs. 5.20 & 5.21), with the maximum value being higher than that of hydraulic heads in the overlying Viking aquifer. Hydraulic heads in the Upper Mannville aquifer generally decrease eastward from highs (700 m) in the northwest, suggesting eastward flow along the northern boundary of the study area, with the flow originating from the north of the study area. In the Lower Mannville aquifer, hydraulic gradients in subzone Ia indicate relatively stagnant flow conditions, with the exception of restricted flow towards the underpressured subzone Ib in the east. Subzone Ib in the Mannville aquifers is relatively small and restricted to a narrow band of low hydraulic heads between the gas-saturated zone and the sub-hydrostatically pressured water in subzone Ia. The gas-saturated zones II in the Upper and Lower Mannville aquifers have a similar configuration as that in the Viking aquifer, except for a closed subzone IIb of sub-hydrostatic gas that can be observed in the northeast in the Upper Mannville aquifer (Fig. 5.20). Pressure variations with depth and elevation in the Upper and Lower Mannville aquifers show the same trend as in the Viking aquifer, indicating a relatively moderate change in pressure from zone Ia to Ib (Figs. 5.22 & 5.23).

The salinity data from the Upper Mannville aquifer generally increase northward from 9 to 36 g/L) (Fig. 5.24) and are slightly higher in value to the salinity range in the overlying Viking aquifer. Formation water salinity in the Lower Mannville aquifer (Fig. 5.26) ranges between 35 g/L in the north and 90 g/L in the northwest, with a general trend of downdip increase in salinity. The bicarbonate concentration in both Mannville aquifers ranges approximately between 0.5 and 2.5 g/L (Figs. 5.25 & 5.27). In the Lower Mannville aquifer the bicarbonate concentration decreases towards the south, opposed to the trend of increasing salinity, whereas in the Upper Mannville aquifer it increases in that direction.



Reproduced with permission of the copyright owner. Further reproduction prohibited without permission.

Reproduced with permission of the copyright owner. Further reproduction prohibited without permission.

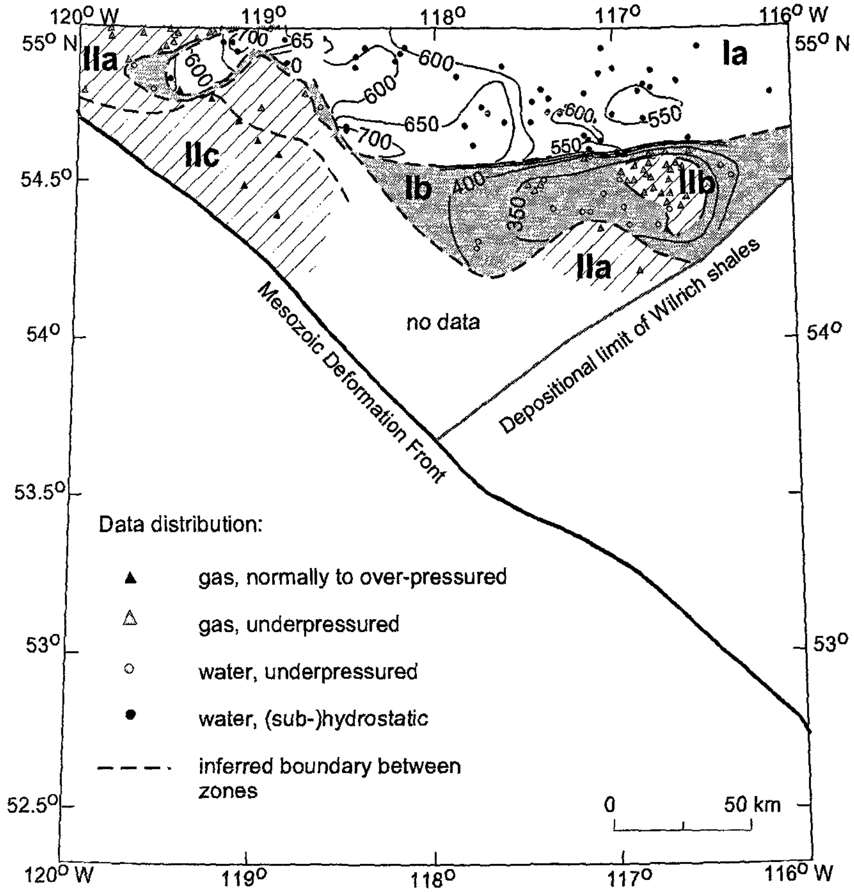


Figure 5.20: Freshwater hydraulic head distribution and aquifer zonation in the Upper Mannville aquifer (50 m contour interval).

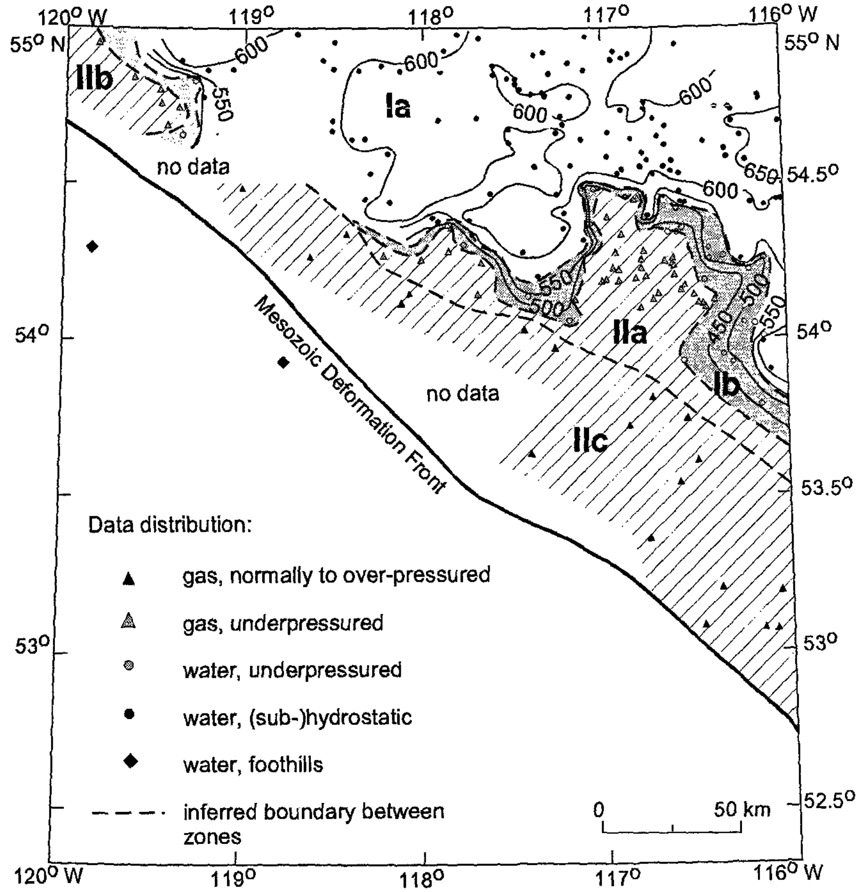


Figure 5.21: Freshwater hydraulic head distribution and aquifer zonation in the Lower Mannville aquifer (50 m contour interval).

Reproduced with permission of the copyright owner. Further reproduction prohibited without permission.



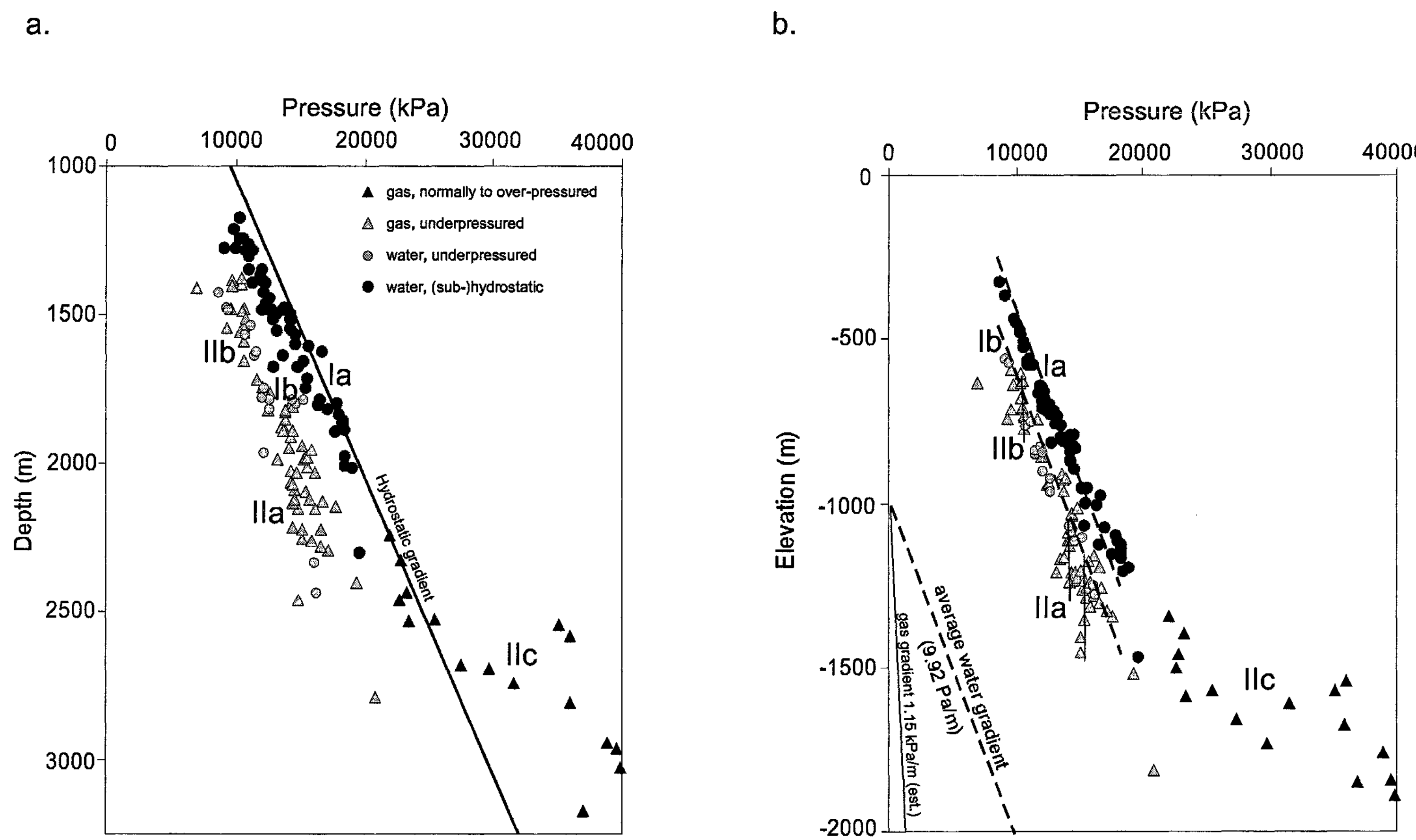


Figure 5.22: Pressure variation with: a) depth and b) elevation in the Upper Mannville aquifer. The data groups denoted by roman numbers correspond to the geographic distributions shown in Figure 5.20.

Reproduced with permission of the copyright owner. Further reproduction prohibited without permission.

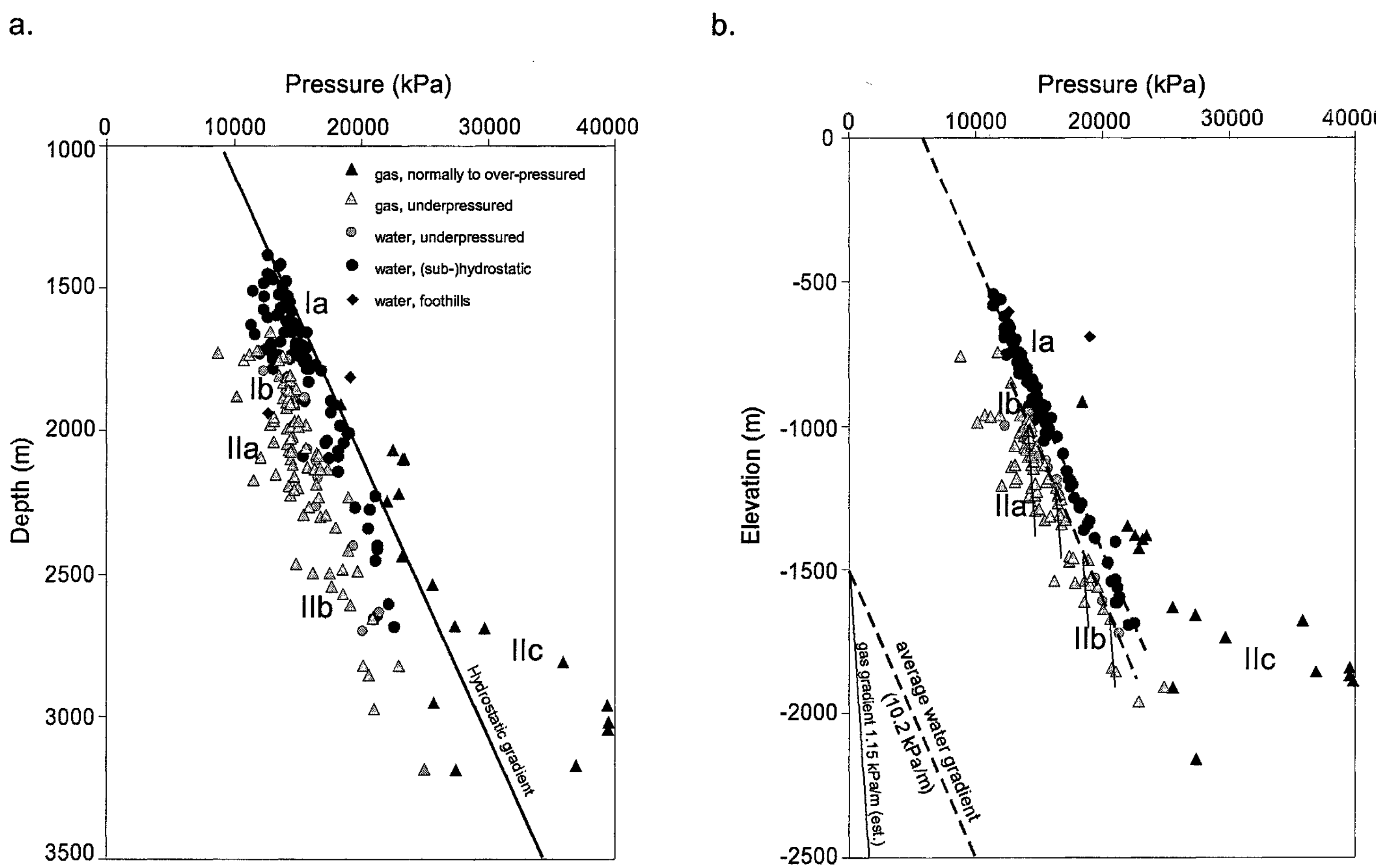


Figure 5.23: Pressure variation with: a) depth and b) elevation in the Lower Mannville aquifer. The data groups denoted by roman numbers correspond to the geographic distributions shown in Figure 5.21.

Reproduced with permission of the copyright owner. Further reproduction prohibited without permission.

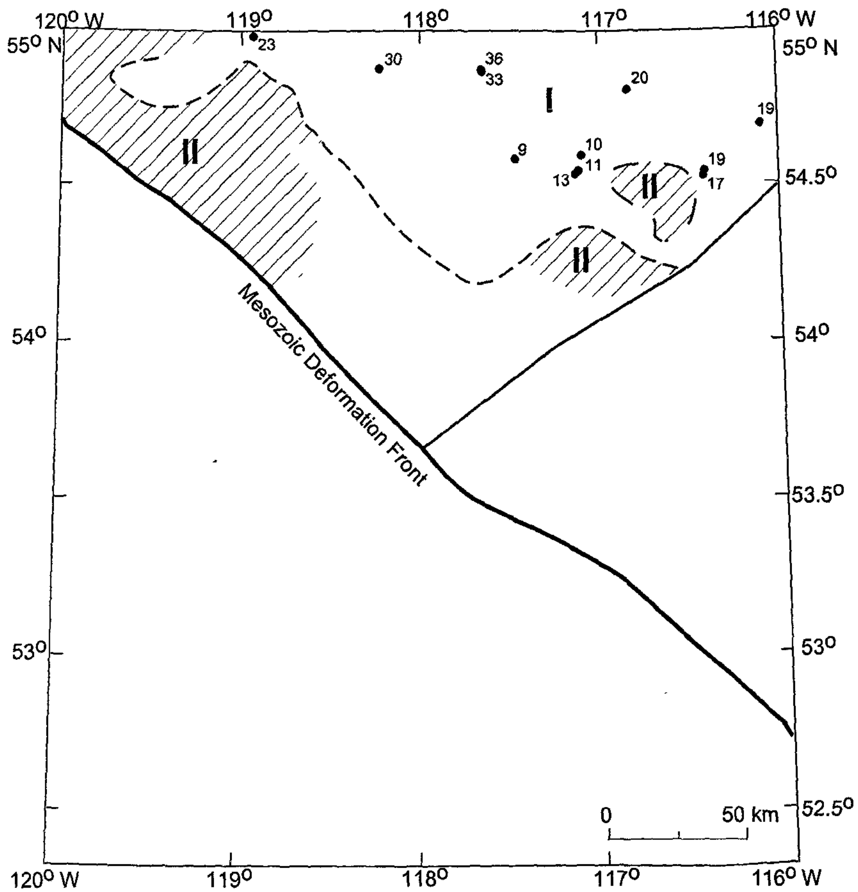


Figure 5.24: Salinity distribution in the Upper Mannville aquifer (point values in g/l). Zones I and II correspond to the zonation in Figure 5.20.

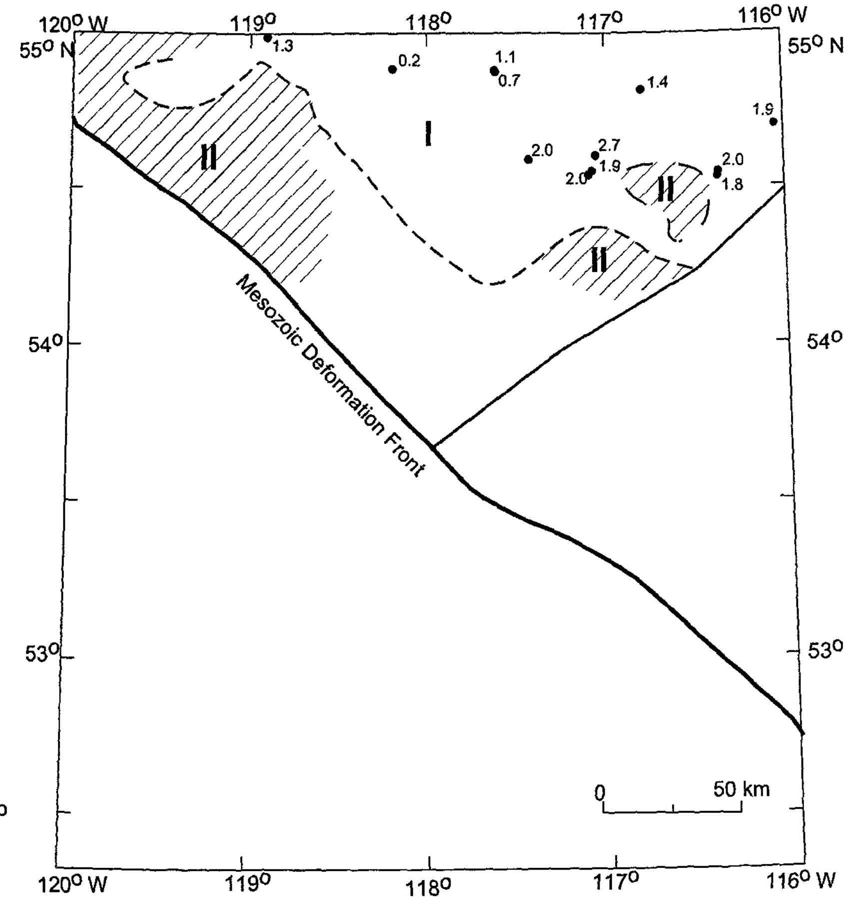


Figure 5.25: Bicarbonate distribution in the Upper Mannville aquifer (point values in g/l). Zones I and II correspond to the zonation in Figure 5.20.

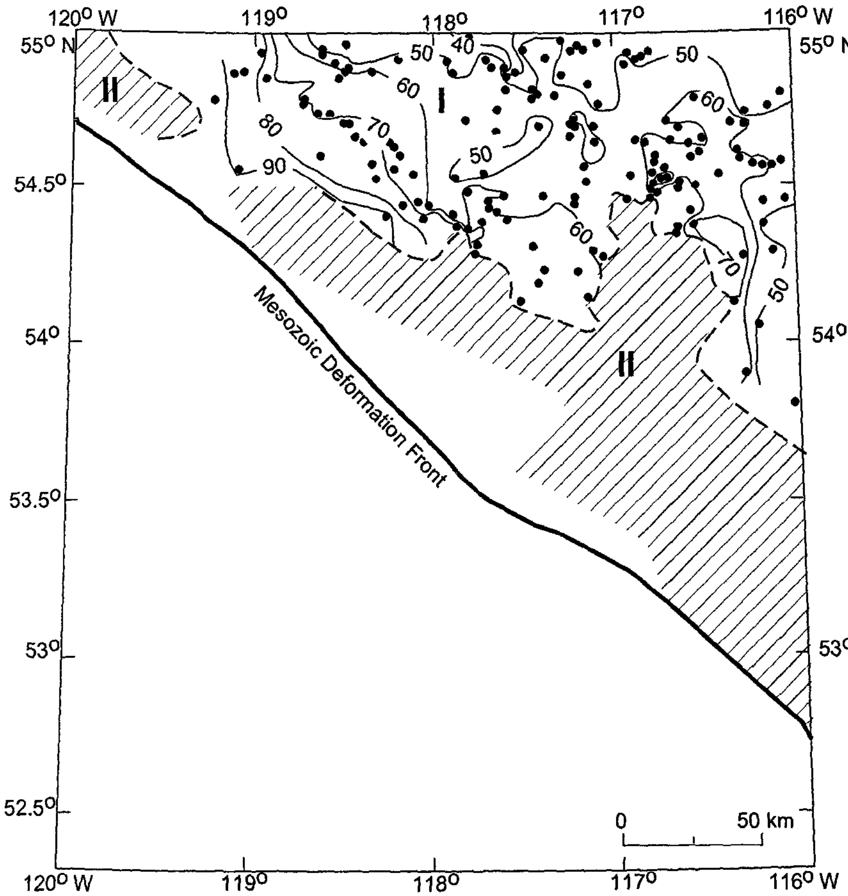


Figure 5.26: Salinity distribution in the Lower Mannville aquifer (10 g/l contour interval). Zones I and II correspond to the zonation in Figure 5.21.

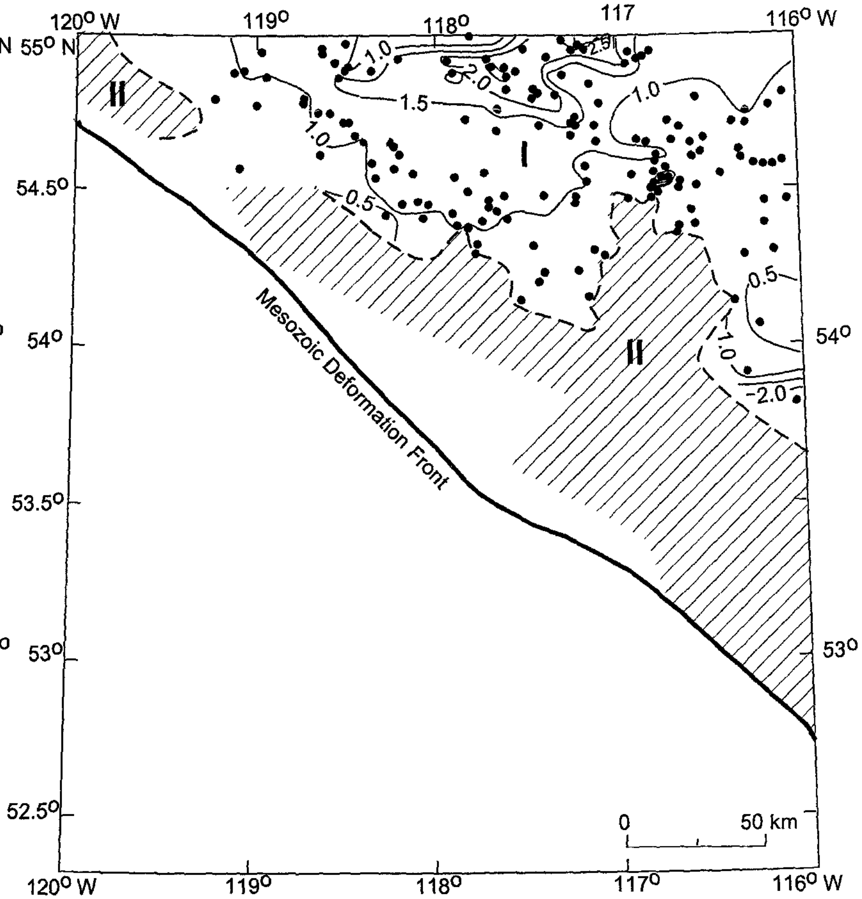


Figure 5.27: Bicarbonate distribution in the Lower Mannville aquifer (0.5 g/l contour interval). Zones I and II correspond to the zonation in Figure 5.21.



Reproduced with permission of the copyright owner. Further reproduction prohibited without permission.

The variation in the major cations with respect to the chloride concentration are shown in Figure 5.28 and are compared to the composition of average seawater and the seawater-dilution curves experimentally derived by McCaffrey et al. (1986). Sodium concentrations in all aquifer units plot along the seawater evaporation-dilution trend (SET) (Fig. 5.28a). In contrast, formation waters are significantly depleted in magnesium in comparison to the SET (Fig. 5.28b), whereas calcium concentrations plot below and above the SET (Fig. 5.28c).

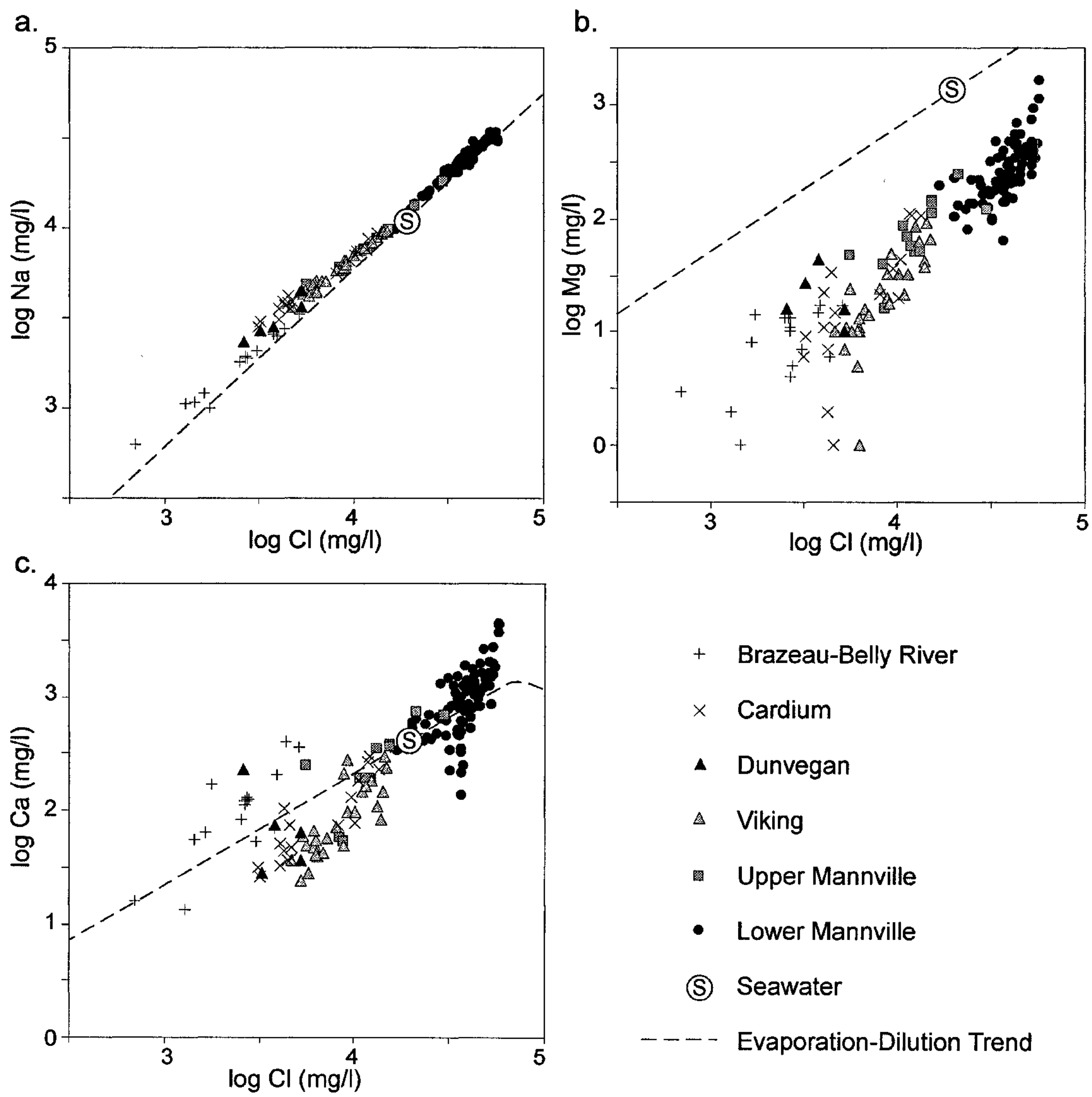


Figure 5.28: Cross plots versus chloride of: a) sodium, b) magnesium, and c) calcium for Cretaceous formation waters in the study area. The various evaporation trends were determined experimentally by McCaffrey et al. (1986).



Reproduced with permission of the copyright owner. Further reproduction prohibited without permission.

*Summary of hydrogeological analysis*

- The Mannville-to Brazeau-Belly River aquifers all have a hydrocarbon-saturated zone (II) downdip of a water-saturated zone (I).
- The hydrostatic to sub-hydrostatically pressured water-saturated subzone (Ia) is separated in most aquifers from the hydrocarbon-saturated zone by an underpressured water subzone (Ib). The only exception is the Cardium aquifer, where subzone Ia lies directly updip of subzone IIb in the northwestern part of the aquifer.
- The areal extent of the underpressured water-saturated subzone Ib successively increases with depth until it reaches its maximum in the Viking aquifer. In the Mannville aquifers it narrows down to a relatively thin band. The average hydraulic head values in subzone Ib also decrease with depth to a minimum of ~200 m in the Dunvegan aquifer, but increase again in the Viking and Mannville aquifers.
- The fluid type and the pressure in the hydrocarbon-saturated zone change (Tab. 5.1), while the area it encompasses increases with depth: Brazeau-Belly River – oil, underpressured; Cardium – oil, overpressured (IIa & b) and gas, normally pressured (IIc); Dunvegan – gas, normally pressured; Viking and Mannville – gas underpressured (IIa & b) and gas, normally to overpressured (IIc).
- The main hydrochemical trend is the increase in salinity with depth. A salinity of formation waters < 15 g/L is observed in the post-Colorado aquifers and in subzone Ia in the Cardium and Dunvegan aquifers. An approximate range of 15 – 30 g/L represents formation waters from the Viking aquifer and isolated parts (zone Ib) in the Colorado aquifers, and a 35 – 90 g/L range characterizes Mannville Group water. For comparison, modern-day seawater has a salinity of approximately 35 g/L.
- Generally, post-Jurassic formation waters are depleted in magnesium compared to evaporated or diluted seawater.



Reproduced with permission of the copyright owner. Further reproduction prohibited without permission.

## 5.4 Interpretation of flow patterns and fluid distributions

Several general conclusions can be drawn from the hydrogeological analysis presented above that will be further discussed in this section.

- The similarity between hydraulic head distributions and the ground surface relief decreases with depth, which suggests that the vertical hydraulic communication between various aquifers and the ground surface decreases with depth.
- The increase of formation water salinity with depth, up to three times higher than that of seawater, suggests that the penetration of fresh meteoric water into deeper aquifers is limited.
- Magnesium and calcium concentrations indicate that other or additional processes than seawater evaporation and dilution must have influenced the evolution of formation waters.
- The subdivision of each aquifer into (sub-)zones, as shown in sharp changes in fluid and pressure distributions, suggests the existence of *lateral permeability or transmissivity changes* in each aquifer (see Chapter 2, 2.3), which results in retardation of pressure equilibration between (sub-)zones and/or the escape of hydrocarbons generally located downdip.
- The hydrogeological similarities between certain adjacent aquifers or parts thereof may indicate areas of *cross-formational flow* across weak aquitards. On the other hand, discontinuous changes in fluid pressure or water chemistry between aquifers imply that the intervening aquitards are effective barriers to flow.
- The existence of large hydrocarbon-saturated zones in the aquifers implies that, at least at some point in time, the rate of hydrocarbon generation was high enough to displace the connate water from the pore space. Therefore, it seems that *hydrocarbon generation and migration* have influenced and continue to influence the flow of formation water.
- Severe underpressuring in parts of the aquifers suggests that at least one alternative *flow-driving mechanism*, different from topography-driven flow, must be active in this part of the Alberta Basin. These underpressures can only be maintained in an overall *low-permeability environment* (see Chapter 2).



Reproduced with permission of the copyright owner. Further reproduction prohibited without permission.

*Aquitard competence and cross-formational flow*

The aquitards in the study area are generally formed by shaly formations that separate or subdivide the various aquifers. The main aquitards are: Battle, Bearpaw, Lea Park, the cumulative Colorado shales, Joli Fou, and Wilrich (Fig. 5.2), which will be discussed in the order of their occurrence from the ground surface downwards.

The relatively fresh water in the Brazeau-Belly River aquifer and the similarity between the hydraulic head distribution and the ground surface relief suggest that the intervening Battle and Bearpaw aquitards are leaky. Nevertheless, they introduce sufficient resistance to flow for hydraulic heads to be below the ground surface, thus indicating semi-confined flow conditions in the Brazeau-Belly River aquifer.

On the other hand, the lack of any similarity between the ground surface topography and the hydraulic head distribution in the underlying Colorado and Mannville aquifers and the offset of fluid pressures in the p(z)-plots in Figure 5.29b & c indicate that the Lea Park aquitard and the cumulatively up to 1500 m thick Colorado shales effectively obstruct vertical hydraulic communication between the ground surface and these aquifers. In addition, the relatively high formation water salinity in the Colorado and Mannville aquifers confirms their isolation from meteoric recharge by the intervening Lea Park and Colorado aquitards.

Regarding the hydraulic communication between aquifers embedded in the Colorado shales, the offset of pressures in the p(z)-plot (Fig. 5.29a) show that the intervening aquitards between the water-saturated (sub-)zones in the Cardium and Dunvegan and between the Dunvegan and Viking aquifers are relatively strong in the northwest of the study area. Farther east on the other hand, pressures plot along a similar gradient (Fig. 5.29b) and cross-formational flow appears to be possible. Nevertheless, it should be noted that the intervening aquitards between the respective aquifers in that area are more than 100 m thick, rendering cross-formational flow rather unlikely. In addition, water pressures in the Cardium to Viking aquifers in the p(z)-plot (Fig. 5.29b) are all from the underpressured subzone Ib, and the similarities in pressure distribution could be explained also by a similar sink in each aquifer that extracts water at the same rate in all three aquifers.



Reproduced with permission of the copyright owner. Further reproduction prohibited without permission.

Reproduced with permission of the copyright owner. Further reproduction prohibited without permission.



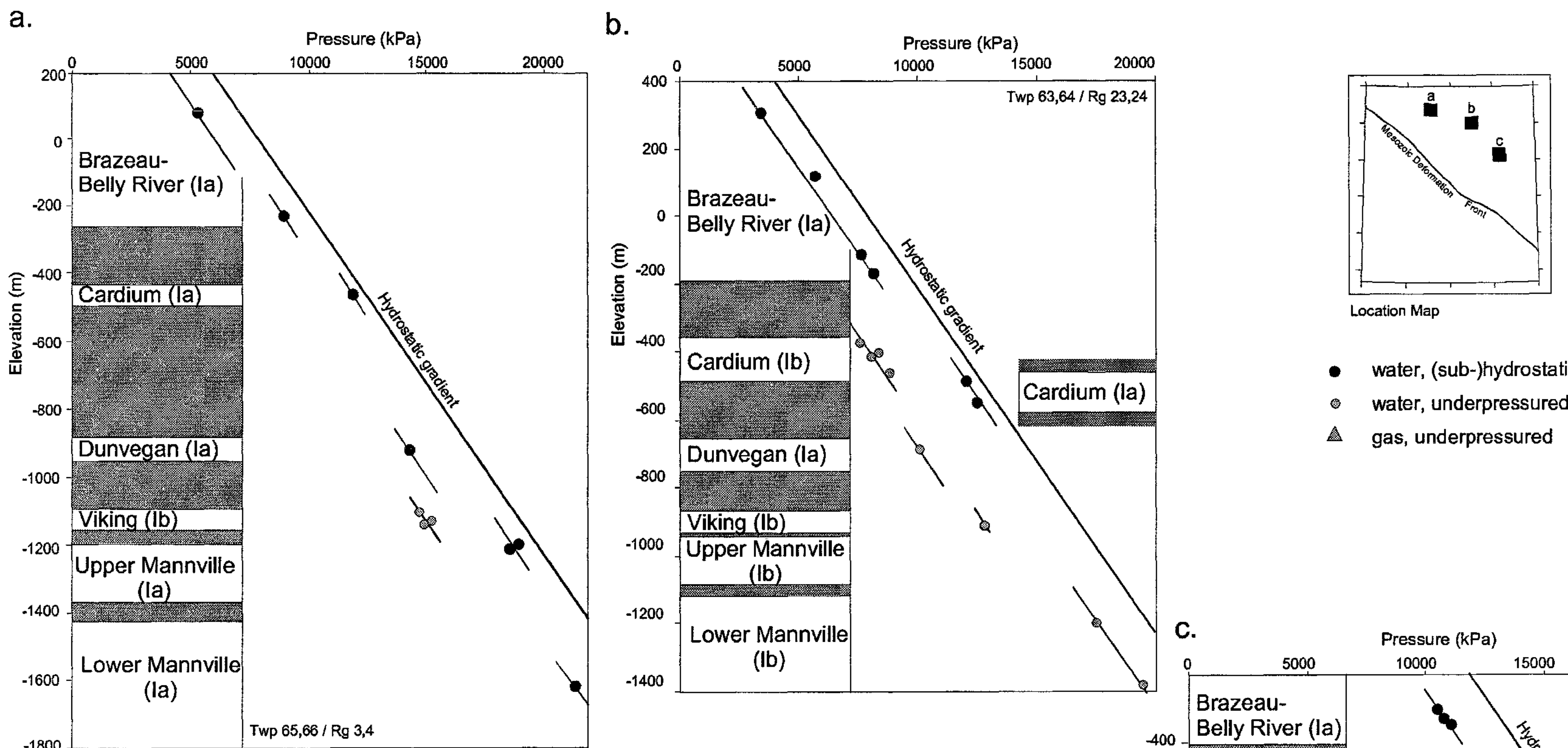


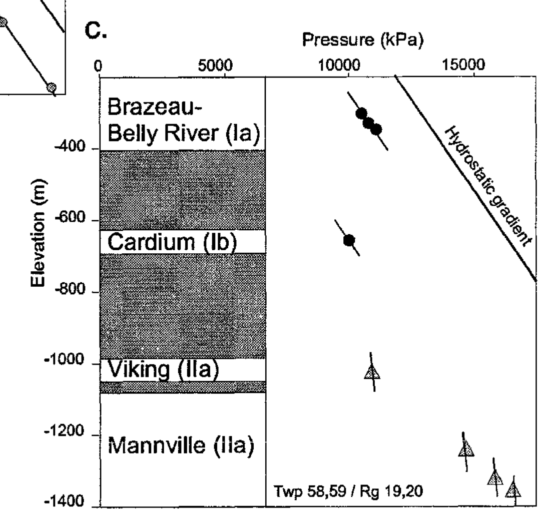


Figure 5.28: Pressure-elevation plots through the post-Jurassic succession in various regions (a, b, c) of the study area (roman numbers indicate aquifer zone) . Large offsets between different lines of static pressure gradient across aquitards show that these aquitards are strong barriers to cross-formational flow in the respective area (see Chapter 2, 2.3). Also note lateral changes over a short distance within the Cardium aquifer (b).

The competence of the Joli Fou aquitard has been demonstrated north and northeast of the study area (Hitchon et al., 1990; Bachu and Underschultz, 1993). To the southeast this aquitard appears to be weak or even absent (Rostron and Tóth, 1997), the transition zone most probably running through the study area. Comparing hydraulic heads in the Viking and the Upper Mannville aquifers indicates that the intervening Joli Fou aquitard is strong in the northwest corner of the study area. This is supported by the distinct offset of respective pressure data from these aquifers in the p(z)-plot for that area (Fig. 5.29a). In the northeast on the other hand, hydraulic heads (~550 m) in subzone Ia in the Upper Mannville aquifer are only slightly higher than hydraulic heads (~500 m) in the directly overlying Viking aquifer, so that upward cross-formational flow through the relatively thin Joli Fou aquitard in that area seems likely. Therefore, it appears that the Joli Fou Formation is a strong aquitard only in the northwestern part of the study area, where it is referred to as the Harmon Formation. The aquitard becomes relatively weak towards the east. The gas-saturated region along the deformation front complicates the interpretation of the Joli Fou aquitard competence in that area. A basin-scale study based on oil-source rock correlations suggests that no oils in the Colorado and post-Colorado succession originate from pre-Colorado source rocks (Allan and Creaney, 1991); i.e., the Joli Fou aquitard is strong. Nevertheless, it is entirely possible that gas in the hydrocarbon-saturated zone has migrated from Mannville to Viking reservoirs, but this needs to be established by comparison of gas analyses.

The differences in hydraulic heads and salinity distribution between the Upper and Lower Mannville aquifers and the p(z)-plot (Fig. 5.29a) suggest that the intervening Wilrich shales represent a relatively strong aquitard in the northwestern half of the study area. In the southeastern half the Wilrich shales are absent, which probably allowed gas to escape upward from subzone IIa in the Lower Mannville aquifer, and to form the closed gas accumulation in subzone IIb in the Upper Mannville aquifer (Fig. 5.20).

The high salinities (70 – 90 g/L) in subzone Ia in the northeast of the Lower Mannville aquifer (Fig. 5.26) at the base of the post-Jurassic hydrostratigraphic group probably can be explained by cross-formational flow across a weak Fernie aquitard from the



Reproduced with permission of the copyright owner. Further reproduction prohibited without permission.

underlying Triassic aquifer that contains formation water in a comparable salinity and pressure range (see Chapter 6).

*Lateral low-permeability barriers*

In addition to the competent shale aquitards that impede hydraulic communication with the ground surface and between various aquifers, the distribution of fluids and pressures in the post-Jurassic succession indicates that large-scale lateral permeability barriers exist within the individual aquifers. The barrier in the Brazeau-Belly River aquifer between zones I and II is possibly caused by the lithological change from fluvial, conglomeratic channel deposits to interbedded, non-marine mudstones and sandstones of floodplain origin (Hamblin and Abrahamson, 1996). These sediments were deposited by an anastomosing fluvial system carrying sediments eastward from the Rocky Mountain region, whereby the grain size decreases with distance from the sediment source (Putnam, 1993). Using pressure distributions, Pendergast (1969) inferred lithological barriers to be responsible for the observed hydraulic discontinuities in the Cardium aquifer. Murray et al. (1994) interpreted the compartmentalization of fluids and pressures in the Cardium Formation on the basis of thin sections and capillary pressure analysis as being due to structural rather than lithological changes.

A comparison of the lateral zonation in the various aquifers with the depositional sediment facies (Hayes et al., 1994; Reinson et al., 1994; Bhatthacharya, 1994; Krause et al., 1994) strongly suggests that lithofacies changes and capillary sealing are the main causes for permeability barriers. The gas- and oil-saturated zones are in a region closer to the western sediment source provided by the Columbian and Laramide orogens than the water -saturated zones. The sand-shale ratio generally decreases east – northeastward in all the units. Depositionally coarser material and assumedly more porous material was deposited in the channel fills of the Mannville and Brazeau groups in a coastal plain environment and in the prograding delta of the Dunvegan Formation. In the Cardium and Viking Formations that were deposited in a more marine-influenced environment, the



Reproduced with permission of the copyright owner. Further reproduction prohibited without permission.

hydrocarbon-saturated zones correspond mainly with the coastal plain sediments, whereby the normally pressured water is observed in the barrier sands, and the underpressured water zone corresponds to offshore bars embedded in fine-grained sediments. Putnam and Ward (2001) speculated that highly pressured fluid moved updip in the Viking aquifer, leaching certain feldspar and rock fragments at depth, and precipitating solutes, thereby reducing pore space, in shallower environments due to a decrease in pressure and temperature. Also, although the permeability of the aquifers is significantly higher than that of the intervening shale aquitards, a capillary seal is formed when the hydrocarbon phase tries to flow from coarser-grained strata into or through finer-grained sediments (Revil et al., 1998) and the flow of both hydrocarbon and water is blocked.

*Topography-driven flow*

Hydrogeological cross sections for the post-Colorado aquifer system show semi - confined flow conditions in the Brazeau-Belly River aquifer (Fig. 5.30 & 5.31). The regional potentiometric surface for the Scollard-Paskapoo aquifer is located above the potentiometric surface of the Brazeau-Belly River aquifer, indicating downward flow, while both potentiometric surfaces follow the ground surface in a subdued manner (Fig. 5.30). This suggests that flow in the post-Colorado aquifer system is mainly driven by gravity and has adjusted to the present-day ground surface topography. A certain degree of underpressuring, referred to as "sub-hydrostatic" in zone Ia (Fig. 5.4), can be explained by hydrodynamic effects like a downward component to flow and a partial isolation of the aquifer by the intervening leaky Battle and Bearpaw aquitards. The salinity of formation water is everywhere less than 10 g/L and can be considered as relatively fresh. The high bicarbonate in the northeast is due to direct replenishment by meteoric water, while along the foothills it is due to recharge at topographic highs. The three pressure measurements from the foothills region (Figs. 5.4 & 5.5) suggest flow from that area into the undeformed basin, with the implication that the deep underpressured zone is relatively isolated and by-passed by this flow system (Fig. 5.31). However, lack of data in that area makes it difficult to substantiate this interpretation. The



Reproduced with permission of the copyright owner. Further reproduction prohibited without permission.

higher salinity plume in the region at $53.8^{O}$ N and $116.8^{O}$ W (Figs. 5.6 & 5.30) at the base of the Brazeau-Belly River aquifer can be explained by a "descending stagnant zone" (Tóth, 1988), that forms a hydraulic trap within the closed high hydraulic head of ~800m (Fig. 5.4). This trapping mechanism is enhanced by the Bearpaw aquitard above the higher salinity plume, which is absent to the northwest. In addition, low bicarbonate concentrations in this area (Fig. 5.7) suggest a very limited influence of meteoric water.

As shown previously, the thick Colorado shales impede vertical fluid flow and pressure transmission, and the current topographic relief does not seem to influence flow in the Colorado and Mannville aquifers. This is substantiated by the hydraulic gradient in subzone Ia of the Cardium aquifer, which is opposed to the slope of the current ground surface and to the flow in the overlying Brazeau-Belly River aquifer, and by the hydrodynamic conditions in the Dunvegan aquifer, which are almost stagnant (Figs. 5.8 & 5.12). In addition, the underpressured subzone Ib in the water-saturated part of each aquifer cannot be explained by a topography-driven flow system. Hence, other flow-driving mechanisms have to be identified that affect fluid pressures in these aquifers.



Reproduced with permission of the copyright owner. Further reproduction prohibited without permission.

Reproduced with permission of the copyright owner. Further reproduction prohibited without permission.



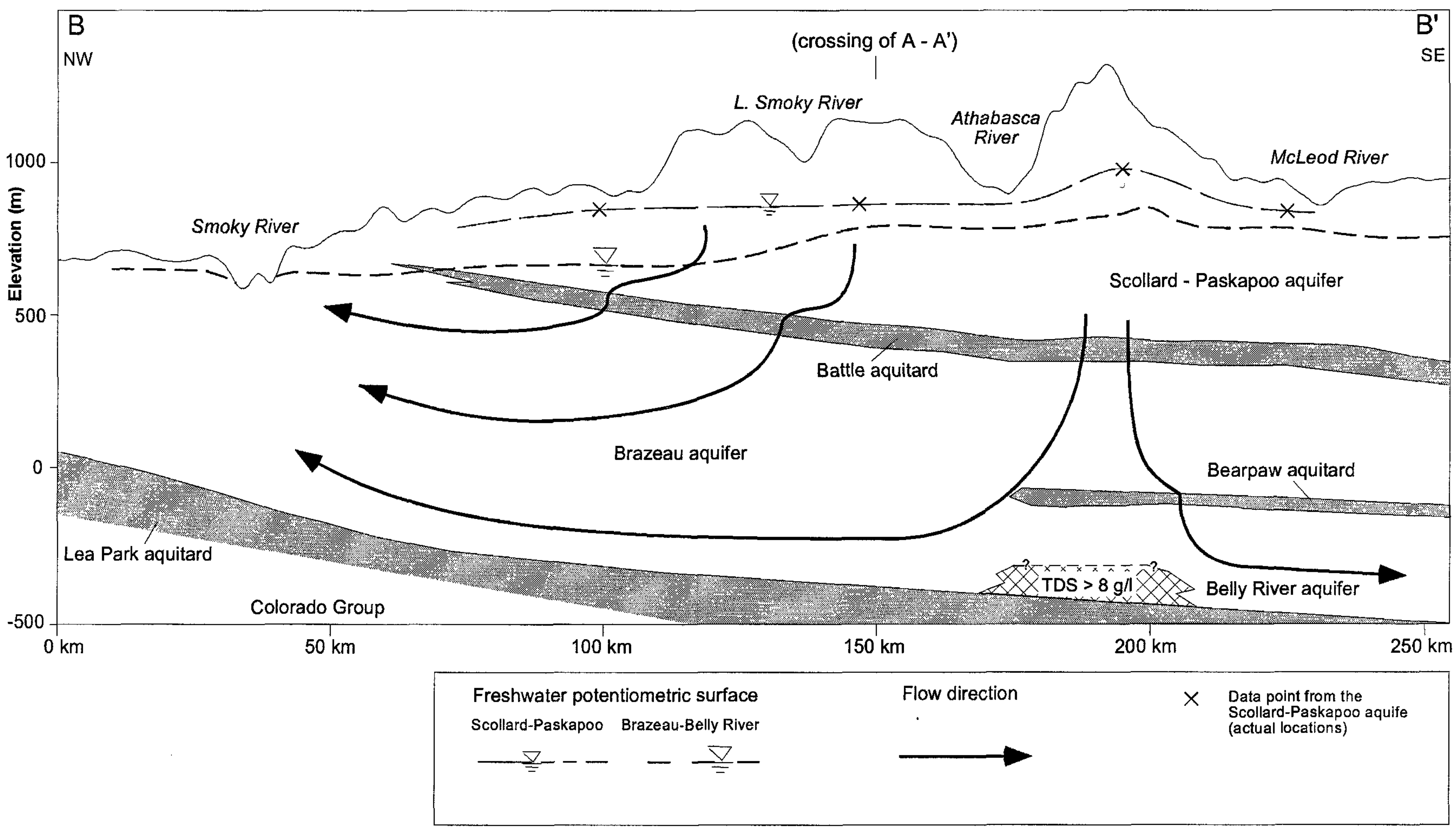


Figure 5.30: Hydrogeological strike cross section of the post-Colorado aquifer system sub-parallel to the deformation front. The potentiometric line of the Scollard-Paskapoo is based on four actual data points ("x"s in cross section), whereas that of the Brazeau-Belly River aquifer is based on the potentiometric surface in Figure 5.4. Also shown is the plume of relatively high salinity in Figure 5.6. See Fig. 5.3 for line of cross section.

Reproduced with permission of the copyright owner. Further reproduction prohibited without permission.



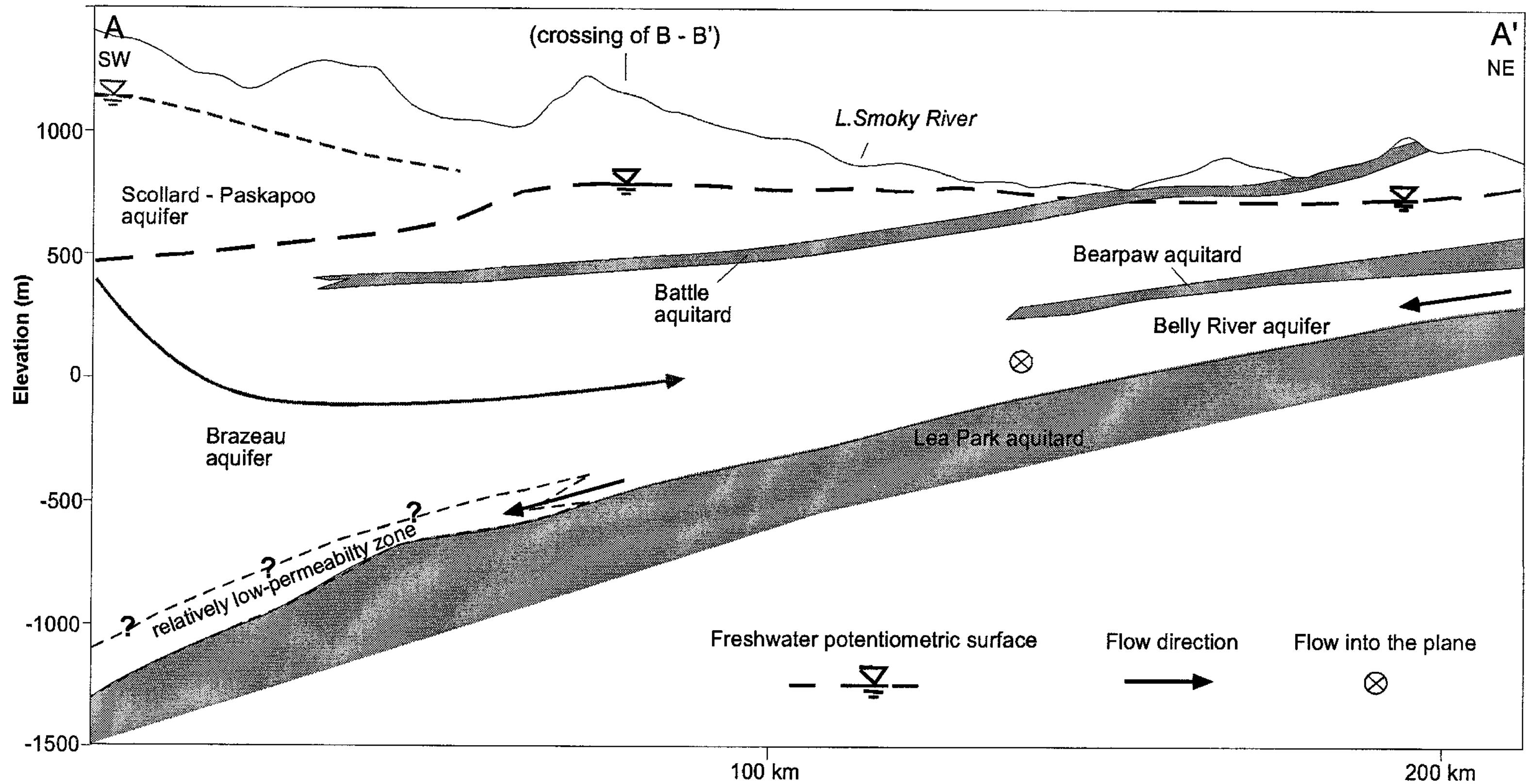


Figure 5.31: Hydrogeological dip cross section of the post-Colorado aquifer system. The potentiometric line and inferred flow directions (black) are based on the potentiometric surface in Figure 5.4. The line and flow arrow in grey represent the extrapolation of hydraulic head values from the foothills region west into the undeformed part of the basin. See Fig. 5.3 for line of cross section.

The existence of a hydrocarbon-saturated region in the deep part of the basin implies that formation water was displaced by hydrocarbons thermally generated during burial. These "deep basin" hydrocarbon accumulations are found only along the deformation front of the Alberta Basin (Figure 5.1), which suggests that this region is significantly influenced by the thermal history of the sedimentary succession. Therefore, the thermal history in this part of the basin is reviewed briefly, and the interaction between hydrocarbon generation and migration and fluid flow is investigated in this section.

Foreland-basin petroleum source rocks in the study area, Mannville Group coals and shales, Colorado Group shales, and post-Colorado shales and coals, show various stages of thermal maturity. Maximum vitrinite reflectance $R_0$max increases with depth and southwestward (Fig. 5.32) from 0.50 % in the coals of the shallow Paskapoo Formation to >2.00 % in Mannville Group coals near the thrust and fold belt (Bustin, 1991; Kalkreuth and McMechan, 1996).

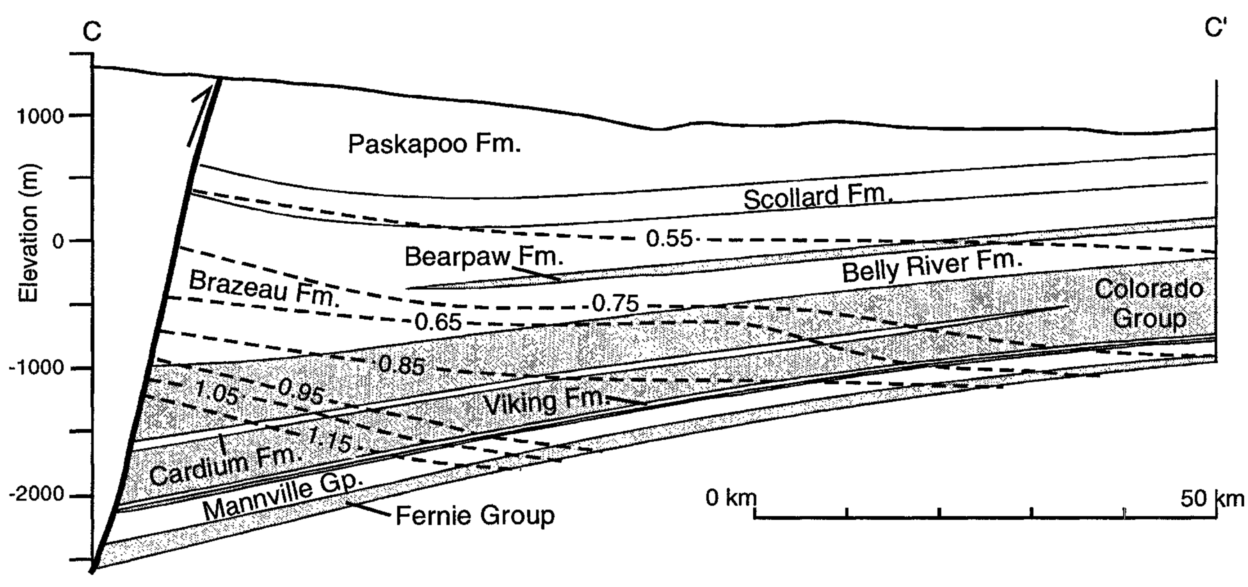


Figure 5.32: Thermal maturity of the foreland-basin strata in the study area (after Bustin, 1991). Isolines represent vitrinite reflectance $R_0$max%. See Fig. 5.3 for line of cross section.



Reproduced with permission of the copyright owner. Further reproduction prohibited without permission.

The burial history based on vitrinite reflectance (Fig. 5.33) and fluid inclusion data indicates that, at the end of the Laramide orogeny about 53.5 Ma ago, the Lower Cretaceous strata near the thrust and fold belt had reached a maximum burial temperature of ~ 200°C at >7 km depth (Tilley et al., 1989; Kalkreuth and McMechan, 1984).

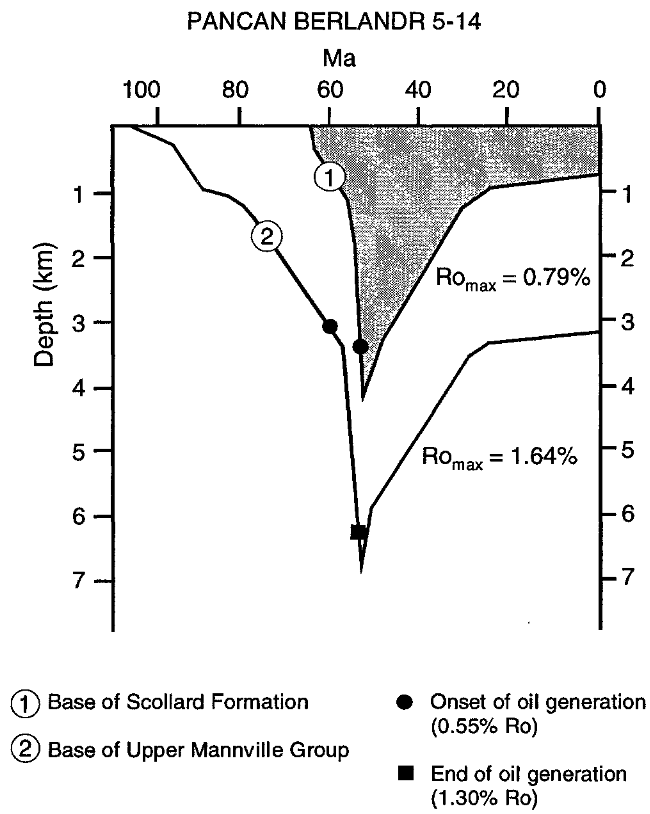


Figure 5.33: Burial history of foreland-basin strata in the PANCAN BERLANDR 5-14 well (from Kalkreuth and McMechan, 1996). See Figure 5.3 for well location.

At the time of maximum burial, the entire Cretaceous succession in the study area was in the oil or gas window. The oil generation window is defined by $R_0$max = 0.5 – 1.0 %, and the gas generation window by $R_0$max = 1.0 – 1.35 %, which approximately translates to temperature ranges of 60 to 115 $^{o}$C and 115 to 130 $^{o}$C respectively (Hunt, 1996). The rate of hydrocarbon generation must have been large enough to compensate for the loss of hydrocarbons due to buoyancy-driven migration out of the reservoirs (Masters, 1979,



Reproduced with permission of the copyright owner. Further reproduction prohibited without permission.

1984). In addition, a lateral permeability barrier must have existed in each aquifer to obstruct the updip escape of hydrocarbons besides stratigraphic trapping. The aquifers also had to be relatively isolated from the ground surface to prevent aquifer and reservoir flushing by meteoric water, which would have counteracted the displacement of formation waters by hydrocarbons.

Gies (1984) generated a "deep basin" gas accumulation in a laboratory experiment by injecting overpressured gas at the base of a water-saturated, layered, fine-to-coarse sand column (Fig. 5.34). This experiment showed that in-place generated gas could displace water from a relatively highly permeable aquifer or reservoir unit, resulting in a very effective permeability barrier for formation water flow (~ zero relative permeability for water in the gas-saturated zone). More importantly, this experiment demonstrates how originally overpressured hydrocarbon reservoirs can develop into underpressured reservoirs during the uplift of a basin, as theoretically suggested by Law and Dickinson (1985). Stage I represents the period after deposition of the Cretaceous sediments and before the onset of hydrocarbon generation (~ late Paleocene), in which the pore fluid is formation water (Fig. 5.34). Stage II corresponds to the time of deepest burial (Eocene), after thermally generated gas had displaced the water from parts of the aquifer and had formed a gas-saturated zone of maximum extent. Since the Eocene, the Alberta Basin underwent rapid uplift and erosion. This caused a relative downward shift of the oil and gas windows and a concurrent decrease in the rate of hydrocarbon generation, which corresponds to Stage III in Gies' laboratory experiment.

The effectively-lower rate of hydrocarbon generation versus hydrocarbon loss caused a drop in pressure in the hydrocarbon-saturated zone. This allowed formation water to partially re-imbibe the formerly hydrocarbon-saturated zones of the aquifer, causing the downdip retreat of the hydrocarbon-water interface and a shrinking of the areal extent of the hydrocarbon-saturated zone. Remaining hydrocarbon accumulations in the newly water-saturated zone would show "conventional" pressure distributions (Stage IV, Fig. 5.34).



Reproduced with permission of the copyright owner. Further reproduction prohibited without permission.

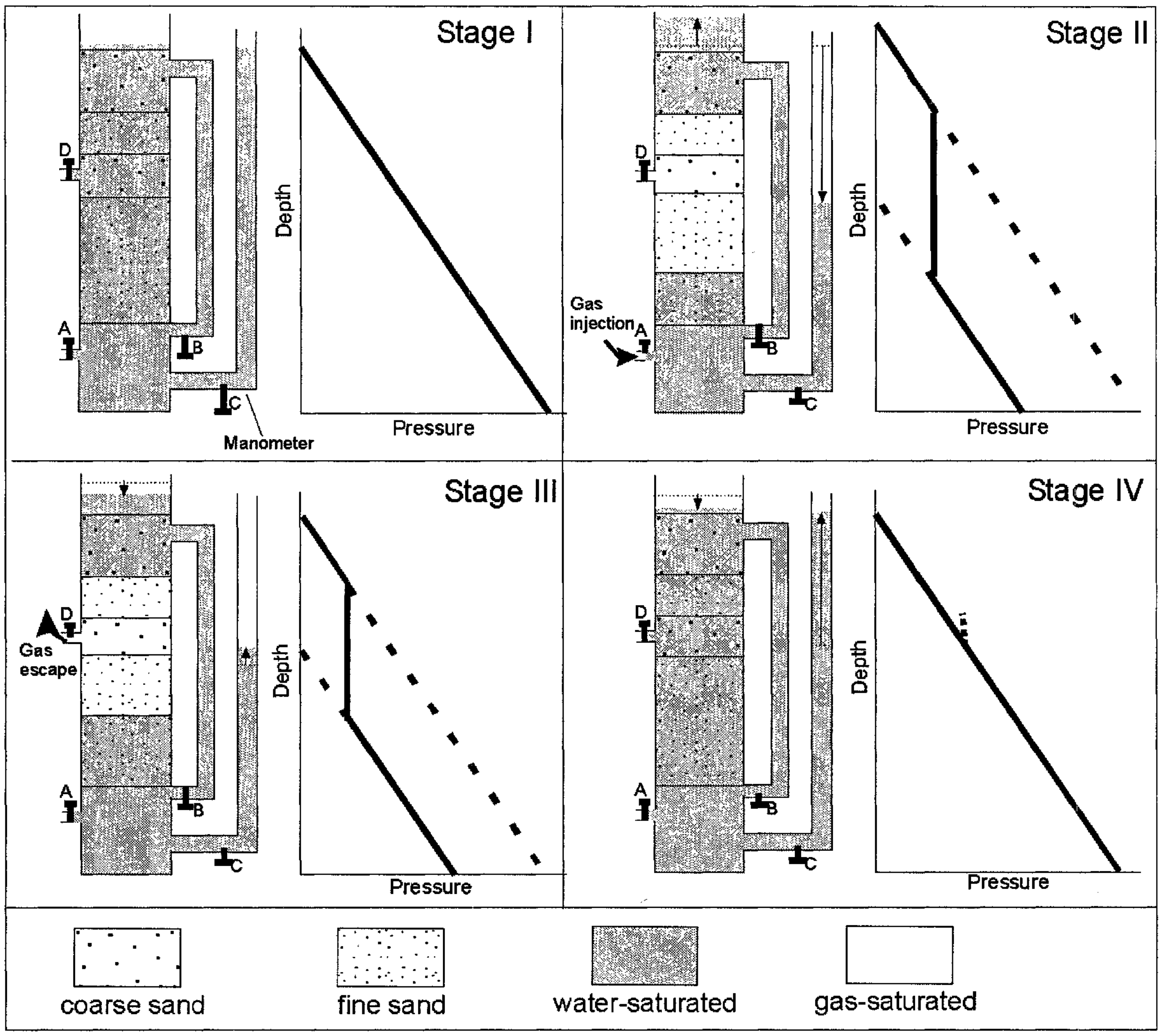

Figure 5.34: Laboratory experiment investigating the hydraulic behavior of "deep basin" gas reservoirs (modified after Gies, 1984): Stage I) initial, water-saturated conditions and pressure distribution; Stage II) pressure conditions after gas injection and water displacement; Stage III) slight change in pressure conditions and fluid saturation after gas escape; Stage IV) return to initial conditions. The dotted line indicates theoretical gas pressure gradient in a (conventional) reservoir unit.

Nevertheless, the advancement of the water front is retarded by the lateral low-permeability barriers, especially in the Cardium and Dunvegan aquifers, which add to the relative permeability barrier. In addition, the amount of water needed to fill the vacated pore space is limited in the Mannville and Colorado aquifers, because they are largely cut off from meteoric recharge that could replenish them. This is probably the main mechanism that created the underpressures in subzone Ib in the Upper and Lower



Reproduced with permission of the copyright owner. Further reproduction prohibited without permission.

Mannville aquifers in the study area. The effect of underpressuring is enhanced or may be dominated by the erosional and post-glaciation rebound of the surrounding shales (see next section).

Presently, only the deep strata along the thrust and fold belt generate hydrocarbons. The present-day subsurface temperature distribution was calculated based on average geothermal gradients in the area and rock thermal conductivity (Bachu, 1993). Temperatures in the $60^{o}$ – $110^{o}$C range indicate that the Cardium-to-Belly River source rocks are in the oil window, while the gas-prone Mannville Group coals (kerogen type III) that are the major source rocks for the "deep basin" gas (Welte et al., 1984), are in the gas window (Fig. 5.35). The above-hydrostatic pressures in the various subzones IIa indicate active hydrocarbon generation in a low-permeability environment (Hedberg, 1974; Spencer, 1987; Osborne and Swarbrick, 1997). The representative isotherms for the oil and gas window generally mimic the observed patterns of fluid distribution in the post-Jurassic succession (Figs. 5.35 & 5.36). In the "isolated" Cardium and Dunvegan aquifers that are embedded in the Colorado shales, the northeastern limit of zone II generally tracks the upper limit of the oil window (Fig. 5.36b & c). Apparently the rate of hydrocarbon generation is high enough to maintain those parts of the aquifers saturated with hydrocarbons that are located within the oil window. On the other hand, the Brazeau-Belly River and Lower Mannville aquifers are not embedded in shales, and large parts of these aquifers, although located in the oil window, are not saturated with hydrocarbons (Fig. 5.36a & d). This suggests that the rate of hydrocarbon generation versus hydrocarbon leakage in these aquifers is not or has not been sufficiently high to maintain or generate a deep basin hydrocarbon accumulation over the entire extent of the part of the aquifer that lies within the oil or gas window. In addition, hydrocarbons have escaped, driven by buoyancy, and have been replaced by formation water.



Reproduced with permission of the copyright owner. Further reproduction prohibited without permission.

Reproduced with permission of the copyright owner. Further reproduction prohibited without permission.



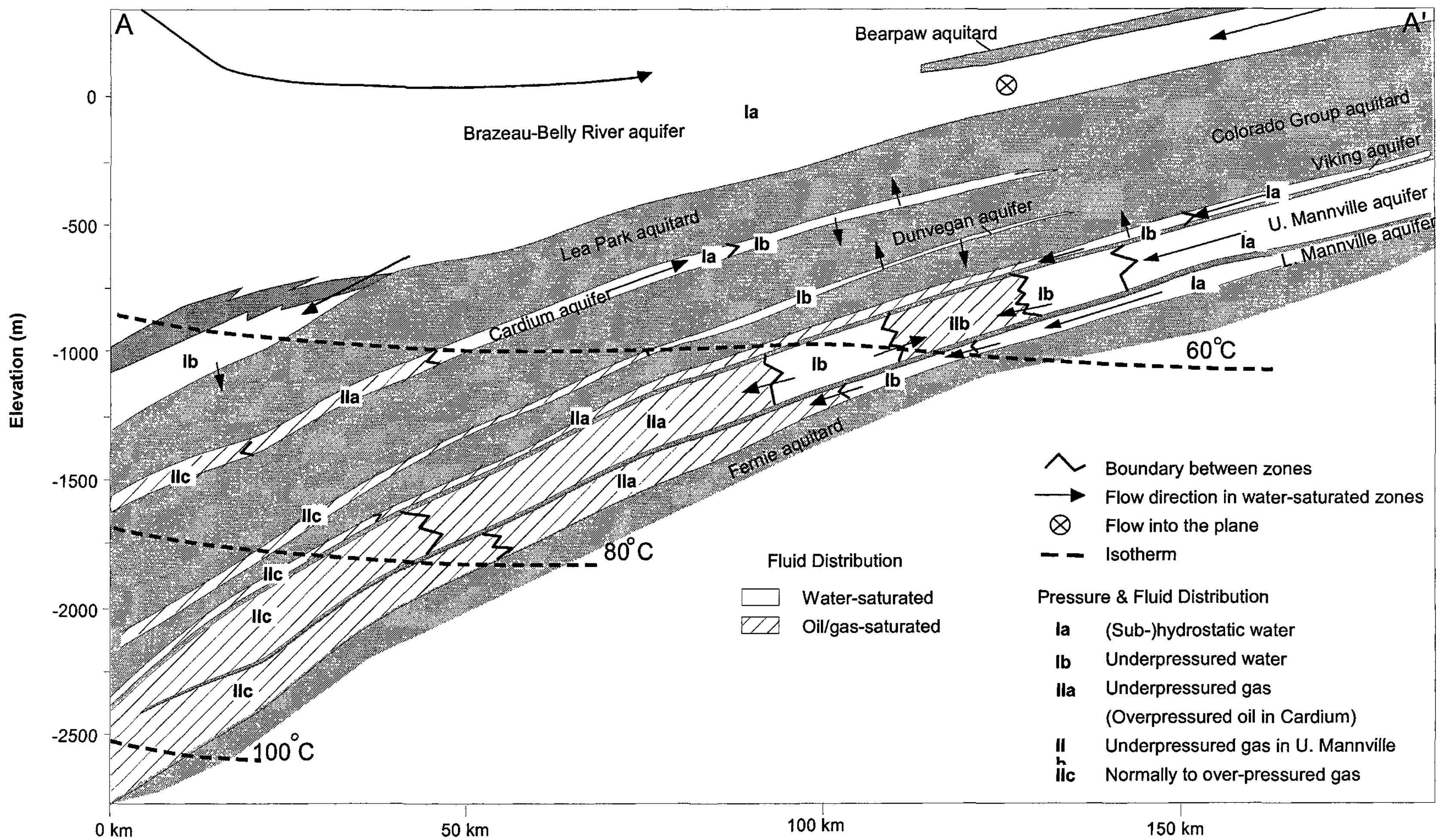


Figure 5.35: Hydrogeological dip cross section (A-A') of the post-Jurassic aquifers showing the inferred flow pattern and fluid, pressure and temperature distributions. (See Fig. 5.3 for line of cross section.)

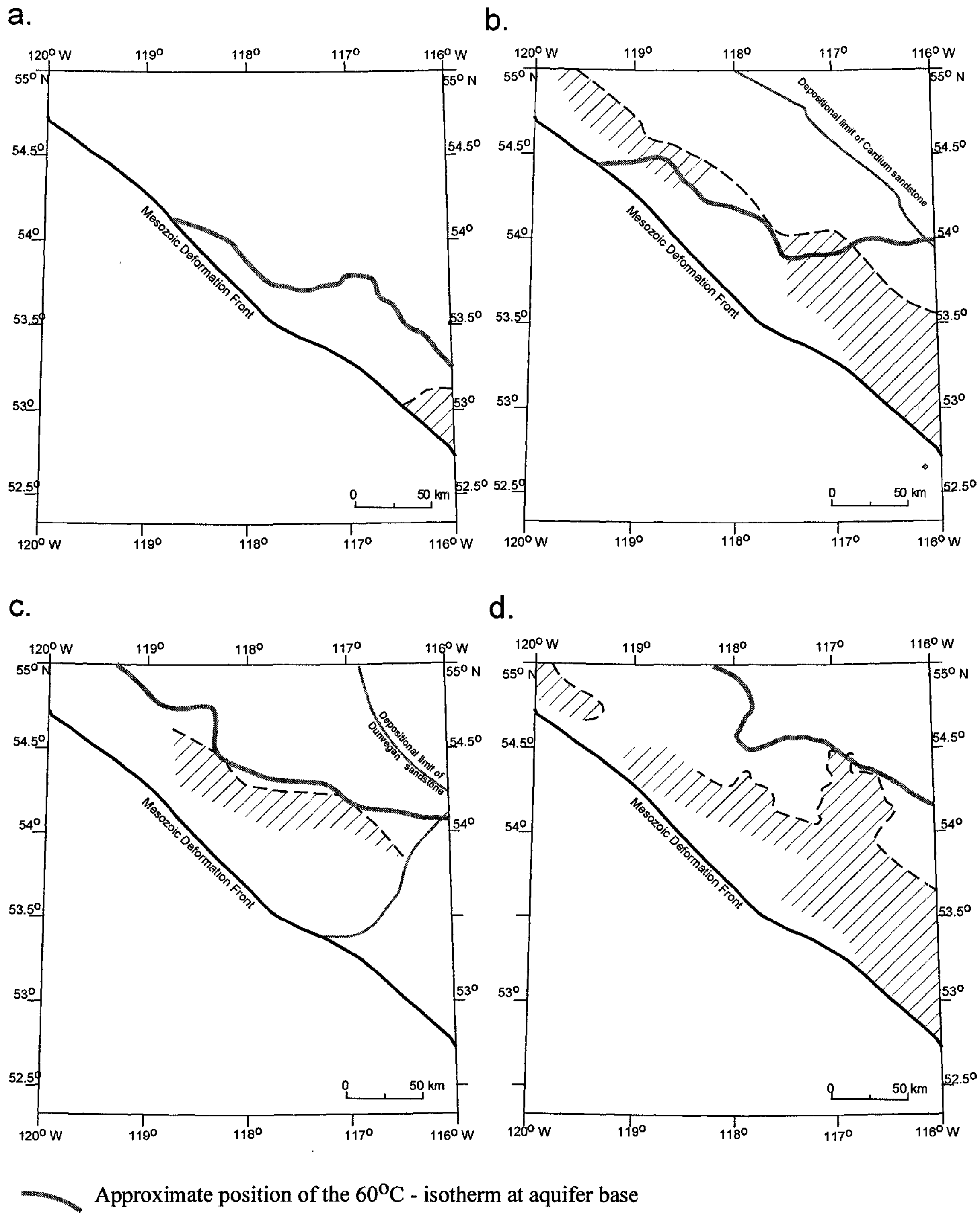


Figure 5.36: Current location of the oil window as inferred from the 60°C isotherm, relative to the aquifer zonation in: a) Brazeau-Belly River, b) Cardium, c) Dunvegan, and d) Lower Mannville, respectively. The hatched area represents the current hydrocarbon-saturated zone. Temperatures are > 60°C west of the isotherm.



Reproduced with permission of the copyright owner. Further reproduction prohibited without permission.

*Erosional and post-glaciation rebound*

The main mechanism currently thought to be responsible for underpressures in the post-Jurassic succession is the "absorbing sponge" effect of thick, low-permeability Colorado shales rebounding after removal of overburden by erosion since the peak of the Laramide orogeny and post-glaciation rebound. This effect has been demonstrated theoretically (Neuzil and Pollock, 1983; Neuzil, 1986), and inferred (Bachu and Underschultz, 1995, Parks and Tóth, 1995), and numerically simulated for the Alberta Basin (Corbet and Bethke, 1992; Bekele et al., 2000). The westward increase in underpressuring can be explained by a greater amount of sediment removal close to the foothills than in the east (Bustin, 1991; Kalkreuth and McMechan, 1996; see also Fig. 4.8a in Chapter 4), which implies an originally higher degree of shale compaction and which necessitates a longer transient time to equilibrate. The permeability of the intervening shales has to be sufficiently low to preserve underpressures in the Cretaceous aquifers. Local- and regional-scale permeability in the order of $10^{-20} - 10^{-21}$ $m^2$ (Neuzil, 1994; Bekele et al., 2000) and an erosional hydraulic diffusivity, defined as hydraulic conductivity divided by the specific storage (Freeze and Cherry, 1979, p. 61), of $10^{-9} - 10^{-8}$ $m^2/s$ (Neuzil and Pollock, 1983; Parks and Tóth, 1995) correspond to a characteristic time for pressure dissipation in the order of 1 – 5 Ma. This is comparable with the period since the start of Tertiary to Holocene erosion and glaciation events. The effect of recent glaciation cycles during which the Laurentide ice sheet in the area reached 1- 2 km in thickness (Matthews, 1974) compounded erosional rebound since the Tertiary (Bachu, 1995a). According to recent numerical modeling results, glacial unloading could be even the dominating mechanism for creating the observed underpressures in the Alberta Basin (Bekele, 1999).

In the study area, the Colorado shales and the lateral permeability changes in each aquifer provide for the low-permeability environment that is necessary to impede fluid and pressure transmission, hence maintain non-hydrostatic pressures in the subsurface. The change in the areal extent of subzone Ib in various aquifers in the succession strongly supports the idea that erosional rebound is an important mechanism for creating underpressures in the post-Jurassic succession in the study area.



Reproduced with permission of the copyright owner. Further reproduction prohibited without permission.

The rebounding Colorado shales represent a pressure sink that "sucks in" fluids from the imbedded (Cardium, Dunvegan, Viking) and over- and underlying Brazeau-Belly River and Mannville aquifers, respectively. The underpressured water-saturated subzone Ib in the Brazeau-Belly River aquifer is relatively small compared to the underlying aquifers, because that aquifer is not imbedded in shales and fluids only are drawn into the Lea Park shales at the base of the aquifer. The existence of this subzone and its persistence in time indicate that there must exist a vertical and lateral barrier to flow that prevents the dissipation of the underpressures from that subzone and equilibration with the topography-driven system in the Brazeau-Belly River aquifer. In the Cardium and Dunvegan aquifers, which are imbedded in the Colorado shales, subzones Ib are more extensive, but these aquifers still are partially, sub-laterally connected hydraulically to the ground surface in areas of aquifer outcrop, and underpressures can easily equilibrate in those areas. An effective combination of isolation from the ground surface and embedding in the rebounding Colorado shales is observed in the Viking aquifer, causing very low hydraulic heads and a maximum areal extent of subzone Ib. There are no significantly thick shale units within the Mannville aquifer system that could draw-in fluids, so that fluids from the Upper and Lower Mannville aquifers can only be "sucked in" by the overlying Colorado shales. This might explain the narrow subzone Ib in both aquifers. An additional mechanism that could be responsible for the underpressures in the Upper and Lower Mannville aquifers is the effect of hydrocarbon generation and migration in the deep parts of the basin as shown in the previous section. The hydrogeological dip cross section A-A' (Fig. 5.35) illustrates these considerations on fluid pressure distributions in the post-Jurassic succession.

*Chemical evolution of formation waters*

Sediments in the post-Jurassic succession were deposited in a marine to marginal-marine environment and, therefore, the respective formation waters probably started out as seawater that was successively altered by water-rock interaction and mixing with



Reproduced with permission of the copyright owner. Further reproduction prohibited without permission.

meteoric water after or during sediment deposition. The sodium and chloride concentrations compared to seawater values suggest that formation waters in the Brazeau-Belly River to Viking aquifers, and the Lower Mannville aquifer, represent diluted and concentrated seawater, respectively, while concentrations from the Upper Mannville aquifer fall in-between the two (Fig. 5.28a). Magnesium and calcium concentrations do not follow the seawater dilution-evaporation trend (Fig. 5.28b & c), which indicates that additional mechanisms must have affected the chemistry of formation waters. The consistently low magnesium concentrations can be explained by the precipitation of dolomite cements shortly after sediment deposition and cation exchange. The relatively high calcium concentrations in the Brazeau-Belly River aquifer are probably due to the shallow depth to the ground surface and mixing with high-calcium waters from shallow aquifers. The low calcium concentrations with respect to the seawater evaporation-dilution curve in the underlying aquifers could be caused by calcite precipitation and cation exchange in montmorillonite shales (Freeze and Cherry, 1979), whereas the excess in calcium, especially in the Lower Mannville aquifer is probably due to the dissolution of calcite and/or sulphate.

Plotting the Na/Cl-ratio versus salinity clearly shows a different grouping of formation waters in the various post-Jurassic aquifers (Fig. 5.37). Waters from aquifers connected to the ground surface (Brazeau-Belly River, Cardium Ia, and Dunvegan Ia) have a relatively wide range in the Na/Cl-ratios and salinities (TDS < 12 g/L) significantly lower than seawater, indicating extensive flushing with meteoric water. The salinity of waters from the isolated parts of the Cardium (zone Ib), the Viking, and the Upper Mannville is slightly higher, and the data follow a tentative mixing trend between seawater and meteoric water (Fig. 5.37). Only data from the Lower Mannville aquifer have a narrow range in Na/Cl-ratios (0.85 - 1.0) and a wide range in salinities, suggesting a relative high degree of halite solution and/or mixing with more-saline brine from the underlying Jurassic-Mississippian aquifers.



Reproduced with permission of the copyright owner. Further reproduction prohibited without permission.

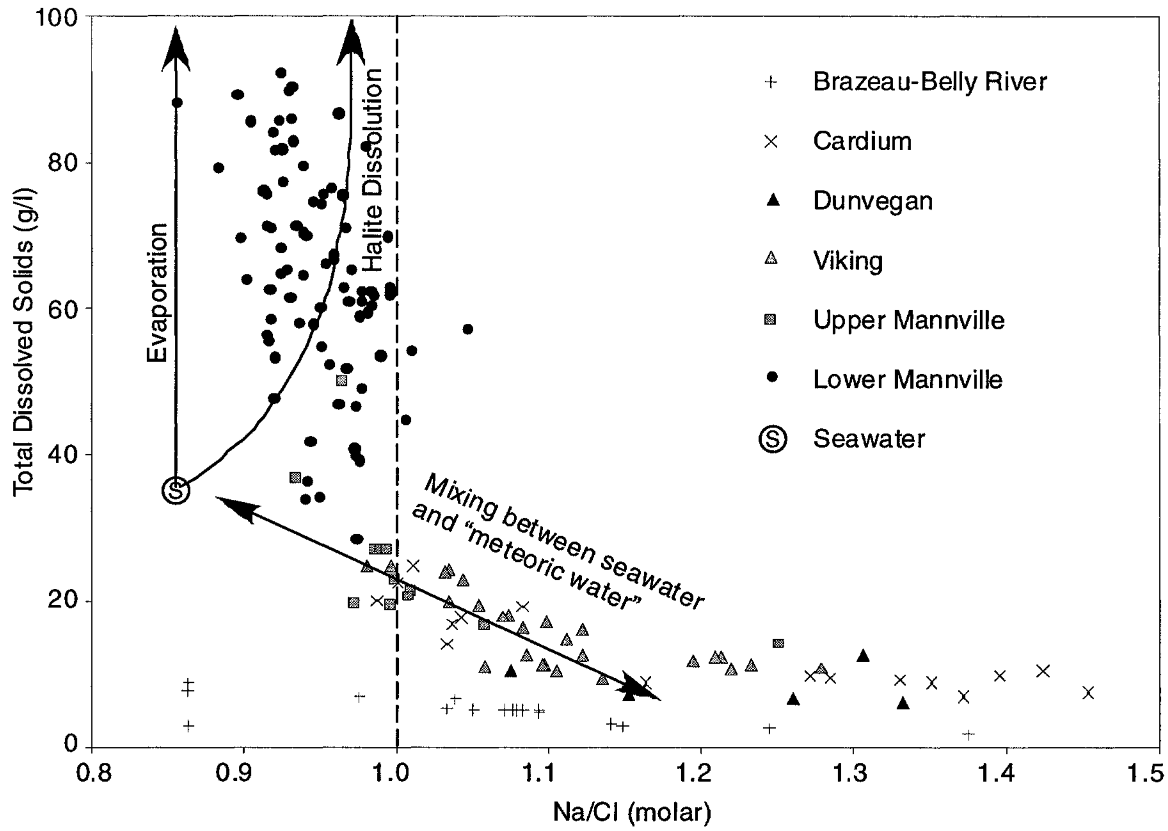


Figure 5.37: Na/Cl-ratio versus salinity plot of Tertiary-Cretaceous formation waters showing tentative trends of evaporation, halite dissolution and mixing.

*Aquifer recharge and flow paths*

So far, it has been shown that flow in the post-Colorado aquifers is driven by topography, and that the respective formation waters are of meteoric origin, as suggested by the low salinity and bicarbonate distribution. On the other hand, erosional and post-glaciation rebound, and the interaction between hydrocarbon- and water-saturated zones, are interpreted to be the main flow driving mechanisms in the Colorado and Mannville aquifers. According to this interpretation, the rebounding Colorado shales and the retreat of the hydrocarbon-saturated zone represent the fluid sinks in these aquifers, whereas the fluid origin and the flow paths still have to be established. This task is complicated by the lateral permeability barriers that restrict fluid flow within each individual aquifer, and that cause their compartmentalization into zones and subzones.



Reproduced with permission of the copyright owner. Further reproduction prohibited without permission.

The generally low salinity and the increase in salinity with distance from aquifer outcrop indicate that subzones Ia in the Cardium and Dunvegan aquifers appear to be the only ones that are laterally connected to the ground surface in areas of formation outcrops outside the study area. Furthermore, the salinity distribution suggests that a plume of meteoric water (TDS < 15 g/L in subzone Ia) has partially penetrated these aquifers that were originally deposited in a marginal-marine environment. Remainders of the connate brackish to marine pore water are represented by salinities > 20 g/L in subzone Ib in the Cardium aquifer. Obviously, this freshwater recharge did not happen as a result of the present-day topographic relief, because the respective aquifers crop out at low elevations, nor can it be explained by cross-formational flow of meteoric water downward through the competent intervening Lea Park aquitard. One possibility would be the lateral pressure-induced intrusion of Pleistocene melt water from the respective aquifer outcrops, similar to an interpretation for the Williston Basin (Grasby and Betcher, 2000). The continental ice sheet, 1- 2 km thick (Matthews, 1974), would have provided the hydraulic drive for this intrusion. Another case of deep recharge of glacial melt water to depths between 700 to 1600 m was demonstrated on the Canadian Shield at the northern edge of the Alberta Basin, by analyzing oxygen isotopes and salinity distributions, and by using numerical flow modeling (Clark et al., 2000). The downward penetration of melt water in the study area could have been facilitated by the existence of an ice-free corridor (see Chapter 4, Fig. 4.7 b) sub-parallel to the deformation front (Rutter, 1984). This area would have been more susceptible to the infiltration of precipitation and surface run-off than the area underneath the Laurentide ice-sheet. Although the latter hypothesis provides a possible explanation, the origin of the relatively fresh water plume in the Cardium and Dunvegan aquifers needs further investigation using isotope data of oxygen and hydrogen.

The cumulative thickness of the Colorado shales (~ 1500 m) and the flow pattern in the Cardium and Dunvegan aquifer suggest that strictly vertical cross-formational flow of recharging meteoric waters into the Viking and lower aquifers is improbable. Direct lateral meteoric recharge of the Viking and Mannville aquifers from the undeformed part



Reproduced with permission of the copyright owner. Further reproduction prohibited without permission.

of the basin is rather unlikely, because these aquifers crop out hundreds of kilometres to the northeast of the study area. Generally, recharge of the Colorado and Mannville aquifer systems by meteoric water from the thrust and fold belt is not possible, because the hydrocarbon-saturated zone along the deformation front in each aquifer represents a continuous lateral pressure and relative-permeability barrier to formation water flow. Although the Mannville to Viking sediments were deposited mainly in a fluvio-deltaic environment, the originally relatively fresh formation waters should have dissolved solutes from the surrounding rock framework with time, and should have mixed with marine waters during and after deposition of the Colorado shales. The relative low salinities < 15 g/L in areas of the Viking and Upper Mannville aquifers can therefore only be explained by either partial flushing of these aquifers by glacial melt water during the Quaternary, as hypothesized for the Dunvegan and Cardium aquifers, or by the isolation of parts of the aquifers, shortly after deposition of the Viking and Mannville sediments before hydrocarbons displaced the formation water. A satisfactory interpretation on the basis of the current flow patterns and salinity distribution is not possible and additional work on isotopes and numerical flow modeling is needed in the future to validate any of these possibilities.

The salinity of formation water (35 – 90 g/L) in the Lower Mannville is significantly higher than that in the overlying aquifers and also higher than seawater, which suggests that the Lower Mannville aquifer in the study area has not been flushed by meteoric water at any time in the basin history. To the contrary, the initially low-salinity water that originated during the time of fluvial and deltaic sedimentation was further concentrated by water-rock interaction and mixing with more saline water. This interpretation makes it also unlikely that formation water in the Upper Mannville aquifer was diluted by meteoric recharge from the emerging front of the Columbian orogen shortly after deposition of the sediments, because such a flow system would have also affected the Lower Mannville aquifer. Therefore, having considered all other possibilities, the relatively low salinity in the Upper Mannville aquifer is most likely the result of a flow system and meteoric recharge originating in the northern Peace River Arch region. In contrast, the Lower Mannville formation water was either further concentrated by cross-



Reproduced with permission of the copyright owner. Further reproduction prohibited without permission.

formational flow of high-salinity Triassic water through a weak Fernie aquitard in the northwest of the study area, or is part of a long-range flow system from the south-southeast, originating in Montana (Bachu and Underschultz, 1995; Bachu, 1995a; Anfort et al., 2001).

### 5.5 Conclusions

Fluid flow in the Tertiary-Cretaceous succession in west-central Alberta is closely related to the basin history. Burial of the basin strata and subsequent hydrocarbon generation during the Laramide orogeny created dominantly hydrocarbon-saturated zones in the deeper parts of the Mannville to Brazeau-Belly River aquifers, the hydrocarbons being located downdip of the water-saturated zones. The extent of these "deep basin" hydrocarbon accumulations, as well as the fluid and the pressure distributions, vary between the various aquifers depending mainly on the subsurface temperature, on the kerogen type and on the degree of water penetration. The water-saturated zone directly updip of the hydrocarbon-saturated zones is generally underpressured, suggesting that the rate of hydrocarbon leakage from the reservoir rocks is presently higher than the rate of hydrocarbon generation, and that formation water can re-imbibe these zones. Therefore, the hydrocarbon-water interface may be characterized as a transient relative permeability barrier that moves downdip towards the deformation front with the uplift of the basin. Overpressures are maintained in the deep parts of those hydrocarbon-saturated zones in which the rate of active thermogenic hydrocarbon generation is sufficiently high.

Only in the post-Colorado aquifers has the flow adjusted to the present-day ground surface topography and pressures are sub-hydrostatic as a result of intervening local- and regional-scale shaly aquitards. The Mannville and Colorado aquifers are mainly cut off from meteoric recharge by the Colorado shales aquitard, except for a tongue of freshwater in subzone Ib of the Cardium and Dunvegan aquifers that are connected to outcrop outside of the study area. The degree of penetration of meteoric water into the Viking and Mannville aquifers needs further investigation. Formation water flow in the



Reproduced with permission of the copyright owner. Further reproduction prohibited without permission.

Mannville and Colorado aquifers is mostly towards the underpressured hydrocarbon-saturated regions and towards the sinks created by erosional and post-glacial rebound of the intervening shales. The discontinuous changes in fluid distributions (gas, oil water) and pressures (underpressured, sub-hydrostatically pressured, sub-hydrostatic, overpressured) between aquifer zones indicate that absolute and relative lateral permeability barriers impede pressure transmission, hydrocarbon migration and water flow. The hydrocarbon-saturated region represents a relative permeability and pressure barrier to potential meteoric recharge from the thrust and fold belt.

In summary, the present-day hydrodynamic regime represents only the latest stage in the fluid flow evolution and is the result of various factors during the basin history: a) hydrocarbon generation and migration leading to "deep basin" hydrocarbon accumulations during burial of the Cretaceous sediments, b) erosion to the present-day ground surface causing uplift of the sedimentary succession with subsequent decrease of hydrocarbon generation and rebound of the shales, c) a low-permeability environment impeding pressure transmission and fluid flow. Hence, a steady-state topography-driven regional flow system does not exist in this part of the basin.



Reproduced with permission of the copyright owner. Further reproduction prohibited without permission.

# CHAPTER 6: FLOW OF FORMATION WATER IN THE JURASSIC-MISSISSIPPIAN SUCCESSION

## 6.1 Introduction

The Jurassic-Mississippian succession represents a transition from dominantly carbonate to siliciclastic sedimentation in the evolution of the WCSB (see Chapter 4). Based on its salinity distribution and flow characteristics, the Mississippian-Jurassic aquifer system was considered as being the upper part of a pre-Cretaceous mega-hydrostratigraphic group (Bachu, 1995a; 1999). Two basin-scale flow systems driven by basin topography and partially flushed by meteoric water are present in this group, hence in this aquifer system: a south-northward one in the south, and a southwest-northeastward one in the north, with a transition zone between the two in the 53°-55°N area (Fig. 6.1a). Based on comprehensive hydrochemical data (e.g., trace and major ion chemistry, and Sr-, O-, H-isotopes), Connolly et al. (1990a,b) divided formation waters in west-central Alberta into three groups. Waters from dominantly Devonian carbonate aquifers (Group 1), which represent water in strata equivalent to Bachu's (1995a) pre-Cretaceous mega-hydrostratigraphic group, and waters from Lower Cretaceous clastic aquifers (Group 2) were interpreted to be composed of evaporated seawater, that was subsequently diluted 50-80% by post-Laramide meteoric water, but has been isolated from further meteoric influences. Triassic to Upper Mississippian formation waters were not considered in the study mentioned above because the respective strata are eroded in the central part of the basin (Fig. 6.1b). It has to be investigated to what extent hydrogeological phenomena in the Tertiary-Cretaceous and Cambrian-Devonian hydrostratigraphic groups influence regional-scale fluid flow in the Jurassic-Mississippian strata in the study area and vice versa.



Reproduced with permission of the copyright owner. Further reproduction prohibited without permission.

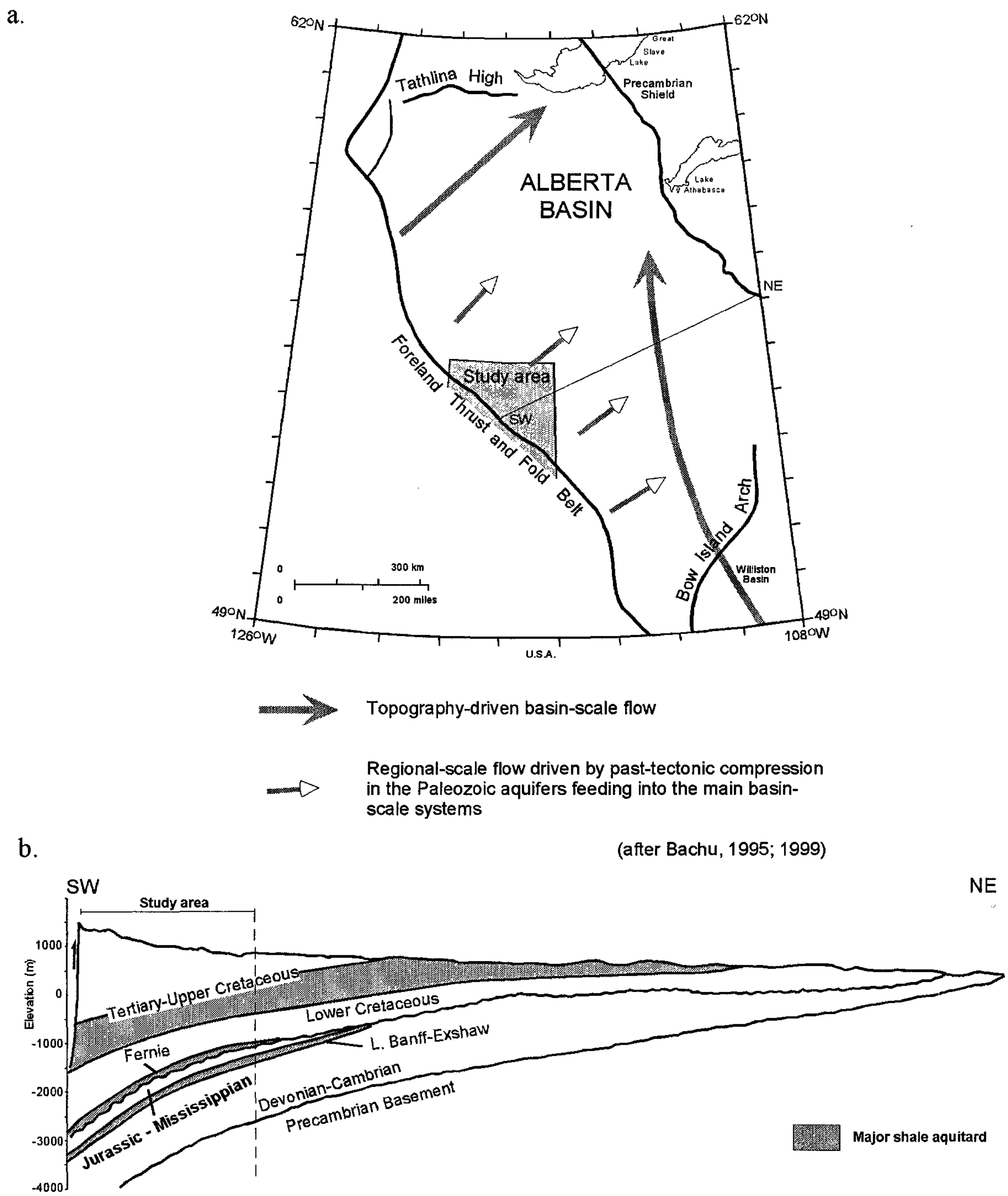


Figure 6.1: Location of the study area in the Alberta Basin: a) in plan view, showing main basin-scale flow systems identified previously by Hitchon et. al (1990), Bachu (1995a, 1997, 1999), and Anfort et al., 2001), and b) in cross-section showing major, basin-wide continuous aquitards.



Reproduced with permission of the copyright owner. Further reproduction prohibited without permission.

Particular issues that need to be addressed are:

(1) The hydraulic competence of the Fernie aquitard at the top of the Jurassic-Mississippian hydrostratigraphic group has to be characterized, in order to identify whether cross-formational flow is responsible for the high salinities observed in parts of the Lower Mannville aquifer (see Chapter 5).

(2) Former regional hydrogeological studies in the Peace River Arch region (Hitchon et al., 1990; Bachu and Underschultz, 1992) and southwestern Alberta (Bachu and Underschultz, 1995), which covered parts of the study area, considered the Jurassic-Mississippian succession as a single, hydraulically continuous aquifer system. A finer resolution of the hydrostratigraphy is required to better understand the regional flow patterns in this part of the Alberta Basin.

(3) What are the hydrochemical characteristics of the Jurassic-Mississippian formation waters in the study area?

(4) Do "deep basin" hydrocarbon accumulations exists in the Jurassic-Mississippian hydrostratigraphic group similar to or as a continuation of, the ones in the overlying Mannville aquifers, as proposed by Masters (1984)?

## 6.2 Hydrostratigraphic framework

Large parts of the Triassic-Mississippian strata were eroded in the study area, and these sediments subcrop below the Jurassic, which complicates the assignment of lateral continuous hydrostratigraphic units. The Jurassic Fernie shales form a laterally continuous aquitard at the top of the Jurassic-Mississippian hydrostratigraphic group, whereas the shales of the Exshaw Formation, in conjunction with the shaly carbonates of the lower Banff Formation, represent the lower confining layer (Fig. 6.2).



Reproduced with permission of the copyright owner. Further reproduction prohibited without permission.

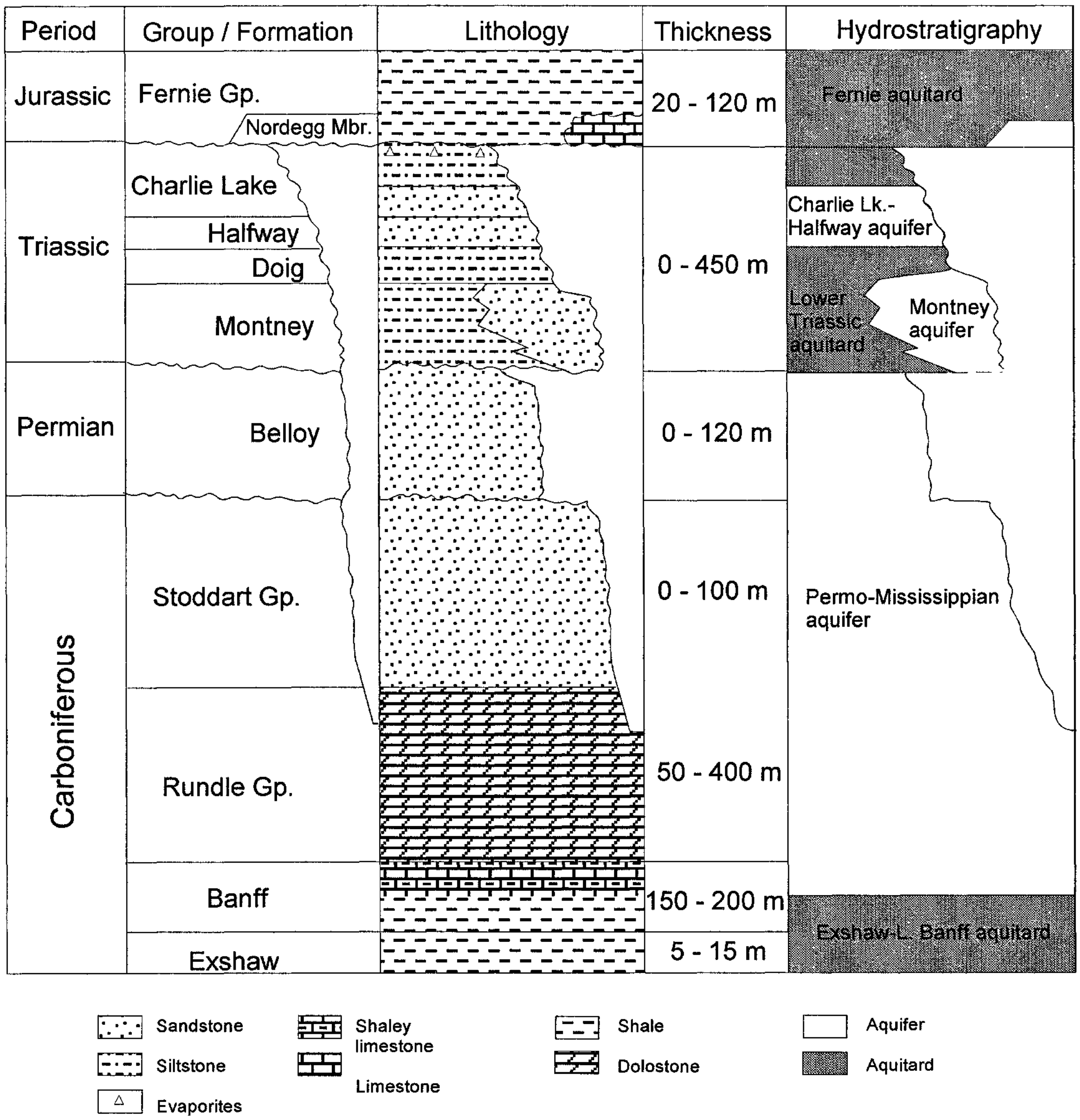


Figure 6.2: General lithology and hydrostratigraphy of the Jurassic-Mississippian succession in the study area.

The limestone aquifer of the Nordegg Member at the bottom of the Fernie Group is only present in the east, where it forms a continuous aquifer system with the underlying sediments of either the Montney Formation, the Belloy Formation or the Rundle Group (Fig. 6.3).



Reproduced with permission of the copyright owner. Further reproduction prohibited without permission.

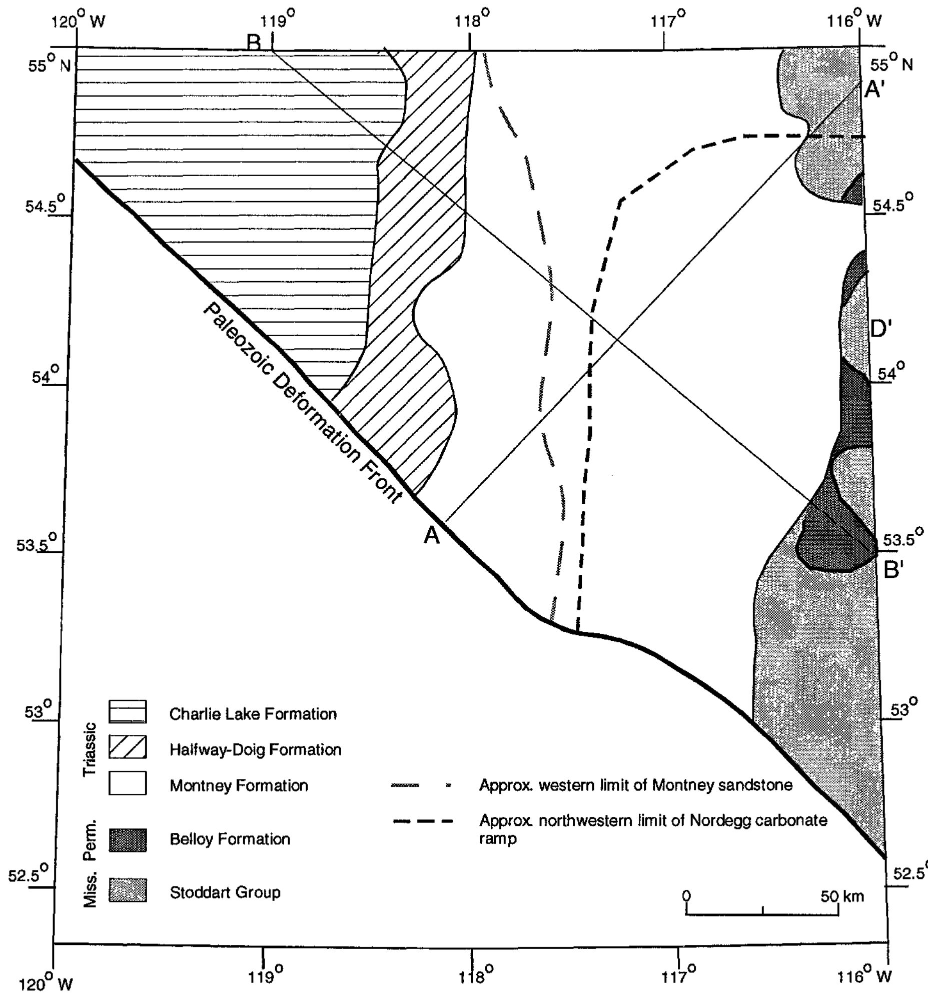


Figure 6.3: Erosional limits of Mississippian to Triassic strata below the Jurassic Fernie Group and limits of the depositional facies of the Montney sandstone (modified from Edwards et al., 1994) and the Nordegg limestone (modified from Poulton et al., 1990). See also Figure 4.7a in Chapter 4, which shows the areal extent of the Triassic and Permian sediments only.

The Triassic Charlie Lake, Halfway, and Doig Formations subcrop below the Fernie shales in the western half of the study area. The shales and minor evaporites in the upper part of the Charlie Lake form an aquitard as a vertical continuation of the Fernie aquitard. The sandstones in the Lower Charlie Lake and Halfway formations represent an aquifer, whereas shales and siltstones in the underlying Doig Formation form another aquitard. The general lithology in the Triassic Montney Formation changes from sandstones in the



Reproduced with permission of the copyright owner. Further reproduction prohibited without permission.

eastern half of the study area to siltstones and shales towards the west (Edwards et al., 1994). Therefore, the Montney Formation successively develops westward into an aquitard, the boundary between aquifer and aquitard zone not being well defined. The Carboniferous Rundle and Stoddart groups consist of dolostones and sandstones, respectively, and form a continuous aquifer with the overlying sandstones of the Permian Belloy Formation.

The hydrostratigraphy in the Jurassic-Mississippian succession is different in the western and eastern halves of the study area. In the east, the Montney aquifer, which includes the Nordegg Member, is for most part in direct hydraulic communication with the underlying Permo-Mississippian aquifer, forming a continuous single Lower Jurassic-Mississippian aquifer. In the west, the Doig-Montney aquitard separates the Permo-Mississippian and Charlie Lake-Halfway aquifers. Therefore, the hydrogeological data are presented separately for the Charlie Lake-Halfway, the Montney and the Permo-Mississippian aquifers. This way, it is also easier to distinguish between possible influences (i.e., cross-formational flow) of hydrogeological phenomena in the overlying Mannville and the underlying Wabamun aquifers on fluid and pressure distributions in the Jurassic-Mississippian hydrostratigraphic group.

## 6.3 Hydrogeological patterns

Similar to the hydrogeology of the Tertiary-Cretaceous succession (Chapter 5), contour maps of equivalent hydraulic heads, and p(d)-and p(z)-plots were used to interpret the flow in the Jurassic-Mississippian succession. Formation water density ranges between approximately 1000 and 1080 kg/m$^3$, and an average reference density $\rho_0$ = 1040 kg/m$^3$ was used to calculate hydraulic heads in order to minimize the DFR and to be able to analyze the flow using hydraulic heads only (see Chapter 2). Maps of salinity and bicarbonate distributions were used in the hydrochemical analysis. The respective ranges



Reproduced with permission of the copyright owner. Further reproduction prohibited without permission.

of hydraulic head and salinity values for the Jurassic-Mississippian hydrostratigraphic group and adjacent aquifers are presented in Table 6.1.

| Aquifer | $H_0$ ($\rho_0 = 1040$ kg/m$^3$) | TDS |
|---|---|---|
| Lower Mannville | 400 – 600 m | 35 – 90 g/l |
| Charlie Lake-Halfway | 415 – 550 m | 115 – 160 g/l |
| Montney | 450 – 650 m | 50 – 155 g/l |
| Permo-Mississippian | 500 – 700 m | 50 – 165 g/l |
| Wabamun | 570 – 950 m | 120 – 260 g/l |

Tab. 6.1: Summary of ranges in hydraulic head and salinity in the Jurassic-Mississippian aquifers. Values for the adjacent Lower Mannville and Wabamun aquifers are listed for reference. Hydraulic heads are calculated with the same reference density of 1040 kg/m$^3$ and their distribution is shown in Figures 6.4 & 6.5 for comparison purposes.

The distribution versus depth of all the pressure data indicates that the aquifers in this succession are underpressured (Fig. 6.6a). The pressure distribution versus elevation, which fits almost entirely on a straight line (Fig. 6.6b), indicates that the Permo-Mississippian and Montney aquifers are in good hydraulic communication, except for a hydrocarbon-saturated low in the Montney aquifer. The distribution of pressure data from the Charlie Lake-Halfway aquifer, present only in the northwest, confirms that this aquifer is not in hydraulic communication with the other aquifers in the succession, as inferred also on the basis of lithology and facies distribution (Figs. 6.2 and 6.3). Similarly, the underpressured hydrocarbon-saturated zone in the Montney aquifer seems to be poorly connected with the surrounding water-saturated zone (Fig. 6.6b).



Reproduced with permission of the copyright owner. Further reproduction prohibited without permission.

Reproduced with permission of the copyright owner. Further reproduction prohibited without permission.



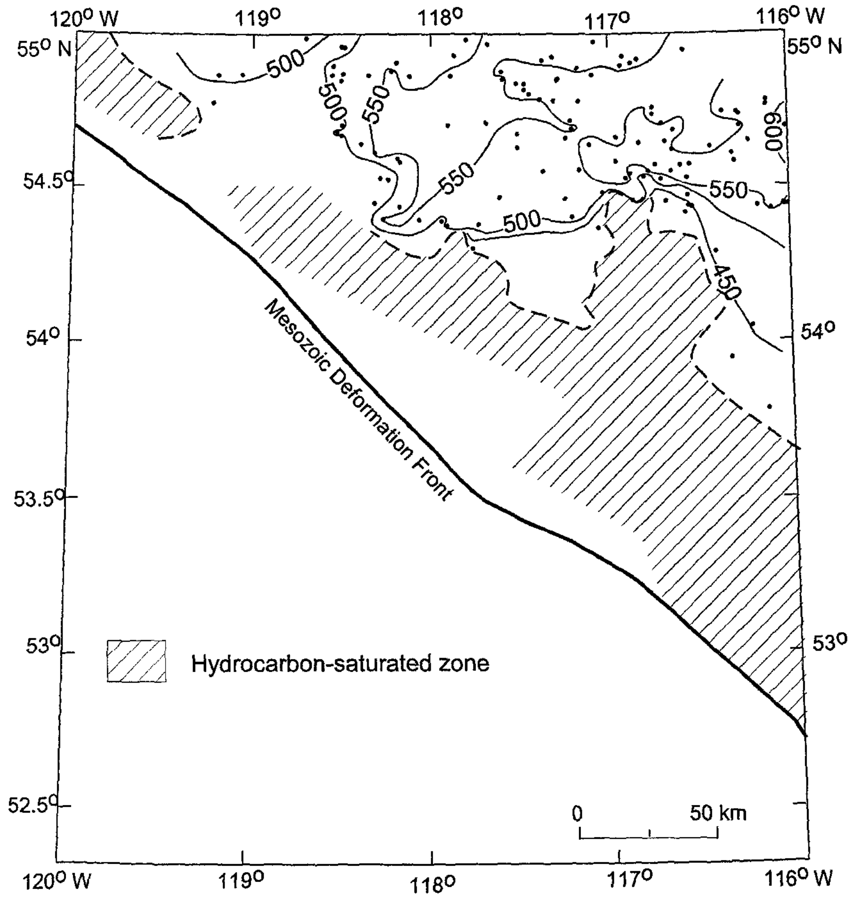


Figure 6.4: Hydraulic head distribution in the Lower Mannville aquifer ($\rho_0$ = 1040 kg/m$^3$, 50 m contour interval).

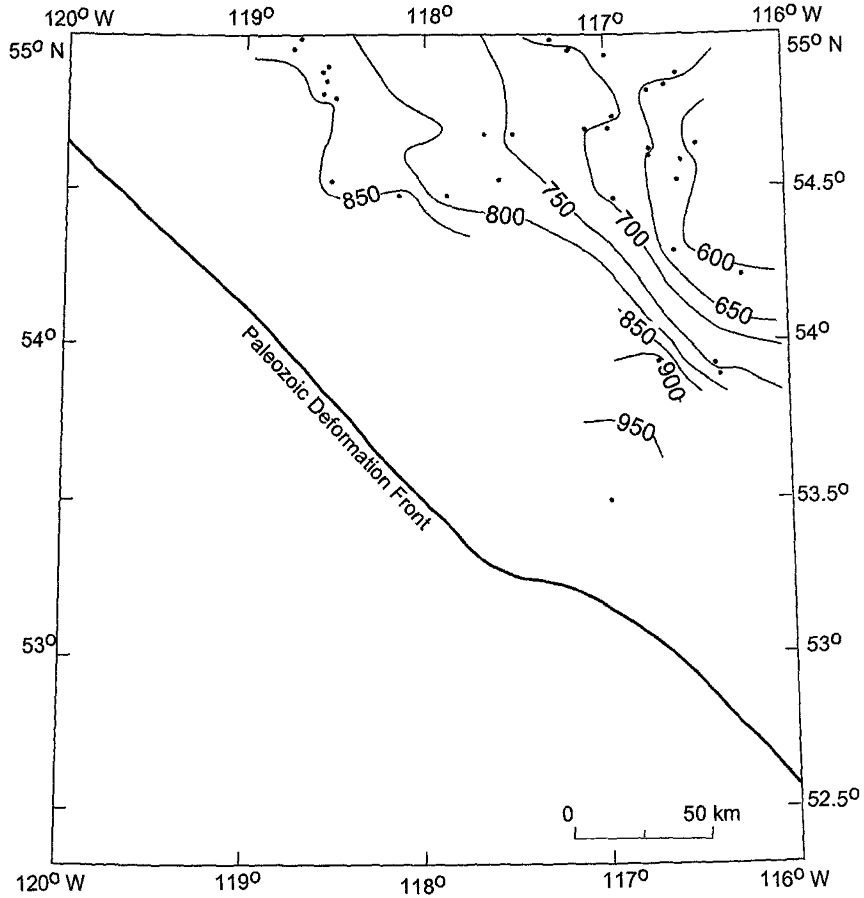


Figure 6.5: Hydraulic head distribution in the Wabamun aquifer ($\rho_0$ = 1040 kg/m$^3$, 50 m contour interval).

Reproduced with permission of the copyright owner. Further reproduction prohibited without permission.

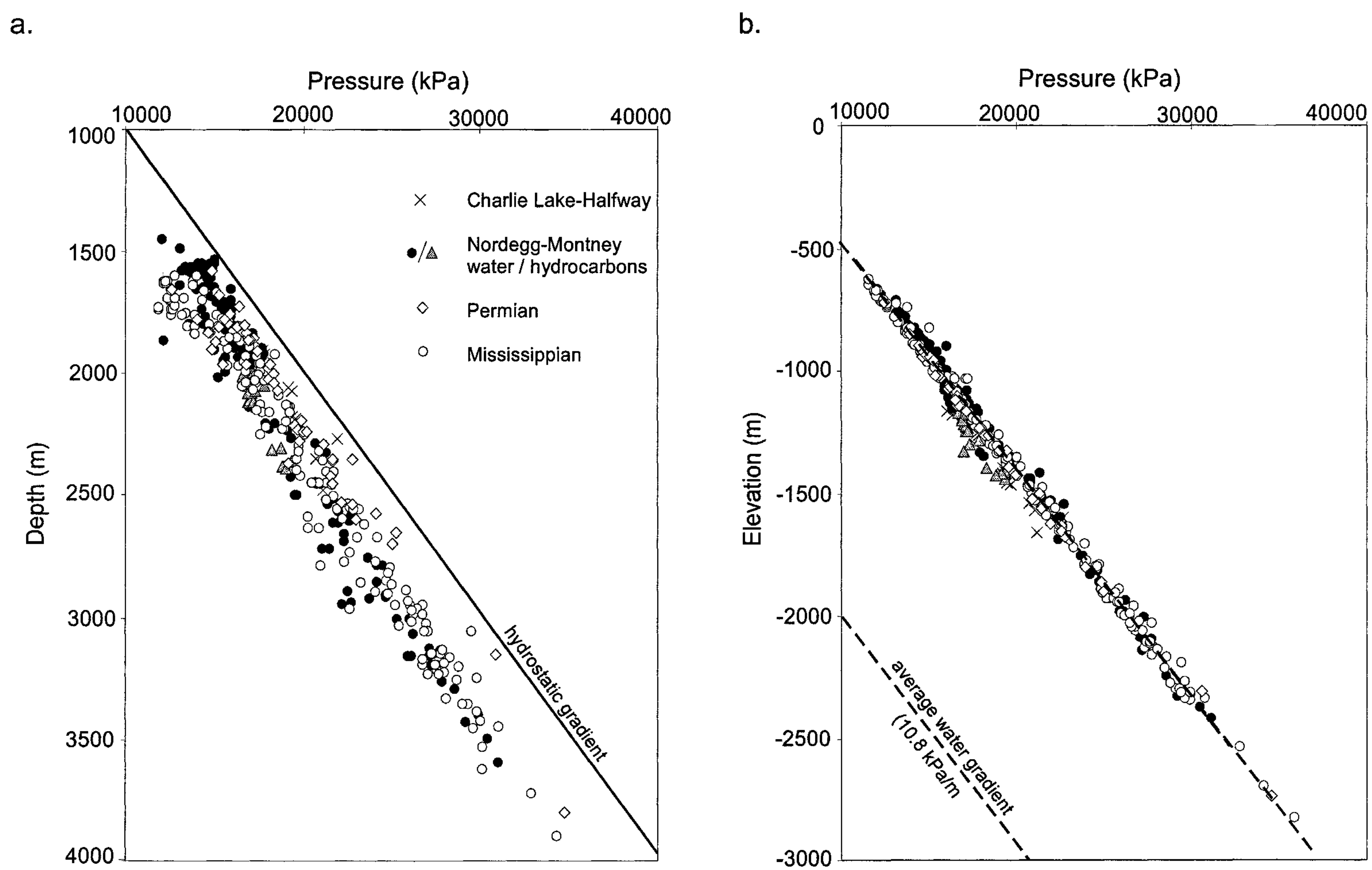


Figure 6.6: Variation of pressure with: a) depth, and b) elevation, for the Jurassic-Mississippian aquifers in the study area.

Figures 6.7 to 6.9 present, respectively, the distribution of hydraulic heads, salinity and bicarbonate in the Charlie Lake-Halfway and Montney aquifers. Because of the location of its subcrop edge, the extent of the Charlie Lake-Halfway aquifer is limited to the northwestern corner of the study area and, therefore, the hydrogeological data are sparse. For better comparison, both aquifers are shown on the same map, because each is confined at the top by the Fernie aquitard. Fluid pressures plot slightly sub-hydrostatic and generally above those of the Montney aquifer at comparable depths (Fig. 6.6a). Hydraulic heads in the Charlie Lake-Halfway are generally at the lower end of the data range in the Triassic aquifers (Fig. 6.7), and the salinity ranges between 115 - 150 g/l (Tab. 6.1).

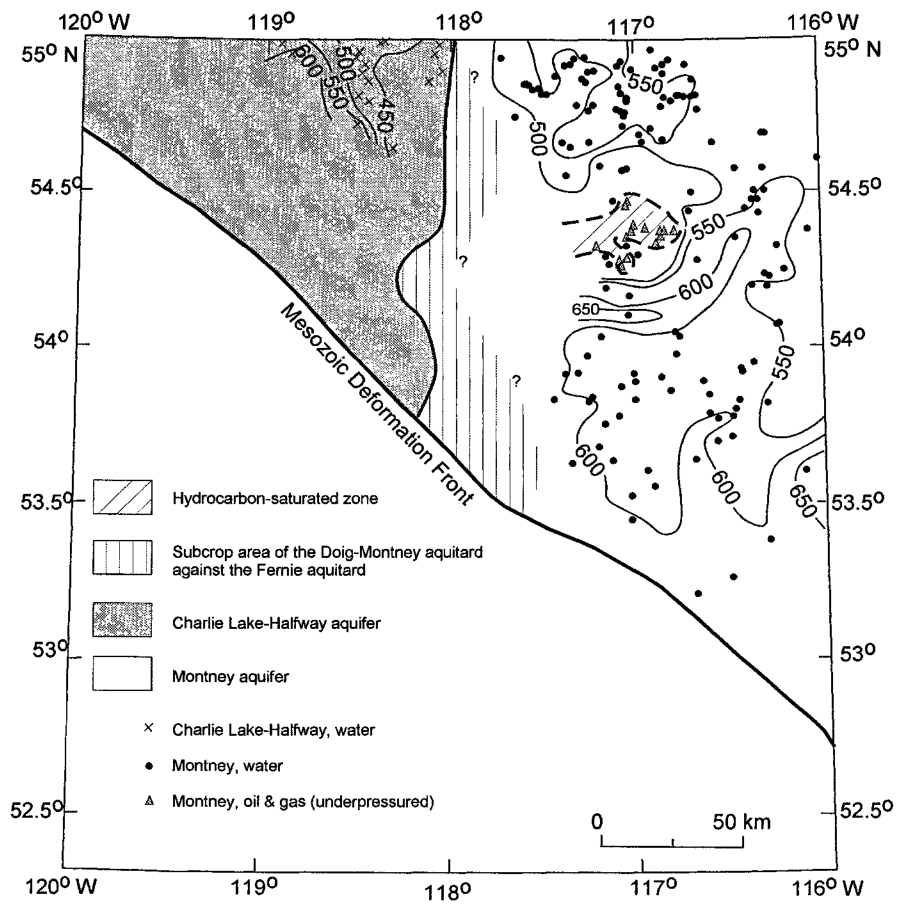


Figure 6.7: Hydraulic head distribution in the Charlie Lake-Halfway and Montney aquifers (50 m contour interval, H calculated with $\rho_0$ = 1040 kg/m3).



Reproduced with permission of the copyright owner. Further reproduction prohibited without permission.

Reproduced with permission of the copyright owner. Further reproduction prohibited without permission.



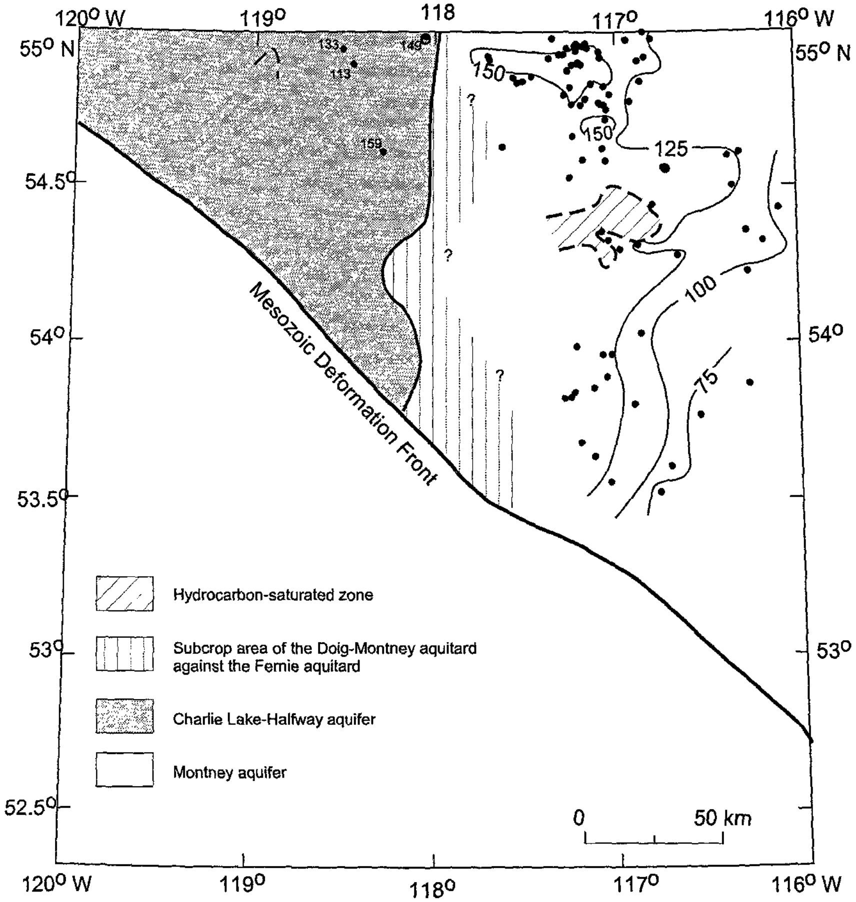


Figure 6.8: Salinity distribution in the Triassic aquifers (25 g/l contour interval in the Montney aquifer, point values in the Charlie L.-Halfway aquifer). Boundaries correspond to zonation in Figure 6.7.

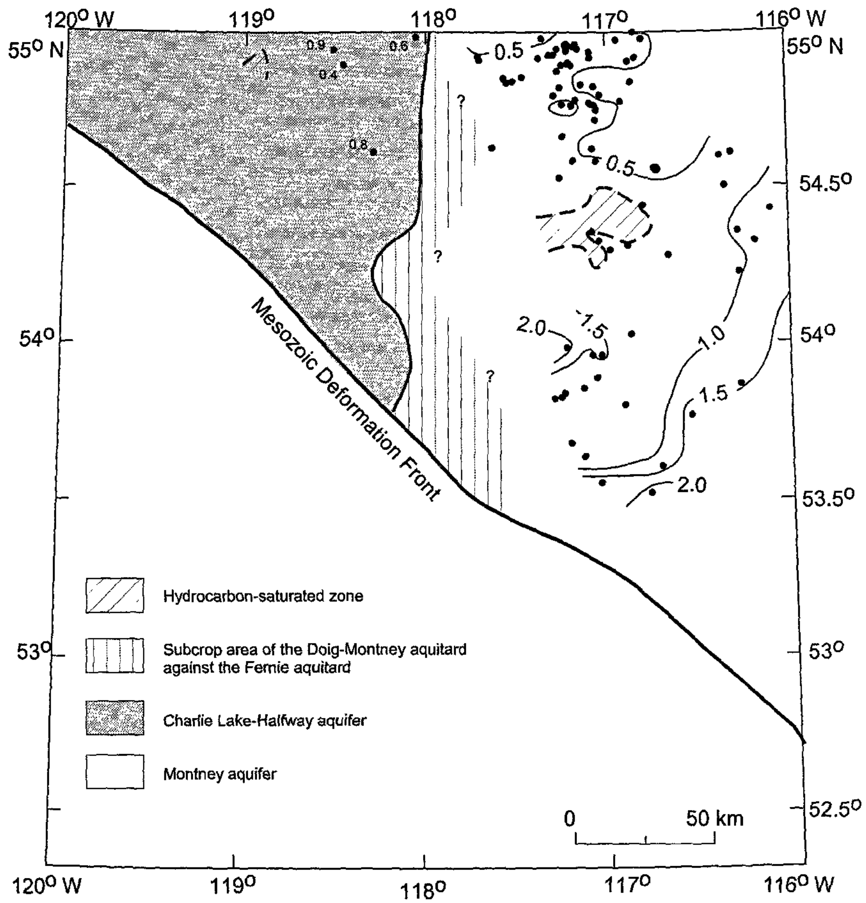


Figure 6.9: Bicarbonate distribution in the Triassic aquifers (0.5 g/l contour interval in the Montney aquifer, point values in the Charlie L.-Halfway aquifer). Boundaries correspond to zonation in Figure 6.7.

Hydraulic heads in the Montney aquifer generally range between 650 and 450 m, and in the north they decrease inwards, towards the centre of the study area. At approximately $117^{O}$ W and $54^{O}$ N, a tongue of hydraulic heads > 600 m forms a potential high, from which hydraulic head values decrease towards the center and northeastward (Fig. 6.7). Flow appears to be focused into a region with hydraulic heads of 450 m, which is adjacent to a hydrocarbon-saturated zone in which fluid pressures plot slightly below the average water gradient (Fig. 6.6b). Lack of data along the northwestern part of the deformation front and towards the center makes it difficult to tell whether the hydrocarbon-saturated zone is closed in that area or if it continues further towards the deformation front.

The salinity in the Montney aquifer increases from 50 g/l in the southeast to 155 g/l in the north (Fig. 6.8). Generally, the lower salinity waters have relatively high bicarbonate concentrations (Fig. 6.9).

*Permo-Mississippian aquifer*

Figures 6.10 to 6.12 present, respectively, the distribution of hydraulic heads, salinity and bicarbonate in the Permo-Mississippian aquifer. Hydraulic heads decrease from approximately 700 m in the southeast corner of the study area to almost 500 m at the northern boundary (Fig. 6.10). A relatively steep hydraulic gradient can be observed in the southeastern and northeastern corners, and along $117^{O}$ W, where hydraulic heads drop by approximately 100 m over a relative short distance (~ 10 km). On the other hand, in an approximately 50 km wide area sub-parallel to $116.5^{O}$ W the hydraulic heads decrease northward by less than 100 m over a 150 km distance. The pressure distribution versus depth (Fig. 6.6a) indicates that the Permo-Mississippian aquifer generally is sub-hydrostatically pressured. In the p(z)-plot (Fig. 6.6b), pressure data follow a relatively straight line, which indicates good hydraulic communication within the aquifer.



Reproduced with permission of the copyright owner. Further reproduction prohibited without permission.

The salinity of formation waters in the Permo-Mississippian aquifer generally increases northwestward in the direction of decreasing hydraulic heads from 50 to 150 g/l and the values stay relatively constant (~ 150 g/l) along the northern boundary of the study area (Fig. 6.11). A relatively abrupt salinity increase from 75 to 125 g/l can be observed northwestward from approximately $54^{O}$ N at the eastern boundary parallel to the deformation front. Along approximately the same line the bicarbonate concentrations rapidly decrease from > 3 g/l in the southeast to < 1 g/l in the north (Fig. 6.12).

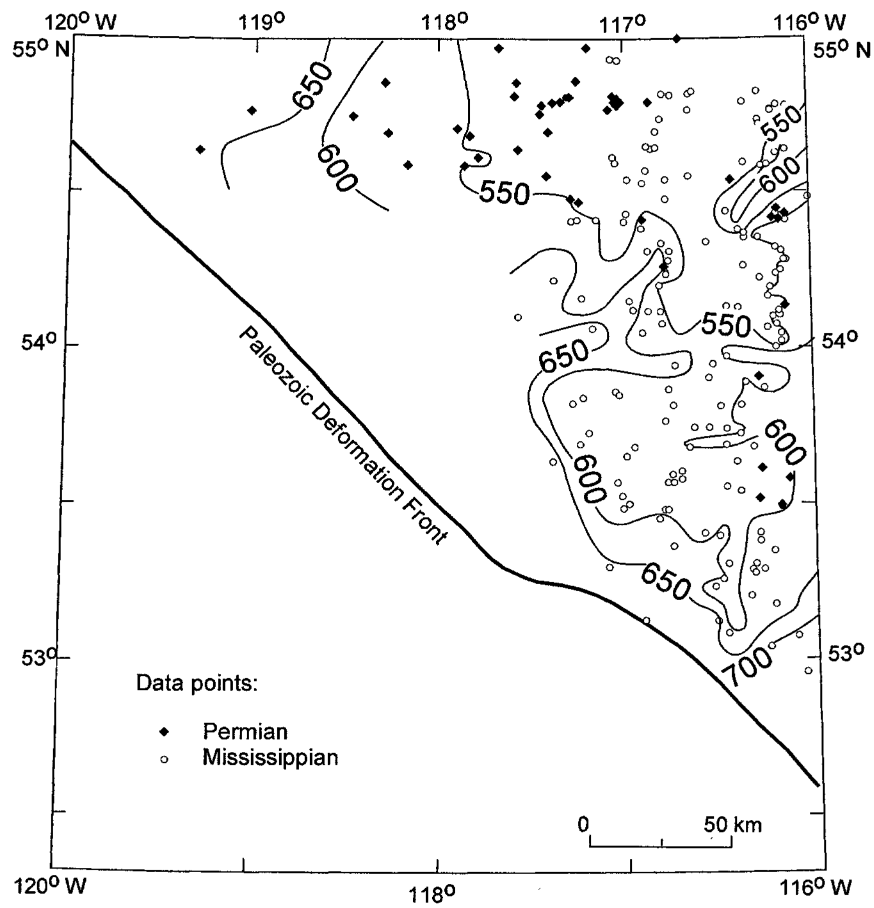


Figure 6.10: Hydraulic head distribution in the Permo-Mississippian aquifer (50 m contour interval, H calculated with $\rho_0 = 1040$ kg/m3).



Reproduced with permission of the copyright owner. Further reproduction prohibited without permission.

Reproduced with permission of the copyright owner. Further reproduction prohibited without permission.



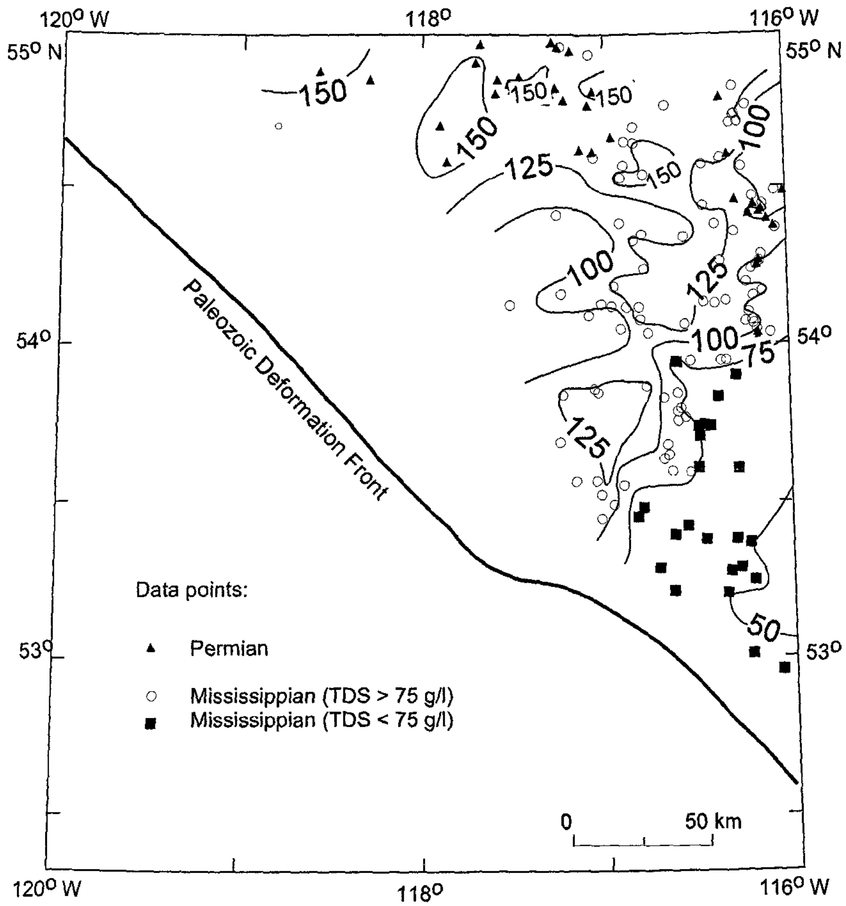


Figure 6.11: Salinity distribution in the Permo-Mississippian aquifer (25 g/l contour interval).

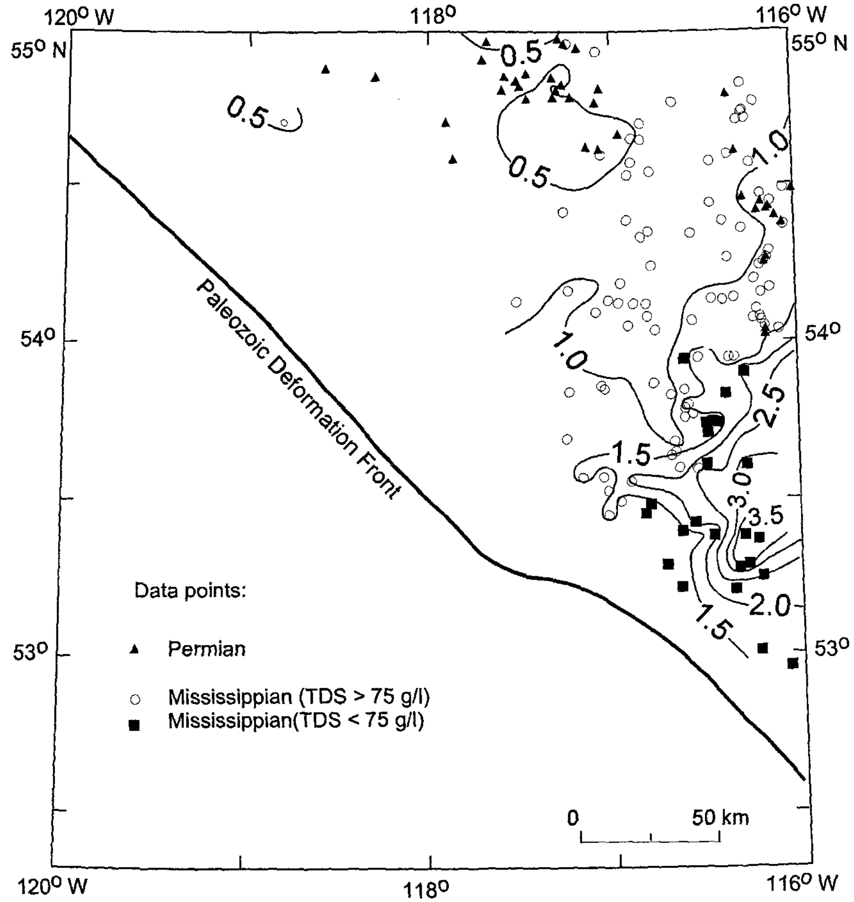


Figure 6.12: Bicarbonate distribution in the Permo-Mississippian aquifer (0.5 g/l contour interval).

*Selected cations in the Jurassic-Mississippian formation waters*

The Jurassic-Mississippian formation waters plot slightly enriched with respect to Na along the seawater-evaporation trajectory (SET) (Fig. 6.13a). The Triassic formation waters and the Mississippian waters from the northern part plot below the SET of Cl versus Br. On the other hand, the low-salinity Mississippian waters from the southeast plot above the SET (Fig. 6.13b).

All of the formation waters are significantly depleted in Mg with respect to the SET (Fig. 6.13c). Conversely, most of the formation waters are enriched in Ca, except for some of the low-salinity Mississippian waters from the southwestern part of the study area, for which concentrations plot below the SET (Fig. 6.13d).

*Summary of hydrogeological observations*

- The hydrostratigraphy of the Jurassic-Mississippian succession and the hydraulic head distribution are different in the western and eastern halves of the study area, approximately W and E of 118$^{O}$ W, respectively.
- Hydraulic heads in the Charlie Lake-Halfway aquifer decrease towards the east, whereas they generally decrease northward in the Montney and Permo-Mississippian aquifers, with the exception of a hydraulic-head low in the center of the Montney aquifer.
- Hydraulic heads less than 500 m in the center of the Montney aquifer indicate a fluid sink, which is not present in the underlying Permo-Mississippian aquifer.
- Generally, the salinity of formation waters in the eastern half of the study area increases northward in the direction of decreasing hydraulic heads in the entire succession.
- There is a zone in the deeper parts of the Triassic aquifers that is saturated with underpressured oil and gas in the Montney aquifer.



Reproduced with permission of the copyright owner. Further reproduction prohibited without permission.

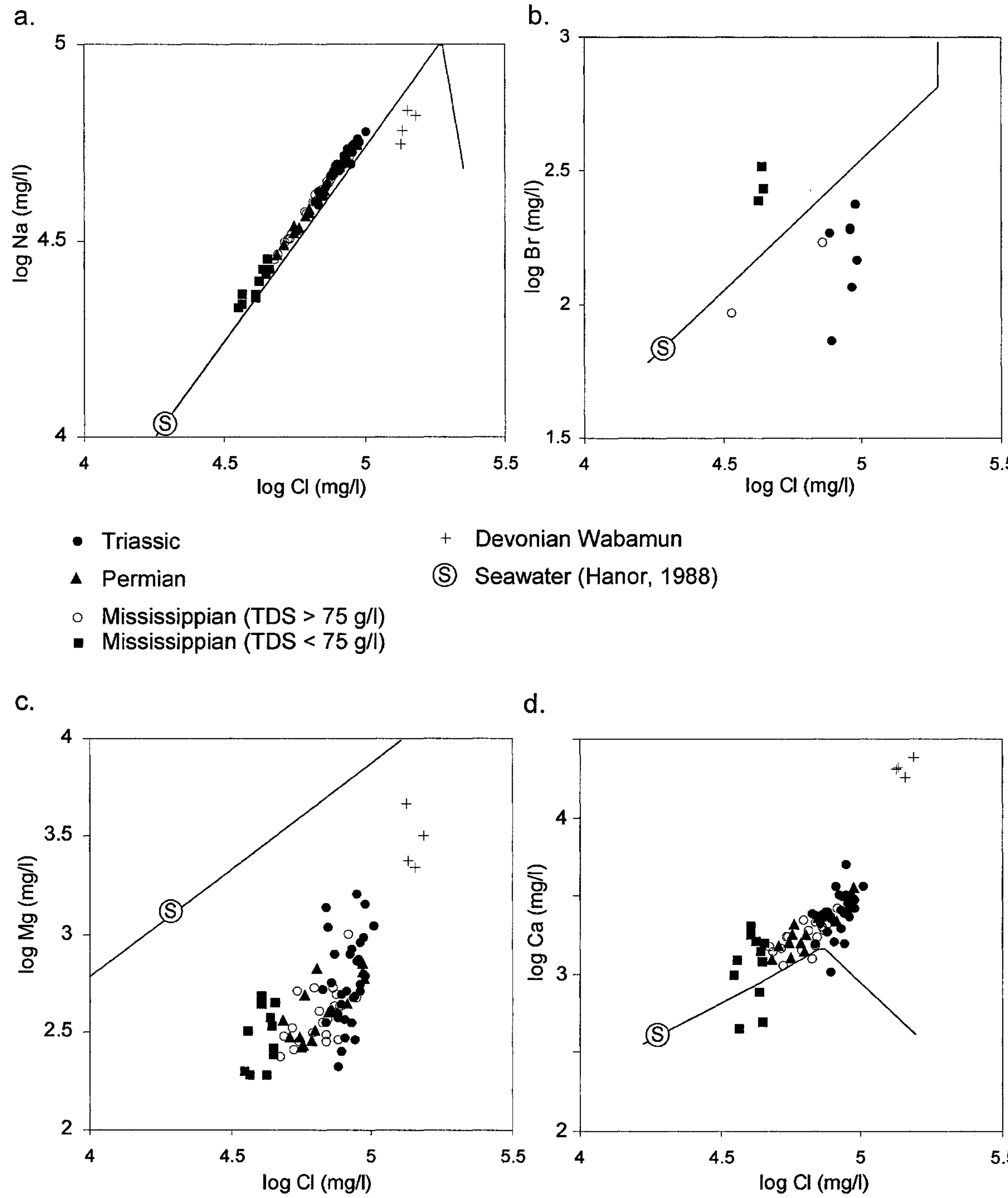


Figure 6.13: Cross plots versus chloride of: a) sodium, b) bromide, c) magnesium, and d) calcium for formation waters in the study area from the Jurassic-Mississippian succession and from the underlying Devonian Wabamun aquifer. Analyses indicating dilution by meteoric water (TDS < 75 g/l) are distinguished from the presumably connate waters. The black line on figures a, b, c, and d represents the respective seawater evaporation curves experimentally determined by McCaffrey et al. (1986).



Reproduced with permission of the copyright owner. Further reproduction prohibited without permission.

## 6.4 Interpretation of flow patterns

*Aquitard competence and lateral barriers to flow*

The confining Fernie aquitard at the top of the Jurassic-Mississippian hydrostratigraphic group thins from 100 m along the deformation front to less than 20 m in the northeastern corner. It separates the overlying Lower Mannville aquifer (Chapter 5) from the Charlie Lake-Halfway and Montney aquifers in the western and eastern halves of the study area, respectively. The Fernie shales are considered to be an effective, regional-scale aquitard in the western Alberta Basin, but they are completely eroded northeast of the study area (Bachu, 1995a).

In the northwestern corner of the study area, the p(z)-plot (Fig. 6.14a) suggests the possibility of cross-formational flow from the Charlie Lake-Halfway aquifer into the Lower Mannville aquifer, which would explain the increased salinity in the Lower Mannville in that area (Fig. 5.26, Chapter 5). Here the Charlie Lake-Halfway aquifer terminates against the Fernie aquitard and the otherwise eastward lateral flow along the Doig aquitard probably is forced upwards into the Lower Mannville aquifer as shown in the hydrogeological cross section (Fig. 6.15). Higher hydraulic heads in the underlying Montney aquifer east of the subcrop edge suggest that flow does not continue sub-laterally across the Doig aquitard and along the base of the Fernie aquitard.

In the southern half the competence of the Fernie aquitard can be inferred from the different fluid saturations in the Lower Mannville (gas) and Montney (water) aquifers. In addition, the offset of fluid pressures in the Lower Mannville and Montney aquifers in the p(z)-plot in Figure 6.14c suggests that there is no hydraulic communication between both aquifers. On the other hand, near the center of the study area the pressure and fluid distributions above and below the Fernie aquitard are similar (Fig. 6.14b), and the "deep basin" gas accumulation in the Lower Mannville aquifer appears to vertically continue into the Montney aquifer.



Reproduced with permission of the copyright owner. Further reproduction prohibited without permission.

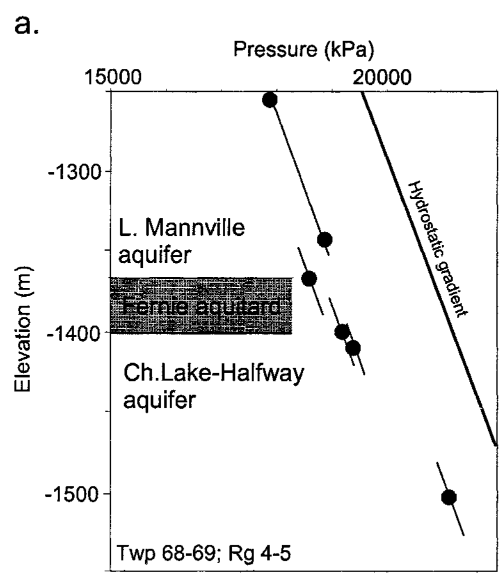


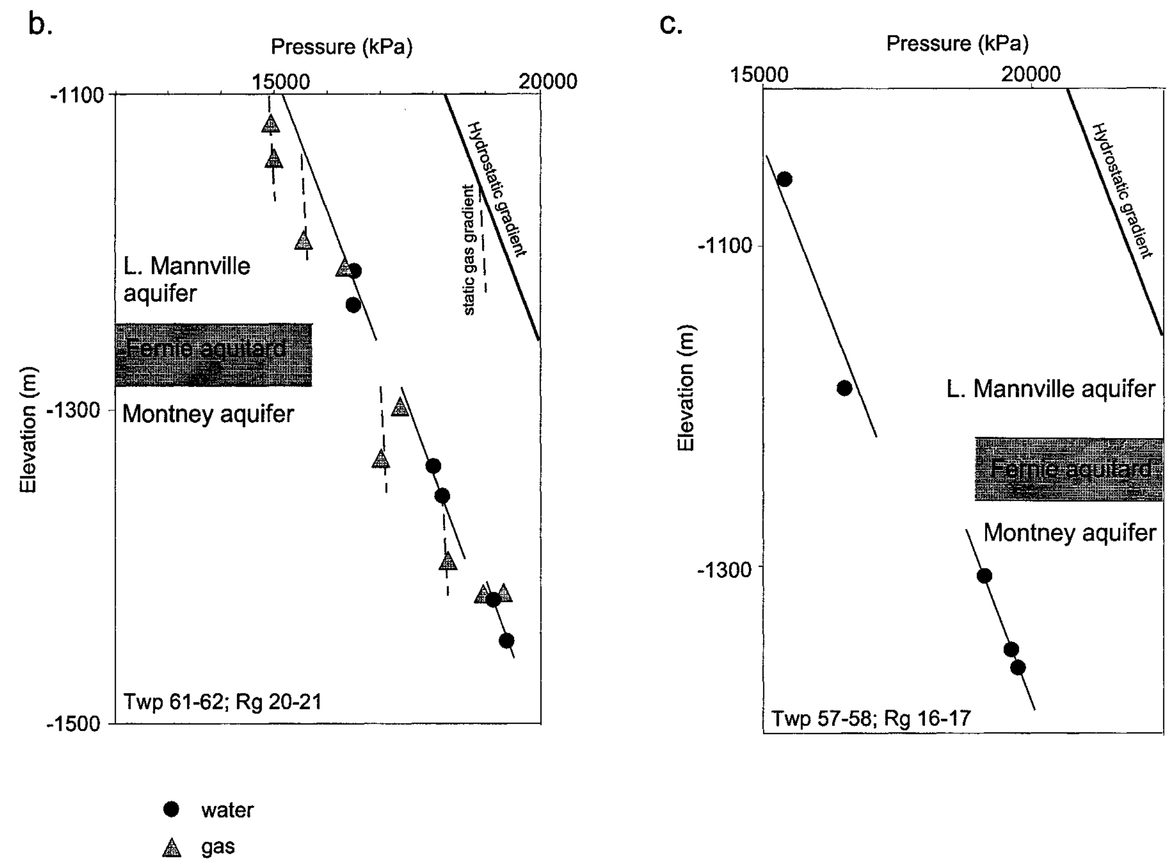


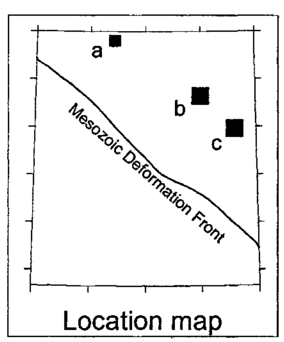


Figure 6.14: Pressure-elevation plots across the Fernie aquitard for the Lower Mannville and Triassic aquifers in various regions of the study area.



Reproduced with permission of the copyright owner. Further reproduction prohibited without permission.

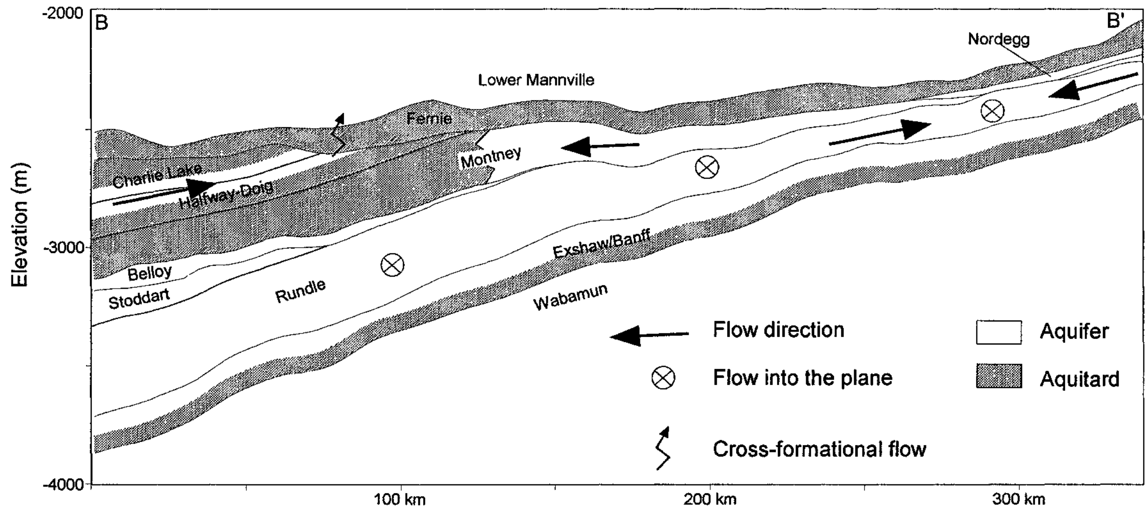


Figure 6.14: Hydrogeological cross section (B - B') sub-parallel to the deformation front showing inferred flow patterns in the Mississippian-Jurassic succession. See Figure 6.1 for line of cross section.

Lack of pressure data towards the deformation front prevents a detailed mapping of this gas-saturated zone in the Montney aquifer. Apparently, the gas-saturated zone does not continue further down into the directly underlying, water-saturated Permo-Mississippian aquifer, which also suggests that there exists a barrier to flow between the latter and the Montney aquifer in that region.

In the northeastern corner of the study area, where the Triassic (and the Permian) strata are eroded and the Nordegg Member consists of carbonates, only approximately 20 m of Fernie aquitard lie between the Lower Mannville and the Mississippian. The hydraulic head distributions in both aquifers are similar (Figs. 6.4 & 6.10) and values decrease westward from above 600 m to less than 550 m, indicating flow from east of the study area. On the other hand, the hydraulic gradient in the Permo-Mississippian aquifer is slightly steeper than in the Lower Mannville aquifer, so that only along a narrow band at the eastern boundary of the study area, flow in the Lower Mannville and Permo-Mississippian aquifers appears to merge. This does not necessarily infer cross-formational



Reproduced with permission of the copyright owner. Further reproduction prohibited without permission.

flow, which would disagree also with the different salinities in both aquifer (Figs. 5.26 and 6.11, but rather is the reflection of a regional SE-NW directed flow system in a continuous Mississippian-Jurassic-Mannville aquifer (Bachu, 1995a, Anfort et al., 2001) extending into the study area from the east, where the Fernie shales are eroded.

The decreasing permeability in the Montney Formation towards the west is inferred from a change in lithology from sandstone to siltstones and shales (Edwards et al., 1994). This is indirectly confirmed by the lack of hydrogeological data in the western part of the Montney Formation, suggesting that this area does not contain substantial reservoir units. The low-permeability part of the Montney Formation also forms an aquitard with respect to flow in the underlying Permo-Mississippian aquifer. In addition, the gas-saturated zone in the Montney aquifer appears to lie in the transition zone from high-to-low permeability, and to be confined at its base (Fig. 6.16), because it is not affected by formation water flow in the underlying Permo-Mississippian aquifer.

Generally, the hydraulic head and salinity distribution in the Permo-Mississippian and Montney aquifers are very similar, except for the hydraulic low associated with the gas-saturated zone in the Montney aquifer. In addition, the pressure variation with elevation in the Montney and Permo-Mississippian aquifer is very similar, as pressure data from both aquifers fall almost on the same straight line. Only in the vicinity of the hydrocarbon-saturated-zone (-1200 to -1500 m elevation) do pressures in the Montney aquifer plot slightly below the line defining the average water gradient in both aquifers (Fig. 6.6). This shows that the Mississippian-to-Lower Jurassic strata form a hydraulically continuous aquifer system in the eastern half of the study area.



Reproduced with permission of the copyright owner. Further reproduction prohibited without permission.

Reproduced with permission of the copyright owner. Further reproduction prohibited without permission.



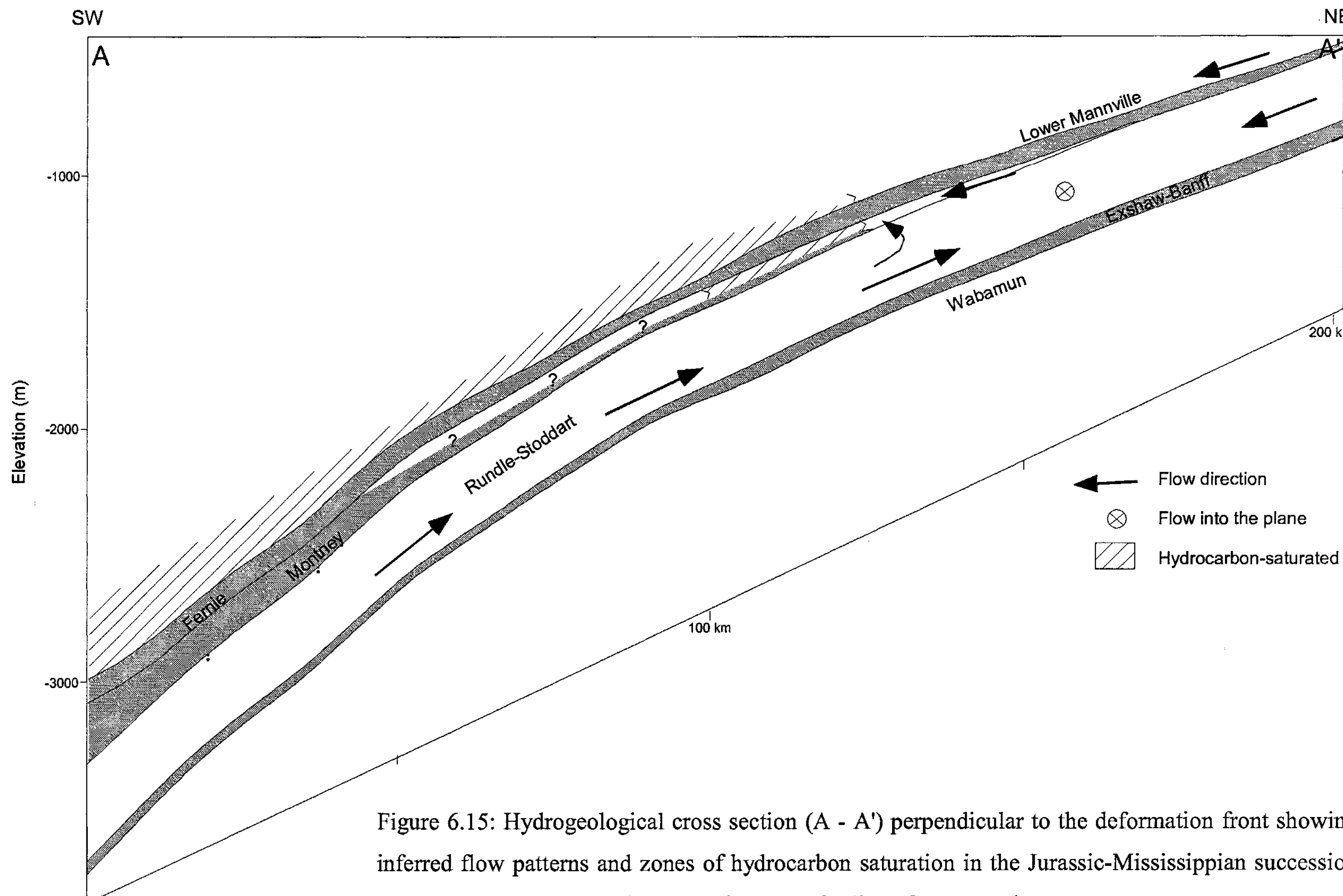


Figure 6.15: Hydrogeological cross section (A - A') perpendicular to the deformation front showing inferred flow patterns and zones of hydrocarbon saturation in the Jurassic-Mississippian succession and Lower Mannville aquifer. See Figure 6.1 for line of cross section.

The Exshaw-Banff aquitard at the base of the succession is considered to be a strong, basin-wide aquitard (Bachu, 1995a). This is confirmed in the study area by lower hydraulic heads in the Permo-Mississippian aquifer (Fig. 6.10) compared to the underlying Wabamun aquifer (Fig. 6.5). The difference in hydraulic heads between the Permo-Mississippian and the Wabamun aquifers is largest along the deformation front in the deeper parts of the aquifers. The difference decreases northeastward along dip, until hydraulic heads are in the same range in the northeast corner of the study area, where pressures in the Permo-Mississippian and the Wabamun aquifers appear to have equilibrated to similar boundary conditions. The analysis of hydrogeological data in the Devonian aquifers is necessary for a more detailed discussion on cross-formational flow across the Exshaw-Banff aquitard and the reader is referred to Chapter 7.

*Fluid origin and evolution*

The Mississippian to Jurassic sediments were deposited mainly in a marine environment, therefore, the original formation water most likely consisted of seawater. The slight excess in Na concentrations compared to evaporated seawater (Fig. 6.13a) and the Br/Cl systematics (Fig. 6.13b) suggests that, in addition to seawater evaporation, the salinity of Mississippian-Jurassic formation waters has been influenced significantly by subsequent evaporite dissolution, for which Charlie Lake Fm evaporites in the northwest of the study area are the main potential source (Kirste et al., 1997).

Mississippian carbonates are largely dolomitized, and therefore replacive dolomitization of limestone is probably the main cause for the depletion of Mg and, at least partly, for the enrichment in Ca in the formation waters. Lewchuk et al. (1998) interpreted the replacive dolomites in Mississippian carbonates in southern Alberta as early diagenetic products that were precipitated along with evaporites from Mg-rich brines during Mississippian time. The exact composition of these brines is not known; however, Ca-ions replace Mg-ions in the formation water in a 1:1-ratio during the replacive



Reproduced with permission of the copyright owner. Further reproduction prohibited without permission.

dolomitization of limestone, and the Ca/Mg-ratio should increase, following the 'dolomitizing' trend in Figure 6.17a. The actually observed positive correlation between Mg and Ca suggests that additional processes must have been involved that led to the chemical composition of formation waters presently observed in the Jurassic-Mississippian succession. The positive correlation of Ca and sulfate (Fig. 6.17b) indicates that gypsum dissolution partly contributed to the Ca content of the formation waters. Higher sulphate concentrations in the Triassic and Permian than in the Mississippian waters probably are related to the distance from the main evaporite deposits in the Triassic succession.

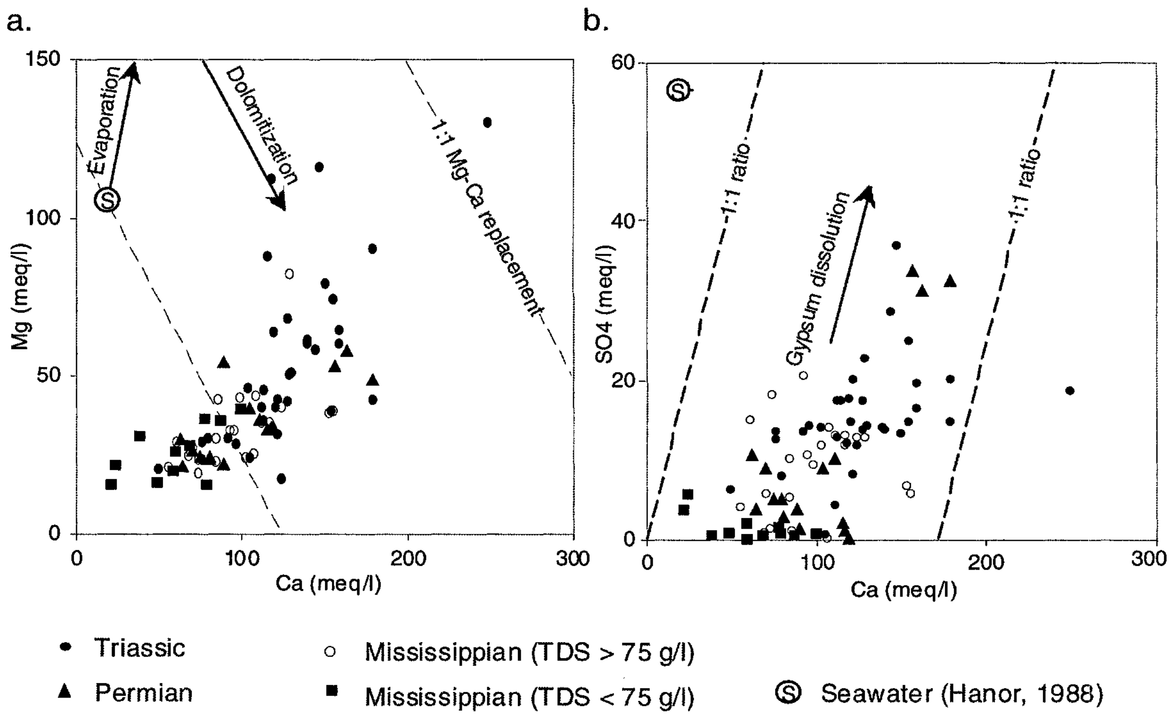


Figure 6.17: Cross plots of calcium versus: a) magnesium, and b) sulfate, for formation waters in the study area from the Jurassic-Mississippian succession.

$Ca_{excess}$ versus $Na_{deficit}$ values of Mississippian-Triassic formation waters in the study area plot around the Basinal Fluid Line (Davisson and Criss, 1996), but there is no distinct 2:1 correlation between Na and Ca that would confirm the albitization trend (Trend 1 in Fig. 6.18). Almost all water samples show excess in Na (negative $Na_{deficit}$) and a deficit-to-excess in Ca. Evaporation of seawater causes the $Ca_{excess}$ values to decrease without



Reproduced with permission of the copyright owner. Further reproduction prohibited without permission.

changing the Na component until the point of halite saturation (following Trend 2a beyond the lower boundary of Figure 6.18). During the precipitation of halite, the $Ca_{excess}$ value stays constant and the $Na_{deficit}$ value increases (Trend 2b). Obviously, the evaporation of seawater alone could not have produced the observed brine composition. However, during the dissolution of halite Na and Cl ions are added to the formation water in a 1:1-ratio, which causes a relative increase in Na over Ca (Trend 3). The dissolution of gypsum and the replacive dolomitization of limestone both cause an increase in Ca without effecting the Na and Cl concentrations (Trend 4).

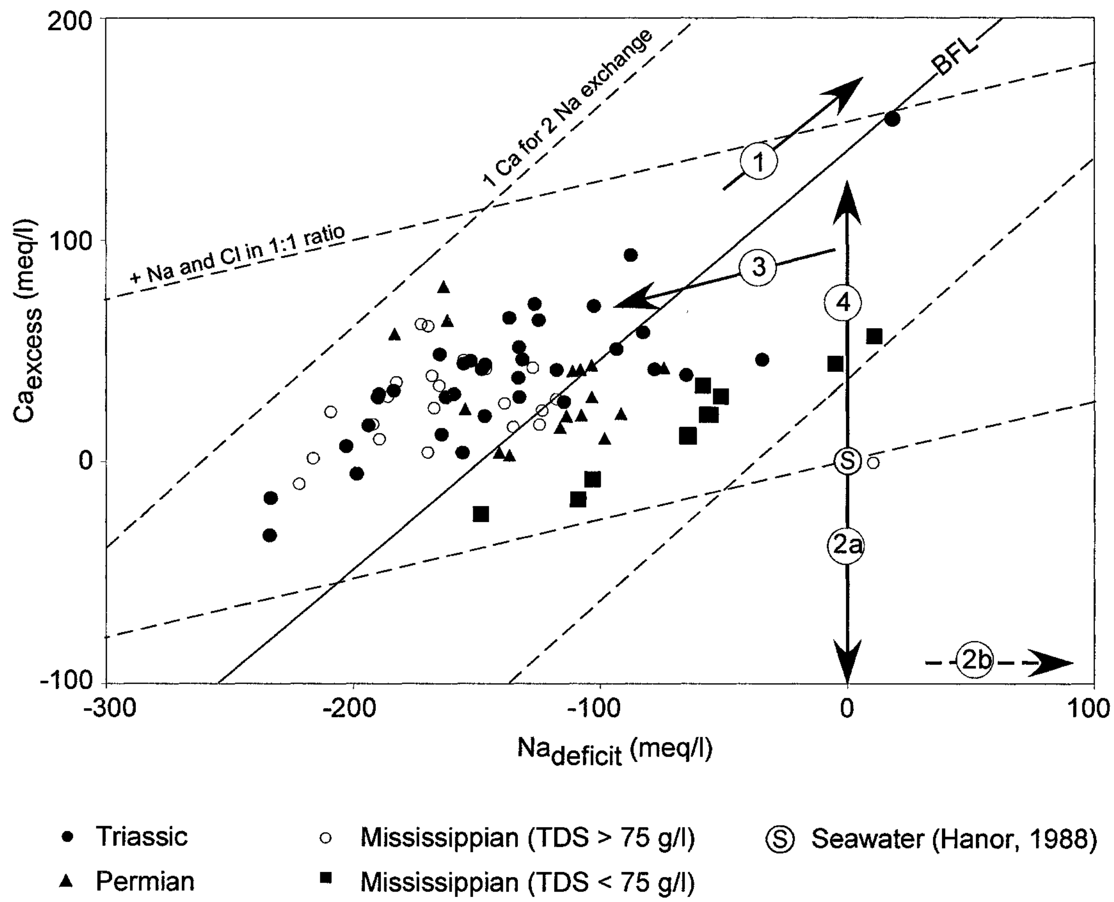


Figure 6.18: Plot of $Ca_{excess}$-$Na_{deficit}$ for Mississippian-Jurassic formation waters in the study area, showing trends for various processes that may have effected the fluid composition. The circled numbers in the figure refer to the trends of: 1) albitization of plagioclase, 2) evaporation of seawater (a) beyond the point of halite saturation (b), 3) halite dissolution, and 4) dolomitization and gypsum dissolution. The Basinal Fluid Line (BFL) from Davisson and Criss (1996) is shown for reference.



Reproduced with permission of the copyright owner. Further reproduction prohibited without permission.

Plotting salinity variations of the Jurassic-Mississippian formation waters versus their Na/Cl-ratios (Fig. 6.19) allows distinguishing between two types of brines and suggests that they have been affected by different processes. Brine I comprises most of the Triassic and Permian, plus some of the Mississippian data, and is characterized by salinities between approximately 75 to 170 g/l and a relatively narrow range of Na/Cl-ratios between 0.875 to 0.95. The high salinities are probably due to the high degree of seawater evaporation, which actually reached beyond the point of halite saturation during the Late Triassic, exemplified by halite deposits in the upper part of the Charlie Lake Formation. The shift towards Na/Cl-ratios higher than observed in seawater probably is due to subsequent halite (Na/Cl=1.0) dissolution in the subsurface.

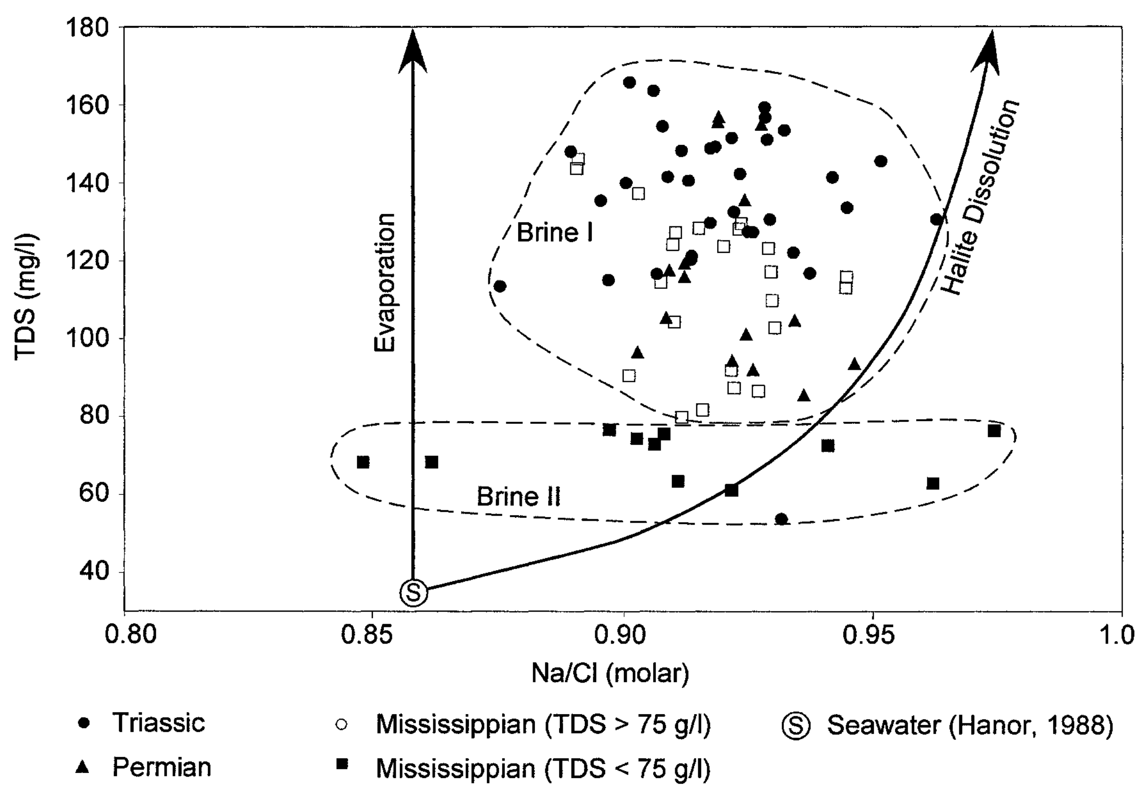


Figure 6.19: Na/Cl-ratio versus salinity plot of Jurassic-Mississippian formation waters showing tentative trends of evaporation and halite dissolution.



Reproduced with permission of the copyright owner. Further reproduction prohibited without permission.

Brine II comprises exclusively Mississippian formation waters, mainly from the south- to southeastern part of the study area. These are relatively fresh waters (TDS = 50 - 75 g/l) with a wide spread in Na/Cl-ratios (0.85 – 0.98), which probably represent the mixing of evaporated seawater with water of more recent meteoric origin to the south of the study area. The degree of evaporation is significantly lower than for the Triassic formation waters, which is not surprising, as there are no significant evaporitic sequences deposited in the Mississippian strata in the study area.

*Flow patterns and driving mechanisms*

Flow in the Charlie Lake-Halfway aquifer, as inferred from hydraulic heads (Fig. 6.7), is eastward where the aquifer terminates against the Fernie aquitard. There it appears to be forced upwards into the Mannville aquifer, as hypothesized in the previous section. Flow could also be deflected northward along the subcrop boundary, but the hydraulic gradient inferred from the hydraulic head distribution north of the study area continues to suggests eastward flow (Hitchon et al., 1990) into the overlying Lower Mannville aquifer across the Fernie aquitard.

Flow in the north-central part of the Montney aquifer is directed inward, towards the hydrocarbon-saturated zone, and therefore differs from the general northward flow direction in the Montney and Permo-Mississippian aquifers. A fluid sink appears to exist in that region, which focuses flow and draws water from the Montney aquifer. The close association with the underpressured hydrocarbon-saturated zone suggests that this sink is created by a higher rate of hydrocarbon escape than hydrocarbon generation in that region, a mechanism that was described for the underpressured water in the overlying Lower Mannville aquifer (s. Chapter 5). The steep drop in hydraulic heads from 550 to less than 500 m in that area appears to delineate a lateral permeability barrier up to which the hydrocarbon-saturated zone probably extended during the period of deep burial and high rate of hydrocarbon generation. This rate decreased during uplift, allowing formation



Reproduced with permission of the copyright owner. Further reproduction prohibited without permission.

water to re-imbibe the formerly hydrocarbon-saturated zone and causing the shrinkage of the latter, a trend that will probably continue with further basin uplift.

In the remainder of the combined Montney-Permo-Mississippian aquifer, hydraulic heads are high (> 600 m) along the eastern boundary and sub-parallel to the deformation front, and decrease towards the northwest and northeast, respectively. Therefore, the respective northwestern and northeastern flow directions merge into a northward flow direction in an approximately 50 km wide area sub- parallel to $116.5^{O}$ W (Figs. 6.7 & 6.10). The steep hydraulic and salinity gradients in that area actually suggest that fresher formation water from the southeast and from the direction of the foothills region encloses a large plume of high-saline brine (TDS > 125 g/l) from all directions except from the north. This brine has a salinity approximately 4 times that of seawater (~ 35 g/l), and is contained within the ranges of brine I (Fig. 6.19). The hydraulic gradient within the area of the high-salinity brine is actually so low that, taking in account higher density brines in the shallow part of the aquifer in the north, and less than 50 m difference in hydraulic heads over a distance of 50 km in a northward direction, flow of brine I can only be inferred to be ± stagnant (see discussion on accuracy an resolution of hydraulic heads in Chapter 3; 3.3.4). The less saline water (brine II) coming from the south-southeast is most probably associated with a long-range, gravity-driven flow system originating in Montana (Bachu and Underschultz, 1995; Anfort et al., 2001). In the southeast, flow appears to be deflected by less permeable strata and forced to by-pass the high-salinity plume northwestward along the deformation front and northward along the eastern boundary of the study area, respectively. Because the Cretaceous aquitards and the hydrocarbon-saturated region in the overlying post-Jurassic succession represent a barrier to meteoric recharge from directly above, the southwestern component of the flow could alternatively be explained only by flow originating in the foothills region. In that case, the relatively low salinity could be due to meteoric recharge in the Rocky Mountains and subsequent downward flow along faults into the Mississippian to Jurassic strata, or caused by expelled water as the result of tectonic loading during the Laramide orogeny. Recharge in the thrust and fold belt, followed by a tortuous flow path, hydraulically connecting



Reproduced with permission of the copyright owner. Further reproduction prohibited without permission.

deformed and undeformed Mississippian strata, has been proposed by Underschultz and Bartlett (1999) in the southern part of the study area. Their study was largely based on industry data not accessible to the public, and it is difficult to evaluate their results. Tectonic expulsion as a possible driving mechanism for regional-scale flow was first introduced theoretically by Oliver (1986), and was proposed to have affected flow in the Cambrian-Devonian hydrostratigraphic group (Bachu, 1995a; Machel and Cavell, 1999). However, considering the relatively low salinity of formation waters along the deformation front, a meteoric origin combined with a long-range, gravity-driven flow system seems to be the most likely explanation for the observed flow pattern in the Mississippian-Jurassic succession. A more detailed discussion on this topic follows in Chapter 7.

### 6.5 Summary and conclusions

In the eastern half of the study area, the Jurassic-Mississippian hydrostratigraphic group represents a single continuous carbonate-sandstone aquifer system, consisting of the Lower Jurassic Nordegg Member, the Triassic Montney Formation, the Permian Belloy Formation and the Mississippian Stoddart and Rundle Groups. The confining units are the competent Fernie and Exshaw-Banff aquitards at the top and base, respectively. The general flow direction is northward, and fresher water, which is part of a basin-scale, gravity-driven flow system originating at high formation outcrops in Montana, flows around and partly displaces a plume of connate brine.

The relatively high salinity, in the 130-150 g/l range, and low bicarbonate content (~0.5 g/l) of formation waters in the northern part of the area indicate a connate origin of these waters. Evaporation of seawater, short of halite saturation, probably took place shortly after sediment deposition, but the Ca-Na-Cl systematics suggest that successive halite and gypsum dissolution, and dolomitization had a more prominent influence in forming the Jurassic-Mississippian brines currently observed in the study area. The only positive



Reproduced with permission of the copyright owner. Further reproduction prohibited without permission.

indication, based on Br, for a brine formed by the evaporation of seawater beyond the point of halite saturation was observed in the low-salinity brine in the southeast. However, no halite deposits exist in the Jurassic-Mississippian strata in this part of the Alberta Basin, and the source for the highly evaporated component in this supposedly highly diluted formation water must be located somewhere along the flow path in the southeast of the study area. A first comparison between the chemical signature of formation waters from the Jurassic-Mississippian and the underlying Wabamun suggest that these brines are different. A detailed discussion on the origin and evolution of formation waters from the entire stratigraphic succession follows in Chapter 8.

Only the Permo-Mississippian aquifer continues westwards, whereas the lithology in the overlying Montney Formation changes to siltstones and shales, which, in combination with the Doig Formation, form an aquitard. A "deep basin" hydrocarbon accumulation with relatively low hydraulic heads in its vicinity is observed in the transition zone from sand- to siltstones in the Montney Formation, similar to directly overlying hydrocarbon reservoirs in the Lower Mannville aquifer, but its exact areal extent is not known. Overlying the Doig-Montney aquitard is the Charlie Lake-Halfway aquifer. Flow in this aquifer is eastward and, at its subcrop edge, is forced upward through the Fernie shales into the Lower Mannville aquifer, where it causes an increase in formation water salinity.

No hydrocarbon-saturated zones were detected in the Permo-Mississippian aquifer, hence hydraulic communication of formation water between the deformed and undeformed parts of the Alberta Basin becomes possible at least from a fluid continuum point of view, but there are insufficient data to corroborate or disprove this. The hydraulic head distribution actually indicates that there is a component of flow from the direction of the thrust and fold belt of the Rocky Mountains, and the nature and origin of this flow will be further investigated in Chapter 7 for the underlying Cambrian-Devonian hydrostratigraphic group.



Reproduced with permission of the copyright owner. Further reproduction prohibited without permission.

# CHAPTER 7: FLOW OF FORMATION WATER IN THE CAMBRIAN-DEVONIAN SUCCESSION

## 7.1 Introduction

Earlier interpretations of the flow in the Alberta Basin suggested a basin-wide, topography-driven flow system that is recharged in the Rocky Mountain foothills in the southwest, channeled updip northeastward mainly along Devonian aquifers, and is discharged along the "feather-edge" of the basin (Hitchon, 1969a, 1984). This interpretation was used to explain the Pine Point Pb-Zn and the Athabasca oil sands deposits northeast of the study area (Garven, 1985, 1989). The main implication of the previous hydrogeological interpretation is that such a basin-scale flow system would have, at least partly, flushed the connate brines from the deep Devonian aquifers within 2 million years (Adams et al., 2000). Also, the flow in Devonian aquifers in the southwest is disconnected from meteoric recharge in the Rocky Mountains, and past tectonic compression was proposed as the mechanism that drives the flow in these aquifers (Bachu, 1995a).

The combination of mainly three mechanisms was proposed to have produced the brines in the Cambrian-Devonian succession in the Alberta Basin (Hitchon et al., 1971; Spencer, 1987; Connolly et al., 1990a): a) dissolution of evaporite deposits, b) evaporation of seawater, and c) shale membrane filtration. Hitchon et al. (1971) suggested that the dissolution of Middle Devonian halite is the major source for the high salinity in the Devonian brines, and that membrane filtration was responsible for further concentrating the brines. According to Spencer (1987) and Connolly et al. (1990a), evaporation of seawater is the main mechanism for the brine production; they argue that halite dissolution could not result in the bromide-chloride ratios observed in the Devonian



Reproduced with permission of the copyright owner. Further reproduction prohibited without permission.

formation waters. On the other hand, according to Land (1987), it is possible to obtain Br-Cl ratios near or slightly greater than seawater from the recrystallization of halite.

The present study of formation water chemistry and flow patterns in Devonian aquifers in the vicinity of the Rocky Mountains deformation front in west-central Alberta (Fig. 7.1a) intends to identify the flow-driving mechanism(s) and to investigate whether there are indications for the displacement of connate brines in these aquifers. Elucidation of these issues is important for understanding hydrocarbon migration pathways and mineralization processes in the basin.

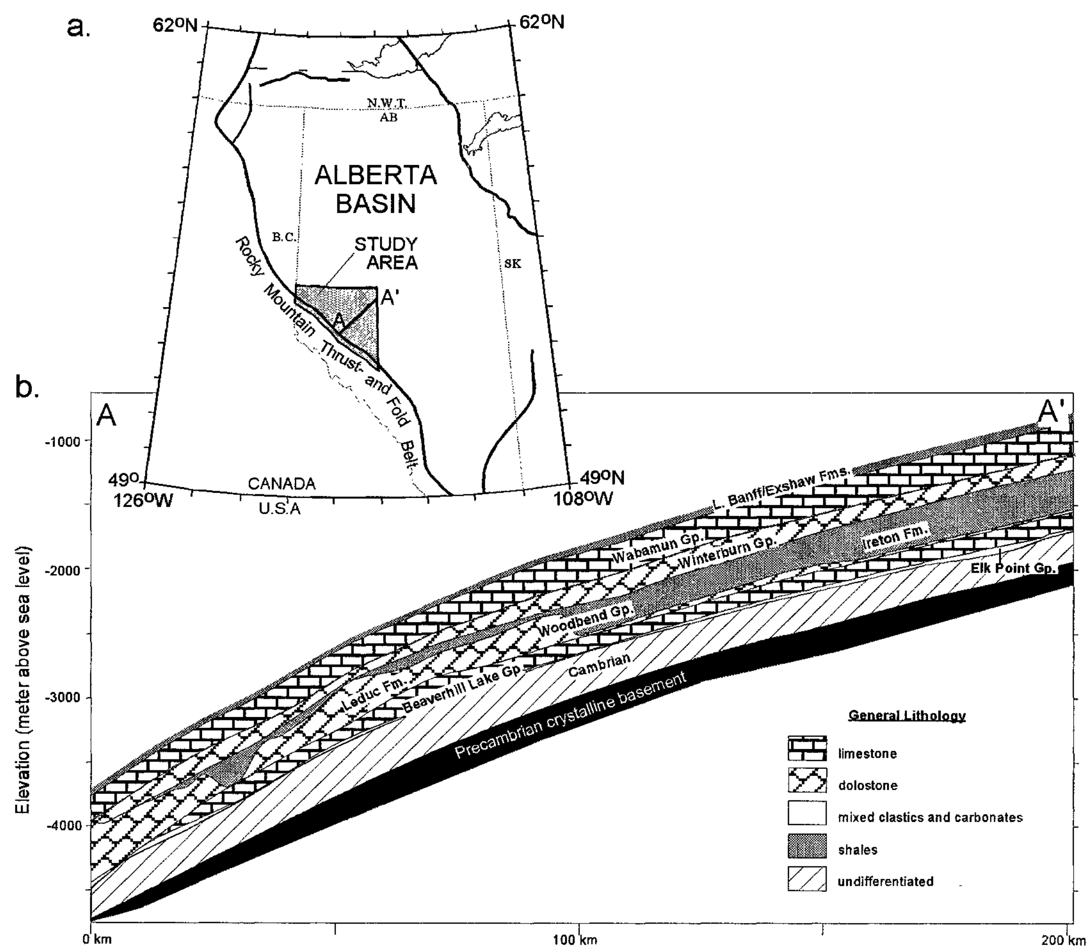


Figure 7.1: a) Location of the study area in the Alberta Basin and b) structural cross section perpendicular to the deformation front showing general lithology distribution in the Cambrian-Devonian succession.



Reproduced with permission of the copyright owner. Further reproduction prohibited without permission.

## 7.2 Hydrostratigraphic framework

The Cambrian-Devonian succession in the study area lies 2000-5000 m below the ground surface, it has an average slope of 15 m/km, and consists mainly of marine carbonates and shales, approximately 1000 m in total thickness (Fig. 7.1b) that were deposited during the passive-margin stage of basin evolution (see Chapter 4). The Cambrian-Devonian hydrostratigraphic group is confined by the underlying crystalline Precambrian basement and the overlying Carboniferous shales of the Exshaw and Lower Banff Formations (Fig. 7.2), which form an aquiclude and an effective aquitard, respectively (Hitchon et al., 1990; Bachu, 1995a). The basal sandstones of Middle Cambrian age form a thin basal aquifer, which is separated from the Upper Cambrian carbonate aquifer by an intervening shale aquitard. In the northwest corner of the study area, where the Cambrian is absent due to non-deposition or erosion, the Devonian lies directly on the Precambrian basement (s. Chapter 4, Fig. 4.4 a). The Devonian succession is comprised, in ascending order, of the following groups: Elk Point, Beaverhill Lake, Woodbend, Winterburn and Wabamun (Fig. 7.2). Mixed near-shore clastics and carbonates of the Elk Point Group and the underlying Upper Cambrian form what, from now on, will be referred to as "Elk Point aquifer". It is overlain by the platform and reef carbonates of the Beaverhill Lake and Woodbend Groups that form the "Woodbend-Beaverhill Lake aquifer" (Fig. 7.1 b and Fig. 7.2). Along the Swan Hills and Cooking Lake platform edges, the intervening Watt Mountain and Waterways shales form local aquitards (Chapter 4, Fig. 4.4 b), where they separate the Elk Point, Beaverhill Lake and Woodbend aquifers, respectively. Thus, on a regional scale these aquifers act as a continuous aquifer system (Middle Devonian). The Woodbend Ireton shales constitute the major aquitard in the study area, separating the Woodbend-Beaverhill Lake aquifer from the overlying Nisku aquifer of the Winterburn Group. The Ireton aquitard thins considerably over several Woodbend Leduc reefs, and cross-formational flow at these locations is very likely, as identified in other parts of the Alberta Basin (Bachu and Underschultz, 1993; Rostron and Toth, 1997; Rostron et al., 1997; Anfort et al., 2001). The siltstones of the Winterburn Graminia Formation form a thin aquitard between the Winterburn and Wabamun aquifers, but these probably form a



Reproduced with permission of the copyright owner. Further reproduction prohibited without permission.

rather continuous aquifer system (Upper Devonian) in most parts of the study area, as observed at the basin-scale (Bachu, 1995a). All shaly aquitards thin out southwestward near the deformation front, where the entire Devonian succession forms a single aquifer system (Skilliter, 1999).

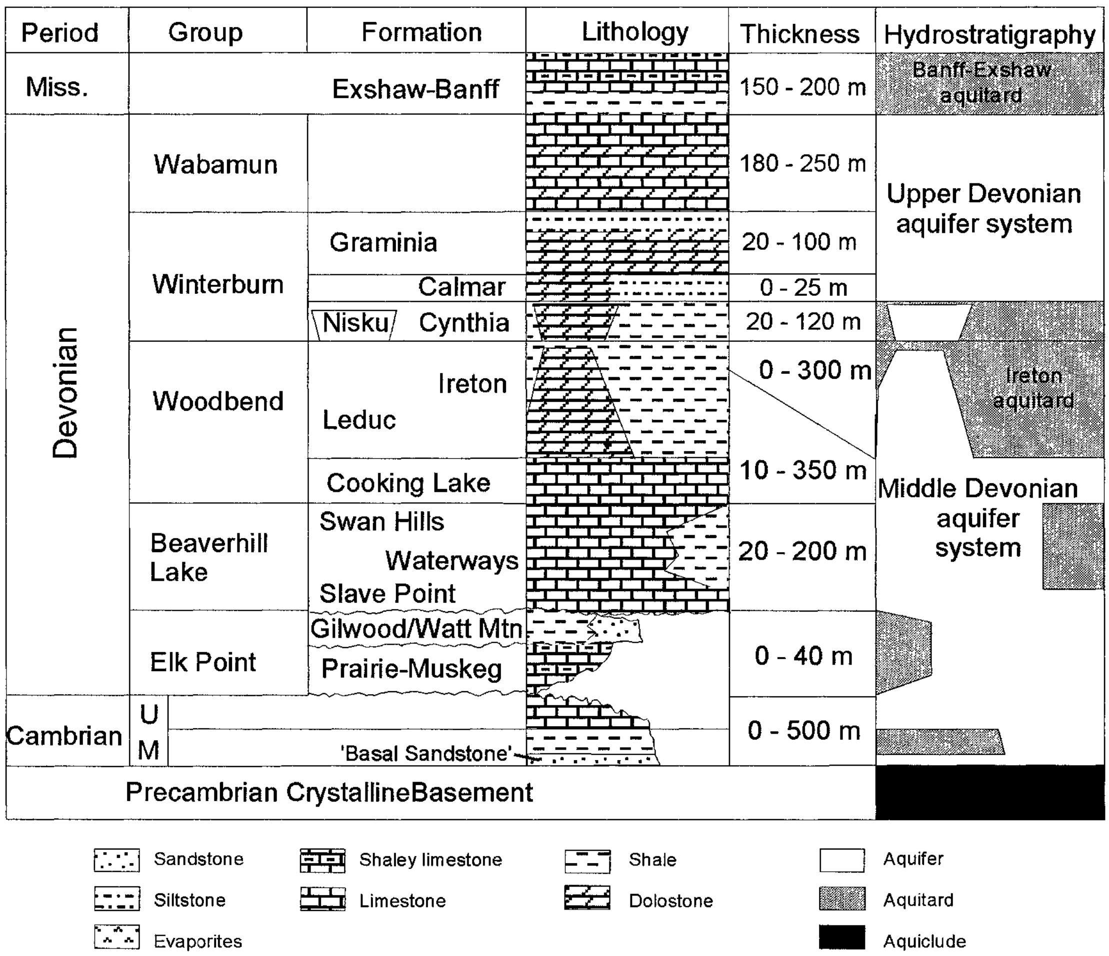


Figure 7.2: General lithology and hydrostratigraphy of the Cambrian-Devonian succession in the study area.

## 7.3 Hydrogeological Patterns

Contour maps of equivalent hydraulic heads, and p(d)-and p(z)-plots were used to interpret the flow in the Cambrian-Devonian hydrostratigraphic group. Formation water density ranges between approximately 1040 and 1140 kg/m$^3$. An average reference



Reproduced with permission of the copyright owner. Further reproduction prohibited without permission.

density $\rho_0$ = 1090 kg/m$^3$ was used to calculate hydraulic heads in order to minimize the DFR, and to be able to analyze the flow using hydraulic heads only (see Chapter 2). Maps of salinity and bicarbonate distributions were used in the hydrochemical analysis. The respective ranges of hydraulic head and salinity values for the Cambrian-Devonian aquifers are presented in Table 7.1.

| Aquifer | $H_0$ ($\rho_0$ = 1090 kg/m$^3$) | TDS |
|---|---|---|
| Wabamun | 480 – 810 m | 116 – 265 g/l |
| Winterburn | 450 – 750 m | 130 – 265 g/l |
| Woodbend-Beaverhill L. | 600 – 750 m | 120 – 262 g/l |
| Elk Point | 605 – 775 m | 178 – 300 g/l |
| 'Basal sandstone aquifer' | 600 – 650 m | 217 – 252 g/l |

Tab. 7.1: Summary of ranges in hydraulic head and salinity in the Cambrian-Devonian aquifers. Hydraulic heads were calculated with a reference density of 1090 kg/m$^3$.

Similar to the previous chapters, the Cambrian-Devonian hydrostratigraphic group will be presented in descending order, starting with the Wabamun aquifer. Hydrogeological data in the 'Basal Sandstone aquifer' are very sparse (3 values) and therefore, only their range is listed in Table 7.1.

The distribution of pressure data from all Devonian aquifers versus depth (Fig. 7.3a) shows that generally the Devonian aquifers are hydrostatically to sub-hydrostatically pressured, except for a small group of pressure data from the Wabamun and Winterburn aquifers that plot above-hydrostatic. In Figure 7.3b, pressure data plot along a line representative of an average brine gradient of 10.7 kPa/m, which approximately corresponds to the pressure gradient in a static column of brine with a density of 1100 kg/m$^3$. This indicates that all Devonian aquifers seem to be in good hydraulic communication or are controlled by similar boundary conditions to flow.



Reproduced with permission of the copyright owner. Further reproduction prohibited without permission.

Reproduced with permission of the copyright owner. Further reproduction prohibited without permission.



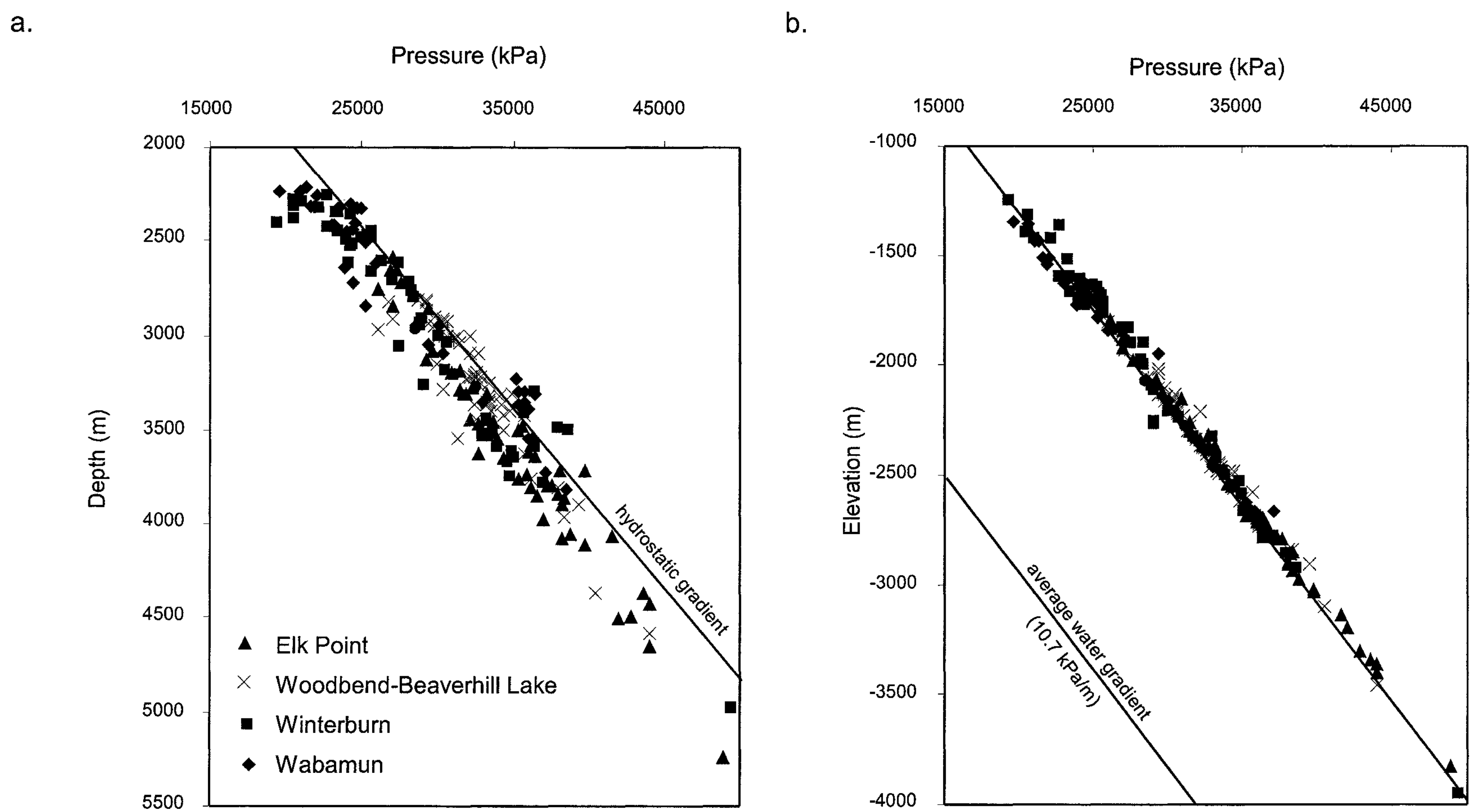


Figure 7.3: Pressure variation with: a) depth, and b) elevation in the Devonian aquifers in the study area.

*Wabamun aquifer*

Hydraulic heads in the Wabamun aquifer generally decrease north-northeastward from > 800 m to less than 500 m (Fig. 7.4). A steep hydraulic gradient is present in the east-central part of the study area, where hydraulic heads drop by approximately 200 m (800 – 600 m) northward over a 20 km distance. In contrast, in the northern half of the study area hydraulic heads decrease eastward with a relatively constant hydraulic gradient of approximately 10 m/km.

The salinity of formation waters in the Wabamun aquifer generally increases northward in the direction of decreasing hydraulic heads from 115 to 265 g/l (Fig. 7.5). The bicarbonate concentrations show a similar, yet reversed, trend, decreasing from > 2.5 g/l to < 0.5 g/l north and northeastward (Fig. 7.6).

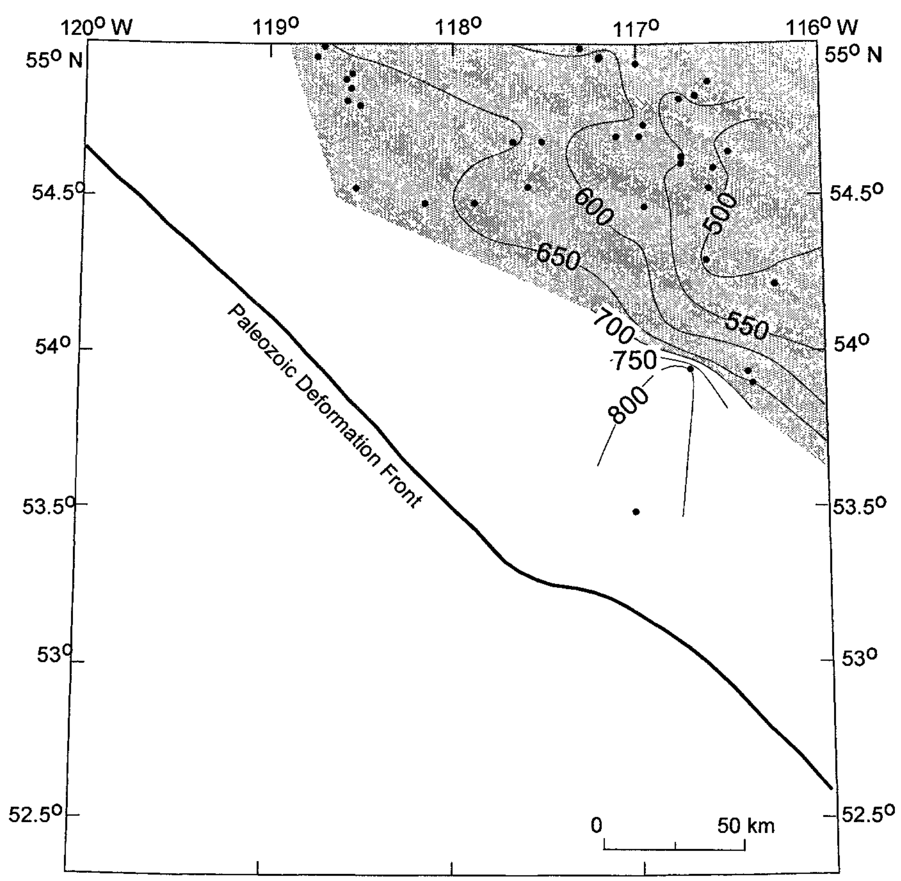


Figure 7.4: Hydraulic head distribution in the Wabamun aquifer (50 m contour interval, H calculated with $\rho_0 = 1090$ kg/m$^3$). For better visualization purposes areas where hydraulic heads < 700 m are shaded in grey.



Reproduced with permission of the copyright owner. Further reproduction prohibited without permission.

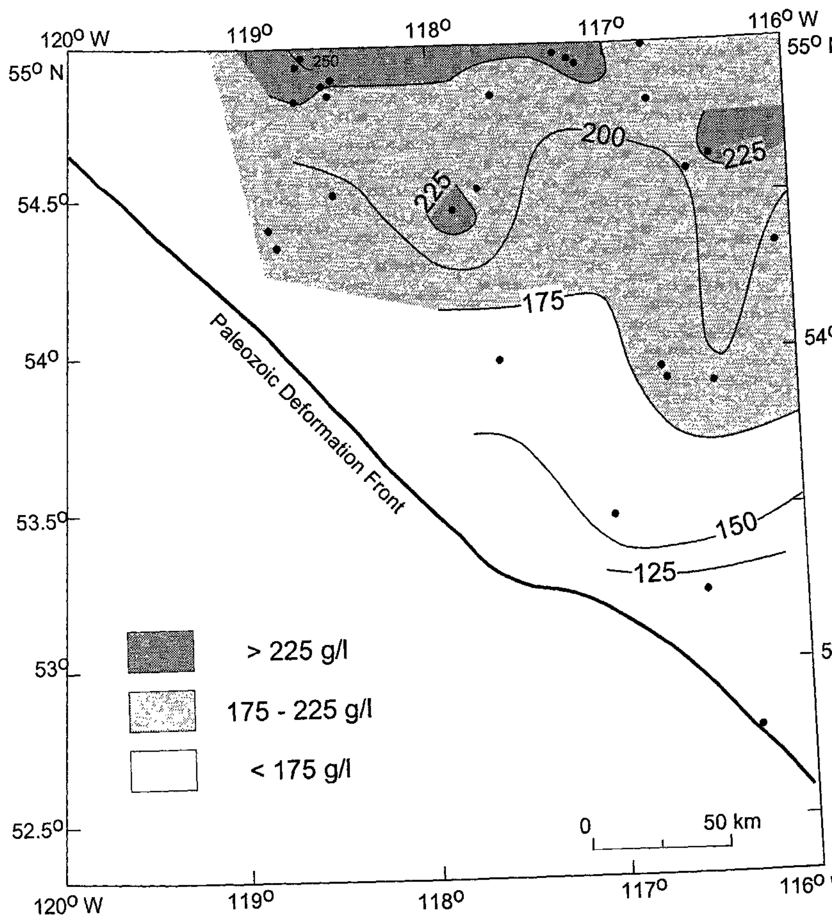


Figure 7.5: Salinity distribution in the Wabamun aquifer (25 g/l contour interval).

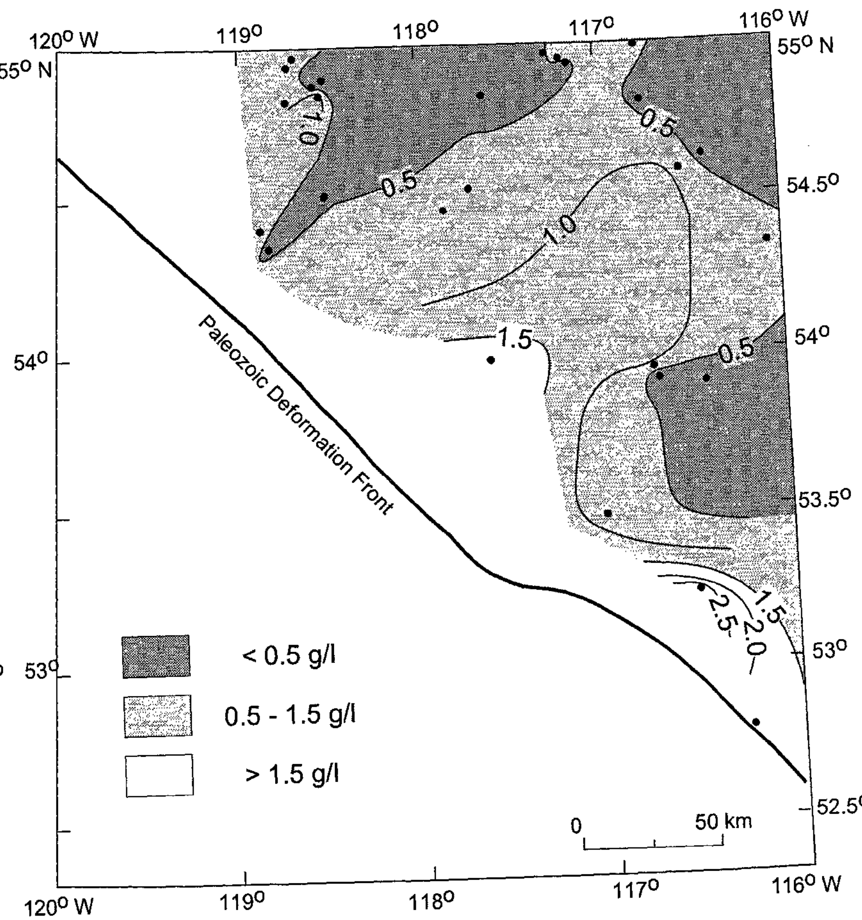


Figure 7.6: Bicarbonate distribution in the Wabamun aquifer (0.5 g/l contour interval).



Reproduced with permission of the copyright owner. Further reproduction prohibited without permission.

Hydraulic heads in the Winterburn aquifer generally decrease from > 700 m along the deformation front to less than 550 m in the northeastern corner of the study area (Fig. 7.7). A "tongue" of relatively high hydraulic heads (> 700 m) and steep hydraulic gradient extents from the deeper parts of the aquifer northward, approximately along 117$^O$ W. Hydraulic heads decrease in a radiating manner, changing from east- to northwestward, away from the high hydraulic-head "tongue".

The salinity of formation waters in the Winterburn aquifer generally increases north-northwestward, from 130 to 265 g/l, with a relatively steep increase from 175 to 200 g/l (Fig. 7.8) along the limit of the tongue with high hydraulic heads (Fig. 7.7). As in the overlying Wabamun aquifer, the bicarbonate concentrations show a similar, yet reversed, trend, decreasing from > 3.0 g/l to < 0.5 g/l (Fig. 7.9).

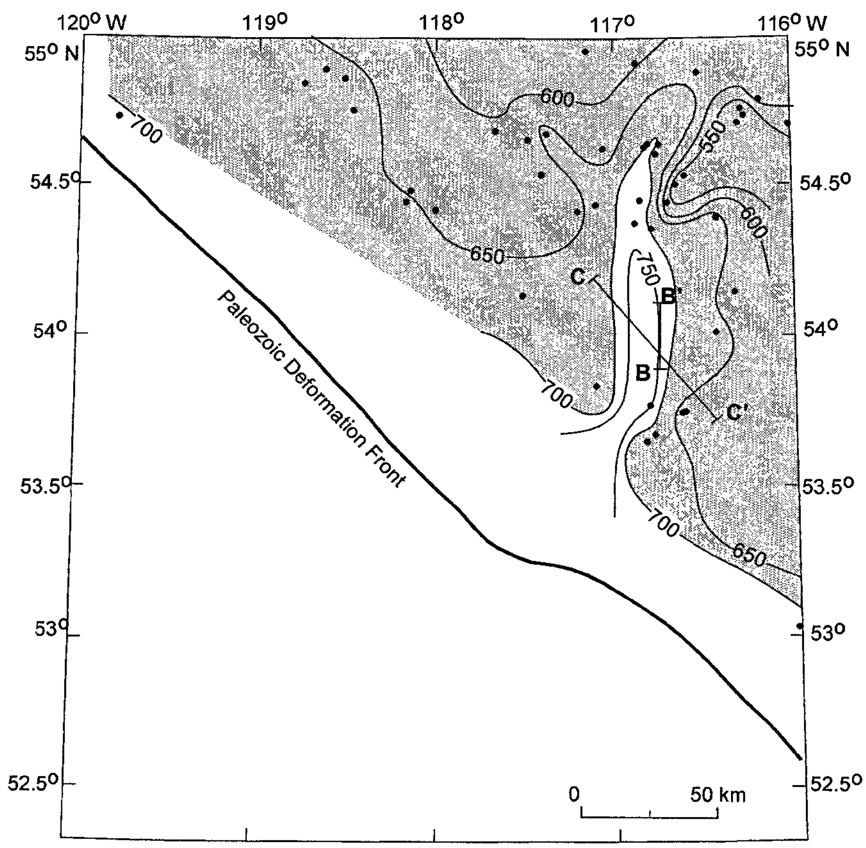


Figure 7.7: Hydraulic head distribution in the Winterburn aquifer (50 m contour interval, H calculated with $\rho_0$ = 1090 kg/m$^3$). Areas where hydraulic heads < 700 m are shaded in grey for better visualization purposes. Lines of cross-sections B-B' and C-C' refer to Figures 7.20 & 7.21, respectively.



Reproduced with permission of the copyright owner. Further reproduction prohibited without permission.

Reproduced with permission of the copyright owner. Further reproduction prohibited without permission.

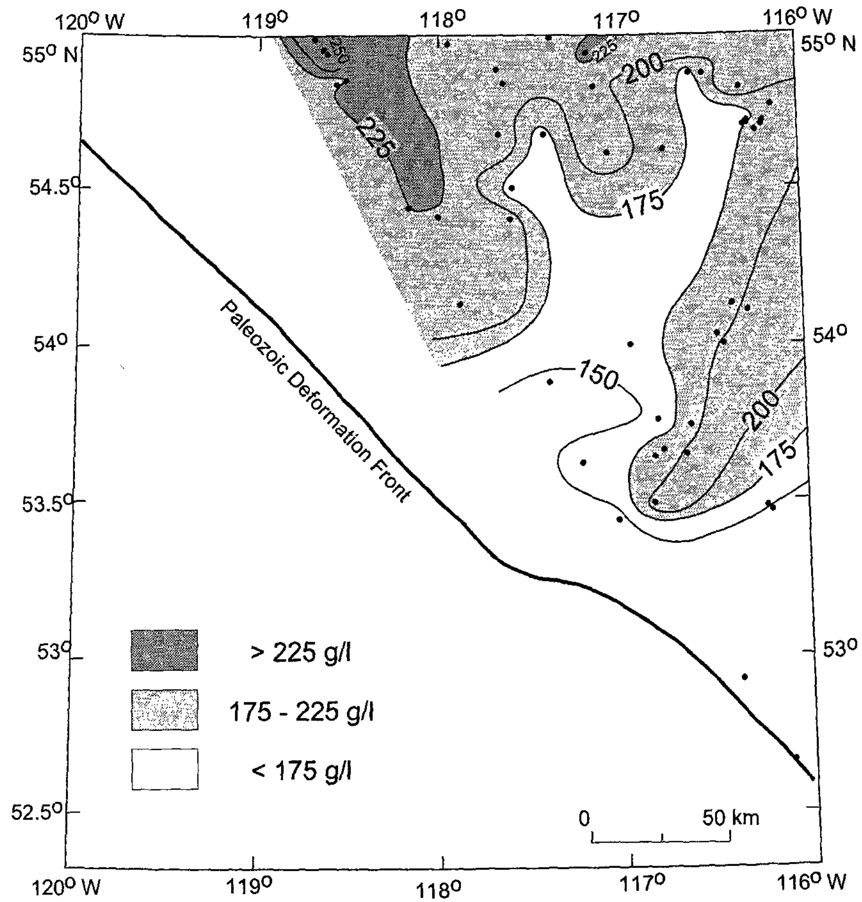


Figure 7.8: Salinity distribution in the Winterburn aquifer (25 g/l contour interval).

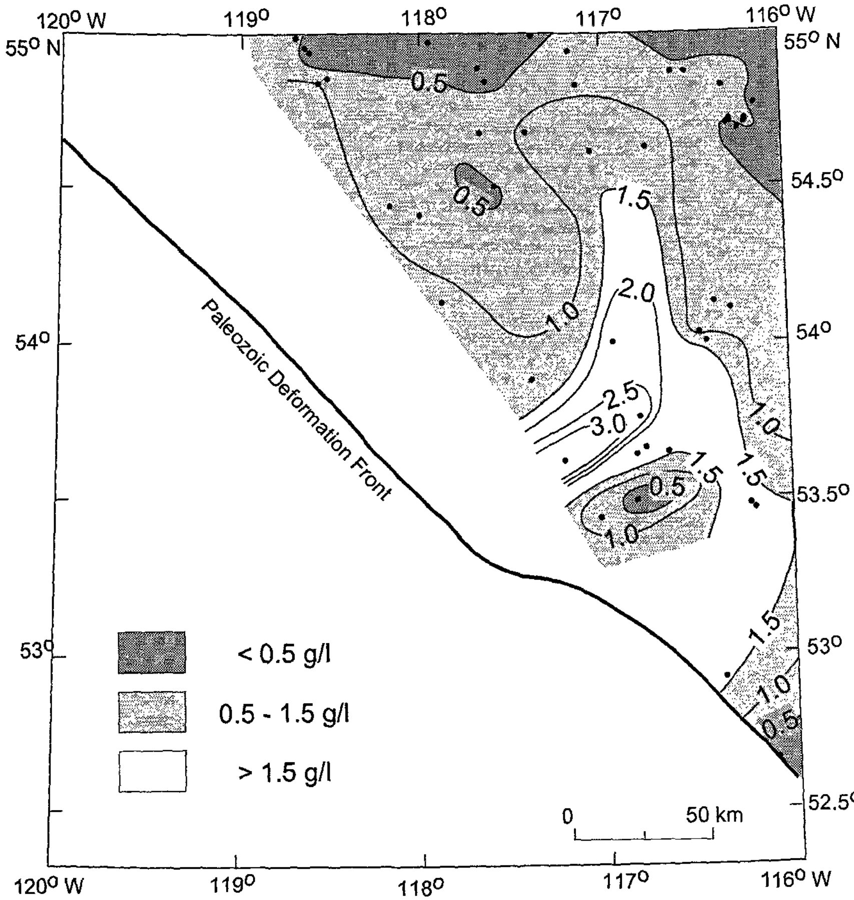


Figure 7.9: Bicarbonate distribution in the Winterburn aquifer (0.5 g/l contour interval).

*Woodbend-Beaverhill Lake aquifer*

Hydraulic heads in the Woodbend-Beaverhill Lake aquifer generally decrease from > 750 m along the deformation front to less than 650 m along the eastern boundary of the study area (Fig. 7.10). "Tongues" of relatively high hydraulic heads (> 700 m) and steep hydraulic gradient extent from the deeper parts of the aquifer northeastward, approximately 150 km away from the deformation front. Excepting the steep hydraulic gradients near the high hydraulic-head tongues, the generally low hydraulic gradients suggest ± stagnant flow conditions.

The salinity of formation waters in the Woodbend-Beaverhill Lake aquifer generally increases north-northwestward from 120 to 260 g/l with a relatively steep increase from 175 to 250 g/l (Fig. 7.11) approximately along the limit of the tongues with high hydraulic heads (Fig. 7.10). Similar to the overlying aquifers, the bicarbonate concentrations show a similar, yet reversed, trend, decreasing from > 2.5 g/l to < 0.5 g/l (Fig. 7.12).



Reproduced with permission of the copyright owner. Further reproduction prohibited without permission.

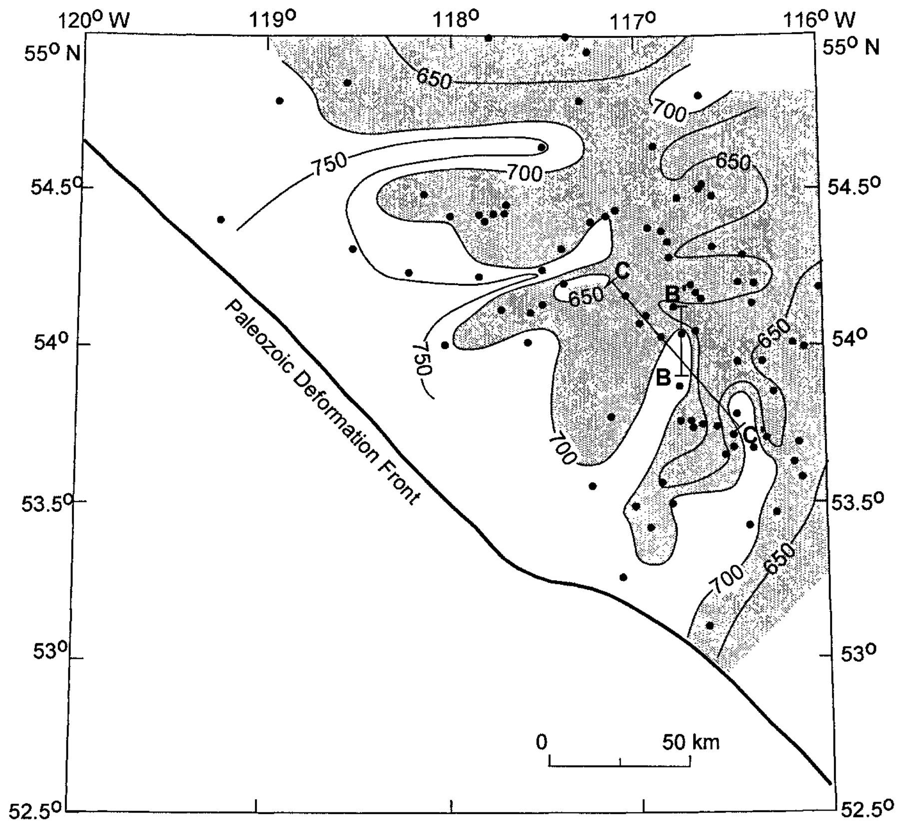


Figure 7.10: Hydraulic head distribution in the Woodbend-Beaverhill Lake aquifer (50 m contour interval; H calculated with $\rho_0$ = 1090 kg/m$^3$). Areas where hydraulic heads < 700 m are shaded in grey for better visualization purposes. Lines of cross-section B-B' and C-C' refer to Figures 7.20 & 7.21, respectively.



Reproduced with permission of the copyright owner. Further reproduction prohibited without permission.

Reproduced with permission of the copyright owner. Further reproduction prohibited without permission.

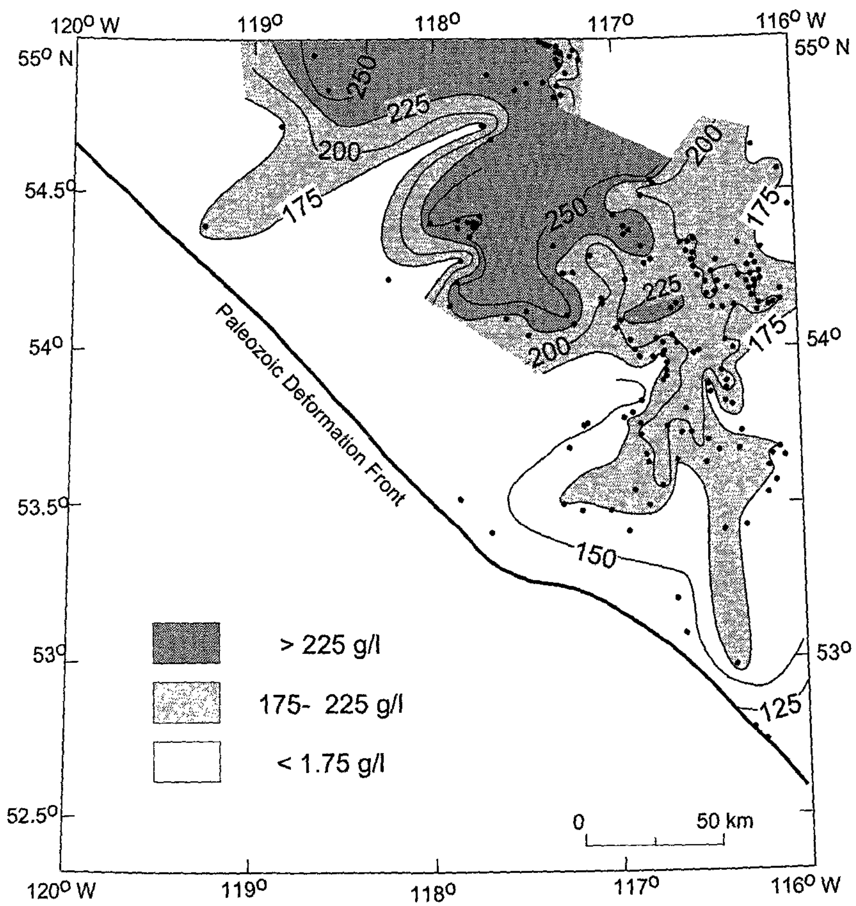


Figure 7.11: Salinity distribution in the Woodbend-Beaverhill Lake aquifer (25 g/l contour interval).

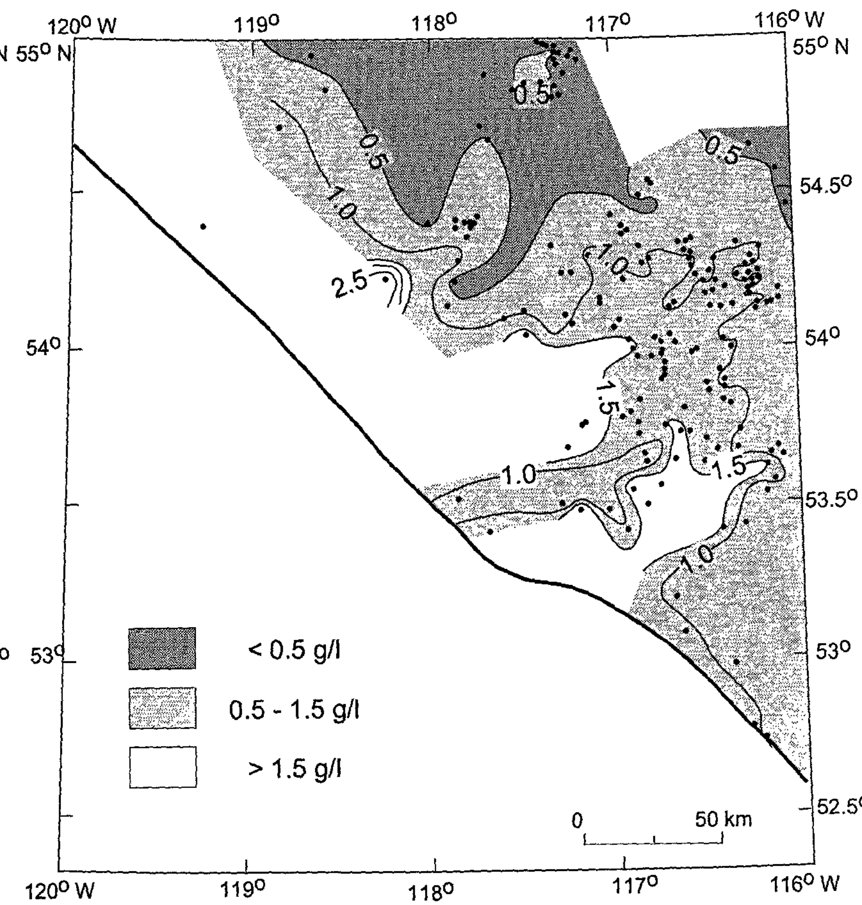


Figure 7.12: Bicarbonate distribution in the Woodbend-Beaverhill Lake aquifer (0.5 g/l contour interval).

*Elk Point aquifer*

Hydraulic heads in the Elk Point aquifer decrease from > 750 m in the southeast to less than 625 m in the northeastern corner of the study area (Fig. 7.13). Sparse data in the south and lack of data in the central part of the study area restrict the representation of the Elk Point aquifer to the northeastern corner of the study area (s. box in Figure 7.13 referring to Chapter 2). The maximum hydraulic gradient can be observed from approximately 670 m in a S-N trending tongue in the centre of the (sub-) study area to less than 625 m at the eastern boundary. However, using a 25 m contour interval probably is beyond the appropriate resolution that should be used in this deep Devonian aquifer (see Chapter 3; 3.3.4). Rather, relatively uniform hydraulic head values around 650 m indicate ± stagnant flow conditions in the northern part of the study area, and potential for northward flow from areas of 750 m in the south can be inferred only on a very regional scale.

The salinity of formation waters in the Elk Point aquifer generally increases northward in the direction of decreasing hydraulic heads from 178 to 300 g/l, with a relatively steep increase from 200 to 250 g/l along 54.25$^{O}$ N, in the centre of the study area (Fig. 7.14). The bicarbonate concentrations show a similar, yet reversed, trend, decreasing northward from > 0,75 g/l to < 0.25 g/l (Fig. 7.15). The exception is an area with a few values < 0.25 g/l between 53.5$^{O}$ and 54.0$^{O}$ N, which creates a tongue of relatively high bicarbonate concentration approximately following the 200 g/l salinity contour line (Fig. 7.15).



Reproduced with permission of the copyright owner. Further reproduction prohibited without permission.

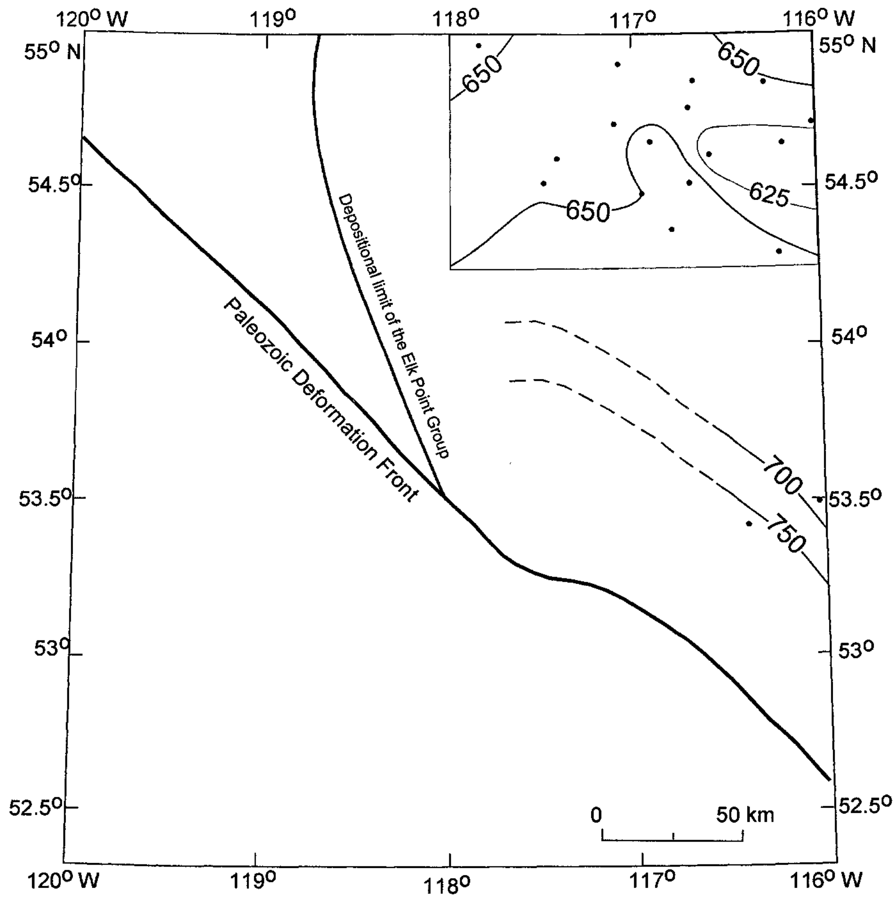

Figure 7.13: Hydraulic head distribution in the Elk Point aquifer (50 m contour interval, except for the addition of the 625 m contour line; H calculated with $\rho_0$ = 1090 kg/m$^3$). The box in the northeastern corner of the map shows the area used in Chapter 2 to examine the effect of different reference densities in the calculation of hydraulic heads on the flow representation.



Reproduced with permission of the copyright owner. Further reproduction prohibited without permission.

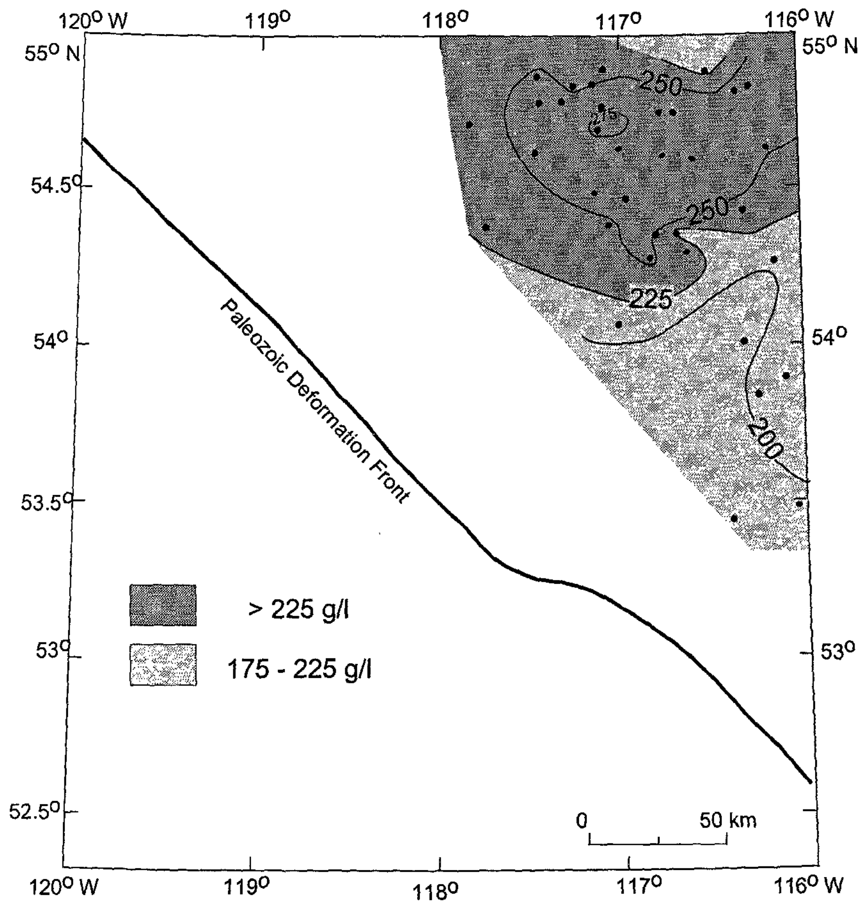


Figure 7.14: Salinity distribution in the Elk Point aquifer (25 g/l contour interval).

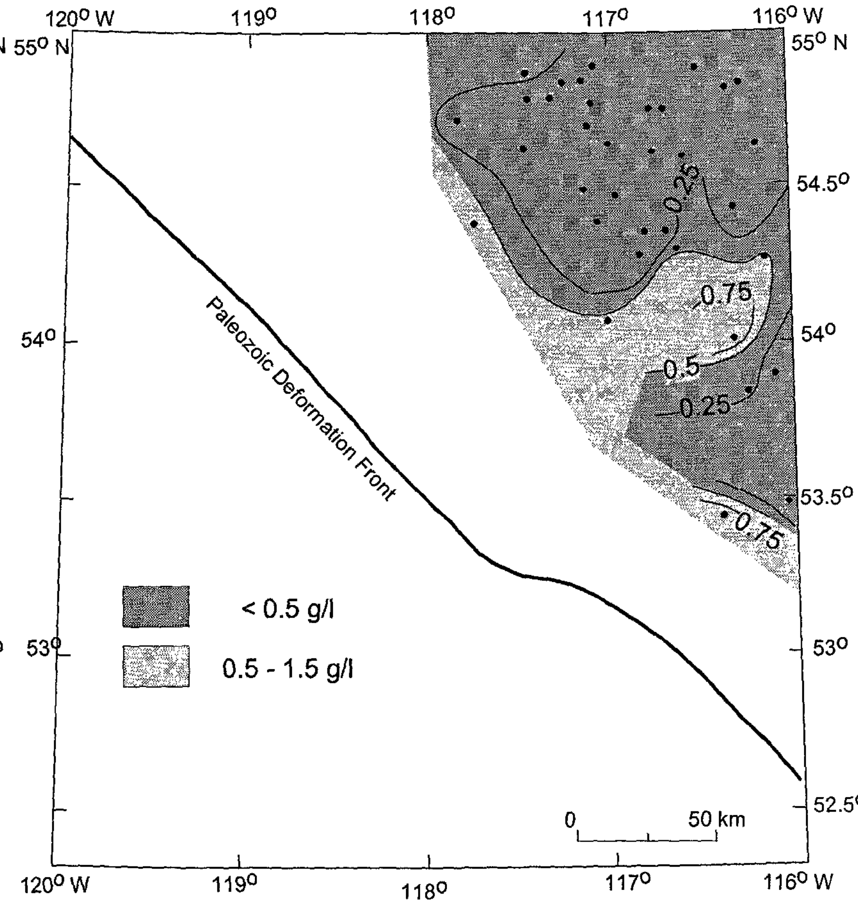


Figure 7.15: Bicarbonate distribution in the Elk Point aquifer (0.25 g/l contour interval).



Reproduced with permission of the copyright owner. Further reproduction prohibited without permission.

*Comparison of selected cations in the Devonian formation waters*

The variation of major cation concentrations (Na, Ca, Mg) and Br of Devonian formation waters in the study area is plotted against their chloride content and against the seawater evaporation-dilution curve (SET). The respective plots show that generally these waters are depleted with respect to sodium, magnesium and bromide, and have excess calcium in comparison to water derived only from the evaporation of seawater (Fig. 7.16). For comparison, the variation of major ions versus chloride in the overlying Mississippian aquifer is offset distinctively from the main group of Devonian data.

*Summary of hydrogeological observations*

- Hydraulic heads generally decrease north-northeastward, updip in all Devonian aquifers;
- Hydraulic head values in the Middle Devonian aquifer system range from 625 to 750 m, which is smaller than the range of $H_0$ in the Upper Devonian aquifer system (500 – 800 m);
- A concurrent, steep change in hydraulic heads, salinity and bicarbonate concentration can be observed in all Devonian aquifers, around the following approximate values: $H_0$ = 700 m, TDS = 175 g/l, $[HCO_3^-]$ = 1.5 g/l;
- Formation waters are depleted with respect to sodium and magnesium and have excess calcium in comparison to water derived only from the evaporation of seawater;
- The discontinuous change in the hydrogeological data has different patterns in the various Devonian aquifers: a) 'interfingering' in the Woodbend-Beaverhill Lake, b) a single tongue in the Winterburn, and c) relatively linear in the Elk Point and Wabamun.



Reproduced with permission of the copyright owner. Further reproduction prohibited without permission.

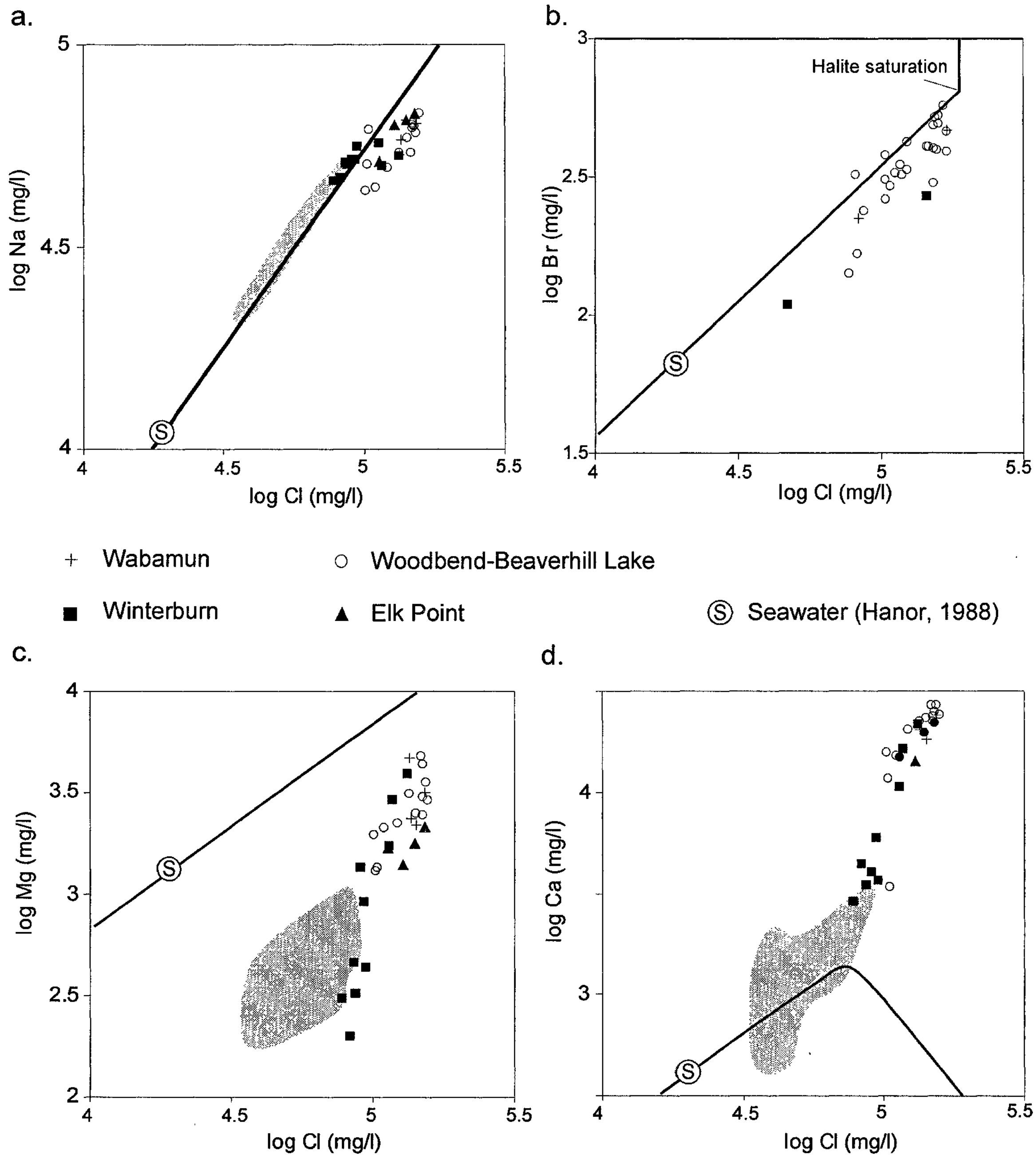


Figure 7.16: Cross plots versus chloride of: a) sodium, b) bromide, c) magnesium, and d) calcium for formation waters in the study area from the Cambrian-Devonian succession. Shaded area represents data distribution in the underlying Mississippian aquifer. The black line on figures a, b, c, and d represents the respective seawater evaporation curves experimentally determined by McCaffrey et al. (1986).



Reproduced with permission of the copyright owner. Further reproduction prohibited without permission.

## 7.4 Interpretation of flow patterns

The general, regional flow patterns are shown in Figure 7.17. The relatively abrupt change in the salinity and bicarbonate concentrations observed in each Devonian aquifer suggests that it is possible to distinguish between a 'light brine' and a 'heavy brine', defined by approximate TDS ranges of < 175 g/l and > 225 g/l, respectively.

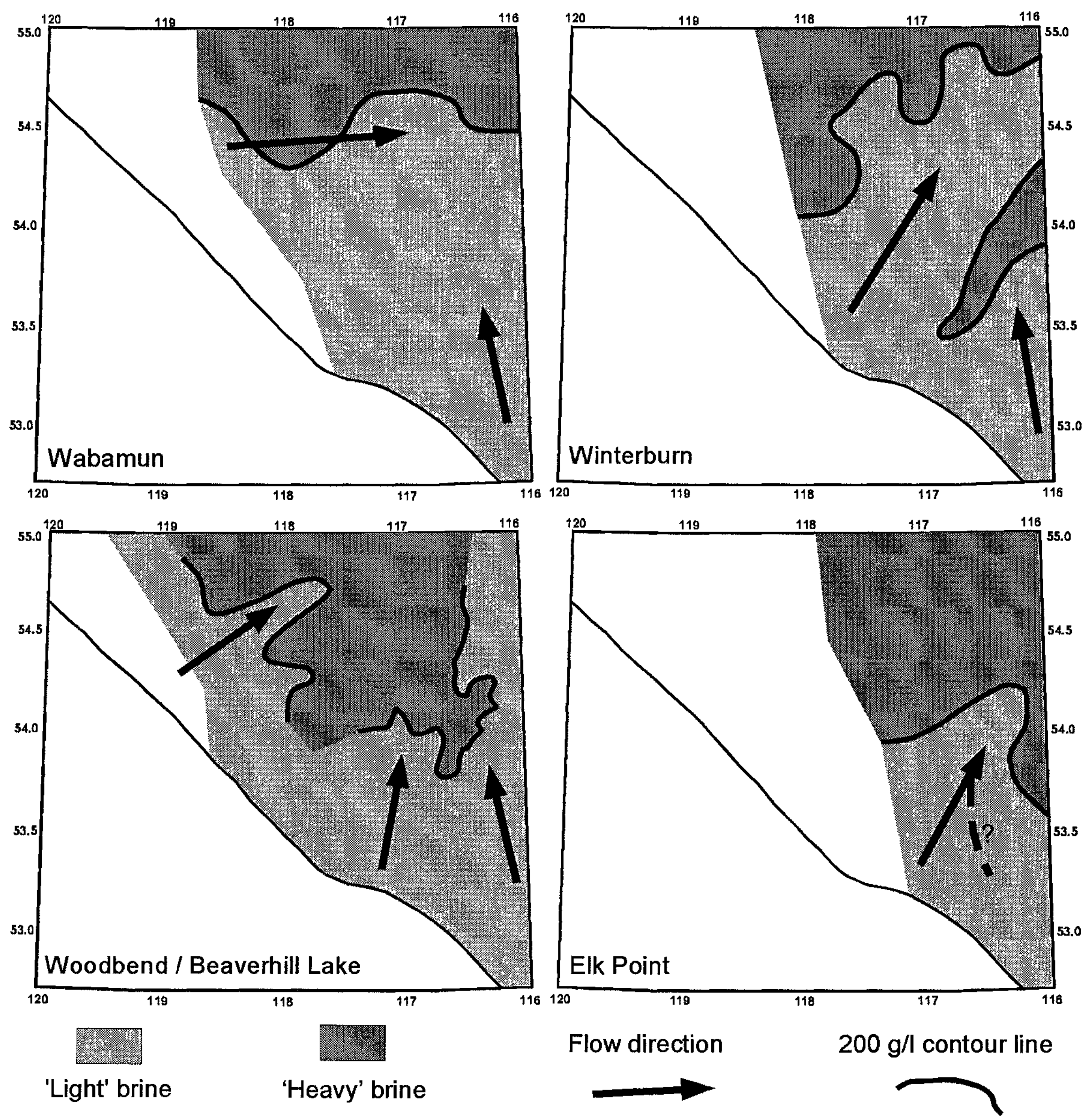


Figure 7.17: Patterns of brine displacement and inferred flow directions in the Devonian aquifers.



Reproduced with permission of the copyright owner. Further reproduction prohibited without permission.

No absolute value for the boundary between these two brines can be defined because of variations between the different aquifers and in data accuracy, so that salinities between 175 and 225 g/l will be referred to as 'intermediate' or 'mixing zone' values. Generally, hydraulic gradients are only high along the boundary between the 'light brine' and a 'heavy brine', suggesting a decrease in permeability or transmissivity across that boundary (see Fig. 2.1c in Chapter 2, and Eqs. 2.16 and 2.18). However, in the area that is taken up by the 'heavy brine', small differences in hydraulic head suggest ± sluggish flow; hence sluggish movement of the 'heavy brine'. Only on a regional scale, the potential for updip, northeastward flow can be inferred from areas of high hydraulic head (> 700 m) along the deformation front. The exception is the northern half of the Wabamun aquifer, where a relatively constant hydraulic gradient of 100 m / 75 km along $54.5^{\circ}$ N suggests eastward flow of formation water

Along the deformation front, in the deep parts of the Cambrian-Devonian hydrostratigraphic group, there are no intervening shaly aquitards, and the stacked Devonian carbonate complexes form a contiguous aquifer (Skilliter, 1999). The light brine is present in this part of the study area and hydraulic heads are high, suggesting updip flow towards hydraulic head lows in the northeast and displacement of the heavy brine. Apart from this general feature, the hydrogeological patterns are different in the various Devonian aquifers, which are caused by the thickening of intervening shale aquitards and variations in permeability within each aquifer. These patterns can be characterized by: a) analysis of the competence of intervening aquitards, b) delineation and characterization of preferential flow paths, and c) investigation of fluid origin and flow driving mechanisms.



Reproduced with permission of the copyright owner. Further reproduction prohibited without permission.

*Preferential flow paths and aquitard competence*

The influence of lateral and vertical permeability variations on flow in the Cambrian-Devonian hydrostratigraphic units have been examined in descending order in the stratigraphic succession, starting at the upper confining boundary. The offset of pressure data in the p(z)-plots (Figs. 7.18 a and c) and the difference in hydraulic heads and in the salinity range of formation waters between the Permo-Mississippian and Wabamun aquifers (s. Tab. 6.2, Chapter 6) indicate that the Exshaw-Banff aquitard is a very effective barrier to flow in the study area. Pressures in the Wabamun aquifer plot closer to hydrostatic than those in the overlying Permo-Mississippian aquifer, which implies higher hydraulic heads and a potentially upward gradient to flow from the Wabamun into the Permo-Mississippian aquifer. In the northeast corner of the study area, however, pressures in both aquifers approximately plot along the same gradient (Fig. 7.18 b) and hydraulic heads are in the same range. This indicates that pressures in both aquifers have adjusted to the same boundary conditions. However, the salinity in the Permo-Mississippian aquifer (100 – 150 g/l Fig. 6.10) is still significantly lower than that in the Wabamun aquifer (200 – 225 g/l, Fig. 7.5) so that cross-formational flow through the Exshaw-Banff aquitard in this area seems unlikely, and formation water only moves laterally in both aquifers.



Reproduced with permission of the copyright owner. Further reproduction prohibited without permission.

Reproduced with permission of the copyright owner. Further reproduction prohibited without permission.



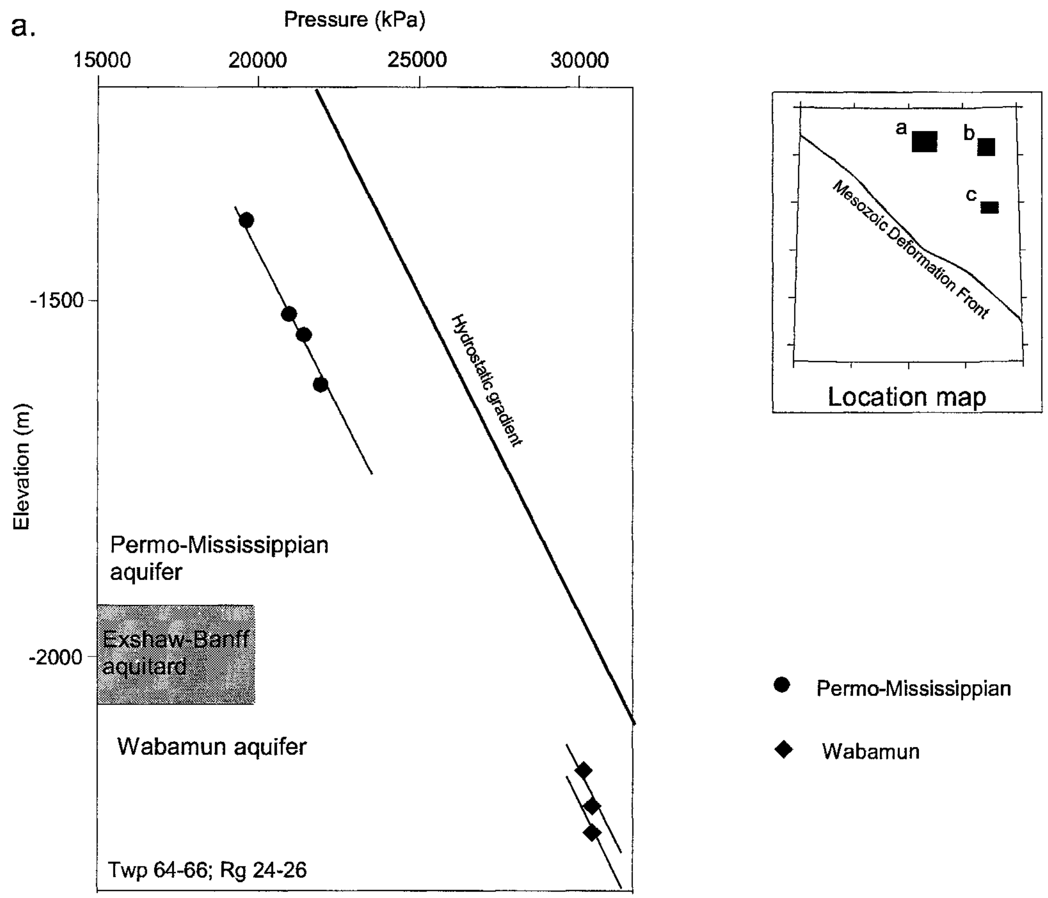


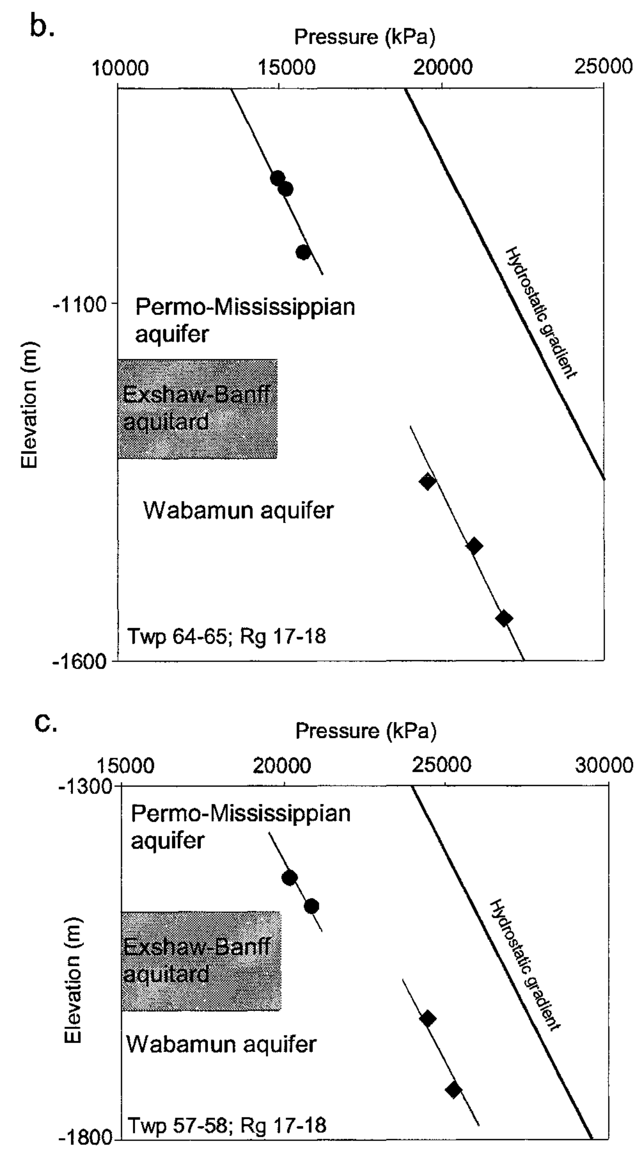


Figure 7.18: Pressure-elevation plots across the Exshaw-Banff aquitard for the Permo-Mississippian and Wabamun aquifers in various regions of the study area.

The hydrogeological patterns in the Wabamun aquifer further suggest that the permeability distribution is more homogeneous than in the Winterburn and Woodbend-Beaverhill Lake aquifers. The limestones in the Wabamun aquifer generally have a fairly low porosity and permeability, but these properties are significantly increased in the dolomitized parts (Saller and Yaremko, 1994). The hydrogeological data resolution in the Wabamun aquifer is relatively poor and the dolomite content is averaged over the entire aquifer thickness. Nevertheless, a general correlation between the degree of dolomitization and salinity distribution appears to be present. The light brine may have displaced the heavy brine from those parts of the aquifer that have a high dolomite content, whereas the less permeable limestone parts obstruct lateral flow (Fig. 7.19).

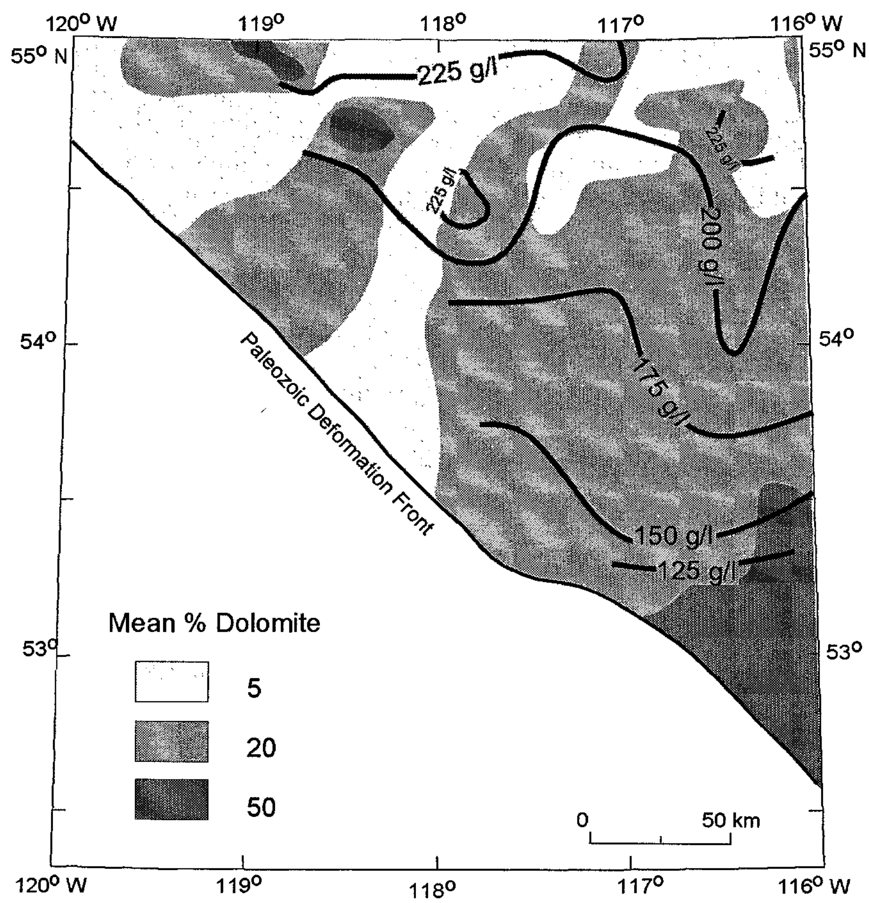


Figure 7.19: Correlation between salinity and average, regional-scale dolomite distribution in the Wabamun aquifer (dolomite-% distribution after Halbertsma, 1994).



Reproduced with permission of the copyright owner. Further reproduction prohibited without permission.

Generally, there is good agreement between hydraulic head and salinity distributions in the Wabamun and Winterburn aquifers, which suggest that the intervening Graminia siltstone is a relatively inefficient aquitard. The only noteworthy difference between these two aquifers can be observed in the area of the high hydraulic head tongue in the Winterburn aquifer, along longitude $117^{O}$ W (Fig. 7.7). Hydraulic heads near the deformation front in the Wabamun aquifer start out at higher values (> 800 m) than in the Winterburn aquifer (~ 750 m), which implies a horizontal barrier to flow. At approximately $53.75^{O}$ W hydraulic heads in both aquifers are at ~ 750 m, but hydraulic heads in the Wabamun aquifer drop rapidly northward to ~ 650 m, while they stay constant in the Winterburn aquifer. According to the hydrostratigraphy, there are no shale aquitards along the deformation front that could impede the vertical hydraulic communication between the Winterburn and Wabamun aquifers, which could explain the difference in hydraulic heads. One possible explanation would be a generally low-permeability layer in this part of the Wabamun Group due to a low degree of dolomitization. Another possibility is that the two pressure data resulting in $H_0$ > 800 m were measured in relatively isolated, fractured reservoirs (Chevron Canada Resources staff, pers. Comm.). More data than currently available, and further study are needed to address this issue of hydraulic continuity (or absence thereof) between and within the Winterburn and Wabamun aquifers in this region. Although the Upper Devonian succession is inferred to be a contiguous aquifer system on a regional- and basin-scale, areas that are not significantly dolomitized in the Wabamun Group and basinal facies in the Winterburn Group appear to be of low permeability, and locally may act as aquitards.

The Ireton shales form the main aquitard in the Cambrian-Devonian hydrostratigraphic group. Hydraulic heads decrease in the Wabamun and Winterburn aquifers to approximately 500 m, whereas hydraulic head values in the Elk Point and Woodbend-Beaverhill Lake aquifers decrease only to approximately 625 m from the southwest to the northeast. In addition, the light brine advanced farther updip in the Upper Devonian aquifer system than in the Middle Devonian aquifer system (Fig. 7.17). This shows that the Ireton shales separate the Woodbend from the overlying Winterburn aquifer and form an effective aquitard in the northeast between the Middle and Upper Devonian aquifer



Reproduced with permission of the copyright owner. Further reproduction prohibited without permission.

systems. Selected stratigraphic cross sections show that the Ireton aquitard thins considerably above Leduc reefs, and that the latter may be even in direct contact with overlying Nisku reefs (Figs. 7.20 and 7.21), where the Ireton is thin or absent. These 'windows' in the Ireton aquitard probably are areas where cross-formational flow between Woodbend-Beaverhill Lake and Winterburn aquifers occurs, which has been identified previously in the same strata in carbonate complexes southeast of the study area (Rostron and Tóth, 1997; Rostron et al., 1997; Anfort et al.; 2001).

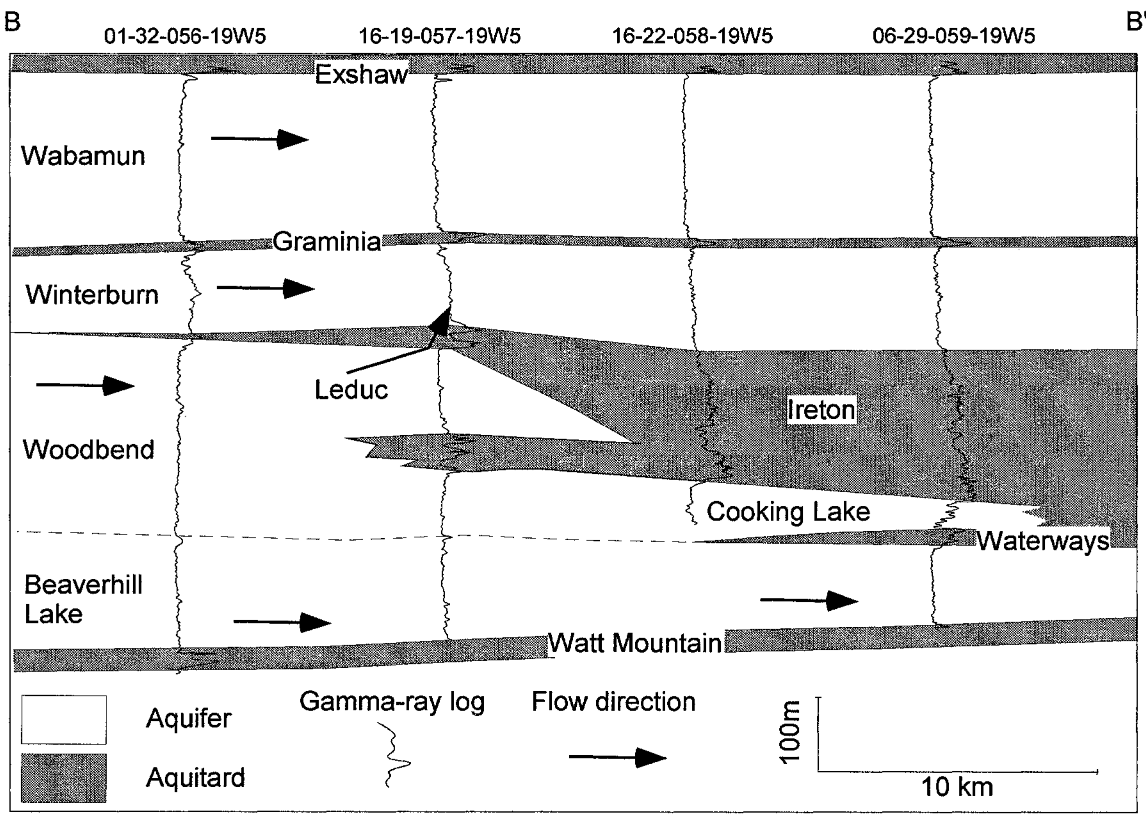

Figure 7.20: (Hydro-)Stratigraphic cross-section perpendicular to the deformation front showing a single Devonian aquifer at the left hand side of the cross-section (S) , which is successively subdivided into two aquifer systems, and cross formational flow across the Ireton aquitard. See Figures 7.7, 7.10 & 7.22 for line of cross section.



Reproduced with permission of the copyright owner. Further reproduction prohibited without permission.

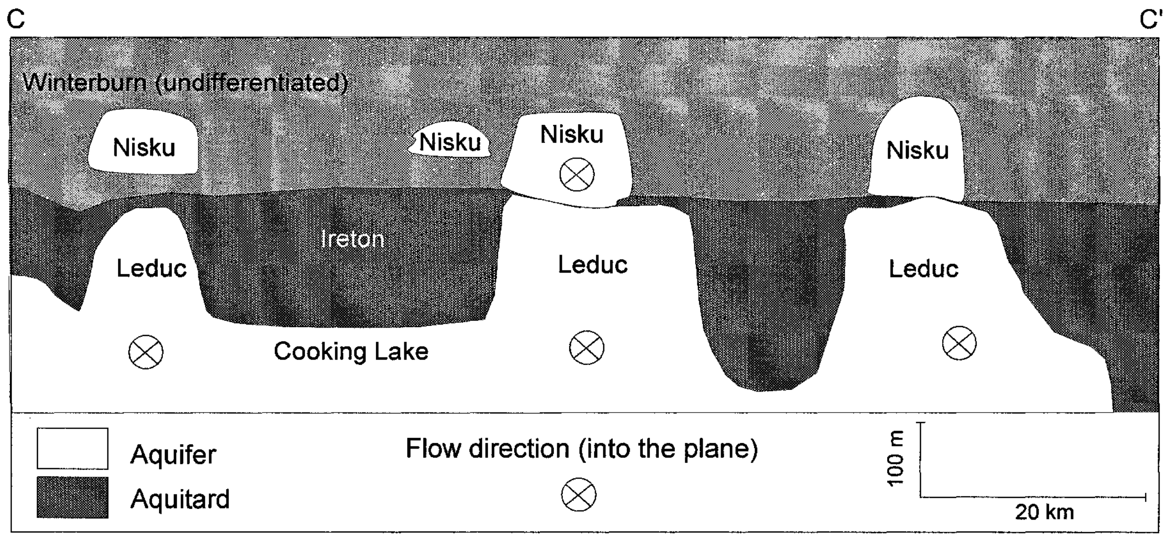


Figure 7.21: (Hydro-)Stratigraphic cross section parallel to the deformation front showing "windows" in the Ireton aquitard and thinning of the Woodbend-Beverhill Lake aquifer between Leduc reef built-ups. [Stratigraphic correlations from Buschkuehle (unpubl.)]. See Figures 7.7, 7.10 & 7.22 for line of cross section.

Flow in the Woodbend-Beaverhill Lake aquifer appears to be preferentially channeled along the platform margins, which probably is a major cause for the differential advancement of the light brine (Fig. 7.22). These flow conduits are due to enhanced porosity and permeability that are associated with the high-energy reef margin facies (Wendte and Stokes, 1982; Oldale and Munday, 1994, Wendte et al., 1998). The fingers of light brine terminate along the northeastern limit of the Cooking Lake platform.



Reproduced with permission of the copyright owner. Further reproduction prohibited without permission.

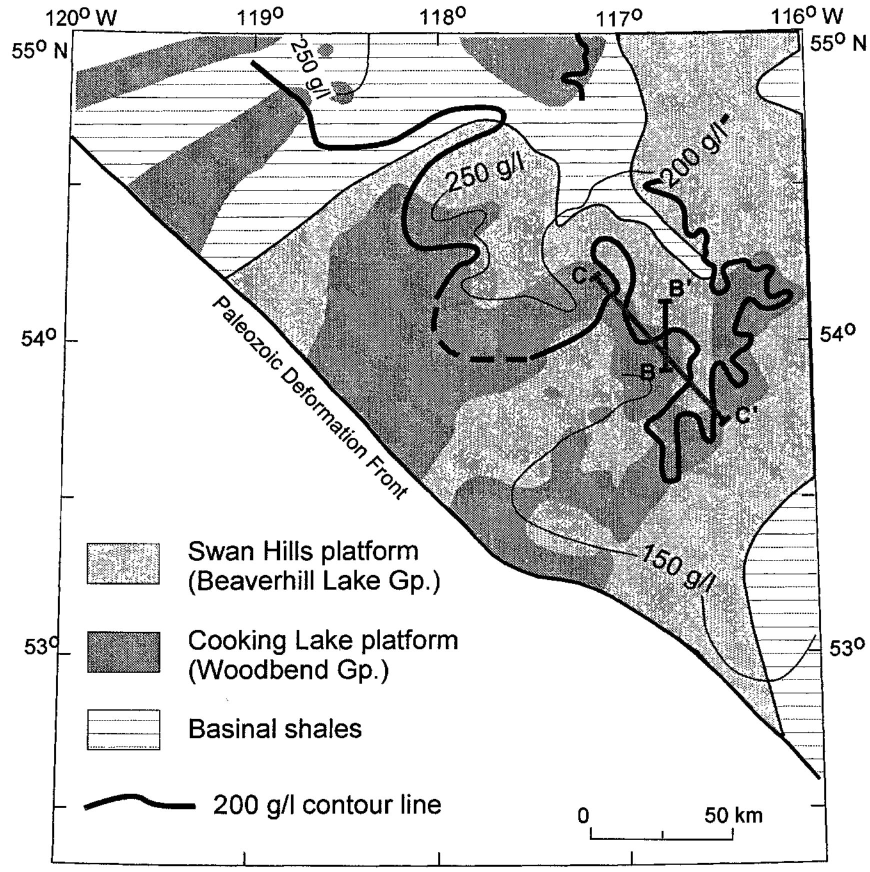

Figure 7.22: Correlation between salinity and facies distribution in the Woodbend-Beaverhill Lake aquifer.

The hydrostratigraphic cross section (Fig. 7.21) shows how the Woodbend-Beaverhill Lake aquifer thins abruptly in this area, permitting formation water flow to be forced upwards, through the 'windows' in the Ireton shales, into the Winterburn aquifer. Along the same line of cross section, the large tongue of light brine in the Winterburn aquifer extends farther to the north (Fig. 7.7) and represents a sub-lateral "continuation" of the 'finger' of light brine, in the Woodbend-Beaverhill Lake aquifer. The 'interfingering' pattern in the Woodbend-Beaverhill Lake aquifer is probably caused by the higher permeability in the Leduc reef carbonates. The high hydraulic head 'fingers' (Fig. 7.10) coincide with the locations of the Leduc reef build-ups (Fig. 7.20), which suggest that formation water flow is channeled through these reefs. Apparently, flow in the Woodbend-Beaverhill Lake aquifer is governed by a combination of the lateral changes of permeability and transmissivity, controlled by depositional facies distribution and



Reproduced with permission of the copyright owner. Further reproduction prohibited without permission.

aquifer thickness, and by hydraulic communication with the Winterburn aquifer at selected locations where the intervening Ireton aquitard is thin or absent.

The hydraulic head distribution in the Elk Point aquifer (Fig. 7.13) suggests relatively stagnant flow conditions in the northeastern corner of the study area, which is filled with the heavy brine. There appears to be a tongue of fresher formation water coming from the south (Fig. 7.14), which is deflected towards the eastern boundary of the study area. The intervening Watt Mountain aquitard is very thin to non-existent in this area, and the heavy brine (> 250 g/l) may continue in the overlying Woodbend-Beaverhill Lake aquifer (this interpretation is tentative and cannot be confirmed due to the lack of data).

Insufficient hydrogeological data exist for the 'Basal sandstone aquifer' in the study area and, therefore, it is difficult to assess the competence of the Middle Cambrian aquitard. The crystalline Precambrian basement is commonly assumed to act as an aquiclude (Hitchon et al., 1990; Bachu, 1995a, 1999), and there is no evidence for the presence of formation waters in the basement in the study area. The nearest occurrence of waters in the crystalline basement are Ca-Cl brines that have been reported from the Precambrian Shield > 500 km to the northeast (Fritz and Frape, 1987). On the other hand, studies on Sr – isotopes from carbonate cements in Devonian reefs suggest that basement fluids may have migrated upwards via faults, which influenced the diagenetic history in the deep parts of the study area (Machel and Cavell, 1999; Mountjoy et al., 1999). Therefore, conduits for fluid flow in the crystalline basement might still exist, but they are most probably restricted to faults and shear zones (Bachu, 1999).

*Fluid origin and flow driving mechanisms*

The Cambrian to Devonian sediments were deposited in a marine environment, which infers that formation waters started out as seawater. The major salt deposits in the Devonian Elk Point Group north of the study area (Meijer Drees, 1994) suggest that parts of the original seawater in the Middle Devonian succession have evaporated beyond the



Reproduced with permission of the copyright owner. Further reproduction prohibited without permission.

point of halite saturation. Other, less evolved evaporitic sediments occur in the Winterburn and Wabamun Groups in the southern part of the Alberta Basin (Switzer et al., 1994; Halbertsma, 1994), but no significant amounts of evaporites were deposited in the study area itself. Connolly et al. (1990a) plotted log Cl versus log Br for formation waters in central Alberta, and all their data fall on or above the seawater evaporation trajectory (Carpenter, 1978), so they concluded that the waters are derived from seawater evaporation or from evaporation and subsequent dilution by freshwater, respectively. However, the bromide concentrations in Figure 7.16b plot on or below the SET, which suggests that the main volume of brines did not reach the point of halite saturation, and halite dissolution played a major role in concentrating the brines in the study area, as was suggested by Hitchon et al. (1971).

The depletion in magnesium with respect to the SET (Fig. 7.16c) probably is caused mainly by the dolomitization of limestone (Land, 1987; Spencer, 1987), according to the reaction:

$$Mg^{2+} + 2CaCO_3 \Rightarrow Ca^{2+} + CaMg(CO_3)_2.$$

The majority of the dolomite in the Devonian carbonates in the deep parts of the Alberta Basin consists of 'burial dolomites', which formed from diagenetically altered Devonian seawater (Machel et al., 1994; Mountjoy et al., 1999). The process of (replacement) dolomitization causes a concurrent increase in Ca with decreasing Mg in the fluid. However, Mg and Ca show a positive correlation (Fig. 7.23a), indicating that an additional process to dolomitization produced the high Ca content currently observed in the Devonian formation waters. The generally low sulfate concentrations (compared to seawater) and the poor correlation between sulfate and calcium in Devonian formation waters (Fig. 7.23b) shows that the dissolution of gypsum, according to the reaction:

$$CaSO_4 \cdot 2H_2O \Leftrightarrow Ca^{2+} + SO_4^{\ 2-} + 2H_2O$$

could not have had an important influence on the calcium content either. Also, sulphate concentrations in the Devonian formation waters are in the same range as in the significantly less saline Mississippian waters.



Reproduced with permission of the copyright owner. Further reproduction prohibited without permission.

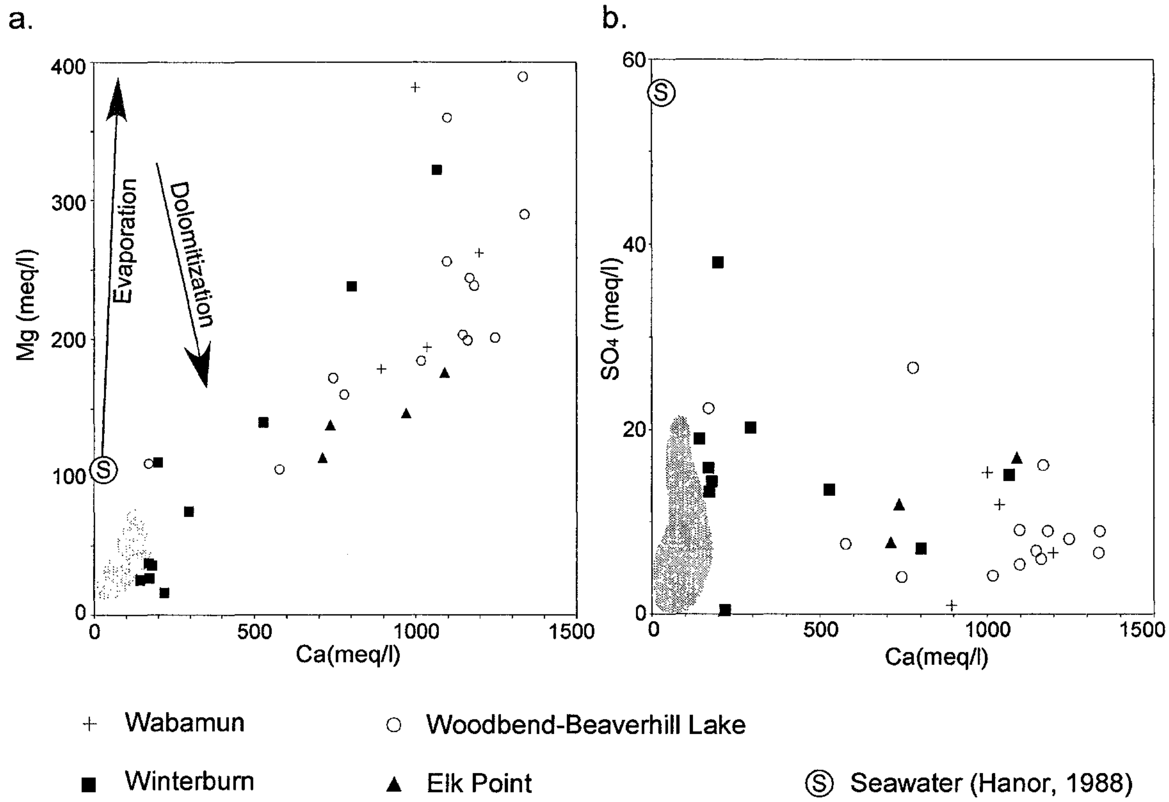


Figure 7.23: Cross plots of calcium versus: a) magnesium, and b) sulfate, for formation waters in the study area from the Cambrian-Devonian succession and the overlying Mississippian aquifer (shaded) for comparison.

The linear correlation between sodium and calcium concentrations with the Basin Fluid Line (BFL) defined by Davisson and Criss (1996) suggests that sodium is replaced by calcium in the formation waters (Fig. 7.24). The mechanisms responsible for this cation exchange is probably the albitization of plagioclase, according to the reaction (Land and Milliken, 1981):

$$CaAl_2Si_2O_8 + 2Na^+ + 4H_4SiO_4 \Rightarrow 2NaAlSi_3O_8 + 8H_2O + Ca^{2+}.$$



Reproduced with permission of the copyright owner. Further reproduction prohibited without permission.

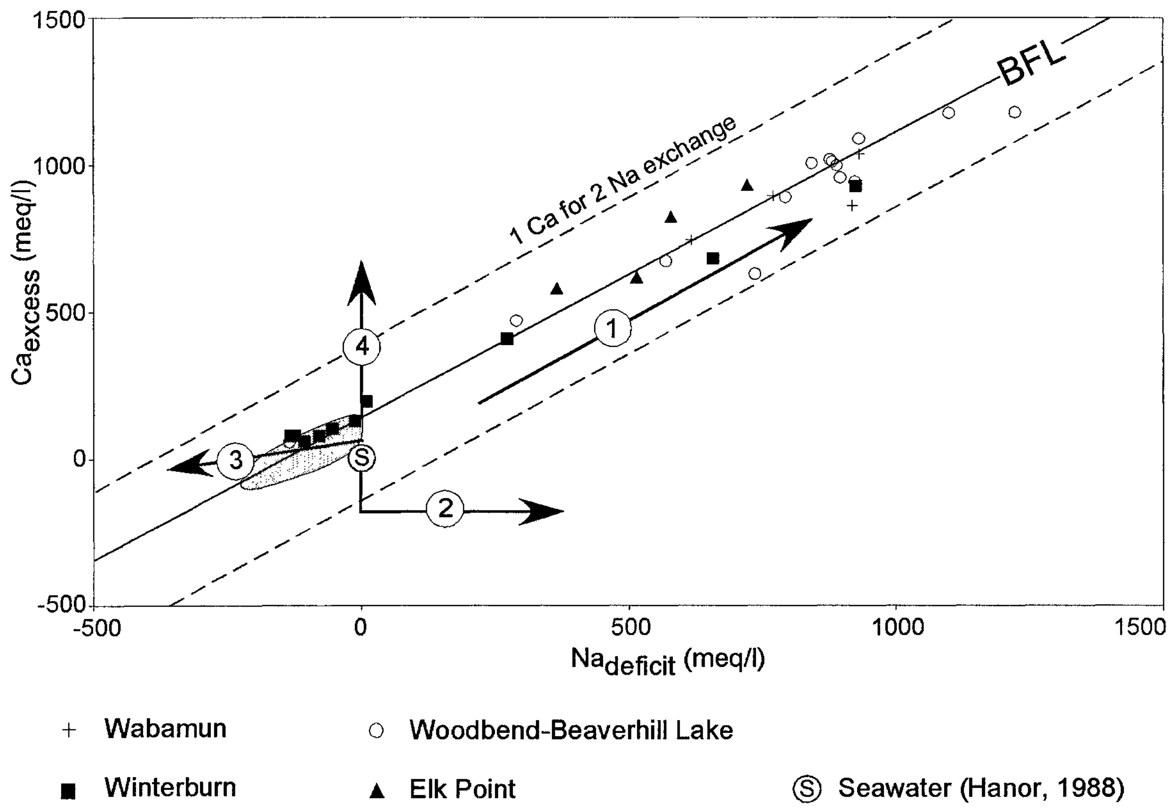


Figure 7.24: Plot of $Ca_{excess}$-$Na_{deficit}$ for Cambrian-Devonian formation waters in the study area, showing trends for various processes that may have effected the fluid composition. The circled numbers in the figure refer to the trends of: 1) albitization of plagioclase, 2) evaporation of seawater, 3) halite dissolution, and 4) dolomitization and gypsum dissolution. The Basinal Fluid Line (BFL) from Davisson and Criss (1996) is shown for reference. The grey shading shows the distribution of overlying Mississippian data for comparison. (See Chapter 2 for definitions of $Ca_{excess}$ and $Na_{deficit}$ values.)

Apparently, the albitization of feldspar left a predominant chemical signature observed in the present-day Devonian brines, although the processes of evaporation and dolomitization must have affected the early stages of brine evolution as indicated in the rock record. Also, the dissolution of halite must have played a role in concentrating the brines, causing a positive intercept of the BFL on the $Ca_{excess}$ axis (positive $Ca_{excess}$ value for $Na_{deficit} = 0$ in Fig. 7.24) and the shift towards Na/Cl-ratios > 0.85 in relatively low-saline Winterburn formation waters (Fig. 7.25). Alternatively, these high Na/Cl-ratios of



Reproduced with permission of the copyright owner. Further reproduction prohibited without permission.

the light brine could be due to mixing with Mississippian formation waters derived from a lateral, regional-scale flow system originating in the south of the study area.

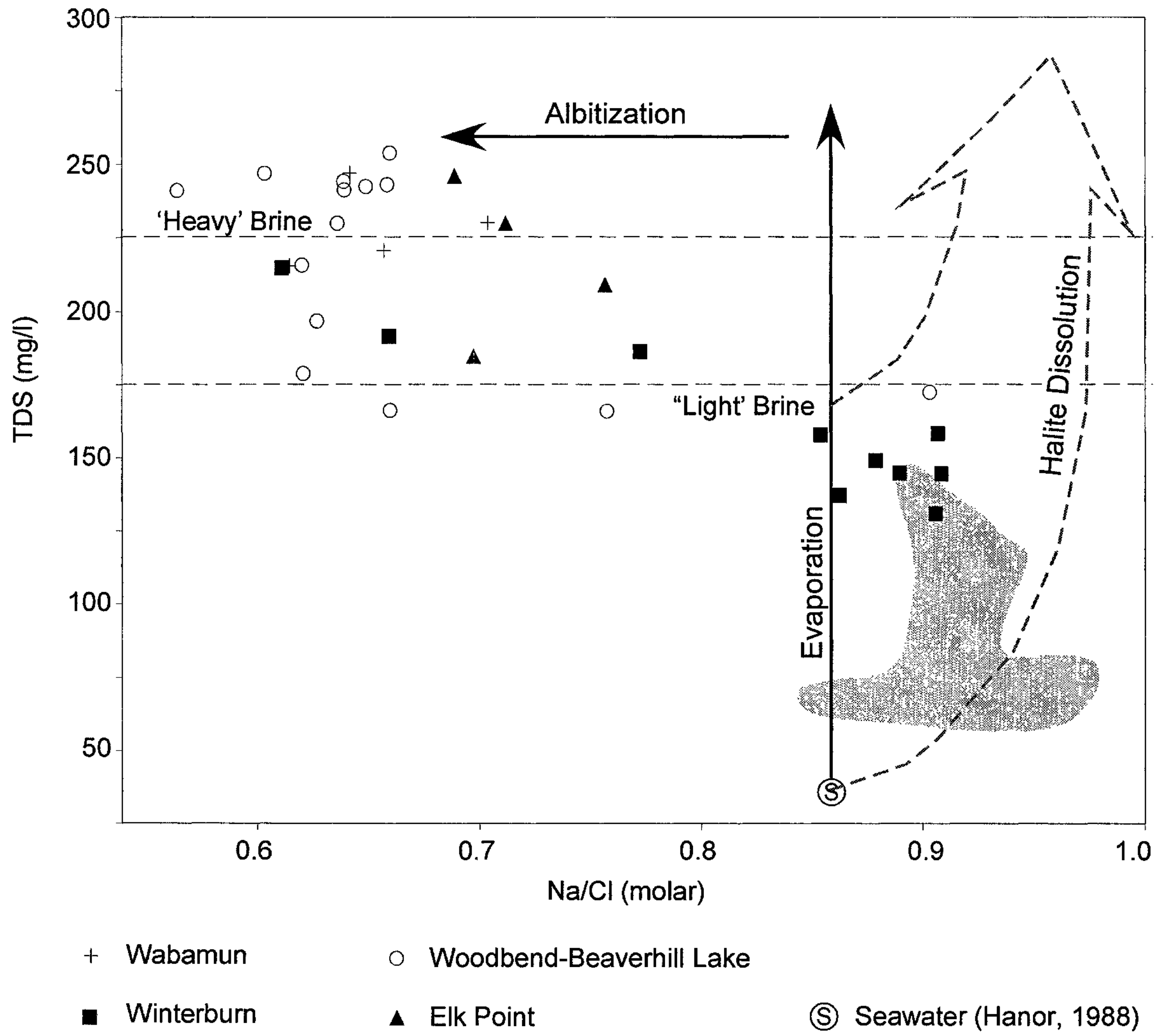


Figure 7.25: Distribution of Na/Cl-ratios versus salinity in Cambrian-Devonian formation waters showing processes that may have produced the brines. The shaded area (grey) shows the distribution of Mississippian data (see Chapter 6) for comparison.



Reproduced with permission of the copyright owner. Further reproduction prohibited without permission.

Following Spencer (1987), the following interpretation for the evolution of the Devonian brines is supported by the presented chemical data: a) starting with an original seawater source, b) concentration due to evaporation, c) syn-depositional loss of residual brines, d) downward migration of dense residual brines and heating, e) water-rock interaction (albitization) with sialic crystalline basement rocks and/or Cambrian clastics, f) upward migration of hot brines along faults, g) formation of carbonate cements, and h) mixing with freshwater. According to this interpretation, the heavy brine supposedly represents formation water that entered the Devonian aquifers at the time of dolomitization (Upper Devonian time), whereas the light brine was formed subsequently by mixing of the residual brine with freshwater of unspecified origin (Spencer, 1987). Similarly, a more recent study of the dolomitized Swan Hills platform carbonates suggested that the brine was derived during the precipitation of Graminia Formation evaporites, which subsequently dolomitized the underlying Beaverhill Lake to Winterburn platform carbonates by a combination of seepage reflux and thermal convection (Wendte et al., 1998). This mechanism would explain how the connate brines could have flowed through Cambrian and maybe even Precambrian rocks, which are the most likely sources for feldspars needed in the albitization process.

The main issue that remains to be addressed is the origin of the freshwater component in the process presented above. According to a study of oxygen and hydrogen isotopes in central Alberta, the observed freshwater component in Devonian-Jurassic formation waters has a post-Laramide, but pre-present day age (Connolly et al., 1990b). Connolly et al. (1990b) suggested that, following Hitchon (1969a,b; 1984) and Garven, (1989), post-Laramide meteoric recharge of the Devonian aquifers occurred through a gravity-driven flow system, with recharge in the mountain ranges and penetration of meteoric water down to the Precambrian basement. However, considering the large amount of residual brine in the deep basin, this flow system could not have been an effective basin-scale flow system with long-distance lateral flow in the Devonian aquifers, and discharging at the exposed Precambrian Shield, as previously suggested (Hitchon 1969a,b; 1984; Garven, 1989). According to numerical simulations, such a flow system would have



Reproduced with permission of the copyright owner. Further reproduction prohibited without permission.

flushed the Alberta Basin of brine within 2 million years (Adams et al., 2000). It appears that the boundary between the light and heavy brines (Fig. 7.17) represents the limit of meteoric freshwater influence (penetration).

The low-salinity waters in the Upper Devonian aquifer system are mainly from the southeastern part of the study area and plot along the respective Mississippian chemistry trends (Figs. 7.16, 7.25). This suggests as a first possibility that the 'light' Devonian brine could be a mixing product of the residual Devonian heavy brine and Mississippian formation waters. However, the intervening Exshaw-Banff aquitard obstructs direct (vertical) mixing between the Devonian and Mississippian aquifers. Therefore, it appears more likely that formation water mixing with meteoric water occurred laterally, along a long-range flow path originating in areas of outcrops at topographic highs in Montana to the south of the study area (Bachu, 1995a; Bachu and Underschultz, 1995; Anfort et al. 2001). Any meteoric recharge had/has to pass either through the Mississippian strata before it reaches the Devonian aquifers, or it has a long flow path from areas of Devonian outcrop in Montana, approximately 500 km south of the study area. In both cases, mixing with residual brine and/or water-rock interaction along the flow path overprinted the meteoric signature.

The relatively low salinity values, in conjunction with low [Na]/[Cl]-ratios < 0.8 (Fig. 7.25), which are predominantly present along the deformation front, suggest the second possibility of a different origin of fresher water in this area, namely from the thrust and fold belt of the Rocky Mountains. However, a hydrogeological study of formation water flow between the deformed and undeformed parts of the Devonian succession in southern Alberta suggests that the present flow systems in the individual thrust sheet are disconnected from each other and from the undeformed part of the Alberta Basin (Wilkinson, 1995). On the other hand, freshwater is believed to have infiltrated down to Mississippian aquifers via convoluted pathways in the over-thrust fault systems (Underschultz and Bartlett, 1999), but maps with the exact locations of such freshwater penetrations have not been published yet. Meteoric recharge through faults could also be



Reproduced with permission of the copyright owner. Further reproduction prohibited without permission.

an explanation for the origin of the light brine in the Devonian aquifers in places along the deformation front in the study area, but insufficient hydrogeological data exist in the thrust and fold belt to verify or disprove this hypothesis.

A third possibility for the origin of the lighter brine is the expulsion of formation water by tectonic compression of sediments during the Laramide orogeny. This flow-driving mechanism was introduced by Oliver (1986), although he expected the expelled fluids to have higher salinity and, after a lateral migration over hundreds of kilometres, to be able to form mineral deposits deep within the continent. Machel and Cavell (1999), using strontium isotopes, suggested that late stage calcite cements in the Woodbend reef complexes in the study area have been precipitated from tectonically expelled fluids, but they have shown that the strontium signal could be detected only within a limit of approximately 100 km from the deformation front. The relatively low salinity of the expelled fluids could also be explained by the involvement of metamorphic water from the Precambrian basement. There is no evidence for the presence of formation waters in the crystalline basement in the study area. The nearest occurrence of waters in the crystalline basement are Ca-Cl brines that have been reported from the Precambrian Shield, > 500 km to the northeast (Fritz and Frape, 1982). On the other hand, studies on Sr – isotopes from carbonate cements in Devonian reefs suggest that basement fluids have migrated upwards via faults, which influenced the diagenetic history in the deep parts of the study area (Machel and Cavell, 1999; Mountjoy et al., 1999). Therefore, conduits for fluid flow in the crystalline basement might exist, but they are most probably restricted to faults and shear zones (Bachu, 1999), not identified in the study area. Diagenetic water from the dehydration of clays appears rather improbable, because the most prevalent clay transformation, smectite to illite, takes place at much shallower depths, early in the burial history, and the volume of fluids released is small (Osborne and Swarbrick, 1997).

While the possible origin of relatively fresher water from metamorphic reactions remains to be further investigated, it seems unlikely that the present-day flow pattern is the remnant of tectonic expulsion. According to numerical modeling studies, the excess



Reproduced with permission of the copyright owner. Further reproduction prohibited without permission.

pressures generated by tectonic loading would have occurred in pulses and have dissipated after only a few million years (Ge and Garven, 1989, 1994).

A fourth mechanism capable of diluting high-salinity brines is the thermogenic reduction of sulfur (TSR), which can produce freshwater during the thermal generation of hydrocarbon gases according to the reaction (Worden et al., 1996):

$$CaSO_4 + CH_4 \rightarrow CaCO_3 + H_2S + H_2O \pm CO_2 \pm S\,.$$

This process is believed to cause the dilution of formation waters by up to 50% locally and up to 30% on a reservoir scale (Worden et al., 1996, 1998; Yang et al., 2001). On the other hand, there might be other reactions involved in TSR, some of them consuming water, and the amount of water produced is probably highly variable and, at least in some cases, negligible and may not affect the regional salinity distribution of formation waters (Machel, 1998).

As a fifth possibility, the updip position of the heavy brine could be the result of the long-range, down-dip migration of heavy evaporitic brines from the Williston Basin more than 500 km to the southeast (Chipley and Kyser, 1991), or, more likely, from the area of up to 600 m thick, laterally extensive Middle Devonian evaporite deposits (Meijer Dress, 1994; Grobe, 1999), 100 - 200 km to the east-northeast of the study area.

### 7.5 Summary and conclusions

The distribution of formation water salinity and hydraulic heads indicates that the Devonian succession in the study area is presently isolated from flow systems in the overlying hydrostratigraphic groups, separated by the competent Exshaw-Banff aquitard. Also, the Devonian aquifers cannot be recharged directly from above because of the hydraulic barriers comprised of thick, competent shales (aquitards), and extensive zones of underpressuring (sinks) and overpressuring (pressure barriers) present in the overlying Cretaceous succession (Chapter 5).



Reproduced with permission of the copyright owner. Further reproduction prohibited without permission.

Hydraulic head distributions and hydrochemical data from this study, in conjunction with previous work on the origin of Devonian formation waters (Spencer, 1987; Connolly et al., 1990a,b) suggest that two brines exist in the Cambrian-Devonian succession (Fig. 7.26). A 'heavy' connate brine (> 200 g/l) was probably generated from evaporated Devonian seawater, halite dissolution and subsequent alteration due to water-rock interaction (e.g., albitization, dolomitization). A 'light' brine (< 200 g/l) is found mainly downdip of the heavy brine and the hydrogeological patterns suggest five possible, not necessarily exclusive, origins. In the first case, the less saline formation water may represent a mixture of meteoric water and/or less saline formation water, originating in the thrust and fault belt, with the original connate ('heavy') brine. Secondly, these waters might contain a metamorphic component because tectonically expelled fluids were probably involved in the mixing process. In the third case, the light brine, flowing updip from the south, may have originated as Mississippian seawater that was mixed with Laramide – Pliocene (or present-day?) meteoric water, and is part of a long-range, gravity-driven flow system originating in Montana (Bachu, 1995a). Thermogenic reduction of sulfur may produce variable amounts of fresh water and therefore, represents a fourth mechanism capable of locally diluting saline brines. Alternatively, as a fifth possibility, the light brine could represent the original connate water, that has been displaced by the downdip migration of heavy brines that originate from partial dissolution of thick Middle Devonian evaporite deposits to the northeast of the study area.

The flow of both brines appears to be sluggish, probably as a result of buoyancy and convergence of the two brines. Although tectonic compression has caused the expulsion of fluids from the sediments in the thrust and fold belt and the crystalline basement, and has driven them laterally up to 100 km into the undeformed part of the basin (Machel and Cavell, 1999; Buschkuehle and Machel, 2001), excess pressures from this process probably have dissipated by now. The light brine advances further updip in the Upper Devonian aquifer system than in the Middle Devonian aquifer system (Fig. 7.26). This shows that the Ireton shales form an effective aquitard between the Middle and Upper



Reproduced with permission of the copyright owner. Further reproduction prohibited without permission.

Devonian aquifer systems. Cross-formational flow between the two Devonian aquifer systems occurs only in places where the Ireton shales thin out or are absent over Leduc reefs. The lighter brine attempts to flow updip, along large-scale "fingers" that are due to channeled flow along high-permeability pathways (Fig. 7.26). These conduits are probably caused by lithology changes, which are controlled by the depositional facies distribution and dolomitization. The density contrast between the light and heavy brines creates buoyancy forces that oppose the flushing of the high-salinity connate brine, so that the flow direction changes from mainly along dip to along strike in the mixing area of the two brines. This suggests that the lighter brine is attempting to displace laterally the heavier brine, which forms a slug of almost stagnant water, similarly to the basin-scale flow pattern in Devonian aquifers in the Williston Basin (Bachu and Hitchon, 1996).

The results of the current hydrogeological study bear two major implications for further studies, particularly numerical modeling, of flow of Devonian brines in the Alberta Basin. First, numerical models of flow in the Alberta Basin need to consider coupled transport and flow processes to account for the high density of the Devonian brines and the general variations in formation water density. Secondly, two-dimensional, cross-sectional numerical modeling of flow, in many cases, inadequately represents the observed flow of formation waters along preferential flow paths due to the heterogeneous permeability distribution in the Devonian aquifers and to the complexity of the flow pattern.



Reproduced with permission of the copyright owner. Further reproduction prohibited without permission.

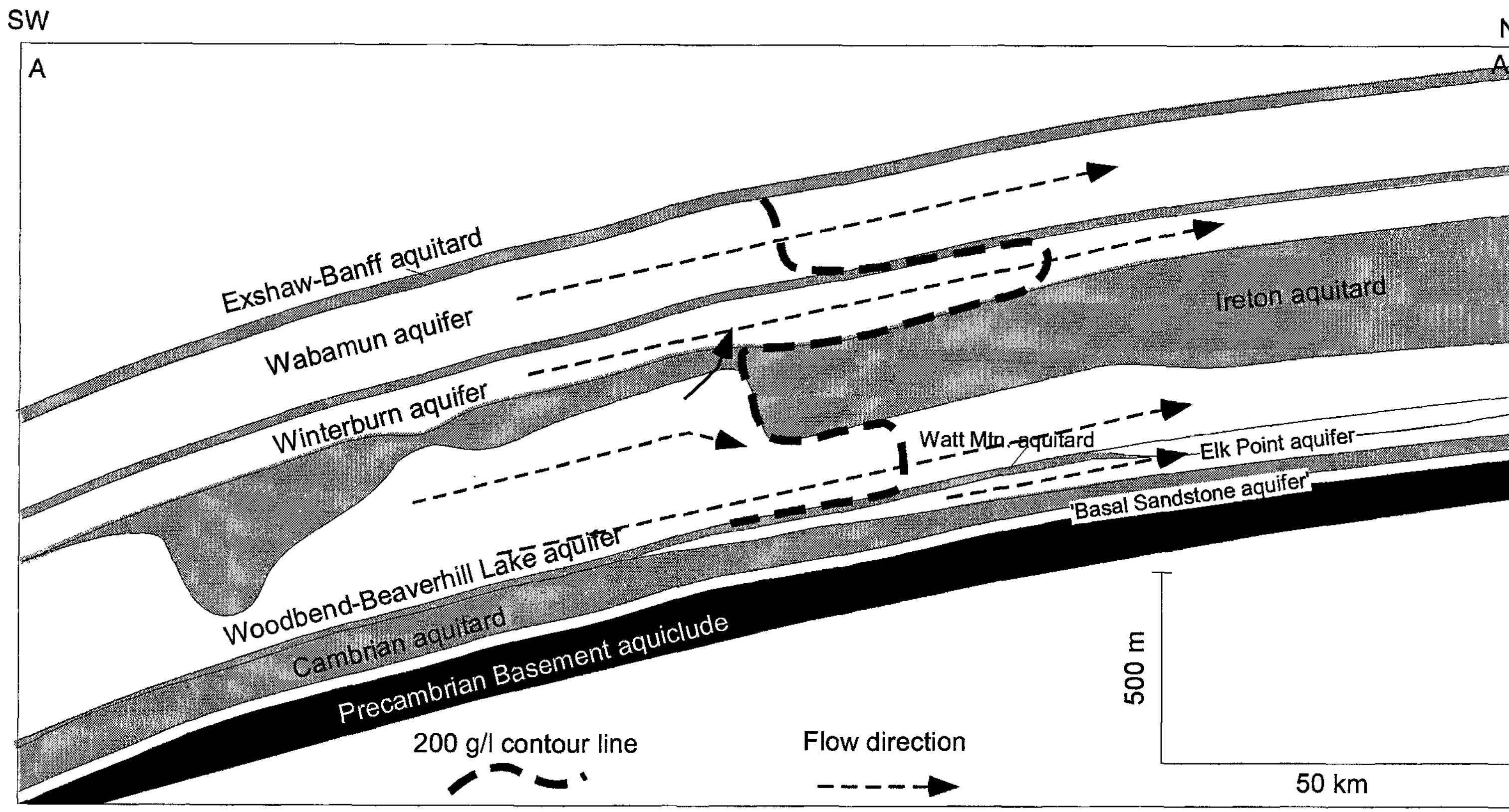


Figure 7.26: Hydrogeological cross section perpendicular to the deformation front showing conceptually the differential advancement of the less saline formation water displacement front against a high-saline connate brine in the Cambrian-Devonian hydrostratigraphic group. The flow arrows are dashed and extent over most of the length of the various aquifers to emphasis the overall sluggish movement of formation water in this succession and the low resolution of differences in hydraulic heads due to the relatively large error associated with pressure data from DSTs. See Figure 7.1 for line of cross section.



Reproduced with permission of the copyright owner. Further reproduction prohibited without permission.

# CHAPTER 8: SYNTHESIS

This chapter intends to summarize the hydrogeological interpretation from the various hydrostratigraphic groups in the study area in a combined conceptual flow model for the entire sedimentary succession. Changes in flow patterns and formation water chemistry from the ground surface to the Precambrian basement reflect the different flow-driving mechanisms that are or were active in the various hydrostratigraphic groups (Tab. 8.1), differing origins and evolution of the formation waters, and how the flow systems interact(ed) with each other. This flow interpretation will be put in perspective to the basin evolution, and will be compared to the prevailing basin-scale interpretations of flow in the Alberta Basin.

| Stratigraphy | Hydrostratigraphic Group (HSG) | Flow-driving Mechanisms | Hydrochemistry | Water Type |
|---|---|---|---|---|
| Belly River Fm. | Tertiary-Cretaceous | Topography-driven flow (local-regional scale) | Meteoric water | Ia |
| Colorado Gp. | | Erosional rebound | Mixing between sea- and meteoric | Ib |
| Mannville Gp. | | Hydrocarbon generation | Evaporated seawater altered by water-rock interaction (dissolution) and mixing with freshwater | Ic |
| Fernie Gp. | Mississippian-Jurassic | Topography-driven flow (basin-scale) | | II |
| Permo-Triassic | | | | |
| Mississippian | | | | |
| Devonian | Cambrian-Devonian | Topography-driven flow (basin-scale)<br>Strong buoyancy effects | Evaporated seawater, altered by water-rock interaction (albitization, dolomitization, halite dissolution) | III |
| Cambrian | | | | |

Table 8.1: Generalized hydrogeological characteristics of the studied sedimentary succession in west-central Alberta. The water types in the last column refer to Figure 8.1.



Reproduced with permission of the copyright owner. Further reproduction prohibited without permission.

## 8.1 Origin and evolution of formation waters in the study area

Most sediments in the stratigraphic succession were deposited in a marine to marginal-marine environment and, therefore, the respective formation waters probably started out as seawater that was successively altered by water-rock interaction and mixing with freshwater during sediment burial. Hence, the main water end members are seawater and freshwater, which have relatively well defined ranges in salinity and Na/Cl-ratio: Seawater: TDS = 35 g/l, Na/Cl = 0.85; meteoric water: TDS ~ 0 - 10 g/l, Na/Cl >> 1 (because typically other anions than $Cl^-$, i.e., $HCO_3^-$, $SO_4^{2-}$, are dominant in shallow groundwater in the study area (Barnes, 1977; 1987; Tokarsky, 1977). The formation waters in the three major hydrostratigraphic groups in the study area have distinctively different ranges in salinity and Na/Cl-ratio, and can be grouped accordingly (Fig. 8.1), confirming the initial hydrostratigraphic delineation based on fluid flow characteristics.

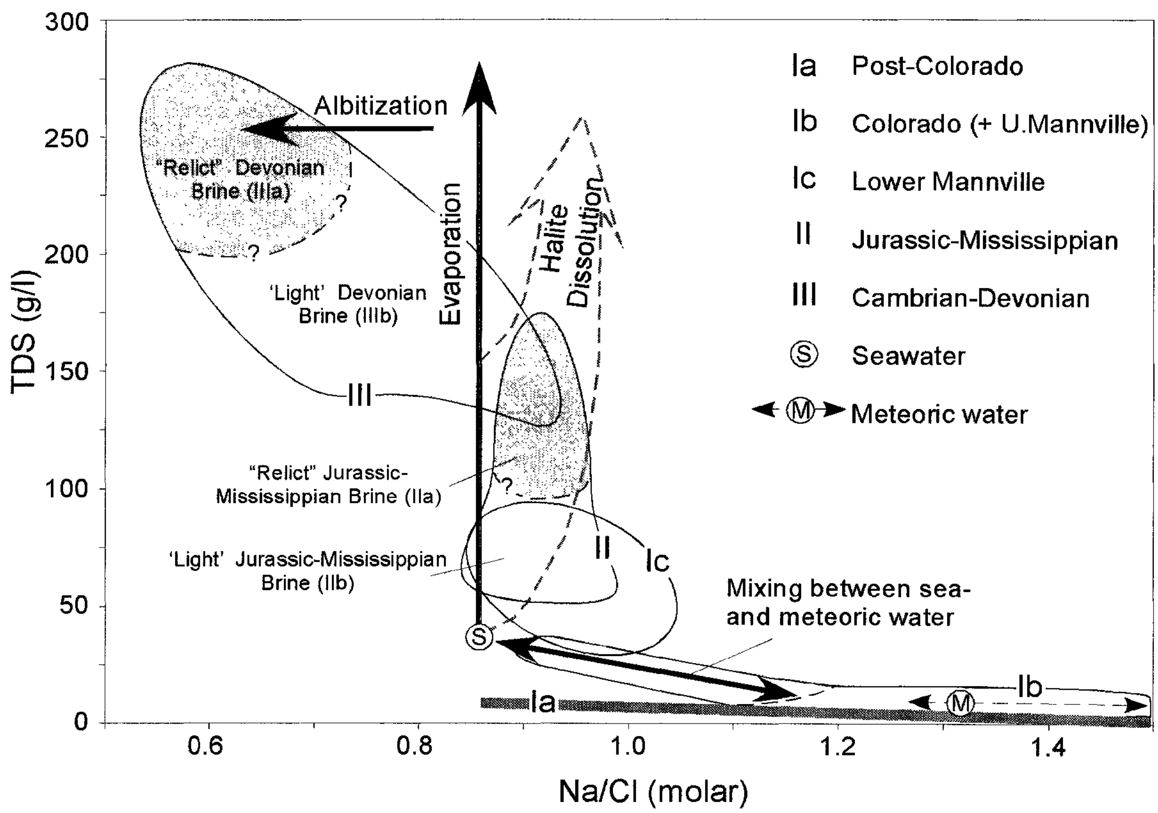


Figure 8.1: Grouping and schematic evolution of formation waters in west-central Alberta with respect to their variations in salinity and Na/Cl-ratio. See Figures 5.37, 6.19 & 7.25 for data distribution.



Reproduced with permission of the copyright owner. Further reproduction prohibited without permission.

Generally, formation waters from the Tertiary-Cretaceous hydrostratigraphic group (Ia and Ib), except in the Lower Mannville, have salinities below that of seawater and a relatively wide range in Na/Cl-ratios (0.85-1.5); those from the Jurassic-Mississippian hydrostratigraphic group (II) and the adjacent Lower Mannville (Ic) have a salinity above that of seawater and a narrow range of Na/Cl-ratios (0.85-1.0); and the Devonian waters (III) have very high salinity and low Na/Cl-ratios (0.5- 0.9). The main processes that cause an increase/decrease in salinity are evaporation/dilution and dissolution/precipitation. The Na/Cl-ratio indicates the relative contents of the main sodium and chloride minerals, e.g., NaCl, $CaCl_2$, and $NaHCO_3$ in solution. Shallow groundwaters are mainly Na-Ca-$HCO_3$ type waters, therefore the Na/Cl-ratio is much larger than 1. Seawater, evaporated seawater, and deep formation water are of the Na-Cl type and have a Na/Cl-ratio around one. Formation waters that contain high concentrations of dissolved $CaCl_2$, hence low Na/Cl-ratio, are mainly found in aquifers in or in contact with crystalline rocks, and are probably formed by the albitization of plagioclase, exchanging Na for Ca.

Originating in a marine to marginal-marine environment, formation waters in the Tertiary-Cretaceous succession (Brazeau-Belly River to Upper Mannville) probably started out as brackish water or seawater that was successively diluted with fresh, meteoric water. The presently relatively high salinities, only slightly lower than seawater salinity, in the Upper Mannville to Cardium aquifers indicates that an effective penetration of meteoric waters did not start before the end of deposition of the Colorado shales, which partly isolate(d) these aquifers from the flushing with meteoric water since pre-Laramide time. Only those parts of the Cardium and Dunvegan aquifers that are connected to the ground surface north of the study area, where these formations crop out, contain waters with significantly lower salinity and a meteoric Na/Cl-signature. On the other hand, the Brazeau-Belly River aquifer has been effectively diluted by meteoric water, and distributions of hydraulic heads show that a flow system driven by regional-to



Reproduced with permission of the copyright owner. Further reproduction prohibited without permission.

local-scale topography is presently active in this aquifer. The Lower Mannville sediments were deposited in a mainly fluvio-deltaic environment, but the current salinity of formation waters is up to three times that of seawater. This high salinity could be explained by leakage of brines from the Mississippian-Jurassic hydrostratigraphic group, driven vertically upward by sediment compaction, and/or mixing with high-saline, ascending Cambrian-to-Jurassic brines in areas where the intervening Exshaw-Banff and Fernie aquitards are missing due to erosion.

Having started out with seawater, aquifers in the Jurassic-Mississippian (II) and Cambrian-Devonian (III) hydrostratigraphic groups probably never were influenced significantly by meteoric water, as indicated by their high salinities. The main reason for that could be the lack of a topographic relief during and shortly after deposition of these sediments, as well as the presence of shale and evaporitic aquitards. Also, halite deposits in the Triassic Charlie Lake Formation indicate that parts of the original seawater had evaporated up to the point of halite precipitation. This suggests that formation waters in the Jurassic-Mississippian succession were partly formed by the evaporation of seawater. Nevertheless, the distribution of other major ions implies that other processes, such as precipitation of dolomite cements and dissolution of sulphate and halite, altered the composition of these waters.

Major salt deposits in the Devonian Elk Point Group northeast of the study area suggest that waters in the Devonian-Cambrian succession have a similar origin and evolution as the Jurassic-Mississippian waters. A higher degree of evaporation and additional dissolution of halite during burial probably caused the much higher salinity of the Devonian formation waters. The shift in the Na/Cl-ratio towards lower values is most likely due to the albitization of feldspar and suggests that these waters might have re-fluxed through the Cambrian clastics and/or the Precambrian crystalline basement. Hydrothermal convection in this part of the basin was invoked to explain the massive replacement of Devonian limestones by dolomite (Spencer, 1987; Wendte et al., 1997).



Reproduced with permission of the copyright owner. Further reproduction prohibited without permission.

## 8.2 Flow patterns from the ground surface to the Precambrian basement

After a critical review and discussion of representation methods for flow of variable-density brines in sloping aquifers (Chapters 2 and 3), equivalent hydraulic heads were calculated based on the mean formation water density in each hydrostratigraphic group (HSG) as reference density, and used to interpret flow in the various aquifers. Freshwater hydraulic heads were used only in the Tertiary-Cretaceous HSG, after driving-force ratio (DFR) calculations confirmed density-effects are negligible. For the Jurassic-Mississippian and Cambrian-Devonian HSGs, the respective average brine density was used as a reference density for calculating hydraulic heads. The results, as presented in Chapters 5-7, confirm that the initial subdivision of the stratigraphic succession into three main hydrostratigraphic groups is correct. The three groups are (Tab. 8.1; Fig. 8.2): 1) Tertiary-Cretaceous, 2) Mississippian-Jurassic, and 3) Cambrian-Devonian. The thick intervening shale aquitards of the Fernie Gp. and the Exshaw-Banff Formations effectively impede cross-formational hydraulic communication between the Tertiary-Cretaceous and the Jurassic-Mississippian, and between the latter and the Cambrian-Devonian HSGs, respectively. This vertical isolation from each other caused flow patterns to evolve separately in the three hydrostratigraphic groups, as the respective flow systems were/are subject to different internal and boundary conditions.

The Tertiary-Cretaceous HSG can be subdivided further into the post-Colorado aquifer system, the Colorado aquitard system (Type Ib water) and the Mannville aquifer system (Fig. 8.2). The flow has adjusted to the present-day ground surface topography only in the post-Colorado aquifer system (Type Ia water). The Colorado and Mannville aquifers (Type Ib & Ic waters) are mainly cut-off from meteoric recharge by the Colorado shales aquitard, except for a tongue of freshwater (Type 1b water, TDS $< 15$ g/l, Na/Cl $> 1.2$) in parts of the Cardium and Dunvegan aquifers (Fig. 8.3) that are connected to outcrop north of the study area.



Reproduced with permission of the copyright owner. Further reproduction prohibited without permission.

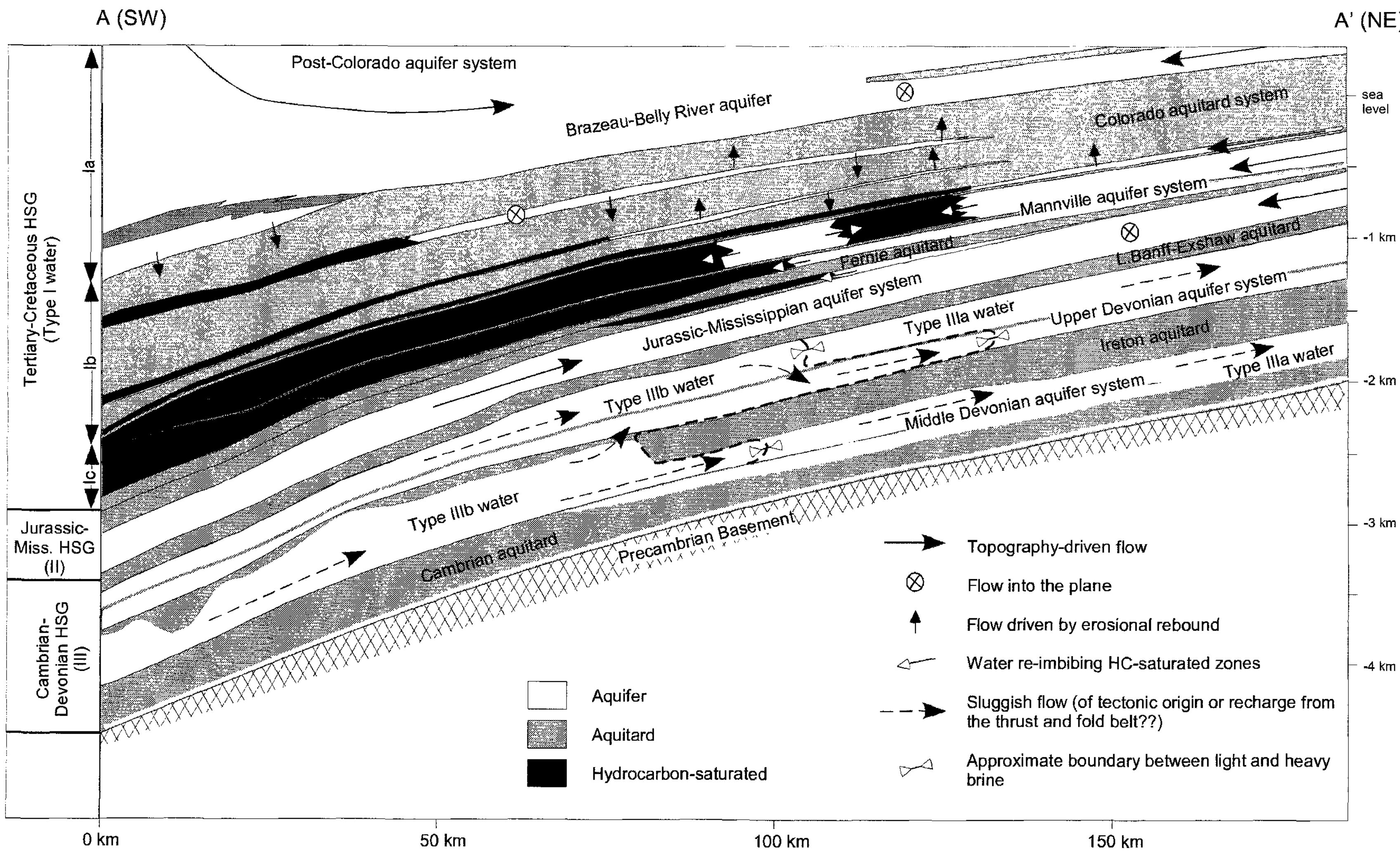


Figure 8.2: Hydrogeological dip cross section (A-A') showing the inferred flow patterns in the three hydrostratigraphic groups in the study area. (See Fig. 8.4 for line of cross section.)



Reproduced with permission of the copyright owner. Further reproduction prohibited without permission.

Reproduced with permission of the copyright owner. Further reproduction prohibited without permission.

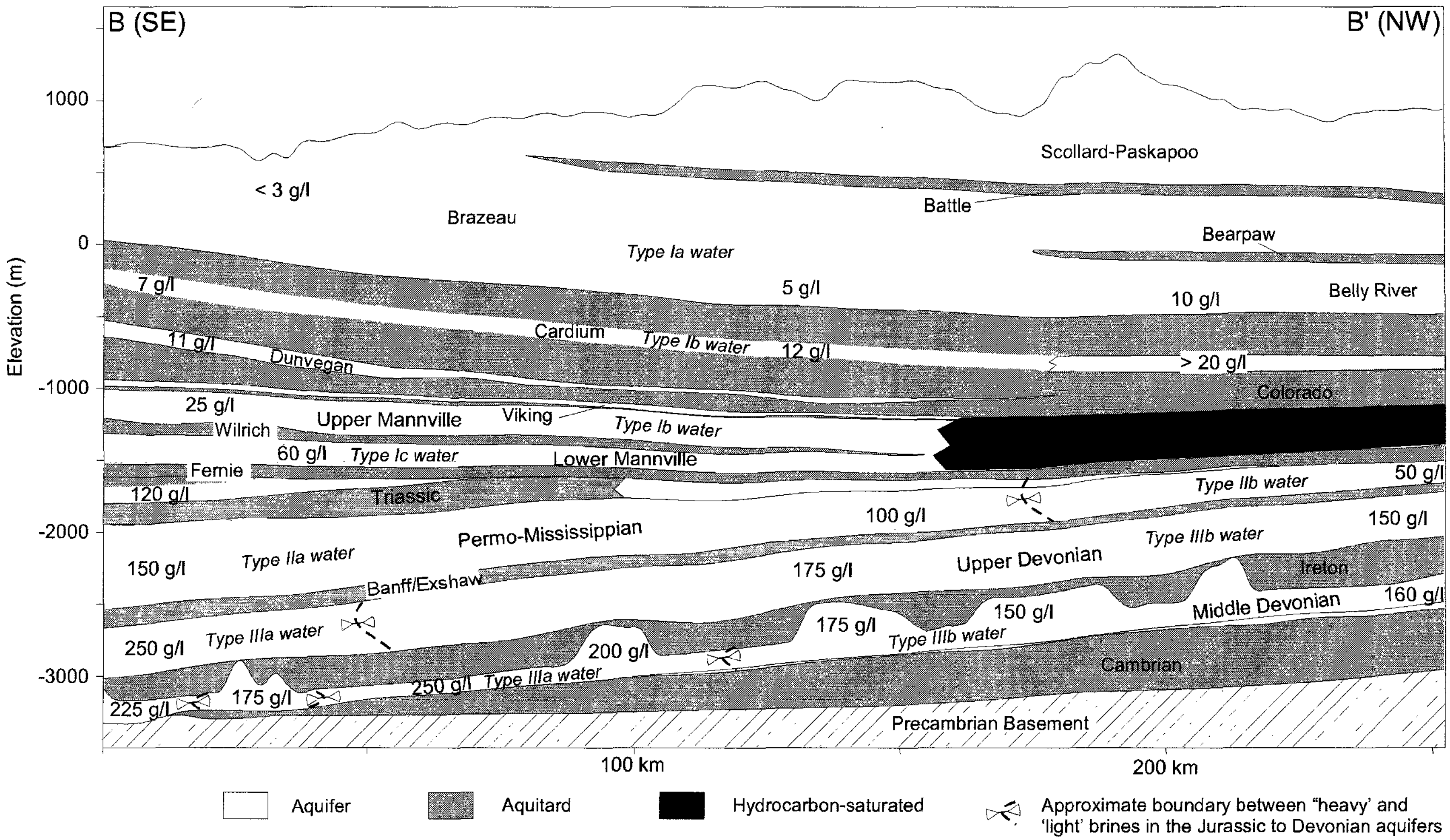


Figure 8.3: Hydrostratigraphic cross section sub-parallel to the deformation front showing general salinity distribution in the study area. (See Fig. 8.4 for line of cross section.)

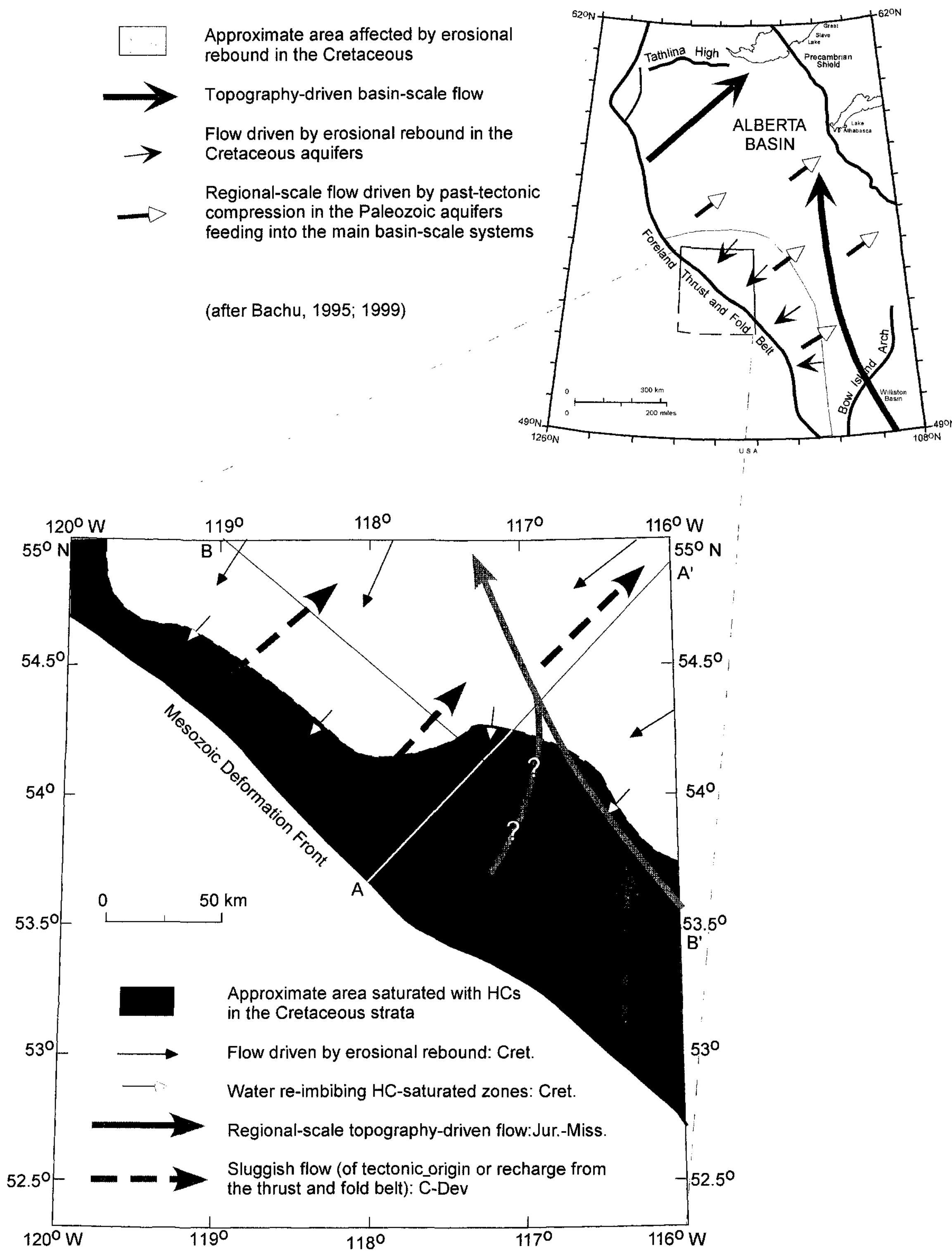


Figure 8.4: Diagrammatic representation of the flow systems and patterns in the study area compared to Bachu's (1995a, 1999) interpretation of flow in the Alberta Basin .



Reproduced with permission of the copyright owner. Further reproduction prohibited without permission.

Burial of the basin strata and subsequent hydrocarbon generation during the Laramide orogeny created dominantly hydrocarbon-saturated zones in the deeper parts of the Mannville to Brazeau-Belly River aquifers, the hydrocarbons being located downdip of the water-saturated zones (Figs. 8.2 and 8.4). The hydrocarbon-water interface appears to be a transient permeability barrier that moves downdip towards the deformation front since the uplift of the basin and a decrease in the rate of hydrocarbon generation, while formation water could re-imbibe formerly hydrocarbon-saturated zones of these strata. Formation water flow in the Mannville and Colorado aquifers is mostly towards the receding hydrocarbon-saturated regions and towards the sinks created by erosional and post-glacial rebound of the intervening shales. In general, the hydrocarbon-saturated region represents a relative-permeability and pressure barrier with respect to lateral hydraulic communication within each aquifer, and to vertical cross-formational flow from the underlying Mississippian-Jurassic hydrostratigraphic group, and to potential meteoric recharge from the thrust and fold belt. As a result of the latter, overpressures in the hydrocarbon-saturated zones in the deep parts of the basin could be due to the weight of the overlying water column in the foothills region. An alternative, frequently employed interpretation for the cause of overpressures in hydrocarbon-saturated regions according to the literature is the active thermogenic generation of hydrocarbons in a low-permeability environment (Hedberg, 1978; Spencer, 1987; Osborne and Swarbrick, 1997).

The Mississippian-Jurassic hydrostratigraphic group represents a single continuous carbonate-sandstone aquifer system in the eastern half of the study area. The general flow direction is northward (Fig. 8.4), while fresher water (Type IIb water, TDS ~ 50 g/l) in the southeast (Fig. 8.3), which is part of a basin-scale, gravity-driven flow system originating at high formation outcrops in Montana, flows around and partly displaces a plume of connate brine (Type IIa water). Only the Permo-Mississippian aquifer continues westwards, whereas the lithology in the overlying Triassic Montney and Doig Formations changes to siltstones and shales, forming an aquitard. Overlying the Doig-Montney aquitard is the Charlie Lake-Halfway aquifer. Flow in this aquifer is eastward and, at its subcrop edge appears to be forced upward through the Fernie shales into the Lower



Reproduced with permission of the copyright owner. Further reproduction prohibited without permission.

Mannville aquifer, where it causes an increase in formation water salinity (Fig. 8.3). A "deep basin" hydrocarbon accumulation with relatively low hydraulic heads in its vicinity is observed in the aquifer-aquitard transition zone in the Montney, similar to directly overlying hydrocarbon reservoirs in the Lower Mannville aquifer. No hydrocarbon-saturated zones were identified in the Permo-Mississippian aquifer; hence hydraulic communication of formation water between the deformed and undeformed parts of the Alberta Basin becomes possible, but has to be confirmed by further research. The hydraulic head distribution actually indicates that there is a component of flow from the direction of the thrust and fold belt of the Rocky Mountains in the central part of the study area (Figs. 6.10 & 8.4). Nevertheless, the nature and origin of this flow is still under debate (Bachu, 1999; Underschultz and Bartlett, 1999).

Similar to the overlying Mississippian-Jurassic HSG, two types of brines were identified in the Cambrian-Devonian HSG, although the salinity is generally much higher. A 'heavy' connate brine (Type IIIa water, Fig. 8.1) was probably generated from evaporated Devonian seawater and subsequent alteration due to water-rock interaction, whereas a 'light' brine (Type IIIb water, Fig. 8.1) is found mainly downdip of the heavy brine. The lighter brine attempts to flow updip, along large-scale "fingers" that are due to channeled flow along high-permeability pathways. These conduits are probably caused by lithology changes, which are controlled by the depositional facies distribution and by dolomitization. The density contrast between the light and heavy brines creates buoyancy forces, which additionally impede the flushing of the high-saline connate brine. Mixing with less saline water from overlying aquifers is only possible through lateral flow from areas southeast of the study area, where the Exshaw-Banff aquitard is absent due to erosion, or through flow from the thrust and fold belt, where faults might represent conduits to flow. In the latter case, the less saline formation water along the deformation front would represent a mixture of meteoric water and/or less saline formation water with the original connate ('heavy') brine. Furthermore, these waters probably contain a metamorphic component, because tectonically expelled fluids were might have been involved in the mixing process (Machel and Cavell, 1999). Alternatively, at least in the southeast of the study area, where the light brine appears to flow updip from the south,



Reproduced with permission of the copyright owner. Further reproduction prohibited without permission.

the formation waters consist of Mississippian seawater mixed with Laramide – Pliocene (or present-day?) meteoric water that is part of a long-range, gravity-driven flow system originating in Montana (Bachu, 1995a). Although tectonic compression has caused the lateral expulsion of fluids from the sediments in the thrust and fold belt and the crystalline basement up to 100 km into the undeformed part of the basin (Machel and Cavell, 1999), excess pressures from this process probably have dissipated by now. Therefore, formation water flow in the Cambrian-Devonian appears to be presently controlled by basin-scale topography and buoyancy, resulting in almost stagnant conditions (Figs. 8.2 and 8.4). The recharge areas are at high elevation in Montana and, probably to a lesser extent, the thrust and fold belt of the Rocky Mountains. Discharge occurs along the sub-Cretaceous unconformity east of the study area, where Devonian and Cretaceous aquifers are in direct hydraulic communication and Devonian brines form a high-saline plume in the Mannville aquifer (Hitchon et al., 1990; Rostron and Tóth, 1997; Anfort et al., 2001).

### 8.3 Basin history and fluid flow evolution

It is difficult to reconstruct flow patterns during the Cambrian to Devonian stage of basin evolution. It is likely that topography-driven flow and meteoric recharge during that time were negligible, because the sediments in the study area were mainly deposited in a marine environment (platform-margin stage). Freshwater that might have accumulated during the period of erosion from the Late Cambrian to the Early Devonian, probably was displaced by descending, heavy evaporitic brines that formed during the Elk Point time. The main indication that large amounts of water must have migrated through the Devonian sediments is the massive dolomitization of limestone observed in this succession, which required an extensive flux of Mg-rich fluids. However, the flow-driving mechanisms behind the dolomitization process and the source of Mg-bearing fluids are still being debated; hence remain unclear (Mountjoy, 1994), and are beyond the scope of this study. The herein presented hydrogeological data only suggest that evaporated Devonian seawater migrated through the Devonian carbonate aquifers, and



Reproduced with permission of the copyright owner. Further reproduction prohibited without permission.

probably also through the Cambrian succession and the Precambrian crystalline basement, where the fluids interacted with the surrounding rock framework. The resulting "relict" brines are still present in most parts of the Cambrian-Devonian hydrostratigraphic group in the study area. These observations agree with dolomitization models that involve a flow system driven by density differences, e.g., a) the long-range, down-dip migration of heavy evaporitic brines from the Williston Basin (Chipley and Kyser, 1991), or b) local-scale hydrothermal convection of evaporitic brines (Spencer, 1987, Wendte et al. 1997). An additional flow-driving mechanism during the Devonian was probably sediment compaction, which also was proposed as a possible hydraulic pumping mechanism for dolomitizing fluids (e.g., Machel and Anderson, 1989).

Marine sedimentation continued during the Mississippian, and buoyancy and sediment compaction are the most likely flow-driving mechanisms that have been active during that time. Similar to the Devonian brines, chemistry of the Triassic to Mississippian brines currently observed in the study area suggest that these represent concentrated evaporated seawater, which was altered mainly by water-rock interaction. However, the salinity of these waters is significantly lower than the salinity of the Devonian brines, one reason being that the degree of evaporation during the Mississippian-Jurassic was relatively low, as indicated by the smaller volume of evaporites in the Triassic compared to the Elk Point Group. Also, the Mississippian to Jurassic formation waters had less time to interact with the rock framework and to dissolve solids. The Triassic-Mississippian aquifers were exposed to potential meteoric recharge during the marine regressions in the Pennsylvanian, Late Permian, and Late Triassic to Early Jurassic. Therefore, mixing of formation water with freshwater during these periods could be an additional cause for the salinity in the Mississippian-Jurassic HSG being significantly lower than in the Cambrian-Devonian HSG. However, the flushing of Mississippian to Cambrian aquifers with freshwater was impeded by presumably low topographic relief; hence low potential for topography-driven flow, combined with the buoyancy between light meteoric water and heavy connate brine.



Reproduced with permission of the copyright owner. Further reproduction prohibited without permission.

The emerging cordillera of the Rocky Mountains in the northwest at the end of the Jurassic and Early Cretaceous started to significantly change the depositional environments, formation water origin, and flow-driving mechanisms in the Alberta Basin. The generally low formation water salinity not only suggests mixing with fresh meteoric water, but also reflects the marginal-marine to marine, and, to a lesser extent, fluvial depositional environments, which result in the lack of evaporitic deposits.

During the late Jurassic, in the early stages of the Columbian orogeny, compaction continued to be the main driving mechanism for fluid flow in the basin fore-deep. Fluids were driven out of the shallow-marine shales and shelf sands, and laterally away from the basin center toward the flanks, in systems characteristic of compacting sand-shale successions (Magara, 1976a; Bredehoeft et al., 1988). In the early Cretaceous, during the deposition of the Mannville Group siliciclastic succession, local gravity-driven flow systems developed after tectonic thrusting provided higher topographic elevations in the west. These flow systems must have been relatively short lived, as the following lull in tectonic activity, represented by the deposition of the marine Colorado shales, again resulted in a compaction-dominated flow system.

The continental post-Colorado Upper Cretaceous and Tertiary strata were deposited during the Laramide orogeny. Tectonic compression, due to successive over-thrusting of foreland basin strata caused by the eastward advancement of the Cordilleran deformation front, drove laterally the flow of connate formation waters in the deeper aquifers (Garven, 1989; Ge and Garven, 1989; Deming et al., 1990). This tectonically-driven flow probably occurred in pulses and was relatively short-lived (Deming and Nunn, 1991), and, therefore, involved low average fluxes, while the respective fluids were expelled only up to 100 km laterally into the basin away from the deformation front (Machel and Cavell, 1999; Buschkuehle and Machel, 2001). Additionally, compaction of the shale-dominated Colorado succession continued to play an important role in expelling formation water (Bekele et al., 2000). Topography became increasingly important as a flow-driving mechanism at least in the post-Colorado aquifer system, setting up a northeastward



Reproduced with permission of the copyright owner. Further reproduction prohibited without permission.

regional flow system (Garven, 1989) sub-parallel to the tectonic expulsion of formation waters.

During the Laramide orogeny, almost the entire sedimentary succession from the Cretaceous to the Cambrian entered the oil and subsequently the gas window, reaching a maximum burial in the Eocene (Bustin, 1991; Kalkreuth and McMechan, 1996). Overpressures developed specifically in the deep Colorado and Mannville strata as a result of compaction and hydrocarbon generation (Hedberg, 1974; Spencer, 1987; Osborne and Swarbrick, 1997; Bekele et al., 2000). Gas and oil displaced the formation water from the pore space in the deep Cretaceous strata adjacent and sub-parallel to the deformation front, forming a pressure and relative-permeability barrier for formation water flow. Since the peak of the Laramide orogeny, the basin has been uplifted due to tectonic relaxation and erosion to the present-day topographic relief. As a result, the oil and gas windows shifted downward, and the rate of hydrocarbon generation decreased in the Cretaceous succession. At present, only the deep part of these strata still generates gas or oil, maintaining high pressures and hydrocarbon saturation in the Cretaceous aquifers. In regions further updip, the rate of hydrocarbon loss and pressure dissipation is higher than the replenishment by hydrocarbon generation, allowing formation water to re-imbibe the "deep basin" reservoirs along the boundary between hydrocarbon – and water-saturated zones (Figs. 8.2 and 8.3). This effect, combined with the erosional rebound of thick shales, led to significant underpressures in hydrocarbon- as well as water-saturated regions because, as a result of very low fluid fluxes in a low-permeability environment, water is not capable of replenishing the expanding pore space. Therefore, the regional flow pattern was reversed from an eastward-directed compaction- and topography-driven system to a westward direction of flow driven by erosional rebound and hydrocarbon leakage in the Colorado and Mannville aquifers.



Reproduced with permission of the copyright owner. Further reproduction prohibited without permission.

## 8.4 Hydraulic communication between deformed and undeformed parts of the Alberta Basin

The interpretation of basin evolution and fluid flow introduced above shows that only in the early stages of the Laramide orogeny there existed the possibility of formation water flow from the deformed into the undeformed parts of the Alberta Basin throughout the entire sedimentary succession. The high elevation of the orogen represented the recharge area of a basin-scale topography-driven flow system, and tectonic compression caused basin-ward expulsion of fluids. Although the topographic high and, therefore, a potential for fluid flow still exist in the foothills and front ranges of the Rocky Mountains, the hydrocarbon-saturated region in the deep Cretaceous strata has formed a permeability barrier for water flow since approximately the Eocene. Only flow above the Colorado shale aquitard is driven by the local to regional topography and the potential flow from the foothills and front ranges in this succession is restricted to the near vicinity of the Cordilleran deformation front. The underpressures observed in the Mannville, Colorado and Brazeau-Belly River aquifers cause formation water to flow from the plains region towards the mountains, opposite to the high fluid potential in the mountains, suggesting that the two regions are hydraulically disconnected.

On the other hand, the present flow in the Mississippian-Jurassic and Cambrian-Devonian HSGs adjacent to the deformation front is directed northeastward, updip, and therefore is coincident with high fluid potential in the foothills and front ranges of the Rocky Mountains. Also, formation water salinity is relatively low, although still higher than that of seawater, suggesting at least the possibility of mixing with meteoric waters that penetrate the deep aquifers via convoluted pathways along faults in the deformed belt. However, hydrogeological data west of the deformation front are too sparse to corroborate this interpretation. One noteworthy argument against a notable influence/effect of meteoric recharge from the area of the Rocky Mountain is the south-north directed basin-scale flow system originating in Montana (Bachu, 1995a; Anfort et al., 2001). Although the topographic highs and the recharge area in Montana are at much



Reproduced with permission of the copyright owner. Further reproduction prohibited without permission.

greater distance from the study area than the directly adjacent Rocky Mountain thrust and fold belt to the southwest, the pattern of relatively fresher water flowing into the study area along the north-to northwest flow direction is dominant or at least equal to the updip flow of water with comparable salinity.

In summary, hydraulic communication between the deformed and undeformed parts of the Alberta Basin is possible according to the presented hydrogeological data, but it only affects the flow in the basin at a distance of approximately 100 km from the deformation front of the Rocky Mountains. Further research and more comprehensive hydrogeological data from the region of the thrust and fold belt of the Rocky Mountains is needed to resolve this issue.

### 8.5 Summary of original scientific contributions

This study tried to resolve remaining questions on fluid flow in the west-central part of the Alberta Basin adjacent to the Rocky Mountain thrust and fold belt. This resulted in original contributions to the understanding of flow, origin and evolution of formation waters in the Alberta Basin, which also has implications for the study of regional fluid flow in foreland basins in general. The following aspects are considered particularly worth mentioning:

(1) Errors in the flow representation of variable-density brines could be minimized using the average formation water density as reference density in the calculation of hydraulic heads, which is an alternative to the calculation of driving-force vectors. A comparison of the two methods, using actual pressure and hydrochemical data, showed that the sum of mechanical and analytical errors associated with the hydrogeological data outweigh the theoretically higher accuracy of driving-force vectors. In most areas where the possibility of flow reversal exists, the accuracy of the hydrogeological data only allows interpreting the respective flow pattern as ±



Reproduced with permission of the copyright owner. Further reproduction prohibited without permission.

stagnant, even when using the theoretically accurate driving force vectors. While driving force vectors are theoretically more accurate than hydraulic heads, additional technical and procedural errors are introduced, because the calculation of driving force vectors requires the computation of water densities from salinity data in addition to the pressure data, and the actual calculation of gradients between wells or within a grid of inter- and extrapolated data.

(2) The formation waters from the various hydrostratigraphic groups in the study area could be subdivided into four groups, and characterized as: 1) mainly fresh, meteoric water, 2) mixing between seawater and meteoric water, 3) evaporated seawater concentrated by halite dissolution and 4) evaporated, concentrated seawater significantly altered by the albitization of feldspar.

(3) This study is the first to identify the interaction between “deep basin” hydrocarbon-saturated and water-saturated zones in the Cretaceous aquifers as an additional mechanism to create underpressuring in the Alberta Basin. Also, the hydrocarbon-saturated zones represent a regionally extensive, effective relative permeability barrier to flow from the Rocky Mountain thrust and fold belt.

(4) Combining the interpretation of flow and formation water chemistry shows that Jurassic-Mississippian and Cambrian-Devonian formation waters in the deep, west-central parts of the Alberta Basin have been influenced less by mixing with meteoric water than in the central, southern and northern parts of the basin, than previously identified by Connolly et al. (1990), Schwartz et al. (1981), and Bachu (1997), respectively. The main reasons for the isolation of “relict” formation waters in the deep Alberta Basin are effective confining aquitards, sluggish flow, and the fact that this area is influenced only marginally by mixing with meteoric water carried by a gravity-driven flow system.

(5) The boundary between a ‘light’ and a ‘heavy’ brine in the Mississippian to Devonian aquifers appears to represent a front of less saline formation water displacing the original connate brines, both along the deformation front and in the southeast of the study area. Similar patterns of formation water salinities and hydraulic-head distributions could be correlated with regional lithofacies maps, which shows that this



Reproduced with permission of the copyright owner. Further reproduction prohibited without permission.

displacement occurs along preferential flow paths, i.e., the platform margins of the Southesk-Cairn and Swan Hills carbonate complexes.

(6) Present flow in the Devonian aquifers is almost stagnant due to buoyancy effects between less saline formation water being located downdip of heavy connate brine counteracting the regional potential for updip flow and the lack of another active flow-driving mechanism.

### 8.6 Future work

There are still remaining issues on the hydrogeology of the Alberta Basin, including the study area, that should be addressed in future research.

- In general, more hydrogeological data is needed from the Rocky Mountain thrust and fold belt to better understand the flow systems within the deformed part, and the hydraulic communication with the undeformed part of the Alberta Basin.
- Future numerical modeling studies of flow in the basin should account for the effectively low permeability of the hydrocarbon-saturated regions and try to quantify their effect on underpressuring.
- Permeability data and parameters describing the two-phase relations between hydrocarbons and formation water (saturation indices, relative permeability) are needed for further quantitative studies on the interaction between hydrocarbon- and water-saturated zones.
- Also, permeability values should be determined from drillstem test data for the Cambrian to Jurassic strata to quantify the sluggish movement of the deep formation waters.
- Additional work on isotope data from deep formation waters adjacent to the deformation front would improve the identification of brine components that are of possible meteoric, metamorphic, hydrothermal or other origin.



Reproduced with permission of the copyright owner. Further reproduction prohibited without permission.

## References:


Adams, J.J., Rostron, B.J., and Mendoza, C.A. (2000): Regional Fluid Flow and the Athabasca Oil Sands: Numerical Simulations Using a Fully-Coupled Heat, Solute and Groundwater Flow Model. Technical Abstract # 476, publ. on CDROM, GeoCananda 2000 Conference, May 29-June2, Calgary, Alberta.

Allan, J., and Creaney, S. (1991): Oil Families of the Western Canada Sedimentary Basin. Bulletin of Canadian Petroleum Geology, v. 39, p. 107-122.

Andrichuk, J.M. (1960): Facies Analysis of Upper Devonian Wabamun Group in West-Central Alberta, Canada. AAPG Bulletin, v. 44(10), p. 1651-1681.

Anfort, S.J., Bachu, S. and Bentley, L.R. (2001): Regional-scale Hydrogeology of the Upper Devonian – Lower Cretaceous Sedimentary Succession, South-Central Alberta Basin, Canada. AAPG Bulletin, v. 85 (4), p. 637-660.

Appold, M.S., and Garven, G. (1999): The Hydrology of Ore Formation in the Southeast Missouri District: Numerical Models of Topography-Driven Fluid Flow During the Ouachita Orogeny. Economic Geology, v. 94, 913-935.

Bachu, S. (1993): Basement Heat Flow in the Western Canada Sedimentary Basin. Tectonophysics, v. 222, p. 119-133.

Bachu, S. (1995a): Synthesis and Model of Formation Water Flow in the Alberta Basin, Canada. AAPG Bulletin, v. 79 (4), 1159-1178.

Bachu, S. (1995b): Flow of Variable-Density Formation Water in Deep Sloping Aquifers: Review of Methods of Representation with Case Studies. Journal of Hydrology, v. 164, p. 19-38.

Bachu, S., (1997): Flow of Formation Water, Aquifer Characteristics, and Their Relation to Hydrocarbon Accumulations, Northern Alberta Basin. AAPG Bulletin, v. 81, 712-733.

Bachu, S., (1999): Flow Systems in the Alberta Basin: Patterns, Types and Driving Mechanisms. Bulletin of Canadian Petroleum Geology, v. 47, 455-474.

Bachu, S., Hitchon, B., and Mortensen, P. (1986): Preliminary Analysis of Transport Processes in the Basal Cambrian Aquifer of South-Central Alberta. ARC/NWWA,




Reproduced with permission of the copyright owner. Further reproduction prohibited without permission.

Proc. Third Canadian/American Conf. Hydrogeology, Banff, AB, Canada, June 22-26, 1986, 118-126.

Bachu, S., and Burwash, R.A. (1991): Regional-scale Analysis of the Geothermal Regime in the Western Canada Sedimentary Basin. Geothermics, 20(5/6), 387-407.

Bachu, S., and Burwash, R.A. (1994): Geothermal Regime in the Western Canada Sedimentary Basin. *In*: Geologic Atlas of the Western Canada Sedimentary Basin; G.D. Mossop & I. Shetsen (comps.), Canadian Society of Petroleum Geologists and Alberta Research Council, p. 447-454.

Bachu, S., and Underschultz, J.R. (1992): Regional-scale Porosity and Permeability Variations, Peace River Arch Area, Alberta, Canada: AAPG Bulletin, v. 76, p. 547-562.

Bachu, S., and Underschultz, J. (1993): Hydrogeology of Formation Waters, Northeastern Alberta Basin. AAPG Bulletin, v. 77, 1745-1768.

Bachu, S., and Underschultz, J.R. (1995): Large-Scale Underpressuring in the Mississippian-Cretaceous Succession, Southwestern Alberta Basin. AAPG Bulletin, v. 79, p. 989-1004.

Bachu, S., and Hitchon, B. (1996): Regional-scale Flow of Formation Waters in the Williston Basin. AAPG Bulletin, v. 80, 248-264.

Bally, A.W., Gordy, P.L., and Stewart, G.A. (1966): Structure, Seismic Data, and Orogenic Evolution of Southern Canadian Rocky Mountains. Bulletin of Canadian Petroleum Geology, v. 14(2), p. 337-381.

Barnes, R.G. (1977): Hydrogeology of the Brazeau - Canoe River Area, Alberta. Alberta Research council, report 77-5, 32 p., Hydrogeological map (1:250,000).

Barnes, R.G. (1987): Hydrogeology of the Mount Robson - Wapiti Area, Alberta. Alberta Research council, report 76-5, 33 p., Hydrogeological map (1: 500,000).

Bear, J. (1972): Dynamics of Fluids in Porous Media. Dover Publications, New York, 764 p.

Bekele, E.B. (1999): Anomalous Pressures and Fluid Migration within the Alberta Basin, Canada. Ph.D. Thesis (unpubl.), University of Minnesota, 189 p.



Reproduced with permission of the copyright owner. Further reproduction prohibited without permission.

Bekele, E.B., Person, M.A., and Rostron, B.J. (2000): Anomalous Pressure Generation within the Alberta Basin: Implications for Oil Charge to the Viking Formation: Journal of Geochemical Exploration, v. 69-70, p. 601-605.

Belitz, K., and Bredehoeft, J.D. (1988): Hydrodynamics of the Denver Basin: Explanation of Subnormal Fluid Pressures. AAPG Bulletin, v.72, p.1334-1359.

Bethke, C.M. (1985): A Numerical Model of Compaction-Driven Groundwater Flow and Heat Transfer and Its Application to the Paleohydrology of Intracratonic Sedimentary Basins. Journal of Geophysical Research, v. 90(B8), p. 6817-6828.

Bethke, C.M. (1989): Modeling Subsurface Flow in Sedimentary Basins. Geologische Rundschau, v. 78(1), p. 129-154.

Bethke, C.M., Harrison, W.J., Upston, C. and Altaner, S.P. (1988): Supercomputer Analysis of Sedimentary Basins. Science, 239, p. 261-267.

Bethke, C.M., and Marshak, S. (1990): Brine Migration Across North America-The Plate Tectonics of Groundwater. Annual Reviews of Earth and Planetary Sciences, v. 18, p. 287-315.

Bhattachcharya, J.P. (1994): Cretaceous Dunvegan Formation of the Western Canada Sedimentary Basin. *In*: Geologic Atlas of the Western Canada Sedimentary Basin; G.D. Mossop & I. Shetsen (comps.), Canadian Society of Petroleum Geologists and Alberta Research Council, p. 365-373.

Billings, G.K., Hitchon, B., and Shaw, D.R. (1969): Geochemistry and Origin of Formation Waters in the Western Canada Sedimentary Basin. 2. Alkali Metals. Chemical Geology, v. 4, p. 211-223.

Bjørlykke, K. (1993): Fluid Flow in Sedimentary Basins: Sedimentary Geology, v. 86, p. 137-158.

Bredehoeft, J.D. (1965): The Drill-Stem Test: The Petroleum Industry's Deep-Well Pumping Test. Ground Water, v. 3 , p. 31-36.

Bredehoeft, J.D., and Hanshaw, B.B. (1968): On the Maintenance of Anomalous Fluid Pressures: I. Thick Sedimentary Sequences. GSA Bulletin, v. 79, p. 1097-1106.

Buschkuhele, B.E. and Machel, H.G. (2001): Diagenese und Palaeoporenwasserfluss in tiefen devonischen Gasfeldern von Alberta, Canada. Zentralblatt der Geologie Palaeontologie, Teil 1, Heft ½, p. 15-32.



Reproduced with permission of the copyright owner. Further reproduction prohibited without permission.

Bustin, R.M. (1991): Organic Maturation of the Western Canada Sedimentary Basin. International Journal of Coal Geology, v. 19, p. 319-358.

Cant, D. (1989): Lower Zuni Sequence: Middle Jurassic to Middle Cretaceous. *In*: B.D Ricketts (ed.): Western Canada Sedimentary Basin - A Case History. Calgary, Canadian Society of Petroleum Geologists, p. 251-267.

Carpenter, A.B. (1978): Origin and Chemical Evolution of Brines in Sedimentary Basins. Oklahoma Geol. Surv. Circular 79, Tulsa, OK, p. 60-77.

Cathles, L.M. (1977): An Analysis of Cooling of Intrusives by Groundwater convection which includes boiling. Economic Geology, v. 72(5), p. 804-826.

Cecile, M.P., Morrow, D.W., and Williams, G.K. (1997): Early Paleozoic (Cambrian to Early Devonian) Tectonic Framework, Canadian Cordillera. Bulletin of Canadian Petroleum Geology, v. 45(1), p. 54-74.

Charlesworth, H.A.K., Johnston, S.T., and Gagnon, L.G. (1986): Evolution of the Triangle Zone in the Rocky Mountain Foothills near Coalspur, Central Alberta. Canadian Journal of Earth Sciences, v. 24, p. 1668-1678.

Chipley, D. and Kyser, T.K. (1991): Large Scale Fluid Movement in the Western Canadian Sedimentary Basin as Recorded by Fluid Inclusions in Evaporites. *In:* J.E. Christopher and F.M. Haidl (eds.), Sixth International Williston Basin Symposium. Saskatchewan Geological Survey Special Publication. Regina, Saskatchewan Geological Society, Regina, Saskatchewan, p. 265-269.

Choquette, L.A. (1955): The Blue Ridge Member of the Graminia Formation. Journal of the Alberta Society of Petroleum Geolgists, v. 3, p. 70-75.

Clark, I.D., Douglas, M., Raven, K., and Bottomley, D. (2000): Recharge and Preservation of Laurentide Glacial Melt Water in the Canadian Shield. Ground Water, v. 38(5), p. 735-742.

Connolly, C.A. (1989): Thermal History and Diagenesis of the Wilrich Member Shale, Spirit River Formation, Northwest Alberta. Bulletin of Canadian Petroleum Geology, v. 37(32), p. 182-197.

Connolly, C.A., Walter, L.M., Baadsgaard, H., and Longstaffe, F.J. (1990a): Origin and Evolution of Formation Waters, Alberta Basin, Western Canada Sedimentary Basin: I. Chemistry. Applied Geochemistry, v. 5, p. 375-395.



Reproduced with permission of the copyright owner. Further reproduction prohibited without permission.

Connolly, C.A., Walter, L.M., Baadsgaard, H., and Longstaffe, F.J. (1990b): Origin and Evolution of Formation Waters, Alberta Basin, Western Canada Sedimentary Basin: II. Isotope Systematics and Water Mixing. Applied Geochemistry, v. 5, p. 397-413.

Corbet, T.F., and Bethke, C.M. (1992): Disequilibrium Fluid pressures and Groundwater Flow in the Western Canada Sedimentary Basin: Journal of Geophysical Research, v. 97(B5), p. 7203-7217.

Cosgrove, J.W. (1991): Fluid Migration and Concentration during the Deformation of a Sedimentary Sequence. *In:* Cosgrove, J. (ed), Neotectonics and Resources: Belhaven Press, p. 268-281.

Dahlberg, E.C. (1995): Applied Hydrodynamics in Petroleum Exploration. Springer-Verlag, 2nd ed., 294 p.

Dahlstrom, C.D.A. (1970): Structural Geology in the Eastern Margin of the Canadian Rocky Mountains. Bulletin of Canadian Petroleum Geology, v. 18(3), p. 332-406.

Davies, P.B. (1987): Modeling Areal, Variable-Density, Groundwater Flow Using Equivalent freshwater head - Analysis of Potentially Significant Errors. Proceedings of NWWA - IGWMC Conference - Solving groundwater Problems with Models, 10 - 12 Feb. 1987, Denver, CO., National Water Well Association, Dublin, OH., p. 888-903.

Davis, S.N. (1969): Porosity and Permeability of Natural Materials. In: Flow Through Porous Media.

Davisson, M.L. and Criss, R.E. (1996): Na-Ca-Cl Relations in Basinal Fluids. Geochimica and Cosmochimica Acta, v. 60, p. 2743-2752.

Deming, D., Nunn, J.A., and Evans, D.G. (1990): Thermal Effects of Compaction-Driven Groundwater Flow from Overthrust Belts. Journal of Geophysical Research, v. 95(B5), p. 6669-6683.

Deming, D., and Nunn, J.A. (1991): Numerical Simulations of Brine Migration by Topographically Driven Recharge. Journal of Geophysical Research, v. 96(B2), p. 2485-2499.

Deming, D. (1994): Factors Necessary to Define a Pressure Seal. AAPG Bulletin, v. 78, p. 1005-1009.



Reproduced with permission of the copyright owner. Further reproduction prohibited without permission.

Dickey, P.A. and Cox, W.C. (1977): Oil and Gas in Reservoirs with Subnormal Pressures. AAPG Bulletin, v. 61 (12), p. 2134-2142.

Domenico, P.A. and Schwartz, F.W. (1998): Physical and Chemical Hydrogeology. 2nd edition, John Wiley & Sons, 506 p.

Domenico, P.A. and Palciauskas, V.V. (1973): Theoretical Analysis of Forced Convective Heat Transfer in Regional Groundwater Flow. GSA Bulletin, v. 84, p. 3803-3814.

Dorgarten, H-W. and Tsang, C-F. (1991): Modeling the Density-Driven Movement of Liquid Wastes in Deep Sloping Aquifers. Groundwater, v. 29(5), p. 655-662.

Edwards, D.E., Barclay, J.E., Gibson, D.W., Krill, G.E and Halton, E. (1994): Triassic Strata of the WCSB. *In*: Geologic Atlas of the Western Canada Sedimentary Basin; G.D. Mossop and I. Shetsen (comps.), Canadian Society of Petroleum Geologists and Alberta Research Council, p. 256-276.

Einsele, G. (1978): Rise of Primary Pore Water (Connate Water) in Compacting Sediments. In: Proc. of Hydrogeology of Great Sedimentary Basins Conference, May/June 1976, Budapest, IASH - AISH Publ. No. 120, p. 134-145.

Fenton, M.M. (1984): Quaternary Stratigraphy of the Canadian Prairies. *In*: Quaternary Stratigraphy of Canada – A Canadian Contribution to the IGCP Project 24; R.J. Fulton (ed.), Geological Survey of Canada, Paper 84-10, p. 57-68.

Fenton, M.M., Schreiner, B.T., Nielson, E., and Pawlowicz, J.G. (1994): Quaternary Geology of the Western Plains. *In*: Geologic Atlas of the Western Canada Sedimentary Basin; G.D. Mossop & I. Shetsen (comps.), Canadian Society of Petroleum Geologists and Alberta Research Council, p. 413-420.

Freeze, R.A. (1975): A Stochastic-Conceptual Analysis of One-Dimensional Groundwater Flow in Nonuniform Homogeneous Media. Water Resources Research, v. 11 (5), p. 725-741.

Freeze, R.A., and Witherspoon, P.A. (1967): Theoretical Analysis of Regional Groundwater Flow: 2. Effect of Water-Table Configuration and Subsurface Permeability Variation. Water Resources Research, v. 3, p. 623-634.

Freeze, R.A., and Cherry, J.A. (1979): Groundwater. Prentice-Hall Inc., 604 p.



Reproduced with permission of the copyright owner. Further reproduction prohibited without permission.

Fritz, P., and Frape, S.K. (1982): Saline Groundwaters in the Canadian Shield – A First Overview. Chemical Geology, v. 36, 179-190.

Fulton, R.J. (1984): Quaternary Glaciation, Canadian Cordillera. *In*: Quaternary Stratigraphy of Canada – A Canadian Contribution to the IGCP Project 24; R.J. Fulton (ed.), Geological Survey of Canada, Paper 84-10, p. 39-48.

Fulton. R.J., Fenton, M.M., and Rutter, N.W. (1984): Summary of Quaternary Stratigraphy and History, Western Canada. *In*: Quaternary Stratigraphy of Canada – A Canadian Contribution to the IGCP Project 24; R.J. Fulton (ed.), Geological Survey of Canada, Paper 84-10, p. 69-83.

Garven, G. (1985): The Role of Regional Fluid Flow in the Genesis of the Pine Point Deposit, Western Canada Sedimentary Basin. Economic Geology, v. 80, p. 307-324.

Garven, G. (1989): A Hydrogeological Model for the Formation of the Giant Oil Sands Deposits of the Western Canada Sedimentary Basin. American Journal of Science, v. 289, p. 105-166.

Garven, G. (1995): Continental-scale Groundwater Flow and Geologic Processes. Annual Review of Earth and Planetary Sciences, v. 23, p. 89-117.

Ge, S., and Garven, G. (1989): Tectonically Induced Transient Groundwater Flow in Foreland Basins. *In:* A.E. Beck, G. Garven and I. Stegena (eds.): The Origin and Evolution of Sedimentary Basins and Their Energy and Mineral Resources. Amer. Geoph. Union Geodyn. Ser. Monograph, 48, 145-157.

Ge, S., and Garven, G. (1992): Hydromechanical Modeling of Tectonically Driven Groundwater Flow with Application to the Arkoma Foreland Basin. Journal of Geophysical Research, v. 97(B6), p. 9119-9144.

Ge, S. and Garven, G. (1994): A Theoretical Model of Thrust-Induced Deep Groundwater Expulsion with Application to the Canadian Rocky Mountains. J. Geophysical Res., v. 99, p. 13851-13868.

Gibson, D.W. and Barclay, J.E. (1989): Middle Absaroka Sequence: The Triassic Stable Craton. *In:* B.D. Ricketts (ed.): Western Canada Sedimentary Basin, A Case History. Canadian Society of Petroleum Geologists, Calgary, AB, p. 219-231.



Reproduced with permission of the copyright owner. Further reproduction prohibited without permission.

Gies, R.M. (1984): Case History for a Major Alberta Deep Basin Gas Trap: The Cadomin Formation. *In:* Masters, J.A. (ed.): Elmworth – Case Study of a Deep Basin Gas Field. AAPG Memoir 38, p. 115-140.

Graf, K.E. and Thomas, M.D. (1988): CPS Subroutine Library USERS Manual, version 1.5. Radian Corporation, Austin, Texas, 435 p.

Grasby, S.E., and Betcher, R. (2000): Pleistocene Recharge and Flow Reversal in the Williston Basin, Central North America. Journal of Geochemical Exploration, v. 69-70, p. 403-407.

Grobe, M. (1999): Distribution and Thickness of Salt within the Devonian Elk Point Group in the Western Canada Sedimentary Basin. Canadian Society of Petroleum Geologists and Petroleum Society Joint Convention, June 14-18, 1999, Calgary, Abstract 99-38O (publ. on CD).

Gupta, N. and Bair, E.S. (1997): Variable-Density Flow in the Midcontinent Basins and Arches Region of the United States. Water Resources Research, v. 33(8), p. 1785-1802.

Halbertsma, H.L. (1994): Devonian Wabamun Group of the Western Canada Sedimentary Basin. *In:* G.D. Mossop and I. Shetsen (comps.): Geological Atlas of the Western Canada Sedimentary Basin. Canadian Society of Petroleum Geologists and Alberta Research Council, p. 203-220.

Hamblin, A.P., and Abrahamson, B.W. (1996): Stratigraphic Architecture of "Basal Belly River" Cycles, Formost Formation, Belly River Group, Subsurface of Southern Alberta and Southwestern Saskatchewan. Bulletin of Canadian Petroleum Geology, v. 44(4), p. 654-673.

Hamilton, W.N., Price, M.C. and Chao, D.K. (1997): Geological Map of Alberta, South Half. Alberta Energy and Utilities Board, Alberta Geological Survey, Scale: 1:1000000.

Hanor, J. (1988): Origin and Migration of Subsurface Sedimentary Brines. SEPM Short Course No. 21 Special Publication, 247 p.

Hanor, J. (1994): Origin of Saline Fluids in Sedimentary Basins. In: J. Parnell (ed.), Geofluids: Origin and Migration of Fluids in Sedimentary Basins. Geological Society of London Special Publication 78, p. 151-174.



Reproduced with permission of the copyright owner. Further reproduction prohibited without permission.

Hardie, L.A. (1987): Dolomitization: A Critical View of Some Current Views. Journal of Sedimentary Petrology, v. 57(1), p. 166-183.

Hayes, B.J.R., Christopher, J.E., Rosenthal, J., Los, G., McKercher, B., Minken, D., Tremblay, Y.M., and Fennel, J. (1994): Cretaceous Mannville Group of the Western Canada Sedimentary Basin. *In*: Geologic Atlas of the Western Canada Sedimentary Basin; G.D. Mossop & I. Shetsen (comps.), Canadian Society of Petroleum Geologists and Alberta Research Council, p. 317-334.

Hedberg, H.D. (1974): Relation of Methane Generation to Undercompacted Shales, Shale Diapirs, and Mud Vulcanoes. AAPG Bulletin, v. 58, p. 661-673.

Hein, F.J. and Nowlan, G.S. (1998): Regional Sedimentology, Conodont Biostratigraphy and Correlation of Middle Cambrian – Early Ordovician(?) Strata of the "Finnegan" and Deadwood Formations, Alberta Subsurface, Western Canada Sedimentary Basin. Bulletin of Canadian Petroleum Geology, v. 46(2), p. 166-188.

Hitchon, B. (1969a): Fluid Flow in the Western Canadian Sedimentary Basin: 1. Effect of Topography. Water Resources Research, v. 5(1/2), p. 187-195.

Hitchon B. (1969b): Fluid Flow in the Western Canadian Sedimentary Basin 2: Effect of Geology. Water Resources Research, v. 5, p. 460-469.

Hitchon, B. (1984): Geothermal Gradients, Hydrodynamics, and Hydrocarbon Occurrences, Alberta, Canada. AAPG Bulletin, v. 68, p. 713-743.

Hitchon, B. and Friedman, I. (1969): Geochemistry and Origin of Formation Waters in the Western Canada Sedimentary Basin. I. Stable isotopes of Hydrogen and Oxygen. Geochimica et Cosmochimica Acta, v. 33, p. 1321-1349.

Hitchon, B., Billings, G.K,, and Klovan, J.E. (1971): Geochemistry and Origin of Formation Waters in the Western Canada Sedimentary Basin III: Factors Controlling Chemical Composition. Geochimica and Cosmochimica Acta, v. 35, p. 567-598.

Hitchon, B., Bachu, S., Sauveplane, A., Lytviak, A.T., and Underschultz, J.R. (1989): Hydrogeological and Geothermal Regimes in the Phanerozoic Succession, Cold Lake Area, Alberta and Saskatchewan. Alberta Research Council Bulletin, v. 59, 84 p.



Reproduced with permission of the copyright owner. Further reproduction prohibited without permission.

Hitchon, B., S. Bachu, and Underschultz, J.R. (1990): Regional Subsurface Hydrogeology, Peace River Arch Area, Alberta and British Columbia. Bulletin of Canadian Petroleum Geology, v. 38A, 196-217.

Hitchon, B., and Brulotte, M. (1994): Culling Criteria for "Standard" Formation Water Analyses. Applied Geochemistry, v. 9, 637-645.

Holzbecher, E.O. (1998): Modeling Density-Driven Flow in Porous Media. Principles, Numerics, Software. Springer, 286 p.

Hubbert, M.K. (1940): The Theory of Groundwater Motion. Journal of Geology, v. 48 (8), p. 785-943.

Hubbert, M.K. (1956): Darcy's Law and the Field Equations of the Flow of Underground Fluids. Journal of Petroleum Technology, American Institute of Mining, Metallurgical, and Petroleum Engineers, v. 207, p. 222-239.

Hubbert, M.K., and Rubey, W.W. (1959): Role of Fluid Pressures in Mechanics of Overthrust Faulting: I. Mechanics of Fluid-Filled Porous Solids and Its Application to Overthrust Faulting. GSA Bulletin, v. 70, p 115-166.

Hunt, J.M. (1990): Generation and Migration of Petroleum from Abnormally Pressured Fluid Compartments. AAPG Bulletin, v. 74, p. 1-12.

Hunt, J.M. (1996): Petroleum Geochemistry and Geology. 2nd ed., W.H. Freeman and Company, New York, 743 p.

Ingebritsen, S.E., and Sanford, W.E. (1998): Groundwater in Geologic Processes. Cambridge University Press, 341 p.

Jorgensen, D.G., Gogel, T., and Signor, D.C. (1982): Determination of Flow in Aquifers Containing Variable-Density Water. Groundwater Monitoring (Spring edition), p. 40-45.

Kalkreuth, W., and McMechan, M. (1984): Regional Pattern of Thermal Maturation as Determined from Coal-Rank Studies, Rocky Mountain Foothills and Front Ranges North of Grande Cache, Alberta – Implications for Petroleum Exploration. Bulletin of Canadian Petroleum Geology, v. 32(3), p. 249-271.

Kalkreuth, W., and McMechan, M. (1996): Coal Rank and Burial History of Cretaceous-Tertiary Strata in the Grande Cache and Hinton Areas, Alberta, Canada: Implications for Fossil Fuel Exploration: Can. J. Earth Sciences., v. 33, p. 938-957.



Reproduced with permission of the copyright owner. Further reproduction prohibited without permission.

Kirste, D., Desrocher, S., Spence, B., Hoyne, W., Tsang, B. and Hutcheon, I. (1997): Fluid Flow, Water Chemistry, Gas Chemistry and Diagenesis in the Subsurface Triassic in Alberta and British Columbia. Bulletin of Canadian Petroleum Geology, v. 45, p. 742-764.

Krause. F.F., Deutsch, K.B., Joiner, S.D., Barclay, J.E., Hall, R.L., and Hills, L.V. (1994): Cretaceous Cardium Formation of the Western Canada Sedimentary Basin. *In*: Geologic Atlas of the Western Canada Sedimentary Basin; G.D. Mossop & I. Shetsen (comps.), Canadian Society of Petroleum Geologists and Alberta Research Council, p. 375-385.

Kreitler, C.W. (1989): Hydrogeology of Sedimentary Basins. Journal of Hydrology, v. 106, p. 29-53.

Kuiper, L. (1983): A Numerical Procedure for the Solution of Steady State Variable Density Groundwater Flow Equation. Water Resources Research, v. 19(1), p. 234-240.

Land, L.S. (1987): The Major Ion Chemistry of Saline Brines in Sedimentary Basins. Proc. 2nd Intern. Symp. on the Physics and Chemistry of Porous Media, American Institute of Physics, p. 160-179.

Land, L.S. and Milliken, K.L. (1981): Feldspar diagenesis in the Frio Formation, Brazoria County, Texas Gulf Coast. Geology, v. 9, p. 314-318.

Langenberg, C.W. (1992): Geological Map: Cadomin, NTS. Mapsheet 83F/3. Alberta Research Council, Geology Map 217, Map with accompanying cross sections.

Langguth, H.-R. and Voigt, R. (1980): Hydrogeologische Methoden. Springer- Verlag, Berlin, 486 p.

Law, B.E., and Dickinson, W.W. (1985): Conceptual Model of Abnormally Pressured Gas Accumulations in Low-Permeability Reservoirs. AAPG Bulletin, v 69, p. 1295-1304.

Lebel, D., Langenberg, W., and Mountjoy, E.W. (1996): Structure of the Central Canadian Cordilleran Thrust-and-Fault Belt, Athabasca-Brazeau Area, Alberta: A Large, Complex Intercutaneous Wedge. Bulletin of Canadian Petroleum Geology, v. 44(2), p. 282-298.



Reproduced with permission of the copyright owner. Further reproduction prohibited without permission.

Leckie, D.A. (1989): Upper Zuni sequence: Middle Cretaceous to Lower Tertiary. *In:* B.D. Ricketts (ed.): Western Canada Sedimentary Basin - A Case History. Calgary, Canadian Society of Petroleum Geologists, p. 269-284.

Lewchuk, M.T., Al-Aasm, I.S., Symons, D.T.A., and Gillen, K.P. (1998): Dolomitization of Mississippian Carbonates in the Shell Waterton Gas Field, Southwestern Alberta: Insights from Paleomagnetism, Petrology and Geochemistry. Bulletin of Canadian Petroleum Geology, v. 46, p. 387-410.

Lusczynski, N.J. (1961): Head and Flow of Ground Water of Variable Density. Journal of Geophysical Research, v. 66(12), p. 4247-4255.

Machel, H.G. (1998): Comment on "The Effects of Thermochemical Sulfate Reduction upon Formation Water Salinity and Oxygen Isotopes in Carbonate Reservoirs" by R.H. Worden, P.C. Smalley, and N.H. Oxtoby. Geochimica and Cosmochimica Acta, v. 62(2), 337-341.

Machel, H.G., and Mountjoy, E.W. (1987): General Constraints on Extensive Pervasive dolomitization and their Application to the Devonian carbonates of Western Canada. Bulletin of Canadian Petroleum Geology, v. 35, p. 143-158.

Machel, H.G., and Andersson, J.H. (1989): Pervasive Dolomitization of the Nisku formation in Central Alberta. Journal of Sedimentary Petrology, v. 59, p. 891-911.

Machel, H.G., Mountjoy, E.W., and Amthor, J.E. (1994): Dolomitisierung von devonischen Riff- und Plattformkarbonaten in West-Kanada. Zentralblatt fuer Geologie und Palaeontologie, Teil I, 1993 (7/8), p. 941-957.

Machel, H.G., Cavell, P.A., and Patey, K.S. (1996): Isotopic Evidence for Carbonate Cementation and Recrystallization, and for Tectonic Expulsion of fluids into the Western Canada Sedimentary Basin. Geological Society of America Bulletin, v. 108, p. 1108-1119.

Machel, H.G., and Cavell, P.A. (1999): Low-Flux, Tectonically Induced Squeegee Fluid Flow ("Hot Flash") into the Rocky Mountain Foreland Basin. Bulletin of Canadian Petroleum Geology, v. 47, p. 510-533.

Magara, K. (1976a): Water Expulsion from Clastic Sediments during Compaction - Directions and Volumes: AAPG Bulletin, v. 60, p. 543-553.



Reproduced with permission of the copyright owner. Further reproduction prohibited without permission.

Magara, K. (1976b): Thickness of Removed Sedimentary Rocks, Paleopore Pressure, and Paleotemperature, Southwestern Part of Western Canada Basin. AAPG Bulletin, v. 60 (4), p. 554-565.

Marine, I.W. and Fritz, S.J. (1981): Osmotic Model to Explain Anomalous Hydraulic Heads. Water Resources Research, v. 17(1), p. 73-82.

Marsily, G. de (1986): Quantitative Hydrogeology. Academic Press, San Diego, CA, 440 p.

Masters, J.A. (1979): Deep Basin Gas Trap, Western Canada. AAPG Bulletin, v. 63, p. 152-181.

Masters, J.A. (1984): Lower Cretaceous Oil and Gas in Western Canada. *In:* J.A Masters (ed.): Elmworth – Case Study of a Deep Basin Gas Field. AAPG Memoir 38, p.1-33.

Matthews, W.H. (1974): Surface Profiles of the Laurentide Ice Sheet in Its Marginal Areas. Journal of Glaciology, v. 13, p. 37-43.

McCaffrey, M.A., Lazar, B., and Holland, H.D. (1986): The Evaporation Path of Seawater and the Coprecipitation of Br- and K+ with Halite. Journal of Sedimentary Petrology, v. 57, p. 928-937.

McCain Jr., W.D. (1991): Reservoir-Fluid Property Correlations – State of the Art. SPE Reservoir Engineering, v.6, p. 266-272.

Meijer Drees, N.C. (1994): Devonian Elkpoint Group of the WCSB. *In*: Geologic Atlas of the Western Canada Sedimentary Basin; G.D. Mossop & I. Shetsen (comps.), Canadian Society of Petroleum Geologists and Alberta Research Council, p.129-148.

Monger, J.W.H. (1989): Overview of Cordilleran Geology. *In*: Western Canada Sedimentary Basin, A case History; B.D. Ricketts (ed.), Canadian Society of Petroleum Geologists, p. 9-32.

Moore, P.F. (1989): The Lower Kaskaskia Sequence - Devonian. *In*: Western Canada Sedimentary Basin, A case History; B.D. Ricketts (ed.), Canadian Society of Petroleum Geologists, p. 139-164.

Morrow, D.W. (1998): Regional Subsurface Dolomitization; Models and Constraints. Geoscience Canada, v. 25(2), p. 57-70.



Reproduced with permission of the copyright owner. Further reproduction prohibited without permission.

Mossop, G.D., and Shetsen, I. (comps) (1994): Geological Atlas of the Western Canada Sedimentary Basin: Canadian Society of Petroleum Geologists and Alberta Research Council, Calgary, 510 p.

Mountjoy, E.W. (1994): Dolomitization and the Character of Hydrocarbon Reservoirs: Devonian of Western Canada. *In:* A. Parker and B.W. Sellwood (eds.); Quantitative Diagenesis: Recent Developments and Applications to Reservoir Geology, Kluwer Academic Publishers, p. 33-93.

Mountjoy, E.W., Machel, H.G., Green, D., Duggan, J., and Williams-Jones, A.E. (1999): Devonian Matrix Dolomites and Deep Burial Carbonate Cements: A Comparison between the Rimbey-Meadowbrook Reef Trend and the Deep Basin of West-Central Alberta. Bulletin of Canadian Petroleum Geology, v. 47, p. 487-509.

Murray, C., Ehrich, R., Mason, E., and Clark, R. (1994): Evaluation of the Diagenetic and Structural Influences on Hydrocarbon Entrapment in the Cardium Formation, Deep Basin, Western Alberta: Bulletin of Canadian Petroleum Geology, v. 42, p. 529-544.

Neuzil, C.E. (1986): Groundwater Flow in Low-Permeability Environments. Water Resources Research, v. 22, p. 1163-1195.

Neuzil, C.E. (1993): Low Fluid Pressures in the Pierre Shale: A Transient Response to Erosion. Water Resources Research, v. 29(7), p. 2007-2020.

Neuzil, C.E. (1994): How Permeable are Clays and Shales? Water Resources Research, v. 30, p. 145-150.

Neuzil, C.E. (1995): Abnormal Pressures as Hydrodynamic Phenomena. American Journal of Science, v. 295, p. 742-786.

Neuzil, C.E., and Pollock, D.W. (1983): Erosional Unloading and Fluid Pressures in Hydraulically "Tight" Rocks. Journal of Geology, v. 91, p. 179-193.

Nield, D.A. and Bejan, A. (1992): Convection in Porous Media. Springer, 408 p.

Nunn, J.A., and Demming, D. (1991): Thermal Constraints on Basin-Scale Flow Systems. Geophysical Research Letters, v. 18(5), p. 967-970.

Nurkowski, J.R. (1984): Coal Quality, Coal Rank Variation and Its Relation to Reconstructed Overburden, Upper Cretaceous and Tertiary Plains Coals, Alberta, Canada. AAPG Bulletin, v. 86, p. 285-295.



Reproduced with permission of the copyright owner. Further reproduction prohibited without permission.

Oldale, H.S., and Munday, R.J. (1994): Devonian Beaverhill Lake Group of the Western Canada Sedimentary Basin. *In:* G.D. Mossop and I. Shetsen (comps.): Geological Atlas of the Western Canada Sedimentary Basin. Can. Soc. Petr. Geol. and Alberta Research Council, p. 149-163.

Oliver, J. (1986): Fluids Expelled Tectonically from Orogenic Belts: Their Role in Hydrocarbon Migration and other Geologic Phenomena. Geology, v. 14, p. 99-102.

Olsen, H W. (1985): Osmosis: A cause for Apparent Deviations from Darcy's Law. Canadian Geotechnical Journal, V. 22, p. 238-241.

Orr, E.D. and Kreitler, C.W. (1985): Interpretation of Pressure-Depth data from Confined Underpressured Aquifers Exemplified by the Deep-Basin Brine, Palo Duro Basin, Texas. Water Resources Research, v. 21 (4), p. 533-544.

Osborne, M.J., and Swarbrick, E. (1997): Mechanisms for Generating Overpressures in Sedimentary Basins: A Reevaluation. AAPG Bulletin, v. 81(6), p. 1023-1041.

Parks, K.P., and Tóth, J. (1995): Field Evidence for Erosion-Induced Underpressuring in Upper Cretaceous and Tertiary Strata, West Central Alberta, Canada. Bulletin of Canadian Petroleum Geology, v. 43(3), p. 281-292.

Pendergast, R.D. (1969): Correlating Cardium Stratigraphy Using Bottom Hole Pressure. Canadian Well Logging Society Journal, v. 2, p. 19-27.

Person, M., and Garven, G. (1994): A Sensitivity Study of the Driving Force Vector on Fluid Flow During Continental-Rift Basin Evolution. GSA Bulletin, v. 106, 461-475.

Person, M., Raffensberger, J.P., Shemin, G., and Garven, G. (1996): Basin-Scale Hydrogeologic Modeling. Reviews of Geophysics, v. 34, p. 61-87.

Phillips, F.M., Bentley, H.W., Davis, S.N., Elmore, D., and Swanick, G.B. (1986): Chlorine 36 Dating of Very Old Groundwater. 2. Milk River Aquifer, Alberta, Canada. Water Resources Research, v. 22, p. 2003-2016.

Porter, J.W., Price, R.A., and McCrossan, R.G. (1982): The Western Canada Sedimentary Basin. Trans. Royal Society of London, A305, p. 169-192.

Poulton, T.P. (1989): Upper Absaroka to Lower Zuni: The Transition to the Foreland Basin. *In*: Western Canada Sedimentary Basin, A case History; B.D. Ricketts (ed.), Canadian Society of Petroleum Geologists, p. 233-246



Reproduced with permission of the copyright owner. Further reproduction prohibited without permission.

Price, R.A. (1986): The Southeastern Canadian Cordillera: Thrust Faulting, Tectonic Wedging, and Delamination of the Lithosphere. Journal of Structural Geology, v. 8(3/4), p. 239-254.

Price, R.A. (1994): Cordilleran Tectonics and the Evolution of the Western Canada Sedimentary Basin. *In*: Geologic Atlas of the Western Canada Sedimentary Basin; G.D. Mossop & I. Shetsen (comps.), Canadian Society of Petroleum Geologists and Alberta Research Council, p. 13-24.

Putnam, P.E. (1993): A Multidisciplinary Analysis of the Belly River-Brazeau (Campanian) Fluvial Channel Reservoirs in West-Central Alberta, Canada. Bulletin of Canadian Petroleum Geology, v. 41, p. 186-217.

Putnam, P.E. and Ward, G.S. (2001): The Relation between Stratigraphic Elements, Pressure Regime, and Hydrocarbons in the Alberta Deep Basin (with Emphasis on Select Mesozoic Units). AAPG Bulletin, v. 85 (4), p. 691-714.

Raffensberger, J.P. (1997): The Potential for Free and Mixed Convection in Sedimentary Basins and Implications for Sandstone Diagenesis. *In:* GSA Annual Meeting, Abtracts with Programs, Boulder, 1997, CO, v. 29 (6), p. 475.

Raffensberger, J.P. and Garven, G. (1995): The Formation of Unconformity-Type Uranium Ore Deposits 1. Coupled Groundwater Flow and Heat Transport Modeling. American Journal of Science, v. 295, p. 581-636.

Ranganathan, V., and Hanor, J.S. (1987): A Numerical Model for the Formation of Saline Waters due to Diffusion of Dissolved NaCl in Subsiding Sedimentary Basins with Evaporites. Journal of Hydrology, v. 92, p. 97-120.

Reinson, G.E., Warters, W.J., Cox, J., and Price, P.R. (1994): Cretaceous Viking Formation of the Western Canada Sedimentary Basin. *In*: Geologic Atlas of the Western Canada Sedimentary Basin; G.D. Mossop & I. Shetsen (comps.), Canadian Society of Petroleum Geologists and Alberta Research Council, p. 353-363.

Revil, A., Cathles III, L.M., Shosa, J.D., Pezard, P.A., and Larouziere, F.D. de (1998): Capillary Sealing in Sedimentary Basins: A Clear Field Example. Geophysical Research Letters, v. 25, p.389-392.



Reproduced with permission of the copyright owner. Further reproduction prohibited without permission.

Richards, B.C. (1989): Upper Kaskaskia Sequence – Uppermost Permian and Lower Carboniferous. *In:* B.D. Ricketts, (ed.): Western Canada Sedimentary Basin, Case History. Canadian Society of Petroleum Geologists, Calgary, AB, p. 165-201.

Richards, B.C., Barclay, J.E., Bryan, D., Hartling, A., Henderson, C.M., and Hinds, R.C. (1994): Carboniferous Strata of the Western Canada Sedimentary Basin. *In*: Geologic Atlas of the Western Canada Sedimentary Basin; G.D. Mossop & I. Shetsen (comps.), Canadian Society of Petroleum Geologists and Alberta Research Council, p. 221-249.

Ricketts, B.D. (1989): Basin Framework, Introduction. *In*: Western Canada Sedimentary Basin, A case History; B.D. Ricketts (ed.), Canadian Society of Petroleum Geologists, p. 3-8.

Ricketts, B.D. (ed.) (1989): Western Canada Sedimentary Basin – A Case History. Calgary, Canadian Society of Petroleum Geologists, 320 p.

Ross, G., McMechan, M.E., and Hein, F.J. (1989): Proterozoic History: The Birth of the Miogeocline. *In*: Western Canada Sedimentary Basin, A case History; B.D. Ricketts (ed.), Canadian Society of Petroleum Geologists, p. 79-104.

Rostron B.J., Wilkinson, K., and Barson, D. (1995): New Methods for Culling Pressure Data. *In:* Abstracts for the CSPG 1995 Annual Convention, Calgary, Alberta.

Rostron, B.J., Tóth, J., and Machel, H.G. (1997): Fluid Flow, Hydrochemistry and Petroleum Entrapment in Devonian Reef Complexes, South-Central Alberta, Canada. In: I.P Montanez, J.M. Gregg, K.L. Shelton (eds.): Basin-Wide Diagenetic Patterns: Integrated Petrologic, Geochemical, and Hydrologic Considerations. SEPM Special Publication No. 57, p. 139-155.

Rostron, B.J., and Tóth, J. (1997): Cross-Formational Fluid Flow and the Generation of a Saline Plume of Formation Waters in the Mannville Group, West-Central Alberta. *In:* S.G. Pemberton and, D.P. James (eds): Petroleum Geology of the Cretaceous Mannville Group, Western Canada. CSPG Memoir 18, Calgary, AB, p. 169-190.

Rowe, A.M., and Chou, J.C.S. (1970): Pressure-Volume-Temperature-Concentration Relation of Aqueous NaCl Solutions. Journal of Chemical and Engineering Data, v. 15(1), p. 61-66.



Reproduced with permission of the copyright owner. Further reproduction prohibited without permission.

Rutter, N.W. (1984): Pleistocene History of the Western Canadian Ice-Free Corridor. *In*: Quaternary Stratigraphy of Canada – A Canadian Contribution to the IGCP Project 24; R.J. Fulton (ed.), Geological Survey of Canada, Paper 84-10, p. 49-56.

Saller, A.H., and Yaremko, K. (1994): Dolomitization and Porosity Development in the Middle and Upper Wabamun Group, Southeast Peace River Arch, Alberta, Canada. AAPG Bulletin, v. 78, p. 1406-1430.

Schwartz, F.W., Muehlenbachs, K. and Chorley, D.W. (1981): Flow-System Controls of the Chemical Evolution of Groundwater. Journal of Hydrology, v. 54, p. 225-243.

Senger, R.K., and Fogg, G.E. (1987): Regional Underpressuring in Deep Brine Aquifers, Palo Duro Basin, Texas 1. Effects of Hydrostratigraphy and Topography. Water Resources Research, v. 23 p. 1481-1493

Sharp, J.M, and Kyle, J.R. (1988): The Role of Groundwater Processes in the Formation of Ore Deposits. In: W. Back, J.S. Rosenheim, and P.R. Seaber (eds.); Hydrogeology. Geology of North America, v. O-2, Geological Society of America, Boulder, Colorado, p. 461-438.

Skilliter, C.C. (1999): Stratigraphic and Geochemical Investigation of Middle to Upper Devonian “Aquitards” in West-Central Alberta, Canada. Unpublished M.Sc. Thesis, University of Alberta.

Slind, O.L., Andrews, G.D., Murray, D.L., Norford, B.S., Paterson, D.F., Salas, C.Y. and Tawadros, E.E. (1994): Middle Cambrian to Lower Ordovician Strata of the WCSB. *In*: Geologic Atlas of the Western Canada Sedimentary Basin; G.D. Mossop & I. Shetsen (comps.), Canadian Society of Petroleum Geologists and Alberta Research Council, p. 87-108.

Smith, D.G. (1994): Paleogeographic Evolution of the Western Canada Foreland Basin. *In*: Geologic Atlas of the Western Canada Sedimentary Basin; G.D. Mossop & I. Shetsen (comps.), Canadian Society of Petroleum Geologists and Alberta Research Council, p. 277-296.

Smith, G.G. (1989): Coal Formation and Reources in the Foreland Basin. *In*: Western Canada Sedimentary Basin, A case History; B.D. Ricketts (ed.), Canadian Society of Petroleum Geologists, p. 307-320.



Reproduced with permission of the copyright owner. Further reproduction prohibited without permission.

Smith, G.G., Cameron, A.R., and Bustin, R.M. (1994): Coal Resources of the Western Canada Sedimentary Basin. *In*: Geologic Atlas of the Western Canada Sedimentary Basin; G.D. Mossop & I. Shetsen (comps.), Canadian Society of Petroleum Geologists and Alberta Research Council, p. 471-481.

Spencer, C.W. (1987): Hydrocarbon Generation as a Mechanism for Overpressuring in the Rocky Mountain Region. AAPG Bulletin, v. 71(4), p. 368-388.

Spencer, R.J. (1987): Origin of Ca-Cl Brines in Devonian Formations, Western Canada Sedimentary Basin. Applied Geochemistry, v. 2, p. 373-384.

Stoessel, R.K., and Moore, C.H. (1983): Chemical Constraints and Origins of Four Groups of Gulf Coast Reservoir Fluids. AAPG Bulletin, v. 67, p. 896-906.

Switzer, S.B., Holland,W.G., Christie, P.S., Graf, G.C., Hedinger, A.S., McAnley, R.J., Wierzbicki, R.A., and Packard, J.J. (1994): Devonian Woodbend - Winterburn Strata of the Western Canada Sedimentary Basin. *In:* S.G. Pemberton and, D.P. James (eds): Petroleum Geology of the Cretaceous Mannville Group, Western Canada. CSPG Memoir 18, Calgary, AB, 165-202.

Thompson, M.J. (1989): Gas Fields, Formation-Fluid Flow and Hydrochemistry in Early Cretaceous Formations, Peace River Region, N.W. Alberta, Canada. Unpublished M.Sc. Thesis, University of Alberta, Edmonton, 160 p.

Tilley, B.J., Nesbitt, B.E., and Longstaffe, F.J. (1989): Thermal History of Alberta Deep Basin: Comparative Study of Fluid Inclusion and Vitrinite Reflectance Data. AAPG Bulletin, v. 73, p. 1206-1222.

Timmerman, E.H. and van Poollen, H.K. (1972): Practical Use of Drill-Stem Tests. Technology, April-June, p. 31-41.

Tokarsky, O. (1977): Hydrogeology of the Iosegun Lake Area, Alberta. Alberta Research Council, report 76-2, 10p., Hydrogeological map (1:250,000).

Tóth, J. (1963): A Theoretical Analysis of Groundwater Flow in Small Drainage Basins. Journal of Geophysical Research, v. 68(16), p. 4795-4811.

Tóth, J. (1978): Gravity-Induced Cross-Formational Flow of Formation Fluids, Red Earth Region, Alberta, Canada: Analysis, Patterns and Evolution. Water Resources Research, v. 14(5), p. 805-843.



Reproduced with permission of the copyright owner. Further reproduction prohibited without permission.

Tóth, J. (1978): Ground Water and Hydrocarbon Migration. In: W. Back, J.S. Rosenheim, and P.R. Seaber (eds.); Hydrogeology. Geology of North America, v. O-2, Geological Society of America, Boulder, Colorado, p. 485-502.

Tóth, J. (1995): Hydraulic Continuity in Large Sedimentary Basins. Hydrogeology Journal, v. 3(4), p. 4-16.

Tóth, J. (1999): Groundwater as a Geologic Agent: An Overview of the Causes, Processes, and Manifestations. Hydrogeology Journal, v. 7, p. 1-14.

Tóth, J. and Millar, R.F. (1983): Possible Effects of Erosional Change of the Topographic Relief on Pore Pressure at Depth. Water Resources Research, v. 19(6), p. 1585-1597.

Tóth, J and Corbet T.F. (1987): Post Paleocene Evolution of Regional Groundwater Flow Systems and their Relation to Petroleum Accumulations, Taber Area, Southern Alberta, Canada. *In:* J.C Geoff & B.P.J. Williams (eds.): Fluid Flow in Sedimentary Basins and Aquifers. Geological Society Special Publication No. 34, Blackwell Scientific Publications, p. 45-77.

Underschultz, J., and Bartlett, R. (1999): Hydrodynamic Controls on Foothills Gas Pools, Mississippian Strata. Abstract, CSPG Reservoir, v. 26, p. 10-11.

Vogwill, R.I.J. (1983): Hydrogeology of the Edson Area, Alberta. Alberta Research Council, report 79-7, 22p., Hydrogeological map (1:250,000).

Welte, D.H., Schaefer, R.G., Stoessinger, W., and Radke, M. (1984): Gas Generation and Migration in the Deep Basin of Western Canada. *In:* J.A Masters (ed.): Elmworth - Case Study of a Deep Basin Gas Field. AAPG Memoir 38, p.35-47.

Wendte, J., and Stokes, F.A. (1982): Evolution and Corresponding Porosity Distribution of the Judy Creek Reef Complex, Upper Devonian, Central Alberta. *In:* W.G. Cutler (ed.): Canada's Giant Hydrocarbon Reservoirs. Canadian Society of Petroleum Geologists, Core Conf. Manual, p. 63-81.

Wendte, J., Quing, H., Dravis, J.F., Moore, S.L.O., Stasiuk, L.D., and Ward, G. (1998): High-Temperature Saline (Thermoflux) Dolomitization of Devonian Swan Hills Platform and Bank Carbonates. Bulletin of Canadian Petroleum Geology, v. 46, p. 210-265.



Reproduced with permission of the copyright owner. Further reproduction prohibited without permission.

Wilkinson, P.K. (1995): Is Fluid Flow in Paleozoic Formations of West Central Alberta Affected by the Rocky Mountain Thrust Belt? M.Sc. Thesis (unpubl.), University of Alberta, Edmonton, 102p.

Wood, J.R., and Hewett, T.A. (1982): Fluid Convection and Mass Transfer in Porous Sandstones; A Theoretical Model. Geochimica and Cosmochimica Acta, v. 46(10), p. 1707-1713.

Worden, R.H., Smalley, P.C., and Oxtoby, N.H. (1996): The Effects of Thermochemical Sulfate Reduction upon Formation Water Salinity and Oxygen Isotopes in Carbonate Reservoirs. Geochimica and Cosmochimica Acta, v. 60, p. 3925-3931.

Worden, R.H., Smalley, P.C., and Oxtoby, N.H., 1998. Reply to the Comment by H.G. Machel on "The Effects of Thermochemical Sulfate Reduction upon Formation Water Salinity and Oxygen Isotopes in Carbonate Reservoirs". Geochimica and Cosmochimica Acta, v. 62(2), p. 343-346.

Wright, G.N., McMechan, M.E., and Potter, D.E.G. (1994): Structure and Architecture of the Western Canada Sedimentary Basin. *In*: Geologic Atlas of the Western Canada Sedimentary Basin; G.D. Mossop & I. Shetsen (comps.), Canadian Society of Petroleum Geologists and Alberta Research Council, p. 25-40.

Yang, C., Hutcheon, I., and Krouse, H.R. (2001): Fluid Inclusion and Stable Isotope Studies of thermochemical Sulphate Reduction from Burnt Timber and Crossfield East Gas Fields in Alberta, Canada. Bulletin of Canadian Petroleum Geology, v. 49, p. 149-164.



Reproduced with permission of the copyright owner. Further reproduction prohibited without permission.

# APPENDIX A: A BRIEF REVIEW OF FLOW DRIVING MECHANISMS FOR AQUEOUS FLUIDS IN SEDIMENTARY BASINS

## Introduction

The purpose of this chapter is to review the driving mechanisms for formation water flow in sedimentary basins and to assess methods of flow representation, especially for variable-density fluids in sloping aquifers.

In contrast to near-surface groundwater flow, which is almost solely driven by gravity in most cases, regional flow in sedimentary basins is driven by a combination of various mechanisms such as: a) topography (gravity), b) sediment compaction, c) tectonic loading, d) erosional rebound, e) buoyancy, f) overpressures due to hydrocarbon generation, and g) osmosis or mineral phase changes. During the geological history of a sedimentary basin various driving mechanisms may be dominant in various stages of basin evolution. Therefore, this review examines the individual driving mechanisms, as well as fluid and rock properties with respect to their influence on basin-scale fluid flow.

## Flow driving mechanisms

It is generally accepted that one of the most important driving mechanisms for fluid flow at various scales in continental sedimentary basins is gravity, and that flow is controlled by the ground surface topography (e.g., Tóth, 1963; 1995; Senger and Fogg, 1987; Kreitler, 1989; Deming and Nunn, 1991; Bjorlykke, 1993; Garven, 1995). Topography-driven flow may be active almost throughout the entire basin history (Fig. A1, a-e) and is generally the main driving mechanism for shallow groundwater flow. Other flow-driving mechanisms become significant only in low-permeability environments and/or at greater depths with increasing temperature and salinity. They usually become important during certain stages of basin evolution.



Reproduced with permission of the copyright owner. Further reproduction prohibited without permission.

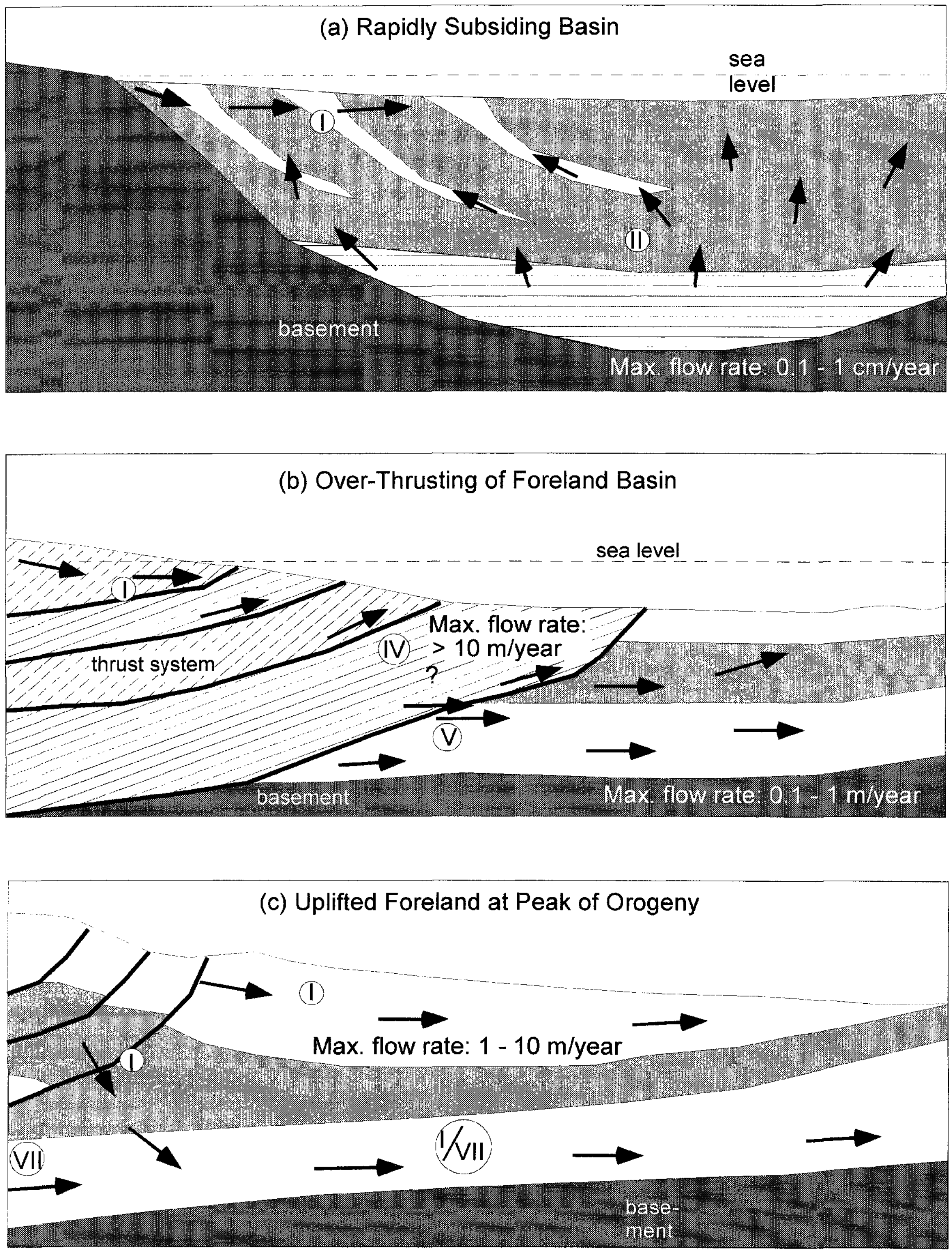


Figure A1: (continued on next page)



Reproduced with permission of the copyright owner. Further reproduction prohibited without permission.

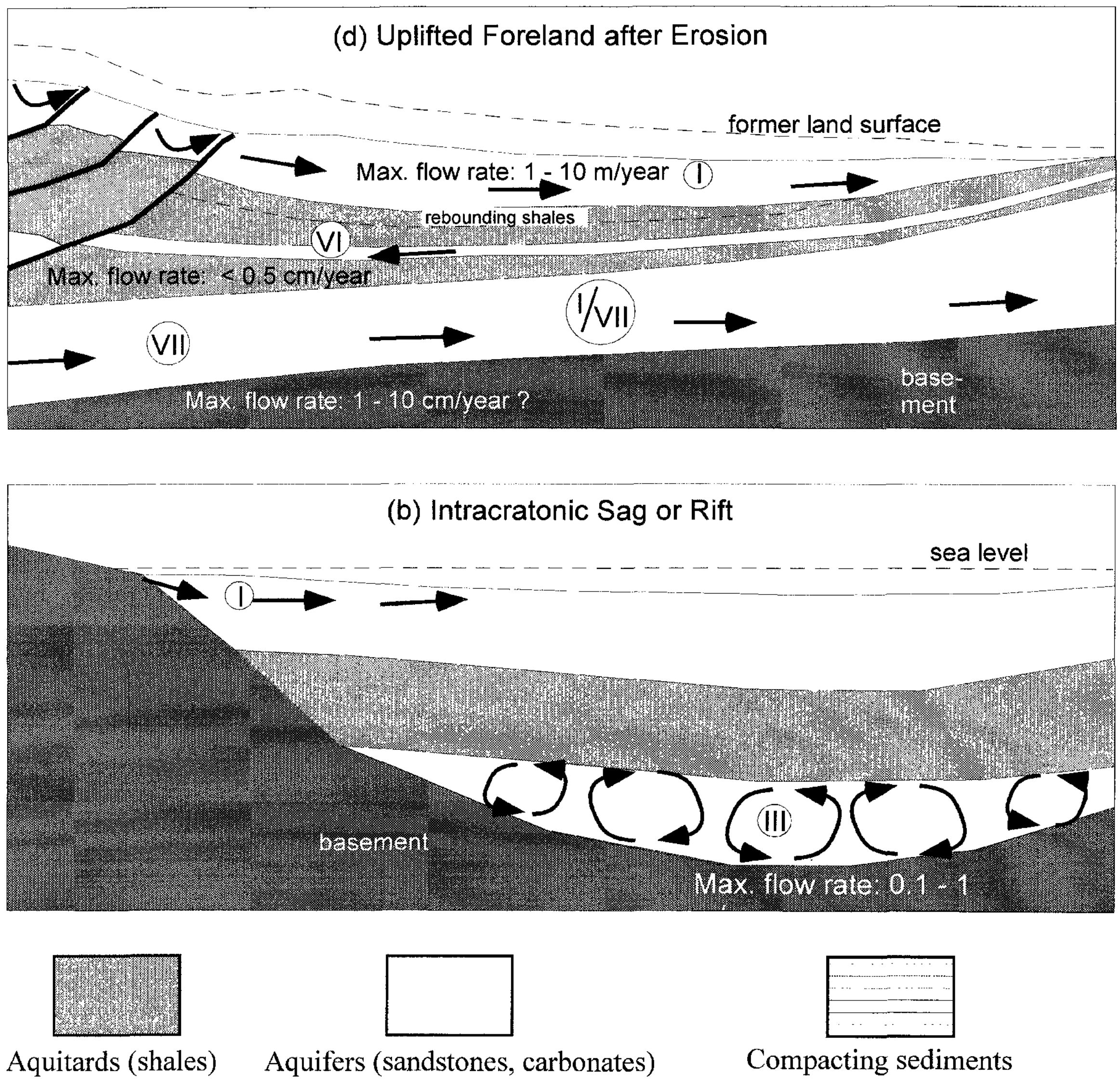


Figure A2: Conceptual representation of regional-scale hydrogeological regimes during the history of a sedimentary basin (modified from Garven, 1995). Arrows represent general flow direction. I Topography-driven flow; II Compaction-driven flow; III Thermally-driven free convection; IV Seismic pumping; V Tectonic expulsion; VI Flow driven by erosional rebound; VII Paleo-flow regime of tectonic origin or paleo-topography.



Reproduced with permission of the copyright owner. Further reproduction prohibited without permission.

*Topography- (gravity) driven flow*

Studies of dominantly topography-driven systems and hydraulic continuity in sedimentary basins are abundant in the literature (e.g., Deming and Nunn, 1991; Garven, 1985; Hitchon, 1969a; Tóth, 1963, 1978, 1995). At least for shallow to intermediate depths, the potentiometric surface of hydraulic heads is generally a smoothed replica of the ground surface. This indicates that there is groundwater recharge in areas of topographic highs and water discharging in areas of topographic lows. With increasing depth the similarity between potentiometric surfaces of various aquifers and topographic relief decreases, which results in local, intermediate, and regional flow systems (Tóth, 1963). Local flow occurs from local topographic highs to adjacent lows, whereas the regional flow patterns are generated by the basin-scale recharge and discharge area(s) (from the highest to the lowest points of elevation in the basin). Hence, when studying only a part of a sedimentary basin, the recharge and/or discharge areas for the deep aquifers might not even lie within the defined study area. In addition, the architecture of the basin and the permeability distribution control the extent of the various flow systems. Thick, regionally extensive aquitards usually impede cross-formational flow, and separate different flow systems above and below. Similarly, high permeability aquifer systems will focus fluid flow in whichever part of the basin, deep or shallow, they are locateded (Freeze and Witherspoon, 1967).

*Compaction-driven flow*

An important driving mechanism in the early stages of basin evolution is compaction due to burial of the sediments and pore fluids (Fig. A1, a). Compaction is a process in which, due to the weight of overburden, porosity decreases, while pressure and temperature increase, and fluids are expelled from the reduced pore space. The increased load on the sediment column is partitioned between the mineral grains (effective stress) and the pore fluid (fluid pressure). "Normal compaction" or "compaction equilibrium" implies concurrent fluid expulsion with loading of the sediments, without apparent increase in pore pressure, in contrast to "disequilibrium compaction", where fluids are expelled some



Reproduced with permission of the copyright owner. Further reproduction prohibited without permission.

time after the deformation process, resulting in above-hydrostatic fluid pressures (Domenico and Schwartz, 1998; p. 25). Whether normal or disequilibrium compaction prevails depends on sedimentation rate and permeability, which govern the drainage rate of the pore fluid, sediment compressibility, and rate of compaction. For normal compaction, the velocity of upward-moving pore water, controlled by the decrease in porosity due to newly added sediment, decreases from top to bottom of the sedimentary sequence and is proportional to the sedimentation rate (Einsele, 1978). In the case of a very high sedimentation rate in fine-grained sediments, the permeability is relatively low. Fluids cannot drain from the reduced pore space fast enough to let fluid pressures equilibrate to the increase in stress, which leads to overpressures in the fluid phase.

During sediment deposition in marine environments, the pore fluid is seawater. Maximum compaction occurs in the basin center, reducing the pore space and driving the pore water upwards and to the basin edges (Magara, 1976a). Meteoric water flows into the basin from topographic highs at its flanks, counteracting the direction of the compaction-driven flow, and forms a freshwater lens above the denser seawater (Fig. A1, a; Bjørlykke, 1993; Person and Garven, 1994). Relative sea level changes may serve as an additional driving mechanism caused by an increase in hydrodynamic head when the sea level is lowered (Bethke et al., 1988). Sedimentation rate, permeability of the sediments, availability of meteoric water, and topographic relief govern the depth of penetrating freshwater and the extent of displacement and replacement of connate waters. Sedimentation stops when the basin subsidence ceases, also causing an end of compaction.

*Tectonic loading*

Aside from the compaction caused by sedimentation, the formation of over-thrust belts (Oliver, 1986) is another mechanism that leads to the deformation of the sediment column, where, in a relatively short time period, sedimentary successions are covered under thick sheets of rocks due to tectonic movements (Fig. A1, b). The maximum flow



Reproduced with permission of the copyright owner. Further reproduction prohibited without permission.

rates under lateral tectonic compression occur when the sediment added to the orogen is entirely accommodated by the compression of pore volume and all pore fluids escape laterally (Bethke and Marshak, 1990). In return, increased fluid pressures reduce the total stress and facilitate the tectonic movement along the fault planes (Hubbert and Rubey, 1959). Some authors (Deming et al., 1990; Bethke and Marshak, 1990; Nunn and Deming, 1991; Ge and Garven, 1992) used numerical modeling techniques and temperature distributions to prove that fluid flow by tectonic expulsion is effective only for a relatively short distance (~ 100 km) from the orogen. Their calculations predict that the induced overpressures quickly dissipate after about $10^3$ to $10^4$ years. As thrust belts commonly form mountain ranges, they also are major topographic highs that develop an asymmetrical topography-driven flow system with regional recharge in the mountains and fluid flow into the undeformed basin (Fig. A1, c), approximately in the same direction as the expelled fluids. A local phenomenon of fluid expulsion may occur with the rapid partial relief of shear stress that accompanies earthquakes, which drives fluids upwards rapidly along faults (Fig. A1, b, IV) in the direction of the easiest pressure release (Cosgrove, 1991).

*Erosional rebound*

Erosional unloading and uplift of the basin at the end and after an orogeny cause a decrease in total stress. Neuzil and Pollock (1983) suggest that this may cause formerly compressed sediments to partly rebound, causing a dilatation of the rock framework, an increase in pore space and, concurrently, a decrease in fluid pressure (Fig. A1, d). According to these authors, the sediment must have a very low permeability and a large compressive storage in order to prevent fluid pressures from equilibrating and to maintain sub-hydrostatic fluid pressures over a certain period of time. The best examples are thick, de-compacting shale units like the Cretaceous Pierre Shales in the Williston Basin (Neuzil and Pollock, 1983; Neuzil, 1993), and the Colorado shales in the Alberta Basin (Corbet and Bethke, 1992; Bachu and Underschultz, 1995; Parks and Tóth, 1995). Furthermore, the sediments should not be fractured or inter-bedded with coarser grained



Reproduced with permission of the copyright owner. Further reproduction prohibited without permission.

layers on a regional scale to an extent that allows pressures to equilibrate via connected high permeability pathways.

It is important to note that the specific storage for compaction is larger than that for erosional rebound, because only a part of the compressive deformation of the rock framework is reversible (mechanical hysteresis). This implies that compaction has a much larger effect on fluid pressures than erosional rebound. Overall, it is relatively hard to quantify the effects of compaction, and especially those of erosional rebound, on fluid flow, because the change of many variables over time is not known. Permeability in particular changes significantly during these processes, and compaction and erosion rates are not constant, neither spatially nor over time.

*Buoyancy-Driven Flow*

Buoyancy-driven flow depends only on density differences within the fluid and is coupled with the hydraulic gradient. Assuming an isotropic porous medium, pressure-related forces drive the fluid in the direction of maximum hydraulic-head gradient, whereas buoyancy drives the fluid in direction of maximum aquifer slope (Bachu, 1995b). Once there is flow due to buoyancy, the pressure field changes. Density differences may be the result of changes in: a) fluid salinity and/or b) pressure and/or c) temperature. As both salinity and temperature vary widely in sedimentary basins, buoyancy definitely has to be considered as a driving mechanism for regional fluid flow. Moving fluids can transport heat and mass by "forced convection", where flow is driven by an external force, or by "free convection", in which case buoyancy is the exclusive driving force (Domenico and Palciauskas, 1973). Cases of free convection in which density variations of the fluid are the dominant driving force have been suggested in areas around salt domes (e.g., Rangathan and Hanor, 1988), or areas associated with magmatic activity (e.g., Cathles, 1977; Sharp and Kyle, 1988). Forced geothermal convection has been invoked to explain diagenetic alterations of sandstones (e.g., Wood and Hewett, 1982) and carbonates (e.g., Hardie, 1987; Morrow, 1998).



Reproduced with permission of the copyright owner. Further reproduction prohibited without permission.

The dimensionless Rayleigh number Ra relates buoyancy to dissipation (viscous and diffusive) forces and is generally defined as (e.g., Holzbecher, 1998, p. 83):

$$Ra = \frac{g\ k\ b\ \Delta\rho}{\mu\ D}$$

where k = permeability ($m^2$), b = aquifer thickness (m), m = viscosity (cp), D = diffusivity ($m^2/s$), thermal or chemical, depending on whether temperature or salinity creates the density difference $\Delta\rho$. There are also cases of double diffusive processes, where both temperature and salinity vary.

For thermal convection only, the previous transforms into (e.g., Bear, 1972, p. 656):

$$Ra = \frac{g\ k\ b\ \rho_0\ \rho\ c_w\ \alpha_f \Delta T}{\mu\ \kappa_e}$$

with $c_w$ = specific heat of the fluid (J/kg/$^O$C), $\alpha_f$ = coefficient of fluid thermal expansion (1/$^O$C), $\kappa_e$ = effective thermal conductivity (W/m/$^O$C).

The onset of free convection in a porous medium is generally accepted to occur for Ra > 10 to 40, depending on the boundary conditions (e.g., Nield and Bejan, 1992). According to Raffensberger (1997), given the right conditions, free thermal convection is favored in a relatively shallow depth range of about 500 - 2000 m, whereas at greater depths high fluid salinity dampens the opposing effect of temperature increase with depth. This is because thin sediment layers of low permeability can already significantly obstruct fluid flow. Thus, it is unlikely for regional-scale free thermal convection cells (Fig. A1, b) to develop, because sedimentary basins generally consist of layered sequences of varying permeability (Bjørlykke, 1993).



Reproduced with permission of the copyright owner. Further reproduction prohibited without permission.

In summary, density differences have to be taken into account when interpreting regional formation water flow, because buoyancy is coupled with the hydraulic gradient and dampens or enhances flow in the direction of maximum aquifer slope. On the other hand, free convection probably is a more local-scale phenomenon and its effect on regional-scale flow is negligible.

*Other flow-driving mechanisms*

This section will review briefly other flow-driving mechanisms that are generally important only on a local scale, but, under certain hydrogeological conditions, may cause "anomalies" in regional flow systems. These conditions are mainly created in low-permeability environments, which are at least partly isolated from a topographic-driven flow system and allow induced pressures to dissipate only slowly. They are most likely to be found in mature sedimentary basins or basins with low topographic relief and extensive shale layers. Possible causes for abnormal fluid pressures are: a) mineral and hydrocarbon phase changes, b) mineral dissolution and precipitation, c) osmosis, and d) water derived from magmatic intrusions or the basement (Osborne and Swarbrick, 1997).

Mineral phase change reactions during increasing burial, such as gypsum to anhydrite and the transformation of clay minerals, result in a fluid volume increase due to the release of water. In the case of dehydration of gypsum to anhydrite, this volume increase is 38% compared to a 5 - 10% increase for the transformation of smectite to illite or the dehydration of montmorillonite (Bjørlykke, 1993). If fluids cannot escape the pore space fast enough, or the porosity is not increased by the expansion of the rock framework, the volume increase will lead to overpressures. According to Osborne and Swarbrick (1997), both processes are probably not responsible for significant overpressures, because the gypsum - anhydrite reaction mainly occurs during shallow burial and therefore cannot produce overpressures at greater depth. The dehydration of smectite is only responsible for a small release of water and is inhibited by a pressure buildup. A more effective source for overpressures seems to be the precipitation of cements due to the release of



Reproduced with permission of the copyright owner. Further reproduction prohibited without permission.

ions during clay transformations, which results in decreases in porosity and permeability (Osborne and Swarbrick, 1997). A much larger volume increase in the fluid phase is generated by the phase changes from kerogen to petroleum, further from kerogen degradation and thermal cracking of liquid to gaseous hydrocarbons, and direct gas generation (Hedberg, 1974; Spencer, 1987). In addition, the effective permeability of the sediment is reduced when a second fluid phase is introduced.

Another process believed to drive fluid flow is chemical osmosis. Osmosis occurs when shales, which act as a semi-permeable membrane, separate two aqueous solutions of different salinity. The passage of anions and cations through the membrane is inhibited because of the positively and negatively charged layers of the shales. To equilibrate the chemical gradient across a membrane, neutral water molecules pass through the shale layer, resulting in a net flow of water to the more saline side of the membrane. Marine and Fritz (1981) explain pressures in excess of hydrostatic of about 100 kPa, or 10 m excess hydraulic head, in a Triassic basin in South Carolina by osmosis, which causes freshwater to pass through 30 - 300 m thick illite - rich shales and dilute the connate Triassic brines. Describing laboratory hydraulic tests on kaolinite, Olsen (1985) proposes that osmosis is responsible for non-Darcyian flow in low-permeability sediments. Like all the other mechanisms involving low-permeability environments, osmosis requires compacted, continuous, and non-fractured shale layers. However, according to Phillips (1983), shales are inefficient semi-permeable membranes. This, coupled with $K_C << K_H$, renders osmosis as a negligible driving mechanism for regional-scale flow (Bachu, 1995b).

**Evolution of flow patterns**

Pressure conditions in deep-basin aquifers do not necessarily reflect the current boundary conditions, including recharge and discharge areas and the present-day surface topography, but instead represent a transient state in which pressures created by paleo-conditions are in the process of equilibrating to the current boundary conditions. In the Alberta Basin for example, adjustment times in the order of $10^3$ - $10^7$ years have been calculated for hydraulic heads in various Cretaceous aquifers embedded in major shale



Reproduced with permission of the copyright owner. Further reproduction prohibited without permission.

aquitards (Tóth and Millar, 1983; Tóth and Corbet, 1987). Critical variables in calculations of such phenomena are the time period a certain topographic relief exists without major changes, the rate of erosion/uplift, and the permeability of the aquifers and aquitards, which change over time. For regional and basin-wide hydrogeological studies this implies that it is very likely to encounter heterochronous flow fields (Tóth, 1995), and that flow in deeper aquifers may be in a different direction than what the present-day topographic relief suggests. As long as the geometry of the sedimentary basin is subject to change due to tectonics and erosion, only fluid pressures and thus fluid flow in the near-surface aquifers would have had the time to equilibrate to the present ground surface topography.

**Summary**

Flow in sedimentary basins is driven by a combination of mechanisms, such as a) topography (gravity), b) sediment compaction, c) tectonic loading, d) erosional rebound, e) buoyancy, f) overpressures due to hydrocarbon generation, g) osmosis and h) mineral phase changes. The internal and boundary conditions for fluid flow change with time and various driving mechanisms may be active during different stages of the basin history. Pressure dissipation and fluid flow as a result of the various flow-driving mechanisms are transient processes, and their rates largely depend on the permeability distribution. Aquitards and lateral low-permeability barriers retard these processes so that the present-day pressures in the subsurface have not necessarily equilibrated to the present-day internal and boundary conditions. Flow systems at shallow depth usually have adjusted to the current ground surface relief and are topography-driven, while flow in deeper, low-permeability environments, which are relatively isolated from the ground surface, may be controlled by other driving mechanisms or reflect a paleo-flow regime. In regional-scale hydrogeological studies, the effect of osmosis is usually negligible and the flow can be represented and analyzed by the driving force acting on the fluid.



Reproduced with permission of the copyright owner. Further reproduction prohibited without permission.

# APPENDIX B: DRILLSTEM TEST DATA

Location in Dominion Land Survey coordinates: MMTTTRRSSLLxxxx
(Meridian, Township, Range, Section, LSD)

Date: date the DST was performed

Well ID: unique well identifier in AGS database

# = DST number

S = shut-in phase of the DST

Q = quality code

z = pressure recorder elevation

dtop = depth to the top of the test interval
dbot = depth to the bottom of the test interval

$H_0$ = freshwater hydraulic head in metres above sea level
$H_{1040}$ = hydraulic head in metres above sea level calculated with reference density of 1040 kg/m$^3$
$H_{1090}$ = hydraulic head in metres above sea level calculated with reference density of 1090 kg/m$^3$

KB = Kelly bushing

Fluid recovery: recovered fluid from the DST in order of volume

Aquifer: aquifer unit in which DST was performed



Reproduced with permission of the copyright owner. Further reproduction prohibited without permission.

Reproduced with permission of the copyright owner. Further reproduction prohibited without permission.



| Location | Date | Well ID | # | S | Q | p [kPa] | z [m] | dtop [m] | dbot [m] | $H_0$ | $H_{1040}$ | $H_{1090}$ | KB [m] | Fluid recovery | Aquifer |
|---|---|---|---|---|---|---|---|---|---|---|---|---|---|---|---|
| 5W0481629060000 | 730802 | 35183 | 1 | 1 | A | 4521 | 446 | 724 | 759 | 906 | | | 1171 | n/a | Pask.-Coalspur |
| 5W0561906110200 | 710323 | -3697 | 1 | 1 | A | 6700 | 531 | 747 | 760 | 1214 | | | 1281 | n/a | Pask.-Coalspur |
| 5W0592202100000 | 761006 | 35692 | 1 | 1 | A | 2063 | 643 | 488 | 518 | 853 | | | 1132 | n/a | Pask.-Coalspur |
| 5W0481636070000 | 730401 | 35187 | 1 | 1 | B | 4844 | 426 | 700 | 725 | 920 | | | 1127 | n/a | Pask.-Coalspur |
| 5W0622618110000 | 770130 | 35573 | 6 | 1 | B | 890 | 749 | 354 | 371 | 840 | | | 1106 | n/a | Pask.-Coalspur |
| 5W0561906110200 | 710323 | -3697 | 2 | 1 | B | 6680 | 559 | 719 | 743 | 1240 | | | 1281 | n/a | Pask.-Coalspur |
| 5W0531530060000 | 731127 | 35070 | 1 | 1 | B | 1643 | 661 | 276 | 285 | 829 | | | 942 | n/a | Pask.-Coalspur |
| 5W0561916160000 | 750721 | 35366 | 7 | 1 | B | 3780 | 579 | 631 | 639 | 964 | | | 1213 | n/a | Pask.-Coalspur |
| 5W0481615100000 | 760204 | 35368 | 2 | 1 | C | 4949 | 431 | 716 | 733 | 936 | | | 1150 | n/a | Pask.-Coalspur |
| 5W0491712110000 | 740621 | 35395 | 1 | 1 | C | 3766 | 459 | 681 | 728 | 843 | | | 1143 | n/a | Pask.-Coalspur |
| 5W0632010100000 | 960809 | -2202 | 4 | 1 | A | 7820 | -31 | 860 | 880 | 767 | 736 | | 831 | water | Brazeau-B.River |
| 5W0662115130000 | 960505 | -2843 | 1 | 1 | A | 3850 | 290 | 440 | 452 | 682 | 667 | | 733 | water+mud | Brazeau-B.River |
| 5W0581911140000 | 950227 | -3017 | 2 | 1 | A | 11100 | -349 | 1590 | 1600 | 783 | 739 | | 1250 | mud | Brazeau-B.River |
| 5W0531814060000 | 720920 | 34879 | 3 | 1 | A | 13500 | -609 | 1580 | 1590 | 769 | 714 | | 975 | water | Brazeau-B.River |
| 5W0531717160000 | 781214 | 35240 | 2 | 1 | A | 10800 | -335 | 1260 | 1270 | 763 | 724 | | 927 | water+cond.+mud | Brazeau-B.River |
| 5W0571725110000 | 810610 | 35415 | 3 | 1 | A | 9870 | -239 | 1340 | 1350 | 767 | 728 | | 1110 | water | Brazeau-B.River |
| 5W0471508140000 | 840717 | 35442 | 3 | 1 | A | 12000 | -794 | 2000 | 2000 | 433 | 382 | | 1190 | oil+mud+cond. | Brazeau-B.River |
| 5W0621917100000 | 700829 | 35601 | 3 | 1 | A | 8060 | -72 | 946 | 961 | 750 | 718 | | 876 | water+oil | Brazeau-B.River |
| 5W0671830110000 | 770923 | 35672 | 2 | 1 | A | 2650 | 411 | 370 | 376 | 681 | 671 | | 783 | water+mud | Brazeau-B.River |
| 5W0682012100000 | 790117 | 35682 | 5 | 1 | A | 2680 | 392 | 351 | 377 | 666 | 655 | | 745 | n/a | Brazeau-B.River |
| 5W0601409060000 | 790407 | 35737 | 4 | 1 | A | 7620 | -17 | 807 | 823 | 760 | 729 | | 792 | water | Brazeau-B.River |
| 5W0642313110000 | 670312 | 36397 | 2 | 1 | A | 3450 | 300 | 555 | 568 | 652 | 638 | | 856 | water | Brazeau-B.River |
| 6W0630320090000 | 840306 | 39279 | 3 | 1 | A | 8050 | -161 | 1130 | 1150 | 660 | 628 | | 968 | water | Brazeau-B.River |
| 5W0471612050000 | 840215 | 68675 | 1 | 1 | A | 11800 | -822 | 2030 | 2040 | 382 | 335 | | 1210 | mud+cond. | Brazeau-B.River |
| 5W0551826060000 | 861024 | 68678 | 1 | 1 | A | 11700 | -420 | 1470 | 1490 | 768 | 727 | | 1050 | n/a | Brazeau-B.River |
| 5W0551736070000 | 880223 | 76709 | 2 | 1 | A | 9900 | -232 | 1130 | 1150 | 776 | 738 | | 904 | water+mud | Brazeau-B.River |
| 6W0650416030020 | 880205 | 80085 | 2 | 1 | A | 8990 | -230 | 1110 | 1120 | 687 | 651 | | 869 | water+cond.+mud | Brazeau-B.River |
| 5W0602124070000 | 891211 | 80705 | 2 | 1 | A | 10200 | -272 | 1240 | 1240 | 770 | 728 | | 966 | water | Brazeau-B.River |
| 5W0471529150000 | 951202 | -3258 | 1 | 1 | B | 9220 | -706 | 1890 | 1910 | 234 | 198 | | 1190 | oil+mud | Brazeau-B.River |
| 5W0471603020000 | 840223 | 34739 | 5 | 1 | B | 12200 | -925 | 2170 | 2180 | 317 | 271 | | 1250 | n/a | Brazeau-B.River |
| 5W0471602030000 | 830919 | 34764 | 4 | 1 | B | 13300 | -948 | 2200 | 2200 | 407 | 356 | | 1250 | n/a | Brazeau-B.River |
| 5W0561408100000 | 760418 | 35202 | 5 | 1 | B | 9370 | -272 | 1190 | 1200 | 683 | 646 | | 921 | water | Brazeau-B.River |
| 5W0461633120000 | 840403 | 35447 | 5 | 1 | B | 9520 | -727 | 1980 | 2000 | 243 | 206 | | 1260 | n/a | Brazeau-B.River |
| 5W0471418130000 | 860115 | 35468 | 3 | 1 | B | 12100 | -822 | 2050 | 2050 | 415 | 364 | | 1230 | water+cond.+mud | Brazeau-B.River |
| 5W0471508050000 | 850115 | 35480 | 1 | 1 | B | 12000 | -795 | 2000 | 2010 | 426 | 381 | | 1200 | mud+cond. | Brazeau-B.River |
| 5W0471514050000 | 860309 | 35488 | 1 | 1 | B | 10700 | -715 | 1980 | 1980 | 372 | 334 | | 1270 | n/a | Brazeau-B.River |
| 5W0471514070000 | 850216 | 35493 | 1 | 1 | B | 12100 | -836 | 2090 | 2100 | 395 | 350 | | 1260 | oil+mud | Brazeau-B.River |

Reproduced with permission of the copyright owner. Further reproduction prohibited without permission.



| Location | Date | Well ID | # | S | Q | p [kPa] | z [m] | dtop [m] | dbot [m] | $H_0$ | $H_{1040}$ | $H_{1090}$ | KB [m] | Fluid recovery | Aquifer |
|---|---|---|---|---|---|---|---|---|---|---|---|---|---|---|---|
| 5W0662132100000 | 770731 | 35567 | 4 | 1 | B | 4350 | 229 | 483 | 493 | 672 | 655 | | 714 | water | Brazeau-B.River |
| 5W0621917100000 | 700829 | 35601 | 2 | 1 | B | 8460 | -99 | 974 | 989 | 763 | 730 | | 876 | water+mud+oil | Brazeau-B.River |
| 5W0622011120000 | 650225 | 35615 | 2 | 1 | B | 8680 | -132 | 967 | 975 | 753 | 719 | | 841 | water+mud | Brazeau-B.River |
| 5W0642034070000 | 790119 | 35738 | 2 | 1 | B | 6540 | 2 | 760 | 779 | 668 | 643 | | 765 | n/a | Brazeau-B.River |
| 5W0642317050000 | 791122 | 35743 | 5 | 1 | B | 7650 | -118 | 934 | 938 | 663 | 632 | | 818 | water | Brazeau-B.River |
| 5W0582023160000 | 671213 | 35781 | 1 | 1 | B | 10500 | -303 | 1220 | 1260 | 766 | 726 | | 913 | water+oil | Brazeau-B.River |
| 5W0612227110000 | 760120 | 35944 | 2 | 1 | B | 9370 | -242 | 1180 | 1190 | 713 | 676 | | 938 | n/a | Brazeau-B.River |
| 5W0611803100000 | 751210 | 36035 | 5 | 1 | B | 9170 | -173 | 1090 | 1100 | 762 | 726 | | 916 | n/a | Brazeau-B.River |
| 5W0632425110000 | 671231 | 36360 | 4 | 1 | B | 8130 | -173 | 1000 | 1010 | 656 | 624 | | 830 | water+mud | Brazeau-B.River |
| 5W0691915090000 | 800301 | 36536 | 6 | 1 | B | 3110 | 343 | 440 | 463 | 660 | 648 | | 785 | water+mud | Brazeau-B.River |
| 5W0592304080020 | 571222 | 36812 | 5 | 1 | B | 12200 | -468 | 1520 | 1540 | 774 | 728 | | 1070 | water+cond.+mud | Brazeau-B.River |
| 5W0622011120020 | 850709 | 36989 | 2 | 1 | B | 8410 | -37 | 880 | 895 | 821 | 787 | | 844 | mud+cond.+water | Brazeau-B.River |
| 6W0640527110000 | 781016 | 38930 | 5 | 1 | B | 9740 | -333 | 1260 | 1270 | 660 | 622 | | 926 | water | Brazeau-B.River |
| 6W0610420110000 | 790315 | 39044 | 5 | 1 | B | 10900 | -560 | 1700 | 1730 | 550 | 508 | | 1140 | n/a | Brazeau-B.River |
| 6W0690905070020 | 770420 | 39157 | 13 | 1 | B | 4850 | 230 | 515 | 524 | 725 | 705 | | 748 | n/a | Brazeau-B.River |
| 6W0630419110000 | 810503 | 39251 | 1 | 1 | B | 10300 | -381 | 1390 | 1390 | 673 | 629 | | 1010 | water+cond.+mud | Brazeau-B.River |
| 6W0630520100000 | 790624 | 39276 | 1 | 1 | B | 10700 | -395 | 1400 | 1430 | 699 | 654 | | 1010 | water+mud | Brazeau-B.River |
| 6W0671128090000 | 860223 | 51239 | 5 | 1 | B | 8300 | -9 | 805 | 828 | 837 | 804 | | 799 | mud+cond. | Brazeau-B.River |
| 5W0562035060000 | 870123 | 68655 | 2 | 1 | B | 11400 | -363 | 1530 | 1540 | 803 | 754 | | 1170 | water+mud | Brazeau-B.River |
| 5W0551835020000 | 870117 | 68656 | 2 | 1 | B | 11700 | -444 | 1510 | 1520 | 749 | 703 | | 1070 | water+mud | Brazeau-B.River |
| 5W0552008080000 | 860101 | 68666 | 1 | 1 | B | 13700 | -592 | 1780 | 1800 | 806 | 751 | | 1190 | water+mud | Brazeau-B.River |
| 5W0552009140000 | 860304 | 68694 | 4 | 1 | B | 13500 | -572 | 1790 | 1800 | 802 | 751 | | 1220 | water+cond. | Brazeau-B.River |
| 5W0552733090000 | 841121 | 68701 | 2 | 1 | B | 12000 | -908 | 2150 | 2180 | 312 | 268 | | 1240 | water+oil+mud | Brazeau-B.River |
| 5W0551736070000 | 880222 | 76709 | 1 | 1 | B | 10800 | -316 | 1220 | 1230 | 779 | 743 | | 904 | water+mud | Brazeau-B.River |
| 5W0602224060020 | 871124 | 80708 | 1 | 1 | B | 10200 | -261 | 1290 | 1310 | 775 | 739 | | 1030 | water+mud | Brazeau-B.River |
| 5W0581934110000 | 900224 | 80754 | 4 | 1 | B | 10700 | -328 | 1230 | 1270 | 759 | 721 | | 906 | water+mud+oil | Brazeau-B.River |
| 5W0562224090000 | 921019 | 83094 | 3 | 1 | B | 12100 | -449 | 1340 | 1360 | 786 | 737 | | 895 | n/a | Brazeau-B.River |
| 5W0592112070000 | 951023 | -1596 | 1 | 1 | C | 11100 | -349 | 1470 | 1500 | 781 | 739 | | 1120 | water | Brazeau-B.River |
| 5W0471529100000 | 950706 | -2338 | 1 | 1 | C | 9420 | -711 | 1900 | 1910 | 249 | 212 | | 1190 | oil+mud | Brazeau-B.River |
| 5W0632626130000 | 960319 | -2907 | 3 | 1 | C | 8730 | -213 | 1110 | 1120 | 677 | 643 | | 903 | water | Brazeau-B.River |
| 5W0471603020000 | 840223 | 34739 | 4 | 1 | C | 13700 | -959 | 2210 | 2220 | 442 | 384 | | 1250 | n/a | Brazeau-B.River |
| 5W0521709140000 | 820326 | 34795 | 4 | 1 | C | 10300 | -486 | 1460 | 1470 | 564 | 524 | | 963 | mud | Brazeau-B.River |
| 5W0531826060000 | 640902 | 34878 | 1 | 1 | C | 10900 | -356 | 1320 | 1320 | 752 | 712 | | 960 | n/a | Brazeau-B.River |
| 5W0562520070000 | 801215 | 34906 | 5 | 1 | C | 12400 | -740 | 2030 | 2050 | 523 | 475 | | 1290 | water+cond. | Brazeau-B.River |
| 5W0571910100000 | 600319 | 34937 | 2 | 1 | C | 11000 | -296 | 1470 | 1480 | 821 | 782 | | 1180 | water+oil | Brazeau-B.River |
| 5W0571507100000 | 800213 | 34983 | 1 | 1 | C | 10400 | -275 | 1520 | 1520 | 787 | 744 | | 1240 | water | Brazeau-B.River |
| 5W0471521040000 | 650823 | 35192 | 1 | 1 | C | 12500 | -880 | 2080 | 2100 | 398 | 345 | | 1220 | oil+mud+cond. | Brazeau-B.River |
| 5W0521836100000 | 760523 | 35304 | 2 | 1 | C | 11900 | -540 | 1440 | 1450 | 674 | 626 | | 903 | n/a | Brazeau-B.River |

| Location | Date | Well ID | # | S | Q | p [kPa] | z [m] | dtop [m] | dbot [m] | $H_0$ | $H_{1040}$ | $H_{1090}$ | KB [m] | Fluid recovery | Aquifer |
|---|---|---|---|---|---|---|---|---|---|---|---|---|---|---|---|
| 5W0561810130000 | 650226 | 35309 | 1 | 1 | C | 11100 | -290 | 1410 | 1430 | 839 | 798 | | 1110 | n/a | Brazeau-B.River |
| 5W0511731070000 | 641130 | 35318 | 1 | 2 | C | 11100 | -583 | 1520 | 1540 | 549 | 505 | | 957 | n/a | Brazeau-B.River |
| 5W0571904100000 | 651031 | 35346 | 1 | 1 | C | 11600 | -366 | 1650 | 1660 | 816 | 771 | | 1220 | n/a | Brazeau-B.River |
| 5W0531715060000 | 830928 | 35424 | 1 | 1 | C | 12100 | -492 | 1400 | 1430 | 745 | 694 | | 912 | water+cond. | Brazeau-B.River |
| 5W0521420160000 | 840108 | 35427 | 3 | 1 | C | 11000 | -373 | 1350 | 1370 | 753 | 705 | | 982 | water+mud | Brazeau-B.River |
| 5W0471601120000 | 840907 | 35448 | 2 | 1 | C | 10700 | -827 | 2050 | 2050 | 265 | 222 | | 1220 | mud | Brazeau-B.River |
| 5W0572301070020 | 850102 | 35462 | 1 | 1 | C | 12200 | -555 | 1630 | 1640 | 684 | 641 | | 1080 | cond.+oil+water+mud | Brazeau-B.River |
| 5W0471513060000 | 850603 | 35469 | 1 | 1 | C | 10500 | -727 | 1980 | 1990 | 346 | 302 | | 1260 | oil+cond. | Brazeau-B.River |
| 5W0502113070000 | 850726 | 35482 | 3 | 1 | C | 10500 | -1010 | 2060 | 2080 | 60 | 19 | | 1060 | water | Brazeau-B.River |
| 5W0572214030000 | 841211 | 35485 | 1 | 1 | C | 12800 | -524 | 1580 | 1590 | 783 | 731 | | 1060 | n/a | Brazeau-B.River |
| 5W0572214030000 | 841214 | 35485 | 2 | 1 | C | 12800 | -552 | 1600 | 1620 | 750 | 703 | | 1060 | water+mud | Brazeau-B.River |
| 5W0471513100000 | 851030 | 35491 | 4 | 2 | C | 10100 | -620 | 1870 | 1880 | 406 | 370 | | 1250 | mud | Brazeau-B.River |
| 5W0621917100000 | 700828 | 35601 | 1 | 1 | C | 9020 | -128 | 1000 | 1020 | 791 | 756 | | 876 | mud | Brazeau-B.River |
| 5W0622011120000 | 650224 | 35615 | 1 | 1 | C | 8380 | -121 | 960 | 966 | 733 | 700 | | 841 | oil | Brazeau-B.River |
| 5W0642024100000 | 630420 | 35626 | 7 | 1 | C | 6670 | 17 | 778 | 780 | 697 | 671 | | 789 | water+mud | Brazeau-B.River |
| 5W0632510060000 | 780920 | 35674 | 9 | 1 | C | 8900 | -245 | 1140 | 1140 | 663 | 627 | | 892 | water | Brazeau-B.River |
| 5W0651921060000 | 780814 | 35723 | 1 | 1 | C | 5130 | 158 | 630 | 638 | 681 | 661 | | 790 | water | Brazeau-B.River |
| 5W0651921060000 | 780815 | 35723 | 2 | 1 | C | 3960 | 279 | 509 | 517 | 683 | 667 | | 790 | water | Brazeau-B.River |
| 5W0622011100000 | 650614 | 35774 | 1 | 1 | C | 8610 | -126 | 989 | 1000 | 752 | 718 | | 870 | water+mud+oil | Brazeau-B.River |
| 5W0621835050000 | 550413 | 35807 | 1 | 1 | C | 5320 | 209 | 654 | 671 | 751 | 730 | | 877 | water | Brazeau-B.River |
| 5W0622014040000 | 651219 | 35844 | 1 | 1 | C | 8480 | -89 | 958 | 974 | 775 | 742 | | 875 | water+cond.+mud | Brazeau-B.River |
| 5W0622024040000 | 600113 | 36575 | 1 | 1 | C | 6710 | 62 | 810 | 830 | 746 | 720 | | 891 | water+mud | Brazeau-B.River |
| 6W0630206120000 | 640120 | 38970 | 4 | 1 | C | 10800 | -440 | 1500 | 1520 | 663 | 619 | | 1080 | n/a | Brazeau-B.River |
| 6W0640520100000 | 570121 | 38980 | 2 | 2 | C | 9320 | -300 | 1210 | 1230 | 650 | 614 | | 928 | n/a | Brazeau-B.River |
| 6W0640604160000 | 561026 | 38982 | 3 | 1 | C | 9910 | -328 | 1170 | 1190 | 682 | 643 | | 860 | n/a | Brazeau-B.River |
| 6W0660301100000 | 770307 | 38995 | 5 | 1 | C | 5340 | 81 | 694 | 708 | 625 | 604 | | 778 | n/a | Brazeau-B.River |
| 6W0691303140000 | 810610 | 39234 | 1 | 1 | C | 6220 | 176 | 711 | 724 | 810 | 786 | | 890 | mud | Brazeau-B.River |
| 5W0632701060000 | 870116 | 50844 | 1 | 1 | C | 9720 | -337 | 1380 | 1400 | 654 | 616 | | 1070 | water+mud | Brazeau-B.River |
| 6W0620415120000 | 860210 | 51228 | 2 | 1 | C | 9340 | -294 | 1320 | 1330 | 658 | 621 | | 1020 | mud+water | Brazeau-B.River |
| 5W0491812110000 | 860402 | 68475 | 2 | 1 | C | 11800 | -911 | 1960 | 1970 | 293 | 246 | | 1050 | mud+water+oil+cond. | Brazeau-B.River |
| 5W0552008080000 | 860101 | 68666 | 2 | 1 | C | 13700 | -600 | 1790 | 1800 | 798 | 743 | | 1190 | water+mud+cond. | Brazeau-B.River |
| 5W0471419020000 | 861231 | 68676 | 1 | 1 | C | 11400 | -716 | 1920 | 1920 | 450 | 401 | | 1190 | oil+mud | Brazeau-B.River |
| 5W0562321020000 | 900119 | 76720 | 2 | 1 | C | 14200 | -673 | 1760 | 1800 | 779 | 719 | | 1090 | water+mud | Brazeau-B.River |
| 5W0521821080000 | 900106 | 76749 | 1 | 1 | C | 12100 | -559 | 1470 | 1490 | 673 | 627 | | 916 | water+mud | Brazeau-B.River |
| 6W0691303110000 | 771207 | 80057 | 1 | 1 | C | 6260 | 191 | 699 | 719 | 828 | 805 | | 891 | water+mud | Brazeau-B.River |
| 5W0552036130000 | 960225 | -2954 | 1 | 1 | A | 22600 | -891 | 2090 | 2120 | 1410 | 1324 | | 1200 | cond. | Cardium |
| 5W0571723100000 | 760318 | 35369 | 7 | 1 | A | 10600 | -586 | 1710 | 1710 | 491 | 453 | | 1120 | water | Cardium |
| 5W0622530100000 | 771015 | 35564 | 6 | 1 | A | 13500 | -608 | 1530 | 1550 | 766 | 715 | | 929 | water+mud | Cardium |



Reproduced with permission of the copyright owner. Further reproduction prohibited without permission.

Reproduced with permission of the copyright owner. Further reproduction prohibited without permission.



| Location | Date | Well ID | # | S | Q | p [kPa] | z [m] | dtop [m] | dbot [m] | $H_0$ | $H_{1040}$ | $H_{1090}$ | KB [m] | Fluid recovery | Aquifer |
|---|---|---|---|---|---|---|---|---|---|---|---|---|---|---|---|
| 5W0642307150000 | 680612 | 35814 | 4 | 1 | A | 8070 | -419 | 1270 | 1280 | 403 | 372 | | 856 | water | Cardium |
| 6W0670432100000 | 650212 | 38894 | 1 | 1 | A | 10100 | -276 | 963 | 978 | 755 | 714 | | 693 | water+mud | Cardium |
| 6W0670508100000 | 670206 | 38913 | 5 | 1 | A | 10700 | -365 | 1140 | 1160 | 729 | 684 | | 778 | water+mud | Cardium |
| 6W0620526160000 | 860305 | 39334 | 1 | 1 | A | 19400 | -818 | 1820 | 1830 | 1162 | 1084 | | 1000 | oil+cond. | Cardium |
| 5W0652701020000 | 860219 | 50857 | 1 | 1 | A | 11800 | -436 | 1380 | 1440 | 763 | 721 | | 947 | water+cond.+mud | Cardium |
| 5W0541706140000 | 820613 | 34808 | 1 | 1 | B | 21200 | -918 | 1900 | 1930 | 1239 | 1160 | | 980 | oil+cond.+mud | Cardium |
| 5W0531729090000 | 810316 | 34859 | 3 | 1 | B | 23300 | -935 | 1890 | 1910 | 1439 | 1349 | | 958 | n/a | Cardium |
| 5W0551809120000 | 780702 | 35018 | 3 | 1 | B | 21100 | -905 | 1900 | 1920 | 1243 | 1163 | | 1010 | oil+cond.+mud | Cardium |
| 5W0531822110000 | 721127 | 35166 | 1 | 1 | B | 23100 | -1020 | 2010 | 2030 | 1337 | 1244 | | 988 | oil | Cardium |
| 5W0471527110000 | 721215 | 35248 | 1 | 1 | B | 26600 | -1290 | 2450 | 2460 | 1424 | 1317 | | 1170 | cond.+oil | Cardium |
| 5W0471418130000 | 860114 | 35468 | 2 | 1 | B | 25800 | -1290 | 2510 | 2520 | 1337 | 1239 | | 1230 | n/a | Cardium |
| 5W0642208070000 | 790219 | 35835 | 8 | 1 | B | 7920 | -395 | 1220 | 1230 | 412 | 381 | | 823 | n/a | Cardium |
| 5W0642130110000 | 770120 | 36353 | 1 | 1 | B | 6630 | -330 | 1140 | 1160 | 346 | 320 | | 816 | mud+cond.+water | Cardium |
| 5W0612516070000 | 750105 | 36359 | 1 | 1 | B | 14600 | -758 | 1900 | 1910 | 732 | 673 | | 1140 | water+mud | Cardium |
| 5W0632429100000 | 670403 | 36361 | 3 | 1 | B | 12100 | -485 | 1370 | 1390 | 743 | 701 | | 888 | water+mud | Cardium |
| 5W0642313110000 | 640314 | 36397 | 5 | 1 | B | 7670 | -376 | 1240 | 1240 | 405 | 376 | | 856 | water | Cardium |
| 5W0632522100000 | 800404 | 36523 | 1 | 1 | B | 12300 | -532 | 1390 | 1400 | 722 | 674 | | 863 | water+cond.+mud | Cardium |
| 5W0642318060000 | 800623 | 36528 | 1 | 1 | B | 8370 | -406 | 1270 | 1290 | 447 | 414 | | 861 | mud+cond.+water | Cardium |
| 5W0632227040000 | 610114 | 36629 | 1 | 1 | B | 8200 | -436 | 1270 | 1270 | 401 | 368 | | 839 | water+cond.+mud | Cardium |
| 5W0612636060000 | 810305 | 36758 | 5 | 1 | B | 14800 | -727 | 1820 | 1840 | 784 | 724 | | 1090 | water+mud | Cardium |
| 5W0591813060000 | 820824 | 36827 | 4 | 1 | B | 9950 | -555 | 1500 | 1500 | 460 | 420 | | 944 | water+mud | Cardium |
| 5W0622503060000 | 811207 | 36829 | 1 | 1 | B | 14100 | -677 | 1760 | 1770 | 765 | 705 | | 1090 | water+cond. | Cardium |
| 6W0670514110000 | 790629 | 39062 | 1 | 1 | B | 10400 | -337 | 1040 | 1060 | 724 | 682 | | 709 | water | Cardium |
| 6W0670733100000 | 800406 | 39085 | 1 | 1 | B | 10800 | -338 | 1110 | 1110 | 765 | 721 | | 757 | water+cond. | Cardium |
| 6W0680316070000 | 810304 | 39184 | 3 | 1 | B | 9050 | -185 | 890 | 935 | 737 | 702 | | 700 | water | Cardium |
| 6W0650222060000 | 830108 | 39212 | 7 | 1 | B | 11800 | -453 | 1240 | 1270 | 750 | 704 | | 789 | water+mud | Cardium |
| 6W0620417060000 | 840609 | 39300 | 1 | 1 | B | 21300 | -836 | 1900 | 1910 | 1331 | 1252 | | 1070 | oil | Cardium |
| 6W0620523080000 | 850906 | 39303 | 1 | 1 | B | 20000 | -837 | 1800 | 1810 | 1199 | 1123 | | 967 | n/a | Cardium |
| 5W0491812110000 | 860321 | 68475 | 1 | 1 | B | 24100 | -1380 | 2430 | 2440 | 1074 | 982 | | 1050 | mud+cond. | Cardium |
| 5W0501804100000 | 870728 | 68713 | 1 | 1 | B | 23400 | -1310 | 2320 | 2330 | 1076 | 984 | | 1010 | mud+cond. | Cardium |
| 5W0672313060000 | 900310 | 80615 | 4 | 1 | B | 5310 | -78 | 791 | 798 | 463 | 443 | | 715 | n/a | Cardium |
| 5W0581702060000 | 960831 | -1223 | 1 | 1 | C | 10700 | -563 | 1750 | 1760 | 529 | 486 | | 1190 | water | Cardium |
| 5W0471530070000 | 810927 | 34755 | 2 | 2 | C | 27900 | -1320 | 2490 | 2490 | 1527 | 1415 | | 1180 | mud+cond. | Cardium |
| 5W0551819010000 | 810822 | 34841 | 1 | 1 | C | 19300 | -888 | 1930 | 1940 | 1075 | 1004 | | 1040 | oil+mud+cond. | Cardium |
| 5W0531814060000 | 720918 | 34879 | 1 | 1 | C | 23100 | -1030 | 2000 | 2030 | 1332 | 1234 | | 975 | oil+cond. | Cardium |
| 5W0541806130000 | 791230 | 34984 | 1 | 1 | C | 21900 | -977 | 1950 | 1960 | 1253 | 1170 | | 975 | cond.+mud+oil | Cardium |
| 5W0541833130000 | 791118 | 34987 | 1 | 1 | C | 20000 | -902 | 1870 | 1890 | 1135 | 1058 | | 974 | mud+oil | Cardium |
| 5W0571606100000 | 761024 | 35001 | 1 | 1 | C | 10700 | -597 | 1660 | 1670 | 494 | 452 | | 1070 | mud | Cardium |

Reproduced with permission of the copyright owner. Further reproduction prohibited without permission.

| Location | Date | Well ID | # | S | Q | p [kPa] | z [m] | dtop [m] | dbot [m] | $H_0$ | $H_{1040}$ | $H_{1090}$ | KB [m] | Fluid recovery | Aquifer |
|---|---|---|---|---|---|---|---|---|---|---|---|---|---|---|---|
| 5W0541812100000 | 690918 | 35003 | 2 | 1 | C | 22000 | -900 | 1870 | 1910 | 1344 | 1256 | | 969 | n/a | Cardium |
| 5W0582102070000 | 760807 | 35010 | 2 | 1 | C | 21400 | -835 | 1770 | 1800 | 1343 | 1263 | | 942 | oil+cond.+mud | Cardium |
| 5W0561929070000 | 760229 | 35047 | 1 | 1 | C | 21500 | -807 | 2130 | 2160 | 1385 | 1300 | | 1320 | oil+cond.+mud | Cardium |
| 5W0561928060000 | 751213 | 35052 | 1 | 1 | C | 19000 | -808 | 2150 | 2190 | 1124 | 1054 | | 1350 | oil+cond. | Cardium |
| 5W0531815100000 | 720115 | 35144 | 1 | 1 | C | 23300 | -1030 | 1980 | 2010 | 1346 | 1254 | | 961 | oil+cond.+mud | Cardium |
| 5W0531619040000 | 630713 | 35160 | 1 | 1 | C | 22500 | -924 | 1820 | 1840 | 1366 | 1281 | | 898 | mud+oil | Cardium |
| 5W0551935150000 | 790108 | 35308 | 1 | 1 | C | 20400 | -871 | 1940 | 1980 | 1207 | 1129 | | 1080 | mud+oil | Cardium |
| 5W0602410110000 | 790102 | 35533 | 2 | 2 | C | 15100 | -782 | 1830 | 1880 | 756 | 698 | | 1050 | water+mud+cond. | Cardium |
| 5W0592434040000 | 630412 | 35534 | 2 | 1 | C | 15400 | -815 | 1950 | 1970 | 752 | 694 | | 1130 | water+mud | Cardium |
| 5W0632208020000 | 640304 | 35622 | 1 | 1 | C | 8730 | -485 | 1340 | 1350 | 404 | 371 | | 859 | mud+water | Cardium |
| 5W0632509120000 | 580831 | 35653 | 1 | 1 | C | 13100 | -579 | 1390 | 1410 | 753 | 705 | | 833 | water+oil | Cardium |
| 5W0581729080000 | 780121 | 35707 | 1 | 1 | C | 10600 | -537 | 1600 | 1620 | 544 | 502 | | 1070 | mud+water | Cardium |
| 5W0642307150000 | 680611 | 35814 | 3 | 1 | C | 8280 | -413 | 1270 | 1280 | 431 | 399 | | 856 | mud+water | Cardium |
| 5W0632120070000 | 781205 | 35815 | 2 | 1 | C | 7820 | -418 | 1230 | 1230 | 380 | 348 | | 808 | mud+water | Cardium |
| 5W0612013100000 | 710308 | 35970 | 7 | 1 | C | 11600 | -483 | 1400 | 1430 | 699 | 654 | | 921 | water+mud | Cardium |
| 5W0622105100000 | 770206 | 36348 | 2 | 1 | C | 8730 | -529 | 1400 | 1420 | 361 | 327 | | 878 | water+mud | Cardium |
| 5W0632425110000 | 671231 | 36360 | 3 | 1 | C | 8870 | -464 | 1290 | 1300 | 440 | 405 | | 830 | mud | Cardium |
| 5W0642609140000 | 570312 | 36362 | 1 | 1 | C | 12500 | -502 | 1360 | 1360 | 773 | 723 | | 852 | water+mud | Cardium |
| 5W0642313110000 | 670313 | 36397 | 3 | 1 | C | 7600 | -381 | 1240 | 1240 | 394 | 364 | | 856 | mud | Cardium |
| 5W0642506060000 | 800818 | 36546 | 1 | 2 | C | 12000 | -487 | 1390 | 1410 | 738 | 689 | | 897 | water+cond.+mud | Cardium |
| 5W0622621100000 | 570112 | 36566 | 10 | 1 | C | 14300 | -652 | 1600 | 1600 | 808 | 750 | | 948 | water | Cardium |
| 5W0591813060000 | 820817 | 36827 | 1 | 1 | C | 9910 | -548 | 1490 | 1500 | 462 | 423 | | 944 | water+mud | Cardium |
| 5W0622735060000 | 811221 | 36834 | 8 | 1 | C | 13800 | -660 | 1710 | 1720 | 742 | 693 | | 1050 | water | Cardium |
| 5W0632403060000 | 820120 | 36836 | 2 | 1 | C | 12600 | -555 | 1430 | 1440 | 732 | 680 | | 876 | water+cond.+mud | Cardium |
| 5W0622227030000 | 840115 | 36906 | 1 | 1 | C | 8260 | -495 | 1380 | 1400 | 347 | 315 | | 883 | mud | Cardium |
| 5W0591904120000 | 840303 | 36920 | 3 | 1 | C | 10000 | -658 | 1520 | 1530 | 366 | 322 | | 859 | mud | Cardium |
| 6W0650523100000 | 781130 | 38860 | 1 | 1 | C | 13000 | -520 | 1340 | 1380 | 802 | 754 | | 820 | water+mud | Cardium |
| 6W0640329100000 | 790301 | 38872 | 5 | 1 | C | 13000 | -570 | 1440 | 1460 | 756 | 704 | | 871 | n/a | Cardium |
| 6W0660629100000 | 740404 | 38895 | 1 | 1 | C | 11500 | -418 | 1240 | 1280 | 750 | 709 | | 826 | mud+oil | Cardium |
| 6W0680709100000 | 780402 | 39008 | 2 | 1 | C | 10100 | -274 | 1000 | 1060 | 754 | 716 | | 731 | water+mud | Cardium |
| 6W0660407110000 | 790710 | 39021 | 2 | 1 | C | 11900 | -467 | 1260 | 1280 | 744 | 699 | | 798 | water | Cardium |
| 6W0660413110000 | 800104 | 39026 | 1 | 1 | C | 11900 | -457 | 1180 | 1210 | 752 | 709 | | 732 | water+mud | Cardium |
| 6W0681307100000 | 800229 | 39055 | 1 | 1 | C | 12000 | -204 | 1170 | 1220 | 1015 | 972 | | 966 | mud+water | Cardium |
| 6W0630631060000 | 820326 | 39205 | 1 | 1 | C | 20900 | -724 | 1730 | 1770 | 1407 | 1325 | | 1010 | oil | Cardium |
| 6W0660719150000 | 840902 | 39296 | 2 | 1 | C | 14500 | -447 | 1270 | 1280 | 1029 | 974 | | 834 | oil+mud | Cardium |
| 6W0650622110000 | 850407 | 39329 | 3 | 1 | C | 13500 | -560 | 1440 | 1450 | 820 | 763 | | 880 | mud | Cardium |
| 6W0690801160000 | 860824 | 51243 | 3 | 1 | C | 9460 | -207 | 934 | 959 | 757 | 720 | | 729 | n/a | Cardium |
| 5W0582123130000 | 890402 | 63298 | 3 | 1 | C | 20600 | -756 | 1720 | 1740 | 1345 | 1263 | | 964 | n/a | Cardium |

Reproduced with permission of the copyright owner. Further reproduction prohibited without permission.



| Location | Date | Well ID | # | S | Q | p [kPa] | z [m] | dtop [m] | dbot [m] | $H_0$ | $H_{1040}$ | $H_{1090}$ | KB [m] | Fluid recovery | Aquifer |
|---|---|---|---|---|---|---|---|---|---|---|---|---|---|---|---|
| 6W0650434100000 | 891105 | 80086 | 2 | 2 | C | 12300 | -482 | 1270 | 1340 | 771 | 724 | | 796 | water+mud+cond. | Cardium |
| 6W0690321160000 | 950127 | -3418 | 2 | 1 | A | 9710 | -440 | 1090 | 1100 | 550 | 512 | | 650 | water | Dunvegan |
| 5W0642317120000 | 830817 | 36850 | 2 | 1 | A | 7470 | -682 | 1510 | 1520 | 79 | 50 | | 820 | mud+oil | Dunvegan |
| 5W0672436110000 | 750325 | 35551 | 6 | 1 | B | 8870 | -350 | 1120 | 1140 | 554 | 519 | | 770 | water+mud | Dunvegan |
| 5W0672309110000 | 710721 | 35555 | 7 | 1 | B | 9330 | -403 | 1170 | 1180 | 548 | 511 | | 770 | water | Dunvegan |
| 5W0672421100000 | 710106 | 35598 | 1 | 1 | B | 9370 | -403 | 1140 | 1180 | 552 | 515 | | 750 | mud+water | Dunvegan |
| 5W0662304110000 | 710415 | 35956 | 7 | 1 | B | 10500 | -517 | 1270 | 1280 | 557 | 512 | | 760 | water+mud+cond. | Dunvegan |
| 5W0682325110000 | 711223 | 36243 | 1 | 1 | B | 7920 | -258 | 975 | 1010 | 550 | 518 | | 720 | water+mud | Dunvegan |
| 5W0662527020000 | 670715 | 36258 | 1 | 1 | B | 10600 | -534 | 1250 | 1270 | 542 | 505 | | 740 | water | Dunvegan |
| 5W0662120100000 | 760621 | 36281 | 1 | 1 | B | 7350 | -416 | 1100 | 1120 | 333 | 304 | | 700 | water+mud | Dunvegan |
| 5W0652123160000 | 850823 | 36998 | 4 | 1 | B | 6040 | -477 | 1250 | 1260 | 138 | 115 | | 780 | water+mud+cond. | Dunvegan |
| 6W0680109110000 | 721204 | 38966 | 1 | 1 | B | 10100 | -480 | 1190 | 1200 | 552 | 510 | | 710 | water+mud | Dunvegan |
| 6W0680123110000 | 671229 | 38990 | 1 | 1 | B | 10100 | -468 | 1120 | 1150 | 560 | 522 | | 680 | water+mud | Dunvegan |
| 6W0660501110000 | 780307 | 39009 | 2 | 1 | B | 12100 | -917 | 1710 | 1720 | 316 | 269 | | 790 | n/a | Dunvegan |
| 6W0660205070000 | 830323 | 39247 | 3 | 1 | B | 10700 | -773 | 1610 | 1640 | 318 | 276 | | 840 | mud+cond. | Dunvegan |
| 6W0630312100000 | 880308 | 80105 | 2 | 1 | B | 20800 | -1100 | 2150 | 2160 | 1018 | 939 | | 1100 | oil+mud+cond. | Dunvegan |
| 5W0692218130020 | 871112 | 80602 | 3 | 1 | B | 7210 | -190 | 909 | 919 | 545 | 517 | | 720 | mud | Dunvegan |
| 5W0652113140000 | 920731 | 83084 | 3 | 1 | B | 6110 | -483 | 1280 | 1290 | 139 | 116 | | 790 | water+mud | Dunvegan |
| 5W0652122080000 | 920624 | 83085 | 1 | 1 | B | 6240 | -495 | 1300 | 1320 | 141 | 117 | | 800 | water+mud | Dunvegan |
| 6W0690327010000 | 960219 | -539 | 2 | 1 | C | 9580 | -467 | 1120 | 1130 | 510 | 472 | | 660 | water | Dunvegan |
| 5W0662307070000 | 960922 | -1563 | 2 | 1 | C | 10400 | -512 | 1310 | 1350 | 552 | 507 | | 800 | mud | Dunvegan |
| 5W0692212110000 | 811104 | 35506 | 2 | 1 | C | 7320 | -196 | 847 | 861 | 550 | 521 | | 650 | water+mud | Dunvegan |
| 5W0622431040000 | 810819 | 35523 | 1 | 1 | C | 10700 | -873 | 1770 | 1780 | 221 | 176 | | 900 | mud+water+oil+cond. | Dunvegan |
| 5W0642603020000 | 710225 | 35542 | 1 | 1 | C | 12800 | -832 | 1770 | 1800 | 470 | 423 | | 940 | water+mud | Dunvegan |
| 5W0672436110000 | 750324 | 35551 | 3 | 1 | C | 8830 | -347 | 1120 | 1130 | 553 | 518 | | 770 | mud | Dunvegan |
| 5W0672309110000 | 710720 | 35555 | 6 | 1 | C | 9140 | -386 | 1150 | 1190 | 545 | 510 | | 770 | n/a | Dunvegan |
| 5W0662132100000 | 770721 | 35567 | 1 | 1 | C | 7340 | -386 | 1090 | 1100 | 362 | 333 | | 710 | water | Dunvegan |
| 5W0622203100000 | 761010 | 35575 | 1 | 2 | C | 10500 | -850 | 1730 | 1760 | 221 | 179 | | 880 | oil+mud | Dunvegan |
| 5W0662115040000 | 641207 | 35617 | 2 | 1 | C | 7620 | -424 | 1160 | 1170 | 353 | 323 | | 740 | mud | Dunvegan |
| 5W0581609100000 | 770416 | 35693 | 7 | 1 | C | 11800 | -730 | 1740 | 1790 | 468 | 427 | | 1000 | mud+water | Dunvegan |
| 5W0672108110000 | 790804 | 35792 | 5 | 1 | C | 7200 | -369 | 1070 | 1070 | 366 | 337 | | 700 | mud+water | Dunvegan |
| 5W0652405100000 | 621106 | 35853 | 2 | 1 | C | 11400 | -653 | 1540 | 1560 | 505 | 464 | | 900 | water+mud | Dunvegan |
| 5W0692619100000 | 730911 | 35957 | 2 | 1 | C | 7950 | -310 | 988 | 1020 | 500 | 469 | | 680 | water+mud+cond. | Dunvegan |
| 5W0662502110000 | 660223 | 36175 | 1 | 1 | C | 10800 | -559 | 1360 | 1410 | 538 | 500 | | 790 | water+mud+cond. | Dunvegan |
| 5W0692302100000 | 770707 | 36199 | 6 | 1 | C | 7810 | -240 | 994 | 1000 | 557 | 526 | | 760 | water+mud | Dunvegan |
| 5W0642521110000 | 731115 | 36332 | 1 | 1 | C | 12100 | -728 | 1560 | 1590 | 501 | 458 | | 840 | water | Dunvegan |
| 5W0662332070000 | 801202 | 36724 | 2 | 1 | C | 9830 | -440 | 1210 | 1210 | 562 | 523 | | 770 | water+mud | Dunvegan |
| 5W0642308090000 | 830127 | 36895 | 1 | 1 | C | 10100 | -689 | 1490 | 1540 | 339 | 301 | | 810 | cond.+mud+oil | Dunvegan |

Reproduced with permission of the copyright owner. Further reproduction prohibited without permission.



| Location | Date | Well ID | # | S | Q | p [kPa] | z [m] | dtop [m] | dbot [m] | $H_0$ | $H_{1040}$ | $H_{1090}$ | KB [m] | Fluid recovery | Aquifer |
|---|---|---|---|---|---|---|---|---|---|---|---|---|---|---|---|
| 6W0680206110000 | 560127 | 38880 | 3 | 1 | C | 10600 | -537 | 1240 | 1250 | 546 | 502 | | 710 | n/a | Dunvegan |
| 6W0680215110000 | 760820 | 38901 | 1 | 1 | C | 10200 | -484 | 1170 | 1200 | 553 | 516 | | 690 | n/a | Dunvegan |
| 6W0660536100000 | 781003 | 38954 | 10 | 1 | C | 11000 | -804 | 1590 | 1610 | 315 | 274 | | 750 | n/a | Dunvegan |
| 6W0680226060000 | 770209 | 38989 | 6 | 1 | C | 10200 | -501 | 1170 | 1180 | 540 | 499 | | 670 | n/a | Dunvegan |
| 6W0680108060000 | 761215 | 38993 | 4 | 1 | C | 10100 | -505 | 1220 | 1250 | 523 | 485 | | 730 | water+mud | Dunvegan |
| 6W0680616060000 | 870211 | 51240 | 2 | 2 | C | 10200 | -767 | 1450 | 1460 | 277 | 233 | | 690 | mud+cond. | Dunvegan |
| 6W0680602100000 | 870312 | 63452 | 2 | 1 | C | 11700 | -738 | 1440 | 1490 | 459 | 409 | | 700 | mud | Dunvegan |
| 6W0660401060000 | 880217 | 80062 | 3 | 1 | C | 14300 | -920 | 1750 | 1750 | 535 | 482 | | 830 | mud | Dunvegan |
| 6W0680127070000 | 780204 | 80075 | 1 | 1 | C | 9520 | -500 | 1200 | 1230 | 470 | 433 | | 710 | mud+water | Dunvegan |
| 6W0680127070000 | 780205 | 80075 | 2 | 1 | C | 9740 | -457 | 1150 | 1170 | 535 | 498 | | 710 | mud+cond.+water | Dunvegan |
| 5W0672129070000 | 900322 | 80614 | 1 | 1 | C | 7500 | -318 | 1020 | 1030 | 447 | 417 | | 700 | water+mud | Dunvegan |
| 5W0672313060000 | 900310 | 80615 | 3 | 1 | C | 9170 | -375 | 1090 | 1100 | 560 | 524 | | 720 | n/a | Dunvegan |
| 5W0571513080000 | 961004 | -1839 | 3 | 1 | A | 11900 | -869 | 1930 | 1940 | 347 | 297 | | 1060 | water | Viking |
| 5W0662116140000 | 960331 | -3041 | 3 | 1 | A | 11800 | -614 | 1340 | 1350 | 594 | 543 | | 729 | water | Viking |
| 5W0581533150000 | 960115 | -3279 | 1 | 1 | A | 11700 | -806 | 1780 | 1800 | 382 | 341 | | 979 | water | Viking |
| 5W0631435060000 | 81227 | 35606 | 1 | 1 | A | 8510 | -482 | 1510 | 1520 | 386 | 352 | | 1020 | water+mud | Viking |
| 5W0631419070000 | 740912 | 35788 | 1 | 1 | A | 9040 | -521 | 1480 | 1490 | 400 | 365 | | 953 | water+mud | Viking |
| 5W0651829110000 | 790225 | 35830 | 4 | 1 | A | 10600 | -546 | 1400 | 1430 | 537 | 493 | | 859 | water | Viking |
| 5W0591523100000 | 760324 | 35881 | 1 | 1 | A | 10800 | -740 | 1660 | 1670 | 359 | 319 | | 922 | water+mud | Viking |
| 5W0691829010000 | 741230 | 35911 | 3 | 1 | A | 6680 | -264 | 1200 | 1210 | 417 | 391 | | 939 | water+mud | Viking |
| 5W0662025100000 | 730226 | 35913 | 2 | 1 | A | 10200 | -525 | 1320 | 1330 | 514 | 475 | | 798 | water+mud | Viking |
| 5W0692619100000 | 730912 | 35957 | 3 | 1 | A | 9170 | -544 | 1220 | 1250 | 391 | 355 | | 679 | water+mud | Viking |
| 5W0611617060000 | 790811 | 36400 | 1 | 1 | A | 10900 | -719 | 1600 | 1620 | 389 | 349 | | 886 | mud+water | Viking |
| 5W0632028020000 | 601117 | 36569 | 3 | 1 | A | 9840 | -797 | 1570 | 1580 | 206 | 167 | | 787 | water | Viking |
| 5W0621521100000 | 760824 | 36807 | 4 | 1 | A | 9660 | -604 | 1620 | 1640 | 381 | 343 | | 1020 | water+mud | Viking |
| 5W0622503060000 | 811224 | 36829 | 5 | 1 | A | 15100 | -1170 | 2260 | 2270 | 374 | 310 | | 1090 | n/a | Viking |
| 5W0591406060000 | 820208 | 36880 | 2 | 1 | A | 11100 | -768 | 1780 | 1810 | 367 | 320 | | 1010 | water+mud | Viking |
| 5W0671533060020 | 830305 | 36899 | 1 | 1 | A | 7930 | -397 | 1210 | 1220 | 411 | 380 | | 916 | water+mud | Viking |
| 5W0641713160020 | 850121 | 36958 | 1 | 1 | A | 9090 | -554 | 1490 | 1500 | 373 | 337 | | 942 | water+mud | Viking |
| 5W0641501120000 | 850312 | 36967 | 1 | 1 | A | 8700 | -506 | 1490 | 1500 | 381 | 347 | | 989 | water | Viking |
| 6W0690705110000 | 780528 | 39032 | 6 | 1 | A | 14300 | -1020 | 1740 | 1760 | 433 | 382 | | 735 | n/a | Viking |
| 6W0660913070000 | 820118 | 39258 | 1 | 1 | A | 17900 | -1410 | 2300 | 2310 | 416 | 344 | | 889 | n/a | Viking |
| 5W0662120020000 | 851114 | 63282 | 1 | 1 | A | 11200 | -622 | 1330 | 1330 | 518 | 476 | | 709 | oil+cond. | Viking |
| 5W0652015040000 | 871207 | 80649 | 1 | 1 | A | 11500 | -651 | 1400 | 1400 | 517 | 476 | | 748 | water+mud | Viking |
| 5W0641722110000 | 920130 | 80668 | 3 | 1 | A | 9240 | -554 | 1370 | 1380 | 388 | 352 | | 819 | water+mud | Viking |
| 6W0671115080000 | 950124 | -1851 | 3 | 1 | B | 18200 | -1450 | 2350 | 2360 | 404 | 334 | | 903 | mud | Viking |
| 5W0591503130000 | 950728 | -2777 | 3 | 1 | B | 11500 | -804 | 1810 | 1810 | 369 | 323 | | 1010 | water | Viking |
| 5W0611516130000 | 961027 | -2853 | 2 | 1 | B | 9880 | -660 | 1550 | 1570 | 347 | 308 | | 894 | oil | Viking |

Reproduced with permission of the copyright owner. Further reproduction prohibited without permission.



| Location | Date | Well ID | # | S | Q | p [kPa] | z [m] | dtop [m] | dbot [m] | $H_0$ | $H_{1040}$ | $H_{1090}$ | KB [m] | Fluid recovery | Aquifer |
|---|---|---|---|---|---|---|---|---|---|---|---|---|---|---|---|
| 5W0611516130000 | 961027 | -2853 | 2 | 2 | B | 9860 | -660 | 1550 | 1570 | 345 | 306 | | 894 | oil | Viking |
| 5W0611624140000 | 960815 | -3084 | 2 | 1 | B | 10400 | -690 | 1580 | 1590 | 374 | 329 | | 891 | water | Viking |
| 5W0581511060000 | 761231 | 35055 | 5 | 1 | B | 11800 | -835 | 1970 | 1990 | 371 | 322 | | 1130 | water+mud | Viking |
| 5W0581405100000 | 760131 | 35227 | 1 | 1 | B | 11800 | -811 | 1850 | 1850 | 396 | 346 | | 1040 | water | Viking |
| 5W0652010100000 | 811118 | 35505 | 2 | 1 | B | 11300 | -631 | 1380 | 1390 | 519 | 477 | | 749 | n/a | Viking |
| 5W0642417100000 | 770811 | 35565 | 2 | 1 | B | 12800 | -912 | 1790 | 1810 | 396 | 343 | | 882 | water | Viking |
| 5W0662011140000 | 660304 | 35610 | 1 | 1 | B | 10800 | -572 | 1330 | 1350 | 527 | 487 | | 759 | water+mud+oil | Viking |
| 5W0661810040000 | 631008 | 35624 | 2 | 1 | B | 10400 | -513 | 1310 | 1330 | 544 | 506 | | 814 | water | Viking |
| 5W0631628120000 | 660116 | 35714 | 1 | 1 | B | 9710 | -596 | 1540 | 1570 | 394 | 356 | | 975 | water+mud | Viking |
| 5W0621625110000 | 781020 | 35852 | 4 | 1 | B | 9840 | -620 | 1640 | 1660 | 383 | 344 | | 1030 | water+mud | Viking |
| 5W0662103120000 | 641230 | 35854 | 1 | 1 | B | 11200 | -626 | 1430 | 1460 | 513 | 472 | | 807 | oil | Viking |
| 5W0632019100000 | 790316 | 35869 | 2 | 1 | B | 11300 | -802 | 1570 | 1590 | 350 | 306 | | 767 | water+mud | Viking |
| 5W0611830070000 | 660331 | 36033 | 3 | 1 | B | 10100 | -827 | 1780 | 1790 | 206 | 163 | | 960 | water | Viking |
| 5W0631410100000 | 751024 | 36127 | 4 | 1 | B | 8960 | -515 | 1460 | 1470 | 398 | 363 | | 938 | water+cond.+mud | Viking |
| 5W0652231100000 | 700103 | 36148 | 3 | 1 | B | 11300 | -697 | 1420 | 1450 | 451 | 411 | | 732 | water+cond.+mud | Viking |
| 5W0652312070000 | 680818 | 36169 | 1 | 1 | B | 11700 | -768 | 1540 | 1550 | 427 | 379 | | 767 | water+mud | Viking |
| 5W0652422040000 | 640111 | 36184 | 2 | 1 | B | 11800 | -783 | 1660 | 1670 | 423 | 374 | | 880 | water+cond. | Viking |
| 5W0662335100000 | 680628 | 36206 | 1 | 1 | B | 10500 | -635 | 1440 | 1450 | 440 | 394 | | 812 | water+mud | Viking |
| 5W0662335100000 | 680629 | 36206 | 2 | 1 | B | 11000 | -621 | 1430 | 1440 | 501 | 457 | | 812 | water+mud | Viking |
| 5W0662527020000 | 670717 | 36258 | 2 | 1 | B | 12200 | -739 | 1440 | 1480 | 509 | 457 | | 736 | water+mud | Viking |
| 5W0662110040000 | 641112 | 36272 | 1 | 1 | B | 11600 | -618 | 1400 | 1430 | 560 | 519 | | 787 | oil | Viking |
| 5W0662109020000 | 650201 | 36275 | 2 | 1 | B | 11200 | -619 | 1380 | 1410 | 527 | 479 | | 764 | oil | Viking |
| 5W0671707060000 | 750204 | 36277 | 1 | 1 | B | 9330 | -411 | 1260 | 1280 | 540 | 503 | | 837 | water+mud | Viking |
| 5W0662123020000 | 650926 | 36280 | 1 | 1 | B | 10900 | -579 | 1300 | 1310 | 537 | 489 | | 724 | water+mud | Viking |
| 5W0621504060000 | 780911 | 36313 | 1 | 1 | B | 10000 | -629 | 1550 | 1570 | 393 | 351 | | 920 | water | Viking |
| 5W0642235070000 | 790126 | 36401 | 2 | 1 | B | 10700 | -763 | 1620 | 1630 | 324 | 286 | | 860 | water | Viking |
| 5W0621602110000 | 800309 | 36494 | 1 | 1 | B | 10200 | -677 | 1650 | 1670 | 367 | 323 | | 989 | water+mud+oil | Viking |
| 5W0662117100000 | 790816 | 36502 | 2 | 1 | B | 11600 | -611 | 1320 | 1320 | 576 | 526 | | 707 | n/a | Viking |
| 5W0652310110000 | 810509 | 36894 | 2 | 1 | B | 11900 | -778 | 1560 | 1580 | 436 | 388 | | 772 | water+mud+cond. | Viking |
| 5W0621904050000 | 840111 | 36907 | 2 | 2 | B | 8790 | -841 | 1740 | 1750 | 55 | 21 | | 904 | mud | Viking |
| 5W0591531080000 | 830307 | 36914 | 1 | 1 | B | 10800 | -747 | 1650 | 1680 | 354 | 312 | | 906 | water+cond. | Viking |
| 5W0641512160000 | 850123 | 36953 | 1 | 1 | B | 8980 | -490 | 1470 | 1490 | 425 | 390 | | 978 | water+mud | Viking |
| 5W0621428100000 | 841229 | 36991 | 1 | 1 | B | 8970 | -552 | 1420 | 1430 | 363 | 327 | | 869 | water+cond.+mud | Viking |
| 6W0660528100000 | 710117 | 38876 | 6 | 1 | B | 15100 | -1140 | 1980 | 1980 | 400 | 340 | | 839 | water+mud | Viking |
| 6W0660407110000 | 790721 | 39021 | 3 | 1 | B | 15000 | -1140 | 1940 | 1960 | 386 | 330 | | 798 | water | Viking |
| 6W0600123110000 | 800529 | 39099 | 1 | 1 | B | 18000 | -1470 | 2760 | 2790 | 366 | 294 | | 1290 | water+mud | Viking |
| 6W0661027150000 | 800526 | 39190 | 2 | 1 | B | 19800 | -1440 | 2460 | 2490 | 579 | 501 | | 1010 | mud | Viking |
| 6W0650222060000 | 830107 | 39212 | 5 | 1 | B | 14400 | -1040 | 1830 | 1840 | 426 | 371 | | 789 | mud+water | Viking |

Reproduced with permission of the copyright owner. Further reproduction prohibited without permission.

| Location | Date | Well ID | # | S | Q | p [kPa] | z [m] | dtop [m] | dbot [m] | $H_0$ | $H_{1040}$ | $H_{1090}$ | KB [m] | Fluid recovery | Aquifer |
|---|---|---|---|---|---|---|---|---|---|---|---|---|---|---|---|
| 6W0680630100000 | 811017 | 39243 | 1 | 1 | B | 14000 | -988 | 1690 | 1710 | 443 | 384 | | 701 | water+mud+cond. | Viking |
| 5W0632321120000 | 860127 | 50842 | 3 | 1 | B | 9010 | -954 | 1780 | 1800 | -36 | -71 | | 832 | mud+cond. | Viking |
| 5W0652233010000 | 860317 | 50856 | 1 | 1 | B | 11400 | -713 | 1430 | 1440 | 448 | 404 | | 723 | water+cond.+mud | Viking |
| 5W0662117060000 | 871226 | 50862 | 1 | 1 | B | 10900 | -628 | 1330 | 1330 | 483 | 440 | | 703 | n/a | Viking |
| 6W0650324100000 | 870206 | 51237 | 1 | 1 | B | 14900 | -1090 | 1940 | 1950 | 433 | 370 | | 856 | mud+water | Viking |
| 5W0661817070000 | 890128 | 63301 | 1 | 1 | B | 10200 | -493 | 1290 | 1300 | 549 | 507 | | 799 | water+cond.+mud | Viking |
| 5W0642521100000 | 890202 | 63310 | 5 | 1 | B | 13200 | -928 | 1770 | 1780 | 418 | 366 | | 844 | water+cond.+mud | Viking |
| 6W0660414110000 | 880225 | 80065 | 2 | 1 | B | 14700 | -1090 | 1810 | 1820 | 407 | 351 | | 718 | water+mud | Viking |
| 6W0660415120000 | 891228 | 80066 | 4 | 1 | B | 14800 | -1100 | 1810 | 1810 | 413 | 351 | | 711 | water+cond.+oil | Viking |
| 5W0652113140000 | 920725 | 83084 | 2 | 1 | B | 11600 | -665 | 1460 | 1460 | 517 | 472 | | 794 | water+mud | Viking |
| 5W0652122080000 | 920703 | 83085 | 2 | 1 | B | 11600 | -672 | 1470 | 1480 | 514 | 465 | | 801 | n/a | Viking |
| 5W0612426130000 | 950129 | -2906 | 2 | 1 | C | 14400 | -1100 | 2130 | 2180 | 367 | 311 | | 1030 | water | Viking |
| 5W0531929070000 | 741008 | 35094 | 2 | 1 | C | 20600 | -1500 | 2500 | 2520 | 592 | 519 | | 1000 | oil+mud+cond. | Viking |
| 5W0531929070000 | 741008 | 35094 | 2 | 2 | C | 20200 | -1500 | 2500 | 2520 | 551 | 480 | | 1000 | oil+mud+cond. | Viking |
| 5W0522013090000 | 760322 | 35200 | 2 | 2 | C | 29500 | -1660 | 2690 | 2710 | 1346 | 1231 | | 1030 | mud | Viking |
| 5W0642603020000 | 710402 | 35542 | 5 | 1 | C | 14600 | -1030 | 1970 | 1970 | 457 | 401 | | 942 | water+cond.+oil | Viking |
| 5W0662109100000 | 611020 | 35619 | 1 | 1 | C | 11700 | -621 | 1350 | 1360 | 571 | 526 | | 741 | oil | Viking |
| 5W0632510060000 | 780918 | 35674 | 4 | 1 | C | 14400 | -1050 | 1940 | 1960 | 419 | 361 | | 892 | water+mud | Viking |
| 5W0662028020000 | 690213 | 35701 | 2 | 1 | C | 10700 | -550 | 1350 | 1360 | 542 | 499 | | 801 | cond.+oil+mud | Viking |
| 5W0661908150000 | 790328 | 35742 | 2 | 1 | C | 10500 | -538 | 1310 | 1320 | 528 | 491 | | 774 | water | Viking |
| 5W0652134100000 | 790321 | 35753 | 3 | 1 | C | 11200 | -630 | 1440 | 1450 | 507 | 468 | | 812 | water+mud | Viking |
| 5W0621506070000 | 761102 | 35756 | 4 | 1 | C | 10200 | -650 | 1610 | 1620 | 394 | 350 | | 959 | water | Viking |
| 5W0621606020000 | 590118 | 35777 | 3 | 1 | C | 10500 | -709 | 1600 | 1620 | 365 | 320 | | 912 | water+mud | Viking |
| 5W0631407070000 | 631115 | 35787 | 1 | 1 | C | 9060 | -542 | 1470 | 1480 | 381 | 346 | | 928 | water+mud | Viking |
| 5W0652004060000 | 761107 | 35833 | 4 | 1 | C | 12000 | -675 | 1440 | 1450 | 546 | 501 | | 761 | water | Viking |
| 5W0622416070000 | 771006 | 35841 | 2 | 1 | C | 14200 | -1090 | 2130 | 2150 | 357 | 302 | | 1040 | water+mud | Viking |
| 5W0692306060000 | 601011 | 35859 | 1 | 1 | C | 9110 | -488 | 1210 | 1220 | 441 | 405 | | 728 | water | Viking |
| 5W0662214100000 | 680615 | 35927 | 1 | 1 | C | 11000 | -632 | 1360 | 1380 | 493 | 446 | | 734 | water+oil | Viking |
| 5W0601421100000 | 770819 | 35995 | 1 | 1 | C | 10400 | -636 | 1500 | 1540 | 419 | 383 | | 869 | water+mud | Viking |
| 5W0662109040000 | 650621 | 36002 | 1 | 1 | C | 11000 | -624 | 1350 | 1350 | 493 | 454 | | 724 | n/a | Viking |
| 5W0671803100000 | 641229 | 36027 | 5 | 1 | C | 9340 | -450 | 1280 | 1280 | 502 | 465 | | 822 | water+mud | Viking |
| 5W0611803100000 | 751209 | 36035 | 3 | 1 | C | 9790 | -836 | 1750 | 1760 | 161 | 124 | | 916 | n/a | Viking |
| 5W0632020110000 | 630809 | 36046 | 1 | 1 | C | 11300 | -806 | 1570 | 1580 | 342 | 302 | | 764 | water+cond. | Viking |
| 5W0662126100000 | 760204 | 36050 | 1 | 1 | C | 11100 | -561 | 1300 | 1310 | 567 | 527 | | 737 | mud | Viking |
| 5W0662226070000 | 670712 | 36051 | 1 | 1 | C | 11100 | -603 | 1320 | 1320 | 526 | 485 | | 707 | water | Viking |
| 5W0611924100000 | 670306 | 36066 | 1 | 1 | C | 10400 | -846 | 1770 | 1780 | 214 | 173 | | 936 | water+mud | Viking |
| 5W0632008130000 | 761212 | 36102 | 4 | 1 | C | 11400 | -823 | 1620 | 1650 | 341 | 294 | | 796 | water+mud | Viking |
| 5W0632136060000 | 740211 | 36115 | 5 | 1 | C | 10800 | -765 | 1560 | 1600 | 333 | 294 | | 797 | water+mud | Viking |

Reproduced with permission of the copyright owner. Further reproduction prohibited without permission.

| Location | Date | Well ID | # | S | Q | p [kPa] | z [m] | dtop [m] | dbot [m] | $H_0$ | $H_{1040}$ | $H_{1090}$ | KB [m] | Fluid recovery | Aquifer |
|---|---|---|---|---|---|---|---|---|---|---|---|---|---|---|---|
| 5W0652415040000 | 630524 | 36182 | 1 | 1 | C | 12100 | -807 | 1680 | 1690 | 428 | 379 | | 884 | water+cond. | Viking |
| 5W0662617120000 | 610113 | 36201 | 1 | 1 | C | 12400 | -844 | 1630 | 1640 | 423 | 371 | | 799 | water+mud | Viking |
| 5W0611725030000 | 771201 | 36239 | 4 | 1 | C | 10700 | -723 | 1650 | 1650 | 368 | 326 | | 924 | water+mud | Viking |
| 5W0662130100000 | 641206 | 36263 | 1 | 1 | C | 11200 | -605 | 1250 | 1270 | 538 | 493 | | 664 | water+mud | Viking |
| 5W0611536080000 | 800807 | 36471 | 4 | 1 | C | 9870 | -616 | 1520 | 1530 | 390 | 351 | | 915 | water+mud | Viking |
| 5W0652135100000 | 790925 | 36498 | 1 | 1 | C | 11400 | -631 | 1390 | 1400 | 536 | 486 | | 769 | water+mud | Viking |
| 5W0601633140000 | 800327 | 36535 | 2 | 1 | C | 10800 | -731 | 1590 | 1620 | 369 | 328 | | 865 | mud+cond.+water | Viking |
| 5W0612403100000 | 590113 | 36565 | 3 | 1 | C | 15300 | -1210 | 2310 | 2340 | 347 | 290 | | 1130 | water+mud | Viking |
| 5W0622021110000 | 611123 | 36574 | 1 | 1 | C | 10200 | -853 | 1690 | 1700 | 191 | 147 | | 851 | mud | Viking |
| 5W0651917100000 | 590129 | 36657 | 1 | 1 | C | 11300 | -615 | 1350 | 1360 | 532 | 493 | | 743 | water+mud | Viking |
| 5W0621614100000 | 600301 | 36684 | 2 | 1 | C | 10200 | -658 | 5300 | 5350 | 382 | 342 | | 970 | water | Viking |
| 5W0611605060000 | 801020 | 36702 | 8 | 1 | C | 10900 | -730 | 1580 | 1610 | 386 | 338 | | 856 | water+mud+oil | Viking |
| 5W0652005100020 | 720723 | 36736 | 1 | 1 | C | 12100 | -662 | 1430 | 1450 | 568 | 524 | | 763 | water | Viking |
| 5W0662220040000 | 810224 | 36745 | 1 | 1 | C | 11000 | -643 | 1400 | 1410 | 478 | 435 | | 760 | water+mud | Viking |
| 5W0592035100000 | 810227 | 36746 | 4 | 1 | C | 10900 | -1020 | 2020 | 2030 | 96 | 48 | | 1000 | water+mud+cond. | Viking |
| 5W0631527070000 | 810224 | 36747 | 4 | 1 | C | 8890 | -523 | 1520 | 1530 | 383 | 348 | | 998 | water+cond.+mud | Viking |
| 5W0662327060000 | 810601 | 36823 | 1 | 1 | C | 10700 | -649 | 1450 | 1460 | 446 | 400 | | 809 | water+mud+cond. | Viking |
| 5W0652123040000 | 810701 | 36868 | 1 | 1 | C | 11900 | -664 | 1460 | 1470 | 551 | 502 | | 794 | mud | Viking |
| 5W0651921100000 | 820213 | 36875 | 1 | 1 | C | 11200 | -594 | 1380 | 1400 | 548 | 504 | | 792 | water+mud | Viking |
| 5W0601403090000 | 821231 | 36909 | 3 | 1 | C | 10200 | -667 | 1470 | 1470 | 374 | 333 | | 787 | water | Viking |
| 6W0680421100000 | 661016 | 38862 | 1 | 1 | C | 12000 | -854 | 1520 | 1550 | 373 | 322 | | 669 | water+mud | Viking |
| 6W0680206110000 | 560315 | 38880 | 4 | 1 | C | 11900 | -803 | 1500 | 1510 | 411 | 363 | | 707 | n/a | Viking |
| 6W0670432100000 | 650224 | 38894 | 2 | 1 | C | 13100 | -927 | 1620 | 1640 | 404 | 357 | | 693 | n/a | Viking |
| 6W0650206060020 | 790207 | 38922 | 1 | 1 | C | 15800 | -1140 | 1990 | 2030 | 468 | 409 | | 856 | water+mud | Viking |
| 6W0660315060000 | 781018 | 38927 | 3 | 1 | C | 14200 | -1030 | 1800 | 1840 | 425 | 362 | | 768 | water+mud | Viking |
| 6W0660526100000 | 710214 | 38975 | 1 | 1 | C | 14800 | -1110 | 1910 | 1930 | 402 | 341 | | 794 | water | Viking |
| 6W0680709100000 | 780410 | 39008 | 6 | 1 | C | 15300 | -1090 | 1820 | 1850 | 467 | 410 | | 731 | n/a | Viking |
| 6W0681133070000 | 780304 | 39011 | 1 | 1 | C | 16800 | -1310 | 2050 | 2060 | 397 | 337 | | 746 | n/a | Viking |
| 6W0681133070000 | 780323 | 39011 | 5 | 1 | C | 16900 | -1300 | 2040 | 2050 | 422 | 356 | | 746 | n/a | Viking |
| 6W0670531070000 | 680126 | 39031 | 2 | 1 | C | 14100 | -1020 | 1700 | 1720 | 419 | 362 | | 685 | water+mud | Viking |
| 6W0681031100000 | 791009 | 39120 | 13 | 1 | C | 16800 | -1230 | 1970 | 1980 | 479 | 417 | | 743 | water+mud | Viking |
| 6W0680402060000 | 790808 | 39167 | 6 | 2 | C | 12700 | -915 | 1610 | 1620 | 376 | 330 | | 700 | water+mud | Viking |
| 6W0640210060000 | 810925 | 39217 | 2 | 1 | C | 16800 | -1200 | 2090 | 2110 | 511 | 447 | | 891 | mud+water | Viking |
| 6W0650232130000 | 840409 | 39281 | 3 | 1 | C | 13600 | -1020 | 1860 | 1870 | 365 | 313 | | 840 | water+mud | Viking |
| 6W0680518160000 | 850908 | 39338 | 1 | 1 | C | 12900 | -958 | 1630 | 1640 | 358 | 306 | | 675 | water+cond. | Viking |
| 5W0662112060000 | 851223 | 50861 | 3 | 1 | C | 11200 | -599 | 1340 | 1340 | 547 | 499 | | 740 | mud | Viking |
| 5W0662223060000 | 800627 | 63281 | 1 | 1 | C | 11200 | -622 | 1360 | 1370 | 515 | 476 | | 734 | mud | Viking |
| 5W0662120020000 | 851116 | 63282 | 4 | 1 | C | 11100 | -606 | 1310 | 1320 | 530 | 482 | | 709 | oil+mud+water+cond. | Viking |

Reproduced with permission of the copyright owner. Further reproduction prohibited without permission.

| Location | Date | Well ID | # | S | Q | p [kPa] | z [m] | dtop [m] | dbot [m] | $H_0$ | $H_{1040}$ | $H_{1090}$ | KB [m] | Fluid recovery | Aquifer |
|---|---|---|---|---|---|---|---|---|---|---|---|---|---|---|---|
| 5W0681428030000 | 890313 | 63316 | 1 | 1 | C | 7000 | -193 | 1070 | 1100 | 520 | 493 | | 879 | water+mud | Viking |
| 6W0650434100000 | 891123 | 80086 | 6 | 1 | C | 15300 | -1130 | 1920 | 1930 | 427 | 370 | | 796 | mud+water | Viking |
| 5W0672313060000 | 900309 | 80615 | 1 | 1 | C | 9970 | -572 | 1290 | 1300 | 444 | 405 | | 715 | water | Viking |
| 5W0632404050000 | 900411 | 80656 | 2 | 1 | C | 13900 | -1040 | 1910 | 1930 | 379 | 322 | | 875 | water+mud | Viking |
| 5W0672634060000 | 960318 | -1494 | 2 | 1 | A | 13600 | -767 | 1490 | 1500 | 615 | 566 | | 723 | water | Upper Mannville |
| 5W0662307070000 | 960923 | -1563 | 3 | 1 | A | 13200 | -758 | 1560 | 1580 | 592 | 536 | | 803 | water | Upper Mannville |
| 6W0671115080000 | 950119 | -1851 | 1 | 1 | A | 9690 | -1540 | 2440 | 2470 | -550 | -590 | | 903 | mud | Upper Mannville |
| 5W0682408110000 | 961007 | -2441 | 5 | 1 | A | 12700 | -702 | 1450 | 1470 | 591 | 543 | | 750 | water+mud | Upper Mannville |
| 5W0661908150000 | 790327 | 35742 | 1 | 1 | A | 11000 | -578 | 1350 | 1360 | 548 | 500 | | 774 | water | Upper Mannville |
| 5W0662228100000 | 750727 | 35914 | 3 | 1 | A | 12300 | -663 | 1400 | 1410 | 587 | 543 | | 734 | water+mud | Upper Mannville |
| 5W0682005160000 | 720206 | 36163 | 3 | 1 | A | 11300 | -577 | 1290 | 1310 | 578 | 531 | | 711 | water+mud | Upper Mannville |
| 5W0681733100000 | 740112 | 36350 | 1 | 1 | A | 9210 | -372 | 1280 | 1370 | 567 | 531 | | 900 | water+mud | Upper Mannville |
| 5W0672135160000 | 790811 | 36470 | 3 | 1 | A | 11100 | -565 | 1270 | 1280 | 569 | 523 | | 705 | water+mud | Upper Mannville |
| 5W0662220040000 | 810226 | 36745 | 7 | 1 | A | 13300 | -738 | 1500 | 1500 | 619 | 566 | | 760 | n/a | Upper Mannville |
| 5W0612636060000 | 810304 | 36758 | 3 | 1 | A | 16100 | -1250 | 2340 | 2360 | 391 | 328 | | 1090 | water+mud | Upper Mannville |
| 5W0612624130000 | 801225 | 36776 | 1 | 1 | A | 16300 | -1280 | 2440 | 2460 | 382 | 318 | | 1160 | water+cond.+mud | Upper Mannville |
| 5W0642004120000 | 850306 | 36980 | 6 | 1 | A | 4840 | -766 | 1570 | 1580 | -272 | -292 | | 809 | water | Upper Mannville |
| 6W0680333100000 | 840120 | 39277 | 3 | 1 | A | 14200 | -824 | 1500 | 1510 | 623 | 568 | | 676 | n/a | Upper Mannville |
| 6W0680307060000 | 860605 | 39322 | 3 | 1 | A | 15600 | -1000 | 1720 | 1720 | 585 | 529 | | 719 | n/a | Upper Mannville |
| 6W0690502100000 | 850914 | 39331 | 7 | 1 | A | 16700 | -982 | 1630 | 1640 | 715 | 655 | | 658 | water+cond. | Upper Mannville |
| 6W0690704080000 | 860630 | 39335 | 6 | 1 | A | 18000 | -1120 | 1840 | 1850 | 714 | 644 | | 721 | n/a | Upper Mannville |
| 6W0690801160000 | 860823 | 51243 | 1 | 1 | A | 18300 | -1140 | 1870 | 1900 | 722 | 654 | | 729 | water+mud | Upper Mannville |
| 5W0671921070020 | 911111 | 80608 | 1 | 1 | A | 10300 | -481 | 1250 | 1260 | 570 | 529 | | 753 | water+cond. | Upper Mannville |
| 5W0671921070020 | 911113 | 80608 | 2 | 1 | A | 10700 | -526 | 1290 | 1310 | 567 | 523 | | 753 | water+cond. | Upper Mannville |
| 5W0641619070000 | 950121 | -1633 | 2 | 1 | B | 9250 | -564 | 1480 | 1490 | 379 | 343 | | 917 | water+mud | Upper Mannville |
| 5W0641609080000 | 950312 | -1805 | 1 | 1 | B | 9510 | -572 | 1490 | 1500 | 397 | 360 | | 922 | water | Upper Mannville |
| 5W0662018150000 | 830204 | 35513 | 2 | 1 | B | 11900 | -666 | 1370 | 1400 | 544 | 500 | | 706 | water+cond.+mud | Upper Mannville |
| 5W0662407070000 | 770227 | 35570 | 5 | 1 | B | 13600 | -798 | 1640 | 1640 | 584 | 535 | | 845 | water+mud+cond. | Upper Mannville |
| 5W0662407070000 | 770301 | 35570 | 6 | 1 | B | 14800 | -837 | 1680 | 1690 | 670 | 614 | | 845 | n/a | Upper Mannville |
| 5W0681902110000 | 741031 | 35586 | 3 | 1 | B | 10100 | -452 | 1280 | 1290 | 573 | 538 | | 840 | water+mud | Upper Mannville |
| 5W0672108110000 | 790803 | 35792 | 4 | 1 | B | 12000 | -653 | 1350 | 1360 | 566 | 523 | | 701 | water+mud | Upper Mannville |
| 5W0672314050000 | 790701 | 35793 | 7 | 1 | B | 12000 | -644 | 1350 | 1350 | 575 | 532 | | 709 | water+mud | Upper Mannville |
| 5W0662323110000 | 781012 | 35826 | 5 | 1 | B | 12900 | -729 | 1520 | 1530 | 590 | 535 | | 795 | water+mud | Upper Mannville |
| 5W0662529100000 | 730917 | 35946 | 1 | 1 | B | 14300 | -795 | 1500 | 1510 | 661 | 607 | | 707 | water | Upper Mannville |
| 5W0671914120000 | 730304 | 35948 | 2 | 1 | B | 10600 | -510 | 1250 | 1260 | 575 | 529 | | 752 | water | Upper Mannville |
| 5W0651824110000 | 750320 | 35979 | 4 | 1 | B | 11400 | -579 | 1400 | 1410 | 584 | 538 | | 822 | water+mud | Upper Mannville |
| 5W0671917030000 | 750106 | 36076 | 5 | 1 | B | 11000 | -571 | 1310 | 1320 | 548 | 507 | | 739 | water | Upper Mannville |
| 5W0621915100000 | 670515 | 36223 | 2 | 1 | B | 12900 | -819 | 1680 | 1690 | 499 | 445 | | 867 | mud | Upper Mannville |

Reproduced with permission of the copyright owner. Further reproduction prohibited without permission.



| Location | Date | Well ID | # | S | Q | p [kPa] | z [m] | dtop [m] | dbot [m] | $H_0$ | $H_{1040}$ | $H_{1090}$ | KB [m] | Fluid recovery | Aquifer |
|---|---|---|---|---|---|---|---|---|---|---|---|---|---|---|---|
| 5W0581533070000 | 751214 | 36405 | 1 | 1 | B | 12000 | -828 | 1780 | 1860 | 397 | 348 | | 955 | water+mud | Upper Mannville |
| 5W0682136060000 | 790907 | 36439 | 2 | 1 | B | 10300 | -476 | 1180 | 1200 | 574 | 534 | | 708 | water | Upper Mannville |
| 5W0652130060000 | 770212 | 36803 | 1 | 1 | B | 12800 | -728 | 1490 | 1510 | 578 | 527 | | 762 | water+mud+cond. | Upper Mannville |
| 5W0642131110000 | 841121 | 36996 | 1 | 1 | B | 10800 | -766 | 1570 | 1580 | 331 | 293 | | 806 | oil+water | Upper Mannville |
| 6W0690803110000 | 781020 | 38868 | 4 | 1 | B | 18400 | -1160 | 1890 | 1900 | 718 | 643 | | 736 | water+mud | Upper Mannville |
| 6W0690710060000 | 770910 | 38881 | 4 | 1 | B | 17900 | -1100 | 1800 | 1820 | 724 | 654 | | 699 | n/a | Upper Mannville |
| 6W0680236110000 | 780221 | 38900 | 3 | 1 | B | 13800 | -811 | 1480 | 1490 | 592 | 542 | | 673 | n/a | Upper Mannville |
| 6W0671029100000 | 790228 | 38904 | 2 | 1 | B | 19700 | -1470 | 2310 | 2330 | 535 | 461 | | 840 | water+mud | Upper Mannville |
| 6W0690805110000 | 781211 | 38951 | 8 | 1 | B | 17700 | -1160 | 1900 | 1910 | 646 | 575 | | 734 | water | Upper Mannville |
| 6W0660526100000 | 710218 | 38975 | 3 | 1 | B | 12300 | -1270 | 2060 | 2100 | -18 | -64 | | 794 | n/a | Upper Mannville |
| 6W0680226060000 | 770128 | 38989 | 1 | 1 | B | 14200 | -1070 | 1520 | 1550 | 379 | 322 | | 675 | water | Upper Mannville |
| 6W0680226060000 | 770208 | 38989 | 4 | 1 | B | 14400 | -845 | 1520 | 1520 | 620 | 566 | | 675 | n/a | Upper Mannville |
| 6W0690705110000 | 780604 | 39032 | 7 | 1 | B | 18300 | -1130 | 1860 | 1870 | 730 | 664 | | 735 | n/a | Upper Mannville |
| 6W0690724100000 | 800831 | 39061 | 6 | 1 | B | 14700 | -1120 | 1800 | 1800 | 370 | 321 | | 676 | water+cond. | Upper Mannville |
| 6W0670535130000 | 800109 | 39105 | 2 | 1 | B | 16600 | -1130 | 1790 | 1790 | 560 | 497 | | 657 | water+mud | Upper Mannville |
| 6W0650435110000 | 810306 | 39181 | 1 | 1 | B | 19000 | -1200 | 2020 | 2020 | 737 | 662 | | 814 | n/a | Upper Mannville |
| 6W0680333100000 | 840120 | 39277 | 2 | 1 | B | 14300 | -875 | 1550 | 1560 | 586 | 527 | | 676 | n/a | Upper Mannville |
| 6W0690512080000 | 841122 | 39294 | 4 | 1 | B | 15700 | -954 | 1610 | 1620 | 646 | 585 | | 658 | n/a | Upper Mannville |
| 6W0680518160000 | 850910 | 39338 | 3 | 1 | B | 15200 | -1110 | 1790 | 1850 | 440 | 380 | | 675 | water+mud+cond. | Upper Mannville |
| 6W0660402060000 | 890330 | 63463 | 3 | 1 | B | 18500 | -1210 | 2010 | 2030 | 677 | 603 | | 803 | water+mud | Upper Mannville |
| 6W0690609080000 | 850904 | 80049 | 1 | 1 | B | 17100 | -1080 | 1820 | 1840 | 667 | 596 | | 749 | water+mud | Upper Mannville |
| 5W0642132100000 | 780118 | 80639 | 1 | 1 | B | 11200 | -754 | 1540 | 1560 | 388 | 344 | | 791 | water+mud+cond. | Upper Mannville |
| 6W0680319100000 | 950915 | -2265 | 1 | 1 | C | 15300 | -958 | 1660 | 1680 | 606 | 542 | | 709 | water | Upper Mannville |
| 5W0641934100300 | 960305 | -3798 | 2 | 1 | C | 2960 | -649 | 1400 | 1410 | -348 | -359 | | 751 | mud | Upper Mannville |
| 5W0542114110000 | 750418 | 35214 | 4 | 1 | C | 31600 | -1620 | 2750 | 2760 | 1601 | 1477 | | 1120 | mud | Upper Mannville |
| 5W0652108060000 | 740126 | 35552 | 2 | 1 | C | 12100 | -713 | 1490 | 1520 | 520 | 473 | | 773 | water+mud | Upper Mannville |
| 5W0671407070000 | 740116 | 35585 | 5 | 1 | C | 8790 | -328 | 1430 | 1460 | 568 | 534 | | 1110 | water | Upper Mannville |
| 5W0662109100000 | 641024 | 35619 | 3 | 1 | C | 12100 | -675 | 1390 | 1420 | 563 | 511 | | 741 | water | Upper Mannville |
| 5W0581514070000 | 790103 | 35794 | 2 | 1 | C | 12200 | -847 | 1970 | 2000 | 399 | 349 | | 1140 | water+cond.+mud | Upper Mannville |
| 5W0632123100000 | 710226 | 36040 | 3 | 1 | C | 11600 | -841 | 1630 | 1670 | 337 | 296 | | 792 | water+mud | Upper Mannville |
| 5W0672301100000 | 641121 | 36160 | 3 | 1 | C | 12200 | -650 | 1390 | 1400 | 593 | 546 | | 752 | water+mud | Upper Mannville |
| 5W0622015120000 | 640703 | 36229 | 2 | 1 | C | 11500 | -886 | 1730 | 1740 | 291 | 241 | | 845 | mud | Upper Mannville |
| 5W0652120060000 | 780208 | 36304 | 3 | 1 | C | 12200 | -687 | 1430 | 1760 | 554 | 509 | | 748 | water+mud+cond.+oil | Upper Mannville |
| 5W0652005100000 | 680208 | 36318 | 1 | 1 | C | 12400 | -718 | 1470 | 1490 | 549 | 497 | | 763 | mud+water | Upper Mannville |
| 5W0622116100000 | 761023 | 36322 | 4 | 1 | C | 19000 | -950 | 1790 | 1800 | 988 | 912 | | 839 | mud | Upper Mannville |
| 5W0662603160000 | 580901 | 36351 | 1 | 1 | C | 14700 | -830 | 1600 | 1680 | 668 | 611 | | 774 | water | Upper Mannville |
| 5W0671827010000 | 791226 | 36476 | 1 | 1 | C | 9860 | -442 | 1220 | 1230 | 563 | 524 | | 783 | water+mud | Upper Mannville |
| 5W0662331160000 | 800331 | 36499 | 5 | 1 | C | 12700 | -701 | 1490 | 1500 | 594 | 544 | | 790 | water | Upper Mannville |

Reproduced with permission of the copyright owner. Further reproduction prohibited without permission.

| Location | Date | Well ID | # | S | Q | p [kPa] | z [m] | dtop [m] | dbot [m] | $H_0$ | $H_{1040}$ | $H_{1090}$ | KB [m] | Fluid recovery | Aquifer |
|---|---|---|---|---|---|---|---|---|---|---|---|---|---|---|---|
| 5W0622131060000 | 711028 | 36701 | 4 | 1 | C | 12700 | -930 | 1790 | 1800 | 361 | 315 | | 864 | n/a | Upper Mannville |
| 5W0632301060000 | 810407 | 36752 | 1 | 1 | C | 12700 | -967 | 1820 | 1840 | 331 | 278 | | 850 | water+mud | Upper Mannville |
| 5W0652613070000 | 810206 | 36814 | 4 | 1 | C | 16500 | -1010 | 1810 | 1830 | 675 | 607 | | 810 | n/a | Upper Mannville |
| 5W0621831130000 | 810418 | 36845 | 5 | 1 | C | 8070 | -747 | 1560 | 1580 | 76 | 44 | | 812 | mud+cond. | Upper Mannville |
| 5W0662522050000 | 830827 | 36848 | 3 | 2 | C | 14700 | -797 | 1570 | 1580 | 697 | 644 | | 770 | water | Upper Mannville |
| 5W0632004080000 | 811023 | 36863 | 3 | 1 | C | 11500 | -851 | 1640 | 1650 | 325 | 276 | | 797 | mud+water | Upper Mannville |
| 5W0652123040000 | 810702 | 36868 | 2 | 1 | C | 13000 | -717 | 1510 | 1520 | 606 | 557 | | 794 | n/a | Upper Mannville |
| 6W0680615060000 | 821216 | 38852 | 4 | 1 | C | 15400 | -1070 | 1750 | 1760 | 503 | 439 | | 682 | water | Upper Mannville |
| 6W0680215110000 | 760824 | 38901 | 2 | 1 | C | 14400 | -871 | 1560 | 1570 | 598 | 540 | | 693 | n/a | Upper Mannville |
| 6W0620631070000 | 790113 | 38950 | 4 | 2 | C | 38900 | -1770 | 2950 | 2970 | 2192 | 2043 | | 1180 | cond.+water+mud | Upper Mannville |
| 6W0680826110000 | 780424 | 39007 | 3 | 1 | C | 18400 | -1170 | 1980 | 2010 | 703 | 633 | | 801 | n/a | Upper Mannville |
| 6W0680734060000 | 580725 | 39121 | 1 | 1 | C | 14400 | -1090 | 1790 | 1800 | 376 | 321 | | 698 | mud+cond. | Upper Mannville |
| 6W0680734060000 | 580724 | 39121 | 5 | 1 | C | 14300 | -1200 | 1790 | 1800 | 262 | 202 | | 698 | n/a | Upper Mannville |
| 6W0680333100000 | 840119 | 39277 | 1 | 1 | C | 14700 | -897 | 1570 | 1590 | 605 | 544 | | 676 | n/a | Upper Mannville |
| 5W0622235100000 | 881215 | 63295 | 4 | 1 | C | 10700 | -930 | 1820 | 1830 | 163 | 119 | | 874 | water+mud | Upper Mannville |
| 6W0681212020000 | 891202 | 63467 | 2 | 1 | C | 10900 | -1610 | 2380 | 2410 | -502 | -542 | | 768 | mud+cond. | Upper Mannville |
| 5W0642303110000 | 880112 | 80640 | 1 | 1 | C | 12200 | -905 | 1750 | 1760 | 342 | 291 | | 842 | mud+water | Upper Mannville |
| 5W0631730120000 | 960129 | -2746 | 4 | 1 | A | 14500 | -930 | 1750 | 1750 | 545 | 491 | | 821 | oil | Lower Mannville |
| 5W0682117130000 | 960806 | -2857 | 1 | 1 | A | 13700 | -758 | 1420 | 1430 | 635 | 585 | | 664 | water | Lower Mannville |
| 5W0661625140000 | 770323 | 35568 | 3 | 1 | A | 12400 | -669 | 1530 | 1540 | 594 | 546 | | 866 | water+mud | Lower Mannville |
| 5W0682404100000 | 750301 | 35584 | 1 | 1 | A | 14600 | -873 | 1630 | 1640 | 615 | 558 | | 760 | water+mud | Lower Mannville |
| 5W0662522020000 | 730915 | 35590 | 1 | 1 | A | 16500 | -1040 | 1770 | 1800 | 638 | 577 | | 735 | water+mud | Lower Mannville |
| 5W0681928110000 | 721130 | 35595 | 1 | 1 | A | 12600 | -653 | 1450 | 1480 | 636 | 582 | | 796 | water+cond. | Lower Mannville |
| 5W0652128020000 | 640718 | 35621 | 3 | 1 | A | 15400 | -943 | 1700 | 1710 | 629 | 566 | | 765 | water | Lower Mannville |
| 5W0661810040000 | 631012 | 35624 | 4 | 1 | A | 13700 | -764 | 1580 | 1580 | 634 | 579 | | 814 | water+mud | Lower Mannville |
| 5W0642024100000 | 630414 | 35626 | 4 | 1 | A | 15700 | -992 | 1770 | 1780 | 608 | 547 | | 789 | water+mud+oil+cond. | Lower Mannville |
| 5W0682416060000 | 601219 | 35630 | 2 | 1 | A | 15200 | -972 | 1700 | 1710 | 574 | 518 | | 735 | water+mud | Lower Mannville |
| 5W0651724060000 | 790329 | 35698 | 3 | 1 | A | 13500 | -793 | 1740 | 1750 | 582 | 530 | | 950 | water+cond. | Lower Mannville |
| 5W0631407070000 | 631118 | 35787 | 2 | 1 | A | 13700 | -764 | 1690 | 1710 | 634 | 579 | | 928 | water+mud | Lower Mannville |
| 5W0651829110000 | 790222 | 35830 | 2 | 1 | A | 14200 | -803 | 1660 | 1680 | 643 | 589 | | 859 | water+mud | Lower Mannville |
| 5W0652004060000 | 761109 | 35833 | 5 | 1 | A | 14900 | -962 | 1720 | 1730 | 556 | 498 | | 761 | oil+mud | Lower Mannville |
| 5W0692513060000 | 761008 | 35862 | 1 | 1 | A | 14200 | -836 | 1570 | 1590 | 613 | 556 | | 758 | water+mud+oil | Lower Mannville |
| 5W0691706100000 | 711207 | 35939 | 1 | 1 | A | 11500 | -589 | 1510 | 1520 | 581 | 538 | | 923 | water | Lower Mannville |
| 5W0651816160000 | 700220 | 35985 | 2 | 1 | A | 14000 | -824 | 1660 | 1710 | 603 | 548 | | 839 | water | Lower Mannville |
| 5W0661625080000 | 660128 | 35990 | 1 | 1 | A | 12300 | -625 | 1490 | 1500 | 630 | 581 | | 875 | water+mud | Lower Mannville |
| 5W0611922120000 | 650111 | 36065 | 4 | 1 | A | 15700 | -1150 | 2060 | 2070 | 453 | 389 | | 920 | water | Lower Mannville |
| 5W0631415110000 | 750218 | 36130 | 3 | 1 | A | 13000 | -754 | 1720 | 1740 | 571 | 520 | | 967 | n/a | Lower Mannville |
| 5W0631415070000 | 770108 | 36138 | 1 | 1 | A | 12500 | -757 | 1720 | 1740 | 521 | 468 | | 966 | oil | Lower Mannville |

Reproduced with permission of the copyright owner. Further reproduction prohibited without permission.



| Location | Date | Well ID | # | S | Q | p [kPa] | z [m] | dtop [m] | dbot [m] | $H_0$ | $H_{1040}$ | $H_{1090}$ | KB [m] | Fluid recovery | Aquifer |
|---|---|---|---|---|---|---|---|---|---|---|---|---|---|---|---|
| 5W0642014100000 | 640804 | 36145 | 2 | 1 | A | 16000 | -975 | 1790 | 1800 | 654 | 593 | | 822 | water+mud | Lower Mannville |
| 5W0662617120000 | 610122 | 36201 | 3 | 1 | A | 18300 | -1290 | 2070 | 2090 | 577 | 504 | | 799 | water+mud | Lower Mannville |
| 5W0631414060000 | 760319 | 36214 | 1 | 1 | A | 13000 | -749 | 1700 | 1710 | 574 | 525 | | 952 | n/a | Lower Mannville |
| 5W0682204070000 | 680426 | 36237 | 1 | 1 | A | 14200 | -858 | 1530 | 1540 | 591 | 534 | | 679 | water+mud | Lower Mannville |
| 5W0682325110000 | 711230 | 36243 | 4 | 1 | A | 13800 | -782 | 1510 | 1520 | 621 | 571 | | 725 | water+mud | Lower Mannville |
| 5W0621809100000 | 760909 | 36328 | 3 | 1 | A | 14400 | -1030 | 1870 | 1890 | 441 | 381 | | 839 | oil | Lower Mannville |
| 5W0661612160000 | 730121 | 36741 | 3 | A1 | A | 12400 | -699 | 1580 | 1610 | 565 | 516 | | 881 | n/a | Lower Mannville |
| 5W0631820060000 | 810325 | 36750 | 3 | 1 | A | 14300 | -975 | 1750 | 1760 | 479 | 427 | | 775 | n/a | Lower Mannville |
| 5W0682036050000 | 830308 | 36917 | 1 | 1 | A | 12900 | -711 | 1460 | 1490 | 604 | 553 | | 755 | water+cond.+mud | Lower Mannville |
| 5W0671406070000 | 840302 | 36945 | 1 | 1 | A | 11400 | -548 | 1630 | 1650 | 613 | 569 | | 1090 | water+mud | Lower Mannville |
| 5W0651529090000 | 840313 | 36946 | 1 | 1 | A | 12700 | -663 | 1610 | 1640 | 634 | 582 | | 945 | water+mud | Lower Mannville |
| 6W0680421100000 | 661230 | 38862 | 7 | 1 | A | 18900 | -1340 | 2010 | 2020 | 584 | 513 | | 669 | water | Lower Mannville |
| 6W0690412120000 | 830117 | 39275 | 1 | 1 | A | 17900 | -1260 | 1910 | 1920 | 569 | 494 | | 658 | water+mud+cond. | Lower Mannville |
| 5W0682204090000 | 860108 | 50872 | 1 | 1 | A | 14100 | -807 | 1480 | 1490 | 628 | 575 | | 679 | n/a | Lower Mannville |
| 5W0682634160000 | 820507 | 63268 | 2 | 1 | A | 15700 | -1030 | 1710 | 1710 | 569 | 509 | | 682 | water+mud+cond. | Lower Mannville |
| 5W0641916150000 | 880222 | 63276 | 1 | 1 | A | 14600 | -984 | 1740 | 1750 | 507 | 447 | | 758 | mud+oil | Lower Mannville |
| 5W0632133100000 | 890303 | 63307 | 2 | 1 | A | 15700 | -1120 | 1890 | 1900 | 477 | 419 | | 770 | water+mud | Lower Mannville |
| 6W0640218160000 | 890120 | 63464 | 1 | 1 | A | 19400 | -1530 | 2400 | 2420 | 449 | 372 | | 874 | mud+cond. | Lower Mannville |
| 6W0660414110000 | 880226 | 80065 | 3 | 1 | A | 20800 | -1540 | 2270 | 2290 | 573 | 499 | | 718 | n/a | Lower Mannville |
| 6W0630213120020 | 880220 | 80104 | 5 | 1 | A | 22600 | -1690 | 2690 | 2700 | 617 | 525 | | 990 | water+mud+oil+cond. | Lower Mannville |
| 5W0651602020000 | 951111 | -586 | 2 | 1 | B | 13100 | -711 | 1740 | 1750 | 626 | 573 | | 1030 | water | Lower Mannville |
| 5W0631717040000 | 950305 | -957 | 2 | 1 | B | 15600 | -934 | 1900 | 1910 | 653 | 595 | | 966 | mud+oil | Lower Mannville |
| 5W0471529100000 | 950712 | -2338 | 2 | 1 | B | 39600 | -1870 | 3050 | 3070 | 2172 | 2011 | | 1190 | water | Lower Mannville |
| 6W0690411140000 | 950209 | -3019 | 2 | 1 | B | 19200 | -1090 | 2040 | 2060 | 873 | 792 | | 961 | oil+mud | Lower Mannville |
| 5W0571629100000 | 610407 | 34938 | 6 | 1 | B | 16500 | -1190 | 2260 | 2270 | 498 | 427 | | 1080 | oil | Lower Mannville |
| 5W0661633040000 | 840302 | 35520 | 2 | 1 | B | 12300 | -626 | 1480 | 1510 | 629 | 580 | | 853 | water+mud+cond. | Lower Mannville |
| 5W0672217060000 | 740225 | 35553 | 1 | 1 | B | 14800 | -929 | 1620 | 1630 | 577 | 522 | | 701 | water+cond.+mud | Lower Mannville |
| 5W0672217060000 | 740225 | 35553 | 2 | 1 | B | 14500 | -857 | 1550 | 1570 | 619 | 564 | | 701 | water+cond.+mud | Lower Mannville |
| 5W0672321060000 | 680318 | 35558 | 5 | 1 | B | 15300 | -976 | 1730 | 1750 | 586 | 524 | | 757 | water+cond. | Lower Mannville |
| 5W0622530100000 | 771010 | 35564 | 3 | 1 | B | 21200 | -1540 | 2460 | 2470 | 619 | 538 | | 929 | n/a | Lower Mannville |
| 5W0621813100000 | 751026 | 35581 | 5 | 1 | B | 14100 | -987 | 1860 | 1870 | 448 | 395 | | 876 | water | Lower Mannville |
| 5W0671407070000 | 750116 | 35585 | 3 | 1 | B | 11700 | -558 | 1660 | 1690 | 630 | 589 | | 1110 | n/a | Lower Mannville |
| 5W0661818100000 | 720312 | 35597 | 4 | 1 | B | 13400 | -787 | 1600 | 1620 | 581 | 526 | | 810 | water+cond.+mud+oil | Lower Mannville |
| 5W0672436100000 | 601231 | 35629 | 2 | 1 | B | 14600 | -868 | 1630 | 1640 | 625 | 563 | | 772 | water+mud | Lower Mannville |
| 5W0672436100000 | 610103 | 35629 | 4 | 1 | B | 15100 | -965 | 1730 | 1740 | 569 | 515 | | 772 | water | Lower Mannville |
| 5W0661926100000 | 590307 | 35634 | 2 | 1 | B | 13600 | -793 | 1570 | 1590 | 596 | 540 | | 775 | water+mud+cond. | Lower Mannville |
| 5W0652423100000 | 630912 | 35733 | 3 | 1 | B | 17400 | -1190 | 2040 | 2050 | 587 | 515 | | 864 | water+mud | Lower Mannville |
| 5W0621811100000 | 660321 | 35744 | 2 | 1 | B | 14500 | -1020 | 1920 | 1930 | 456 | 401 | | 908 | mud | Lower Mannville |

Reproduced with permission of the copyright owner. Further reproduction prohibited without permission.

| Location | Date | Well ID | # | S | Q | p [kPa] | z [m] | dtop [m] | dbot [m] | $H_0$ | $H_{1040}$ | $H_{1090}$ | KB [m] | Fluid recovery | Aquifer |
|---|---|---|---|---|---|---|---|---|---|---|---|---|---|---|---|
| 5W0641718120000 | 611212 | 35758 | 1 | 1 | B | 14600 | -852 | 1650 | 1670 | 640 | 579 | | 805 | water+mud | Lower Mannville |
| 5W0672329060000 | 611222 | 35766 | 2 | 1 | B | 15500 | -986 | 1750 | 1760 | 595 | 533 | | 778 | water+cond. | Lower Mannville |
| 5W0672329060000 | 611229 | 35766 | 3 | 1 | B | 15600 | -998 | 1770 | 1780 | 593 | 531 | | 778 | water | Lower Mannville |
| 5W0641927020000 | 600308 | 35770 | 1 | 1 | B | 14900 | -898 | 1640 | 1660 | 618 | 562 | | 745 | water+mud | Lower Mannville |
| 5W0672108110000 | 790802 | 35792 | 3 | 1 | B | 14100 | -850 | 1550 | 1560 | 592 | 532 | | 701 | water+cond.+mud | Lower Mannville |
| 5W0692114090000 | 751127 | 35799 | 5 | 1 | B | 12700 | -678 | 1380 | 1390 | 617 | 567 | | 709 | mud | Lower Mannville |
| 5W0662025100000 | 730225 | 35913 | 1 | 1 | B | 14100 | -821 | 1620 | 1620 | 613 | 561 | | 798 | water+mud | Lower Mannville |
| 5W0632202020000 | 630220 | 35972 | 1 | 1 | B | 18200 | -1280 | 2140 | 2150 | 578 | 504 | | 871 | water+mud | Lower Mannville |
| 5W0681919160000 | 620210 | 35998 | 1 | 1 | B | 13000 | -720 | 1480 | 1480 | 608 | 554 | | 759 | water | Lower Mannville |
| 5W0622725070000 | 701114 | 36043 | 3 | 1 | B | 21400 | -1590 | 2650 | 2660 | 585 | 508 | | 1050 | water+mud+cond. | Lower Mannville |
| 5W0641828020000 | 600202 | 36099 | 7 | 1 | B | 14600 | -864 | 1630 | 1630 | 627 | 567 | | 769 | water+mud | Lower Mannville |
| 5W0632136060000 | 740210 | 36115 | 2 | 1 | B | 14900 | -1080 | 1870 | 1880 | 436 | 380 | | 797 | n/a | Lower Mannville |
| 5W0631515020000 | 691118 | 36159 | 5 | 1 | B | 13500 | -805 | 1740 | 1740 | 572 | 518 | | 940 | water+mud | Lower Mannville |
| 5W0611725030000 | 771205 | 36239 | 6 | 1 | B | 14700 | -984 | 1910 | 1910 | 517 | 457 | | 924 | water+mud | Lower Mannville |
| 5W0682232070000 | 720605 | 36242 | 1 | 1 | B | 13600 | -753 | 1420 | 1470 | 630 | 580 | | 701 | water+mud | Lower Mannville |
| 5W0682023070000 | 710127 | 36289 | 1 | 1 | B | 12900 | -702 | 1470 | 1470 | 612 | 562 | | 768 | water+cond.+mud | Lower Mannville |
| 5W0682111060000 | 730103 | 36292 | 1 | 1 | B | 13800 | -803 | 1490 | 1500 | 601 | 550 | | 698 | water+mud+cond.+oil | Lower Mannville |
| 5W0622508030000 | 780702 | 36305 | 3 | 1 | B | 23300 | -1470 | 2440 | 2460 | 900 | 814 | | 967 | n/a | Lower Mannville |
| 5W0631718060000 | 690122 | 36324 | 1 | 1 | B | 14300 | -936 | 1820 | 1830 | 521 | 466 | | 881 | water | Lower Mannville |
| 5W0632430100000 | 770501 | 36346 | 3 | 1 | B | 19500 | -1390 | 2270 | 2280 | 596 | 521 | | 881 | water+mud | Lower Mannville |
| 5W0642130110000 | 770306 | 36353 | 3 | 1 | B | 15900 | -1010 | 1830 | 1850 | 609 | 548 | | 816 | water+cond.+mud | Lower Mannville |
| 5W0672332110000 | 771107 | 36373 | 6 | 1 | B | 15400 | -968 | 1750 | 1750 | 598 | 541 | | 782 | n/a | Lower Mannville |
| 5W0672332110000 | 771107 | 36373 | 7 | 1 | B | 14900 | -927 | 1710 | 1710 | 591 | 533 | | 782 | n/a | Lower Mannville |
| 5W0662211100000 | 780211 | 36380 | 2 | 1 | B | 15300 | -930 | 1660 | 1670 | 634 | 570 | | 734 | water+mud | Lower Mannville |
| 5W0692519070020 | 760329 | 36382 | 1 | 1 | B | 15000 | -934 | 1700 | 1720 | 592 | 536 | | 773 | water | Lower Mannville |
| 5W0661411120000 | 590126 | 36392 | 1 | 1 | B | 12000 | -568 | 1730 | 1750 | 659 | 608 | | 1160 | water+mud | Lower Mannville |
| 5W0652234110000 | 731212 | 36402 | 1 | 1 | B | 15800 | -1030 | 1750 | 1780 | 575 | 519 | | 722 | water+mud | Lower Mannville |
| 5W0581531110000 | 791208 | 36463 | 3 | 1 | B | 15400 | -1060 | 2090 | 2130 | 517 | 449 | | 1030 | cond.+water+oil+mud | Lower Mannville |
| 5W0652033100000 | 790128 | 36554 | 6 | 1 | B | 14900 | -912 | 1650 | 1680 | 602 | 548 | | 742 | water+mud | Lower Mannville |
| 5W0662402100000 | 620721 | 36619 | 1 | 1 | B | 17200 | -1160 | 2040 | 2060 | 598 | 526 | | 897 | water+mud | Lower Mannville |
| 5W0641731100000 | 620308 | 36623 | 4 | 1 | B | 14100 | -803 | 1620 | 1630 | 634 | 579 | | 820 | water+mud | Lower Mannville |
| 5W0632227040000 | 610128 | 36629 | 5 | 1 | B | 18200 | -1270 | 2090 | 2110 | 585 | 514 | | 839 | water+cond.+mud | Lower Mannville |
| 5W0642326060000 | 590302 | 36685 | 5 | 1 | B | 17500 | -1200 | 2100 | 2110 | 587 | 515 | | 912 | water+mud | Lower Mannville |
| 5W0602703130000 | 801127 | 36698 | 2 | 1 | B | 25000 | -1910 | 3200 | 3200 | 633 | 540 | | 1270 | n/a | Lower Mannville |
| 5W0651911040000 | 600813 | 36733 | 5 | 1 | B | 14500 | -864 | 1660 | 1660 | 615 | 557 | | 794 | mud+water | Lower Mannville |
| 5W0651929070000 | 780402 | 36734 | 1 | 1 | B | 14600 | -843 | 1620 | 1650 | 645 | 588 | | 786 | water+mud | Lower Mannville |
| 5W0671901020000 | 600119 | 36740 | 2 | 1 | B | 13500 | -776 | 1520 | 1540 | 603 | 547 | | 753 | water+cond. | Lower Mannville |
| 5W0612636060000 | 810303 | 36758 | 2 | 1 | B | 20100 | -1610 | 2700 | 2720 | 440 | 360 | | 1090 | water+mud | Lower Mannville |

Reproduced with permission of the copyright owner. Further reproduction prohibited without permission.

| Location | Date | Well ID | # | S | Q | p [kPa] | z [m] | dtop [m] | dbot [m] | $H_0$ | $H_{1040}$ | $H_{1090}$ | KB [m] | Fluid recovery | Aquifer |
|---|---|---|---|---|---|---|---|---|---|---|---|---|---|---|---|
| 5W0682610050000 | 810204 | 36763 | 1 | 1 | B | 15700 | -977 | 1660 | 1680 | 623 | 562 | | 688 | water+mud | Lower Mannville |
| 5W0622735060000 | 811217 | 36834 | 4 | 1 | B | 21100 | -1610 | 2660 | 2710 | 537 | 458 | | 1050 | water+mud | Lower Mannville |
| 5W0641835070000 | 811129 | 36869 | 2 | 1 | B | 13600 | -825 | 1590 | 1610 | 559 | 508 | | 771 | water+cond.+mud | Lower Mannville |
| 5W0641823050000 | 811105 | 36870 | 3 | 1 | B | 14800 | -868 | 1640 | 1660 | 641 | 583 | | 789 | water+mud | Lower Mannville |
| 5W0622032040000 | 840205 | 36901 | 3 | 1 | B | 10500 | -1130 | 1960 | 1970 | -59 | -101 | | 822 | water+mud+cond. | Lower Mannville |
| 5W0651611130000 | 840320 | 36943 | 3 | 1 | B | 13100 | -742 | 1790 | 1790 | 595 | 542 | | 1050 | oil+water+cond. | Lower Mannville |
| 5W0651611130000 | 840321 | 36943 | 4 | 1 | B | 13200 | -704 | 1750 | 1780 | 638 | 590 | | 1050 | water+mud | Lower Mannville |
| 5W0672314010S00 | 840310 | 36944 | 4 | 1 | B | 14500 | -868 | 1580 | 1600 | 615 | 553 | | 717 | water+cond.+mud | Lower Mannville |
| 5W0672208160000 | 841003 | 36962 | 5 | 1 | B | 14600 | -908 | 1620 | 1630 | 584 | 523 | | 718 | water+mud | Lower Mannville |
| 5W0631801150000 | 850215 | 36978 | 3 | 1 | B | 14200 | -956 | 1850 | 1860 | 495 | 436 | | 894 | water+mud | Lower Mannville |
| 5W0641818060000 | 841201 | 36997 | 4 | 1 | B | 15100 | -954 | 1730 | 1740 | 588 | 526 | | 777 | water+cond.+mud | Lower Mannville |
| 5W0631919120000 | 850927 | 37001 | 3 | 1 | B | 15700 | -1000 | 1780 | 1790 | 597 | 539 | | 781 | mud+water | Lower Mannville |
| 6W0680421100000 | 670101 | 38862 | 8 | 1 | B | 19100 | -1330 | 2010 | 2020 | 611 | 542 | | 669 | water | Lower Mannville |
| 6W0680215110000 | 760829 | 38901 | 4 | 1 | B | 17000 | -1100 | 1790 | 1800 | 629 | 566 | | 693 | n/a | Lower Mannville |
| 6W0680215110000 | 760902 | 38901 | 6 | 1 | B | 17600 | -1210 | 1900 | 1910 | 583 | 515 | | 693 | n/a | Lower Mannville |
| 6W0630324070000 | 781130 | 38903 | 4 | 1 | B | 21400 | -1720 | 2640 | 2750 | 460 | 378 | | 914 | water+oil | Lower Mannville |
| 6W0630324070000 | 781201 | 38903 | 5 | 1 | B | 22200 | -1700 | 2610 | 2620 | 568 | 476 | | 914 | mud+water | Lower Mannville |
| 6W0620308060000 | 790402 | 38947 | 4 | 1 | B | 25700 | -1920 | 2950 | 2970 | 704 | 599 | | 1040 | n/a | Lower Mannville |
| 6W0680108060000 | 761214 | 38993 | 3 | 1 | B | 17700 | -1200 | 1940 | 1940 | 602 | 535 | | 734 | n/a | Lower Mannville |
| 6W0670531070000 | 680327 | 39031 | 5 | 1 | B | 22000 | -1370 | 2050 | 2070 | 870 | 786 | | 685 | water+mud | Lower Mannville |
| 6W0650535100000 | 791221 | 39104 | 5 | 1 | B | 25100 | -1690 | 2460 | 2480 | 869 | 770 | | 778 | water+cond.+mud | Lower Mannville |
| 6W0680311110000 | 590814 | 39116 | 3 | 1 | B | 18400 | -1270 | 1980 | 1990 | 605 | 533 | | 714 | water | Lower Mannville |
| 6W0650211070000 | 811119 | 39225 | 2 | 1 | B | 20600 | -1480 | 2340 | 2350 | 621 | 539 | | 867 | water+cond.+mud | Lower Mannville |
| 6W0610513060000 | 840216 | 39285 | 3 | 1 | B | 27500 | -2170 | 3200 | 3270 | 641 | 525 | | 1040 | water+cond.+mud | Lower Mannville |
| 6W0680411160000 | 840713 | 39290 | 4 | 1 | B | 18600 | -1370 | 2050 | 2060 | 532 | 453 | | 691 | water+mud | Lower Mannville |
| 5W0622122110000 | 860313 | 50826 | 4 | 1 | B | 16500 | -1210 | 2100 | 2110 | 468 | 407 | | 877 | mud+cond. | Lower Mannville |
| 5W0631927080000 | 880209 | 50839 | 1 | 2 | B | 12300 | -1000 | 1790 | 1820 | 258 | 206 | | 800 | n/a | Lower Mannville |
| 5W0641936120000 | 870128 | 50850 | 4 | 1 | B | 14900 | -870 | 1630 | 1650 | 645 | 590 | | 763 | water | Lower Mannville |
| 5W0662223060000 | 800628 | 63281 | 3 | 1 | B | 14900 | -962 | 1700 | 1710 | 559 | 498 | | 734 | water+mud+cond. | Lower Mannville |
| 5W0632133100000 | 890304 | 63307 | 3 | 1 | B | 15600 | -1120 | 1890 | 1900 | 475 | 409 | | 770 | water+mud+cond. | Lower Mannville |
| 6W0660402060000 | 890329 | 63463 | 2 | 1 | B | 21300 | -1620 | 2420 | 2430 | 553 | 468 | | 803 | water+mud | Lower Mannville |
| 5W0551534070000 | 861220 | 68707 | 1 | 1 | B | 16600 | -1240 | 2160 | 2170 | 452 | 387 | | 921 | oil+water+cond. | Lower Mannville |
| 6W0650325100000 | 891104 | 80081 | 1 | 1 | B | 21100 | -1410 | 2230 | 2250 | 746 | 658 | | 822 | mud+cond. | Lower Mannville |
| 6W0650328100000 | 900623 | 80082 | 2 | 1 | B | 21300 | -1560 | 2400 | 2420 | 605 | 528 | | 846 | mud+water | Lower Mannville |
| 5W0642136110000 | 831123 | 36904 | 1 | 1 | A | 16200 | -1110 | 1880 | 1890 | 537 | 478 | 405 | 778 | water+mud | Nordegg |
| 5W0621420140000 | 840317 | 36939 | 4 | 1 | A | 14500 | -893 | 1800 | 1800 | 587 | 528 | 463 | 896 | oil+water+cond. | Nordegg |
| 5W0561930110000 | 810824 | 34793 | 5 | 1 | A | 22300 | -1610 | 2950 | 2960 | 671 | 576 | 475 | 1350 | water+mud | Nordegg |
| 5W0572317100000 | 710625 | 35402 | 3 | 1 | A | 26300 | -1940 | 2990 | 3010 | 740 | 638 | 520 | 1050 | water | Nordegg |

Reproduced with permission of the copyright owner. Further reproduction prohibited without permission.

| Location | Date | Well ID | # | S | Q | p [kPa] | z [m] | dtop [m] | dbot [m] | $H_0$ | $H_{1040}$ | $H_{1090}$ | KB [m] | Fluid recovery | Aquifer |
|---|---|---|---|---|---|---|---|---|---|---|---|---|---|---|---|
| 5W0572114060000 | 770406 | 34902 | 10 | 1 | B | 22400 | -1690 | 2660 | 2690 | 590 | 506 | 405 | 963 | water+mud+cond. | Nordegg |
| 5W0651411100000 | 820923 | 36882 | 2 | 1 | B | 12300 | -694 | 1870 | 1880 | 562 | 512 | 456 | 1180 | water | Nordegg |
| 5W0692205030000 | 910915 | 80601 | 5 | 1 | B | 14500 | -894 | 1590 | 1610 | 585 | 527 | 462 | 696 | water+mud+oil | Nordegg |
| 5W0561610120000 | 671107 | 35138 | 1 | 1 | B | 19200 | -1340 | 2240 | 2270 | 612 | 542 | 456 | 903 | water+mud | Nordegg |
| 5W0662009050000 | 880111 | 80630 | 1 | 1 | B | 15100 | -934 | 1660 | 1680 | 600 | 546 | 478 | 736 | water+mud | Nordegg |
| 5W0661612040000 | 821222 | 36820 | 4 | 1 | B | 13200 | -717 | 1640 | 1660 | 624 | 577 | 517 | 927 | water+mud+oil | Nordegg |
| 5W0511609110000 | 650324 | 35039 | 5 | 1 | B | 24700 | -1820 | 2910 | 2930 | 692 | 601 | 490 | 1110 | mud | Nordegg |
| 5W0561704060000 | 910617 | 76718 | 2 | 1 | B | 20700 | -1440 | 2450 | 2470 | 674 | 589 | 496 | 1010 | mud+cond. | Nordegg |
| 5W0581932110020 | 890206 | 63313 | 2 | 1 | B | 20800 | -1440 | 2290 | 2300 | 680 | 599 | 505 | 845 | water | Nordegg |
| 5W0572011110000 | 770419 | 34900 | 3 | 1 | B | 22600 | -1600 | 2900 | 2930 | 703 | 615 | 514 | 1300 | water | Nordegg |
| 5W0531526110000 | 781101 | 35239 | 2 | 1 | B | 21400 | -1420 | 2330 | 2350 | 769 | 678 | 581 | 916 | water | Nordegg |
| 5W0491836060000 | 660404 | 35165 | 2 | 1 | C | 27800 | -2100 | 3140 | 3150 | 560 | 625 | 500 | 1040 | water | Nordegg |
| 5W0641805050000 | 570720 | 36626 | 7 | 1 | C | 16000 | -1080 | 1880 | 1890 | 550 | 488 | 416 | 793 | water+oil | Nordegg |
| 5W0631818020000 | 591214 | 36330 | 6 | 1 | C | 15700 | -1030 | 1820 | 1840 | 576 | 509 | 438 | 799 | water+mud | Nordegg |
| 5W0661611020000 | 620326 | 36618 | 4 | 1 | C | 12700 | -735 | 1660 | 1680 | 562 | 510 | 453 | 916 | water+mud+cond. | Nordegg |
| 5W0691915090000 | 800229 | 36536 | 4 | 2 | C | 12100 | -671 | 1450 | 1480 | 559 | 515 | 461 | 785 | water+mud | Nordegg |
| 5W0591507010004 | 960331 | -441 | 4 | 1 | C | 17100 | -1130 | 2140 | 2160 | 607 | 546 | 469 | 1010 | water | Nordegg |
| 5W0552223050000 | 671011 | 34901 | 3 | 1 | C | 26100 | -1990 | 3010 | 3040 | 674 | 568 | 451 | 1030 | water+cond.+mud | Nordegg |
| 5W0532008100000 | 630216 | 35350 | 2 | 1 | A | 27168 | -2089.7 | 3130 | 3190 | 680 | 573 | 451 | 1040 | water+gas | Triassic |
| 5W0541834060000 | 850929 | 35498 | 3 | 1 | A | 22712 | -1655.9 | 2610 | 2620 | 659 | 570 | 468 | 960 | n/a | Triassic |
| 5W0551705060000 | 760425 | 35370 | 5 | 1 | A | 21808 | -1580.4 | 2520 | 2530 | 643 | 557 | 459 | 946 | water | Triassic |
| 5W0551826060000 | 811113 | 68678 | 3 | 1 | A | 22124 | -1562.0 | 2620 | 2640 | 693 | 607 | 507 | 1050 | n/a | Triassic |
| 5W0551833100000 | 760112 | 35348 | 6 | 1 | A | 22349 | -1598.1 | 2690 | 2690 | 680 | 592 | 492 | 1090 | n/a | Triassic |
| 5W0561715050000 | 950910 | -1113 | 1 | 1 | A | 20890 | -1458.1 | 2460 | 2460 | 671 | 589 | 496 | 1000 | oil+water | Triassic |
| 5W0571715090000 | 950618 | -2044 | 1 | 1 | A | 19765 | -1364.1 | 2500 | 2510 | 650 | 573 | 484 | 1140 | water | Triassic |
| 5W0571722070000 | 960317 | -1649 | 1 | 1 | A | 19629 | -1353.2 | 2500 | 2510 | 648 | 571 | 482 | 1140 | water | Triassic |
| 5W0572102100000 | 761024 | 34899 | 2 | 1 | A | 23848 | -1762.0 | 2930 | 2940 | 669 | 575 | 468 | 1170 | water+gas+mud | Triassic |
| 5W0572314110000 | 951104 | -2487 | 2 | 1 | A | 25354 | -1936.0 | 3010 | 3030 | 649 | 549 | 435 | 1080 | water | Triassic |
| 5W0601620120000 | 630823 | 35936 | 2 | 1 | A | 16637 | -1117.4 | 1930 | 1940 | 579 | 513 | 439 | 816 | water+mud | Triassic |
| 5W0601623060000 | 701005 | 35876 | 1 | 1 | A | 16652 | -1083.9 | 1900 | 1920 | 614 | 548 | 473 | 822 | water | Triassic |
| 5W0602224070000 | 960324 | -1659 | 1 | 1 | A | 21484 | -1516.3 | 2540 | 2550 | 674 | 589 | 493 | 1030 | oil | Triassic |
| 5W0621715070000 | 720302 | 36029 | 1 | 1 | A | 17190 | -1079.6 | 1970 | 1970 | 673 | 605 | 528 | 891 | water+mud | Triassic |
| 5W0631627110000 | 731216 | 80678 | 1 | 1 | A | 15582 | -922.3 | 1950 | 1980 | 666 | 605 | 535 | 1030 | water | Triassic |
| 5W0631628120000 | 660124 | 35714 | 4 | 1 | A | 15126 | -950.4 | 1910 | 1930 | 592 | 532 | 464 | 975 | water+mud | Triassic |
| 5W0641602090000 | 830317 | 36885 | 7 | 1 | A | 16076 | -902.7 | 1890 | 1900 | 736 | 673 | 601 | 989 | n/a | Triassic |
| 5W0641604100000 | 661001 | 36106 | 4 | 1 | A | 14789 | -921.4 | 1830 | 1840 | 586 | 528 | 462 | 921 | water+mud+gas | Triassic |
| 5W0641635100000 | 660110 | 36370 | 5 | 1 | A | 13734 | -836.7 | 1800 | 1810 | 563 | 510 | 448 | 968 | water | Triassic |
| 5W0641735100000 | 790313 | 35739 | 5 | 1 | A | 14368 | -894.6 | 1740 | 1760 | 570 | 514 | 449 | 846 | water+mud+gas | Triassic |

Reproduced with permission of the copyright owner. Further reproduction prohibited without permission.

| Location | Date | Well ID | # | S | Q | p [kPa] | z [m] | dtop [m] | dbot [m] | $H_0$ | $H_{1040}$ | $H_{1090}$ | KB [m] | Fluid recovery | Aquifer |
|---|---|---|---|---|---|---|---|---|---|---|---|---|---|---|---|
| 5W0662014100000 | 960118 | -2231 | 3 | 1 | A | 15511 | -958.8 | 1740 | 1740 | 622 | 561 | 492 | 781 | water+mud | Triassic |
| 5W0671821110000 | 960123 | -2521 | 1 | 1 | A | 13720 | -811.8 | 1580 | 1590 | 587 | 533 | 471 | 769 | water | Triassic |
| 5W0671924140000 | 740205 | 35702 | 4 | 1 | A | 13953 | -817.2 | 1580 | 1620 | 605 | 550 | 488 | 768 | water+mud | Triassic |
| 5W0672006040000 | 840119 | 36925 | 2 | 1 | A | 15547 | -963.9 | 1730 | 1740 | 621 | 560 | 490 | 766 | water+oil+gas | Triassic |
| 5W0672101060000 | 860228 | 50868 | 1 | 1 | A | 15700 | -959.6 | 1720 | 1760 | 641 | 579 | 509 | 770 | water+mud | Triassic |
| 5W0672125060000 | 890220 | 63304 | 1 | 1 | A | 15111 | -917.5 | 1650 | 1660 | 623 | 564 | 496 | 736 | water+oil+mud+gas | Triassic |
| 5W0672135160000 | 790811 | 36470 | 2 | 1 | A | 14858 | -904.6 | 1610 | 1620 | 610 | 552 | 485 | 705 | water+mud | Triassic |
| 5W0672212140000 | 651229 | 35611 | 1 | 1 | A | 16048 | -997.9 | 1660 | 1670 | 638 | 575 | 503 | 664 | water+mud+oil | Triassic |
| 5W0672436100020 | 850630 | 37009 | 2 | 1 | A | 15938 | -1068.6 | 1830 | 1850 | 548 | 494 | 422 | 772 | n/a | Triassic |
| 5W0682210120000 | 660908 | 35646 | 4 | 1 | A | 14943 | -942.8 | 1610 | 1620 | 580 | 522 | 455 | 673 | water+mud+oil | Triassic |
| 5W0682210120000 | 661017 | 35646 | 1 | 1 | A | 14708 | -934.8 | 1610 | 1630 | 564 | 507 | 441 | 673 | water+oil+mud+gas | Triassic |
| 5W0682223030020 | 630812 | 36813 | 1 | 1 | A | 14842 | -915.0 | 1570 | 1570 | 598 | 540 | 473 | 658 | water+mud+gas+oil | Triassic |
| 5W0682230150000 | 951231 | -3263 | 3 | 1 | A | 14600 | -927.5 | 1650 | 1660 | 561 | 504 | 438 | 727 | water+mud | Triassic |
| 5W0682325110000 | 720103 | 36243 | 6 | 1 | A | 15261 | -949.8 | 1670 | 1690 | 606 | 546 | 477 | 725 | water+mud+oil+gas | Triassic |
| 6W0680423010000 | 840710 | 39286 | 1 | 1 | A | 19423 | -1456.4 | 2180 | 2190 | 524 | 447 | 360 | 728 | oil+mud | Triassic |
| 6W0690321160000 | 950128 | -3418 | 3 | 1 | A | 17897 | -1266.3 | 1920 | 1920 | 558 | 488 | 407 | 652 | water+mud | Triassic |
| 5W0522104070000 | 750313 | 35035 | 5 | 1 | B | 29243 | -2328.1 | 3430 | 3450 | 653 | 538 | 407 | 1100 | n/a | Triassic |
| 5W0561821100000 | 840413 | 35440 | 2 | 1 | B | 21570 | -1539.9 | 2720 | 2740 | 659 | 574 | 477 | 1190 | n/a | Triassic |
| 5W0562114100000 | 800623 | 34869 | 2 | 1 | B | 24787 | -1862.9 | 2920 | 2940 | 664 | 567 | 455 | 1060 | water+gas+mud | Triassic |
| 5W0562218070000 | 740330 | 35109 | 2 | 1 | B | 27300 | -2010.2 | 3200 | 3240 | 793 | 666 | 543 | 1190 | water+gas | Triassic |
| 5W0562220060000 | 750327 | 35060 | 1 | 1 | B | 26190 | -1984.9 | 3160 | 3160 | 669 | 582 | 464 | 1180 | water | Triassic |
| 5W0562413130000 | 801223 | 34905 | 2 | 1 | B | 27931 | -2132.7 | 3270 | 3280 | 714 | 605 | 479 | 1140 | water+gas | Triassic |
| 5W0571715090000 | 950620 | -2044 | 2 | 1 | B | 19751 | -1363.1 | 2500 | 2510 | 651 | 573 | 484 | 1140 | water+mud | Triassic |
| 5W0571805110000 | 770705 | 35286 | 1 | 1 | B | 21202 | -1525.2 | 2720 | 2720 | 636 | 553 | 458 | 1190 | water+mud+gas | Triassic |
| 5W0581905100000 | 650106 | 35103 | 5 | 1 | B | 21808 | -1573.4 | 2620 | 2630 | 650 | 564 | 466 | 1050 | water+mud | Triassic |
| 5W0582227110000 | 720709 | 36338 | 2 | 1 | B | 23671 | -1758.4 | 2760 | 2770 | 655 | 562 | 455 | 999 | n/a | Triassic |
| 5W0592123060000 | 760317 | 35908 | 1 | 1 | B | 22781 | -1548.7 | 2590 | 2620 | 774 | 684 | 582 | 1050 | n/a | Triassic |
| 5W0601635090000 | 610422 | 36579 | 1 | 1 | B | 16224 | -1050.0 | 1810 | 1840 | 604 | 540 | 467 | 764 | water | Triassic |
| 5W0611603010000 | 730314 | 36024 | 2 | 1 | B | 16411 | -1050.0 | 1860 | 1890 | 623 | 558 | 485 | 816 | water+mud | Triassic |
| 5W0612118110000 | 761106 | 35574 | 1 | 1 | B | 19414 | -1446.9 | 2430 | 2440 | 532 | 456 | 369 | 990 | water+gas | Triassic |
| 5W0632128110000 | 720111 | 36333 | 1 | 1 | B | 17238 | -1232.9 | 2020 | 2030 | 524 | 457 | 379 | 794 | water+mud+gas+oil | Triassic |
| 5W0642135060000 | 740102 | 35804 | 1 | 1 | B | 16238 | -1133.9 | 1900 | 1900 | 521 | 458 | 385 | 767 | water+mud+oil+gas | Triassic |
| 5W0642326060000 | 590308 | 36685 | 6 | 1 | B | 19442 | -1373.4 | 2270 | 2290 | 608 | 532 | 445 | 912 | water+mud+gas | Triassic |
| 5W0652201070000 | 730308 | 35803 | 6 | 1 | B | 16417 | -1156.7 | 1940 | 1960 | 517 | 452 | 379 | 787 | water+gas+mud | Triassic |
| 5W0652325110000 | 761102 | 35929 | 2 | 1 | B | 17919 | -1172.0 | 1920 | 1940 | 655 | 584 | 504 | 748 | water+mud | Triassic |
| 5W0652334100000 | 721020 | 35746 | 7 | 1 | B | 17767 | -1161.3 | 1900 | 1940 | 650 | 580 | 500 | 742 | water+mud+oil | Triassic |
| 5W0662014100000 | 960117 | -2231 | 1 | 1 | B | 15817 | -1022.8 | 1800 | 1810 | 590 | 528 | 456 | 781 | oil | Triassic |
| 5W0662123020000 | 651005 | 36280 | 3 | 1 | B | 15957 | -1000.1 | 1720 | 1730 | 627 | 564 | 492 | 724 | water | Triassic |

Reproduced with permission of the copyright owner. Further reproduction prohibited without permission.



| Location | Date | Well ID | # | S | Q | p [kPa] | z [m] | dtop [m] | dbot [m] | $H_0$ | $H_{1040}$ | $H_{1090}$ | KB [m] | Fluid recovery | Aquifer |
|---|---|---|---|---|---|---|---|---|---|---|---|---|---|---|---|
| 5W0662135080000 | 850314 | 36969 | 3 | 1 | B | 15636 | -961.9 | 1730 | 1740 | 632 | 571 | 500 | 756 | n/a | Triassic |
| 5W0671822140000 | 810227 | 36767 | 1 | 1 | B | 13978 | -816.5 | 1600 | 1630 | 608 | 554 | 491 | 789 | water+mud | Triassic |
| 5W0671908080000 | 710411 | 36314 | 1 | 1 | B | 14738 | -881.8 | 1640 | 1650 | 621 | 563 | 496 | 758 | water | Triassic |
| 5W0671914120000 | 730305 | 35948 | 4 | 1 | B | 14260 | -845.2 | 1600 | 1620 | 608 | 553 | 488 | 752 | water | Triassic |
| 5W0671921070000 | 721121 | 35945 | 5 | 1 | B | 14527 | -899.8 | 1650 | 1670 | 581 | 524 | 459 | 753 | n/a | Triassic |
| 5W0671924160000 | 960128 | -3439 | 3 | 1 | B | 14035 | -825.5 | 1600 | 1600 | 605 | 550 | 487 | 773 | water+mud | Triassic |
| 5W0672018100000 | 711222 | 35731 | 4 | 1 | B | 15236 | -922.6 | 1710 | 1720 | 630 | 571 | 502 | 786 | mud+water | Triassic |
| 5W0672018100020 | 870724 | 63292 | 1 | 1 | B | 15195 | -930.9 | 1710 | 1720 | 618 | 558 | 490 | 787 | water+mud+gas+oil | Triassic |
| 5W0672102140000 | 880307 | 80612 | 3 | 1 | B | 15670 | -968.4 | 1710 | 1720 | 629 | 567 | 497 | 744 | water+mud+oil | Triassic |
| 5W0672202110000 | 740331 | 36042 | 1 | 1 | B | 16179 | -1027.8 | 1730 | 1740 | 621 | 558 | 485 | 704 | water+oil | Triassic |
| 5W0672208160000 | 841001 | 36962 | 3 | 1 | B | 16471 | -1090.0 | 1810 | 1810 | 589 | 524 | 450 | 718 | n/a | Triassic |
| 5W0672330060000 | 841124 | 37004 | 1 | 1 | B | 16632 | -1071.7 | 1840 | 1860 | 624 | 559 | 484 | 775 | n/a | Triassic |
| 5W0681829120000 | 700318 | 36295 | 1 | 1 | B | 13155 | -764.1 | 1640 | 1680 | 577 | 525 | 466 | 879 | water+mud | Triassic |
| 5W0681919160000 | 620212 | 35998 | 2 | 1 | B | 13821 | -813.2 | 1570 | 1570 | 596 | 541 | 479 | 759 | water+gas | Triassic |
| 5W0682126070000 | 740316 | 36285 | 1 | 1 | B | 14611 | -862.6 | 1570 | 1580 | 627 | 570 | 504 | 720 | water+gas+oil+mud | Triassic |
| 5W0682136060000 | 790909 | 36439 | 4 | 1 | B | 14161 | -844.1 | 1550 | 1550 | 599 | 544 | 480 | 708 | water+gas+oil+mud | Triassic |
| 5W0682203160000 | 840626 | 50871 | 1 | 1 | B | 14803 | -940.8 | 1620 | 1640 | 568 | 510 | 444 | 669 | water+oil | Triassic |
| 5W0682223030020 | 630814 | 36813 | 2 | 1 | B | 14822 | -907.1 | 1560 | 1570 | 604 | 546 | 479 | 658 | water+mud | Triassic |
| 5W0682232070000 | 720608 | 36242 | 3 | 1 | B | 14927 | -909.5 | 1610 | 1620 | 612 | 554 | 486 | 701 | water+oil+mud+gas | Triassic |
| 5W0682234110000 | 580911 | 35801 | 2 | 1 | B | 14988 | -894.3 | 1570 | 1570 | 634 | 575 | 507 | 677 | water+mud+gas+oil | Triassic |
| 5W0682404100000 | 750309 | 35584 | 3 | 1 | B | 17554 | -1177.1 | 1940 | 1940 | 612 | 543 | 465 | 760 | oil+mud | Triassic |
| 5W0692012160000 | 950323 | -3354 | 1 | 1 | B | 13201 | -765.0 | 1490 | 1500 | 581 | 529 | 470 | 726 | n/a | Triassic |
| 6W0650325100000 | 891115 | 80081 | 2 | 1 | B | 21141 | -1661.8 | 2480 | 2490 | 493 | 410 | 315 | 822 | mud+gas | Triassic |
| 6W0680108060000 | 761213 | 38993 | 2 | 1 | B | 17640 | -1303.6 | 2040 | 2050 | 495 | 425 | 346 | 734 | water+mud | Triassic |
| 6W0680436020000 | 850707 | 39327 | 2 | 1 | B | 19220 | -1401.0 | 2060 | 2070 | 558 | 483 | 397 | 664 | water+gas+mud | Triassic |
| 6W0690109070000 | 701226 | 39197 | 1 | 1 | B | 16374 | -1182.6 | 1840 | 1890 | 486 | 422 | 349 | 667 | water+mud | Triassic |
| 6W0690122070000 | 720313 | 38997 | 1 | 1 | B | 16070 | -1163.4 | 1820 | 1860 | 475 | 412 | 339 | 651 | water+gas+mud | Triassic |
| 6W0690327010000 | 960218 | -539 | 1 | 1 | B | 17760 | -1252.3 | 1910 | 1910 | 558 | 489 | 409 | 657 | water | Triassic |
| 5W0491910150000 | 720413 | 34837 | 1 | 1 | C | 30480 | -2375.9 | 3500 | 3510 | 731 | 612 | 475 | 1140 | mud | Triassic |
| 5W0522104070000 | 750303 | 35035 | 1 | 1 | C | 29978 | -2322.9 | 3400 | 3420 | 733 | 615 | 481 | 1100 | water+mud | Triassic |
| 5W0522133100000 | 760214 | 35013 | 15 | 1 | C | 28593 | -2249.1 | 3300 | 3390 | 666 | 553 | 425 | 1050 | water+mud | Triassic |
| 5W0532031040000 | 771211 | 35076 | 6 | 1 | C | 27390 | -2100.7 | 3150 | 3160 | 691 | 584 | 461 | 1050 | water | Triassic |
| 5W0541911070000 | 820906 | 34781 | 2 | 1 | C | 24564 | -1805.1 | 2790 | 2810 | 699 | 603 | 492 | 993 | water+mud+gas | Triassic |
| 5W0542211070000 | 741007 | 35143 | 1 | 1 | C | 27652 | -2128.0 | 3200 | 3310 | 691 | 582 | 458 | 1070 | water | Triassic |
| 5W0542229070000 | 800328 | 34985 | 1 | 2 | C | 27204 | -2140.1 | 3160 | 3180 | 633 | 526 | 404 | 1030 | water | Triassic |
| 5W0542305160000 | 810807 | 34805 | 4 | 1 | C | 31126 | -2418.3 | 3600 | 3630 | 755 | 633 | 493 | 1190 | mud+water+gas | Triassic |
| 5W0551729150000 | 540809 | 34923 | 15 | 1 | C | 22036 | -1530.7 | 2570 | 2590 | 716 | 629 | 530 | 1060 | water | Triassic |
| 5W0552132040000 | 690825 | 35292 | 1 | 1 | C | 26310 | -1996.7 | 3070 | 3080 | 685 | 582 | 464 | 1070 | water+gas+mud | Triassic |

Reproduced with permission of the copyright owner. Further reproduction prohibited without permission.

| Location | Date | Well ID | # | S | Q | p [kPa] | z [m] | dtop [m] | dbot [m] | $H_0$ | $H_{1040}$ | $H_{1090}$ | KB [m] | Fluid recovery | Aquifer |
|---|---|---|---|---|---|---|---|---|---|---|---|---|---|---|---|
| 5W0562132100000 | 740315 | 35059 | 1 | 2 | C | 24242 | -1821.5 | 2790 | 2800 | 650 | 555 | 446 | 963 | water | Triassic |
| 5W0562220060000 | 750404 | 35060 | 3 | 1 | C | 26001 | -1981.5 | 3160 | 3180 | 685 | 567 | 450 | 1180 | water | Triassic |
| 5W0571630110000 | 950207 | -2579 | 1 | 1 | C | 19087 | -1306.7 | 2380 | 2390 | 639 | 564 | 478 | 1080 | water | Triassic |
| 5W0572011110000 | 770330 | 34900 | 2 | 1 | C | 22839 | -1638.9 | 2940 | 2950 | 689 | 600 | 497 | 1300 | mud | Triassic |
| 5W0581928110000 | 591229 | 35708 | 2 | 1 | C | 21078 | -1501.8 | 2460 | 2470 | 647 | 564 | 469 | 966 | water | Triassic |
| 5W0582206060000 | 810203 | 80757 | 2 | 1 | C | 24279 | -1832.3 | 2860 | 2860 | 643 | 547 | 438 | 1030 | water | Triassic |
| 5W0591506140000 | 781210 | 36406 | 4 | 1 | C | 17321 | -1136.8 | 2150 | 2170 | 629 | 561 | 483 | 1020 | water+mud+oil | Triassic |
| 5W0602111100000 | 780310 | 35791 | 4 | 1 | C | 21552 | -1532.2 | 2530 | 2530 | 665 | 580 | 483 | 996 | n/a | Triassic |
| 5W0611509040000 | 721215 | 36422 | 4 | 1 | C | 16105 | -1017.1 | 1830 | 1850 | 625 | 561 | 489 | 817 | water | Triassic |
| 5W0611820060000 | 570107 | 36656 | 3 | 1 | C | 18521 | -1239.0 | 2210 | 2220 | 649 | 576 | 493 | 980 | water+mud | Triassic |
| 5W0621506070000 | 761031 | 35756 | 3 | 1 | C | 15700 | -985.4 | 1940 | 1970 | 615 | 553 | 483 | 959 | water+oil | Triassic |
| 5W0631610100000 | 961003 | -2201 | 1 | 1 | C | 15710 | -962.3 | 2000 | 2010 | 639 | 578 | 507 | 1040 | mud+water | Triassic |
| 5W0631618100000 | 680311 | 36110 | 1 | 1 | C | 15326 | -974.5 | 2020 | 2020 | 588 | 528 | 459 | 1050 | water+oil+mud | Triassic |
| 5W0612030100000 | 631020 | 36335 | 1 | 1 | C | 18171 | -1354.8 | 2230 | 2240 | 497 | 426 | 345 | 877 | water+mud | Triassic |
| 5W0612225070000 | 770219 | 35750 | 3 | 1 | C | 19181 | -1429.2 | 2390 | 2400 | 526 | 451 | 365 | 964 | water+mud+gas | Triassic |
| 5W0622102120000 | 631005 | 36233 | 1 | 1 | C | 17958 | -1336.2 | 2210 | 2260 | 494 | 424 | 343 | 880 | water+mud | Triassic |
| 5W0651836080000 | 641228 | 36198 | 1 | 1 | C | 14575 | -906.5 | 1770 | 1800 | 579 | 522 | 457 | 888 | water+mud+oil | Triassic |
| 5W0652033100000 | 781220 | 36554 | 2 | 1 | C | 16146 | -1074.2 | 1820 | 1830 | 572 | 508 | 436 | 742 | water+oil+mud | Triassic |
| 5W0652234110000 | 731217 | 36402 | 2 | 1 | C | 17236 | -1121.7 | 1840 | 1860 | 635 | 568 | 490 | 722 | water+gas | Triassic |
| 5W0661905040000 | 720719 | 35912 | 1 | 1 | C | 15476 | -954.0 | 1720 | 1730 | 624 | 563 | 493 | 765 | water+mud | Triassic |
| 5W0662123020000 | 651001 | 36280 | 2 | 2 | C | 15892 | -1005.8 | 1730 | 1750 | 614 | 552 | 480 | 724 | water+oil+gas | Triassic |
| 5W0662536060000 | 810321 | 36762 | 2 | 1 | C | 16925 | -1196.7 | 1940 | 1960 | 529 | 462 | 386 | 748 | mud | Triassic |
| 5W0671803100020 | 871230 | 80606 | 2 | 1 | C | 14142 | -838.7 | 1660 | 1670 | 603 | 547 | 484 | 823 | water+mud | Triassic |
| 5W0671819090000 | 930727 | 83059 | 1 | 1 | C | 14209 | -828.2 | 1600 | 1610 | 620 | 565 | 501 | 773 | water+mud+oil | Triassic |
| 5W0672019070000 | 820121 | 35502 | 3 | 1 | C | 14952 | -919.4 | 1690 | 1700 | 605 | 546 | 479 | 773 | mud | Triassic |
| 5W0672108110020 | 911201 | 80613 | 2 | 1 | C | 16064 | -1005.5 | 1700 | 1710 | 632 | 569 | 497 | 703 | water+gas+mud | Triassic |
| 5W0672329060000 | 611228 | 35766 | 6 | 1 | C | 17359 | -1156.1 | 1930 | 1930 | 613 | 545 | 467 | 778 | mud+water+oil | Triassic |
| 5W0672330060000 | 841215 | 37004 | 6 | 1 | C | 17735 | -1167.6 | 1940 | 1950 | 640 | 571 | 491 | 775 | water+mud+oil+gas | Triassic |
| 5W0672435060000 | 750426 | 35582 | 2 | 1 | C | 17103 | -1173.2 | 1940 | 1960 | 570 | 503 | 426 | 768 | water+mud+oil | Triassic |
| 5W0672435060000 | 750528 | 35582 | 3 | 1 | C | 16681 | -1086.6 | 1850 | 1860 | 614 | 548 | 473 | 768 | water+oil | Triassic |
| 5W0681809070000 | 830227 | 36913 | 1 | 1 | C | 13450 | -763.6 | 1570 | 1600 | 607 | 555 | 494 | 811 | water+gas+mud | Triassic |
| 5W0681916110000 | 700212 | 36294 | 1 | 1 | C | 13780 | -818.7 | 1590 | 1640 | 586 | 532 | 470 | 782 | water+oil+mud | Triassic |
| 5W0681928110000 | 721204 | 35595 | 2 | 1 | C | 13608 | -788.8 | 1580 | 1600 | 598 | 545 | 484 | 796 | water+oil+gas | Triassic |
| 5W0681928110000 | 721228 | 35595 | 8 | 1 | C | 13744 | -779.1 | 1570 | 1590 | 622 | 568 | 506 | 796 | water+gas+oil | Triassic |
| 5W0681934100000 | 750214 | 35583 | 3 | 1 | C | 13273 | -759.3 | 1580 | 1600 | 594 | 542 | 482 | 815 | water+mud | Triassic |
| 5W0682020100000 | 740310 | 36299 | 1 | 1 | C | 14062 | -843.1 | 1580 | 1590 | 590 | 535 | 472 | 750 | water+mud | Triassic |
| 5W0682136060000 | 790903 | 36439 | 1 | 1 | C | 14420 | -848.3 | 1550 | 1560 | 622 | 565 | 500 | 708 | water+mud+oil | Triassic |
| 5W0682224070000 | 590603 | 36593 | 3 | 1 | C | 14881 | -901.6 | 1550 | 1560 | 615 | 557 | 490 | 648 | water | Triassic |

Reproduced with permission of the copyright owner. Further reproduction prohibited without permission.



| Location | Date | Well ID | # | S | Q | p [kPa] | z [m] | dtop [m] | dbot [m] | $H_0$ | $H_{1040}$ | $H_{1090}$ | KB [m] | Fluid recovery | Aquifer |
|---|---|---|---|---|---|---|---|---|---|---|---|---|---|---|---|
| 5W0682224070000 | 580603 | 36593 | 2 | 1 | C | 15101 | -897.9 | 1550 | 1550 | 641 | 582 | 514 | 648 | n/a | Triassic |
| 5W0682224090000 | 570606 | 35809 | 1 | 2 | C | 15152 | -906.8 | 1540 | 1550 | 638 | 578 | 510 | 645 | oil | Triassic |
| 5W0682315060000 | 650303 | 36287 | 2 | 1 | C | 16077 | -1013.8 | 1770 | 1790 | 625 | 562 | 490 | 761 | water+mud | Triassic |
| 5W0682403070000 | 831221 | 36937 | 3 | 1 | C | 16221 | -1045.8 | 1810 | 1830 | 608 | 544 | 471 | 749 | water+oil+mud | Triassic |
| 5W0682403120000 | 900316 | 80594 | 1 | 1 | C | 17402 | -1168.7 | 1910 | 1920 | 605 | 537 | 459 | 737 | water+mud+oil | Triassic |
| 5W0692203050000 | 591008 | 36279 | 1 | 1 | C | 14785 | -892.8 | 1560 | 1570 | 614 | 556 | 490 | 677 | oil+water | Triassic |
| 5W0692203070000 | 591130 | 36207 | 1 | 2 | C | 14570 | -884.5 | 1560 | 1560 | 601 | 544 | 478 | 673 | water+mud+oil | Triassic |
| 5W0692503070000 | 721210 | 36381 | 3 | 1 | C | 17282 | -1175.0 | 1890 | 1900 | 587 | 519 | 441 | 707 | water+oil+gas+mud | Triassic |
| 6W0670318140000 | 850411 | 39320 | 1 | 1 | C | 20731 | -1541.6 | 2350 | 2380 | 572 | 490 | 397 | 809 | water+gas | Triassic |
| 6W0670426040000 | 840912 | 39287 | 2 | 1 | C | 21085 | -1574.2 | 2300 | 2310 | 575 | 492 | 398 | 730 | water+gas+mud | Triassic |
| 6W0680123110000 | 680111 | 38990 | 2 | 1 | C | 17087 | -1231.7 | 1920 | 1930 | 510 | 443 | 366 | 680 | water+mud+gas+oil | Triassic |
| 6W0680307060000 | 860605 | 39322 | 1 | 1 | C | 19659 | -1469.4 | 2190 | 2190 | 535 | 458 | 369 | 719 | mud+water+oil+gas | Triassic |
| 6W0690403100000 | 850122 | 39313 | 3 | 2 | C | 19412 | -1410.0 | 2070 | 2080 | 569 | 493 | 405 | 666 | water+mud+gas | Triassic |
| 6W0690608080000 | 840830 | 39289 | 4 | 1 | C | 22645 | -1601.1 | 2290 | 2300 | 707 | 618 | 517 | 689 | gas+water+oil+mud | Triassic |
| 6W0690724100000 | 800830 | 39061 | 5 | 1 | C | 21982 | -1597.7 | 2270 | 2290 | 643 | 557 | 458 | 676 | water+gas | Triassic |
| 6W0680618060000 | 831013 | 39356 | 1 | 1 | C | 28086 | -1723.8 | 2430 | 2430 | 1139 | 1029 | 903 | 704 | oil | Triassic |
| 6W0680630050000 | 810123 | 39179 | 5 | 1 | C | 31085 | -1694.8 | 2400 | 2430 | 1474 | 1352 | 1212 | 706 | oil | Triassic |
| 6W0680619100000 | 790309 | 38948 | 2 | 1 | C | 32325 | -1701.0 | 2400 | 2410 | 1594 | 1467 | 1322 | 695 | oil | Triassic |
| 6W0680631100000 | 830909 | 39235 | 1 | 1 | C | 34103 | -1657.3 | 2360 | 2370 | 1819 | 1685 | 1532 | 703 | oil | Triassic |
| 5W0692118040000 | 840918 | 36942 | 2 | 1 | A | 14800 | -936 | 1580 | 1590 | 569 | 515 | 448 | 647 | water | Permian |
| 5W0672124100000 | 660328 | 35810 | 2 | 1 | A | 15800 | -1020 | 1750 | 1770 | 591 | 529 | 458 | 742 | water+oil+mud | Permian |
| 5W0672018100000 | 711221 | 35731 | 3 | 1 | A | 15700 | -1010 | 1790 | 1830 | 591 | 529 | 458 | 786 | water | Permian |
| 5W0611916030020 | 920703 | 83075 | 1 | 1 | A | 19600 | -1320 | 2230 | 2230 | 683 | 601 | 513 | 914 | - | Permian |
| 6W0650921110000 | 701223 | 38935 | 2 | 1 | A | 34600 | -2740 | 3810 | 3850 | 791 | 651 | 496 | 1080 | - | Permian |
| 5W0672007110000 | 731208 | 36028 | 4 | 1 | B | 15500 | -1010 | 1780 | 1800 | 569 | 509 | 440 | 763 | water + mud + oil | Permian |
| 5W0682403120000 | 900317 | 80594 | 2 | 1 | B | 18000 | -1240 | 1980 | 1980 | 594 | 524 | 443 | 737 | - | Permian |
| 5W0672102100000 | 660222 | 36376 | 3 | 1 | B | 16200 | -1070 | 1810 | 1820 | 588 | 518 | 445 | 748 | water + oil + cond. | Permian |
| 5W0652604100000 | 630123 | 36372 | 1 | 1 | B | 22000 | -1620 | 2530 | 2540 | 623 | 536 | 437 | 915 | water+mud | Permian |
| 5W0632227040000 | 610201 | 36629 | 6 | 1 | B | 19900 | -1410 | 2240 | 2250 | 616 | 541 | 451 | 839 | water + mud + oil + cond. | Permian |
| 5W0692513060000 | 761015 | 35862 | 2 | 1 | B | 17300 | -1160 | 1910 | 1930 | 605 | 536 | 458 | 758 | water+oil+mud | Permian |
| 5W0591535040000 | 610303 | 36319 | 1 | 1 | B | 16700 | -1100 | 1960 | 1990 | 604 | 537 | 462 | 886 | - | Permian |
| 5W0672309110000 | 710719 | 35555 | 4 | 1 | B | 18100 | -1230 | 1960 | 2000 | 613 | 544 | 463 | 767 | water + oil + mud + cond. | Permian |
| 5W0631504100000 | 630102 | 36162 | 1 | 1 | B | 14800 | -913 | 1900 | 1910 | 598 | 538 | 471 | 990 | water+mud | Permian |
| 5W0672218060000 | 700120 | 35602 | 2 | 1 | B | 17100 | -1130 | 1850 | 1860 | 609 | 546 | 469 | 719 | water | Permian |
| 5W0642328040000 | 840401 | 36940 | 1 | 1 | B | 19800 | -1400 | 2190 | 2210 | 623 | 541 | 452 | 793 | water+mud | Permian |
| 5W0632232030000 | 850725 | 37000 | 2 | 1 | B | 20100 | -1420 | 2240 | 2250 | 633 | 550 | 460 | 828 | water+mud | Permian |

Reproduced with permission of the copyright owner. Further reproduction prohibited without permission.



| Location | Date | Well ID | # | S | Q | p [kPa] | z [m] | dtop [m] | dbot [m] | $H_0$ | $H_{1040}$ | $H_{1090}$ | KB [m] | Fluid recovery | Aquifer |
|---|---|---|---|---|---|---|---|---|---|---|---|---|---|---|---|
| 5W0652613070000 | 810204 | 36814 | 1 | 1 | B | 21500 | -1550 | 2360 | 2370 | 644 | 557 | 461 | 810 | water+mud | Permian |
| 5W0521628100000 | 620914 | 34885 | 6 | 1 | B | 22900 | -1680 | 2600 | 2630 | 652 | 565 | 462 | 944 | water | Permian |
| 6W0660436060000 | 680320 | 38864 | 4 | 1 | B | 25100 | -1900 | 2650 | 2700 | 663 | 560 | 447 | 753 | - | Permian |
| 5W0521520040020 | 650127 | 34839 | 3 | 1 | B | 22700 | -1630 | 2540 | 2550 | 678 | 595 | 493 | 921 | water+mud | Permian |
| 5W0531522040000 | 630322 | 35096 | 2 | 1 | B | 21400 | -1500 | 2420 | 2450 | 684 | 598 | 501 | 927 | water + mud + cond. | Permian |
| 6W0680530090000 | 810303 | 39183 | 2 | 1 | C | 24870 | -1837 | 2510 | 2530 | 675 | 698 | 489 | | water+mud+gas | Permian |
| 5W0672314010S00 | 840308 | 36944 | 2 | 1 | C | 16900 | -1140 | 1860 | 1880 | 577 | 516 | 440 | 717 | water + oil + cond. + mud | Permian |
| 5W0672202020000 | 651205 | 36519 | 6 | 1 | C | 16700 | -1140 | 1830 | 1830 | 569 | 497 | 422 | 693 | water + mud + oil | Permian |
| 5W0672314010S00 | 840306 | 36944 | 1 | 1 | C | 16800 | -1140 | 1860 | 1870 | 563 | 507 | 431 | 717 | - | Permian |
| 5W0672221060000 | 850717 | 50869 | 1 | 2 | C | 16600 | -1110 | 1800 | 1810 | 583 | 517 | 442 | 699 | water+mud | Permian |
| 5W0662603160000 | 580915 | 36351 | 3 | 1 | C | 21000 | -1520 | 2290 | 2300 | 612 | 538 | 444 | 774 | water + oil | Permian |
| 5W0691829010000 | 741230 | 35911 | 2 | 1 | C | 12600 | -714 | 1650 | 1660 | 572 | 521 | 464 | 939 | water+mud | Permian |
| 5W0631410110000 | 691021 | 36368 | 3 | 2 | C | 14000 | -844 | 1780 | 1790 | 579 | 528 | 465 | 935 | water + cond. + oil | Permian |
| 5W0662331160000 | 800330 | 36499 | 4 | 1 | C | 18000 | -1230 | 2020 | 2030 | 602 | 534 | 453 | 790 | water + cond. + oil + mud | Permian |
| 5W0682203160000 | 840717 | 50871 | 3 | 1 | C | 16300 | -1060 | 1720 | 1730 | 596 | 538 | 464 | 669 | water + mud + oil | Permian |
| 5W0672421100000 | 710120 | 35598 | 3 | 1 | C | 18300 | -1260 | 2000 | 2010 | 606 | 534 | 451 | 751 | water + mud + oil | Permian |
| 5W0662309100000 | 761013 | 35745 | 3 | 1 | C | 18300 | -1260 | 2040 | 2050 | 609 | 534 | 451 | 779 | water+mud | Permian |
| 5W0631502060000 | 891119 | 80677 | 1 | 1 | C | 14700 | -907 | 1830 | 1840 | 593 | 534 | 468 | 928 | water + cond. | Permian |
| 5W0631515100000 | 650131 | 35784 | 3 | 1 | C | 14600 | -892 | 1830 | 1840 | 595 | 539 | 473 | 946 | water + mud + cond. | Permian |
| 5W0652421130000 | 820305 | 36867 | 1 | 1 | C | 19700 | -1390 | 2280 | 2280 | 620 | 541 | 452 | 885 | mud + water + cond. | Permian |
| 5W0671917030000 | 750105 | 36076 | 2 | 1 | C | 15200 | -945 | 1680 | 1690 | 602 | 545 | 477 | 739 | water+mud | Permian |
| 6W0660207090000 | 790704 | 38905 | 1 | 1 | C | 24000 | -1800 | 2580 | 2650 | 644 | 552 | 444 | 785 | water + mud + cond. | Permian |
| 5W0571610070000 | 770909 | 35000 | 4 | 1 | C | 19100 | -1320 | 2370 | 2380 | 623 | 552 | 466 | 1050 | water + cond. + mud + oil | Permian |
| 5W0662617120000 | 610201 | 36201 | 5 | 1 | C | 21500 | -1550 | 2350 | 2350 | 635 | 557 | 461 | 799 | water + mud + oil | Permian |
| 5W0531634040000 | 661101 | 35272 | 2 | 1 | C | 21500 | -1560 | 2450 | 2460 | 637 | 547 | 451 | 899 | water | Permian |
| 5W0641713160000 | 720326 | 36374 | 3 | 1 | C | 15000 | -926 | 1870 | 1880 | 607 | 544 | 477 | 941 | water | Permian |
| 5W0641607060000 | 720407 | 36211 | 1 | 1 | C | 15200 | -940 | 1810 | 1820 | 611 | 550 | 482 | 875 | water+mud | Permian |
| 5W0632002020000 | 701212 | 36336 | 2 | 1 | C | 18500 | -1260 | 2070 | 2090 | 628 | 553 | 470 | 818 | mud + oil + water | Permian |
| 5W0631611150000 | 701224 | 36044 | 1 | 1 | C | 15400 | -949 | 1960 | 1970 | 625 | 560 | 491 | 1010 | - | Permian |
| 6W0680206110000 | 560305 | 38880 | 10 | 1 | C | 22700 | -1650 | 2350 | 2360 | 670 | 575 | 473 | 707 | water | Permian |
| 6W0650201120000 | 621124 | 38985 | 5 | 1 | C | 24900 | -1860 | 2700 | 2710 | 688 | 581 | 469 | 852 | - | Permian |
| 6W0670705070000 | 770801 | 38883 | 1 | 1 | C | 30700 | -2310 | 3150 | 3170 | 823 | 699 | 561 | 840 | - | Permian |
| 5W0671503110000 | 810117 | 36771 | 1 | 1 | A | 12100 | -676 | 1620 | 1640 | 552 | 510 | 456 | 940 | cond. + oil + mud + water | Mississippian |
| 5W0641828020000 | 600209 | 36099 | 10 | 1 | A | 15800 | -1030 | 1790 | 1800 | 576 | 519 | 448 | 769 | water | Mississippian |

Reproduced with permission of the copyright owner. Further reproduction prohibited without permission.



| Location | Date | Well ID | # | S | Q | p [kPa] | z [m] | dtop [m] | dbot [m] | $H_0$ | $H_{1040}$ | $H_{1090}$ | KB [m] | Fluid recovery | Aquifer |
|---|---|---|---|---|---|---|---|---|---|---|---|---|---|---|---|
| 5W0652111010000 | 751109 | 35579 | 3 | 1 | A | 17400 | -1190 | 1960 | 1970 | 584 | 515 | 437 | 769 | water + mud + cond. + oil | Mississippian |
| 5W0671615060000 | 880219 | 80605 | 2 | 1 | A | 12400 | -708 | 1700 | 1710 | 561 | 507 | 452 | 997 | - | Mississippian |
| 5W0671827010000 | 791227 | 36476 | 2 | 1 | A | 13800 | -834 | 1620 | 1620 | 568 | 519 | 457 | 783 | water | Mississippian |
| 5W0661509100000 | 780723 | 35762 | 3 | 1 | A | 12500 | -715 | 1760 | 1770 | 564 | 510 | 454 | 1050 | water + cond. + mud | Mississippian |
| 5W0671826100000 | 740107 | 36799 | 1 | 1 | A | 13800 | -834 | 1640 | 1650 | 570 | 519 | 457 | 810 | water+mud | Mississippian |
| 5W0671803100020 | 871229 | 80606 | 1 | 1 | A | 14300 | -884 | 1700 | 1720 | 573 | 518 | 453 | 823 | water+mud | Mississippian |
| 5W0671503060000 | 690125 | 35729 | 1 | 1 | A | 12300 | -685 | 1620 | 1630 | 564 | 521 | 465 | 939 | water + cond. + oil + mud | Mississippian |
| 5W0671511100000 | 710315 | 36008 | 1 | 1 | A | 11800 | -644 | 1740 | 1760 | 563 | 513 | 460 | 1100 | water+mud | Mississippian |
| 5W0661928100000 | 800408 | 36496 | 4 | 1 | A | 15100 | -959 | 1760 | 1770 | 580 | 521 | 453 | 806 | water+mud | Mississippian |
| 5W0661510050000 | 701221 | 35918 | 1 | 1 | A | 12600 | -715 | 1740 | 1750 | 569 | 520 | 463 | 1030 | water + mud + cond. | Mississippian |
| 5W0642020060000 | 641121 | 36180 | 4 | 1 | A | 17800 | -1220 | 2030 | 2040 | 595 | 525 | 445 | 823 | water+mud | Mississippian |
| 5W0581517060000 | 830124 | 36915 | 4 | 1 | A | 17600 | -1200 | 2250 | 2280 | 594 | 525 | 446 | 1050 | - | Mississippian |
| 5W0581521100000 | 660413 | 36409 | 5 | 1 | A | 17600 | -1200 | 2150 | 2160 | 596 | 525 | 446 | 962 | water+mud | Mississippian |
| 5W0661521100000 | 951105 | -2285 | 3 | 1 | A | 12700 | -721 | 1740 | 1750 | 578 | 524 | 467 | 1020 | water+mud | Mississippian |
| 5W0631435060000 | 690102 | 35606 | 2 | 1 | A | 13500 | -796 | 1810 | 1830 | 583 | 527 | 467 | 1020 | cond. + oi + water + mudl | Mississippian |
| 5W0601929040000 | 650203 | 35812 | 5 | 1 | A | 19600 | -1380 | 2350 | 2380 | 619 | 541 | 453 | 964 | water+mud | Mississippian |
| 5W0542115070000 | 770318 | 35139 | 1 | 1 | A | 27400 | -2130 | 3220 | 3240 | 658 | 556 | 432 | 1090 | mud | Mississippian |
| 5W0642014100000 | 640809 | 36145 | 3 | 1 | A | 17500 | -1170 | 1990 | 2000 | 612 | 545 | 467 | 822 | water+mud | Mississippian |
| 5W0601635090000 | 610424 | 36579 | 2 | 1 | A | 17200 | -1150 | 1890 | 1910 | 610 | 536 | 459 | 764 | - | Mississippian |
| 5W0652025100000 | 780924 | 35740 | 5 | 1 | A | 16600 | -1080 | 1810 | 1820 | 620 | 547 | 472 | 743 | water + oil + cond. + mud | Mississippian |
| 5W0551929040000 | 650118 | 35057 | 4 | 1 | A | 24000 | -1790 | 2900 | 2920 | 658 | 562 | 454 | 1130 | water | Mississippian |
| 5W0611934110000 | 670109 | 36069 | 5 | 1 | A | 18900 | -1290 | 2230 | 2240 | 633 | 563 | 478 | 944 | water+mud | Mississippian |
| 5W0621617100000 | 760828 | 36431 | 3 | 1 | A | 16300 | -1050 | 1970 | 1980 | 621 | 548 | 474 | 925 | - | Mississippian |
| 5W0562220060000 | 750407 | 35060 | 4 | 1 | A | 26900 | -2060 | 3240 | 3260 | 677 | 577 | 456 | 1180 | water | Mississippian |
| 5W0591520020000 | 610704 | 35641 | 1 | 1 | A | 17100 | -1110 | 2070 | 2090 | 631 | 566 | 489 | 985 | water + cond. + mud | Mississippian |
| 5W0522116160000 | 770412 | 35331 | 1 | 1 | A | 29900 | -2340 | 3430 | 3440 | 704 | 591 | 456 | 1100 | - | Mississippian |
| 5W0471731060000 | 750224 | 35367 | 6 | 1 | A | 30000 | -2350 | 3540 | 3550 | 707 | 590 | 456 | 1200 | water | Mississippian |
| 5W0602209060000 | 720913 | 35891 | 1 | 1 | A | 22600 | -1630 | 2740 | 2760 | 674 | 585 | 484 | 1090 | - | Mississippian |
| 5W0531929070000 | 741030 | 35094 | 3 | 1 | A | 26600 | -2000 | 2950 | 3010 | 710 | 607 | 488 | 1000 | water + mud + cond. | Mississippian |
| 5W0631714070000 | 730331 | 36003 | 1 | 1 | A | 16500 | -1020 | 2050 | 2070 | 665 | 597 | 523 | 1040 | water+mud | Mississippian |
| 5W0461514110000 | 920119 | 80923 | 1 | 1 | A | 28000 | -2130 | 3340 | 3340 | 725 | 614 | 489 | 1210 | - | Mississippian |
| 5W0501635070000 | 720411 | 35232 | 3 | 1 | A | 24600 | -1800 | 2850 | 2870 | 714 | 611 | 501 | 1060 | - | Mississippian |
| 5W0511905100000 | 670209 | 35360 | 1 | 1 | A | 29700 | -2270 | 3250 | 3270 | 760 | 641 | 508 | 992 | - | Mississippian |
| 5W0651524150000 | 920226 | 80644 | 1 | 1 | A | 13900 | -735 | 1760 | 1760 | 685 | 627 | 565 | 1020 | - | Mississippian |

Reproduced with permission of the copyright owner. Further reproduction prohibited without permission.



| Location | Date | Well ID | # | S | Q | p [kPa] | z [m] | dtop [m] | dbot [m] | $H_0$ | $H_{1040}$ | $H_{1090}$ | KB [m] | Fluid recovery | Aquifer |
|---|---|---|---|---|---|---|---|---|---|---|---|---|---|---|---|
| 5W0541925060000 | 750108 | 35218 | 5 | 1 | A | 24800 | -1790 | 2800 | 2800 | 740 | 641 | 529 | 1010 | water | Mississippian |
| 5W0621630060000 | 800420 | 36399 | 4 | 3 | A | 17300 | -1030 | 2010 | 2020 | 731 | 666 | 588 | 973 | water+mud | Mississippian |
| 5W0641532030000 | 801106 | 36704 | 3 | 1 | A | 15200 | -824 | 1810 | 1850 | 721 | 666 | 598 | 990 | - | Mississippian |
| 5W0501606110000 | 661031 | 35127 | 2 | 2 | A | 26800 | -1960 | 3030 | 3040 | 781 | 667 | 546 | 1080 | water | Mississippian |
| 5W0621630060000 | 800420 | 36399 | 4 | 1 | A | 17400 | -1030 | 2010 | 2020 | 741 | 675 | 597 | 973 | water+mud | Mississippian |
| 5W0661908150000 | 790329 | 35742 | 4 | 1 | B | 15400 | -1000 | 1780 | 1780 | 572 | 509 | 440 | 774 | water+mud | Mississippian |
| 5W0651609020000 | 740120 | 35589 | 2 | 1 | B | 13900 | -846 | 1810 | 1820 | 570 | 516 | 454 | 964 | water + mud + cond. | Mississippian |
| 5W0682136130000 | 650311 | 35614 | 2 | 1 | B | 15100 | -963 | 1670 | 1670 | 577 | 517 | 449 | 704 | water | Mississippian |
| 5W0661534070000 | 710313 | 35919 | 1 | 1 | B | 12100 | -666 | 1630 | 1640 | 565 | 520 | 466 | 969 | water + mud + cond. | Mississippian |
| 5W0651505100000 | 680213 | 35768 | 2 | 1 | B | 13400 | -796 | 1750 | 1760 | 572 | 517 | 457 | 958 | water+mud | Mississippian |
| 5W0631510140000 | 640803 | 35785 | 2 | 1 | B | 14700 | -915 | 1830 | 1840 | 579 | 526 | 460 | 914 | water | Mississippian |
| 5W0632008130000 | 761212 | 36102 | 3 | 1 | B | 18600 | -1300 | 2090 | 2110 | 598 | 523 | 439 | 796 | water+mud | Mississippian |
| 5W0631934020000 | 581110 | 36573 | 2 | 1 | B | 17300 | -1180 | 1930 | 1970 | 592 | 516 | 438 | 788 | water | Mississippian |
| 5W0661625080000 | 660202 | 35990 | 2 | 1 | B | 12800 | -735 | 1600 | 1610 | 571 | 520 | 462 | 875 | water + mud + oil | Mississippian |
| 5W0611922120000 | 540117 | 36065 | 5 | 1 | B | 18800 | -1310 | 2230 | 2240 | 605 | 533 | 448 | 920 | water | Mississippian |
| 5W0581521100000 | 660402 | 36409 | 4 | 1 | B | 17400 | -1180 | 2140 | 2150 | 597 | 525 | 447 | 962 | oil + water | Mississippian |
| 5W0652114060000 | 670807 | 36738 | 3 | 1 | B | 17500 | -1180 | 1960 | 1980 | 598 | 535 | 457 | 780 | water+mud | Mississippian |
| 5W0642036060000 | 610207 | 35561 | 4 | 1 | B | 16900 | -1130 | 1890 | 1900 | 597 | 526 | 450 | 768 | water | Mississippian |
| 5W0661518150000 | 700317 | 36196 | 1 | 1 | B | 12800 | -728 | 1720 | 1730 | 577 | 527 | 469 | 990 | water + cond. + mud + oil | Mississippian |
| 5W0671407070000 | 750115 | 35585 | 2 | 1 | B | 11800 | -624 | 1730 | 1750 | 574 | 533 | 480 | 1110 | cond. + oil + water | Mississippian |
| 5W0581533070000 | 751216 | 36405 | 2 | 1 | B | 17600 | -1180 | 2130 | 2140 | 608 | 545 | 466 | 955 | - | Mississippian |
| 5W0601520120000 | 651010 | 36419 | 1 | 1 | B | 16400 | -1070 | 1870 | 1880 | 603 | 537 | 464 | 807 | water+mud | Mississippian |
| 5W0562128110000 | 800123 | 34911 | 2 | 1 | B | 25100 | -1910 | 2950 | 2960 | 651 | 550 | 437 | 1040 | water+mud | Mississippian |
| 5W0591631040000 | 650218 | 36411 | 3 | 1 | B | 17700 | -1190 | 2160 | 2170 | 615 | 545 | 465 | 975 | water | Mississippian |
| 5W0651506060000 | 800110 | 36472 | 2 | 1 | B | 13900 | -822 | 1840 | 1850 | 598 | 540 | 478 | 1020 | water + cond. + mud | Mississippian |
| 5W0661536120000 | 840115 | 36921 | 1 | 1 | B | 12300 | -667 | 1690 | 1700 | 589 | 539 | 483 | 1030 | water+mud | Mississippian |
| 5W0611504110000 | 760321 | 36420 | 7 | 1 | B | 16000 | -1020 | 1830 | 1830 | 609 | 548 | 476 | 807 | water + oil | Mississippian |
| 5W0632006020000 | 630330 | 36119 | 6 | 1 | B | 19200 | -1330 | 2140 | 2150 | 625 | 552 | 466 | 812 | water | Mississippian |
| 5W0591509060000 | 760322 | 63291 | 1 | 1 | B | 17300 | -1140 | 2150 | 2160 | 617 | 556 | 478 | 1010 | water + oil | Mississippian |
| 5W0591734070000 | 790118 | 36412 | 3 | 1 | B | 18100 | -1230 | 2160 | 2170 | 623 | 544 | 463 | 937 | water + cond. | Mississippian |
| 5W0631501060000 | 701210 | 35786 | 1 | 1 | B | 14700 | -892 | 1800 | 1830 | 608 | 549 | 483 | 914 | water | Mississippian |
| 5W0671924160000 | 960128 | -3439 | 3 | 1 | B | 14000 | -826 | 1600 | 1600 | 605 | 546 | 483 | 773 | water+mud | Mississippian |
| 5W0611534100000 | 760908 | 36428 | 2 | 1 | B | 15500 | -965 | 1870 | 1890 | 613 | 554 | 485 | 907 | water | Mississippian |
| 5W0522123130000 | 810224 | 34860 | 1 | 1 | B | 29200 | -2300 | 3360 | 3370 | 680 | 562 | 431 | 1060 | mud + cond. + water | Mississippian |

Reproduced with permission of the copyright owner. Further reproduction prohibited without permission.



| Location | Date | Well ID | # | S | Q | p [kPa] | z [m] | dtop [m] | dbot [m] | $H_0$ | $H_{1040}$ | $H_{1090}$ | KB [m] | Fluid recovery | Aquifer |
|---|---|---|---|---|---|---|---|---|---|---|---|---|---|---|---|
| 5W0551712060000 | 740707 | 35287 | 2 | 1 | B | 21600 | -1550 | 2510 | 2540 | 643 | 567 | 470 | 965 | water + mud + cond. | Mississippian |
| 5W0621504060000 | 780924 | 36313 | 3 | 1 | B | 15700 | -987 | 1900 | 1920 | 616 | 552 | 481 | 920 | - | Mississippian |
| 5W0581834100000 | 680928 | 35932 | 2 | 1 | B | 19800 | -1380 | 2420 | 2430 | 639 | 561 | 472 | 1040 | water + mud + cond. | Mississippian |
| 5W0561708050000 | 771229 | 35091 | 4 | 1 | B | 20800 | -1470 | 2640 | 2650 | 650 | 569 | 475 | 1170 | - | Mississippian |
| 5W0651929070000 | 780406 | 36734 | 4 | 1 | B | 16500 | -1050 | 1830 | 1850 | 630 | 567 | 493 | 786 | water + mud + cond. | Mississippian |
| 5W0531702110000 | 640716 | 34883 | 1 | 1 | B | 23400 | -1720 | 2620 | 2650 | 664 | 574 | 468 | 905 | water+mud | Mississippian |
| 5W0591908100000 | 771015 | 36150 | 3 | 1 | B | 21200 | -1500 | 2410 | 2430 | 659 | 578 | 483 | 913 | water + cond. | Mississippian |
| 5W0611510060000 | 890828 | 80687 | 1 | 1 | B | 16200 | -1020 | 1850 | 1860 | 636 | 568 | 495 | 834 | water + mud + cond. | Mississippian |
| 5W0592026070000 | 771211 | 36722 | 2 | 1 | B | 21200 | -1500 | 2520 | 2540 | 665 | 578 | 483 | 1010 | water + cond. | Mississippian |
| 5W0531708110000 | 650707 | 34882 | 12 | 1 | B | 24100 | -1780 | 2680 | 2700 | 680 | 582 | 474 | 916 | mud | Mississippian |
| 5W0501718100000 | 650128 | 35258 | 1 | 1 | B | 26900 | -2050 | 3060 | 3090 | 694 | 587 | 466 | 1050 | water + cond. | Mississippian |
| 5W0551814100000 | 750303 | 35134 | 1 | 1 | B | 22100 | -1580 | 2600 | 2620 | 672 | 586 | 487 | 1020 | water | Mississippian |
| 5W0551817110000 | 761215 | 35412 | 5 | 1 | B | 23000 | -1660 | 2680 | 2690 | 685 | 594 | 491 | 1010 | - | Mississippian |
| 5W0621620100000 | 760202 | 36375 | 1 | 1 | B | 16600 | -1030 | 1950 | 1960 | 662 | 597 | 522 | 927 | mud + water | Mississippian |
| 5W0571927060000 | 800623 | 34949 | 1 | 1 | B | 22200 | -1560 | 2780 | 2800 | 701 | 616 | 516 | 1220 | water + cond. | Mississippian |
| 5W0602006100000 | 800311 | 36556 | 2 | 1 | B | 22000 | -1540 | 2540 | 2560 | 704 | 616 | 517 | 1000 | mud + water | Mississippian |
| 5W0541729140000 | 820412 | 34751 | 1 | 2 | B | 23100 | -1640 | 2560 | 2570 | 715 | 624 | 520 | 923 | water + cond. | Mississippian |
| 5W0581704070000 | 770809 | 34997 | 3 | 1 | B | 20200 | -1350 | 2590 | 2630 | 705 | 630 | 539 | 1240 | mud + cond. + water | Mississippian |
| 5W0561712100000 | 800709 | 34959 | 4 | 1 | B | 21600 | -1480 | 2410 | 2430 | 718 | 637 | 540 | 927 | water + cond. + mud | Mississippian |
| 5W0592029110000 | 770128 | 36339 | 5 | 1 | B | 22400 | -1560 | 2540 | 2550 | 725 | 636 | 535 | 978 | water+mud | Mississippian |
| 5W0671614070000 | 710116 | 35599 | 1 | 1 | C | 12200 | -693 | 1630 | 1650 | 547 | 503 | 448 | 943 | - | Mississippian |
| 5W0612035100000 | 640119 | 36061 | 1 | 1 | C | 19000 | -1340 | 2200 | 2210 | 597 | 522 | 437 | 872 | water + mud + cond. | Mississippian |
| 5W0611617060000 | 790822 | 36400 | 5 | 1 | C | 16700 | -1120 | 1990 | 2010 | 590 | 517 | 442 | 886 | water + cond. + mud | Mississippian |
| 5W0651522020000 | 590322 | 36729 | 4 | 1 | C | 13200 | -775 | 1760 | 1770 | 573 | 519 | 459 | 993 | water | Mississippian |
| 5W0671926040000 | 640811 | 35703 | 8 | 1 | C | 14400 | -888 | 1660 | 1670 | 584 | 523 | 459 | 761 | water+oil+mud | Mississippian |
| 5W0671530100000 | 650128 | 35616 | 1 | 1 | C | 12200 | -666 | 1620 | 1630 | 574 | 530 | 475 | 956 | water + mud + oil | Mississippian |
| 5W0661519050000 | 700304 | 36049 | 2 | 2 | C | 12800 | -724 | 1690 | 1710 | 580 | 531 | 473 | 972 | water+mud | Mississippian |
| 5W0661527100000 | 810308 | 36753 | 5 | 1 | C | 12600 | -703 | 1660 | 1680 | 580 | 532 | 475 | 967 | water+mud | Mississippian |
| 5W0621812110000 | 690717 | 36451 | 2 | 1 | C | 17200 | -1150 | 2030 | 2050 | 603 | 536 | 459 | 888 | water | Mississippian |
| 5W0621614100000 | 600307 | 36684 | 3 | 1 | C | 15700 | -1000 | 1970 | 1980 | 596 | 539 | 468 | 970 | - | Mississippian |
| 5W0651930020000 | 810108 | 36735 | 3 | 1 | C | 16300 | -1060 | 1810 | 1810 | 601 | 538 | 464 | 747 | water + cond. | Mississippian |
| 5W0591528080002 | 601229 | 35864 | 1 | 1 | C | 17100 | -1130 | 2070 | 2090 | 606 | 546 | 469 | 951 | oil + mud | Mississippian |
| 5W0632006020000 | 630329 | 36119 | 5 | 1 | C | 19100 | -1330 | 2140 | 2150 | 618 | 542 | 456 | 812 | oil + water | Mississippian |
| 5W0641922070000 | 570310 | 35719 | 6 | 1 | C | 16800 | -1110 | 1850 | 1860 | 608 | 537 | 461 | 746 | water | Mississippian |

Reproduced with permission of the copyright owner. Further reproduction prohibited without permission.



| Location | Date | Well ID | # | S | Q | p [kPa] | z [m] | dtop [m] | dbot [m] | $H_0$ | $H_{1040}$ | $H_{1090}$ | KB [m] | Fluid recovery | Aquifer |
|---|---|---|---|---|---|---|---|---|---|---|---|---|---|---|---|
| 5W0541629060000 | 681009 | 35004 | 4 | 1 | C | 21200 | -1530 | 2450 | 2470 | 630 | 548 | 453 | 921 | water+mud | Mississippian |
| 5W0632106100000 | 640106 | 35759 | 4 | 1 | C | 20000 | -1410 | 2250 | 2260 | 624 | 550 | 460 | 836 | water+mud | Mississippian |
| 5W0571825100000 | 770129 | 34998 | 9 | 1 | C | 20200 | -1430 | 2640 | 2650 | 627 | 550 | 459 | 1200 | water | Mississippian |
| 5W0611523100000 | 771025 | 36425 | 2 | 2 | C | 15500 | -980 | 1870 | 1880 | 604 | 539 | 470 | 881 | water + mud + cond. | Mississippian |
| 5W0611523120000 | 630729 | 36426 | 4 | 1 | C | 15800 | -1010 | 1850 | 1860 | 607 | 539 | 468 | 853 | water+mud | Mississippian |
| 5W0582033110000 | 641211 | 35618 | 1 | 1 | C | 21800 | -1590 | 2560 | 2570 | 637 | 547 | 449 | 978 | water | Mississippian |
| 5W0542336020000 | 660222 | 35073 | 2 | 2 | C | 28900 | -2280 | 3360 | 3380 | 673 | 553 | 423 | 1100 | water | Mississippian |
| 5W0531934020000 | 740919 | 35136 | 11 | 1 | C | 24900 | -1890 | 2870 | 2880 | 653 | 551 | 439 | 985 | water | Mississippian |
| 5W0591929060000 | 610831 | 36542 | 5 | 1 | C | 20800 | -1480 | 2450 | 2480 | 633 | 559 | 465 | 991 | water | Mississippian |
| 5W0562122130000 | 770726 | 35284 | 3 | 1 | C | 25300 | -1930 | 3040 | 3060 | 658 | 550 | 436 | 1120 | water | Mississippian |
| 5W0522133100000 | 760206 | 35013 | 12 | 1 | C | 29700 | -2340 | 3390 | 3400 | 680 | 571 | 438 | 1050 | water+mud | Mississippian |
| 5W0632205060000 | 620202 | 35716 | 6 | 1 | C | 21000 | -1500 | 2360 | 2380 | 638 | 558 | 464 | 881 | mud + water + cond. | Mississippian |
| 5W0622027110000 | 610815 | 36576 | 6 | 1 | C | 19000 | -1310 | 2130 | 2160 | 629 | 552 | 467 | 838 | mud + water + cond. | Mississippian |
| 5W0591506110000 | 560713 | 36548 | 5 | 1 | C | 17900 | -1200 | 2220 | 2220 | 625 | 554 | 474 | 1020 | water+mud | Mississippian |
| 5W0621614100000 | 600310 | 36684 | 4 | 1 | C | 16700 | -1080 | 2040 | 2050 | 620 | 557 | 482 | 970 | water+mud | Mississippian |
| 5W0481814040000 | 650524 | 35168 | 1 | 1 | C | 30900 | -2340 | 3450 | 3490 | 808 | 689 | 550 | 1140 | water + cond. | Mississippian |
| 5W0601507100000 | 661001 | 36417 | 2 | 1 | C | 16700 | -1080 | 1930 | 1960 | 622 | 557 | 482 | 853 | water + cond. | Mississippian |
| 5W0632204100000 | 770317 | 36045 | 2 | 1 | C | 20800 | -1480 | 2320 | 2350 | 643 | 559 | 465 | 841 | water+mud | Mississippian |
| 5W0591801110000 | 681003 | 36072 | 1 | 1 | C | 19600 | -1360 | 2400 | 2410 | 638 | 561 | 473 | 1040 | water | Mississippian |
| 5W0511821060000 | 860128 | 68690 | 1 | 1 | C | 26700 | -2050 | 3060 | 3070 | 673 | 567 | 447 | 1010 | - | Mississippian |
| 5W0561932010000 | 560321 | 35411 | 4 | 1 | C | 22600 | -1650 | 2970 | 2980 | 654 | 565 | 464 | 1330 | - | Mississippian |
| 5W0531918100000 | 750322 | 35249 | 3 | 1 | C | 26100 | -1990 | 2990 | 3000 | 673 | 568 | 451 | 994 | water | Mississippian |
| 5W0552209100000 | 830510 | 34742 | 1 | 1 | C | 27900 | -2160 | 3230 | 3250 | 684 | 575 | 449 | 1060 | - | Mississippian |
| 5W0532117100000 | 760408 | 35083 | 5 | 1 | C | 29400 | -2300 | 3060 | 3390 | 696 | 582 | 449 | 1070 | - | Mississippian |
| 5W0542125060000 | 710313 | 35281 | 8 | 1 | C | 26600 | -2030 | 3200 | 3260 | 683 | 577 | 458 | 1170 | mud | Mississippian |
| 5W0611904100000 | 660304 | 36059 | 7 | 1 | C | 19700 | -1350 | 2300 | 2320 | 652 | 581 | 492 | 955 | water + mud + cond. | Mississippian |
| 5W0682031100000 | 890809 | 63321 | 1 | 1 | C | 14200 | -820 | 1530 | 1540 | 626 | 572 | 508 | 715 | water + mud + cond. + oil | Mississippian |
| 5W0571811100000 | 770404 | 35054 | 5 | 2 | C | 20900 | -1470 | 2790 | 2800 | 660 | 579 | 485 | 1320 | water + cond. + mud | Mississippian |
| 5W0562313040000 | 650210 | 35269 | 3 | 1 | C | 27500 | -2110 | 3240 | 3300 | 694 | 585 | 462 | 1130 | water+mud | Mississippian |
| 5W0531917090000 | 641102 | 35413 | 8 | 1 | C | 26300 | -2000 | 2970 | 2980 | 689 | 578 | 460 | 985 | - | Mississippian |
| 5W0491822100000 | 660419 | 35256 | 2 | 1 | C | 28600 | -2220 | 3260 | 3270 | 702 | 583 | 455 | 1050 | - | Mississippian |
| 5W0561635070000 | 950120 | -1736 | 1 | 1 | C | 19700 | -1350 | 2320 | 2330 | 659 | 581 | 492 | 979 | water | Mississippian |
| 5W0531922070000 | 731227 | 35264 | 3 | 1 | C | 25700 | -1930 | 2890 | 2930 | 689 | 589 | 473 | 963 | water | Mississippian |
| 5W0541710020000 | 650519 | 34873 | 4 | 1 | C | 22600 | -1630 | 2550 | 2560 | 674 | 585 | 484 | 922 | water | Mississippian |

Reproduced with permission of the copyright owner. Further reproduction prohibited without permission.

| Location | Date | Well ID | # | S | Q | p [kPa] | z [m] | dtop [m] | dbot [m] | $H_0$ | $H_{1040}$ | $H_{1090}$ | KB [m] | Fluid recovery | Aquifer |
|---|---|---|---|---|---|---|---|---|---|---|---|---|---|---|---|
| 5W0661519050000 | 700304 | 36049 | 2 | 1 | C | 13300 | -724 | 1690 | 1710 | 630 | 580 | 520 | 972 | water+mud | Mississippian |
| 5W0522013090000 | 760320 | 35200 | 1 | 1 | C | 27700 | -2120 | 3150 | 3160 | 700 | 595 | 471 | 1030 | mud | Mississippian |
| 5W0672220100000 | 720315 | 35650 | 3 | 1 | C | 18400 | -1220 | 1920 | 1940 | 655 | 583 | 501 | 701 | - | Mississippian |
| 5W0561909090000 | 740128 | 35174 | 8 | 1 | C | 23200 | -1690 | 2860 | 2910 | 680 | 584 | 480 | 1170 | mud | Mississippian |
| 5W0501609060000 | 670609 | 35121 | 3 | 2 | C | 25900 | -1950 | 2950 | 3010 | 694 | 589 | 472 | 1060 | water + cond. + oil | Mississippian |
| 5W0551716060000 | 770212 | 35071 | 1 | 2 | C | 21500 | -1510 | 2460 | 2490 | 677 | 597 | 501 | 953 | water + mud + cond. | Mississippian |
| 5W0521520040020 | 650128 | 34839 | 4 | 1 | C | 22800 | -1640 | 2560 | 2570 | 685 | 595 | 492 | 921 | mud | Mississippian |
| 5W0501712080000 | 681001 | 35245 | 1 | 1 | C | 26000 | -1950 | 2980 | 3030 | 701 | 598 | 482 | 1040 | water + mud + cond. | Mississippian |
| 5W0491836060000 | 660404 | 35165 | 2 | 1 | C | 27800 | -2110 | 3140 | 3180 | 721 | 615 | 490 | 1040 | water + cond. | Mississippian |
| 6W0610204070000 | 700619 | 38988 | 2 | 1 | C | 30000 | -2320 | 3630 | 3640 | 733 | 620 | 486 | 1310 | mud | Mississippian |
| 5W0511621060000 | 740428 | 35102 | 1 | 1 | C | 24700 | -1810 | 2820 | 2860 | 709 | 611 | 500 | 1020 | water | Mississippian |
| 5W0511609110000 | 650411 | 35039 | 6 | 1 | C | 24700 | -1800 | 2910 | 2920 | 715 | 621 | 510 | 1110 | water + cond. + mud | Mississippian |
| 5W0592419070000 | 620407 | 36582 | 7 | 1 | C | 26600 | -1990 | 3180 | 3230 | 725 | 617 | 498 | 1190 | mud + water + cond. | Mississippian |
| 5W0491712110000 | 740917 | 35395 | 8 | 1 | C | 27300 | -2060 | 3200 | 3220 | 731 | 616 | 493 | 1140 | - | Mississippian |
| 5W0521918100000 | 811005 | 34810 | 7 | 1 | C | 28200 | -2140 | 3170 | 3180 | 737 | 624 | 497 | 1030 | mud + cond. | Mississippian |
| 5W0481635100000 | 711016 | 35072 | 4 | 1 | C | 27100 | -2020 | 3150 | 3160 | 741 | 636 | 514 | 1130 | water + cond. | Mississippian |
| 5W0621908070000 | 830830 | 36849 | 1 | 1 | C | 19150 | -1260 | 2160 | 2190 | 705 | 617 | 531 | 907 | water+gas | Mississippian |
| 5W0602333060000 | 731016 | 35761 | 4 | 1 | C | 24000 | -1710 | 2780 | 2790 | 735 | 642 | 534 | 1070 | mud + water + cond. | Mississippian |
| 5W0502214020000 | 710808 | 35385 | 11 | 1 | C | 34200 | -2700 | 3910 | 3910 | 788 | 652 | 498 | 1200 | water | Mississippian |
| 5W0522002100000 | 810114 | 34799 | 2 | 1 | C | 28700 | -2170 | 3210 | 3260 | 762 | 643 | 514 | 1040 | water + cond. | Mississippian |
| 5W0592202100000 | 770107 | 35692 | 8 | 1 | C | 26000 | -1890 | 3020 | 3030 | 764 | 658 | 542 | 1130 | water+mud | Mississippian |
| 5W0542412070000 | 730417 | 35040 | 8 | 1 | C | 32800 | -2540 | 3730 | 3800 | 800 | 675 | 527 | 1260 | water | Mississippian |
| 5W0501618100000 | 630927 | 35158 | 1 | 1 | C | 25800 | -1910 | 2940 | 2980 | 786 | 619 | 503 | 1040 | water | Mississippian |
| 5W0481814040000 | 650714 | 35168 | 2 | 1 | C | 29500 | -2320 | 3460 | 3520 | 684 | 571 | 439 | 1140 | water+mud | Mississippian |
| 5W0482018060000 | 600305 | 35254 | 10 | 1 | C | 35900 | -2830 | 4110 | 4150 | 833 | 689 | 527 | 1320 | water + cond. | Mississippian |
| 5W0571606100000 | 761214 | 35001 | 12 | 1 | C | 20400 | -1390 | 2450 | 2470 | 769 | 610 | 518 | 1070 | water | Mississippian |
| 5W0471615060020 | 620501 | 34840 | 6 | 1 | C | 29500 | -2190 | 3460 | 3610 | 814 | 701 | 569 | 1270 | water + cond. + mud | Mississippian |
| 5W0471527110000 | 730211 | 35248 | 12 | 1 | C | 27900 | -2030 | 3190 | 3190 | 814 | 705 | 579 | 1170 | water | Mississippian |
| 5W0511813150000 | 641231 | 35140 | 1 | 1 | C | 26600 | -1990 | 2990 | 3000 | 825 | 617 | 498 | 1010 | mud | Mississippian |
| 5W0671924140000 | 740203 | 35702 | 2 | 1 | A | 22000 | -1510 | 2260 | 2300 | 734 | 646 | 547 | 768 | water | Wabamun |
| 5W0682033120000 | 670221 | 35609 | 5 | 1 | A | 23400 | -1600 | 2330 | 2350 | 786 | 694 | 588 | 744 | water | Wabamun |
| 5W0571723100000 | 760304 | 35369 | 4 | 1 | A | 25200 | -1730 | 2850 | 2860 | 838 | 740 | 627 | 1120 | mud + water | Wabamun |
| 5W0642417100000 | 770917 | 35565 | 5 | 1 | A | 30400 | -2210 | 3090 | 3090 | 895 | 770 | 633 | 882 | water + cond. + mud | Wabamun |
| 6W0690508050000 | 701013 | 38861 | 3 | 1 | A | 35200 | -2630 | 3230 | 3310 | 956 | 820 | 662 | 660 | water + mud | Wabamun |

| Location | Date | Well ID | # | S | Q | p [kPa] | z [m] | dtop [m] | dbot [m] | $H_0$ | $H_{1040}$ | $H_{1090}$ | KB [m] | Fluid recovery | Aquifer |
|---|---|---|---|---|---|---|---|---|---|---|---|---|---|---|---|
| 6W0680421100000 | 661223 | 38862 | 6 | 1 | A | 35800 | -2660 | 3300 | 3330 | 983 | 849 | 688 | 669 | water | Wabamun |
| 5W0611828080000 | 600305 | 36562 | 3 | 1 | B | 23800 | -1730 | 2640 | 2640 | 697 | 603 | 496 | 910 | water + cond. | Wabamun |
| 5W0651801100000 | 610116 | 36633 | 10 | 1 | B | 21900 | -1540 | 2320 | 2340 | 696 | 607 | 508 | 803 | mud + cond. + water | Wabamun |
| 5W0651911100000 | 601124 | 36620 | 5 | 1 | B | 23000 | -1630 | 2420 | 2440 | 719 | 624 | 521 | 812 | water | Wabamun |
| 5W0641814020000 | 640211 | 36104 | 1 | 1 | B | 21000 | -1440 | 2240 | 2260 | 707 | 618 | 524 | 821 | water + mud | Wabamun |
| 5W0651923020000 | 610309 | 36621 | 1 | 1 | B | 23100 | -1610 | 2420 | 2450 | 741 | 654 | 550 | 839 | water + mud | Wabamun |
| 5W0662109100000 | 641112 | 35619 | 5 | 1 | B | 25300 | -1780 | 2510 | 2520 | 807 | 700 | 586 | 741 | water | Wabamun |
| 5W0662028020000 | 690302 | 35701 | 5 | 1 | B | 24000 | -1650 | 2450 | 2480 | 791 | 702 | 594 | 801 | water + cond. + mud | Wabamun |
| 5W0692107030000 | 570405 | 36666 | 7 | 1 | B | 24700 | -1690 | 2330 | 2350 | 820 | 731 | 620 | 651 | water + cond. | Wabamun |
| 5W0571712020000 | 860402 | 68685 | 2 | 1 | B | 24400 | -1630 | 2720 | 2730 | 858 | 762 | 652 | 1100 | water + cond. + mud | Wabamun |
| 6W0680417060000 | 650321 | 38917 | 2 | 1 | B | 35700 | -2670 | 3350 | 3380 | 975 | 829 | 669 | 687 | water + mud | Wabamun |
| 6W0670414110000 | 820709 | 39215 | 3 | 1 | B | 36000 | -2680 | 3390 | 3460 | 989 | 849 | 687 | 718 | water + mud | Wabamun |
| 5W0651728010000 | 820226 | 36871 | 1 | 1 | C | 19600 | -1350 | 2240 | 2250 | 640 | 571 | 483 | 885 | mud + water + cond. | Wabamun |
| 5W0601625150000 | 570109 | 36691 | 6 | 1 | C | 21600 | -1510 | 2320 | 2330 | 699 | 607 | 510 | 814 | water + cond. | Wabamun |
| 5W0671834040000 | 630225 | 35540 | 4 | 1 | C | 21300 | -1440 | 2210 | 2230 | 731 | 648 | 552 | 775 | cond. + water + mud | Wabamun |
| 5W0681812100000 | 660419 | 35544 | 4 | 1 | C | 20600 | -1360 | 2290 | 2300 | 740 | 659 | 567 | 917 | water | Wabamun |
| 5W0692221040000 | 580623 | 36647 | 2 | 2 | C | 24500 | -1720 | 2410 | 2420 | 783 | 681 | 571 | 698 | water | Wabamun |
| 5W0662008100000 | 720321 | 36007 | 2 | 1 | C | 24400 | -1700 | 2440 | 2460 | 793 | 692 | 582 | 742 | water | Wabamun |
| 5W0632028020000 | 601212 | 36569 | 7 | 1 | C | 25900 | -1840 | 2620 | 2630 | 802 | 699 | 582 | 787 | water + cond. + mud | Wabamun |
| 5W0662402100000 | 620815 | 36619 | 3 | 1 | C | 28500 | -2060 | 2950 | 2960 | 841 | 733 | 605 | 897 | water + cond. + mud | Wabamun |
| 5W0692107030000 | 570403 | 36666 | 6 | 1 | C | 24300 | -1660 | 2300 | 2310 | 826 | 722 | 613 | 651 | water + mud + cond. | Wabamun |
| 5W0692106130000 | 560924 | 35684 | 3 | 1 | C | 25000 | -1710 | 2330 | 2350 | 844 | 740 | 628 | 643 | water + mud | Wabamun |
| 5W0632633040000 | 641201 | 35697 | 2 | 1 | C | 33000 | -2460 | 3350 | 3360 | 910 | 775 | 626 | 899 | oil | Wabamun |
| 5W0662502110000 | 660321 | 36175 | 2 | 1 | C | 30100 | -2160 | 2950 | 2980 | 914 | 790 | 655 | 792 | mud | Wabamun |
| 6W0690521100000 | 690320 | 38920 | 2 | 1 | C | 35300 | -2650 | 3300 | 3320 | 947 | 810 | 651 | 661 | water + mud + cond. | Wabamun |
| 6W0680404060000 | 681129 | 38919 | 2 | 2 | C | 35400 | -2650 | 3370 | 3420 | 959 | 820 | 661 | 727 | water + cond. | Wabamun |
| 6W0640415060000 | 621215 | 38878 | 7 | 2 | C | 38500 | -2930 | 3820 | 3830 | 1000 | 844 | 671 | 887 | water + cond. | Wabamun |
| 6W0670420100000 | 660411 | 38916 | 1 | 1 | C | 36400 | -2720 | 3310 | 3350 | 990 | 848 | 684 | 601 | water + cond. + mud | Wabamun |
| 6W0630131040000 | 670915 | 38974 | 2 | 1 | C | 36000 | -2670 | 3550 | 3570 | 998 | 859 | 697 | 889 | water | Wabamun |
| 5W0571926040000 | 651122 | 35122 | 1 | 1 | C | 29400 | -1950 | 3050 | 3060 | 1045 | 932 | 799 | 1100 | water | Wabamun |
| 5W0522123130000 | 810308 | 34860 | 4 | 1 | C | 37100 | -2660 | 3730 | 3760 | 1121 | 976 | 810 | 1060 | water + mud + cond. | Wabamun |
| 5W0661519050000 | 700301 | 36049 | 1 | 1 | A | 20600 | -1400 | 2380 | 2390 | 703 | 619 | 527 | 972 | oil + cond. + mud | Winterburn |
| 5W0671502010000 | 710308 | 35728 | 1 | 1 | A | 20600 | -1320 | 2320 | 2360 | 779 | 699 | 607 | 990 | oil | Winterburn |
| 5W0652114060000 | 670818 | 36738 | 5 | 1 | A | 26300 | -1840 | 2610 | 2620 | 840 | 738 | 620 | 780 | water + mud | Winterburn |



Reproduced with permission of the copyright owner. Further reproduction prohibited without permission.

Reproduced with permission of the copyright owner. Further reproduction prohibited without permission.



| Location | Date | Well ID | # | S | Q | p [kPa] | z [m] | dtop [m] | dbot [m] | $H_0$ | $H_{1040}$ | $H_{1090}$ | KB [m] | Fluid recovery | Aquifer |
|---|---|---|---|---|---|---|---|---|---|---|---|---|---|---|---|
| 5W0681709100000 | 650310 | 35757 | 4 | 1 | A | 22200 | -1430 | 2330 | 2340 | 836 | 746 | 646 | 907 | water + mud | Winterburn |
| 5W0562118060000 | 780510 | 35405 | 3 | 1 | A | 34900 | -2590 | 3610 | 3630 | 970 | 831 | 674 | 1020 | water + cond. + mud | Winterburn |
| 5W0501520060000 | 780713 | 35384 | 2 | 1 | B | 29100 | -2260 | 3260 | 3320 | 706 | 592 | 461 | 1020 | water | Winterburn |
| 5W0641804020000 | 611103 | 36624 | 5 | 1 | B | 23500 | -1670 | 2450 | 2460 | 728 | 633 | 528 | 791 | water + cond. | Winterburn |
| 5W0642316100000 | 760209 | 36093 | 2 | 1 | B | 29000 | -2110 | 2920 | 2940 | 839 | 732 | 602 | 805 | water + cond. + mud | Winterburn |
| 5W0632202020000 | 630315 | 35972 | 3 | 1 | B | 28900 | -2090 | 2950 | 2960 | 855 | 743 | 613 | 871 | water + oil | Winterburn |
| 6W0630131040000 | 671025 | 38974 | 5 | 1 | B | 36400 | -2790 | 3590 | 3790 | 919 | 778 | 614 | 889 | mud + water | Winterburn |
| 5W0641802040000 | 590328 | 36085 | 6 | 1 | B | 30700 | -2240 | 3040 | 3070 | 889 | 769 | 631 | 821 | water + mud | Winterburn |
| 6W0680513110000 | 640418 | 38908 | 3 | 1 | B | 36400 | -2750 | 3300 | 3330 | 961 | 818 | 654 | 578 | water + mud | Winterburn |
| 6W0680403100000 | 660302 | 38912 | 5 | 1 | B | 35800 | -2690 | 3410 | 3480 | 954 | 819 | 658 | 728 | water | Winterburn |
| 5W0581715060000 | 590212 | 35635 | 2 | 1 | B | 27500 | -1900 | 3060 | 3080 | 900 | 795 | 672 | 1180 | water | Winterburn |
| 5W0541919020000 | 660412 | 35215 | 4 | 1 | B | 33700 | -2480 | 3520 | 3540 | 948 | 823 | 672 | 1040 | water + mud | Winterburn |
| 5W0651917100000 | 590304 | 36657 | 8 | 1 | B | 25700 | -1720 | 2450 | 2460 | 900 | 799 | 683 | 743 | water + oil + mud | Winterburn |
| 6W0630213120000 | 641114 | 38969 | 4 | 1 | B | 37000 | -2780 | 3780 | 3850 | 989 | 847 | 680 | 991 | water + mud | Winterburn |
| 6W0670531070000 | 680322 | 39031 | 4 | 1 | B | 38600 | -2930 | 3500 | 3610 | 1014 | 853 | 680 | 685 | water + mud | Winterburn |
| 5W0651921060000 | 780903 | 35723 | 4 | 1 | B | 25500 | -1690 | 2470 | 2490 | 910 | 809 | 695 | 790 | water | Winterburn |
| 6W0660436060000 | 680314 | 38864 | 3 | 1 | B | 37900 | -2860 | 3490 | 3610 | 1007 | 855 | 684 | 753 | water | Winterburn |
| 5W0651911040000 | 600901 | 36733 | 8 | 1 | B | 25400 | -1680 | 2470 | 2480 | 907 | 810 | 695 | 794 | water + mud + oil + cond. | Winterburn |
| 5W0471408040000 | 800205 | 34966 | 5 | 1 | B | 34800 | -2530 | 3750 | 3780 | 1021 | 881 | 724 | 1230 | mud + water + cond. | Winterburn |
| 5W0501520090000 | 810923 | 34758 | 1 | 1 | C | 29100 | -2270 | 3260 | 3270 | 701 | 582 | 451 | 993 | water | Winterburn |
| 5W0661625080000 | 660222 | 35990 | 3 | 1 | C | 20500 | -1400 | 2280 | 2280 | 683 | 609 | 517 | 875 | oil + mud + water + cond. | Winterburn |
| 5W0641814020000 | 640215 | 36104 | 2 | 1 | C | 22700 | -1600 | 2430 | 2460 | 711 | 625 | 523 | 821 | water + cond. | Winterburn |
| 5W0661614020000 | 660405 | 36774 | 1 | 1 | C | 21100 | -1430 | 2290 | 2300 | 720 | 638 | 543 | 856 | water | Winterburn |
| 5W0641804020000 | 611106 | 36624 | 6 | 1 | C | 24000 | -1700 | 2500 | 2510 | 741 | 652 | 544 | 791 | water + cond. + mud | Winterburn |
| 5W0631818020000 | 591121 | 36330 | 7 | 1 | C | 24400 | -1730 | 2520 | 2530 | 758 | 662 | 552 | 799 | water + mud | Winterburn |
| 5W0661411120000 | 590214 | 36392 | 5 | 1 | C | 19400 | -1250 | 2410 | 2420 | 733 | 652 | 564 | 1160 | water + mud | Winterburn |
| 5W0692105090020 | 571124 | 36811 | 2 | 1 | C | 24200 | -1700 | 2360 | 2360 | 767 | 672 | 563 | 663 | water + cond. | Winterburn |
| 5W0681919160000 | 620227 | 35998 | 3 | 1 | C | 23500 | -1600 | 2350 | 2360 | 796 | 703 | 598 | 759 | mud + water + cond. | Winterburn |
| 5W0662502110000 | 660323 | 36175 | 3 | 1 | C | 30100 | -2210 | 3000 | 3050 | 856 | 740 | 605 | 792 | water + mud | Winterburn |
| 5W0652425100000 | 651003 | 36070 | 2 | 1 | C | 28900 | -2090 | 2940 | 2970 | 851 | 743 | 613 | 856 | water + mud | Winterburn |
| 6W0630101100000 | 601016 | 39110 | 7 | 2 | C | 35100 | -2660 | 3650 | 3690 | 916 | 780 | 623 | 1010 | mud + cond. + water | Winterburn |
| 5W0551817020000 | 800909 | 34993 | 3 | 1 | C | 31700 | -2330 | 3320 | 3360 | 901 | 777 | 635 | 989 | water + cond. | Winterburn |
| 5W0662008100000 | 720305 | 36007 | 1 | 1 | C | 25700 | -1760 | 2490 | 2500 | 859 | 759 | 643 | 742 | mud + water | Winterburn |
| 5W0591633100000 | 660119 | 35665 | 2 | 1 | C | 25600 | -1750 | 2670 | 2680 | 851 | 759 | 644 | 924 | water | Winterburn |

Reproduced with permission of the copyright owner. Further reproduction prohibited without permission.



| Location | Date | Well ID | # | S | Q | p [kPa] | z [m] | dtop [m] | dbot [m] | $H_0$ | $H_{1040}$ | $H_{1090}$ | KB [m] | Fluid recovery | Aquifer |
|---|---|---|---|---|---|---|---|---|---|---|---|---|---|---|---|
| 5W0551816060000 | 590326 | 35356 | 5 | 1 | C | 30500 | -2210 | 3180 | 3190 | 899 | 779 | 642 | 977 | water | Winterburn |
| 5W0621726100000 | 640214 | 35962 | 2 | 1 | C | 24200 | -1610 | 2530 | 2550 | 850 | 762 | 653 | 932 | water + cond. | Winterburn |
| 5W0601622090002 | 950816 | -2075 | 1 | 1 | C | 23300 | -1520 | 2350 | 2500 | 852 | 764 | 659 | 824 | water + mud | Winterburn |
| 5W0632109100000 | 680126 | 35997 | 3 | 1 | C | 28400 | -2000 | 2800 | 2860 | 890 | 784 | 656 | 808 | mud | Winterburn |
| 5W0652334100000 | 721009 | 35746 | 3 | 1 | C | 28200 | -1980 | 2720 | 2760 | 885 | 784 | 657 | 742 | water+ mud + cond. | Winterburn |
| 5W0542011100000 | 700308 | 35389 | 2 | 1 | C | 33900 | -2500 | 3590 | 3620 | 949 | 823 | 670 | 1090 | water | Winterburn |
| 6W0661219080000 | 700901 | 80070 | 1 | 2 | C | 49400 | -3950 | 4980 | 5180 | 1086 | 892 | 670 | 1010 | water+ mud + cond. | Winterburn |
| 5W0592434040000 | 630614 | 35534 | 5 | 1 | C | 34600 | -2550 | 3670 | 3760 | 974 | 841 | 686 | 1130 | water + cond. | Winterburn |
| 5W0621916040000 | 590426 | 35775 | 11 | 1 | C | 27000 | -1830 | 2710 | 2720 | 921 | 816 | 695 | 874 | mud + water | Winterburn |
| 5W0651923080000 | 830216 | 35509 | 3 | 1 | C | 25000 | -1640 | 2490 | 2520 | 907 | 810 | 698 | 849 | water + cond. + mud | Winterburn |
| 5W0541919020000 | 660414 | 35215 | 5 | 1 | C | 33300 | -2420 | 3450 | 3490 | 974 | 844 | 694 | 1040 | water | Winterburn |
| 5W0651923080000 | 830212 | 35509 | 2 | 2 | C | 25200 | -1650 | 2490 | 2520 | 923 | 820 | 707 | 849 | mud + oil + cond. | Winterburn |
| 5W0631918100000 | 621019 | 35999 | 3 | 1 | C | 27400 | -1830 | 2620 | 2640 | 964 | 856 | 732 | 791 | water + cond. + mud | Winterburn |
| 5W0622023060000 | 670901 | 35989 | 3 | 1 | C | 28300 | -1900 | 2770 | 2790 | 985 | 874 | 747 | 880 | water + cond. + mud | Winterburn |
| 5W0551919140020 | 690221 | 35337 | 3 | 1 | C | 33000 | -2330 | 3520 | 3620 | 1034 | 905 | 756 | 1150 | water | Winterburn |
| 5W0681714060000 | 770307 | 35571 | 3 | 1 | C | 22700 | -1370 | 2260 | 2290 | 944 | 855 | 753 | 893 | water + mud | Winterburn |
| 5W0591626070000 | 770206 | 35879 | 4 | 1 | C | 24100 | -1730 | 2620 | 2640 | 722 | 632 | 524 | 891 | mud + water | Winterburn |
| 5W0582026040000 | 630222 | 36354 | 8 | 1 | A | 32300 | -2360 | 3280 | 3290 | 932 | 806 | 661 | 929 | water + cond. | Woodbend |
| 6W0630131040000 | 671026 | 38974 | 6 | 1 | A | 38100 | -2900 | 3720 | 3790 | 982 | 834 | 663 | 889 | water + mud | Woodbend |
| 5W0602110060000 | 650228 | 35658 | 1 | 1 | A | 33700 | -2470 | 3460 | 3480 | 963 | 833 | 682 | 1010 | water + cond. | Woodbend |
| 5W0591631040000 | 650312 | 36411 | 6 | 1 | B | 27000 | -1880 | 2850 | 2870 | 872 | 766 | 645 | 975 | water | Woodbend |
| 5W0561622090000 | 691113 | 35293 | 3 | 1 | B | 29600 | -2120 | 3080 | 3120 | 901 | 781 | 648 | 962 | water + cond. | Woodbend |
| 5W0551817100000 | 650412 | 35290 | 3 | 1 | B | 31900 | -2330 | 3310 | 3330 | 915 | 797 | 653 | 988 | water | Woodbend |
| 5W0592007110000 | 620516 | 35890 | 1 | 1 | B | 32100 | -2340 | 3450 | 3460 | 935 | 806 | 662 | 1110 | water + cond. | Woodbend |
| 5W0592017100000 | 610418 | 35898 | 5 | 1 | B | 33000 | -2420 | 3520 | 3530 | 945 | 815 | 666 | 1100 | water | Woodbend |
| 5W0571629100000 | 610516 | 34938 | 9 | 1 | B | 29200 | -2060 | 3130 | 3140 | 912 | 802 | 671 | 1080 | water + cond. | Woodbend |
| 5W0632522040000 | 850330 | 36983 | 1 | 1 | B | 36200 | -2720 | 3580 | 3600 | 975 | 828 | 665 | 869 | water + mud | Woodbend |
| 5W0592434040000 | 630623 | 35534 | 8 | 1 | B | 36600 | -2730 | 3850 | 3900 | 1008 | 857 | 693 | 1130 | water + cond. | Woodbend |
| 5W0592434040000 | 630618 | 35534 | 7 | 1 | B | 36200 | -2690 | 3810 | 3830 | 994 | 858 | 695 | 1130 | water + cond. | Woodbend |
| 5W0522116160000 | 770515 | 35331 | 6 | 1 | B | 39700 | -3020 | 4110 | 4120 | 1021 | 871 | 693 | 1100 | water + cond. | Woodbend |
| 5W0602632100000 | 690905 | 36692 | 6 | 1 | B | 38300 | -2850 | 4080 | 4090 | 1055 | 904 | 732 | 1240 | water | Woodbend |
| 6W0670712120000 | 701231 | 38976 | 1 | 1 | B | 41500 | -3140 | 4070 | 4080 | 1086 | 928 | 741 | 928 | water | Woodbend |
| 5W0692325030000 | 560111 | 35849 | 1 | 1 | C | 27600 | -1980 | 2720 | 2730 | 835 | 725 | 601 | 748 | water | Woodbend |
| 5W0692210070000 | 560526 | 36265 | 1 | 1 | C | 27000 | -1920 | 2590 | 2590 | 831 | 726 | 605 | 668 | oil | Woodbend |

| Location | Date | Well ID | # | S | Q | p [kPa] | z [m] | dtop [m] | dbot [m] | $H_0$ | $H_{1040}$ | $H_{1090}$ | KB [m] | Fluid recovery | Aquifer |
|---|---|---|---|---|---|---|---|---|---|---|---|---|---|---|---|
| 5W0632509120000 | 581101 | 35653 | 3 | 1 | C | 35300 | -2680 | 3500 | 3510 | 921 | 780 | 621 | 833 | oil + mud | Woodbend |
| 5W0602320100000 | 600319 | 36581 | 4 | 1 | C | 34000 | -2540 | 3550 | 3560 | 935 | 793 | 640 | 1030 | water + cond. | Woodbend |
| 5W0541814070000 | 860419 | 68686 | 1 | 1 | C | 31500 | -2300 | 3290 | 3300 | 912 | 788 | 646 | 984 | mud | Woodbend |
| 5W0591631040000 | 650308 | 36411 | 5 | 2 | C | 26100 | -1790 | 2760 | 2770 | 870 | 768 | 651 | 975 | water | Woodbend |
| 5W0552226080020 | 660719 | 34891 | 8 | 1 | C | 38000 | -2910 | 3840 | 3850 | 959 | 815 | 644 | 929 | n/a | Woodbend |
| 5W0532008100000 | 630330 | 35350 | 3 | 1 | C | 35900 | -2710 | 3740 | 3750 | 950 | 809 | 647 | 1040 | water | Woodbend |
| 5W0552226080020 | 660707 | 34891 | 3 | 1 | C | 38400 | -2940 | 3860 | 3900 | 982 | 824 | 651 | 929 | n/a | Woodbend |
| 5W0601415060000 | 700116 | 35691 | 6 | 1 | C | 27300 | -1890 | 2660 | 2670 | 889 | 786 | 663 | 764 | oil + cond. + mud | Woodbend |
| 5W0551920100000 | 660223 | 35391 | 5 | 1 | C | 34300 | -2550 | 3650 | 3670 | 955 | 812 | 658 | 1130 | water + cond. | Woodbend |
| 5W0512030060000 | 710604 | 35386 | 5 | 1 | C | 38800 | -2970 | 4050 | 4200 | 994 | 833 | 659 | 1080 | water | Woodbend |
| 5W0551914020000 | 580223 | 34941 | 5 | 2 | C | 33200 | -2440 | 3440 | 3470 | 940 | 814 | 665 | 990 | water | Woodbend |
| 5W0551923120000 | 690124 | 35283 | 1 | 1 | C | 33200 | -2440 | 3520 | 3520 | 946 | 814 | 665 | 1080 | water | Woodbend |
| 5W0601722100000 | 581015 | 35935 | 4 | 1 | C | 29400 | -2080 | 2860 | 2870 | 921 | 802 | 669 | 792 | water + cond. | Woodbend |
| 5W0601620120000 | 630924 | 35936 | 3 | 1 | C | 26900 | -1840 | 2660 | 2660 | 896 | 797 | 676 | 816 | water | Woodbend |
| 5W0632509120000 | 581031 | 35653 | 2 | 1 | C | 35600 | -2660 | 3480 | 3500 | 968 | 829 | 669 | 833 | cond. + oil + mud | Woodbend |
| 5W0592434040000 | 630616 | 35534 | 6 | 1 | C | 35400 | -2640 | 3760 | 3780 | 971 | 830 | 671 | 1130 | water + cond. | Woodbend |
| 5W0541719110000 | 711012 | 34872 | 3 | 1 | C | 31400 | -2260 | 3190 | 3200 | 942 | 818 | 677 | 942 | mud | Woodbend |
| 5W0622633100000 | 590910 | 36250 | 2 | 1 | C | 36400 | -2730 | 3640 | 3650 | 988 | 838 | 674 | 924 | water + mud | Woodbend |
| 5W0632604160000 | 600317 | 35633 | 4 | 1 | C | 36000 | -2690 | 3610 | 3630 | 972 | 839 | 677 | 934 | water + cond. + mud | Woodbend |
| 5W0592419070000 | 620527 | 36582 | 15 | 1 | C | 37000 | -2780 | 3980 | 3990 | 993 | 847 | 680 | 1190 | water | Woodbend |
| 6W0670432100000 | 650521 | 38894 | 10 | 1 | C | 39700 | -3030 | 3720 | 3760 | 1008 | 861 | 683 | 693 | water + cond. + mud | Woodbend |
| 5W0592007110000 | 620518 | 35890 | 2 | 2 | C | 32700 | -2360 | 3470 | 3480 | 966 | 845 | 698 | 1110 | mud | Woodbend |
| 6W0630101100000 | 601022 | 39110 | 9 | 1 | C | 37300 | -2790 | 3790 | 3820 | 1011 | 866 | 698 | 1010 | water + cond. + mud | Woodbend |
| 5W0632509070000 | 860212 | 50843 | 1 | 1 | C | 36300 | -2690 | 3530 | 3550 | 1011 | 868 | 705 | 836 | water + mud | Woodbend |
| 6W0580114060000 | 790303 | 39196 | 1 | 1 | C | 42800 | -3300 | 4490 | 4520 | 1060 | 895 | 703 | 1190 | water + cond. | Woodbend |
| 5W0582513130000 | 680322 | 35668 | 6 | 1 | C | 38200 | -2860 | 3900 | 3970 | 1031 | 884 | 712 | 1050 | water + cond. | Woodbend |
| 5W0492235070000 | 810307 | -1735 | 7 | 1 | C | 44000 | -3400 | 4650 | 4840 | 1092 | 913 | 715 | 1240 | mud | Woodbend |
| 5W0522023060000 | 800514 | 34944 | 5 | 2 | C | 37600 | -2790 | 3800 | 3810 | 1045 | 895 | 726 | 1020 | mud | Woodbend |
| 6W0610204070000 | 700720 | 38988 | 4 | 1 | C | 42000 | -3200 | 4510 | 4550 | 1076 | 917 | 728 | 1310 | water | Woodbend |
| 5W0551729150000 | 541013 | 34923 | 18 | 1 | C | 30900 | -2150 | 3200 | 3200 | 1005 | 879 | 740 | 1060 | cond. | Woodbend |
| 5W0581928110000 | 600207 | 35708 | 4 | 1 | C | 33200 | -2360 | 3310 | 3320 | 1029 | 894 | 745 | 966 | water + cond. | Woodbend |
| 5W0532312060000 | 781203 | 35388 | 7 | 1 | C | 43600 | -3340 | 4370 | 4380 | 1101 | 934 | 737 | 1020 | n/a | Woodbend |
| 6W0620934090000 | 761217 | 38873 | 5 | 1 | C | 48900 | -3830 | 5240 | 5530 | 1150 | 963 | 743 | 1410 | water + cond. + mud | Woodbend |
| 6W0610433070000 | 730514 | 39146 | 1 | 1 | C | 44000 | -3360 | 4430 | 4460 | 1128 | 953 | 755 | 1100 | water | Woodbend |



Reproduced with permission of the copyright owner. Further reproduction prohibited without permission.

Reproduced with permission of the copyright owner. Further reproduction prohibited without permission.



| Location | Date | Well ID | # | S | Q | p [kPa] | z [m] | dtop [m] | dbot [m] | $H_0$ | $H_{1040}$ | $H_{1090}$ | KB [m] | Fluid recovery | Aquifer |
|---|---|---|---|---|---|---|---|---|---|---|---|---|---|---|---|
| 5W0561932010000 | 560517 | 35411 | 17 | 1 | C | 32700 | -2320 | 3630 | 3650 | 1010 | 885 | 738 | 1330 | water + cond. | Woodbend |
| 5W0571728070000 | 680408 | 35294 | 3 | 1 | B | 31300 | -2300 | 3550 | 3610 | 900 | 768 | 627 | 1260 | water | Beaverhill Lake |
| 5W0591929060000 | 611008 | 36542 | 8 | 1 | B | 33400 | -2490 | 3460 | 3480 | 912 | 784 | 634 | 991 | water | Beaverhill Lake |
| 5W0611828080000 | 600325 | 36562 | 4 | 1 | B | 31900 | -2340 | 3230 | 3250 | 912 | 787 | 643 | 910 | water | Beaverhill Lake |
| 5W0581516060000 | 790308 | 35789 | 3 | 1 | B | 29900 | -2140 | 3150 | 3180 | 907 | 791 | 656 | 1010 | water | Beaverhill Lake |
| 5W0601807100000 | 680127 | 36712 | 5 | 1 | B | 33400 | -2470 | 3340 | 3360 | 925 | 804 | 654 | 864 | water | Beaverhill Lake |
| 5W0541719110000 | 711024 | 34872 | 5 | 1 | B | 34400 | -2560 | 3500 | 3540 | 951 | 812 | 657 | 942 | mud | Beaverhill Lake |
| 5W0612332060000 | 700902 | 35955 | 2 | 1 | B | 36100 | -2720 | 3760 | 3790 | 960 | 818 | 656 | 1060 | water + mud | Beaverhill Lake |
| 5W0601722100000 | 581021 | 35935 | 5 | 1 | B | 31000 | -2230 | 3020 | 3030 | 934 | 809 | 669 | 792 | water | Beaverhill Lake |
| 5W0521610060000 | 690415 | 34886 | 2 | 1 | B | 35800 | -2680 | 3630 | 3660 | 971 | 829 | 668 | 953 | water + cond. + mud | Beaverhill Lake |
| 5W0641804020000 | 611122 | 36624 | 7 | 1 | B | 30300 | -2160 | 2910 | 2950 | 933 | 810 | 674 | 791 | water | Beaverhill Lake |
| 5W0632109100000 | 680115 | 35997 | 1 | 1 | B | 33400 | -2450 | 3250 | 3260 | 954 | 824 | 674 | 808 | water+ mud + cond. | Beaverhill Lake |
| 5W0581511060000 | 761219 | 35055 | 3 | 1 | B | 30300 | -2150 | 3290 | 3300 | 938 | 820 | 684 | 1130 | water | Beaverhill Lake |
| 5W0531522040000 | 630427 | 35096 | 7 | 1 | B | 33400 | -2440 | 3360 | 3370 | 969 | 834 | 684 | 927 | water + cond. | Beaverhill Lake |
| 5W0621906140000 | 380803 | 36253 | 1 | 1 | B | 32600 | -2360 | 3220 | 3290 | 970 | 835 | 689 | 869 | water + cond. | Beaverhill Lake |
| 5W0641804100000 | 610908 | 36625 | 1 | 1 | B | 30400 | -2130 | 2930 | 2960 | 972 | 850 | 713 | 797 | oil | Beaverhill Lake |
| 5W0692519070030 | 820920 | 35510 | 1 | 1 | C | 32900 | -2460 | 3220 | 3230 | 898 | 765 | 617 | 769 | water+ mud + cond. | Beaverhill Lake |
| 5W0631825100000 | 630412 | 36343 | 7 | 2 | C | 29800 | -2160 | 2950 | 2980 | 883 | 761 | 627 | 821 | water+ mud + cond. | Beaverhill Lake |
| 5W0541632100000 | 691121 | 34874 | 1 | 1 | C | 33300 | -2480 | 3370 | 3390 | 918 | 784 | 634 | 890 | water + mud | Beaverhill Lake |
| 5W0581936060000 | 610414 | 36543 | 3 | 1 | C | 32600 | -2400 | 3440 | 3450 | 923 | 795 | 649 | 1050 | water | Beaverhill Lake |
| 5W0631927080000 | 880305 | 50839 | 3 | 1 | C | 30600 | -2210 | 3010 | 3020 | 909 | 789 | 652 | 800 | mud + oil + water | Beaverhill Lake |
| 5W0611919020000 | 580313 | 35712 | 9 | 1 | C | 32300 | -2370 | 3270 | 3270 | 922 | 796 | 651 | 897 | water | Beaverhill Lake |
| 5W0601805070000 | 680820 | 35557 | 3 | 1 | C | 32200 | -2360 | 3220 | 3230 | 923 | 796 | 651 | 862 | water+ mud + cond. | Beaverhill Lake |
| 5W0652023100000 | 790121 | 36737 | 3 | B1 | C | 31300 | -2270 | 3010 | 3040 | 922 | 798 | 657 | 768 | water+ mud + cond. | Beaverhill Lake |
| 5W0622021110000 | 620106 | 36574 | 9 | 1 | C | 32400 | -2370 | 3210 | 3220 | 936 | 806 | 660 | 851 | water | Beaverhill Lake |
| 5W0622024040000 | 600224 | 36575 | 3 | 2 | C | 32400 | -2370 | 3250 | 3260 | 942 | 806 | 660 | 891 | water + cond. | Beaverhill Lake |
| 5W0601807100000 | 680123 | 36712 | 4 | 1 | C | 32400 | -2370 | 3220 | 3230 | 935 | 806 | 660 | 864 | cond. + water | Beaverhill Lake |
| 5W0481901060000 | 730215 | 35167 | 3 | 1 | C | 44000 | -3460 | 4580 | 4590 | 1016 | 853 | 655 | 1120 | water + mud | Beaverhill Lake |
| 5W0541528100000 | 710627 | 35280 | 2 | 1 | C | 32800 | -2400 | 3250 | 3260 | 945 | 815 | 667 | 861 | mud + cond. | Beaverhill Lake |
| 5W0531522040000 | 650502 | 35096 | 9 | 1 | C | 33200 | -2430 | 3350 | 3360 | 955 | 824 | 675 | 927 | water + mud | Beaverhill Lake |
| 5W0672208160000 | 840928 | 36962 | 1 | 1 | C | 32700 | -2380 | 3100 | 3130 | 950 | 825 | 678 | 718 | water + mud | Beaverhill Lake |
| 5W0601924060000 | 680122 | 35993 | 1 | 1 | C | 32400 | -2350 | 3370 | 3370 | 952 | 826 | 680 | 1020 | mud + water + cond. | Beaverhill Lake |
| 5W0641810040000 | 611224 | 36627 | 6 | 1 | C | 30400 | -2160 | 2950 | 2960 | 945 | 820 | 683 | 804 | mud + cond. + oil | Beaverhill Lake |
| 5W0531522040000 | 630423 | 35096 | 4 | 1 | C | 33600 | -2460 | 3400 | 3400 | 963 | 833 | 682 | 927 | water + mud | Beaverhill Lake |

Reproduced with permission of the copyright owner. Further reproduction prohibited without permission.



| Location | Date | Well ID | # | S | Q | p [kPa] | z [m] | dtop [m] | dbot [m] | $H_0$ | $H_{1040}$ | $H_{1090}$ | KB [m] | Fluid recovery | Aquifer |
|---|---|---|---|---|---|---|---|---|---|---|---|---|---|---|---|
| 5W0541505070000 | 690414 | 35279 | 3 | 1 | C | 33400 | -2440 | 3320 | 3370 | 969 | 834 | 684 | 891 | water + cond. + mud | Beaverhill Lake |
| 5W0631825120000 | 731017 | 36109 | 1 | 1 | C | 29800 | -2100 | 2900 | 2990 | 933 | 821 | 687 | 805 | cond. + mud + water | Beaverhill Lake |
| 5W0592519140000 | 800518 | 36486 | 3 | 1 | C | 40500 | -3100 | 4370 | 4380 | 1029 | 870 | 688 | 1270 | water+ mud + cond. | Beaverhill Lake |
| 5W0632202020000 | 630325 | 35972 | 4 | 1 | C | 34200 | -2500 | 3370 | 3380 | 982 | 852 | 698 | 871 | water | Beaverhill Lake |
| 5W0632106100000 | 640203 | 35759 | 5 | 1 | C | 34100 | -2480 | 3320 | 3320 | 990 | 862 | 709 | 836 | water | Beaverhill Lake |
| 5W0671815100000 | 630122 | 36317 | 1 | 1 | C | 29300 | -2020 | 2820 | 2860 | 973 | 852 | 720 | 814 | water + oil + cond. | Beaverhill Lake |
| 5W0511727100000 | 580520 | 34920 | 9 | 1 | C | 38000 | -2840 | 3810 | 3850 | 1032 | 885 | 714 | 1000 | water | Beaverhill Lake |
| 5W0541723100000 | 720327 | 35098 | 5 | 1 | C | 34400 | -2480 | 3420 | 3450 | 1028 | 892 | 737 | 942 | mud + water + cond. | Beaverhill Lake |
| 5W0612403100000 | 590501 | 36565 | 11 | 1 | C | 38400 | -2840 | 3960 | 3970 | 1075 | 924 | 751 | 1130 | water + mud | Beaverhill Lake |
| 5W0652423100000 | 631016 | 35733 | 4 | 1 | C | 35700 | -2580 | 3420 | 3440 | 1058 | 919 | 759 | 864 | cond. + oil | Beaverhill Lake |
| 5W0671803040000 | 631013 | 36274 | 2 | 1 | C | 29300 | -2040 | 2810 | 2860 | 941 | 832 | 700 | 813 | oil + mud | Beaverhill Lake |
| 5W0631933070000 | 570921 | 35637 | 6 | 2 | C | 32200 | -2210 | 3000 | 3020 | 1071 | 946 | 801 | 793 | mud + cond. | Beaverhill Lake |
| 5W0652023100000 | 790117 | 36737 | 5 | 1 | A | 31400 | -2280 | 3040 | 3050 | 925 | 798 | 657 | 768 | water + cond. + mud | Elk Point |
| 5W0521418080000 | 810405 | 34796 | 6 | 1 | B | 34400 | -2530 | 3500 | 3530 | 970 | 842 | 687 | 961 | water + cond. | Elk Point |
| 5W0651801100000 | 610204 | 36633 | 14 | 1 | B | 29400 | -2130 | 2940 | 2950 | 864 | 752 | 619 | 803 | cond. | Elk Point |
| 5W0661411120000 | 590226 | 36392 | 9 | 1 | B | 26000 | -1800 | 2970 | 2970 | 857 | 748 | 632 | 1160 | water | Elk Point |
| 5W0661832040000 | 641204 | 35620 | 3 | 1 | B | 29300 | -2100 | 2870 | 2880 | 879 | 772 | 640 | 765 | water + mud | Elk Point |
| 5W0662109100000 | 641125 | 35619 | 6 | 1 | B | 32100 | -2360 | 3090 | 3100 | 918 | 786 | 642 | 741 | water + mud | Elk Point |
| 5W0682114160000 | 850901 | 37007 | 2 | 1 | B | 30600 | -2220 | 2930 | 2930 | 900 | 779 | 642 | 709 | oil + cond. + water | Elk Point |
| 5W0511727100000 | 580520 | 34920 | 10 | 1 | C | 39400 | -2910 | 3900 | 3920 | 1106 | 952 | 775 | 1000 | - | Elk Point |
| 5W0611517150000 | 740119 | 35657 | 2 | 1 | C | 30100 | -2160 | 3010 | 3020 | 908 | 790 | 655 | 862 | - | Elk Point |
| 5W0621916040000 | 590420 | 35775 | 6 | 1 | C | 32600 | -2380 | 3250 | 3260 | 937 | 815 | 669 | 874 | water | Elk Point |
| 5W0632028020000 | 601230 | 36569 | 8 | 1 | C | 32600 | -2400 | 3200 | 3200 | 923 | 795 | 649 | 787 | water | Elk Point |
| 5W0641805050000 | 570914 | 36626 | 10 | 1 | C | 31000 | -2230 | 3030 | 3030 | 928 | 809 | 669 | 793 | water + cond. + oil | Elk Point |
| 5W0642401120000 | 611027 | 36683 | 3 | 1 | C | 36100 | -2730 | 3580 | 3600 | 947 | 808 | 646 | 861 | mud + oil + water | Elk Point |
| 5W0651522020000 | 590321 | 36729 | 3 | A1 | C | 27100 | -1930 | 2910 | 2920 | 832 | 726 | 604 | 993 | water | Elk Point |
| 5W0652304040000 | 641116 | 36795 | 2 | 1 | C | 34800 | -2620 | 3400 | 3410 | 926 | 791 | 634 | 780 | water + oil + mud + cond. | Elk Point |
| 5W0671530100000 | 650221 | 35616 | 2 | 1 | C | 26800 | -1860 | 2820 | 2820 | 870 | 767 | 646 | 956 | water | Elk Point |
| 5W0671834040000 | 630219 | 35540 | 2 | 1 | C | 28700 | -2050 | 2810 | 2830 | 870 | 763 | 634 | 775 | water | Elk Point |
| 5W0692611060000 | 830821 | 36926 | 1 | 1 | C | 34900 | -2610 | 3310 | 3350 | 945 | 811 | 654 | 702 | water + mud | Elk Point |
| 5W0571512010000 | 760404 | 35312 | 5 | 1 | C | 31200 | -2280 | 3210 | 3220 | 906 | 778 | 638 | 937 | water | Cambrian |
| 5W0681709100000 | 650322 | 35757 | 5 | 1 | C | 28500 | -2070 | 2970 | 3010 | 839 | 723 | 595 | 907 | water + mud | Cambrian |
| 5W0621818020000 | 590320 | 36561 | 10 | 1 | C | 32500 | -2390 | 3280 | 3290 | 924 | 796 | 649 | 880 | water + mud + oil + cond. | Cambrian |

# APPENDIX C: HYDROCHEMICAL DATA

All ion concentrations are measured in mg/l. The calculated sodium concentration ($Na_c$) was derived by charge balance calculation. See Chapter 3 for the equations to calculate $Ca_{excess}$ and $Na_{deficit}$ values. The Na/Cl ratios were calculated with the respective molar concentrations of sodium and chloride.



Reproduced with permission of the copyright owner. Further reproduction prohibited without permission.

Reproduced with permission of the copyright owner. Further reproduction prohibited without permission.



| DLS | ID | # | elev | dtop | dbot | TDS | Cl | Na | $Na_c$ | K | pH | $SO_4$ | Mg | Ca | $HCO_3$ | $Ca_{ex}$ | $Na_{df}$ | Na/Cl | Aquifer |
|---|---|---|---|---|---|---|---|---|---|---|---|---|---|---|---|---|---|---|---|
| 0635250306000 | 121463 | | 866 | 1122 | 1137 | 1855 | 698 | 620 | 623 | 4 | 8.4 | 26 | 3 | 16 | 488 | 0 | -10 | 1.375 | Brazeau-B. River |
| 0605192314000 | 152209 | 1 | 994 | 1218 | 1233 | 2670 | 1300 | 1051 | 1048 | 4 | 8.4 | 22 | 2 | 13 | 573 | -1 | -14 | 1.244 | Brazeau-B. River |
| 0565252007000 | 89469 | 2 | 1290 | 2028 | 2048 | 2860 | 1436 | 1081 | 1069 | 20 | 8.2 | 25 | 1 | 54 | 535 | 1 | -12 | 1.148 | Brazeau-B. River |
| 0565232102000 | 169597 | 3 | 1093 | 1764 | 1797 | 3289 | 1645 | 1218 | 1217 | 2 | 6.7 | 115 | 8 | 63 | 488 | 1 | -13 | 1.141 | Brazeau-B. River |
| 0575221403000 | 90858 | 3 | 1063 | 1576 | 1588 | 5190 | 2660 | 1905 | 1886 | 14 | 7.8 | 95 | 13 | 114 | 742 | 3 | -18 | 1.094 | Brazeau-B. River |
| 0575221403000 | 90858 | 2 | 1063 | 1576 | 1588 | 4886 | 2530 | 1815 | 1794 | 20 | 8.2 | 103 | 13 | 83 | 625 | 1 | -17 | 1.093 | Brazeau-B. River |
| 0575221403000 | 90858 | 6 | 1063 | 1576 | 1588 | 5225 | 2700 | 1913 | 1894 | 11 | 7.8 | 103 | 10 | 120 | 683 | 3 | -17 | 1.082 | Brazeau-B. River |
| 0575221403000 | 90858 | 5 | 1063 | 1576 | 1588 | 5215 | 2700 | 1907 | 1889 | 12 | 7.9 | 119 | 4 | 128 | 644 | 4 | -17 | 1.079 | Brazeau-B. River |
| 0575221403000 | 90858 | 4 | 1063 | 1576 | 1588 | 5236 | 2700 | 1903 | 1885 | 12 | 7.8 | 123 | 13 | 127 | 671 | 3 | -17 | 1.077 | Brazeau-B. River |
| 0575221403000 | 90858 | 7 | 1063 | 1576 | 1588 | 5151 | 2690 | 1884 | 1867 | 10 | 7.8 | 78 | 11 | 119 | 659 | 3 | -16 | 1.070 | Brazeau-B. River |
| 0575221403000 | 90858 | 8 | 1063 | 1576 | 1588 | 5170 | 2760 | 1900 | 1880 | 14 | 7.8 | 27 | 5 | 124 | 630 | 3 | -15 | 1.050 | Brazeau-B. River |
| 0555183502000 | 140021 | 2 | 1069 | 1511 | 1517 | 6749 | 3800 | 2568 | 2559 | 15 | 7.9 | 66 | 15 | 68 | 473 | -1 | -19 | 1.038 | Brazeau-B. River |
| 0535171506000 | 83819 | 1 | 912 | 1402 | 1427 | 5391 | 3063 | 2058 | 2050 | 12 | 7.5 | 61 | 7 | 52 | 305 | -1 | -15 | 1.032 | Brazeau-B. River |
| 0465163312000 | 64896 | 1 | 1259 | 2072 | 2094 | 6925 | 3910 | 2481 | 2472 | 14 | 7.8 | 80 | 17 | 207 | 468 | 6 | -13 | 0.975 | Brazeau-B. River |
| 0585193411000 | 177298 | 1 | 907 | 1232 | 1264 | 3070 | 1753 | 1002 | 982 | 35 | 8.3 | 72 | 14 | 166 | 127 | 6 | 0 | 0.863 | Brazeau-B. River |
| 0545142016000 | 85094 | 10 | 849 | 1166 | 1169 | 8880 | 5166 | 3314 | 2892 | 29 | 7.0 | 0 | 17 | 363 | 20 | 13 | -1 | 0.863 | Brazeau-B. River |
| 0545200808000 | 113854 | | 1059 | 1757 | 1760 | 7888 | 4336 | 2732 | 2427 | 71 | 5.6 | 20 | 6 | 403 | 320 | 16 | -1 | 0.863 | Brazeau-B. River |
| 0455142904000 | 150898 | 3 | 1140 | 1879 | 1892 | 7310 | 3180 | 2300 | | | 7.8 | 274 | 36 | 238 | 1064 | | | | Brazeau-B. River |
| 0455162710020 | 63192 | 1 | 1244 | 2235 | 2239 | 7107 | 4120 | 2593 | | | 7.9 | 26 | 15 | 175 | 364 | | | | Brazeau-B. River |
| 0455162710020 | 63192 | 5 | 1244 | 2235 | 2239 | 6441 | 3800 | 2292 | | | 7.1 | 22 | 13 | 208 | 214 | | | | Brazeau-B. River |
| 0475151601000 | 67723 | 1 | 1265 | 2153 | 2161 | 3400 | 1873 | 1195 | | | 8.1 | 13 | 36 | 52 | 244 | | | | Brazeau-B. River |
| 0475152605000 | 67744 | 1 | 1183 | n/a | n/a | 2408 | 1027 | 951 | | | 8.4 | 6 | 4 | 17 | 745 | | | | Brazeau-B. River |
| 0505211307000 | 79053 | 2 | 1057 | 2065 | 2076 | 4471 | 2050 | 1670 | | | 8.5 | 288 | 6 | 71 | 756 | | | | Brazeau-B. River |
| 0515173107000 | 81243 | 1 | 957 | 1525 | 1540 | 3776 | 2184 | 1423 | | | 8.1 | 38 | 3 | 54 | 150 | | | | Brazeau-B. River |
| 0525183610000 | 82715 | 2 | 903 | 1442 | 1455 | 2940 | 1268 | 1138 | | | 9.2 | 224 | 2 | 12 | 566 | | | | Brazeau-B. River |
| 0535181406000 | 83872 | 1 | 973 | 1582 | 1591 | 10420 | 6256 | 3900 | | | 8.2 | 0 | 15 | 147 | 102 | | | | Brazeau-B. River |
| 0545192111000 | 85247 | 5 | 1008 | 1577 | 1582 | 10363 | 5960 | 3850 | | | 8.2 | 5 | 27 | 192 | 665 | | | | Brazeau-B. River |
| 0545220210000 | 85278 | 5 | 1061 | 1776 | 1785 | 5639 | 3014 | 2075 | | | 7.5 | 25 | 1 | 152 | 742 | | | | Brazeau-B. River |
| 0545220210000 | 85278 | 6 | 1061 | 1776 | 1785 | 4234 | 2269 | 1529 | | | 7.5 | 20 | 1 | 140 | 535 | | | | Brazeau-B. River |
| 0555182606000 | 140019 | 1 | 1051 | 1467 | 1494 | 5571 | 3070 | 2155 | | | 7.5 | 11 | 5 | 44 | 580 | | | | Brazeau-B. River |
| 0555200808000 | 140024 | 1 | 1189 | 1780 | 1801 | 2512 | 1210 | 957 | | | 9.0 | 172 | 1 | 21 | 210 | | | | Brazeau-B. River |
| 0555200808000 | 140024 | 2 | 1189 | 1780 | 1801 | 2524 | 1270 | 970 | | | 8.8 | 94 | 1 | 23 | 263 | | | | Brazeau-B. River |
| 0555200808000 | 140024 | 4 | 1189 | 1780 | 1801 | 2440 | 1240 | 937 | | | 8.8 | 68 | 1 | 25 | 268 | | | | Brazeau-B. River |
| 0555200914000 | 140025 | 8 | 1224 | 1794 | 1804 | 2744 | 1553 | 1061 | | | 8.1 | 11 | 1 | 21 | 197 | | | | Brazeau-B. River |
| 0555200914000 | 140025 | 9 | 1224 | 1794 | 1804 | 2391 | 1129 | 885 | | | 8.0 | 251 | 1 | 32 | 189 | | | | Brazeau-B. River |
| 0555200914000 | 140025 | 10 | 1224 | 1794 | 1804 | 2517 | 1199 | 936 | | | 7.8 | 263 | 1 | 30 | 180 | | | | Brazeau-B. River |
| 0555230101000 | 114964 | | 1208 | 1905 | 1929 | 2990 | 1400 | 1080 | | | 7.7 | 25 | 2 | 61 | 415 | | | | Brazeau-B. River |
| 0555230101000 | 114965 | | 1208 | 1905 | 1929 | 2995 | 1350 | 1090 | | | 7.6 | 42 | 3 | 58 | 442 | | | | Brazeau-B. River |

Reproduced with permission of the copyright owner. Further reproduction prohibited without permission.



| DLS | ID | # | elev | dtop | dbot | TDS | Cl | Na | $Na_c$ | K | pH | $SO_4$ | Mg | Ca | $HCO_3$ | $Ca_{ex}$ | $Na_{df}$ | Na/Cl | Aquifer |
|---|---|---|---|---|---|---|---|---|---|---|---|---|---|---|---|---|---|---|---|
| 0555230101000 | 114969 | | 1208 | 1905 | 1929 | 2950 | 875 | 1010 | | | 7.7 | 537 | 4 | 48 | 458 | | | | Brazeau-B. River |
| 0555273309000 | 87512 | 1 | 1237 | 2157 | 2183 | 3383 | 1250 | 1257 | | | 7.7 | 118 | 2 | 97 | 1340 | | | | Brazeau-B. River |
| 0565162807000 | 151987 | 2 | 971 | 1283 | 1293 | 5441 | 3120 | 2071 | | | 8.1 | 15 | 3 | 68 | 326 | | | | Brazeau-B. River |
| 0565222409000 | 115882 | | 895 | 1313 | 1329 | 1870 | 800 | 604 | | | 7.6 | 175 | 19 | 42 | 203 | | | | Brazeau-B. River |
| 0565230807000 | 115895 | | 1095 | 1737 | 1764 | 2726 | 908 | 955 | | | 7.6 | 148 | 3 | 19 | 683 | | | | Brazeau-B. River |
| 0575190410000 | 90808 | 1 | 1224 | 1647 | 1662 | 4368 | 2520 | 1669 | | | 8.0 | 10 | 3 | 48 | 240 | | | | Brazeau-B. River |
| 0575221403000 | 90858 | 12 | 1063 | 1576 | 1588 | 4578 | 2490 | 1670 | | | 7.8 | 46 | 3 | 128 | 490 | | | | Brazeau-B. River |
| 0575221403000 | 90858 | 15 | 1063 | 1576 | 1588 | 4788 | 2640 | 1696 | | | 7.8 | 19 | 4 | 181 | 504 | | | | Brazeau-B. River |
| 0606051710000 | 162554 | 1 | 1180 | 1874 | 1883 | 3134 | 1020 | 1164 | | | 8.6 | 292 | 10 | 60 | 1171 | | | | Brazeau-B. River |
| 0615192212000 | 94962 | 2 | 920 | 1103 | 1108 | 2298 | 910 | 897 | | | 8.9 | 160 | 2 | 10 | 500 | | | | Brazeau-B. River |
| 0625201112000 | 95927 | 1 | 841 | 967 | 975 | 1703 | 707 | 677 | | | 8.5 | 5 | 2 | 10 | 590 | | | | Brazeau-B. River |
| 0625201112020 | 95928 | 1 | 844 | 909 | 910 | 1706 | 686 | 679 | | | 8.2 | 79 | 0 | 2 | 526 | | | | Brazeau-B. River |
| 0645202410000 | 98573 | 6 | 789 | 778 | 780 | 1821 | 564 | 725 | | | 8.4 | 63 | 3 | 12 | 900 | | | | Brazeau-B. River |
| 0666040711000 | 102429 | 7 | 798 | 1263 | 1278 | 7609 | 3212 | 3037 | 3027 | 16 | 8.0 | 51 | 9 | 26 | 2591 | -2 | -54 | 1.453 | Cardium |
| 0635252210000 | 97272 | 1 | 863 | 1393 | 1398 | 10582 | 4482 | 4184 | 4138 | 29 | 8.2 | 103 | 34 | 37 | 3467 | -3 | -72 | 1.433 | Cardium |
| 0635242803000 | 97244 | 5 | 906 | 1396 | 1437 | 9906 | 4277 | 3887 | 3871 | 12 | 8.4 | 25 | 7 | 102 | 3245 | 1 | -65 | 1.396 | Cardium |
| 0666051111000 | 102439 | 5 | 903 | 1381 | 1396 | 7076 | 3151 | 2813 | 2803 | 16 | 8.1 | 29 | 6 | 31 | 2129 | -2 | -46 | 1.372 | Cardium |
| 0656022206000 | 101065 | 1 | 789 | 1240 | 1265 | 8977 | 4050 | 3573 | 3548 | 4 | 8.6 | 2 | 11 | 32 | 2603 | -3 | -56 | 1.351 | Cardium |
| 0615263606000 | 95040 | 4 | 1094 | 1820 | 1836 | 9369 | 4304 | 3720 | 3712 | 13 | 7.9 | 43 | 2 | 44 | 2554 | -2 | -57 | 1.330 | Cardium |
| 0635242803000 | 97244 | 3 | 906 | 1396 | 1437 | 9701 | 4574 | 3817 | 3809 | 13 | 8.1 | 24 | 1 | 75 | 2461 | -1 | -55 | 1.284 | Cardium |
| 0635240306000 | 97234 | 1 | 876 | 1429 | 1442 | 9873 | 4730 | 3910 | 3897 | 21 | 7.6 | 4 | 11 | 38 | 2401 | -3 | -55 | 1.270 | Cardium |
| 0645231806000 | 98614 | 1 | 860 | 1265 | 1285 | 9035 | 4650 | 3521 | 3507 | 23 | 8.0 | 86 | 15 | 48 | 1454 | -3 | -40 | 1.163 | Cardium |
| 0645231705000 | 98611 | 2 | 818 | 1230 | 1234 | 8073 | 4078 | 3125 | 3067 | 20 | 8.4 | 104 | 22 | 51 | 1287 | -2 | -35 | 1.160 | Cardium |
| 0595181306000 | 92856 | 1 | 944 | 1490 | 1504 | 19325 | 10540 | 7416 | 7399 | 27 | 7.8 | 37 | 43 | 180 | 2257 | -2 | -67 | 1.083 | Cardium |
| 0595180208000 | 92847 | 1 | 961 | 1539 | 1544 | 17884 | 10200 | 6962 | 6889 | 124 | 7.5 | 25 | 20 | 76 | 1222 | -7 | -53 | 1.041 | Cardium |
| 0565163306000 | 89380 | 1 | 977 | 1595 | 1612 | 17039 | 9650 | 6535 | 6479 | 55 | 8.8 | 119 | 36 | 130 | 1098 | -4 | -48 | 1.035 | Cardium |
| 0625241412000 | 96062 | 1 | 1003 | 1598 | 1603 | 14346 | 8210 | 5558 | 5496 | 105 | 7.8 | 33 | 21 | 75 | 913 | -5 | -40 | 1.032 | Cardium |
| 0575160610000 | 116331 | | 1070 | 1673 | 1679 | 24916 | 13600 | 9420 | 8906 | 44 | 7.9 | 38 | 107 | 227 | 1480 | -3 | -81 | 1.010 | Cardium |
| 0575172310000 | 116384 | | 1122 | 1704 | 1711 | 22703 | 12100 | 8670 | 7848 | 51 | 8.0 | 54 | 105 | 292 | 1430 | 2 | -84 | 1.000 | Cardium |
| 0555153616000 | 87392 | 3 | 936 | 1553 | 1558 | 20269 | 11790 | 7559 | 7541 | 29 | 7.3 | 19 | 109 | 260 | 1083 | 0 | -43 | 0.986 | Cardium |
| 0555141716000 | 87368 | 1 | 865 | 1495 | 1506 | 15723 | 8960 | 6057 | | | 8.3 | 118 | 34 | 90 | 915 | | | | Cardium |
| 0565162807000 | 151987 | 1 | 971 | 1596 | 1606 | 28179 | 15580 | 10682 | | | 7.3 | 31 | 74 | 358 | 2957 | | | | Cardium |
| 0575150606000 | 90767 | 1 | 1091 | 1685 | 1688 | 24338 | 14400 | 9224 | | | 8.0 | 30 | 62 | 243 | 582 | | | | Cardium |
| 0575161511000 | 116341 | | 1117 | 1701 | 1706 | 20687 | 11300 | 7880 | | | 8.1 | 2 | 69 | 275 | 1050 | | | | Cardium |
| 0575173602000 | 161148 | | 1130 | 1692 | 1690 | 22613 | 12400 | 8730 | | | 7.8 | 2 | 42 | 133 | 1270 | | | | Cardium |
| 0575173602000 | 161991 | | 1130 | 1692 | 1698 | 23050 | 12700 | 8690 | | | 7.8 | 2 | 43 | 181 | 1400 | | | | Cardium |
| 0595182516000 | 118008 | | 928 | 1447 | 1462 | 18674 | 10000 | 7020 | | | 8.0 | 11 | 50 | 168 | 1390 | | | | Cardium |
| 0595182516000 | 118011 | | 928 | 1447 | 1462 | 19646 | 10800 | 7160 | | | 7.8 | 16 | 50 | 163 | 1420 | | | | Cardium |

| DLS | ID | # | elev | dtop | dbot | TDS | Cl | Na | $Na_c$ | K | pH | $SO_4$ | Mg | Ca | $HCO_3$ | $Ca_{ex}$ | $Na_{df}$ | Na/Cl | Aquifer |
|---|---|---|---|---|---|---|---|---|---|---|---|---|---|---|---|---|---|---|---|
| 0595182516000 | 118015 | | 928 | 1447 | 1462 | 17966 | 9590 | 6790 | | | 7.6 | 11 | 49 | 162 | 1330 | | | | Cardium |
| 0595183602000 | 162470 | 2 | 921 | 1440 | 1444 | 20610 | 11700 | 7893 | | | 7.5 | 21 | 35 | 187 | 1510 | | | | Cardium |
| 0605201716000 | 118819 | | 952 | 1558 | 1568 | 11094 | 5400 | 4180 | | | 8.1 | 661 | 10 | 90 | 697 | | | | Cardium |
| 0605242703000 | 118944 | | 1124 | 1892 | 1907 | 16007 | 7750 | 6060 | | | 7.7 | 33 | 26 | 73 | 2030 | | | | Cardium |
| 0605242703000 | 118945 | | 1124 | 1892 | 1907 | 15193 | 7750 | 5400 | | | 8.1 | 38 | 27 | 76 | 1880 | | | | Cardium |
| 0605242703000 | 118946 | | 1124 | 1892 | 1907 | 14969 | 7500 | 5270 | | | 7.8 | 57 | 26 | 91 | 2000 | | | | Cardium |
| 0605242703000 | 118947 | | 1124 | 1892 | 1907 | 15887 | 8000 | 5660 | | | 7.8 | 49 | 26 | 80 | 2040 | | | | Cardium |
| 0615251607000 | 95031 | 1 | 1141 | 1899 | 1913 | 10734 | 5480 | 4178 | | | 8.1 | 82 | 25 | 58 | 1854 | | | | Cardium |
| 0625253010000 | 96076 | 3 | 929 | 1535 | 1554 | 8685 | 3958 | 3460 | | | 7.9 | 6 | 10 | 26 | 2492 | | | | Cardium |
| 0625260909000 | 96081 | 2 | 949 | 1627 | 1632 | 10330 | 4510 | 4097 | | | 8.2 | 25 | 21 | 44 | 3320 | | | | Cardium |
| 0625262110000 | 96088 | 1 | 948 | 1597 | 1601 | 7741 | 3178 | 3078 | | | 8.3 | 53 | 17 | 32 | 2814 | | | | Cardium |
| 0635242710000 | 97242 | 4 | 848 | 1337 | 1346 | 9902 | 4780 | 3328 | | | 7.7 | 20 | 132 | 413 | 2500 | | | | Cardium |
| 0635242910000 | 97245 | 1 | 888 | 1372 | 1393 | 9085 | 4228 | 3601 | | | 7.6 | 25 | 6 | 42 | 2406 | | | | Cardium |
| 0645231311000 | 98607 | 2 | 857 | 1242 | 1243 | 11343 | 6200 | 4360 | | | 7.2 | 38 | 26 | 94 | 1270 | | | | Cardium |
| 0676043210000 | 103599 | 7 | 693 | 963 | 978 | 7555 | 3320 | 3015 | | | 8.4 | 12 | 9 | 24 | 2270 | | | | Cardium |
| 0606020806000 | 93882 | 1 | 1267 | 2742 | 2750 | 6423 | 2595 | 2340 | 2240 | 170 | 7.5 | 8 | 16 | 229 | 2511 | 9 | -35 | 1.331 | Dunvegan |
| 0655212208000 | 122906 | 0 | 801 | 1295 | 1315 | 12890 | 5270 | 4500 | 4462 | 20 | 8.1 | 205 | 16 | 63 | 2816 | -2 | -67 | 1.306 | Dunvegan |
| 0626013411000 | 96111 | 5 | 1059 | 2097 | 2102 | 7028 | 3230 | 2663 | 2637 | 20 | 8.8 | 612 | 27 | 28 | 915 | -2 | -37 | 1.259 | Dunvegan |
| 0655240110000 | 101023 | 1 | 860 | 1486 | 1492 | 7551 | 3785 | 2844 | 2825 | 24 | 8.4 | 218 | 43 | 73 | 1183 | 0 | -31 | 1.151 | Dunvegan |
| 0645241106000 | 122252 | 0 | 877 | 1602 | 1608 | 10617 | 5276 | 3660 | 3673 | 332 | 7.0 | 173 | 10 | 37 | 1129 | -4 | -32 | 1.073 | Dunvegan |
| 0636010110000 | 97310 | 2 | 1012 | 1986 | 1996 | 10777 | 5400 | 4245 | | | 8.3 | 20 | 13 | 44 | 2085 | | | | Dunvegan |
| 0655211413000 | 122863 | 0 | 794 | 1276 | 1292 | 12690 | 5354 | 4300 | | | 8.3 | 165 | 18 | 43 | 2790 | | | | Dunvegan |
| 0655232010020 | 101017 | 1 | 786 | 1362 | 1368 | 12028 | 6415 | 4724 | | | 8.5 | 66 | 10 | 37 | 1548 | | | | Dunvegan |
| 0665252702000 | 102411 | 1 | 736 | 1250 | 1271 | 10615 | 5700 | 4156 | | | 7.5 | 20 | 13 | 43 | 1390 | | | | Dunvegan |
| 0685221014000 | 163677 | 14 | 669 | 950 | 961 | 3733 | 1800 | 1429 | | | 8.3 | 200 | 5 | 28 | 551 | | | | Dunvegan |
| 0685232511000 | 104531 | 1 | 725 | 975 | 1012 | 6939 | 3550 | 2702 | | | 8.4 | 102 | 11 | 36 | 1010 | | | | Dunvegan |
| 0686010911000 | 104551 | 1 | 711 | 1194 | 1202 | 11112 | 5980 | 4355 | | | 8.4 | 71 | 14 | 32 | 1270 | | | | Dunvegan |
| 0686010911000 | 104551 | 2 | 711 | 1204 | 1215 | 9310 | 5020 | 3660 | | | 8.6 | 26 | 8 | 26 | 1040 | | | | Dunvegan |
| 0686012311000 | 104553 | 1 | 680 | 1119 | 1149 | 8032 | 4377 | 3107 | | | 8.4 | 46 | 11 | 57 | 854 | | | | Dunvegan |
| 0646032710000 | 177719 | 2 | 858 | 2043 | 2046 | 11100 | 5250 | 4411 | 4351 | 23 | 8.5 | 113 | 7 | 24 | 2513 | -4 | -62 | 1.278 | Viking |
| 0625251805000 | 96072 | 4 | 923 | 2079 | 2094 | 11371 | 5575 | 4467 | 4455 | 20 | 7.5 | 25 | 24 | 50 | 2501 | -3 | -59 | 1.232 | Viking |
| 0615272610000 | 95043 | 4 | 1167 | 2451 | 2452 | 10924 | 5410 | 4297 | 4273 | 42 | 7.7 | 4 | 11 | 59 | 2324 | -3 | -55 | 1.218 | Viking |
| 0666040711000 | 102429 | 2 | 798 | 1937 | 1958 | 12705 | 6380 | 5026 | 5017 | 16 | 7.7 | 8 | 11 | 39 | 2523 | -5 | -64 | 1.213 | Viking |
| 0666040711000 | 102429 | 1 | 798 | 1937 | 1958 | 12523 | 6300 | 4944 | 4933 | 19 | 8.0 | 10 | 10 | 48 | 2462 | -4 | -62 | 1.207 | Viking |
| 0655201410000 | 100975 | 1 | 767 | 1390 | 1400 | 12120 | 6101 | 4783 | 4723 | 33 | 8.6 | 15 | 10 | 47 | 2260 | -4 | -58 | 1.194 | Viking |
| 0665221816000 | 123504 | 0 | 711 | 1367 | 1373 | 9739 | 4700 | 3654 | 3458 | 14 | 7.4 | 49 | 10 | 36 | 1208 | -3 | -37 | 1.135 | Viking |
| 0645241710000 | 98634 | 2 | 882 | 1786 | 1806 | 12824 | 6837 | 5037 | 4972 | 34 | 8.5 | 9 | 16 | 42 | 1679 | -5 | -51 | 1.121 | Viking |
| 0635201910000 | 97191 | 2 | 767 | 1567 | 1593 | 16504 | 8900 | 6482 | 6470 | 21 | 7.6 | 6 | 20 | 49 | 2128 | -7 | -66 | 1.121 | Viking |



Reproduced with permission of the copyright owner. Further reproduction prohibited without permission.

Reproduced with permission of the copyright owner. Further reproduction prohibited without permission.

| DLS | ID | # | elev | dtop | dbot | TDS | Cl | Na | $Na_c$ | K | pH | $SO_4$ | Mg | Ca | $HCO_3$ | $Ca_{ex}$ | $Na_{df}$ | Na/Cl | Aquifer |
|---|---|---|---|---|---|---|---|---|---|---|---|---|---|---|---|---|---|---|---|
| 0635141614000 | 141087 | 2 | 966 | 1484 | 1490 | 14983 | 8100 | 5840 | 5832 | 13 | 7.9 | 35 | 24 | 72 | 1854 | -5 | -58 | 1.110 | Viking |
| 0605152307000 | 93710 | 2 | 799 | 1489 | 1512 | 10735 | 5784 | 4196 | 4143 | 37 | 8.5 | 185 | 10 | 28 | 1000 | -5 | -40 | 1.105 | Viking |
| 0685103512000 | 137913 | 0 | 723 | 1907 | 1933 | 17426 | 8899 | 5900 | 6332 | 37 | 7.7 | 25 | 32 | 212 | 2321 | 1 | -60 | 1.097 | Viking |
| 0665181707000 | 163487 | 1 | 799 | 1290 | 1300 | 11530 | 6333 | 4513 | 4501 | 20 | 7.8 | 40 | 1 | 54 | 1197 | -4 | -43 | 1.096 | Viking |
| 0665181707000 | 163487 | 2 | 799 | 1290 | 1300 | 11366 | 6223 | 4433 | 4421 | 20 | 7.8 | 17 | 5 | 67 | 1263 | -3 | -42 | 1.096 | Viking |
| 0655192907000 | 100962 | 2 | 786 | 1370 | 1371 | 12919 | 7155 | 5045 | 5030 | 26 | 8.1 | 5 | 14 | 56 | 1310 | -5 | -46 | 1.084 | Viking |
| 0686063010000 | 104611 | 1 | 699 | 1686 | 1707 | 16731 | 9220 | 6507 | 6467 | 69 | 7.6 | 27 | 18 | 97 | 1753 | -5 | -58 | 1.081 | Viking |
| 0685103512000 | 137912 | 0 | 723 | 1907 | 1933 | 18212 | 9252 | 6300 | 6436 | 35 | 7.2 | 16 | 48 | 279 | 2282 | 4 | -56 | 1.073 | Viking |
| 0615153608000 | 94872 | 1 | 915 | 1503 | 1527 | 18120 | 10120 | 7030 | 7014 | 27 | 7.6 | 29 | 32 | 96 | 1655 | -6 | -60 | 1.069 | Viking |
| 0655192907000 | 100962 | 1 | 786 | 1370 | 1371 | 11250 | 6356 | 4393 | 4358 | 41 | 8.6 | 5 | 13 | 40 | 872 | -5 | -36 | 1.057 | Viking |
| 0605140309000 | 93672 | 2 | 787 | 1467 | 1471 | 19481 | 10985 | 7520 | 7502 | 30 | 8.1 | 71 | 21 | 144 | 1505 | -4 | -61 | 1.053 | Viking |
| 0615171602000 | 94909 | 2 | 864 | 1615 | 1635 | 23228 | 13180 | 8975 | 8916 | 100 | 8.3 | 60 | 64 | 108 | 1710 | -9 | -69 | 1.043 | Viking |
| 0595142112000 | 162115 | 0 | 967 | 1682 | 1696 | 23070 | 12500 | 8365 | 8452 | 33 | 7.8 | 138 | 85 | 180 | 1769 | -4 | -65 | 1.043 | Viking |
| 0615161706000 | 94892 | 1 | 886 | 1600 | 1618 | 24594 | 14160 | 9503 | 9487 | 27 | 7.7 | 8 | 42 | 146 | 1495 | -8 | -70 | 1.033 | Viking |
| 0595140606000 | 92776 | 2 | 1011 | 1777 | 1812 | 20179 | 11550 | 7756 | 7738 | 30 | 7.5 | 16 | 32 | 164 | 1344 | -4 | -57 | 1.033 | Viking |
| 0615161706000 | 94892 | 2 | 886 | 1600 | 1618 | 24184 | 14040 | 9407 | 9389 | 29 | 7.9 | 14 | 38 | 83 | 1226 | -11 | -69 | 1.031 | Viking |
| 0595203510000 | 92907 | 2 | 1001 | 2019 | 2030 | 25050 | 14600 | 9437 | 9418 | 32 | 7.6 | 33 | 90 | 292 | 1216 | -1 | -57 | 0.995 | Viking |
| 0675153306020 | 103454 | 1 | 916 | 1209 | 1215 | 25186 | 15020 | 9568 | 9543 | 42 | 7.1 | 12 | 66 | 236 | 577 | -4 | -52 | 0.980 | Viking |
| 0585183405000 | 117115 | 0 | 999 | 1963 | 1977 | 25003 | 14100 | 9810 | | | 7.2 | 17 | 27 | 178 | 811 | | | | Viking |
| 0595181013000 | 117966 | 0 | 1073 | 2028 | 2037 | 10923 | 4500 | 3450 | | | 7.8 | 2000 | 12 | 275 | 456 | | | | Viking |
| 0595182115000 | 117994 | 0 | 923 | 1482 | 2235 | 22826 | 13800 | 7950 | | | 7.8 | 340 | 73 | 274 | 311 | | | | Viking |
| 0615151404000 | 94861 | 1 | 831 | 1494 | 1501 | 19545 | 10769 | 7572 | | | 7.5 | 16 | 43 | 113 | 2100 | | | | Viking |
| 0615181011000 | 94921 | 2 | 900 | 1734 | 1740 | 23095 | 13000 | 8958 | | | 8.3 | 27 | 35 | 127 | 1928 | | | | Viking |
| 0615192410000 | 94963 | 1 | 936 | 1772 | 1782 | 19875 | 11160 | 7678 | | | 7.5 | 28 | 33 | 135 | 1710 | | | | Viking |
| 0615240310000 | 95025 | 1 | 1130 | 2311 | 2344 | 15105 | 7750 | 5922 | | | 8.8 | 87 | 28 | 54 | 2450 | | | | Viking |
| 0615242613000 | 161605 | 0 | 1034 | 2133 | 2184 | 10062 | 3600 | 3670 | | | 8.1 | 729 | 17 | 40 | 1970 | | | | Viking |
| 0625142810000 | 95790 | 3 | 869 | 1420 | 1429 | 16787 | 9040 | 6542 | | | 7.8 | 10 | 33 | 80 | 2200 | | | | Viking |
| 0625152110000 | 95798 | 4 | 1016 | 1616 | 1640 | 13352 | 7003 | 5218 | | | 8.2 | 4 | 22 | 68 | 2109 | | | | Viking |
| 0625252607000 | 96075 | 12 | 947 | 2032 | 2043 | 12534 | 6200 | 4967 | | | 8.0 | 8 | 20 | 24 | 2674 | | | | Viking |
| 0625260909000 | 96081 | 3 | 949 | 2142 | 2158 | 12595 | 5825 | 4996 | | | 7.9 | 22 | 12 | 54 | 3430 | | | | Viking |
| 0625260909000 | 96081 | 4 | 949 | 2142 | 2158 | 12581 | 5825 | 4984 | | | 8.1 | 20 | 14 | 57 | 3420 | | | | Viking |
| 0635142010000 | 97062 | 1 | 1003 | 1514 | 1531 | 14767 | 7730 | 5770 | | | 7.6 | 56 | 21 | 74 | 2269 | | | | Viking |
| 0635161904000 | 121100 | 0 | 1044 | 1648 | 1653 | 15255 | 8160 | 4960 | | | 8.0 | 307 | 23 | 49 | 1720 | | | | Viking |
| 0635162612000 | 121104 | 0 | 1035 | 1604 | 1622 | 13683 | 6830 | 5190 | | | 7.5 | 21 | 16 | 47 | 1550 | | | | Viking |
| 0635202802000 | 97195 | 1 | 787 | 1572 | 1584 | 23527 | 13021 | 9020 | | | 7.5 | 15 | 53 | 218 | 2440 | | | | Viking |
| 0645160908000 | 161003 | 0 | 922 | 1473 | 1480 | 16712 | 8250 | 6410 | | | 7.6 | 8 | 21 | 57 | 1930 | | | | Viking |
| 0655191710000 | 100955 | 1 | 743 | 1353 | 1359 | 11936 | 6579 | 4625 | | | 8.4 | 49 | 15 | 78 | 1140 | | | | Viking |
| 0655200510020 | 100973 | 1 | 763 | 1430 | 1452 | 13826 | 7000 | 5451 | | | 7.9 | 91 | 15 | 40 | 2500 | | | | Viking |

Reproduced with permission of the copyright owner. Further reproduction prohibited without permission.

| DLS | ID | # | elev | dtop | dbot | TDS | Cl | Na | $Na_c$ | K | pH | $SO_4$ | Mg | Ca | $HCO_3$ | $Ca_{ex}$ | $Na_{df}$ | Na/Cl | Aquifer |
|---|---|---|---|---|---|---|---|---|---|---|---|---|---|---|---|---|---|---|---|
| 0655211314000 | 122861 | 0 | 794 | 1458 | 1462 | 12492 | 6480 | 4600 | | | 7.7 | 99 | 14 | 18 | 1264 | | | | Viking |
| 0655212006000 | 100987 | 4 | 748 | 1433 | 1452 | 12334 | 5732 | 4905 | | | 7.5 | 12 | 12 | 41 | 3321 | | | | Viking |
| 0665161216000 | 102285 | 2 | 881 | 1284 | 1295 | 16979 | 8758 | 6604 | | | 7.5 | 23 | 30 | 119 | 2938 | | | | Viking |
| 0665181004000 | 102312 | 1 | 814 | 1314 | 1329 | 11521 | 6283 | 4491 | | | 7.4 | 22 | 16 | 55 | 1324 | | | | Viking |
| 0665181810000 | 102314 | 1 | 810 | 1305 | 1319 | 12544 | 6910 | 4904 | | | 7.7 | 16 | 21 | 40 | 1328 | | | | Viking |
| 0665193506000 | 102328 | 3 | 760 | 1243 | 1251 | 14032 | 7905 | 5436 | | | 0.0 | 22 | 34 | 64 | 1160 | | | | Viking |
| 0665200102000 | 163493 | 1 | 769 | 1342 | 1346 | 12707 | 6980 | 4974 | | | 7.9 | 21 | 13 | 35 | 1310 | | | | Viking |
| 0665210312000 | 102338 | 1 | 807 | 1441 | 1443 | 9865 | 4748 | 3886 | | | 8.2 | 22 | 14 | 49 | 2332 | | | | Viking |
| 0665210312000 | 102338 | 2 | 807 | 1441 | 1443 | 10729 | 5410 | 4212 | | | 8.0 | 22 | 11 | 57 | 2068 | | | | Viking |
| 0665222607000 | 102379 | 1 | 707 | 1316 | 1320 | 10371 | 4337 | 4097 | | | 7.9 | 6 | 20 | 76 | 3733 | | | | Viking |
| 0665233510000 | 102391 | 3 | 812 | 1428 | 1433 | 19234 | 10827 | 7404 | | | 8.4 | 271 | 25 | 126 | 1132 | | | | Viking |
| 0666041512000 | 170259 | 1 | 711 | 1807 | 1814 | 11504 | 5810 | 4562 | | | 8.2 | 20 | 13 | 17 | 2120 | | | | Viking |
| 0666052610000 | 102440 | 1 | 794 | 1899 | 1908 | 18552 | 10300 | 7221 | | | 7.8 | 15 | 29 | 88 | 1830 | | | | Viking |
| 0666052810000 | 102441 | 5 | 839 | 1975 | 1980 | 17220 | 9530 | 6713 | | | 7.0 | 28 | 26 | 73 | 1730 | | | | Viking |
| 0685262901000 | 104546 | 1 | 671 | 1299 | 1311 | 24097 | 14207 | 9182 | | | 8.0 | 7 | 85 | 181 | 885 | | | | Viking |
| 0695220201000 | 105434 | 1 | 657 | 1073 | 1087 | 28055 | 16283 | 10647 | | | 7.5 | 30 | 126 | 226 | 1513 | | | | Viking |
| 0695230606000 | 105514 | 1 | 728 | 1205 | 1216 | 19344 | 11150 | 7431 | | | 7.6 | 3 | 66 | 109 | 1190 | | | | Viking |
| 0686112707000 | 137938 | 0 | 757 | 2208 | 2228 | 14346 | 5680 | 4784 | 4605 | 31 | 7.8 | 26 | 46 | 249 | 3450 | 6 | -63 | 1.250 | Upper Mannville |
| 0645161811000 | 121917 | 0 | 912 | 1488 | 1494 | 16794 | 8780 | 5745 | 6018 | 430 | 7.8 | 2 | 16 | 52 | 1769 | -7 | -49 | 1.057 | Upper Mannville |
| 0645161811000 | 121916 | 0 | 912 | 1488 | 1494 | 17071 | 8500 | 5929 | 5717 | 641 | 7.8 | 15 | 39 | 56 | 1891 | -6 | -43 | 1.037 | Upper Mannville |
| 0635171704000 | 161762 | 0 | 966 | 1624 | 1908 | 21607 | 12447 | 7800 | 8140 | 62 | 8.1 | 103 | 51 | 183 | 961 | -4 | -53 | 1.008 | Upper Mannville |
| 0675192107000 | 123963 | 0 | 752 | 1249 | 1264 | 20835 | 12020 | 7498 | 7854 | 39 | 7.4 | 132 | 57 | 186 | 903 | -3 | -51 | 1.008 | Upper Mannville |
| 0696072410000 | 105575 | 3 | 676 | 1799 | 1807 | 23193 | 13430 | 8718 | 8685 | 55 | 7.7 | 4 | 50 | 344 | 1316 | 3 | -53 | 0.997 | Upper Mannville |
| 0675192107000 | 123956 | 0 | 752 | 1249 | 1264 | 19505 | 10900 | 7317 | 7035 | 35 | 8.0 | 23 | 86 | 192 | 952 | -2 | -42 | 0.995 | Upper Mannville |
| 0675192107000 | 123958 | 0 | 752 | 1293 | 1307 | 27161 | 15450 | 9660 | 9950 | 54 | 7.9 | 64 | 109 | 360 | 1464 | 2 | -59 | 0.993 | Upper Mannville |
| 0675192107000 | 123961 | 0 | 752 | 1293 | 1307 | 27255 | 15600 | 9476 | 9997 | 63 | 7.5 | 41 | 137 | 376 | 1562 | 2 | -58 | 0.988 | Upper Mannville |
| 0675192107000 | 123957 | 0 | 752 | 1293 | 1307 | 27203 | 15550 | 9568 | 9935 | 63 | 7.2 | 51 | 143 | 364 | 1464 | 2 | -56 | 0.985 | Upper Mannville |
| 0675192107000 | 123960 | 0 | 752 | 1249 | 1264 | 19784 | 11600 | 7475 | 7310 | 35 | 7.5 | 35 | 69 | 192 | 378 | -3 | -37 | 0.972 | Upper Mannville |
| 0565171107000 | 115742 | 0 | 916 | 2239 | 2253 | 50300 | 30000 | 18200 | 18749 | 192 | 8.1 | 8 | 121 | 681 | 1098 | 2 | -90 | 0.964 | Upper Mannville |
| 0685240715000 | 161706 | 0 | 753 | 1475 | 1480 | 36913 | 21480 | 13241 | 13008 | 102 | 7.1 | 13 | 243 | 721 | 1113 | 13 | -46 | 0.934 | Upper Mannville |
| 0525192904000 | 112389 | 0 | 1000 | 2656 | 2665 | 31871 | 18200 | 11000 | | | 6.9 | 2 | 90 | 640 | 1930 | | | | Upper Mannville |
| 0555141712000 | 114626 | 0 | 870 | 2080 | 2098 | 11575 | 6770 | 4250 | | | 6.5 | 5 | 27 | 141 | 320 | | | | Upper Mannville |
| 0565150706000 | 115661 | 0 | 927 | 2159 | 2162 | 30255 | 15100 | 10300 | | | 7.8 | 29 | 43 | 126 | 4120 | | | | Upper Mannville |
| 0575182102000 | 116414 | 0 | 1285 | 2565 | 2575 | 63292 | 33200 | 23803 | | | 8.1 | 337 | 233 | 256 | 5002 | | | | Upper Mannville |
| 0605152704000 | 118636 | 0 | 794 | 1505 | 1523 | 14480 | 7970 | 5200 | | | 7.3 | 128 | 24 | 80 | 1010 | | | | Upper Mannville |
| 0635130707000 | 120988 | 0 | 928 | 1713 | 1725 | 61460 | 36143 | 22962 | | | 8.0 | 291 | 58 | 827 | 1179 | | | | Upper Mannville |
| 0645161907000 | 161335 | 0 | 917 | 1479 | 1489 | 19671 | 9770 | 7540 | | | 7.9 | 7 | 24 | 72 | 2230 | | | | Upper Mannville |
| 0645161907000 | 161340 | 0 | 917 | 1477 | 1482 | 16575 | 8220 | 6190 | | | 8.1 | 14 | 23 | 64 | 2040 | | | | Upper Mannville |

Reproduced with permission of the copyright owner. Further reproduction prohibited without permission.

| DLS | ID | # | elev | dtop | dbot | TDS | Cl | Na | $Na_c$ | K | pH | $SO_4$ | Mg | Ca | $HCO_3$ | $Ca_{ex}$ | $Na_{df}$ | Na/Cl | Aquifer |
|---|---|---|---|---|---|---|---|---|---|---|---|---|---|---|---|---|---|---|---|
| 0645161907000 | 161341 | 0 | 917 | 1477 | 1482 | 18339 | 9250 | 6650 | | | 8.2 | 4 | 32 | 80 | 2300 | | | | Upper Mannville |
| 0645161907000 | 161342 | 0 | 917 | 1477 | 1482 | 18368 | 9250 | 6760 | | | 7.7 | 9 | 29 | 88 | 2210 | | | | Upper Mannville |
| 0645212001000 | 122158 | 0 | 798 | 1563 | 1599 | 13631 | 6500 | 4830 | | | 8.3 | 202 | 27 | 79 | 1970 | | | | Upper Mannville |
| 0645212115000 | 122164 | 0 | 782 | 1558 | 1563 | 11291 | 4970 | 4300 | | | 8.0 | 46 | 9 | 24 | 1920 | | | | Upper Mannville |
| 0645212115000 | 122855 | 0 | 761 | 1480 | 1487 | 10838 | 4270 | 3720 | | | 8.0 | 46 | 11 | 24 | 2750 | | | | Upper Mannville |
| 0655230610000 | 122955 | 0 | 852 | 1661 | 1670 | 9604 | 4300 | 3220 | | | 8.3 | 12 | 8 | 24 | 1970 | | | | Upper Mannville |
| 0665140812000 | 123297 | 0 | 1143 | 1510 | 1523 | 14458 | 7000 | 5500 | | | 8.0 | 888 | 32 | 71 | 924 | | | | Upper Mannville |
| 0665140812000 | 123298 | 0 | 1143 | 1510 | 1523 | 19206 | 10500 | 7430 | | | 7.5 | 5 | 36 | 95 | 1100 | | | | Upper Mannville |
| 0665140812000 | 123299 | 0 | 1143 | 1510 | 1523 | 19970 | 11000 | 7630 | | | 7.6 | 3 | 40 | 89 | 1170 | | | | Upper Mannville |
| 0685240710000 | 104534 | 1 | 747 | 1622 | 1626 | 33446 | 20025 | 12268 | | | 7.9 | 8 | 109 | 685 | 715 | | | | Upper Mannville |
| 0686021511000 | 104557 | 3 | 694 | 1650 | 1667 | 30085 | 18150 | 11591 | | | 7.1 | 26 | 46 | 164 | 220 | | | | Upper Mannville |
| 0686112707000 | 137939 | 0 | 757 | 2208 | 2228 | 14426 | 5780 | 4738 | | | 7.5 | 12 | 32 | 334 | 3428 | | | | Upper Mannville |
| 0686130910000 | 138007 | 0 | 926 | 2633 | 2643 | 15885 | 7500 | 5660 | | | 7.2 | 86 | 66 | 77 | 2280 | | | | Upper Mannville |
| 0696091910000 | 105601 | 2 | 703 | 1908 | 1918 | 29930 | 18030 | 10041 | | | 7.9 | 2 | 284 | 1213 | 732 | | | | Upper Mannville |
| 0625182001000 | 120220 | 0 | 872 | 1890 | 1899 | 57251 | 32000 | 21142 | 21709 | 125 | 7.4 | 831 | 98 | 218 | 2837 | -23 | -170 | 1.046 | Lower Mannville |
| 0675230914000 | 161941 | 0 | 765 | 1768 | 1795 | 54388 | 32000 | 19683 | 20953 | 102 | 7.1 | 23 | 95 | 332 | 2153 | -17 | -137 | 1.010 | Lower Mannville |
| 0565140412000 | 115622 | 0 | 1208 | 2098 | 2104 | 44872 | 25800 | 15950 | 16830 | 153 | 8.0 | 78 | 131 | 420 | 2340 | -6 | -108 | 1.006 | Lower Mannville |
| 0646012007000 | 98652 | 8 | 865 | 2405 | 2409 | 62327 | 37200 | 24123 | 24022 | 170 | 7.2 | 30 | 136 | 210 | 1279 | -29 | -145 | 0.996 | Lower Mannville |
| 0645153203000 | 98449 | 1 | 990 | 1695 | 1709 | 62034 | 37300 | 24181 | 24077 | 175 | 6.3 | 19 | 63 | 136 | 683 | -33 | -145 | 0.995 | Lower Mannville |
| 0646012007000 | 98652 | 9 | 865 | 2405 | 2409 | 63098 | 37600 | 24383 | 24258 | 210 | 7.2 | 20 | 140 | 250 | 1435 | -27 | -146 | 0.995 | Lower Mannville |
| 0665222306000 | 102376 | 3 | 734 | 1695 | 1712 | 69900 | 41500 | 26770 | 26730 | 67 | 7.8 | 25 | 146 | 521 | 1908 | -18 | -159 | 0.993 | Lower Mannville |
| 0636011408000 | 135630 | 0 | 884 | 2476 | 2486 | 53674 | 30600 | 20800 | 19625 | 134 | 7.0 | 432 | 124 | 439 | 1040 | -11 | -113 | 0.989 | Lower Mannville |
| 0686031111000 | 104561 | 3 | 715 | 1982 | 1990 | 61952 | 37000 | 23673 | 23611 | 103 | 7.0 | 5 | 241 | 345 | 1400 | -22 | -132 | 0.984 | Lower Mannville |
| 0656021107000 | 101060 | 9 | 850 | 2340 | 2351 | 60545 | 36100 | 23090 | 23012 | 131 | 8.0 | 6 | 194 | 440 | 1454 | -16 | -128 | 0.983 | Lower Mannville |
| 0656022806000 | 152869 | 1 | 784 | 2257 | 2264 | 62383 | 37000 | 23952 | 23577 | 635 | 6.9 | 263 | 170 | 320 | 1379 | -23 | -131 | 0.983 | Lower Mannville |
| 0656021107000 | 101060 | 8 | 850 | 2340 | 2351 | 59612 | 35600 | 22716 | 22640 | 128 | 8.0 | 2 | 182 | 460 | 1327 | -15 | -124 | 0.981 | Lower Mannville |
| 0615191603000 | 119571 | 0 | 914 | 2062 | 2235 | 82221 | 43000 | 30500 | 27296 | 1330 | 7.4 | 2500 | 220 | 1540 | 3130 | 31 | -147 | 0.979 | Lower Mannville |
| 0656021107000 | 101060 | 10 | 850 | 2340 | 2351 | 61043 | 36500 | 23202 | 23112 | 151 | 8.0 | 10 | 219 | 476 | 1293 | -15 | -122 | 0.976 | Lower Mannville |
| 0685203605000 | 104432 | 1 | 755 | 1460 | 1492 | 49153 | 29050 | 18455 | 18393 | 104 | 7.1 | 8 | 160 | 637 | 1714 | 1 | -97 | 0.976 | Lower Mannville |
| 0635251014000 | 97260 | 1 | 913 | 2368 | 2391 | 62504 | 37350 | 23693 | 23645 | 80 | 6.8 | 4 | 194 | 591 | 1366 | -10 | -125 | 0.976 | Lower Mannville |
| 0645252106000 | 177710 | 2 | 848 | 2076 | 2088 | 39291 | 23412 | 14863 | 14803 | 100 | 6.8 | 4 | 120 | 407 | 987 | -5 | -78 | 0.975 | Lower Mannville |
| 0635252210000 | 97272 | 4 | 863 | 2296 | 2318 | 59095 | 35400 | 22431 | 22382 | 82 | 8.0 | 58 | 202 | 492 | 1042 | -13 | -117 | 0.975 | Lower Mannville |
| 0685240903000 | 124538 | 0 | 755 | 1695 | 1702 | 28612 | 16900 | 9670 | 10669 | 212 | 6.9 | 746 | 190 | 328 | 564 | -2 | -55 | 0.973 | Lower Mannville |
| 0696041212000 | 105542 | 2 | 658 | 1912 | 1920 | 46668 | 27750 | 17551 | 17507 | 73 | 7.0 | 72 | 214 | 472 | 1238 | -6 | -90 | 0.973 | Lower Mannville |
| 0645252106000 | 177710 | 3 | 848 | 2076 | 2088 | 40017 | 23770 | 15055 | 14996 | 100 | 6.9 | 12 | 79 | 554 | 1113 | 2 | -77 | 0.973 | Lower Mannville |
| 0675141601000 | 103438 | 1 | 1036 | 1550 | 1574 | 40906 | 24300 | 15436 | 15316 | 204 | 7.9 | 156 | 135 | 426 | 921 | -5 | -78 | 0.972 | Lower Mannville |
| 0666042912000 | 136541 | 0 | 818 | 2348 | 2357 | 65350 | 39350 | 23586 | 24764 | 227 | 6.6 | 62 | 155 | 721 | 1249 | -6 | -125 | 0.970 | Lower Mannville |
| 0646022711000 | 162880 | 1 | 885 | 2434 | 2447 | 61170 | 36500 | 23147 | 22917 | 390 | 7.1 | 86 | 194 | 601 | 1305 | -9 | -114 | 0.968 | Lower Mannville |

Reproduced with permission of the copyright owner. Further reproduction prohibited without permission.



| DLS | ID | # | elev | dtop | dbot | TDS | Cl | Na | $Na_c$ | K | pH | $SO_4$ | Mg | Ca | $HCO_3$ | $Ca_{ex}$ | $Na_{df}$ | Na/Cl | Aquifer |
|---|---|---|---|---|---|---|---|---|---|---|---|---|---|---|---|---|---|---|---|
| 0665253606000 | 102413 | 2 | 748 | 1789 | 1794 | 51969 | 30750 | 19575 | 19276 | 507 | 8.3 | 84 | 170 | 601 | 1604 | -3 | -95 | 0.967 | Lower Mannville |
| 0646033510000 | 141248 | 5 | 860 | 2454 | 2465 | 71117 | 42700 | 26850 | 26766 | 141 | 6.6 | 4 | 211 | 773 | 1176 | -7 | -131 | 0.967 | Lower Mannville |
| 0686053610000 | 137522 | 0 | 665 | 1991 | 1997 | 62964 | 38700 | 22080 | 24203 | 141 | 7.5 | 7 | 199 | 741 | 1096 | -4 | -117 | 0.964 | Lower Mannville |
| 0656032810000 | 177777 | 1 | 846 | 2404 | 2417 | 75615 | 45500 | 28527 | 28446 | 136 | 7.2 | 64 | 243 | 801 | 976 | -8 | -137 | 0.964 | Lower Mannville |
| 0665250112000 | 162599 | 0 | 769 | 1944 | 1947 | 86719 | 52900 | 31050 | 32989 | 528 | 7.3 | 77 | 243 | 857 | 1064 | -13 | -155 | 0.962 | Lower Mannville |
| 0685220409000 | 141836 | 2 | 679 | 1480 | 1487 | 46996 | 28000 | 17531 | 17461 | 117 | 6.5 | 31 | 194 | 641 | 1220 | 2 | -82 | 0.962 | Lower Mannville |
| 0655160202000 | 163335 | 0 | 1034 | 1743 | 1752 | 66819 | 41200 | 23700 | 25601 | 253 | 7.5 | 4 | 233 | 641 | 549 | -12 | -117 | 0.958 | Lower Mannville |
| 0636012106000 | 162766 | 1 | 978 | 2613 | 2624 | 67491 | 40500 | 25245 | 25152 | 156 | 8.3 | 134 | 267 | 841 | 1025 | -1 | -114 | 0.958 | Lower Mannville |
| 0666041311000 | 102431 | 1 | 732 | 2289 | -1000 | 76564 | 46380 | 28797 | 28789 | 11 | 7.9 | 12 | 304 | 801 | 549 | -9 | -130 | 0.957 | Lower Mannville |
| 0635141614000 | 141087 | 1 | 966 | 1736 | 1770 | 52514 | 31500 | 19617 | 19535 | 138 | 7.6 | 31 | 160 | 757 | 915 | 4 | -88 | 0.956 | Lower Mannville |
| 0625243104000 | 96068 | 2 | 897 | 2352 | 2369 | 66206 | 39900 | 24747 | 24671 | 128 | 6.5 | 23 | 292 | 805 | 893 | -2 | -108 | 0.953 | Lower Mannville |
| 0656033110000 | 152870 | 2 | 810 | 2391 | 2435 | 75760 | 45500 | 28370 | 28070 | 508 | 6.9 | 128 | 267 | 961 | 1086 | 0 | -120 | 0.951 | Lower Mannville |
| 0615152310000 | 94867 | 3 | 881 | 1763 | 1778 | 54817 | 32926 | 20449 | 20306 | 243 | 7.7 | 4 | 172 | 810 | 927 | 5 | -87 | 0.951 | Lower Mannville |
| 0666041411000 | 153213 | 1 | 718 | 2274 | 2287 | 74319 | 44500 | 27523 | 27421 | 172 | 6.6 | 249 | 388 | 1041 | 1257 | 5 | -116 | 0.950 | Lower Mannville |
| 0686041116000 | 104572 | 2 | 691 | 2049 | 2056 | 60285 | 36200 | 22340 | 22293 | 79 | 7.8 | 95 | 355 | 785 | 1037 | 1 | -94 | 0.950 | Lower Mannville |
| 0545163210020 | 169474 | 1 | 890 | 2265 | 2275 | 34293 | 20400 | 12711 | 12559 | 258 | 7.2 | 92 | 104 | 586 | 813 | 8 | -53 | 0.949 | Lower Mannville |
| 0646031306000 | 177717 | 1 | 889 | 2562 | 2571 | 74643 | 45000 | 27688 | 27586 | 172 | 6.6 | 35 | 413 | 985 | 1061 | 1 | -111 | 0.945 | Lower Mannville |
| 0625181703000 | 120213 | 0 | 886 | 1936 | 1948 | 57997 | 35800 | 20400 | 21936 | 148 | 5.8 | 5 | 182 | 870 | 392 | 5 | -88 | 0.945 | Lower Mannville |
| 0665153612000 | 102276 | 2 | 1028 | 1585 | 1606 | 41887 | 25100 | 15429 | 15350 | 133 | 7.1 | 16 | 219 | 681 | 900 | 7 | -61 | 0.943 | Lower Mannville |
| 0605220101000 | 118884 | 0 | 1061 | 2581 | 2588 | 36545 | 21200 | 13700 | 12935 | 115 | 6.6 | 19 | 129 | 635 | 580 | 9 | -50 | 0.941 | Lower Mannville |
| 0625182412000 | 120237 | 0 | 875 | 1896 | 1906 | 70149 | 43346 | 24000 | 26437 | 190 | 5.9 | 5 | 449 | 1002 | 1157 | 4 | -102 | 0.940 | Lower Mannville |
| 0685261005000 | 104544 | 1 | 688 | 1660 | 1679 | 33938 | 20350 | 12468 | 12397 | 120 | 7.6 | 27 | 222 | 517 | 720 | 4 | -47 | 0.939 | Lower Mannville |
| 0636021312020 | 152350 | 9 | 990 | 2686 | 2698 | 79582 | 48250 | 29455 | 29380 | 125 | 7.8 | 26 | 364 | 1201 | 580 | 9 | -111 | 0.939 | Lower Mannville |
| 0645152710000 | 177702 | 2 | 1027 | 1785 | 1790 | 70473 | 42500 | 26036 | 25879 | 260 | 6.1 | 35 | 225 | 1250 | 834 | 17 | -98 | 0.939 | Lower Mannville |
| 0645170608000 | 121931 | 0 | 817 | 1740 | 1753 | 64680 | 39500 | 23000 | 24049 | 259 | 7.5 | 4 | 217 | 1080 | 621 | 12 | -91 | 0.939 | Lower Mannville |
| 0635180115000 | 97101 | 2 | 892 | 1847 | 1855 | 58079 | 35000 | 21317 | 21254 | 106 | 7.7 | 6 | 335 | 961 | 935 | 11 | -78 | 0.936 | Lower Mannville |
| 0686070107000 | 104618 | 3 | 722 | 2306 | 2310 | 71424 | 43100 | 26215 | 26108 | 180 | 7.0 | 16 | 340 | 1277 | 968 | 18 | -93 | 0.934 | Lower Mannville |
| 0636021312020 | 152350 | 12 | 990 | 2686 | 2698 | 82946 | 50000 | 30482 | 30228 | 430 | 6.2 | 74 | 425 | 1401 | 1147 | 17 | -105 | 0.932 | Lower Mannville |
| 0656051205000 | 101082 | 2 | 841 | 2578 | 2584 | 90489 | 54600 | 33440 | 32979 | 781 | 6.7 | 148 | 335 | 1522 | 903 | 18 | -114 | 0.931 | Lower Mannville |
| 0656051205000 | 101082 | 4 | 841 | 2578 | 2584 | 86125 | 52000 | 31799 | 31396 | 684 | 6.5 | 222 | 471 | 1249 | 781 | 7 | -108 | 0.931 | Lower Mannville |
| 0575161007000 | 90776 | 1 | 1051 | 2301 | 2321 | 61696 | 37244 | 22636 | 22459 | 300 | 6.7 | 27 | 385 | 981 | 859 | 9 | -76 | 0.930 | Lower Mannville |
| 0645180709000 | 121993 | 0 | 708 | 1755 | 1760 | 89862 | 53000 | 34100 | 31953 | 418 | 6.2 | 29 | 340 | 1500 | 476 | 19 | -108 | 0.930 | Lower Mannville |
| 0645170608000 | 121932 | 0 | 817 | 1740 | 1753 | 65515 | 41000 | 22400 | 24666 | 238 | 7.4 | 4 | 204 | 1330 | 340 | 23 | -81 | 0.928 | Lower Mannville |
| 0645191303000 | 141240 | 1 | 759 | 1732 | 1738 | 77457 | 46900 | 28213 | 28143 | 118 | 6.7 | 27 | 365 | 1578 | 759 | 29 | -90 | 0.925 | Lower Mannville |
| 0636021312020 | 152350 | 11 | 990 | 2686 | 2698 | 81830 | 49500 | 29928 | 29685 | 410 | 6.2 | 37 | 425 | 1502 | 891 | 22 | -94 | 0.925 | Lower Mannville |
| 0645181806000 | 98479 | 1 | 777 | 1729 | 1743 | 92281 | 56000 | 33650 | 33575 | 126 | 7.2 | 23 | 462 | 1802 | 700 | 30 | -106 | 0.924 | Lower Mannville |
| 0645171309000 | 121941 | 0 | 940 | 1764 | 1767 | 64938 | 39420 | 22796 | 23625 | 156 | 6.7 | 8 | 466 | 1153 | 939 | 16 | -74 | 0.924 | Lower Mannville |
| 0615192412000 | 119585 | 0 | 919 | 2040 | 2058 | 68366 | 39700 | 26100 | 23780 | 151 | 6.5 | 1 | 313 | 1350 | 702 | 25 | -74 | 0.924 | Lower Mannville |

Reproduced with permission of the copyright owner. Further reproduction prohibited without permission.



| DLS | ID | # | elev | dtop | dbot | TDS | Cl | Na | $Na_c$ | K | pH | $SO_4$ | Mg | Ca | $HCO_3$ | $Ca_{ex}$ | $Na_{df}$ | Na/Cl | Aquifer |
|---|---|---|---|---|---|---|---|---|---|---|---|---|---|---|---|---|---|---|---|
| 0645181806000 | 98479 | 2 | 777 | 1728 | 1744 | 85698 | 51900 | 31133 | 31057 | 126 | 7.9 | 84 | 294 | 1966 | 654 | 43 | -96 | 0.923 | Lower Mannville |
| 0665161602000 | 123366 | 0 | 831 | 1545 | 1559 | 81796 | 49800 | 29400 | 29727 | 581 | 6.9 | 48 | 388 | 1350 | 88 | 14 | -88 | 0.920 | Lower Mannville |
| 0665221507000 | 102373 | 3 | 730 | 1691 | 1693 | 53408 | 31620 | 19051 | 18862 | 320 | 7.5 | 58 | 316 | 1409 | 1940 | 37 | -56 | 0.920 | Lower Mannville |
| 0635202210000 | 97193 | 1 | 801 | 1829 | 1840 | 47945 | 28850 | 17300 | 17203 | 164 | 6.8 | 2 | 131 | 1273 | 791 | 33 | -50 | 0.919 | Lower Mannville |
| 0616011103000 | 95045 | 1 | 1243 | 3110 | 3127 | 84226 | 50500 | 31061 | 30099 | 1635 | 7.0 | 76 | 401 | 1381 | 1640 | 15 | -88 | 0.919 | Lower Mannville |
| 0615263606000 | 95040 | 2 | 1094 | 2704 | 2718 | 58748 | 35400 | 21133 | 21062 | 118 | 6.2 | 2 | 250 | 1493 | 956 | 37 | -60 | 0.917 | Lower Mannville |
| 0625262014000 | 96086 | 1 | 1036 | 2572 | 2588 | 71220 | 43000 | 25938 | 25578 | 610 | 6.6 | 10 | 433 | 1329 | 1037 | 21 | -73 | 0.917 | Lower Mannville |
| 0635193309000 | 97170 | 1 | 784 | 1774 | 1787 | 62676 | 37900 | 23024 | 22537 | 827 | 7.6 | 23 | 194 | 1241 | 598 | 22 | -64 | 0.917 | Lower Mannville |
| 0635192612020 | 162755 | 3 | 794 | 1786 | 1799 | 55605 | 33500 | 20226 | 19912 | 531 | 7.4 | 62 | 206 | 1241 | 754 | 26 | -56 | 0.917 | Lower Mannville |
| 0595162910000 | 92823 | 1 | 1007 | 2074 | 2082 | 75765 | 45935 | 27439 | 27264 | 296 | 6.6 | 3 | 209 | 1895 | 577 | 46 | -75 | 0.915 | Lower Mannville |
| 0626013411000 | 96111 | 4 | 1059 | 2725 | 2735 | 71302 | 43250 | 25725 | 25651 | 125 | 7.8 | 2 | 680 | 1201 | 903 | 14 | -70 | 0.915 | Lower Mannville |
| 0655161113000 | 100916 | 4 | 1049 | 1749 | 1775 | 56449 | 34100 | 20338 | 20222 | 196 | 6.9 | 95 | 471 | 1065 | 773 | 17 | -55 | 0.914 | Lower Mannville |
| 0656051205000 | 101082 | 3 | 841 | 2578 | 2584 | 76159 | 46100 | 27950 | 27289 | 1123 | 6.5 | 128 | 554 | 1073 | 720 | 5 | -72 | 0.913 | Lower Mannville |
| 0686081106000 | 104634 | 1 | 811 | 2466 | 2469 | 85680 | 52000 | 30851 | 30492 | 609 | 6.0 | 16 | 748 | 1592 | 961 | 24 | -69 | 0.904 | Lower Mannville |
| 0615262413000 | 95036 | 2 | 1156 | 2802 | 2812 | 64060 | 38800 | 22759 | 22681 | 130 | 6.5 | 14 | 289 | 1854 | 699 | 51 | -48 | 0.901 | Lower Mannville |
| 0615263606000 | 95040 | 1 | 1094 | 2757 | 2767 | 69748 | 42400 | 24749 | 24678 | 118 | 6.2 | 2 | 552 | 1710 | 681 | 40 | -48 | 0.897 | Lower Mannville |
| 0686070710000 | 104619 | 4 | 749 | 2363 | 2376 | 89300 | 54300 | 31636 | 31541 | 160 | 6.8 | 2 | 938 | 1914 | 1037 | 38 | -59 | 0.896 | Lower Mannville |
| 0615161509000 | 94890 | 1 | 858 | 1808 | 1819 | 79343 | 48200 | 27843 | 27618 | 380 | 6.5 | 80 | 356 | 2600 | 537 | 79 | -35 | 0.884 | Lower Mannville |
| 0646082506000 | 98707 | 1 | 1046 | 3141 | 3149 | 88241 | 53700 | 31241 | 29786 | 2471 | 7.1 | 12 | 391 | 2650 | 503 | 75 | 3 | 0.855 | Lower Mannville |
| 0676080706000 | 103643 | 19 | 868 | 2665 | 2682 | 93824 | 57400 | 31210 | 31061 | 250 | 6.7 | 21 | 1115 | 3680 | 810 | 123 | 37 | 0.834 | Lower Mannville |
| 0676080706000 | 103643 | 17 | 868 | 2665 | 2682 | 93663 | 57500 | 30492 | 30360 | 222 | 6.6 | 10 | 1113 | 4276 | 553 | 152 | 70 | 0.814 | Lower Mannville |
| 0676080706000 | 103643 | 18 | 868 | 2665 | 2682 | 94166 | 58000 | 29835 | 29687 | 249 | 6.5 | 21 | 1614 | 4356 | 692 | 156 | 112 | 0.789 | Lower Mannville |
| 0485181404000 | 71559 | 1 | 1138 | 3380 | 3390 | 42643 | 25100 | 14853 | | | 6.4 | 288 | 243 | 1441 | 1460 | | | | Lower Mannville |
| 0525191612000 | 112368 | 0 | 602 | 2018 | 2028 | 48553 | 28500 | 16000 | | | 7.3 | 465 | 265 | 1740 | 961 | | | | Lower Mannville |
| 0565170406000 | 115735 | 0 | 1013 | 2449 | 2468 | 16965 | 7600 | 5610 | | | 8.3 | 1572 | 78 | 175 | 1879 | | | | Lower Mannville |
| 0575191507000 | 140392 | 1 | 1164 | 2518 | 2533 | 26298 | 15700 | 9310 | | | 6.7 | 70 | 187 | 701 | 671 | | | | Lower Mannville |
| 0585153111000 | 91959 | 1 | 1035 | 2097 | 2100 | 45955 | 28000 | 15776 | | | 7.2 | 41 | 338 | 1642 | 321 | | | | Lower Mannville |
| 0595243404000 | 92941 | 2 | 1132 | 2835 | 2844 | 63518 | 38480 | 22401 | | | 6.5 | 31 | 218 | 2083 | 620 | | | | Lower Mannville |
| 0605223513000 | 93859 | 2 | 984 | 2401 | 2426 | 35587 | 21300 | 12826 | | | 8.0 | 12 | 316 | 660 | 961 | | | | Lower Mannville |
| 0605232010000 | 93861 | 1 | 1028 | 2599 | 2609 | 68651 | 41500 | 24623 | | | 7.1 | 40 | 406 | 1639 | 900 | | | | Lower Mannville |
| 0605233306000 | 93863 | 4 | 1072 | 2619 | 2625 | 67418 | 41000 | 23888 | | | 6.6 | 8 | 430 | 1826 | 540 | | | | Lower Mannville |
| 0615183007000 | 94932 | 3 | 960 | 2054 | 2086 | 56717 | 34000 | 21102 | | | 8.2 | 15 | 143 | 941 | 1050 | | | | Lower Mannville |
| 0615190403020 | 177502 | 1 | 974 | 2129 | 2139 | 41710 | 24991 | 15125 | | | 6.2 | 4 | 73 | 1102 | 844 | | | | Lower Mannville |
| 0615212207000 | 95003 | 2 | 967 | 2251 | 2276 | 43298 | 25881 | 15914 | | | 7.4 | 6 | 217 | 754 | 1069 | | | | Lower Mannville |
| 0615212910000 | 95007 | 1 | 951 | 2293 | 2305 | 54601 | 32900 | 19934 | | | 6.8 | 14 | 151 | 1229 | 760 | | | | Lower Mannville |
| 0615243607000 | 95028 | 3 | 1046 | 2533 | 2541 | 68755 | 41600 | 25189 | | | 6.4 | 14 | 175 | 1477 | 610 | | | | Lower Mannville |
| 0625152110000 | 95798 | 1 | 1016 | 1857 | 1885 | 48581 | 29225 | 18020 | | | 7.5 | 8 | 322 | 574 | 879 | | | | Lower Mannville |
| 0625253010000 | 96076 | 1 | 929 | 2467 | 2480 | 69847 | 41900 | 26825 | | | 7.3 | 2 | 100 | 492 | 1074 | | | | Lower Mannville |

Reproduced with permission of the copyright owner. Further reproduction prohibited without permission.



| DLS | ID | # | elev | dtop | dbot | TDS | Cl | Na | $Na_c$ | K | pH | $SO_4$ | Mg | Ca | $HCO_3$ | $Ca_{ex}$ | $Na_{df}$ | Na/Cl | Aquifer |
|---|---|---|---|---|---|---|---|---|---|---|---|---|---|---|---|---|---|---|---|
| 0625262206000 | 96089 | 6 | 930 | 2532 | 2537 | 56039 | 33600 | 20800 | | | 6.8 | 199 | 224 | 833 | 780 | | | | Lower Mannville |
| 0626023214000 | 96121 | 2 | 1052 | 2830 | 2845 | 96639 | 59000 | 34622 | | | 6.4 | 10 | 553 | 2341 | 230 | | | | Lower Mannville |
| 0635151510000 | 97080 | 1 | 946 | 1740 | 1747 | 52498 | 31500 | 19614 | | | 6.6 | 7 | 190 | 715 | 960 | | | | Lower Mannville |
| 0635192110000 | 97139 | 1 | 786 | 1777 | 1818 | 58768 | 35300 | 21631 | | | 7.2 | 11 | 300 | 951 | 968 | | | | Lower Mannville |
| 0635192212000 | 97148 | 4 | 787 | 1806 | 1810 | 54857 | 33000 | 20214 | | | 7.4 | 5 | 185 | 1021 | 880 | | | | Lower Mannville |
| 0635221411000 | 152344 | 2 | 853 | 2100 | 2103 | 56048 | 33800 | 20813 | | | 7.4 | 7 | 197 | 878 | 717 | | | | Lower Mannville |
| 0635222312000 | 170061 | 2 | 841 | 1974 | 1978 | 36493 | 22000 | 13573 | | | 7.1 | 49 | 146 | 521 | 415 | | | | Lower Mannville |
| 0635232706000 | 97229 | 2 | 852 | 2150 | 2173 | 59961 | 35700 | 23080 | | | 8.1 | 14 | 114 | 350 | 1430 | | | | Lower Mannville |
| 0635243010000 | 97246 | 3 | 882 | 2271 | 2281 | 61941 | 37000 | 23621 | | | 6.2 | 2 | 129 | 545 | 1311 | | | | Lower Mannville |
| 0635251204000 | 97262 | 1 | 892 | 2351 | 2370 | 52100 | 30995 | 19706 | | | 6.9 | 4 | 91 | 640 | 1352 | | | | Lower Mannville |
| 0635260511000 | 97286 | 3 | 997 | 2530 | 2544 | 52022 | 31000 | 19675 | | | 7.6 | 132 | 120 | 577 | 1054 | | | | Lower Mannville |
| 0635263510000 | 97305 | 1 | 936 | 2395 | 2402 | 65537 | 39250 | 25229 | | | 7.7 | 4 | 153 | 328 | 1165 | | | | Lower Mannville |
| 0636010110000 | 97310 | 3 | 1012 | 2613 | 2635 | 84263 | 51000 | 31101 | | | 7.5 | 16 | 264 | 1528 | 720 | | | | Lower Mannville |
| 0645143202000 | 98440 | 1 | 1076 | 1743 | 1747 | 54977 | 33140 | 20221 | | | 6.8 | 54 | 254 | 950 | 727 | | | | Lower Mannville |
| 0645152510000 | 98448 | 1 | 1064 | 1747 | 1770 | 59779 | 36100 | 21938 | | | 6.6 | 23 | 218 | 1161 | 690 | | | | Lower Mannville |
| 0645180402000 | 98467 | 2 | 791 | 1763 | 1769 | 52182 | 31250 | 19944 | | | 7.7 | 16 | 114 | 403 | 925 | | | | Lower Mannville |
| 0645181004000 | 98473 | 1 | 804 | 1756 | 1765 | 49164 | 29500 | 18274 | | | 6.8 | 13 | 182 | 750 | 905 | | | | Lower Mannville |
| 0645181004000 | 98473 | 2 | 804 | 1756 | 1765 | 56308 | 33980 | 20735 | | | 7.6 | 16 | 314 | 880 | 780 | | | | Lower Mannville |
| 0645183004000 | 122031 | 0 | 779 | 1689 | 1698 | 32662 | 19000 | 12300 | | | 8.0 | 178 | 91 | 329 | 680 | | | | Lower Mannville |
| 0645190306000 | 98490 | 1 | 758 | 1740 | 1744 | 70682 | 43000 | 25554 | | | 6.7 | 21 | 516 | 1351 | 488 | | | | Lower Mannville |
| 0645192207000 | 98540 | 1 | 747 | 1651 | 1658 | 67475 | 40840 | 24088 | | | 7.2 | 15 | 466 | 1623 | 900 | | | | Lower Mannville |
| 0645193410000 | 98559 | 2 | 747 | 1672 | 1686 | 62011 | 37500 | 22523 | | | 7.5 | 9 | 462 | 1092 | 865 | | | | Lower Mannville |
| 0645201410000 | 98570 | 1 | 818 | 1786 | 1799 | 54815 | 32920 | 20100 | | | 7.3 | 18 | 190 | 1105 | 980 | | | | Lower Mannville |
| 0645210702000 | 98579 | 1 | 791 | 1911 | 1935 | 56890 | 34100 | 21204 | | | 6.6 | 12 | 183 | 855 | 1090 | | | | Lower Mannville |
| 0645213011000 | 98589 | 3 | 819 | 1829 | 1847 | 59056 | 35750 | 21627 | | | 6.5 | 62 | 170 | 1241 | 420 | | | | Lower Mannville |
| 0645261612000 | 122322 | 0 | 888 | 2285 | 2302 | 38532 | 21500 | 15600 | | | 8.0 | 112 | 30 | 49 | 1170 | | | | Lower Mannville |
| 0646082506000 | 98707 | 2 | 1046 | 3141 | 3149 | 85654 | 52100 | 30365 | | | 7.0 | 10 | 376 | 2542 | 531 | | | | Lower Mannville |
| 0655160202000 | 163334 | 0 | 1034 | 1776 | 1885 | 66203 | 40600 | 23300 | | | 6.9 | 3 | 231 | 964 | 505 | | | | Lower Mannville |
| 0655170810000 | 100920 | 1 | 815 | 1586 | 1594 | 61790 | 37289 | 22556 | | | 7.6 | 7 | 298 | 1187 | 709 | | | | Lower Mannville |
| 0655172811000 | 100926 | 1 | 882 | 1667 | 1709 | 53085 | 31853 | 19679 | | | 7.3 | 4 | 144 | 932 | 961 | | | | Lower Mannville |
| 0655180110000 | 100931 | 3 | 803 | 1606 | 1617 | 65627 | 39565 | 24110 | | | 7.8 | 84 | 393 | 1032 | 900 | | | | Lower Mannville |
| 0655182411000 | 100938 | 1 | 822 | 1639 | 1658 | 60315 | 36300 | 22483 | | | 6.6 | 10 | 255 | 811 | 928 | | | | Lower Mannville |
| 0655182911000 | 100940 | 2 | 859 | 1660 | 1680 | 56624 | 34000 | 21329 | | | 8.0 | 19 | 177 | 646 | 920 | | | | Lower Mannville |
| 0655191104000 | 100953 | 2 | 794 | 1655 | 1660 | 66787 | 40334 | 24641 | | | 7.7 | 9 | 464 | 872 | 950 | | | | Lower Mannville |
| 0655191104000 | 100953 | 3 | 794 | 1693 | 1706 | 67059 | 40334 | 24904 | | | 7.5 | 7 | 384 | 850 | 1180 | | | | Lower Mannville |
| 0655192907000 | 100962 | 3 | 786 | 1625 | 1650 | 61969 | 37500 | 22381 | | | 7.0 | 23 | 608 | 1001 | 927 | | | | Lower Mannville |
| 0655202510000 | 100979 | 6 | 743 | 1601 | 1613 | 55940 | 33600 | 21087 | | | 8.1 | 29 | 193 | 597 | 883 | | | | Lower Mannville |
| 0655212802000 | 100991 | 2 | 765 | 1760 | 1771 | 65786 | 39480 | 24869 | | | 7.1 | 3 | 194 | 689 | 1120 | | | | Lower Mannville |

Reproduced with permission of the copyright owner. Further reproduction prohibited without permission.



| DLS | ID | # | elev | dtop | dbot | TDS | Cl | Na | $Na_c$ | K | pH | $SO_4$ | Mg | Ca | $HCO_3$ | $Ca_{ex}$ | $Na_{df}$ | Na/Cl | Aquifer |
|---|---|---|---|---|---|---|---|---|---|---|---|---|---|---|---|---|---|---|---|
| 0655212802000 | 100991 | 1 | 765 | 1704 | 1710 | 59361 | 35960 | 21030 | | | 6.4 | 18 | 866 | 941 | 1110 | | | | Lower Mannville |
| 0655223411000 | 101004 | 1 | 722 | 1753 | 1777 | 53528 | 31900 | 20416 | | | 7.1 | 2 | 129 | 448 | 1288 | | | | Lower Mannville |
| 0656022206000 | 101065 | 3 | 789 | 2155 | 2174 | 37939 | 22500 | 14443 | | | 7.8 | 20 | 93 | 344 | 1090 | | | | Lower Mannville |
| 0665161216000 | 102285 | 1 | 881 | 1578 | 1606 | 65359 | 39396 | 23824 | | | 6.8 | 176 | 256 | 1376 | 673 | | | | Lower Mannville |
| 0665162508000 | 102297 | 1 | 875 | 1490 | 1501 | 40637 | 24024 | 15265 | | | 6.8 | 45 | 131 | 516 | 1335 | | | | Lower Mannville |
| 0665181004000 | 102312 | 2 | 814 | 1576 | 1585 | 58210 | 35060 | 21555 | | | 7.0 | 10 | 188 | 994 | 820 | | | | Lower Mannville |
| 0665181810000 | 102314 | 3 | 810 | 1600 | 1616 | 78371 | 47500 | 28232 | | | 6.6 | 13 | 479 | 1734 | 840 | | | | Lower Mannville |
| 0665181810000 | 102314 | 2 | 810 | 1568 | 1578 | 68477 | 41400 | 25083 | | | 6.7 | 18 | 260 | 1357 | 730 | | | | Lower Mannville |
| 0665210910000 | 102346 | 3 | 741 | 1630 | 1648 | 56603 | 33750 | 20890 | | | 6.5 | 178 | 189 | 1018 | 1175 | | | | Lower Mannville |
| 0665221110000 | 102366 | 1 | 734 | 1661 | 1665 | 50751 | 30600 | 18788 | | | 7.0 | 16 | 236 | 768 | 698 | | | | Lower Mannville |
| 0665230910000 | 102384 | 2 | 779 | 1747 | 1760 | 46922 | 28400 | 16699 | | | 7.1 | 33 | 457 | 989 | 701 | | | | Lower Mannville |
| 0665262303000 | 102417 | 2 | 760 | 2005 | 2010 | 55616 | 33150 | 21383 | | | 7.5 | 25 | 145 | 289 | 1270 | | | | Lower Mannville |
| 0666052610000 | 102440 | 4 | 794 | 2210 | 2242 | 65923 | 39450 | 24887 | | | 6.5 | 33 | 182 | 741 | 1280 | | | | Lower Mannville |
| 0675170810000 | 103463 | 1 | 831 | 1522 | 1527 | 61337 | 37010 | 22598 | | | 6.8 | 24 | 268 | 1050 | 787 | | | | Lower Mannville |
| 0675210210000 | 103526 | 1 | 748 | 1579 | 1590 | 46413 | 27600 | 17507 | | | 6.9 | 18 | 145 | 524 | 1260 | | | | Lower Mannville |
| 0675212815000 | 103533 | 1 | 707 | 1500 | 1506 | 48100 | 28770 | 18008 | | | 0.0 | 2 | 293 | 462 | 1150 | | | | Lower Mannville |
| 0675221706000 | 103541 | 1 | 701 | 1625 | 1631 | 55016 | 32400 | 20955 | | | 7.6 | 8 | 122 | 524 | 2048 | | | | Lower Mannville |
| 0675221706000 | 103541 | 2 | 701 | 1554 | 1570 | 43664 | 26200 | 16001 | | | 7.5 | 16 | 197 | 827 | 860 | | | | Lower Mannville |
| 0675231511000 | 103565 | 7 | 749 | 1726 | 1729 | 52498 | 30783 | 20071 | | | 8.0 | 35 | 160 | 374 | 2185 | | | | Lower Mannville |
| 0675231511000 | 103565 | 4 | 749 | 1622 | 1629 | 42994 | 25818 | 15783 | | | 7.5 | 34 | 431 | 456 | 960 | | | | Lower Mannville |
| 0675232106000 | 103567 | 3 | 757 | 1661 | 1669 | 45304 | 26940 | 16888 | | | 7.3 | 7 | 154 | 681 | 1290 | | | | Lower Mannville |
| 0675242110000 | 103573 | 2 | 751 | 1798 | 1818 | 51242 | 29990 | 19613 | | | 7.1 | 18 | 136 | 379 | 2250 | | | | Lower Mannville |
| 0676050510000 | 103602 | 2 | 785 | 2220 | 2223 | 82047 | 49435 | 30579 | | | 6.8 | 50 | 210 | 1289 | 986 | | | | Lower Mannville |
| 0676050810000 | 103604 | 7 | 778 | 2191 | 2198 | 63634 | 38391 | 23446 | | | 7.5 | 70 | 112 | 1312 | 617 | | | | Lower Mannville |
| 0685040306000 | 161914 | 0 | 745 | 2105 | 2252 | 72867 | 44000 | 26105 | | | 6.8 | 58 | 209 | 857 | 1513 | | | | Lower Mannville |
| 0685040306000 | 161917 | 0 | 745 | 2105 | 2252 | 69407 | 41500 | 25738 | | | 7.7 | 86 | 243 | 721 | 994 | | | | Lower Mannville |
| 0685191916000 | 104422 | 1 | 759 | 1475 | 1480 | 41069 | 23814 | 15969 | | | 7.4 | 13 | 59 | 157 | 2151 | | | | Lower Mannville |
| 0685192811000 | 104423 | 3 | 796 | 1454 | 1481 | 47259 | 28210 | 17502 | | | 7.0 | 3 | 167 | 801 | 1171 | | | | Lower Mannville |
| 0685193410000 | 104424 | 2 | 814 | 1490 | 1503 | 47655 | 28550 | 17492 | | | 6.8 | 10 | 200 | 901 | 1020 | | | | Lower Mannville |
| 0685202307000 | 104430 | 2 | 768 | 1498 | 1506 | 57333 | 33800 | 22120 | | | 6.8 | 13 | 172 | 220 | 2050 | | | | Lower Mannville |
| 0685232511000 | 104531 | 3 | 725 | 1506 | 1518 | 36809 | 21800 | 13633 | | | 7.2 | 10 | 190 | 549 | 1274 | | | | Lower Mannville |
| 0685232511000 | 104531 | 4 | 725 | 1579 | 1593 | 52414 | 30500 | 19796 | | | 6.7 | 18 | 156 | 620 | 2692 | | | | Lower Mannville |
| 0685240410000 | 104533 | 1 | 759 | 1629 | 1642 | 41559 | 23540 | 15342 | | | 7.5 | 132 | 187 | 753 | 3265 | | | | Lower Mannville |
| 0685241110000 | 104536 | 1 | 743 | 1602 | 1611 | 38310 | 23000 | 14048 | | | 8.1 | 15 | 284 | 562 | 815 | | | | Lower Mannville |
| 0685241606000 | 104537 | 1 | 736 | 1679 | 1689 | 52485 | 30750 | 20041 | | | 7.8 | 4 | 134 | 440 | 2270 | | | | Lower Mannville |
| 0685251314000 | 104540 | 3 | 754 | 1748 | 1757 | 55103 | 32064 | 21317 | | | 8.0 | 17 | 138 | 222 | 2735 | | | | Lower Mannville |
| 0685252606000 | 104542 | 3 | 708 | 1670 | 1684 | 57246 | 33620 | 22029 | | | 6.5 | 44 | 111 | 361 | 2200 | | | | Lower Mannville |
| 0685262901000 | 104546 | 2 | 671 | 1711 | 1718 | 51190 | 30159 | 19579 | | | 8.0 | 13 | 171 | 331 | 1905 | | | | Lower Mannville |

Reproduced with permission of the copyright owner. Further reproduction prohibited without permission.

| DLS | ID | # | elev | dtop | dbot | TDS | Cl | Na | $Na_c$ | K | pH | $SO_4$ | Mg | Ca | $HCO_3$ | $Ca_{ex}$ | $Na_{df}$ | Na/Cl | Aquifer |
|---|---|---|---|---|---|---|---|---|---|---|---|---|---|---|---|---|---|---|---|
| 0685262901000 | 104546 | 3 | 671 | 1734 | 1740 | 53107 | 31156 | 20512 | | | 8.0 | 9 | 158 | 195 | 2190 | | | | Lower Mannville |
| 0686022606000 | 104558 | 2 | 675 | 1858 | 1869 | 54169 | 32090 | 20985 | | | 7.0 | 5 | 127 | 170 | 1611 | | | | Lower Mannville |
| 0686041310000 | 153263 | 1 | 738 | 2063 | 2073 | 51771 | 31041 | 19590 | | | 7.5 | 13 | 187 | 477 | 941 | | | | Lower Mannville |
| 0686042110000 | 104576 | 2 | 669 | 1999 | 2023 | 57107 | 34200 | 21461 | | | 6.5 | 32 | 228 | 633 | 1125 | | | | Lower Mannville |
| 0686042110000 | 104576 | 6 | 669 | 2012 | 2016 | 58385 | 34960 | 22360 | | | 7.0 | 21 | 112 | 431 | 1020 | | | | Lower Mannville |
| 0686073511000 | 104629 | 5 | 674 | 2232 | 2238 | 83910 | 50761 | 30649 | | | 6.6 | 7 | 540 | 1437 | 1051 | | | | Lower Mannville |
| 0686081106000 | 104634 | 7 | 811 | 2467 | 2484 | 89917 | 55000 | 31352 | | | 6.1 | 107 | 841 | 2499 | 240 | | | | Lower Mannville |
| 0695210507000 | 105382 | 1 | 658 | 1358 | 1362 | 47116 | 27567 | 17780 | | | 7.1 | 10 | 207 | 470 | 2200 | | | | Lower Mannville |
| 0695210704000 | 105405 | 1 | 642 | 1345 | 1350 | 44050 | 25250 | 16771 | | | 6.7 | 6 | 241 | 270 | 3075 | | | | Lower Mannville |
| 0695211110000 | 105417 | 1 | 695 | 1377 | 1407 | 45989 | 26430 | 17800 | | | 6.9 | 4 | 131 | 177 | 2943 | | | | Lower Mannville |
| 0695220201000 | 105434 | 2 | 657 | 1381 | 1399 | 42875 | 24963 | 16152 | | | 7.6 | 37 | 171 | 481 | 2178 | | | | Lower Mannville |
| 0695221609000 | 105490 | 2 | 686 | 1463 | 1472 | 50303 | 29294 | 19238 | | | 7.5 | 22 | 155 | 365 | 2500 | | | | Lower Mannville |
| 0695230606000 | 105514 | 2 | 728 | 1535 | 1546 | 35158 | 20950 | 12914 | | | 7.8 | 7 | 264 | 502 | 1060 | | | | Lower Mannville |
| 0695230606000 | 105514 | 3 | 728 | 1639 | 1646 | 52796 | 31250 | 19279 | | | 7.3 | 5 | 396 | 873 | 2020 | | | | Lower Mannville |
| 0695251306000 | 105527 | 1 | 758 | 1573 | 1594 | 38635 | 23125 | 14245 | | | 7.4 | 3 | 209 | 609 | 903 | | | | Lower Mannville |
| 0695251907000 | 105528 | 4 | 772 | 1603 | 1609 | 36425 | 21846 | 13316 | | | 7.3 | 16 | 206 | 662 | 770 | | | | Lower Mannville |
| 0696050107000 | 138058 | 0 | 662 | 1998 | 2002 | 47757 | 27000 | 19100 | | | 7.9 | 103 | 78 | 255 | 1120 | | | | Lower Mannville |
| 0695220503000 | 124829 | 0 | 696 | 1588 | 1611 | 110066 | 66600 | 38985 | 41019 | 156 | 6.9 | 1646 | 471 | 1842 | 366 | 21 | -173 | 0.950 | Nordegg |
| 0525213310000 | 82752 | 1 | 1050 | 3296 | 3391 | 122460 | 74000 | 45598 | | | 6.9 | 224 | 461 | 1722 | 925 | | | | Nordegg |
| 0555181410000 | 87433 | 3 | 1023 | 2595 | 2622 | 67922 | 40500 | 24945 | | | 6.8 | 64 | 194 | 1402 | 1660 | | | | Nordegg |
| 0565162404000 | 89377 | 3 | 939 | 2239 | 2243 | 50866 | 30225 | 18731 | | | 7.5 | 67 | 223 | 900 | 1465 | | | | Nordegg |
| 0565213210000 | 89451 | 2 | 964 | 2783 | 2789 | 129286 | 78466 | 47979 | | | 7.4 | 198 | 638 | 1741 | 537 | | | | Nordegg |
| 0585220606000 | 92045 | 2 | 1027 | 2857 | 2863 | 120140 | 72600 | 44669 | | | 6.4 | 27 | 228 | 2090 | 1070 | | | | Nordegg |
| 0615222507000 | 95018 | 3 | 964 | 2393 | 2397 | 108053 | 65450 | 40128 | | | 6.9 | 284 | 401 | 1602 | 381 | | | | Nordegg |
| 0645213611000 | 98595 | 1 | 778 | 1882 | 1893 | 156820 | 94800 | 57431 | | | 6.1 | 492 | 559 | 3103 | 885 | | | | Nordegg |
| 0665152804002 | 123331 | 0 | 1026 | 1692 | 1702 | 26600 | 15000 | 9450 | | | 6.0 | 1210 | 103 | 606 | 22.3 | | | | Nordegg |
| 0675220211000 | 103536 | 1 | 704 | 1730 | 1739 | 155078 | 93900 | 56750 | | | 7.3 | 604 | 646 | 2951 | 460 | | | | Nordegg |
| 0685193410000 | 104424 | 3 | 814 | 1580 | 1596 | 127660 | 77300 | 46801 | | | 6.8 | 436 | 559 | 2323 | 490 | | | | Nordegg |
| 0655252408000 | 123010 | 0 | 900 | 2204 | 2218 | 130619 | 78700 | 48600 | 49135 | 1120 | 6.9 | 293 | 247 | 1010 | 648 | -33 | -234 | 0.963 | Triassic |
| 0675201810020 | 141776 | 1 | 787 | 1712 | 1720 | 145492 | 87800 | 55072 | 54188 | 1500 | 6.4 | 601 | 284 | 1540 | 396 | -16 | -233 | 0.952 | Triassic |
| 0696040310000 | 105539 | 1 | 666 | 2074 | 2082 | 133578 | 80540 | 50237 | 49352 | 1500 | 6.9 | 380 | 363 | 1603 | 927 | -6 | -199 | 0.945 | Triassic |
| 0645221610000 | 98597 | 4 | 811 | 2053 | 2056 | 141339 | 85186 | 52891 | 52036 | 1450 | 6.9 | 681 | 346 | 1953 | 573 | 7 | -203 | 0.942 | Triassic |
| 0675193206000 | 123976 | 0 | 753 | 1610 | 1621 | 116654 | 69100 | 43500 | 42007 | 1230 | 5.9 | 647 | 348 | 1550 | 125 | 4 | -156 | 0.937 | Triassic |
| 0675201204000 | 123992 | 0 | 799 | 1698 | 1708 | 122025 | 76000 | 41100 | 46042 | 1550 | 6.3 | 650 | 368 | 1860 | 497 | 12 | -164 | 0.934 | Triassic |
| 0685253504000 | 161175 | 0 | 711 | 1744 | 1764 | 153387 | 91800 | 56200 | 55506 | 1440 | 6.8 | 610 | 552 | 2280 | 503 | 16 | -194 | 0.932 | Triassic |
| 0525193205000 | 160933 | 0 | 957 | 3027 | 3040 | 53756 | 31096 | 18000 | 18790 | 920 | 8.2 | 55 | 24 | 1440 | 2221 | 39 | -65 | 0.932 | Triassic |
| 0675210214000 | 153245 | 1 | 744 | 1716 | 1722 | 130534 | 78500 | 48147 | 47316 | 1410 | 7.1 | 832 | 428 | 2280 | 706 | 30 | -159 | 0.929 | Triassic |
| 0675212506000 | 163649 | 4 | 736 | 1650 | 1657 | 151007 | 91200 | 55736 | 54940 | 1350 | 6.6 | 834 | 508 | 2580 | 302 | 32 | -184 | 0.929 | Triassic |

| DLS | ID | # | elev | dtop | dbot | TDS | Cl | Na | $Na_c$ | K | pH | $SO_4$ | Mg | Ca | $HCO_3$ | $Ca_{ex}$ | $Na_{df}$ | Na/Cl | Aquifer |
|---|---|---|---|---|---|---|---|---|---|---|---|---|---|---|---|---|---|---|---|
| 0675243610020 | 103579 | 2 | 775 | 1833 | 1851 | 156668 | 94700 | 57769 | 57023 | 1264 | 6.5 | 683 | 620 | 2623 | 556 | 30 | -190 | 0.928 | Triassic |
| 0656021806000 | 136004 | 0 | 858 | 2537 | 2542 | 159190 | 95100 | 56980 | 57256 | 1838 | 6.9 | 1095 | 607 | 2603 | 732 | 29 | -190 | 0.928 | Triassic |
| 0675210214000 | 153245 | 3 | 744 | 1716 | 1722 | 127314 | 76500 | 46737 | 45941 | 1350 | 7.3 | 960 | 382 | 2460 | 560 | 42 | -148 | 0.926 | Triassic |
| 0655211516000 | 177770 | 15 | 749 | 1868 | 1876 | 127411 | 76916 | 47025 | 46141 | 1500 | 6.4 | 558 | 206 | 2512 | 394 | 44 | -147 | 0.925 | Triassic |
| 0645183004000 | 122026 | 0 | 779 | 1795 | 1799 | 142308 | 87400 | 49300 | 52341 | 1710 | 6.4 | 705 | 481 | 2440 | 107 | 29 | -163 | 0.923 | Triassic |
| 0545222907000 | 85284 | 1 | 1027 | 3160 | 3180 | 132490 | 80400 | 49377 | 48084 | 2195 | 7.1 | 23 | 292 | 2122 | 563 | 21 | -147 | 0.922 | Triassic |
| 0685212610000 | 141832 | 2 | 723 | 1579 | 1585 | 151444 | 91000 | 55205 | 54398 | 1369 | 5.8 | 1374 | 705 | 2903 | 522 | 48 | -165 | 0.922 | Triassic |
| 0685240307000 | 104532 | 3 | 749 | 1807 | 1832 | 149221 | 90250 | 54478 | 53758 | 1220 | 7.4 | 667 | 729 | 2803 | 598 | 44 | -155 | 0.918 | Triassic |
| 0665213508000 | 102362 | 2 | 756 | 1758 | 1760 | 148811 | 90000 | 54279 | 53552 | 1232 | 7.4 | 656 | 741 | 2823 | 634 | 45 | -152 | 0.918 | Triassic |
| 0635191608000 | 141089 | 1 | 786 | 1920 | 1925 | 129676 | 78500 | 47824 | 46705 | 1900 | 7.0 | 203 | 485 | 2250 | 842 | 29 | -133 | 0.917 | Triassic |
| 0675210811000 | 124018 | 0 | 702 | 1688 | 1698 | 121181 | 74100 | 41515 | 43907 | 938 | 6.9 | 839 | 777 | 2402 | 610 | 41 | -118 | 0.914 | Triassic |
| 0565200410000 | 89432 | 6 | 1208 | 3013 | 3037 | 120200 | 72500 | 44108 | 42952 | 1962 | 7.4 | 667 | 559 | 2082 | 577 | 27 | -115 | 0.914 | Triassic |
| 0695201406000 | 105356 | 1 | 709 | 1474 | 1494 | 140540 | 85000 | 51177 | 50329 | 1438 | 6.5 | 658 | 826 | 2563 | 641 | 38 | -133 | 0.913 | Triassic |
| 0695221813020 | 153317 | 1 | 722 | 1597 | 1607 | 148195 | 89500 | 53607 | 52914 | 1173 | 6.5 | 942 | 728 | 3203 | 439 | 65 | -137 | 0.912 | Triassic |
| 0645192511000 | 163354 | 0 | 773 | 1894 | 1898 | 141487 | 86100 | 48900 | 50747 | 1860 | 7.0 | 706 | 471 | 3110 | 336 | 64 | -125 | 0.909 | Triassic |
| 0675210106000 | 141777 | 1 | 770 | 1720 | 1762 | 154458 | 93600 | 55946 | 55103 | 1428 | 7.0 | 638 | 960 | 3023 | 593 | 51 | -133 | 0.908 | Triassic |
| 0685252606000 | 124561 | 0 | 708 | 1755 | 1762 | 116547 | 67300 | 44100 | 39571 | 1170 | 6.5 | 388 | 517 | 2450 | 580 | 51 | -93 | 0.907 | Triassic |
| 0685213514000 | 124419 | 0 | 715 | 1560 | 1565 | 163503 | 96000 | 59340 | 56405 | 1447 | 6.8 | 1769 | 1408 | 2963 | 576 | 46 | -131 | 0.906 | Triassic |
| 0656021806000 | 136008 | 0 | 858 | 2537 | 2542 | 165677 | 102500 | 54388 | 59906 | 1955 | 6.8 | 963 | 1093 | 3604 | 866 | 71 | -126 | 0.901 | Triassic |
| 0695221211000 | 105482 | 1 | 653 | 1504 | 1508 | 139928 | 84500 | 50303 | 49344 | 1627 | 7.2 | 790 | 778 | 3203 | 720 | 70 | -102 | 0.900 | Triassic |
| 0655160802000 | 122723 | 0 | 908 | 1759 | 1767 | 114946 | 70100 | 38500 | 40775 | 1254 | 7.0 | 829 | 1063 | 2322 | 878 | 41 | -78 | 0.897 | Triassic |
| 0655161113000 | 100916 | 2 | 1049 | 1860 | 1875 | 135402 | 81800 | 48502 | 47500 | 1700 | 7.0 | 704 | 510 | 3604 | 573 | 93 | -88 | 0.895 | Triassic |
| 0645183004000 | 122028 | 0 | 779 | 1795 | 1799 | 147970 | 91700 | 47300 | 52893 | 3390 | 7.3 | 1190 | 903 | 3120 | 366 | 58 | -83 | 0.889 | Triassic |
| 0695191509000 | 105328 | 2 | 785 | 1513 | 1551 | 113391 | 68900 | 39879 | 39106 | 1310 | 6.2 | 570 | 1361 | 2382 | 610 | 46 | -34 | 0.875 | Triassic |
| 0535193402000 | 83939 | 2 | 985 | 2872 | 2881 | 92106 | 55334 | 34264 | | | 7.6 | 37 | 134 | 1659 | 1377 | | | | Triassic |
| 0545221107000 | 85280 | 1 | 1071 | 3203 | 3307 | 134002 | 81500 | 49306 | | | 6.5 | 39 | 753 | 2082 | 654 | | | | Triassic |
| 0565221807000 | 89454 | 1 | 1191 | 3207 | 3210 | 130030 | 79060 | 47959 | | | 6.7 | 12 | 594 | 2110 | 600 | | | | Triassic |
| 0565222006000 | 89455 | 2 | 1178 | 3157 | 3162 | 131800 | 79800 | 48841 | | | 6.5 | 309 | 456 | 2106 | 586 | | | | Triassic |
| 0565222006000 | 89455 | 3 | 1178 | 3161 | 3180 | 124778 | 75800 | 45609 | | | 6.1 | 128 | 563 | 2402 | 561 | | | | Triassic |
| 0565222507000 | 89456 | 1 | 897 | 2822 | 2841 | 127129 | 76912 | 47116 | | | 7.2 | 154 | 298 | 2248 | 815 | | | | Triassic |
| 0565231304000 | 89458 | 1 | 1131 | 3165 | 3196 | 140565 | 85200 | 52356 | | | 6.4 | 20 | 347 | 2234 | 830 | | | | Triassic |
| 0575213210000 | 90853 | 1 | 965 | 2676 | 2691 | 126626 | 76360 | 47329 | | | 7.1 | 56 | 328 | 1857 | 1415 | | | | Triassic |
| 0575213410000 | 90854 | 1 | 984 | 2670 | 2684 | 125844 | 76000 | 47119 | | | 6.6 | 152 | 156 | 1985 | 880 | | | | Triassic |
| 0585202604000 | 92025 | 7 | 929 | 2489 | 2494 | 105751 | 63900 | 39205 | | | 7.6 | 188 | 316 | 1760 | 776 | | | | Triassic |
| 0605163509000 | 93736 | 1 | 764 | 1812 | 1845 | 90134 | 54670 | 31330 | | | 7.7 | 16 | 438 | 3200 | 976 | | | | Triassic |
| 0615182006000 | 94927 | 4 | 980 | 2215 | 2221 | 126661 | 76575 | 46188 | | | 6.5 | 446 | 414 | 2733 | 620 | | | | Triassic |
| 0615203010000 | 94983 | 1 | 877 | 2228 | 2242 | 137484 | 83200 | 51419 | | | 6.1 | 100 | 340 | 1986 | 893 | | | | Triassic |
| 0615203510000 | 94992 | 1 | 872 | 2199 | 2214 | 116526 | 70430 | 43464 | | | 7.4 | 113 | 339 | 1722 | 933 | | | | Triassic |



Reproduced with permission of the copyright owner. Further reproduction prohibited without permission.

Reproduced with permission of the copyright owner. Further reproduction prohibited without permission.

| DLS | ID | # | elev | dtop | dbot | TDS | Cl | Na | $Na_c$ | K | pH | $SO_4$ | Mg | Ca | $HCO_3$ | $Ca_{ex}$ | $Na_{df}$ | Na/Cl | Aquifer |
|---|---|---|---|---|---|---|---|---|---|---|---|---|---|---|---|---|---|---|---|
| 0625150406000 | 95795 | 2 | 920 | 1900 | 1916 | 121065 | 73500 | 44819 | | | 6.5 | 218 | 414 | 1979 | 273 | | | | Triassic |
| 0625161410000 | 95807 | 2 | 971 | 1974 | 1984 | 115330 | 69580 | 41827 | | | 7.3 | 308 | 437 | 2640 | 1093 | | | | Triassic |
| 0625161410000 | 95807 | 3 | 971 | 1974 | 1984 | 114699 | 69225 | 42012 | | | 7.8 | 283 | 122 | 2680 | 766 | | | | Triassic |
| 0625210212000 | 96015 | 1 | 880 | 2213 | 2256 | 122551 | 73997 | 45926 | | | 6.9 | 211 | 248 | 1754 | 845 | | | | Triassic |
| 0625211412000 | 96027 | 1 | 796 | 2120 | 2135 | 144519 | 87600 | 53989 | | | 6.8 | 257 | 391 | 2066 | 440 | | | | Triassic |
| 0625211610000 | 96028 | 1 | 839 | 2169 | 2195 | 115389 | 70031 | 42952 | | | 7.5 | 14 | 335 | 1784 | 556 | | | | Triassic |
| 0635140707000 | 120993 | 0 | 928 | 1803 | 1809 | 87076 | 51118 | 31985 | | | 7.9 | 1069 | 251 | 1443 | 1210 | | | | Triassic |
| 0645160410000 | 98452 | 2 | 921 | 1829 | 1844 | 128325 | 77257 | 47054 | | | 7.5 | 580 | 432 | 2460 | 681 | | | | Triassic |
| 0655220107000 | 100995 | 2 | 786 | 1942 | 1957 | 148332 | 90000 | 54385 | | | 6.8 | 403 | 790 | 2503 | 510 | | | | Triassic |
| 0655223411000 | 101004 | 2 | 722 | 1841 | 1856 | 147527 | 89158 | 54793 | | | 6.2 | 319 | 270 | 2591 | 805 | | | | Triassic |
| 0655223411000 | 101004 | 3 | 722 | 1841 | 1856 | 146243 | 88453 | 54337 | | | 6.2 | 259 | 270 | 2550 | 761 | | | | Triassic |
| 0665212302000 | 102357 | 2 | 724 | 1725 | 1750 | 154693 | 93500 | 56967 | | | 6.3 | 455 | 243 | 3204 | 660 | | | | Triassic |
| 0675210210000 | 103526 | 2 | 748 | 1721 | 1727 | 145037 | 87340 | 52868 | | | 6.6 | 940 | 565 | 2980 | 701 | | | | Triassic |
| 0675210210000 | 103526 | 3 | 748 | 1721 | 1727 | 147833 | 89400 | 53532 | | | 6.3 | 668 | 661 | 3267 | 620 | | | | Triassic |
| 0675210606000 | 103527 | 1 | 661 | 1664 | 1677 | 145440 | 87985 | 53442 | | | 6.5 | 592 | 522 | 2683 | 438 | | | | Triassic |
| 0675210811000 | 124012 | 0 | 702 | 1704 | 1714 | 144983 | 89500 | 46345 | | | 7.4 | 889 | 1578 | 5005 | 610 | | | | Triassic |
| 0675212815000 | 103533 | 2 | 707 | 1721 | 1725 | 149778 | 90340 | 54214 | | | 0.0 | 1080 | 660 | 3298 | 378 | | | | Triassic |
| 0675220211000 | 103536 | 2 | 704 | 1730 | 1739 | 151238 | 91370 | 55642 | | | 7.4 | 576 | 468 | 2790 | 370 | | | | Triassic |
| 0675221610000 | 103540 | 2 | 694 | 1689 | 1702 | 143982 | 86900 | 53000 | | | 6.6 | 474 | 491 | 2635 | 980 | | | | Triassic |
| 0675243506000 | 103577 | 3 | 767 | 1939 | 1960 | 149925 | 89859 | 54657 | | | 7.3 | 1455 | 515 | 3123 | 644 | | | | Triassic |
| 0675243506000 | 103577 | 4 | 767 | 1939 | 1960 | 149197 | 89386 | 54406 | | | 7.2 | 1457 | 477 | 3144 | 664 | | | | Triassic |
| 0675243506000 | 103577 | 5 | 767 | 1850 | 1857 | 148706 | 89623 | 54856 | | | 7.1 | 701 | 490 | 2613 | 859 | | | | Triassic |
| 0675243610020 | 103579 | 4 | 775 | 1839 | 1844 | 152851 | 92450 | 56013 | | | 7.2 | 611 | 710 | 2739 | 666 | | | | Triassic |
| 0685191916000 | 104422 | 2 | 759 | 1568 | 1573 | 129938 | 78658 | 47605 | | | 7.2 | 492 | 683 | 2229 | 551 | | | | Triassic |
| 0685192811000 | 104423 | 6 | 796 | 1578 | 1597 | 136326 | 82344 | 50346 | | | 6.4 | 539 | 429 | 2376 | 595 | | | | Triassic |
| 0685211903000 | 124406 | 0 | 656 | 1562 | 1564 | 152161 | 91818 | 54205 | | | 6.6 | 798 | 918 | 3691 | 519 | | | | Triassic |
| 0685212607000 | 104444 | 1 | 720 | 1573 | 1585 | 148337 | 89500 | 53262 | | | 6.8 | 858 | 790 | 3504 | 859 | | | | Triassic |
| 0685212607000 | 104444 | 2 | 720 | 1573 | 1585 | 148929 | 89890 | 53842 | | | 7.4 | 877 | 685 | 3270 | 302 | | | | Triassic |
| 0685221014000 | 163677 | 12 | 669 | 1609 | 1614 | 156623 | 95000 | 56823 | | | 6.8 | 683 | 1093 | 2803 | 451 | | | | Triassic |
| 0685221014000 | 163677 | 13 | 669 | 1610 | 1612 | 151659 | 92000 | 54302 | | | 6.5 | 702 | 1165 | 3223 | 542 | | | | Triassic |
| 0685222303020 | 104474 | 1 | 658 | 1565 | 1575 | 159757 | 96600 | 58651 | | | 6.5 | 644 | 588 | 2979 | 600 | | | | Triassic |
| 0685222303020 | 104474 | 2 | 658 | 1558 | 1567 | 152167 | 92000 | 55678 | | | 6.6 | 642 | 608 | 2939 | 610 | | | | Triassic |
| 0685222407000 | 104481 | 1 | 648 | 1547 | 1549 | 151903 | 91818 | 54211 | | | 6.6 | 798 | 918 | 3691 | 519 | | | | Triassic |
| 0685222407000 | 104481 | 2 | 648 | 1547 | 1549 | 151903 | 91818 | 54211 | | | 6.6 | 798 | 918 | 3691 | 519 | | | | Triassic |
| 0685222409000 | 104482 | 1 | 645 | 1544 | 1551 | 150459 | 91410 | 54347 | | | 6.8 | 4 | 462 | 3763 | 520 | | | | Triassic |
| 0685223207000 | 104499 | 2 | 701 | 1606 | 1623 | 148848 | 90000 | 54173 | | | 6.6 | 685 | 632 | 3083 | 560 | | | | Triassic |
| 0685223307000 | 104501 | 6 | 688 | 1591 | 1597 | 151299 | 91853 | 54311 | | | 6.8 | 671 | 974 | 3350 | 285 | | | | Triassic |
| 0685223307000 | 104501 | 8 | 688 | 1591 | 1597 | 155909 | 94335 | 56995 | | | 7.1 | 700 | 406 | 3350 | 250 | | | | Triassic |

| DLS | ID | # | elev | dtop | dbot | TDS | Cl | Na | $Na_c$ | K | pH | $SO_4$ | Mg | Ca | $HCO_3$ | $Ca_{ex}$ | $Na_{df}$ | Na/Cl | Aquifer |
|---|---|---|---|---|---|---|---|---|---|---|---|---|---|---|---|---|---|---|---|
| 0685230510000 | 104524 | 1 | 789 | 1833 | 1855 | 149553 | 90385 | 54266 | | | 6.4 | 693 | 784 | 3043 | 776 | | | | Triassic |
| 0685232511000 | 104531 | 5 | 725 | 1670 | 1688 | 152789 | 92400 | 55359 | | | 6.5 | 700 | 797 | 3187 | 704 | | | | Triassic |
| 0686042408000 | 104579 | 1 | 733 | 2171 | 2177 | 113640 | 69000 | 40574 | | | 6.6 | 347 | 610 | 2910 | 405 | | | | Triassic |
| 0695192804000 | 105337 | 1 | 744 | 1470 | 1473 | 132779 | 80500 | 48376 | | | 6.2 | 546 | 904 | 2226 | 460 | | | | Triassic |
| 0695210509020 | 105388 | 2 | 663 | 1505 | 1508 | 153425 | 92700 | 55645 | | | 6.9 | 866 | 765 | 3179 | 550 | | | | Triassic |
| 0695210509020 | 105388 | 3 | 663 | 1505 | 1508 | 154107 | 93023 | 55519 | | | 6.7 | 867 | 532 | 3836 | 393 | | | | Triassic |
| 0695210701000 | 105401 | 2 | 651 | 1498 | 1501 | 151009 | 91315 | 54166 | | | 6.2 | 791 | 888 | 3448 | 387 | | | | Triassic |
| 0695210701000 | 105401 | 1 | 651 | 1440 | 1498 | 151202 | 91362 | 54788 | | | 6.7 | 558 | 827 | 3067 | 784 | | | | Triassic |
| 0695210811000 | 105413 | 1 | 642 | 1495 | 1498 | 132410 | 80000 | 47096 | | | 6.8 | 823 | 1047 | 3051 | 800 | | | | Triassic |
| 0695220103000 | 105426 | 2 | 653 | 1521 | 1525 | 119619 | 72000 | 43183 | | | 6.8 | 883 | 486 | 2803 | 537 | | | | Triassic |
| 0695220311000 | 105447 | 1 | 675 | 1560 | 1562 | 137078 | 83000 | 49509 | | | 6.2 | 668 | 938 | 2683 | 570 | | | | Triassic |
| 0695221201020 | 105474 | 1 | 641 | 1487 | 1495 | 157060 | 94874 | 57094 | | | 6.7 | 728 | 629 | 3352 | 623 | | | | Triassic |
| 0695221201020 | 105474 | 2 | 641 | 1487 | 1495 | 150051 | 90681 | 54357 | | | 6.3 | 746 | 662 | 3302 | 616 | | | | Triassic |
| 0695221205000 | 105477 | 1 | 654 | 1504 | 1507 | 150890 | 91356 | 53995 | | | 7.4 | 713 | 840 | 3688 | 605 | | | | Triassic |
| 0695221207000 | 105479 | 4 | 652 | 1497 | 1503 | 152936 | 93100 | 52977 | | | 6.8 | 719 | 1495 | 4430 | 439 | | | | Triassic |
| 0696012207000 | 105538 | 1 | 651 | 1820 | 1859 | 149970 | 90897 | 55558 | | | 6.5 | 396 | 798 | 2011 | 630 | | | | Triassic |
| 0585152810000 | 152086 | 4 | 966 | 2130 | 2145 | 93563 | 56200 | 35029 | 34491 | 912 | 7.3 | 190 | 264 | 1280 | 1220 | 4 | -141 | 0.946 | Permian |
| 0585152810000 | 152086 | 2 | 966 | 2130 | 2145 | 85498 | 51200 | 31571 | 31085 | 824 | 7.8 | 244 | 294 | 1500 | 1400 | 20 | -114 | 0.936 | Permian |
| 0585152602000 | 91956 | 4 | 1106 | 2254 | 2262 | 104626 | 63000 | 39119 | 38177 | 1598 | 7.4 | 431 | 322 | 1400 | 720 | 3 | -137 | 0.934 | Permian |
| 0625153608000 | 162674 | 1 | 894 | 1799 | 1803 | 81080 | 48500 | 29965 | 29228 | 1251 | 7.4 | 518 | 364 | 1241 | 1000 | 10 | -98 | 0.929 | Permian |
| 0675243610020 | 103579 | 3 | 775 | 1934 | 1944 | 154885 | 92600 | 56403 | 55711 | 1173 | 6.3 | 1630 | 644 | 3123 | 986 | 57 | -183 | 0.928 | Permian |
| 0585152810000 | 152086 | 3 | 966 | 2130 | 2145 | 91969 | 55600 | 33969 | 33391 | 980 | 7.4 | 248 | 299 | 1600 | 515 | 21 | -108 | 0.926 | Permian |
| 0635150216000 | 97074 | 1 | 922 | 1816 | 1834 | 101139 | 61300 | 37591 | 36758 | 1415 | 7.6 | 144 | 287 | 1610 | 421 | 15 | -116 | 0.925 | Permian |
| 0675161506000 | 153240 | 4 | 998 | 1704 | 1714 | 135634 | 82000 | 50229 | 49157 | 1820 | 7.3 | 488 | 440 | 2220 | 522 | 24 | -155 | 0.924 | Permian |
| 0585152110002 | 91953 | 1 | 962 | 2150 | 2153 | 94318 | 56900 | 34766 | 34017 | 1270 | 7.3 | 75 | 271 | 1790 | 1050 | 29 | -103 | 0.922 | Permian |
| 0675222106000 | 103544 | 1 | 699 | 1800 | 1811 | 156970 | 94100 | 56792 | 56088 | 1193 | 6.2 | 1568 | 595 | 3584 | 673 | 79 | -164 | 0.919 | Permian |
| 0675233006000 | 103571 | 5 | 776 | 1940 | 1945 | 155607 | 93400 | 56438 | 55660 | 1319 | 7.3 | 1514 | 705 | 3263 | 583 | 64 | -162 | 0.919 | Permian |
| 0625142014000 | 95787 | 1 | 896 | 1797 | 1801 | 119302 | 72000 | 43785 | 42595 | 2020 | 7.1 | 56 | 410 | 2350 | 1425 | 41 | -111 | 0.912 | Permian |
| 0625142014000 | 95787 | 3 | 896 | 1797 | 1801 | 115913 | 70000 | 42489 | 41411 | 1830 | 7.1 | 101 | 400 | 2320 | 1228 | 41 | -108 | 0.912 | Permian |
| 0625142014000 | 95787 | 2 | 896 | 1797 | 1801 | 117541 | 71000 | 43063 | 41861 | 2040 | 7.2 | 12 | 410 | 2380 | 1376 | 43 | -104 | 0.909 | Permian |
| 0635151206000 | 162746 | 1 | 911 | 1792 | 1806 | 105386 | 63600 | 38513 | 37473 | 1766 | 7.0 | 193 | 665 | 1786 | 1279 | 22 | -92 | 0.909 | Permian |
| 0615151006000 | 169979 | 4 | 833 | 1848 | 1855 | 96586 | 58200 | 34965 | 34073 | 1515 | 7.3 | 432 | 486 | 2082 | 856 | 42 | -74 | 0.903 | Permian |
| 0655161113000 | 100916 | 2 | 1049 | 1860 | 1875 | 135402 | 81800 | 48502 | 47500 | 1700 | 7.0 | 704 | 510 | 3604 | 573 | 93 | -88 | 0.895 | Permian |
| 0615151508000 | 182960 | 1 | 845 | 1845 | 1850 | 119265 | 72000 | 43828 | | | 6.7 | 280 | 563 | 2050 | 1108 | | | | Permian |
| 0635143506000 | 97070 | 2 | 1027 | 1811 | 1834 | 90564 | 54385 | 33448 | | | 6.7 | 250 | 270 | 1633 | 1176 | | | | Permian |
| 0635150410000 | 97075 | 1 | 990 | 1902 | 1912 | 90013 | 53980 | 33179 | | | 6.9 | 230 | 252 | 1714 | 1340 | | | | Permian |
| 0635151510000 | 97080 | 2 | 946 | 1830 | 1839 | 105052 | 63400 | 38850 | | | 6.3 | 155 | 467 | 1634 | 1110 | | | | Permian |
| 0635162410000 | 177632 | 1 | 1034 | 1952 | 1964 | 120582 | 72600 | 44915 | | | 6.2 | 327 | 289 | 1910 | 1100 | | | | Permian |



Reproduced with permission of the copyright owner. Further reproduction prohibited without permission.

Reproduced with permission of the copyright owner. Further reproduction prohibited without permission.



| DLS | ID | # | elev | dtop | dbot | TDS | Cl | Na | $Na_c$ | K | pH | $SO_4$ | Mg | Ca | $HCO_3$ | $Ca_{ex}$ | $Na_{df}$ | Na/Cl | Aquifer |
|---|---|---|---|---|---|---|---|---|---|---|---|---|---|---|---|---|---|---|---|
| 0655203310000 | 100980 | 3 | 742 | 1815 | 1830 | 133222 | 80300 | 48909 | | | 6.4 | 885 | 495 | 2441 | 390 | | | | Permian |
| 0655211406000 | 100983 | 2 | 780 | 1958 | 1976 | 134963 | 81600 | 49145 | | | 6.2 | 805 | 554 | 2771 | 180 | | | | Permian |
| 0655211715000 | 100986 | 7 | 729 | 1933 | 1937 | 141226 | 85398 | 50097 | | | 7.2 | 869 | 560 | 4149 | 313 | | | | Permian |
| 0655260410000 | 101047 | 1 | 915 | 2532 | 2544 | 150342 | 90170 | 54847 | | | 7.2 | 1508 | 462 | 3161 | 395 | | | | Permian |
| 0655260410000 | 101047 | 2 | 915 | 2532 | 2544 | 152797 | 91590 | 55559 | | | 7.1 | 1545 | 486 | 3360 | 522 | | | | Permian |
| 0665261712000 | 102416 | 4 | 799 | 2345 | 2354 | 154713 | 94075 | 56456 | | | 7.3 | 40 | 510 | 3340 | 595 | | | | Permian |
| 0675210210000 | 103526 | 5 | 748 | 1812 | 1822 | 104229 | 62600 | 37274 | | | 6.7 | 950 | 535 | 2595 | 560 | | | | Permian |
| 0675212410000 | 103530 | 3 | 742 | 1753 | 1770 | 151967 | 91620 | 54784 | | | 6.4 | 1020 | 695 | 3530 | 646 | | | | Permian |
| 0675220815000 | 103537 | 3 | 704 | 1804 | 1809 | 148926 | 89580 | 53833 | | | 0.0 | 1360 | 586 | 3416 | 307 | | | | Permian |
| 0675221214000 | 103539 | 1 | 664 | 1762 | 1772 | 128513 | 77000 | 46201 | | | 6.8 | 1430 | 575 | 3065 | 492 | | | | Permian |
| 0675222710000 | 103551 | 4 | 676 | 1743 | 1746 | 139536 | 83920 | 50499 | | | 0.0 | 1260 | 624 | 3044 | 385 | | | | Permian |
| 0675230809000 | 103559 | 2 | 776 | 1973 | 1984 | 146839 | 88377 | 51700 | | | 7.0 | 1465 | 883 | 4195 | 445 | | | | Permian |
| 0675242110000 | 103573 | 3 | 751 | 2004 | 2012 | 147286 | 88347 | 52634 | | | 7.0 | 1298 | 340 | 4293 | 761 | | | | Permian |
| 0685220503000 | 104466 | 1 | 700 | 1778 | 1782 | 151078 | 90860 | 54218 | | | 6.9 | 1379 | 650 | 3752 | 445 | | | | Permian |
| 0685230801000 | 104525 | 3 | 792 | 1931 | 1938 | 149658 | 89730 | 54202 | | | 8.0 | 1442 | 487 | 3484 | 635 | | | | Permian |
| 0685240312000 | 177859 | 1 | 737 | 1914 | 1925 | 128643 | 76805 | 46941 | | | 6.4 | 1414 | 332 | 2786 | 742 | | | | Permian |
| 0685252606000 | 104542 | 6 | 708 | 1907 | 1920 | 161429 | 96400 | 59244 | | | 6.4 | 1625 | 333 | 3320 | 1031 | | | | Permian |
| 0686020611000 | 104556 | 4 | 707 | 2325 | 2331 | 145175 | 87384 | 51353 | | | 6.9 | 1419 | 1098 | 3618 | 615 | | | | Permian |
| 0686041706000 | 104574 | 8 | 687 | 2475 | 2497 | 165409 | 99400 | 60392 | | | 6.2 | 1159 | 593 | 3379 | 990 | | | | Permian |
| 0695210609000 | 105396 | 3 | 650 | 1583 | 1590 | 140461 | 85398 | 50442 | | | 6.2 | 257 | 840 | 3227 | 605 | | | | Permian |
| 0695221112000 | 105472 | 4 | 658 | 1603 | 1610 | 145578 | 88176 | 52982 | | | 7.7 | 401 | 548 | 3144 | 665 | | | | Permian |
| 0695221609000 | 105490 | 3 | 686 | 1608 | 1625 | 148891 | 90363 | 54384 | | | 6.5 | 107 | 144 | 3648 | 500 | | | | Permian |
| 0695251306000 | 105527 | 3 | 758 | 1912 | 1943 | 138412 | 83585 | 48420 | | | 7.5 | 1320 | 1159 | 3781 | 298 | | | | Permian |
| 0575161007000 | 90776 | 3 | 1051 | 2370 | 2383 | 76252 | 44981 | 29130 | 28423 | 1200 | 8.0 | 273 | 257 | 481 | 2299 | -24 | -148 | 0.974 | Mississippian |
| 0575161007000 | 90776 | 4 | 1051 | 2377 | 2380 | 62782 | 36884 | 23989 | 23012 | 1660 | 7.8 | 173 | 187 | 442 | 2250 | -17 | -109 | 0.962 | Mississippian |
| 0615152310000 | 94867 | 2 | 881 | 1885 | 1894 | 115681 | 69091 | 43392 | 42332 | 1800 | 6.7 | 862 | 280 | 1501 | 1128 | 2 | -170 | 0.945 | Mississippian |
| 0615152310000 | 94867 | 1 | 881 | 1885 | 1894 | 112905 | 67292 | 42519 | 41223 | 2200 | 7.4 | 716 | 350 | 1231 | 1621 | -10 | -165 | 0.945 | Mississippian |
| 0495162511000 | 75191 | 2 | 1071 | 2984 | 2987 | 72442 | 43694 | 27126 | 26665 | 782 | 7.6 | 24 | 369 | 766 | 942 | -8 | -103 | 0.941 | Mississippian |
| 0605151110000 | 93702 | 1 | 818 | 1879 | 1880 | 102585 | 62000 | 38383 | 37411 | 1650 | 7.7 | 31 | 310 | 1400 | 937 | 4 | -128 | 0.930 | Mississippian |
| 0645173510000 | 98463 | 4 | 846 | 1740 | 1755 | 109609 | 65700 | 40381 | 39619 | 1293 | 7.4 | 979 | 395 | 1880 | 556 | 24 | -134 | 0.930 | Mississippian |
| 0595150701002 | 169791 | 1 | 1008 | 2200 | 2202 | 117007 | 70547 | 43589 | 42534 | 1790 | 7.3 | 480 | 364 | 1702 | 662 | 10 | -144 | 0.930 | Mississippian |
| 0645173510000 | 98463 | 3 | 846 | 1775 | 1790 | 123025 | 74200 | 45677 | 44711 | 1640 | 7.5 | 502 | 394 | 1914 | 686 | 17 | -150 | 0.929 | Mississippian |
| 0635143310000 | 121020 | 0 | 1029 | 1846 | 1853 | 86367 | 53300 | 29400 | 32047 | 1690 | 7.2 | 185 | 251 | 1120 | 393 | -1 | -105 | 0.927 | Mississippian |
| 0675180310020 | 153241 | 4 | 823 | 1700 | 1719 | 129436 | 78200 | 47764 | 46844 | 1560 | 6.3 | 620 | 424 | 2250 | 363 | 29 | -146 | 0.924 | Mississippian |
| 0675180310020 | 153241 | 1 | 823 | 1700 | 1719 | 128096 | 77200 | 47129 | 46222 | 1540 | 6.9 | 624 | 424 | 2360 | 730 | 36 | -143 | 0.923 | Mississippian |
| 0635151309000 | 97078 | 3 | 923 | 1800 | 1805 | 87198 | 52400 | 32252 | 31339 | 1550 | 7.8 | 274 | 326 | 1430 | 1050 | 16 | -96 | 0.922 | Mississippian |
| 0465151411000 | 107995 | 0 | 1210 | 3336 | 3340 | 61137 | 35500 | 21000 | 21221 | 1680 | 7.4 | 35 | 194 | 978 | 1750 | 11 | -64 | 0.922 | Mississippian |
| 0635152707000 | 97085 | 2 | 997 | 1885 | 1893 | 91739 | 55100 | 33830 | 32934 | 1520 | 7.0 | 245 | 277 | 1698 | 1198 | 26 | -100 | 0.922 | Mississippian |

Reproduced with permission of the copyright owner. Further reproduction prohibited without permission.

| DLS | ID | # | elev | dtop | dbot | TDS | Cl | Na | $Na_c$ | K | pH | $SO_4$ | Mg | Ca | $HCO_3$ | $Ca_{ex}$ | $Na_{df}$ | Na/Cl | Aquifer |
|---|---|---|---|---|---|---|---|---|---|---|---|---|---|---|---|---|---|---|---|
| 0675180310020 | 153241 | 2 | 823 | 1700 | 1719 | 123579 | 74600 | 45353 | 44516 | 1420 | 7.2 | 564 | 424 | 2360 | 566 | 39 | -132 | 0.920 | Mississippian |
| 0555182110000 | 87446 | 1 | 1041 | 2651 | 2667 | 81565 | 49100 | 30166 | 29165 | 1700 | 6.8 | 29 | 299 | 1377 | 1208 | 17 | -81 | 0.916 | Mississippian |
| 0605201716000 | 118818 | 0 | 952 | 2440 | 2459 | 128264 | 73600 | 48700 | 43681 | 2180 | 7.6 | 443 | 524 | 2000 | 817 | 22 | -120 | 0.915 | Mississippian |
| 0565182110000 | 89399 | 2 | 1190 | 2724 | 2736 | 79688 | 47800 | 29420 | 28262 | 1967 | 7.1 | 58 | 233 | 1481 | 1415 | 23 | -73 | 0.912 | Mississippian |
| 0565180306000 | 115769 | 0 | 1095 | 2645 | 2685 | 63342 | 36750 | 22061 | 21711 | 1337 | 6.9 | 91 | 316 | 1201 | 1586 | 21 | -55 | 0.911 | Mississippian |
| 0565212811000 | 89450 | 1 | 1043 | 2951 | 2960 | 127141 | 76400 | 47293 | 45108 | 3714 | 7.2 | 568 | 287 | 2074 | 1055 | 22 | -114 | 0.910 | Mississippian |
| 0675150311000 | 103448 | 1 | 940 | 1615 | 1638 | 104132 | 62600 | 37737 | 36953 | 1330 | 7.2 | 667 | 530 | 2178 | 854 | 42 | -93 | 0.910 | Mississippian |
| 0675180310020 | 153241 | 5 | 823 | 1700 | 1719 | 124063 | 75000 | 45277 | 44257 | 1730 | 6.4 | 604 | 484 | 2510 | 383 | 46 | -111 | 0.910 | Mississippian |
| 0575163011000 | 160941 | 0 | 1078 | 2382 | 2386 | 75446 | 45200 | 26200 | 26621 | 1930 | 7.8 | 5 | 238 | 1190 | 683 | 11 | -65 | 0.908 | Mississippian |
| 0595173407000 | 92839 | 6 | 937 | 2160 | 2166 | 114323 | 69057 | 42201 | 40641 | 2650 | 7.1 | 3 | 305 | 2153 | 1228 | 34 | -97 | 0.907 | Mississippian |
| 0555171506000 | 163212 | 0 | 940 | 2479 | 2490 | 72795 | 42500 | 24380 | 24979 | 1740 | 6.7 | 30 | 189 | 1586 | 1603 | 34 | -59 | 0.906 | Mississippian |
| 0665153012000 | 102268 | 1 | 884 | 1593 | 1609 | 137224 | 83100 | 49575 | 48662 | 1548 | 6.9 | 609 | 996 | 2603 | 695 | 42 | -107 | 0.903 | Mississippian |
| 0615151006000 | 169979 | 4 | 833 | 1848 | 1855 | 96586 | 58200 | 34965 | 34073 | 1515 | 7.3 | 432 | 486 | 2082 | 856 | 42 | -74 | 0.903 | Mississippian |
| 0555171704000 | 163162 | 0 | 993 | 2526 | 2530 | 74277 | 44500 | 24495 | 26049 | 1720 | 7.6 | 26 | 335 | 1369 | 1047 | 21 | -57 | 0.903 | Mississippian |
| 0545191107000 | 85216 | 1 | 993 | 2787 | 2810 | 90415 | 54400 | 32957 | 31789 | 1984 | 6.5 | 51 | 510 | 1722 | 1576 | 28 | -67 | 0.901 | Mississippian |
| 0555182606000 | 140019 | 3 | 1051 | 2621 | 2637 | 76447 | 45900 | 27744 | 26704 | 1766 | 6.6 | 74 | 437 | 1562 | 1486 | 29 | -51 | 0.897 | Mississippian |
| 0666061406000 | 102444 | 6 | 847 | 3096 | 3115 | 146023 | 88700 | 53294 | 51248 | 3476 | 6.6 | 265 | 471 | 3129 | 332 | 62 | -84 | 0.891 | Mississippian |
| 0666061406000 | 102444 | 7 | 847 | 3096 | 3115 | 143587 | 87200 | 52393 | 50365 | 3446 | 6.5 | 317 | 465 | 3078 | 271 | 61 | -82 | 0.891 | Mississippian |
| 0505190906000 | 79046 | 5 | 1052 | 3389 | 3392 | 68255 | 41023 | 24326 | 22925 | 2380 | 7.5 | 23 | 432 | 1751 | 1424 | 44 | -5 | 0.862 | Mississippian |
| 0505190906000 | 79046 | 3 | 1052 | 3389 | 3392 | 68150 | 41023 | 23938 | 22561 | 2340 | 7.6 | 35 | 478 | 2001 | 1372 | 56 | 11 | 0.848 | Mississippian |
| 0475160207000 | 67762 | 3 | 1257 | 3451 | 3463 | 66934 | 40212 | 23661 | | | 8.0 | 49 | 441 | 1869 | 1428 | | | | Mississippian |
| 0475160207000 | 67762 | 1 | 1257 | 3451 | 3463 | 67414 | 40491 | 23754 | | | 8.1 | 40 | 466 | 1925 | 1501 | | | | Mississippian |
| 0475160207000 | 67762 | 2 | 1257 | 3451 | 3463 | 68018 | 41050 | 23270 | | | 7.2 | 105 | 729 | 2204 | 1342 | | | | Mississippian |
| 0495171211000 | 75197 | 4 | 1142 | 3197 | 3219 | 50486 | 29559 | 18755 | | | 7.1 | 96 | 201 | 793 | 2201 | | | | Mississippian |
| 0495191306000 | 75217 | 3 | 1077 | 3423 | 3438 | 55441 | 33126 | 20844 | | | 7.2 | 27 | 167 | 687 | 1200 | | | | Mississippian |
| 0495191306000 | 75217 | 2 | 1077 | 3423 | 3438 | 56785 | 33831 | 21320 | | | 7.4 | 163 | 107 | 805 | 1137 | | | | Mississippian |
| 0505160611000 | 79026 | 2 | 1079 | 3025 | 3038 | 58680 | 33700 | 22906 | | | 6.8 | 103 | 40 | 210 | 3500 | | | | Mississippian |
| 0505160611000 | 79026 | 1 | 1079 | 3041 | 3071 | 59366 | 34200 | 23170 | | | 6.9 | 99 | 43 | 207 | 3350 | | | | Mississippian |
| 0505160906000 | 79027 | 2 | 1061 | 2950 | 2973 | 57697 | 33200 | 22558 | | | 7.2 | 76 | 31 | 185 | 3350 | | | | Mississippian |
| 0505160906000 | 79027 | 1 | 1061 | 2952 | 3010 | 57980 | 33200 | 22638 | | | 8.1 | 184 | 50 | 182 | 3510 | | | | Mississippian |
| 0505190906000 | 79046 | 4 | 1052 | 3389 | 3392 | 68478 | 41203 | 24255 | | | 7.7 | 39 | 478 | 1828 | 1372 | | | | Mississippian |
| 0515160111000 | 81215 | 2 | 1056 | 2853 | 2875 | 50049 | 28362 | 19539 | | | 7.9 | 16 | 91 | 132 | 3881 | | | | Mississippian |
| 0515160911000 | 81220 | 1 | 1106 | 2908 | 2931 | 55467 | 31700 | 21690 | | | 6.8 | 91 | 40 | 171 | 3610 | | | | Mississippian |
| 0515170810000 | 81230 | 1 | 990 | 2926 | 2936 | 61733 | 37363 | 22021 | | | 7.0 | 14 | 773 | 1020 | 1103 | | | | Mississippian |
| 0515181810000 | 81249 | 1 | 974 | 3049 | 3074 | 52857 | 31524 | 19455 | | | 8.4 | 142 | 207 | 960 | 1157 | | | | Mississippian |
| 0515181810000 | 81249 | 2 | 974 | 3049 | 3074 | 56075 | 33548 | 20648 | | | 8.2 | 30 | 207 | 1040 | 1225 | | | | Mississippian |
| 0515181810000 | 81249 | 4 | 974 | 3049 | 3074 | 64129 | 38163 | 23676 | | | 7.3 | 2 | 243 | 1140 | 1840 | | | | Mississippian |
| 0515181810000 | 81249 | 3 | 974 | 3049 | 3074 | 65160 | 39050 | 24016 | | | 7.4 | 21 | 316 | 1080 | 1376 | | | | Mississippian |

Reproduced with permission of the copyright owner. Further reproduction prohibited without permission.

| DLS | ID | # | elev | dtop | dbot | TDS | Cl | Na | $Na_c$ | K | pH | $SO_4$ | Mg | Ca | $HCO_3$ | $Ca_{ex}$ | $Na_{df}$ | Na/Cl | Aquifer |
|---|---|---|---|---|---|---|---|---|---|---|---|---|---|---|---|---|---|---|---|
| 0515182710000 | 81252 | 2 | 1001 | 2970 | 2989 | 52074 | 30530 | 19857 | | | 7.6 | 16 | 146 | 440 | 2206 | | | | Mississippian |
| 0515182710000 | 81252 | 1 | 1001 | 2970 | 2989 | 52155 | 30530 | 19897 | | | 7.3 | 33 | 170 | 400 | 2289 | | | | Mississippian |
| 0525200210000 | 82732 | 4 | 1040 | 3214 | 3257 | 65736 | 39300 | 24107 | | | 7.2 | 86 | 253 | 1289 | 1425 | | | | Mississippian |
| 0525201309000 | 82736 | 2 | 1036 | 3159 | 3161 | 60811 | 36500 | 22077 | | | 7.1 | 25 | 313 | 1289 | 1235 | | | | Mississippian |
| 0525210407000 | 82744 | 1 | 1100 | 3400 | 3424 | 108457 | 64906 | 42008 | | | 7.8 | 181 | 172 | 396 | 1615 | | | | Mississippian |
| 0525212406000 | 82750 | 1 | 1035 | 3313 | 3358 | 103655 | 62480 | 38674 | | | 7.3 | 4 | 292 | 1560 | 1313 | | | | Mississippian |
| 0525213310000 | 82752 | 3 | 1050 | 3394 | 3397 | 127026 | 76600 | 47406 | | | 6.7 | 196 | 291 | 1962 | 1161 | | | | Mississippian |
| 0535163404000 | 83808 | 1 | 899 | 2452 | 2460 | 63708 | 37000 | 24528 | | | 6.6 | 140 | 136 | 384 | 3090 | | | | Mississippian |
| 0535173106000 | 83845 | 5 | 966 | 2668 | 2694 | 67047 | 39600 | 25313 | | | 7.0 | 115 | 136 | 841 | 2120 | | | | Mississippian |
| 0535182606000 | 83898 | 2 | 960 | 2729 | 2743 | 79473 | 47000 | 30397 | | | 7.0 | 49 | 179 | 619 | 2500 | | | | Mississippian |
| 0535183011000 | 83906 | 1 | 978 | 2797 | 2806 | 80406 | 47900 | 30801 | | | 6.8 | 257 | 107 | 633 | 1440 | | | | Mississippian |
| 0535200810000 | 83949 | 1 | 1036 | 3131 | 3192 | 77624 | 45795 | 28474 | | | 7.5 | 528 | 219 | 1600 | 2050 | | | | Mississippian |
| 0535211710000 | 83965 | 2 | 1066 | 3365 | 3392 | 120226 | 72500 | 44810 | | | 7.1 | 163 | 267 | 1926 | 1140 | | | | Mississippian |
| 0535221512000 | 83969 | 4 | 1068 | 3414 | 3459 | 109865 | 65943 | 40972 | | | 7.4 | 165 | 202 | 1813 | 1566 | | | | Mississippian |
| 0535221512000 | 83969 | 3 | 1068 | 3414 | 3459 | 124835 | 75087 | 46787 | | | 7.1 | 154 | 265 | 1792 | 1527 | | | | Mississippian |
| 0545191302000 | 85227 | 2 | 995 | 2740 | 2755 | 87245 | 52400 | 32281 | | | 7.3 | 51 | 316 | 1469 | 1480 | | | | Mississippian |
| 0545192506000 | 85252 | 1 | 981 | 2795 | 2802 | 97527 | 58770 | 36011 | | | 6.9 | 443 | 187 | 1825 | 220 | | | | Mississippian |
| 0545233602000 | 85296 | 1 | 1099 | 3359 | 3376 | 121849 | 73094 | 44716 | | | 7.4 | 413 | 303 | 2492 | 1318 | | | | Mississippian |
| 0555170506000 | 87406 | 4 | 946 | 2525 | 2533 | 75537 | 44700 | 28121 | | | 6.5 | 693 | 261 | 1074 | 1399 | | | | Mississippian |
| 0555171606000 | 87409 | 1 | 953 | 2462 | 2485 | 75649 | 45826 | 27990 | | | 7.1 | 18 | 357 | 1139 | 649 | | | | Mississippian |
| 0555183310000 | 87451 | 2 | 1094 | 2686 | 2695 | 77232 | 46300 | 28508 | | | 7.7 | 33 | 347 | 1277 | 1559 | | | | Mississippian |
| 0565171310000 | 89388 | 2 | 984 | 2414 | 2429 | 70436 | 42000 | 26472 | | | 7.0 | 37 | 213 | 885 | 1686 | | | | Mississippian |
| 0565191310000 | 89412 | 3 | 1194 | 2807 | 2815 | 95823 | 58000 | 35944 | | | 7.2 | 163 | 141 | 1405 | 347 | | | | Mississippian |
| 0565193201000 | 89428 | 6 | 1330 | 2971 | 2977 | 127571 | 77454 | 46910 | | | 7.7 | 191 | 560 | 2213 | 495 | | | | Mississippian |
| 0565212213000 | 89448 | 1 | 1115 | 3037 | 3057 | 92790 | 55500 | 34640 | | | 7.0 | 514 | 250 | 1343 | 1103 | | | | Mississippian |
| 0565222006000 | 89455 | 7 | 1178 | 3240 | 3264 | 119290 | 71400 | 44373 | | | 7.1 | 464 | 295 | 1890 | 1387 | | | | Mississippian |
| 0565222006000 | 89455 | 4 | 1178 | 3240 | 3264 | 124321 | 75000 | 46011 | | | 6.4 | 206 | 306 | 2243 | 1130 | | | | Mississippian |
| 0575162710000 | 90782 | 5 | 1175 | 2472 | 2499 | 73483 | 43698 | 27732 | | | 6.7 | 39 | 160 | 911 | 1918 | | | | Mississippian |
| 0575162710000 | 90782 | 1 | 1175 | 2474 | 2475 | 82914 | 49691 | 30976 | | | 7.8 | 26 | 270 | 1174 | 1581 | | | | Mississippian |
| 0575162910000 | 90784 | 1 | 1076 | 2390 | 2401 | 83683 | 49878 | 30781 | | | 7.8 | 40 | 535 | 1280 | 2377 | | | | Mississippian |
| 0575182510000 | 90804 | 1 | 1205 | 2637 | 2652 | 87341 | 52000 | 33482 | | | 7.4 | 142 | 236 | 521 | 1953 | | | | Mississippian |
| 0575182806000 | 90806 | 1 | 1289 | 2751 | 2761 | 71449 | 42760 | 26290 | | | 7.2 | 191 | 247 | 1342 | 1260 | | | | Mississippian |
| 0585152510000 | 91955 | 2 | 1047 | 2182 | 2192 | 98374 | 59006 | 36157 | | | 7.0 | 575 | 534 | 1560 | 1102 | | | | Mississippian |
| 0585153307000 | 91960 | 1 | 955 | 2135 | 2136 | 108279 | 65375 | 39944 | | | 7.0 | 252 | 440 | 1818 | 915 | | | | Mississippian |
| 0585192811000 | 92016 | 1 | 966 | 2457 | 2470 | 116284 | 70219 | 43074 | | | 7.7 | 369 | 372 | 1913 | 685 | | | | Mississippian |
| 0585203311000 | 92033 | 1 | 978 | 2557 | 2571 | 93769 | 56600 | 34820 | | | 7.0 | 125 | 260 | 1546 | 850 | | | | Mississippian |
| 0595150410000 | 92784 | 1 | 1021 | 2167 | 2180 | 103603 | 62210 | 38129 | | | 7.3 | 326 | 289 | 1965 | 995 | | | | Mississippian |
| 0595150906000 | 92788 | 1 | 1008 | 2150 | 2157 | 108343 | 65588 | 38458 | | | 7.6 | 15 | 411 | 3278 | 1206 | | | | Mississippian |

Reproduced with permission of the copyright owner. Further reproduction prohibited without permission.



| DLS | ID | # | elev | dtop | dbot | TDS | Cl | Na | $Na_c$ | K | pH | $SO_4$ | Mg | Ca | $HCO_3$ | $Ca_{ex}$ | $Na_{df}$ | Na/Cl | Aquifer |
|---|---|---|---|---|---|---|---|---|---|---|---|---|---|---|---|---|---|---|---|
| 0595152002000 | 92791 | 1 | 985 | 2073 | 2094 | 98231 | 59413 | 35931 | | | 7.3 | 163 | 447 | 1869 | 830 | | | | Mississippian |
| 0595163104000 | 92824 | 2 | 975 | 2179 | 2184 | 115182 | 70000 | 41745 | | | 7.4 | 51 | 680 | 2332 | 760 | | | | Mississippian |
| 0595163310000 | 92825 | 1 | 924 | 2073 | 2097 | 105536 | 63700 | 38047 | | | 6.5 | 168 | 428 | 2603 | 1200 | | | | Mississippian |
| 0595180111000 | 92844 | 1 | 1041 | 2399 | 2405 | 140918 | 85500 | 50699 | | | 6.2 | 126 | 741 | 3323 | 1075 | | | | Mississippian |
| 0595190810000 | 92880 | 3 | 911 | 2414 | 2429 | 134141 | 81000 | 49581 | | | 7.4 | 446 | 420 | 2316 | 769 | | | | Mississippian |
| 0595192906000 | 92893 | 4 | 991 | 2455 | 2477 | 116622 | 70497 | 43037 | | | 7.4 | 369 | 420 | 1999 | 610 | | | | Mississippian |
| 0595192906000 | 92893 | 3 | 991 | 2455 | 2477 | 129772 | 78554 | 47996 | | | 7.5 | 395 | 368 | 2260 | 405 | | | | Mississippian |
| 0595192906000 | 92893 | 1 | 991 | 2455 | 2477 | 133098 | 80568 | 49162 | | | 7.4 | 301 | 473 | 2260 | 680 | | | | Mississippian |
| 0595192906000 | 92893 | 2 | 991 | 2455 | 2477 | 134804 | 81575 | 49730 | | | 7.3 | 367 | 473 | 2347 | 635 | | | | Mississippian |
| 0595202607000 | 92903 | 2 | 1009 | 2518 | 2536 | 125731 | 76100 | 46856 | | | 7.3 | 45 | 352 | 1920 | 932 | | | | Mississippian |
| 0595202911000 | 92906 | 1 | 978 | 2506 | 2551 | 89682 | 54174 | 32592 | | | 6.7 | 68 | 262 | 2121 | 945 | | | | Mississippian |
| 0595211611000 | 92913 | 2 | 1088 | 2660 | 2665 | 95030 | 57700 | 34255 | | | 6.9 | 78 | 656 | 1962 | 770 | | | | Mississippian |
| 0595211611000 | 92913 | 1 | 1088 | 2660 | 2665 | 97564 | 59288 | 35256 | | | 7.2 | 8 | 572 | 2082 | 727 | | | | Mississippian |
| 0595213604000 | 92919 | 2 | 1034 | 2595 | 2601 | 115067 | 69509 | 42487 | | | 8.0 | 119 | 227 | 2250 | 965 | | | | Mississippian |
| 0595243404000 | 92941 | 3 | 1132 | 3024 | 3049 | 92891 | 55780 | 34332 | | | 7.8 | 461 | 272 | 1629 | 850 | | | | Mississippian |
| 0605150410000 | 93693 | 1 | 854 | 1930 | 1944 | 108513 | 65300 | 40215 | | | 6.4 | 239 | 384 | 1746 | 1280 | | | | Mississippian |
| 0605152012000 | 93709 | 2 | 807 | 1872 | 1879 | 90143 | 54400 | 32404 | | | 6.4 | 194 | 467 | 2162 | 1050 | | | | Mississippian |
| 0605220906000 | 93853 | 2 | 1086 | 2739 | 2761 | 128358 | 77300 | 48015 | | | 7.2 | 8 | 318 | 1881 | 1700 | | | | Mississippian |
| 0605220906000 | 93853 | 1 | 1086 | 2739 | 2761 | 131146 | 79075 | 48999 | | | 6.4 | 15 | 411 | 1850 | 1620 | | | | Mississippian |
| 0615150411000 | 94851 | 4 | 807 | 1829 | 1832 | 59485 | 35808 | 20035 | | | 7.5 | 246 | 731 | 2072 | 1206 | | | | Mississippian |
| 0615151404000 | 94861 | 2 | 831 | 1830 | 1838 | 106436 | 64245 | 39737 | | | 7.4 | 400 | 363 | 1425 | 540 | | | | Mississippian |
| 0615161706000 | 94892 | 4 | 886 | 1994 | 2006 | 125604 | 76200 | 44810 | | | 6.8 | 383 | 589 | 3371 | 509 | | | | Mississippian |
| 0615190410000 | 94943 | 1 | 955 | 2298 | 2318 | 123010 | 74300 | 44440 | | | 7.1 | 588 | 593 | 2755 | 680 | | | | Mississippian |
| 0625142008000 | 95784 | 2 | 897 | 1800 | 1814 | 100704 | 60705 | 37266 | | | 7.7 | 208 | 462 | 1520 | 1105 | | | | Mississippian |
| 0625142008000 | 95784 | 2 | 897 | 1800 | 1814 | 100704 | 60705 | 37266 | | | 7.7 | 208 | 462 | 1520 | 1105 | | | | Mississippian |
| 0625161410000 | 95807 | 4 | 971 | 2041 | 2053 | 123065 | 74195 | 45057 | | | 7.3 | 771 | 583 | 2200 | 527 | | | | Mississippian |
| 0625163006000 | 95814 | 3 | 954 | 2006 | 2017 | 130918 | 79400 | 48007 | | | 7.4 | 165 | 316 | 2763 | 542 | | | | Mississippian |
| 0625181211000 | 95836 | 2 | 888 | 2030 | 2047 | 113037 | 68205 | 41405 | | | 7.2 | 352 | 167 | 2565 | 698 | | | | Mississippian |
| 0625190614000 | 95858 | 2 | 869 | 2149 | 2190 | 139226 | 84000 | 51273 | | | 6.7 | 617 | 467 | 2515 | 720 | | | | Mississippian |
| 0625191604000 | 95870 | 2 | 874 | 2149 | 2156 | 104778 | 63339 | 38279 | | | 8.2 | 579 | 405 | 2078 | 200 | | | | Mississippian |
| 0625202711000 | 95994 | 1 | 838 | 2131 | 2164 | 120514 | 72511 | 44901 | | | 7.2 | 658 | 355 | 1760 | 670 | | | | Mississippian |
| 0635171407000 | 97097 | 1 | 1039 | 2053 | 2070 | 104765 | 63000 | 38579 | | | 6.9 | 609 | 389 | 1834 | 720 | | | | Mississippian |
| 0635220410000 | 97215 | 3 | 840 | 2316 | 2347 | 97806 | 58700 | 35867 | | | 6.5 | 741 | 292 | 1930 | 561 | | | | Mississippian |
| 0645153203000 | 98449 | 2 | 990 | 1809 | 1851 | 94546 | 56900 | 34837 | | | 6.9 | 323 | 340 | 1682 | 943 | | | | Mississippian |
| 0645192207000 | 98540 | 2 | 747 | 1846 | 1858 | 150006 | 90869 | 53284 | | | 6.8 | 826 | 1140 | 3587 | 610 | | | | Mississippian |
| 0645201410000 | 98570 | 2 | 818 | 1986 | 1996 | 150875 | 91000 | 55284 | | | 6.3 | 851 | 617 | 2803 | 650 | | | | Mississippian |
| 0645203606000 | 98576 | 3 | 768 | 1887 | 1900 | 134223 | 81000 | 49243 | | | 6.9 | 693 | 452 | 2579 | 520 | | | | Mississippian |
| 0655160902000 | 100915 | 1 | 962 | 1807 | 1820 | 140072 | 84800 | 51439 | | | 7.4 | 574 | 680 | 2362 | 442 | | | | Mississippian |

Reproduced with permission of the copyright owner. Further reproduction prohibited without permission.

| DLS | ID | # | elev | dtop | dbot | TDS | Cl | Na | $Na_c$ | K | pH | $SO_4$ | Mg | Ca | $HCO_3$ | $Ca_{ex}$ | $Na_{df}$ | Na/Cl | Aquifer |
|---|---|---|---|---|---|---|---|---|---|---|---|---|---|---|---|---|---|---|---|
| 0655192907000 | 100962 | 6 | 786 | 1829 | 1850 | 154786 | 93600 | 56441 | | | 6.8 | 741 | 729 | 3003 | 555 | | | | Mississippian |
| 0655202510000 | 100979 | 8 | 743 | 1808 | 1824 | 148388 | 89800 | 53681 | | | 6.8 | 770 | 826 | 3083 | 464 | | | | Mississippian |
| 0655211101000 | 100982 | 3 | 769 | 1958 | 1966 | 148017 | 89300 | 53942 | | | 6.6 | 1040 | 519 | 3090 | 107 | | | | Mississippian |
| 0665151815000 | 102251 | 1 | 990 | 1724 | 1733 | 131690 | 79483 | 48140 | | | 6.9 | 517 | 657 | 2418 | 966 | | | | Mississippian |
| 0665161409000 | 102291 | 3 | 859 | 1608 | 1628 | 132426 | 80478 | 48316 | | | 7.2 | 10 | 388 | 2939 | 600 | | | | Mississippian |
| 0665161409000 | 102291 | 1 | 859 | 1608 | 1628 | 138592 | 84000 | 50558 | | | 7.9 | 538 | 705 | 2603 | 384 | | | | Mississippian |
| 0665162508000 | 102297 | 2 | 875 | 1597 | 1612 | 123754 | 74880 | 45485 | | | 6.1 | 422 | 530 | 2165 | 554 | | | | Mississippian |
| 0665190815000 | 102323 | 4 | 773 | 1775 | 1782 | 134293 | 80900 | 49443 | | | 6.4 | 819 | 489 | 2358 | 576 | | | | Mississippian |
| 0675153010000 | 103452 | 1 | 956 | 1618 | 1631 | 154933 | 93740 | 57740 | | | 6.6 | 465 | 430 | 2310 | 504 | | | | Mississippian |
| 0685213613000 | 104462 | 1 | 704 | 1666 | 1670 | 113665 | 68200 | 41883 | | | 6.5 | 838 | 510 | 1826 | 830 | | | | Mississippian |
| 0695221109000 | 105469 | 1 | 655 | 1658 | 1682 | 83060 | 50419 | 29899 | | | 6.6 | 61 | 476 | 1890 | 640 | | | | Mississippian |
| 0655172406000 | 100923 | 1 | 944.5 | 2222 | 2224 | 230037 | 142178 | 67629 | 64873 | 4680 | 5.7 | 44 | 2169 | 17926 | 185 | 744 | 617 | 0.704 | Wabamun |
| 0695192602000 | 105335 | 1 | 822.6 | 2250 | 2270 | 220572 | 136100 | 60468 | 57964 | 4251 | 6 | 570 | 2357 | 20780 | 604 | 892 | 771 | 0.657 | Wabamun |
| 0635262812000 | 97303 | 1 | 897.6 | 3357 | 3360 | 246848 | 153000 | 66029 | 63641 | 4055 | 6.6 | 317 | 3183 | 24020 | 608 | 1036 | 933 | 0.641 | Wabamun |
| 0675243116000 | 103576 | 3 | 755.3 | 2751 | 2777 | 215334 | 134100 | 55645 | 53437 | 3750 | 6.4 | 737 | 4641 | 20060 | 307 | 859 | 919 | 0.614 | Wabamun |
| 0445162006000 | 61039 | 3 | 1191 | 4155 | 4164 | 116467 | 69500 | 37442 | | | 7.5 | 1350 | 593 | 6775 | 1641 | | | | Wabamun |
| 0495182210000 | 75209 | 1 | 1041 | 3725 | 3766 | 120792 | 71583 | 39921 | | | 7.6 | 1300 | 619 | 6062 | 2658 | | | | Wabamun |
| 0525211616000 | 82748 | 4 | 1095 | 3850 | 3901 | 169938 | 104000 | 55874 | | | 6.9 | 158 | 1162 | 8440 | 618 | | | | Wabamun |
| 0575170915000 | 90788 | 4 | 1156 | 3001 | 3016 | 198833 | 123825 | 49877 | | | 7.7 | 197 | 3024 | 21736 | 355 | | | | Wabamun |
| 0575191411000 | 90816 | 1 | 1136 | 3014 | 3077 | 176438 | 108800 | 49239 | | | 5.2 | 769 | 2029 | 15576 | 49 | | | | Wabamun |
| 0575193411000 | 90832 | 4 | 1201 | 3182 | 3185 | 194739 | 119800 | 56889 | | | 6.2 | 33 | 1555 | 15936 | 1070 | | | | Wabamun |
| 0585251010000 | 92062 | 1 | 1124 | 3735 | 3762 | 159736 | 97900 | 43024 | | | 6.8 | 173 | 1226 | 16500 | 1855 | | | | Wabamun |
| 0625140710000 | 95782 | 2 | 1063 | 2324 | 2331 | 189796 | 117480 | 51344 | | | 7.2 | 477 | 2976 | 17178 | 695 | | | | Wabamun |
| 0645252111000 | 98642 | 1 | 837 | 3057 | 3082 | 212603 | 131200 | 58473 | | | 7.4 | 517 | 2391 | 19692 | 670 | | | | Wabamun |
| 0646041506000 | 98680 | 2 | 887.3 | 3822 | 3830 | 194456 | 120520 | 47661 | | | 5.65 | 380 | 1710 | 24000 | 138 | | | | Wabamun |
| 0655180110000 | 100931 | 4 | 802.8 | 2316 | 2339 | 196539 | 121590 | 51386 | | | 7.1 | 366 | 2650 | 20056 | 1000 | | | | Wabamun |
| 0675192414000 | 103513 | 1 | 767.5 | 2265 | 2304 | 211759 | 131750 | 54992 | | | 6.5 | 448 | 3718 | 20701 | 305 | | | | Wabamun |
| 0676053107000 | 103618 | 3 | 684.6 | 3498 | 3611 | 226303 | 139800 | 62865 | | | 6.2 | 617 | 3256 | 19379 | 785 | | | | Wabamun |
| 0686040406000 | 104568 | 5 | 727.3 | 3374 | 3423 | 212093 | 130600 | 56226 | | | 6.3 | 698 | 2211 | 21822 | 1090 | | | | Wabamun |
| 0686041706000 | 104574 | 9 | 686.7 | 3369 | 3380 | 253153 | 156600 | 71103 | | | 5.7 | 216 | 2746 | 22262 | 460 | | | | Wabamun |
| 0686042110000 | 104576 | 4 | 669.3 | 3303 | 3335 | 227830 | 140800 | 63041 | | | 5.9 | 574 | 2819 | 20380 | 440 | | | | Wabamun |
| 0695210510000 | 105389 | 1 | 660.2 | 2284 | 2288 | 261291 | 162400 | 69804 | | | 6.3 | 318 | 4131 | 24424 | 435 | | | | Wabamun |
| 0695210703000 | 105402 | 3 | 650.7 | 2333 | 2345 | 232641 | 144500 | 61030 | | | 7.4 | 279 | 3770 | 22659 | 820 | | | | Wabamun |
| 0695221609000 | 105490 | 5 | 685.8 | 2391 | 2405 | 228075 | 142992 | 54382 | | | 6.5 | 316 | 5520 | 24624 | 490 | | | | Wabamun |
| 0696050805000 | 105548 | 2 | 660.2 | 3231 | 3307 | 237796 | 148200 | 59326 | | | 5.8 | 178 | 3985 | 25785 | 655 | | | | Wabamun |
| 0696051610000 | 105551 | 5 | 659.6 | 3294 | 3316 | 265297 | 164400 | 72829 | | | 5.3 | 146 | 2381 | 24024 | 720 | | | | Wabamun |
| 0525150706000 | 139132 | 1 | 920 | 3068 | 3073 | 144324 | 86500 | 52339 | 50954 | 2350 | 7.0 | 762 | 457 | 3411 | 1739 | 78 | -124 | 0.908 | Winterburn |
| 0525161306000 | 82662 | 2 | 946 | 3084 | 3105 | 158086 | 95000 | 57575 | 55873 | 2890 | 7.1 | 690 | 437 | 3604 | 1586 | 79 | -133 | 0.907 | Winterburn |

Reproduced with permission of the copyright owner. Further reproduction prohibited without permission.



| DLS | ID | # | elev | dtop | dbot | TDS | Cl | Na | $Na_c$ | K | pH | $SO_4$ | Mg | Ca | $HCO_3$ | $Ca_{ex}$ | $Na_{df}$ | Na/Cl | Aquifer |
|---|---|---|---|---|---|---|---|---|---|---|---|---|---|---|---|---|---|---|---|
| 0465170306000 | 64906 | 3 | 1307 | 4381 | 4384 | 130674 | 78460 | 47746 | 46089 | 2813 | 8.0 | 914 | 304 | 2869 | 776 | 60 | -107 | 0.906 | Winterburn |
| 0465170306000 | 64906 | 6 | 1307 | 4380 | 4383 | 144657 | 87300 | 52624 | 50356 | 3853 | 7.1 | 636 | 323 | 3437 | 686 | 79 | -79 | 0.889 | Winterburn |
| 0665151602000 | 123314 | 0 | 1007 | 2395 | 2408 | 148967 | 90900 | 49060 | 51785 | 1672 | 7.7 | 1827 | 1348 | 3984 | 176 | 102 | -54 | 0.878 | Winterburn |
| 0435150406000 | 59848 | 4 | 1400 | 4618 | 4627 | 137054 | 83465 | 48851 | 46673 | 3700 | 7.0 | 19 | 197 | 4379 | 292 | 130 | -11 | 0.862 | Winterburn |
| 0665151616000 | 123316 | 0 | 968 | 2250 | 2421 | 157787 | 93800 | 53500 | 51931 | 1920 | 7.4 | 970 | 914 | 5920 | 763 | 196 | 10 | 0.854 | Winterburn |
| 0665150513000 | 153203 | 1 | 936 | 2352 | 2368 | 186212 | 114000 | 59028 | 57129 | 3225 | 7.6 | 646 | 1700 | 10610 | 464 | 408 | 272 | 0.773 | Winterburn |
| 0695261810000 | 124954 | 0 | 664 | 2846 | 2853 | 191507 | 117500 | 50600 | 50220 | 3860 | 6.1 | 340 | 2890 | 16100 | 170 | 679 | 658 | 0.659 | Winterburn |
| 0675243116000 | 103576 | 2 | 755 | 2798 | 2815 | 214594 | 133300 | 55047 | 52819 | 3782 | 6.8 | 724 | 3912 | 21380 | 471 | 925 | 927 | 0.611 | Winterburn |
| 0515213311000 | 81274 | 2 | 1128 | 4019 | 4075 | 131567 | 79500 | 43025 | | | 7.3 | 881 | 633 | 7068 | 935 | | | | Winterburn |
| 0545191302000 | 85227 | 8 | 995 | 3445 | 3462 | 202090 | 124000 | 58846 | | | 6.5 | 583 | 2503 | 15415 | 1510 | | | | Winterburn |
| 0545191902000 | 85246 | 3 | 1041 | 3453 | 3493 | 192444 | 118400 | 54415 | | | 6.7 | 432 | 2211 | 16416 | 1160 | | | | Winterburn |
| 0545220607000 | 85279 | 6 | 1017 | 3919 | 3928 | 160575 | 96816 | 51564 | | | 7.6 | 117 | 751 | 9688 | 3333 | | | | Winterburn |
| 0555191914020 | 87459 | 3 | 1147 | 3516 | 3625 | 152753 | 91850 | 49875 | | | 7.7 | 506 | 849 | 8226 | 2943 | | | | Winterburn |
| 0565211806000 | 89447 | 1 | 1020 | 3606 | 3627 | 119031 | 72220 | 39006 | | | 7.9 | 342 | 1703 | 4801 | 1950 | | | | Winterburn |
| 0575230607000 | 90862 | 1 | 1060 | 3776 | 3787 | 147290 | 89425 | 49086 | | | 6.8 | 396 | 719 | 7113 | 1122 | | | | Winterburn |
| 0585171506000 | 91970 | 2 | 1177 | 3063 | 3079 | 205805 | 125696 | 57560 | | | 6.6 | 1249 | 2025 | 18550 | 1475 | | | | Winterburn |
| 0585172908000 | 91976 | 1 | 1066 | 2910 | 2918 | 183345 | 112960 | 52372 | | | 7.1 | 58 | 1593 | 15907 | 926 | | | | Winterburn |
| 0585201807000 | 92022 | 1 | 872 | 3080 | 3088 | 170473 | 105600 | 41223 | | | 6.6 | 564 | 4301 | 17660 | 2288 | | | | Winterburn |
| 0595162210000 | 92821 | 2 | 923 | 2665 | 2673 | 201775 | 124539 | 58642 | | | 7.6 | 14 | 2059 | 16147 | 762 | | | | Winterburn |
| 0595163104000 | 92824 | 5 | 975 | 2735 | 2758 | 198614 | 122400 | 58192 | | | 7.0 | 385 | 2503 | 14755 | 770 | | | | Winterburn |
| 0635240601000 | 97236 | 5 | 878 | 3239 | 3246 | 206606 | 127270 | 55462 | | | 7.4 | 457 | 1362 | 21750 | 620 | | | | Winterburn |
| 0636010110000 | 97310 | 4 | 1012 | 3651 | 3689 | 211593 | 130500 | 57325 | | | 6.7 | 517 | 1980 | 20962 | 630 | | | | Winterburn |
| 0636021312000 | 97326 | 2 | 991 | 3780 | 3853 | 223783 | 138200 | 62051 | | | 6.1 | 410 | 2673 | 20060 | 790 | | | | Winterburn |
| 0645240514000 | 98627 | 1 | 853 | 3111 | 3138 | 172468 | 106932 | 46805 | | | 6.9 | 148 | 2184 | 16226 | 350 | | | | Winterburn |
| 0655192302000 | 100959 | 2 | 839 | 2493 | 2500 | 190731 | 117730 | 52387 | | | 7.1 | 481 | 3144 | 16340 | 1320 | | | | Winterburn |
| 0655211406000 | 100983 | 4 | 780 | 2613 | 2623 | 215597 | 133000 | 59408 | | | 6.5 | 420 | 2673 | 19540 | 1130 | | | | Winterburn |
| 0665161306000 | 102286 | 1 | 881 | 2309 | 2329 | 178942 | 109421 | 56769 | | | 6.5 | 550 | 1417 | 10473 | 634 | | | | Winterburn |
| 0665161314000 | 102288 | 2 | 902 | 2332 | 2377 | 174251 | 106336 | 56502 | | | 6.1 | 539 | 1126 | 9437 | 634 | | | | Winterburn |
| 0665161402000 | 102290 | 3 | 857 | 2289 | 2300 | 192317 | 118000 | 59988 | | | 7.5 | 671 | 2066 | 11411 | 370 | | | | Winterburn |
| 0665230411000 | 102381 | 8 | 755 | 2769 | 2783 | 172653 | 106044 | 46610 | | | 6.6 | 660 | 1997 | 16718 | 1269 | | | | Winterburn |
| 0665250211000 | 102401 | 3 | 793 | 3002 | 3048 | 219715 | 135600 | 61045 | | | 5.9 | 487 | 2474 | 19785 | 660 | | | | Winterburn |
| 0675150107000 | 103442 | 2 | 1004 | 2327 | 2338 | 190666 | 117676 | 55675 | | | 6.4 | 408 | 2163 | 14655 | 180 | | | | Winterburn |
| 0675162607000 | 103460 | 5 | 943 | 2248 | 2254 | 210537 | 130700 | 53728 | | | 0.0 | 470 | 3430 | 21840 | 750 | | | | Winterburn |
| 0675212815000 | 103533 | 5 | 707 | 2467 | 2473 | 205837 | 127280 | 55244 | | | 0.0 | 390 | 2610 | 19920 | 800 | | | | Winterburn |
| 0676043210000 | 103599 | 9 | 693 | 3374 | 3520 | 219423 | 134600 | 61238 | | | 6.5 | 1035 | 2304 | 19705 | 1100 | | | | Winterburn |
| 0685170910000 | 104409 | 2 | 907 | 2330 | 2338 | 193477 | 119280 | 54930 | | | 6.1 | 384 | 2360 | 16100 | 860 | | | | Winterburn |
| 0685181210000 | 104414 | 1 | 917 | 2365 | 2377 | 162884 | 100000 | 47527 | | | 7.5 | 728 | 1843 | 12535 | 510 | | | | Winterburn |
| 0685230801000 | 104525 | 5 | 792 | 2777 | 2797 | 150257 | 92846 | 38420 | | | 6.4 | 633 | 2030 | 16080 | 505 | | | | Winterburn |

| DLS | ID | # | elev | dtop | dbot | TDS | Cl | Na | $Na_c$ | K | pH | $SO_4$ | Mg | Ca | $HCO_3$ | $Ca_{ex}$ | $Na_{df}$ | Na/Cl | Aquifer |
|---|---|---|---|---|---|---|---|---|---|---|---|---|---|---|---|---|---|---|---|
| 0686040310000 | 104565 | 14 | 729 | 3485 | 3487 | 225140 | 139744 | 58476 | | | 6.0 | 254 | 3013 | 23360 | 595 | | | | Winterburn |
| 0695210505000 | 105381 | 1 | 653 | 2342 | 2353 | 236423 | 146850 | 60530 | | | 7.3 | 344 | 3388 | 25011 | 610 | | | | Winterburn |
| 0695232413000 | 105517 | 4 | 746 | 2539 | 2556 | 206413 | 128500 | 52151 | | | 6.6 | 329 | 3517 | 21680 | 480 | | | | Winterburn |
| 0696050107000 | 105546 | 1 | 662 | 3356 | 3389 | 264089 | 163800 | 71878 | | | 5.9 | 321 | 3492 | 24431 | 340 | | | | Winterburn |
| 0696051107000 | 105549 | 3 | 667 | 3435 | 3456 | 254434 | 157700 | 69700 | | | 6.8 | 272 | 3159 | 23420 | 372 | | | | Winterburn |
| 0696052110000 | 105552 | 1 | 661 | 3301 | 3334 | 254173 | 157200 | 69676 | | | 5.6 | 206 | 2406 | 24424 | 530 | | | | Winterburn |
| 0696051107000 | 105549 | 7 | 667 | 3484 | 3489 | 253687 | 157100 | 69470 | 67184 | 3880 | 6.4 | 432 | 2897 | 23710 | 159 | 1016 | 878 | 0.659 | Woodbend |
| 0635260109000 | 141102 | 5 | 874 | 3527 | 3542 | 242983 | 150000 | 66485 | 64017 | 4190 | 6.6 | 286 | 2420 | 23300 | 1000 | 1003 | 844 | 0.658 | Woodbend |
| 0675233006000 | 103571 | 2 | 776 | 2797 | 2810 | 242322 | 149700 | 65189 | 62967 | 3771 | 6.4 | 776 | 2965 | 23420 | 554 | 1010 | 882 | 0.649 | Woodbend |
| 0675222106000 | 103544 | 2 | 699 | 2705 | 2726 | 241137 | 150000 | 64107 | 62154 | 3314 | 6.2 | 436 | 4374 | 22020 | 407 | 940 | 925 | 0.639 | Woodbend |
| 0595243507000 | 92942 | 1 | 1092 | 3839 | 3849 | 229921 | 142500 | 61563 | 58771 | 4742 | 6.2 | 329 | 2469 | 23000 | 122 | 996 | 890 | 0.636 | Woodbend |
| 0695220111000 | 105431 | 1 | 654 | 2557 | 2565 | 206888 | 129090 | 50087 | 49591 | 3550 | 6.5 | 232 | 3360 | 23972 | 300 | 888 | 794 | 0.627 | Woodbend |
| 0685221414002 | 177858 | 1 | 659 | 2576 | 2594 | 215601 | 134000 | 56047 | 53892 | 3660 | 6.6 | 258 | 3110 | 22000 | 377 | 955 | 897 | 0.620 | Woodbend |
| 0675231208000 | 103562 | 1 | 725 | 2685 | 2707 | 246826 | 153500 | 62412 | 60062 | 3989 | 6.5 | 430 | 3523 | 26830 | 266 | 1176 | 1100 | 0.603 | Woodbend |
| 0625263305000 | 120516 | 0 | 947 | 3784 | 3804 | 240862 | 147700 | 56210 | 53998 | 4389 | 5.6 | 317 | 4735 | 26750 | 761 | 1178 | 1224 | 0.564 | Woodbend |
| 0515203006000 | 81270 | 2 | 1085 | 4047 | 4203 | 157833 | 96396 | 45883 | | | 6.6 | 910 | 1734 | 12376 | 1087 | | | | Woodbend |
| 0515253011000 | 81285 | 15 | 1344 | 5357 | 5615 | 135741 | 84000 | 34885 | | | 6.0 | 301 | 3003 | 12773 | 1585 | | | | Woodbend |
| 0525202306000 | 82739 | 4 | 1017 | 3788 | 3824 | 210729 | 130100 | 58943 | | | 7.0 | 364 | 1944 | 19220 | 323 | | | | Woodbend |
| 0525211616000 | 82748 | 5 | 1095 | 4105 | 4119 | 175752 | 108600 | 49622 | | | 6.9 | 240 | 1770 | 15400 | 244 | | | | Woodbend |
| 0525222103000 | 82755 | 1 | 1195 | 4321 | 4339 | 159255 | 94600 | 56616 | | | 7.0 | 339 | 802 | 4528 | 4820 | | | | Woodbend |
| 0525232604000 | 161891 | 2 | 1151 | 4464 | 4473 | 183110 | 113900 | 51680 | | | 6.9 | 319 | 4419 | 12430 | 737 | | | | Woodbend |
| 0525273614000 | 82771 | 17 | 1280 | 5200 | 5260 | 144018 | 90000 | 36956 | | | 6.7 | 150 | 3600 | 13000 | 634 | | | | Woodbend |
| 0535191709000 | 83930 | 2 | 985 | 3697 | 3751 | 212693 | 129800 | 60425 | | | 7.4 | 1353 | 2527 | 17698 | 1810 | | | | Woodbend |
| 0545191302000 | 85227 | 5 | 995 | 3481 | 3492 | 174546 | 104800 | 50663 | | | 7.9 | 1473 | 1487 | 14398 | 3510 | | | | Woodbend |
| 0545201110000 | 85256 | 28 | 1095 | 3712 | 3716 | 182028 | 113597 | 42106 | | | 6.3 | 314 | 3829 | 21673 | 1035 | | | | Woodbend |
| 0545202307000 | 169475 | 1 | 1139 | 3724 | -1000 | 198591 | 124000 | 49398 | | | 6.3 | 330 | 4500 | 20000 | 737 | | | | Woodbend |
| 0545233602000 | 85296 | 2 | 1099 | 4051 | 4053 | 157132 | 95420 | 52734 | | | 6.8 | 37 | 661 | 7452 | 1684 | | | | Woodbend |
| 0545233602000 | 85296 | 9 | 1099 | 4141 | 4143 | 168676 | 102479 | 55392 | | | 7.4 | 82 | 747 | 9061 | 1861 | | | | Woodbend |
| 0555170506000 | 87406 | 5 | 946 | 3338 | 3399 | 184456 | 112400 | 53785 | | | 7.1 | 1286 | 1652 | 14815 | 1052 | | | | Woodbend |
| 0555181507000 | 87434 | 4 | 970 | 3273 | 3283 | 215556 | 132600 | 62132 | | | 6.2 | 265 | 1895 | 18138 | 1070 | | | | Woodbend |
| 0555181702000 | 87437 | 1 | 989 | 3320 | 3360 | 151175 | 91631 | 42015 | | | 6.9 | 1057 | 786 | 14867 | 1664 | | | | Woodbend |
| 0555181710000 | 87439 | 1 | 988 | 3314 | 3334 | 197695 | 121400 | 55719 | | | 6.4 | 734 | 2260 | 17017 | 1150 | | | | Woodbend |
| 0555192010000 | 87462 | 3 | 1127 | 3676 | 3744 | 207561 | 128400 | 55046 | | | 6.8 | 200 | 2430 | 21002 | 981 | | | | Woodbend |
| 0555192211000 | 140022 | 1 | 1077 | 3482 | 3488 | 175026 | 107000 | 49457 | | | 6.5 | 730 | 1400 | 15800 | 1300 | | | | Woodbend |
| 0555192312000 | 87463 | 2 | 1081 | 3516 | 3523 | 198275 | 122581 | 51509 | | | 6.7 | 187 | 2006 | 21497 | 1005 | | | | Woodbend |
| 0555201111000 | 87478 | 5 | 1158 | 3944 | 3984 | 219987 | 135800 | 56043 | | | 7.0 | 128 | 1701 | 25626 | 1401 | | | | Woodbend |
| 0555202607000 | 87481 | 3 | 1194 | 3752 | 3780 | 177707 | 108657 | 47354 | | | 6.6 | 506 | 1346 | 18822 | 2079 | | | | Woodbend |
| 0555203109000 | 87486 | 3 | 1379 | 4068 | 4085 | 180294 | 110600 | 48582 | | | 7.7 | 595 | 1390 | 18530 | 1214 | | | | Woodbend |



Reproduced with permission of the copyright owner. Further reproduction prohibited without permission.

Reproduced with permission of the copyright owner. Further reproduction prohibited without permission.



| DLS | ID | # | elev | dtop | dbot | TDS | Cl | Na | $Na_c$ | K | pH | $SO_4$ | Mg | Ca | $HCO_3$ | $Ca_{ex}$ | $Na_{df}$ | Na/Cl | Aquifer |
|---|---|---|---|---|---|---|---|---|---|---|---|---|---|---|---|---|---|---|---|
| 0555222305000 | 87500 | 7 | 1031 | 3841 | 3844 | 137624 | 82000 | 44866 | | | 6.7 | 267 | 770 | 7543 | 4430 | | | | Woodbend |
| 0555222605002 | 151888 | 3 | 979 | 3760 | 3779 | 151249 | 92200 | 49274 | | | 7.1 | 8 | 1321 | 7576 | 1769 | | | | Woodbend |
| 0555222608020 | 87503 | 10 | 929 | 3865 | 3867 | 133695 | 81200 | 40419 | | | 6.5 | 349 | 1604 | 8953 | 2380 | | | | Woodbend |
| 0565161801000 | 89373 | 7 | 931 | 2930 | 2963 | 211681 | 130000 | 62315 | | | 6.9 | 290 | 1660 | 16900 | 1050 | | | | Woodbend |
| 0565171310000 | 89388 | 4 | 984 | 3064 | 3079 | 199122 | 122400 | 60484 | | | 6.6 | 420 | 1702 | 13950 | 337 | | | | Woodbend |
| 0565172813000 | 177196 | 2 | 1120 | 3196 | 3205 | 172975 | 106200 | 47641 | | | 7.8 | 837 | 2428 | 15260 | 1237 | | | | Woodbend |
| 0565173615000 | 89393 | 1 | 1054 | 3078 | 3080 | 228383 | 141000 | 63463 | | | 6.2 | 302 | 2200 | 21100 | 647 | | | | Woodbend |
| 0565200410000 | 89432 | 5 | 1208 | 3804 | 3850 | 144978 | 88300 | 36743 | | | 7.1 | 1251 | 1944 | 15820 | 1871 | | | | Woodbend |
| 0565202307000 | 89439 | 4 | 1358 | 3886 | 3980 | 148181 | 90750 | 40400 | | | 6.0 | 642 | 1179 | 14730 | 976 | | | | Woodbend |
| 0575170509000 | 90786 | 2 | 1127 | 3170 | 3226 | 174988 | 107500 | 48484 | | | 7.3 | 831 | 2406 | 15240 | 1072 | | | | Woodbend |
| 0575171202000 | 140389 | 2 | 1096 | 3078 | 3087 | 201878 | 124000 | 57350 | | | 6.4 | 428 | 1520 | 18100 | 976 | | | | Woodbend |
| 0575172310000 | 90792 | 5 | 1122 | 3130 | 3138 | 186930 | 115222 | 51850 | | | 6.7 | 44 | 1714 | 17519 | 1181 | | | | Woodbend |
| 0575191010000 | 90810 | 4 | 1178 | 3430 | 3450 | 191052 | 118016 | 51583 | | | 7.2 | 48 | 2385 | 18312 | 1440 | | | | Woodbend |
| 0575191411000 | 90816 | 2 | 1136 | 3375 | 3398 | 192217 | 118400 | 55618 | | | 6.3 | 40 | 1993 | 15576 | 1200 | | | | Woodbend |
| 0575192310000 | 90822 | 6 | 1138 | 3397 | 3418 | 193734 | 119000 | 54543 | | | 7.3 | 120 | 1590 | 17600 | 1100 | | | | Woodbend |
| 0575192310000 | 90822 | 2 | 1138 | 3397 | 3418 | 199461 | 123000 | 57554 | | | 6.4 | 28 | 2333 | 15936 | 1240 | | | | Woodbend |
| 0575193506000 | 90835 | 5 | 1130 | 3315 | 3365 | 155794 | 95600 | 45210 | | | 6.4 | 267 | 1701 | 12372 | 1310 | | | | Woodbend |
| 0585161706000 | 91964 | 1 | 1040 | 2920 | 2938 | 238333 | 145783 | 72731 | | | 6.6 | 407 | 1406 | 17322 | 1391 | | | | Woodbend |
| 0585172506000 | 91975 | 1 | 1160 | 3155 | 3174 | 196744 | 121017 | 56625 | | | 6.6 | 572 | 1920 | 16320 | 591 | | | | Woodbend |
| 0585190510000 | 92002 | 1 | 1053 | 3352 | 3353 | 170752 | 105000 | 49352 | | | 6.3 | 72 | 1983 | 13598 | 1520 | | | | Woodbend |
| 0585191002000 | 92004 | 4 | 1227 | 3456 | 3486 | 175407 | 108000 | 52148 | | | 6.4 | 63 | 1871 | 12853 | 960 | | | | Woodbend |
| 0585191016000 | 92008 | 1 | 1117 | 3375 | 3390 | 194692 | 119600 | 56996 | | | 6.5 | 222 | 1920 | 15295 | 1340 | | | | Woodbend |
| 0585192216000 | 92014 | 4 | 1040 | 3348 | 3380 | 180519 | 110800 | 51181 | | | 7.3 | 447 | 816 | 17000 | 335 | | | | Woodbend |
| 0585192811000 | 92016 | 2 | 966 | 3315 | 3324 | 207719 | 127581 | 56911 | | | 7.2 | 242 | 1314 | 20938 | 1490 | | | | Woodbend |
| 0585200210000 | 92019 | 1 | 921 | 3383 | 3412 | 187507 | 115245 | 52241 | | | 6.6 | 370 | 1587 | 17515 | 1115 | | | | Woodbend |
| 0585201511000 | 92020 | 5 | 922 | 3271 | 3279 | 211091 | 129400 | 56225 | | | 6.9 | 869 | 1871 | 21942 | 1594 | | | | Woodbend |
| 0585202806000 | 92029 | 4 | 963 | 3319 | 3329 | 219323 | 135272 | 57068 | | | 6.6 | 216 | 1962 | 24071 | 1493 | | | | Woodbend |
| 0585243416000 | 177306 | 1 | 1044 | 3840 | 3848 | 200067 | 122500 | 58563 | | | 6.9 | 527 | 1457 | 16420 | 1220 | | | | Woodbend |
| 0585243416000 | 177306 | 4 | 1044 | 3773 | 3818 | 230617 | 143000 | 58811 | | | 7.0 | 422 | 3156 | 24820 | 830 | | | | Woodbend |
| 0595152910000 | 92806 | 1 | 935 | 2706 | 2707 | 200906 | 123418 | 57754 | | | 6.5 | 283 | 1736 | 17007 | 727 | | | | Woodbend |
| 0595153514000 | 92813 | 1 | 850 | 2570 | 2575 | 203398 | 125900 | 57242 | | | 6.8 | 317 | 2649 | 17140 | 305 | | | | Woodbend |
| 0595163104000 | 92824 | 4 | 975 | 2853 | 2868 | 201926 | 124400 | 58273 | | | 6.5 | 349 | 2527 | 15856 | 1060 | | | | Woodbend |
| 0595163310000 | 92825 | 3 | 924 | 2742 | 2786 | 198516 | 122200 | 57101 | | | 6.5 | 507 | 2576 | 15616 | 1050 | | | | Woodbend |
| 0595173407000 | 92839 | 5 | 937 | 2863 | 2892 | 204487 | 125000 | 62268 | | | 7.4 | 741 | 1906 | 13960 | 1244 | | | | Woodbend |
| 0595200707000 | 92899 | 3 | 1116 | 3441 | 3453 | 200056 | 123376 | 47440 | | | 7.2 | 226 | 1051 | 27239 | 1474 | | | | Woodbend |
| 0595201710000 | 92901 | 5 | 1099 | 3523 | 3526 | 238285 | 148610 | 58109 | | | 6.6 | 391 | 5502 | 24940 | 1490 | | | | Woodbend |
| 0595221503000 | 92927 | 8 | 1141 | 3781 | 3795 | 249344 | 154420 | 66126 | | | 7.1 | 295 | 3089 | 24977 | 890 | | | | Woodbend |
| 0595222902000 | 92930 | 2 | 1145 | 3781 | 3799 | 251829 | 155400 | 70441 | | | 7.0 | 179 | 1823 | 23704 | 574 | | | | Woodbend |

| DLS | ID | # | elev | dtop | dbot | TDS | Cl | Na | $Na_c$ | K | pH | $SO_4$ | Mg | Ca | $HCO_3$ | $Ca_{ex}$ | $Na_{df}$ | Na/Cl | Aquifer |
|---|---|---|---|---|---|---|---|---|---|---|---|---|---|---|---|---|---|---|---|
| 0595241907000 | 92940 | 3 | 1190 | 3979 | 3988 | 213493 | 132000 | 59768 | | | 6.3 | 370 | 3360 | 17480 | 1046 | | | | Woodbend |
| 0595263111000 | 92952 | 1 | 1187 | 4101 | 4108 | 211338 | 130000 | 53651 | | | 5.3 | 1222 | 2697 | 23180 | 1196 | | | | Woodbend |
| 0605140616000 | 93674 | 2 | 799 | 2691 | 2704 | 197144 | 121073 | 57294 | | | 6.8 | 461 | 1803 | 16038 | 966 | | | | Woodbend |
| 0605150103002 | 93686 | 1 | 824 | 2568 | 2621 | 205022 | 125565 | 61157 | | | 7.0 | 294 | 866 | 16677 | 942 | | | | Woodbend |
| 0605150404000 | 93692 | 1 | 873 | 2637 | 2641 | 177440 | 108642 | 50477 | | | 6.7 | 689 | 1492 | 15603 | 1093 | | | | Woodbend |
| 0605150404000 | 93692 | 2 | 873 | 2618 | 2635 | 194795 | 119750 | 55794 | | | 6.7 | 308 | 1595 | 16875 | 961 | | | | Woodbend |
| 0605150710000 | 93698 | 2 | 853 | 2609 | 2615 | 189866 | 117000 | 53720 | | | 6.1 | 212 | 1830 | 16673 | 876 | | | | Woodbend |
| 0605151906000 | 93708 | 2 | 823 | 2571 | 2591 | 162768 | 100000 | 47063 | | | 6.5 | 162 | 1104 | 14028 | 835 | | | | Woodbend |
| 0605151906000 | 93708 | 5 | 823 | 2594 | 2597 | 204891 | 125692 | 62481 | | | 7.0 | 346 | 1799 | 14091 | 980 | | | | Woodbend |
| 0605152012000 | 93709 | 4 | 807 | 2656 | 2672 | 185457 | 113600 | 54163 | | | 6.1 | 805 | 2012 | 14366 | 1040 | | | | Woodbend |
| 0605153203000 | 93716 | 1 | 766 | 2594 | 2646 | 188359 | 116201 | 46519 | | | 6.9 | 616 | 2280 | 22080 | 1347 | | | | Woodbend |
| 0605153306000 | 93717 | 2 | 757 | 2609 | 2640 | 186851 | 114817 | 53468 | | | 6.9 | 517 | 1835 | 15780 | 883 | | | | Woodbend |
| 0605162012000 | 93726 | 2 | 816 | 2657 | 2665 | 222966 | 136965 | 63625 | | | 7.4 | 381 | 1798 | 19575 | 1263 | | | | Woodbend |
| 0605162515000 | 93729 | 3 | 814 | 2580 | 2583 | 188996 | 116000 | 53940 | | | 7.0 | 319 | 1720 | 16200 | 695 | | | | Woodbend |
| 0605171414000 | 93742 | 3 | 846 | 2657 | 2665 | 190255 | 117000 | 52632 | | | 7.2 | 389 | 1610 | 18000 | 365 | | | | Woodbend |
| 0605171414000 | 93742 | 2 | 846 | 2657 | 2665 | 204180 | 126000 | 58104 | | | 6.5 | 351 | 2177 | 17302 | 500 | | | | Woodbend |
| 0605173604000 | 93753 | 4 | 840 | 2865 | 2884 | 232936 | 143000 | 68443 | | | 8.3 | 356 | 1750 | 18820 | 1153 | | | | Woodbend |
| 0605210311000 | 93836 | 1 | 1015 | 3384 | 3398 | 192715 | 121000 | 41704 | | | 7.0 | 195 | 5270 | 23800 | 839 | | | | Woodbend |
| 0605210311000 | 93836 | 6 | 1015 | 3347 | 3355 | 196006 | 120500 | 51845 | | | 6.8 | 265 | 1700 | 20820 | 1781 | | | | Woodbend |
| 0605211006000 | 93839 | 1 | 1008 | 3457 | 3487 | 217414 | 133684 | 59451 | | | 6.6 | 245 | 1239 | 22204 | 1202 | | | | Woodbend |
| 0605263210000 | 93872 | 2 | 1245 | 4075 | 4092 | 250075 | 155000 | 66985 | | | 6.5 | 219 | 2772 | 24892 | 420 | | | | Woodbend |
| 0615150602000 | 94852 | 5 | 762 | 2518 | 2520 | 202579 | 123879 | 61329 | | | 6.8 | 364 | 614 | 15983 | 834 | | | | Woodbend |
| 0615150906000 | 94858 | 2 | 829 | 2705 | 2726 | 194350 | 119358 | 55118 | | | 7.1 | 533 | 1503 | 17439 | 811 | | | | Woodbend |
| 0615151715000 | 94864 | 6 | 862 | 2736 | 2747 | 188168 | 115400 | 54602 | | | 7.1 | 545 | 1560 | 15500 | 315 | | | | Woodbend |
| 0615151715000 | 94864 | 1 | 862 | 2745 | 2745 | 202953 | 125731 | 56620 | | | 6.9 | 218 | 3314 | 16638 | 879 | | | | Woodbend |
| 0615160301002 | 94882 | 2 | 816 | 2599 | 2602 | 198844 | 121783 | 56890 | | | 7.0 | 1075 | 1546 | 17313 | 483 | | | | Woodbend |
| 0615161307000 | 94889 | 7 | 832 | 2709 | 2728 | 182809 | 112700 | 52377 | | | 6.6 | 407 | 1774 | 15400 | 307 | | | | Woodbend |
| 0615220805000 | 95013 | 1 | 1035 | 3408 | 3411 | 210724 | 130532 | 54721 | | | 6.5 | 123 | 1984 | 23069 | 600 | | | | Woodbend |
| 0615221006000 | 95015 | 2 | 996 | 3459 | 3470 | 221985 | 138300 | 56879 | | | 8.0 | 156 | 3578 | 22890 | 370 | | | | Woodbend |
| 0615262806000 | 95038 | 4 | 1158 | 3895 | 3953 | 168719 | 103750 | 44339 | | | 6.5 | 688 | 1823 | 17618 | 1020 | | | | Woodbend |
| 0616020407000 | 95050 | 4 | 1313 | 4512 | 4555 | 157962 | 96192 | 41526 | | | 7.2 | 675 | 1847 | 16340 | 2810 | | | | Woodbend |
| 0625262310000 | 96090 | 2 | 933 | 3594 | 3600 | 254931 | 157049 | 70396 | | | 7.1 | 228 | 2155 | 24314 | 767 | | | | Woodbend |
| 0625263610000 | 96102 | 1 | 879 | 3531 | -1000 | 254931 | 157049 | 70396 | | | 7.1 | 228 | 2155 | 24314 | 767 | | | | Woodbend |
| 0625263612000 | 96104 | 4 | 872 | 3541 | 3546 | 254931 | 157049 | 70396 | | | 7.1 | 228 | 2155 | 24314 | 767 | | | | Woodbend |
| 0626093409000 | 96192 | 1 | 1409 | 5243 | 5532 | 182816 | 111200 | 48898 | | | 7.6 | 82 | 1555 | 19059 | 4111 | | | | Woodbend |
| 0635250510000 | 97249 | 1 | 899 | 3569 | 3572 | 254931 | 157049 | 70396 | | | 7.1 | 228 | 2155 | 24314 | 767 | | | | Woodbend |
| 0635250512000 | 97250 | 3 | 883 | 3535 | 3543 | 242454 | 149926 | 65106 | | | 7.0 | 230 | 2261 | 24595 | 683 | | | | Woodbend |
| 0635250512000 | 97250 | 2 | 883 | 3535 | 3543 | 254931 | 157049 | 70396 | | | 7.1 | 228 | 2155 | 24314 | 767 | | | | Woodbend |



Reproduced with permission of the copyright owner. Further reproduction prohibited without permission.

Reproduced with permission of the copyright owner. Further reproduction prohibited without permission.

| DLS | ID | # | elev | dtop | dbot | TDS | Cl | Na | $Na_c$ | K | pH | $SO_4$ | Mg | Ca | $HCO_3$ | $Ca_{ex}$ | $Na_{df}$ | Na/Cl | Aquifer |
|---|---|---|---|---|---|---|---|---|---|---|---|---|---|---|---|---|---|---|---|
| 0635250610000 | 97254 | 1 | 871 | 3514 | 3533 | 250588 | 154984 | 69245 | | | 7.0 | 246 | 2966 | 22739 | 830 | | | | Woodbend |
| 0635250612000 | 97255 | 1 | 860 | 3494 | 3523 | 256914 | 159173 | 70147 | | | 7.1 | 220 | 3305 | 23715 | 720 | | | | Woodbend |
| 0635250912000 | 97258 | 3 | 833 | 3493 | 3503 | 239868 | 148003 | 66358 | | | 6.8 | 249 | 2204 | 22599 | 927 | | | | Woodbend |
| 0635251604000 | 97266 | 3 | 825 | 3417 | 3488 | 249160 | 153588 | 69318 | | | 6.3 | 241 | 1865 | 23715 | 879 | | | | Woodbend |
| 0635260110000 | 97276 | 1 | 873 | 3528 | 3539 | 216164 | 133482 | 58167 | | | 6.8 | 213 | 1661 | 22320 | 653 | | | | Woodbend |
| 0635260110000 | 97276 | 2 | 873 | 3493 | 3539 | 261924 | 161965 | 72099 | | | 6.8 | 206 | 2627 | 24692 | 683 | | | | Woodbend |
| 0635261003000 | 97300 | 3 | 934 | 3589 | 3592 | 245567 | 150795 | 72323 | | | 7.2 | 336 | 1356 | 20367 | 793 | | | | Woodbend |
| 0636010110000 | 97310 | 5 | 1012 | 3792 | 3819 | 256587 | 159000 | 69615 | | | 6.5 | 247 | 3036 | 24455 | 475 | | | | Woodbend |
| 0666062212000 | 102445 | 3 | 785 | 3907 | 3916 | 171615 | 105400 | 51371 | | | 6.9 | 412 | 1116 | 13208 | 220 | | | | Woodbend |
| 0675221806000 | 103542 | 1 | 719 | 2722 | 2739 | 234444 | 145200 | 62306 | | | 6.2 | 399 | 2819 | 23463 | 524 | | | | Woodbend |
| 0675222010000 | 103543 | 4 | 701 | 2902 | 2926 | 192587 | 119000 | 51356 | | | 6.6 | 593 | 2540 | 18779 | 650 | | | | Woodbend |
| 0675222707000 | 103550 | 1 | 676 | 2654 | 2655 | 278357 | 171835 | 76598 | | | 6.3 | 269 | 2708 | 26270 | 412 | | | | Woodbend |
| 0675222707000 | 103550 | 4 | 676 | 2654 | 2655 | 278623 | 172000 | 76667 | | | 6.3 | 269 | 2710 | 26300 | 412 | | | | Woodbend |
| 0676043210000 | 103599 | 10 | 693 | 3720 | 3755 | 271324 | 168400 | 71028 | | | 6.7 | 272 | 3177 | 28275 | 350 | | | | Woodbend |
| 0685213214000 | 183296 | 1 | 654 | 2525 | 2534 | 184129 | 114000 | 47602 | | | 7.3 | 470 | 2240 | 19600 | 442 | | | | Woodbend |
| 0685220407000 | 104465 | 2 | 679 | 2659 | 2672 | 169944 | 104730 | 44902 | | | 6.8 | 607 | 1952 | 17281 | 314 | | | | Woodbend |
| 0685222301020 | 163678 | 3 | 659 | 2611 | 2618 | 190865 | 118000 | 50087 | | | 6.4 | 608 | 2410 | 19500 | 528 | | | | Woodbend |
| 0685222303000 | 104473 | 1 | 658 | 2587 | 2601 | 254894 | 158200 | 66608 | | | 6.6 | 301 | 3118 | 26481 | 380 | | | | Woodbend |
| 0685222713000 | 104497 | 1 | 676 | 2605 | 2612 | 248595 | 154000 | 63806 | | | 6.9 | 373 | 2890 | 27000 | 194 | | | | Woodbend |
| 0685223307000 | 104501 | 1 | 688 | 2624 | 2628 | 249142 | 154299 | 64629 | | | 6.4 | 259 | 2916 | 26425 | 401 | | | | Woodbend |
| 0685230801000 | 104525 | 8 | 792 | 2824 | 2833 | 229678 | 142992 | 57906 | | | 6.5 | 316 | 3549 | 24750 | 335 | | | | Woodbend |
| 0685230801000 | 104525 | 6 | 792 | 2802 | 2809 | 229952 | 142992 | 56930 | | | 6.1 | 286 | 3045 | 26465 | 475 | | | | Woodbend |
| 0685230801000 | 104525 | 9 | 792 | 2841 | 2852 | 230264 | 142992 | 58981 | | | 6.0 | 319 | 3003 | 24750 | 445 | | | | Woodbend |
| 0685231207000 | 104528 | 1 | 715 | 2693 | 2705 | 235812 | 146800 | 57977 | | | 7.0 | 438 | 3937 | 26350 | 632 | | | | Woodbend |
| 0685251314000 | 104540 | 4 | 754 | 2809 | 2817 | 217133 | 134422 | 56962 | | | 7.7 | 597 | 2634 | 22354 | 335 | | | | Woodbend |
| 0685251314000 | 104540 | 8 | 754 | 3001 | 3031 | 233116 | 144306 | 65086 | | | 6.5 | 379 | 2900 | 20310 | 275 | | | | Woodbend |
| 0695210704020 | 177883 | 2 | 650 | 2575 | 2605 | 210903 | 130866 | 52705 | | | 5.8 | 514 | 2848 | 23722 | 504 | | | | Woodbend |
| 0695211804000 | 105419 | 1 | 646 | 2700 | 2705 | 196658 | 122000 | 51681 | | | 7.3 | 200 | 2240 | 20400 | 279 | | | | Woodbend |
| 0695220407000 | 105451 | 2 | 685 | 2618 | 2619 | 246757 | 153400 | 63637 | | | 6.2 | 280 | 3548 | 25666 | 460 | | | | Woodbend |
| 0695220915000 | 105458 | 1 | 679 | 2623 | 2626 | 207853 | 128646 | 50975 | | | 6.5 | 319 | 1452 | 26202 | 525 | | | | Woodbend |
| 0695221011000 | 105462 | 1 | 672 | 2594 | 2602 | 237047 | 146973 | 59530 | | | 6.9 | 288 | 2982 | 26641 | 421 | | | | Woodbend |
| 0695221615000 | 105493 | 1 | 693 | 2612 | 2622 | 249000 | 153755 | 62798 | | | 6.0 | 438 | 1865 | 29505 | 287 | | | | Woodbend |
| 0695221615000 | 105493 | 2 | 693 | 2614 | 2624 | 269996 | 166759 | 73171 | | | 6.7 | 269 | 2845 | 26179 | 377 | | | | Woodbend |
| 0695221615000 | 124881 | 0 | 693 | 2614 | 2624 | 192751 | 117863 | 59368 | | | 6.4 | 491 | 1494 | 12818 | 347 | | | | Woodbend |
| 0695221901000 | 105499 | 1 | 717 | 2639 | 2646 | 232296 | 144978 | 56207 | | | 7.9 | 259 | 3920 | 26738 | 395 | | | | Woodbend |
| 0695221905000 | 105501 | 1 | 737 | 2556 | 2567 | 231408 | 143600 | 61800 | | | 7.1 | 350 | 3164 | 22340 | 312 | | | | Woodbend |
| 0695232413000 | 105517 | 5 | 746 | 2690 | 2697 | 218413 | 136000 | 55497 | | | 6.2 | 329 | 3777 | 22574 | 480 | | | | Woodbend |
| 0665252115000 | 102407 | 2 | 738 | 3392 | 3396 | 172321 | 104500 | 61919 | 61199 | 1220 | 6.5 | 1072 | 1337 | 3403 | 183 | 59 | -134 | 0.903 | Beaverhill Lake |

Reproduced with permission of the copyright owner. Further reproduction prohibited without permission.

| DLS | ID | # | elev | dtop | dbot | TDS | Cl | Na | $Na_c$ | K | pH | $SO_4$ | Mg | Ca | $HCO_3$ | $Ca_{ex}$ | $Na_{df}$ | Na/Cl | Aquifer |
|---|---|---|---|---|---|---|---|---|---|---|---|---|---|---|---|---|---|---|---|
| 0645190405000 | 122054 | 0 | 789 | 3041 | 3043 | 165913 | 103000 | 47725 | 50602 | 1420 | 6.3 | 364 | 1287 | 11590 | 527 | 469 | 290 | 0.758 | Beaverhill Lake |
| 0655152909000 | 100913 | 1 | 947 | 2823 | 2850 | 166174 | 102000 | 45237 | 43625 | 2736 | 6.9 | 1282 | 1944 | 15620 | 185 | 671 | 570 | 0.659 | Beaverhill Lake |
| 0635192312000 | 97152 | 1 | 794 | 3039 | 3051 | 244032 | 151000 | 64985 | 62540 | 4150 | 6.9 | 392 | 2440 | 25000 | 438 | 1087 | 932 | 0.639 | Beaverhill Lake |
| 0465173402000 | 64912 | 1 | 1298 | 4714 | 4717 | 178745 | 110300 | 50843 | 44401 | 10950 | 6.6 | 193 | 2090 | 14930 | 793 | 628 | 737 | 0.621 | Beaverhill Lake |
| 0445160212000 | 61037 | 5 | 1242 | 4870 | 4876 | 119344 | 74500 | 29596 | | | 6.6 | 74 | 2843 | 11930 | 817 | | | | Beaverhill Lake |
| 0445162006000 | 61039 | 6 | 1191 | 4813 | 4820 | 120366 | 73400 | 36226 | | | 8.0 | 119 | 1108 | 8689 | 1676 | | | | Beaverhill Lake |
| 0485190106000 | 71567 | 3 | 1116 | 4603 | 4615 | 149206 | 91063 | 46406 | | | 7.1 | 187 | 942 | 9975 | 1288 | | | | Beaverhill Lake |
| 0495191015000 | 75215 | 2 | 1135 | 4469 | 4526 | 147832 | 91633 | 40051 | | | 7.0 | 163 | 2480 | 13123 | 776 | | | | Beaverhill Lake |
| 0515163311000 | 81228 | 1 | 969 | 3698 | 3718 | 167220 | 102300 | 49672 | | | 6.6 | 570 | 1196 | 13072 | 834 | | | | Beaverhill Lake |
| 0515172710000 | 81239 | 1 | 1003 | 3837 | 3847 | 191747 | 118000 | 53521 | | | 6.3 | 420 | 2579 | 16477 | 1525 | | | | Beaverhill Lake |
| 0535150511000 | 83781 | 2 | 907 | 3402 | 3417 | 179302 | 109941 | 52169 | | | 6.7 | 54 | 475 | 16214 | 913 | | | | Beaverhill Lake |
| 0535152204000 | 83785 | 7 | 927 | 3361 | 3366 | 173519 | 105790 | 51240 | | | 7.2 | 814 | 1409 | 13600 | 1354 | | | | Beaverhill Lake |
| 0535200810000 | 83949 | 5 | 1036 | 4171 | 4209 | 181391 | 110099 | 50787 | | | 7.4 | 1164 | 1246 | 17079 | 2067 | | | | Beaverhill Lake |
| 0545150507000 | 85102 | 1 | 891 | 3319 | 3366 | 189336 | 115800 | 56580 | | | 6.8 | 337 | 1385 | 14494 | 1505 | | | | Beaverhill Lake |
| 0545151311000 | 85104 | 5 | 867 | 3255 | 3260 | 172346 | 106000 | 55934 | | | 6.7 | 74 | 1604 | 8625 | 222 | | | | Beaverhill Lake |
| 0545152111000 | 85107 | 1 | 829 | 3217 | 3223 | 169889 | 106921 | 39815 | | | 5.7 | 352 | 5161 | 17482 | 322 | | | | Beaverhill Lake |
| 0545152611000 | 85110 | 1 | 819 | 3180 | 3182 | 179172 | 112241 | 47091 | | | 6.3 | 83 | 4786 | 14717 | 517 | | | | Beaverhill Lake |
| 0545162906000 | 85121 | 1 | 921 | 3399 | 3434 | 183057 | 112400 | 54401 | | | 7.0 | 241 | 1385 | 14214 | 845 | | | | Beaverhill Lake |
| 0545172807000 | 85136 | 4 | 924 | 3456 | 3485 | 193516 | 116000 | 66420 | | | 7.7 | 242 | 923 | 7728 | 4480 | | | | Beaverhill Lake |
| 0545181210000 | 85166 | 1 | 969 | 3560 | 3584 | 196038 | 121000 | 53738 | | | 6.1 | 282 | 2432 | 18036 | 1120 | | | | Beaverhill Lake |
| 0555161606000 | 87399 | 1 | 893 | 3296 | 3353 | 159850 | 96800 | 55399 | | | 6.7 | 538 | 622 | 5974 | 1050 | | | | Beaverhill Lake |
| 0555192312000 | 87463 | 3 | 1081 | 3829 | 3841 | 194464 | 118438 | 49720 | | | 7.3 | 622 | 1775 | 22133 | 3611 | | | | Beaverhill Lake |
| 0565180911000 | 89396 | 1 | 1129 | 3708 | 3734 | 215009 | 132600 | 57434 | | | 6.3 | 166 | 1555 | 22743 | 1040 | | | | Beaverhill Lake |
| 0585181110000 | 91979 | 1 | 1225 | 3573 | 3594 | 211406 | 131238 | 52891 | | | 6.6 | 123 | 2750 | 23924 | 976 | | | | Beaverhill Lake |
| 0585181306000 | 91981 | 1 | 1116 | 3490 | 3499 | 212585 | 131407 | 54535 | | | 7.1 | 176 | 2077 | 23795 | 1210 | | | | Beaverhill Lake |
| 0585181910000 | 91983 | 2 | 1063 | 3431 | 3433 | 200859 | 123972 | 51860 | | | 7.0 | 169 | 2465 | 21488 | 1840 | | | | Beaverhill Lake |
| 0585193606000 | 92017 | 3 | 1046 | 3438 | 3446 | 218311 | 134694 | 51327 | | | 6.8 | 382 | 2286 | 28460 | 1832 | | | | Beaverhill Lake |
| 0595183110000 | 92875 | 1 | 871 | 3236 | 3239 | 233556 | 144600 | 62710 | | | 6.1 | 122 | 2552 | 23183 | 790 | | | | Beaverhill Lake |
| 0605141907000 | 93680 | 1 | 794 | 2802 | 2817 | 188081 | 117055 | 44422 | | | 6.6 | 352 | 3302 | 22473 | 971 | | | | Beaverhill Lake |
| 0605171607000 | 93743 | 5 | 796 | 2938 | 2966 | 173021 | 106822 | 45732 | | | 6.9 | 7 | 1546 | 18353 | 1142 | | | | Beaverhill Lake |
| 0605172810000 | 93748 | 2 | 920 | 3045 | 3071 | 167297 | 102200 | 48268 | | | 6.9 | 648 | 1094 | 14535 | 1123 | | | | Beaverhill Lake |
| 0605173305000 | 93750 | 5 | 922 | 3091 | 3095 | 185465 | 114159 | 53243 | | | 7.0 | 16 | 1257 | 16351 | 893 | | | | Beaverhill Lake |
| 0605180507000 | 93756 | 2 | 862 | 3232 | 3264 | 239945 | 148400 | 64994 | | | 6.1 | 95 | 2163 | 23944 | 710 | | | | Beaverhill Lake |
| 0605203311000 | 93833 | 3 | 908 | 3373 | 3392 | 198470 | 122913 | 51980 | | | 6.7 | 47 | 2239 | 20818 | 962 | | | | Beaverhill Lake |
| 0615153007000 | 94870 | 1 | 907 | 2896 | 2917 | 184840 | 113400 | 53616 | | | 6.3 | 309 | 1239 | 15784 | 1000 | | | | Beaverhill Lake |
| 0615170610000 | 94904 | 4 | 943 | 3176 | 3191 | 207328 | 128390 | 54695 | | | 6.9 | 53 | 2164 | 21625 | 815 | | | | Beaverhill Lake |
| 0615171006000 | 94905 | 1 | 831 | 3011 | 3017 | 195121 | 120100 | 58652 | | | 7.0 | 249 | 1620 | 14320 | 366 | | | | Beaverhill Lake |
| 0615172310000 | 94912 | 2 | 946 | 3092 | 3107 | 187176 | 115000 | 53370 | | | 6.6 | 451 | 1823 | 16016 | 1050 | | | | Beaverhill Lake |

Reproduced with permission of the copyright owner. Further reproduction prohibited without permission.



| DLS | ID | # | elev | dtop | dbot | TDS | Cl | Na | $Na_c$ | K | pH | $SO_4$ | Mg | Ca | $HCO_3$ | $Ca_{ex}$ | $Na_{df}$ | Na/Cl | Aquifer |
|---|---|---|---|---|---|---|---|---|---|---|---|---|---|---|---|---|---|---|---|
| 0615181307000 | 94923 | 2 | 889 | 3074 | 3085 | 169095 | 103877 | 47463 | | | 6.6 | 183 | 1576 | 15296 | 1425 | | | | Beaverhill Lake |
| 0615182414000 | 140927 | 4 | 827 | 3027 | 3040 | 200576 | 123000 | 57613 | | | 6.9 | 376 | 1740 | 17100 | 1520 | | | | Beaverhill Lake |
| 0615183512000 | 94936 | 1 | 832 | 3030 | 3062 | 205969 | 127300 | 59497 | | | 6.4 | 60 | 2090 | 16817 | 417 | | | | Beaverhill Lake |
| 0615183605000 | 94937 | 2 | 869 | 3034 | 3070 | 213088 | 131500 | 61329 | | | 6.5 | 202 | 1944 | 17900 | 433 | | | | Beaverhill Lake |
| 0615183607000 | 94938 | 1 | 881 | 3096 | 3109 | 153624 | 94160 | 42967 | | | 7.3 | 778 | 1630 | 13600 | 316 | | | | Beaverhill Lake |
| 0615191902000 | 94953 | 5 | 897 | 3267 | 3273 | 210104 | 130207 | 50549 | | | 6.6 | 420 | 2270 | 26250 | 830 | | | | Beaverhill Lake |
| 0615192803000 | 94965 | 1 | 918 | 3292 | 3300 | 224769 | 139082 | 58095 | | | 6.8 | 227 | 2403 | 24455 | 1030 | | | | Beaverhill Lake |
| 0615213107000 | 95008 | 2 | 930 | 3491 | 3493 | 176049 | 108304 | 48915 | | | 6.4 | 63 | 1546 | 16527 | 1411 | | | | Beaverhill Lake |
| 0625150406000 | 95795 | 3 | 920 | 2910 | 2925 | 171651 | 105451 | 49241 | | | 6.6 | 23 | 924 | 15511 | 1020 | | | | Beaverhill Lake |
| 0625161006000 | 162675 | 1 | 983 | 3045 | 3048 | 182028 | 112000 | 51412 | | | 7.4 | 751 | 2695 | 14690 | 976 | | | | Beaverhill Lake |
| 0625180910000 | 95829 | 4 | 839 | 3021 | 3082 | 197694 | 122200 | 53963 | | | 6.5 | 313 | 2428 | 18418 | 756 | | | | Beaverhill Lake |
| 0625181110020 | 95834 | 1 | 907 | 3106 | 3114 | 211015 | 130000 | 60320 | | | 6.1 | 72 | 1580 | 18619 | 864 | | | | Beaverhill Lake |
| 0625181310000 | 95839 | 1 | 875 | 3077 | 3104 | 193751 | 119122 | 55631 | | | 6.5 | 158 | 983 | 17519 | 688 | | | | Beaverhill Lake |
| 0625181310000 | 95839 | 4 | 875 | 3077 | 3104 | 203098 | 125100 | 59375 | | | 6.8 | 155 | 2010 | 15900 | 232 | | | | Beaverhill Lake |
| 0625190614000 | 95858 | 1 | 869 | 3223 | 3291 | 210383 | 130640 | 52098 | | | 6.2 | 243 | 2527 | 24575 | 610 | | | | Beaverhill Lake |
| 0625200116000 | 95887 | 1 | 875 | 3231 | 3238 | 242502 | 149800 | 65335 | | | 6.1 | 206 | 2138 | 24585 | 890 | | | | Beaverhill Lake |
| 0625202111000 | 95969 | 1 | 851 | 3214 | 3221 | 236224 | 146318 | 63195 | | | 6.7 | 229 | 3035 | 23012 | 886 | | | | Beaverhill Lake |
| 0625202711000 | 95994 | 4 | 838 | 3196 | 3202 | 234388 | 145550 | 60692 | | | 7.8 | 10 | 2795 | 25000 | 693 | | | | Beaverhill Lake |
| 0625203306000 | 96012 | 1 | 835 | 3188 | 3194 | 239478 | 148400 | 63974 | | | 6.1 | 137 | 2673 | 23984 | 630 | | | | Beaverhill Lake |
| 0625231107000 | 96055 | 3 | 1005 | 3624 | 3639 | 238716 | 147400 | 63789 | | | 7.5 | 213 | 2250 | 24370 | 460 | | | | Beaverhill Lake |
| 0625231107000 | 96055 | 1 | 1005 | 3624 | 3639 | 241465 | 149600 | 63266 | | | 6.1 | 232 | 2673 | 25345 | 710 | | | | Beaverhill Lake |
| 0635142207000 | 97064 | 1 | 995 | 2812 | 2830 | 170122 | 102539 | 63097 | | | 6.6 | 957 | 374 | 2910 | 498 | | | | Beaverhill Lake |
| 0635200813000 | 97188 | 4 | 796 | 3203 | 3247 | 211353 | 130800 | 57163 | | | 7.0 | 187 | 2661 | 20100 | 898 | | | | Beaverhill Lake |
| 0645143202000 | 98440 | 4 | 1076 | 2869 | 2905 | 185088 | 111480 | 68720 | | | 6.2 | 1190 | 495 | 2960 | 495 | | | | Beaverhill Lake |
| 0645191412000 | 98519 | 3 | 749 | 2961 | 2978 | 212136 | 131200 | 52994 | | | 7.2 | 374 | 4468 | 21700 | 2847 | | | | Beaverhill Lake |
| 0645192207000 | 98540 | 4 | 747 | 2986 | 3012 | 252979 | 157234 | 66489 | | | 6.2 | 173 | 3108 | 25916 | 120 | | | | Beaverhill Lake |
| 0665250211000 | 102401 | 2 | 793 | 3420 | 3455 | 204964 | 123600 | 75892 | | | 6.1 | 1160 | 461 | 3605 | 500 | | | | Beaverhill Lake |
| 0575151201000 | 90771 | 4 | 939 | 3211 | 3222 | 209086 | 128455 | 64518 | 63044 | 2500 | 6.2 | 373 | 1390 | 14285 | 134 | 576 | 365 | 0.757 | Elk Point |
| 0625262609000 | 161564 | 0 | 896 | 3698 | 4181 | 229858 | 140590 | 60000 | 64888 | 4100 | 7.1 | 3325 | 1779 | 19462 | 602 | 822 | 578 | 0.712 | Elk Point |
| 0525141808000 | 82645 | 5 | 961 | 3495 | 3532 | 184706 | 113700 | 53934 | 51403 | 4300 | 6.3 | 572 | 1677 | 14770 | 106 | 616 | 514 | 0.697 | Elk Point |
| 0685211416000 | 104435 | 1 | 709 | 2926 | 2934 | 245866 | 151500 | 69534 | 67645 | 3206 | 5.7 | 815 | 2138 | 21860 | 39 | 930 | 722 | 0.688 | Elk Point |
| 0515172710000 | 81239 | 2 | 1003 | 3897 | 3918 | 177708 | 108000 | 52595 | | | 6.9 | 1267 | 903 | 14526 | 850 | | | | Elk Point |
| 0565162404000 | 89377 | 1 | 939 | 3322 | 3363 | 203509 | 125775 | 55586 | | | 6.0 | 399 | 1984 | 19632 | 270 | | | | Elk Point |
| 0595210115000 | 92909 | 3 | 1118 | 3854 | 3868 | 204562 | 127270 | 46453 | | | 7.6 | 384 | 2420 | 27790 | 500 | | | | Elk Point |
| 0615151404000 | 94861 | 4 | 831 | 2897 | 2907 | 201636 | 125312 | 54018 | | | 6.7 | 69 | 3178 | 18750 | 630 | | | | Elk Point |
| 0615182808000 | 94928 | 2 | 910 | 3231 | 3246 | 239878 | 148350 | 63751 | | | 7.4 | 247 | 2056 | 25193 | 570 | | | | Elk Point |
| 0615191902000 | 94953 | 6 | 897 | 3372 | 3375 | 254165 | 158598 | 60248 | | | 6.6 | 700 | 4540 | 30000 | 160 | | | | Elk Point |
| 0615191902000 | 94953 | 7 | 897 | 3372 | 3375 | 253651 | 158598 | 60079 | | | 6.6 | 370 | 4540 | 30000 | 130 | | | | Elk Point |

Reproduced with permission of the copyright owner. Further reproduction prohibited without permission.



| DLS | ID | # | elev | dtop | dbot | TDS | Cl | Na | $Na_c$ | K | pH | $SO_4$ | Mg | Ca | $HCO_3$ | $Ca_{ex}$ | $Na_{df}$ | Na/Cl | Aquifer |
|---|---|---|---|---|---|---|---|---|---|---|---|---|---|---|---|---|---|---|---|
| 0625181802000 | 95846 | 2 | 880 | 3296 | 3302 | 211584 | 131588 | 58148 | | | 7.2 | 25 | 3038 | 18736 | 100 | | | | Elk Point |
| 0625191604000 | 95870 | 3 | 874 | 3252 | 3263 | 246694 | 154174 | 57545 | | | 6.4 | 173 | 3600 | 31160 | 85 | | | | Elk Point |
| 0625212710000 | 96041 | 2 | 892 | 3410 | 3427 | 244019 | 152724 | 56195 | | | 6.4 | 168 | 4086 | 30750 | 195 | | | | Elk Point |
| 0635161106000 | 97089 | 1 | 1049 | 3109 | 3120 | 247250 | 154160 | 60651 | | | 6.1 | 200 | 3350 | 28860 | 60 | | | | Elk Point |
| 0635202802000 | 97195 | 3 | 787 | 3197 | 3205 | 265910 | 164472 | 71813 | | | 6.6 | 219 | 1855 | 27468 | 170 | | | | Elk Point |
| 0635202802000 | 97195 | 4 | 787 | 3197 | 3205 | 272424 | 169367 | 72470 | | | 6.6 | 198 | 3710 | 26596 | 170 | | | | Elk Point |
| 0635213210000 | 97210 | 4 | 771 | 3258 | 3272 | 268717 | 167444 | 62640 | | | 6.9 | 138 | 2590 | 35868 | 75 | | | | Elk Point |
| 0635213210000 | 97210 | 5 | 771 | 3258 | 3272 | 250993 | 157234 | 56058 | | | 7.1 | 201 | 4144 | 33306 | 100 | | | | Elk Point |
| 0655152202000 | 100911 | 1 | 993 | 2908 | 2922 | 255025 | 158960 | 64067 | | | 7.2 | 200 | 3800 | 27900 | 200 | | | | Elk Point |
| 0655180110000 | 100931 | 5 | 803 | 2938 | 2954 | 265351 | 165015 | 71155 | | | 6.6 | 193 | 3930 | 24940 | 240 | | | | Elk Point |
| 0655191110000 | 100954 | 1 | 812 | 3023 | 3028 | 265637 | 164472 | 72311 | | | 5.6 | 235 | 2385 | 26160 | 150 | | | | Elk Point |
| 0655202006000 | 100976 | 3 | 743 | 3071 | 3086 | 267034 | 165502 | 71355 | | | 6.0 | 222 | 2436 | 27470 | 100 | | | | Elk Point |
| 0655231810000 | 101015 | 4 | 846 | 3458 | 3469 | 263726 | 164200 | 65509 | | | 5.9 | 43 | 2935 | 30956 | 170 | | | | Elk Point |
| 0665183204000 | 102318 | 2 | 765 | 2865 | 2883 | 252428 | 157900 | 63038 | | | 5.3 | 195 | 5020 | 26181 | 190 | | | | Elk Point |
| 0665193506000 | 102328 | 1 | 760 | 2899 | 2902 | 258358 | 160140 | 68381 | | | n/a | 200 | 2230 | 27360 | 96 | | | | Elk Point |
| 0665193506000 | 102328 | 2 | 760 | 3010 | 3038 | 242482 | 151000 | 57896 | | | n/a | 230 | 2665 | 30635 | 114 | | | | Elk Point |
| 0665210910000 | 102346 | 1 | 741 | 3094 | 3100 | 300914 | 186000 | 87170 | | | 5.8 | 420 | 3320 | 23920 | 171 | | | | Elk Point |
| 0675153010000 | 103452 | 2 | 956 | 2817 | 2821 | 263540 | 162700 | 77839 | | | 5.9 | 240 | 2360 | 20360 | 82 | | | | Elk Point |
| 0675162607000 | 103460 | 2 | 943 | 2864 | 2874 | 256075 | 158000 | 74876 | | | n/a | 290 | 2070 | 20790 | 98 | | | | Elk Point |
| 0675162607000 | 103460 | 1 | 943 | 2823 | 2829 | 258708 | 160140 | 70389 | | | n/a | 190 | 2070 | 25870 | 99 | | | | Elk Point |
| 0675210210000 | 103526 | 6 | 748 | 3045 | 3060 | 267071 | 166400 | 70004 | | | 5.8 | 318 | 4540 | 25740 | 140 | | | | Elk Point |
| 0675212815000 | 103533 | 6 | 707 | 2989 | 2997 | 256375 | 158820 | 69631 | | | n/a | 190 | 2320 | 25370 | 90 | | | | Elk Point |
| 0675220815000 | 103537 | 4 | 704 | 3121 | 3126 | 258987 | 161000 | 64988 | | | n/a | 210 | 2640 | 30120 | 59 | | | | Elk Point |
| 0675230809000 | 103559 | 5 | 776 | 3275 | 3284 | 261336 | 164838 | 53698 | | | 6.5 | 211 | 6072 | 36480 | 75 | | | | Elk Point |
| 0685230801020 | 104526 | 1 | 790 | 3231 | 3231 | 241319 | 152922 | 46862 | | | 5.9 | 253 | 7320 | 33768 | 395 | | | | Elk Point |
| 0685230906000 | 104527 | 1 | 789 | 3218 | 3227 | 264522 | 166100 | 53744 | | | 5.5 | 359 | 4613 | 39640 | 134 | | | | Elk Point |
| 0635161106000 | 97089 | 2 | 1049 | 3456 | 3479 | 216584 | 134300 | 55487 | | | 6.4 | 175 | 1760 | 24780 | 167 | | | | Cambrian |
| 0655202006000 | 100976 | 4 | 743 | 3171 | 3181 | 251911 | 157526 | 56228 | | | 6.0 | 267 | 3654 | 34170 | 135 | | | | Cambrian |
| 0665262303000 | 102417 | 3 | 760 | 3536 | 3546 | 228823 | 143568 | 50311 | | | 6.0 | 440 | 4818 | 29602 | 170 | | | | Cambrian |
| 0675222701000 | 103545 | 2 | 681 | 3090 | 3094 | 241113 | 150480 | 54671 | | | n/a | 170 | 2690 | 33070 | 66 | | | | Cambrian |
| 0675222701000 | 103545 | 3 | 681 | 3113 | 3119 | 240506 | 149940 | 56440 | | | n/a | 150 | 2690 | 31230 | 114 | | | | Cambrian |
| 0685170910000 | 104409 | 1 | 907 | 2972 | 3008 | 220669 | 136680 | 58676 | | | 5.4 | 480 | 2480 | 22280 | 149 | | | | Cambrian |

## Appendix D: Equations for the density calculation of formation waters (Rowe & Chow, 1970; Kestin et al., 1981)

$\rho^{-1} = A - B\cdot p - C\cdot p^2 + w\cdot D + w^2\cdot E - w\cdot F\cdot p - w^2\cdot G\cdot p - 0.5\cdot w\cdot H\cdot p^2$,

where $\rho$ = density (kg/m3), p = pressure (MPa), T = temperature ($^oK$), w = weight percent salinity (kg/kg)

The coefficients A to H are functions of temperature:

$A = 1.00674\cdot 10^2T^{-2} - 1.127522T^{-1} + 2.84851\cdot 10^{-3} - 1.5106\cdot 10^{-5}T + 9.270048\cdot 10^{-9}T^2$

$B = 1.042948T^{-2} - 1.1933677\cdot 10^{-2}T^{-1} + 5.30753\cdot 10^{-5} - 1.0688768\cdot 10^{-7}T + 8.492739\cdot 10^{-11}T^2$

$C = 1.23268\cdot 10^{-9} - 6.861928\cdot 10^{-12}T$

$D = -2.5166\cdot 10^{-3} + 1.11766\cdot 10^{-5}T - 1.70552\cdot 10^{-8}T^2$

$E = 2.84851\cdot 10^{-3} - 1.54305\cdot 10^{-5}T + 2.23982\cdot 10^{-8}T^2$

$F = -1.5106\cdot 10^{-5} + 8.4605\cdot 10^{-8}T - 1.2715\cdot 10^{-10}T^2$

$G = 2.7676\cdot 10^{-5} - 1.5694\cdot 10^{-7}T + 2.3102\cdot 10^{-10}T^2$

$H = 6.4633\cdot 10^{-8} - 4.1671\cdot 10^{-10}T + 6.8599\cdot 10^{-13}T^2$



Reproduced with permission of the copyright owner. Further reproduction prohibited without permission.